UNIVERSIDAD COMPLUTENSE DE MADRID
FACULTAD DE CIENCIAS QUIMICAS

TESIS DOCTORAL

Alternativas para facilitar el uso de nanocelulosas en la producción de papel reciclado

Alternatives to facilitate the use of nanocellulloses in the production of recycled paper

MEMORIA PARA OPTAR AL GRADO DE DOCTOR

PRESENTADA POR

Cristina Campano Tiedra

Directora

Mª Ángeles Blanco Suárez

Madrid

UNIVERSIDAD COMPLUTENSE DE MADRID

FACULTAD DE CIENCIAS QUÍMICAS

Departamento de Ingeniería Química y de Materiales

TESIS DOCTORAL

Alternativas para facilitar el uso de nanocelulosas en la producción de papel reciclado

Alternatives to facilitate the use of nanocelluloses in the production of recycled paper

MEMORIA PARA OPTAR AL GRADO DE DOCTOR

PRESENTADA POR

Cristina Campano Tiedra

Directora

Mª Ángeles Blanco Suárez

Madrid, 2019

UNIVERSIDAD COMPLUTENSE MADRID

DECLARACIÓN DE AUTORÍA Y ORIGINALIDAD DE LA TESIS PRESENTADA PARA OBTENER EL TÍTULO DE DOCTOR

D./Dña. Cristina Campano Tiedra,
estudiante en el Programa de Doctorado D9BN - Doctorado en Ingeniería Química,
de la Facultad de Ciencias Químicas de la Universidad Complutense de Madrid, como autor/a de la tesis presentada para la obtención del título de Doctor y titulada:

Alternativas para facilitar el uso de nanocelulosas en la producción de papel reciclado /
Alternatives to facilitate the use of nanocelluloses in the production of recycled paper

y dirigida por: Mª Ángeles Blanco Suárez

DECLARO QUE:

La tesis es una obra original que no infringe los derechos de propiedad intelectual ni los derechos de propiedad industrial u otros, de acuerdo con el ordenamiento jurídico vigente, en particular, la Ley de Propiedad Intelectual (R.D. legislativo 1/1996, de 12 de abril, por el que se aprueba el texto refundido de la Ley de Propiedad Intelectual, modificado por la Ley 2/2019, de 1 de marzo, regularizando, aclarando y armonizando las disposiciones legales vigentes sobre la materia), en particular, las disposiciones referidas al derecho de cita.

Del mismo modo, asumo frente a la Universidad cualquier responsabilidad que pudiera derivarse de la autoría o falta de originalidad del contenido de la tesis presentada de conformidad con el ordenamiento jurídico vigente.

En Madrid, a 11 de junio de 2019

Fdo.: CRISTINA CAMPANO TIEDRA

Esta DECLARACIÓN DE AUTORÍA Y ORIGINALIDAD debe ser insertada en la primera página de la tesis presentada para la obtención del título de Doctor.

COMPLUTENSE UNIVERSITY OF MADRID

FACULTY OF CHEMICAL SCIENCES

DEPARTMENT OF CHEMICAL ENGINEERING AND MATERIALS

DOCTORAL DISSERTATION

Alternativas para facilitar el uso de nanocelulosas en la producción de papel reciclado/ Alternatives to facilitate the use of nanocelluloses in the production of recycled paper

Submitted to the Complutense University of Madrid for the degree of Doctor in Chemical Engineering by

Cristina Campano Tiedra

Directed by

Mª Ángeles Blanco Suárez

Madrid, 2019

MARIA ÁNGELES BLANCO SUÁREZ, CATEDRÁTICA DEL DEPARTAMENTO DE INGENIERÍA QUÍMICA Y DE MATERIALES DE LA UNIVERSIDAD COMPLUTENSE DE MADRID

INFORMA

Que el trabajo de investigación titulado "ALTERNATIVAS PARA FACILITAR EL USO DE NANOCELULOSAS EN LA PRODUCCIÓN DE PAPEL RECICLADO / ALTERNATIVES TO FACILITATE THE USE OF NANOCELLULOSES IN THE PRODUCTION OF RECYCLED PAPER" ha sido realizado bajo su dirección en el Departamento de Ingeniería Química y Materiales, dentro del Grupo de Investigación de Celulosa, Papel y Tratamientos Avanzados de Agua de la Universidad Complutense de Madrid, y constituye la memoria que presenta Dña. Cristina Campano Tiedra para optar al Grado de Doctor.

Y para que conste a los efectos oportunos, firman la presente, en Madrid a 11 de junio de 2019.

AGRADECIMIENTOS

En primer lugar, me gustaría agradecer a mi directora de tesis, la Prof. Ángeles Blanco por toda la dedicación y apoyo que he recibido durante todos estos años. Gracias por todos los conocimientos que me has transmitido y por haberme guiado y aconsejado numerosas veces durante el transcurso de mi tesis doctoral. También, agradecer al Prof. Carlos Negro por su ayuda y sus consejos. Gracias por haber confiado en mí todo este tiempo.

I would also like to express my gratitude to the Prof. Theo van de Ven and his research group in the University of McGill. Thank you for the huge knowledge I have learnt from you and for offering me your help and advice. Thanks also to Roya Koshani: I have been really lucky for finding your friendship. You are one of those friends that it is difficult to find. Thank you very much for all your help and support during all this time.

Me gustaría agradecer al Ministerio de Economía y Competitividad por la beca de formación de personal investigador concedida para la realización de esta tesis, por la ayuda para la realización de estancias breves y por el proyecto NANOSOLPAPELREC. Gracias también a Holmen Paper Madrid en cuyas instalaciones, dentro del laboratorio UCM-Holmen, se ha llevado a cabo parte de la experimentación de esta tesis. Gracias también al grupo LEPAMAP de la UdG, al grupo de Interacciones planta-bacteria, de la EEZ-CSIC y al CIFOR-INIA.

Quisiera agradecer también a todos los que han sido y los que siguen siendo miembros del Grupo de Investigación de Celulosa, Papel y Tratamientos Avanzados de Agua. Gracias a la Prof. Mª Concepción Monte, Prof. Elena de la Fuente, Prof. Rubén Miranda, Noemi y Ana por todo el asesoramiento recibido. Gracias también al Prof. Julio Tijero, Antonio, Sara, Luis, Helen, Isabel, Giovanni, Roberto y Jhiret. Querría hacer una mención especial a los grandes científicos del futuro Javi y Pep, con los que he pasado muy buenos momentos.

Quiero dar mil gracias al que ha sido mi mayor apoyo en el día a día de esta tesis: gracias Patricio, he aprendido muchísimo de ti y creo que hemos formado un equipo maravilloso. Has demostrado ser un investigador y un escritor extraordinario, además de un genial amigo, de esos que es difícil de encontrar. Gracias por estar ahí en todo momento, por animarme en los malos momentos y por reírnos juntos en los buenos. También, gracias por tus ideas felices de última hora, que sin duda han sido clave en muchas ocasiones. Una gran parte de esta tesis te la debo a ti.

También, quiero mencionar al gran grupo de personas que he encontrado en esta universidad: Marcos, Noemi, Pablo y Sandra. Gracias por tantas risas chicos y por tanta ayuda desinteresada, esto no habría sido posible sin vosotros. En especial a Gonzalo, gracias por ser tan buena persona, espero que no cambies nunca; a Antonio, gracias por los buenos momentos que nos has dado, me he reído muchísimo contigo; y a Jesús, gracias por tu gran disponibilidad, ayuda y buen humor.

Mil gracias a Mari y Vicky por todo vuestro apoyo incondicional, por esos afterwork maravillosos, que han supuesto una inyección de ánimo y motivación, y por el gran equipo divulgativo que hemos formado. Esta tesis no habría tenido ningún sentido si vosotras no hubierais estado ahí. Vicky, eres una gran persona, me he reído muchísimo contigo todo este tiempo y desde luego que eres una gran amiga. Mari, infinitas gracias por todo el apoyo que me has dado todo este tiempo. Siempre te estaré agradecida por tanto cariño y comprensión. Habéis estado ahí tanto en los buenos como en los malos momentos, muchas gracias por todo!

Además me gustaría agradecer a todas las personas que han contribuido a que pueda presentar esta tesis doctoral: gracias a mis amigos de toda la vida de Nava, en especial a Sara, me ha encantado recuperar esa complicidad que teníamos antes, gracias por todos los ratos que hemos pasado juntas y que me han ayudado a desconectar. También gracias a mis mejores compañeros de carrera y ya doctores, Rut y Álvaro. Gracias a mis profesores de la Universidad de Valladolid, que me transmitieron su pasión por la ciencia. Gracias a mi compi de piso y amiga Nieves, fue una suerte encontrarte, y quiero agradecerte el infinito apoyo diario y todos los momentos buenísimos que hemos pasado. También quiero dar las gracias a Rober por enseñarme a ser mejor persona y por todo el cariño, confianza y apoyo que me ha dado en los primeros años de tesis.

Por último, me gustaría dedicar esta tesis doctoral a mi familia. Ellos me han dado la vida y me han aportado una educación excelente. Siempre me habéis animado a que siga hacia adelante y que luche por lo que quiero. Mami, infinitas gracias por todo, estoy muy orgullosa de tenerte como madre. Gracias por todos los cuidados, por todo el cariño y por la ilusión con la que me recibes cada vez que voy a verte. Papi, también estoy muy orgullosa de tenerte como padre. Siempre me has apoyado y has confiado en mí. Gracias por todo tu cariño y amor. Y Sonia (la chica), de esas personas con las que se tiene complicidad incluso con mar de por medio. Gracias por ser como eres, por todo tu cariño incondicional. Me siento orgullosa de ser vuestra hija y hermana, os quiero mucho.

Success is not the key to happiness. Happiness is the key to success. If you love what you are doing, you will be successful.

-Albert Schweitzer-

ORIGINAL PUBLICATION LIST

I. C. Campano, A. Balea, A. Blanco, C. Negro. Enhancement of the fermentation process and properties of bacterial cellulose: a review. *Cellulose* 23 (2016) 57-91.

II. C. Campano, N. Merayo, C. Negro, A. Blanco. Low-fibrillated bacterial cellulose nanofibers as a sustainable additive to enhance recycled paper quality. *International Journal of Biological Macromolecules* 114 (2018) 1077-1083.

III. C. Campano, N. Merayo, C. Negro, A. Blanco. In situ production of bacterial cellulose to economically improve recycled paper properties. *International Journal of Biological Macromolecules* 118 (2018), 1532-1541

IV. C. Campano, R. Miranda, N. Merayo, C. Negro, A. Blanco. Direct production of cellulose nanocrystals from old newspapers and recycled newsprint. *Carbohydrate Polymers* 173 (2017) 489-496.

V. C. Campano, N. Merayo, A. Balea, Q. Tarrés, M. Delgado-Aguilar, P. Mutjé, C. Negro, A. Blanco. Mechanical and chemical dispersion of nanocelluloses to improve their reinforcing effect on recycled paper. *Cellulose* 25 (2018) 269-280.

VI. C. Campano, P. Lopez-Exposito, A. Blanco, C. Negro, T. G. M. van de Ven. Hairy cationic nanocrystalline cellulose as a novel flocculant of clay. *Journal of Colloid and Interface science,* 545 (2019) pp. 153-161.

VII. C. Campano, P. Lopez-Exposito, A. Blanco, C. Negro, T. G. M. van de Ven. Hairy cationic nanocrystalline cellulose as retention additive in recycled paper. *Cellulose.* https://doi.org/10.1007/s10570-019-02494-x

ADDITIONAL PUBLICATIONS

VIII. C. Campano, P. Lopex-Exposito, P. Bolivar, C. Negro, A. Blanco. Toward an online monitoring of the nanocrystalline cellulose aggregation state: correlating image analysis and Dynamic Light Scattering data. In preparation

IX. A. Blanco, M. C. Monte, C. Campano, A. Balea, N. Merayo, C. Negro. Handbook of nanomaterials for industrial applications. Nanocellulose for industrial use: cellulose nanofibers (CNF), cellulose nanocrystals (CNC) and bacterial cellulose (BC). *Elsevier* (2018).

INDEX

FIGURES CAPTION

TABLES LEGEND

NOMENCLATURE

ACD	Average crystalline dimension
AFM	Atomic Force Microscopy
BC	Bacterial cellulose
BCNF	Bacterial cellulose nanofibers
Cel^-	Mutant cells that do not produce cellulose
Cel^+	Cellulose producing cells
CD	Cationic demand
CDAMC	Cationic dialdehyde modified cellulose
CECT	Spanish Type Culture Collection
CH	Chitosan
CMC	Carboxymethyl cellulose
CNC	Cellulose Nanocrystals
CNCC	Hairy cationic nanocrystalline cellulose
CNF	Cellulose nanofibers
COD	Chemical oxygen demand
CPAMB	Three-component retention system
Cr.I	Crystallinity index
D1	Dispersant 1: A mixture of a moisturizing and a detergent surfactant
D2	Dispersant 2: A moisturizing agent
D_2	2D fractal dimension
D_f	3D fractal dimension
DAC	Dissolved amorphous cellulose
DAMC	Dialdehyde modified cellulose
DLS	Dynamic Light Scattering
ENCC	Electrosterically stabilized hairy nanocrystalline cellulose
EUC	*Eucalyptus globulus* ECF bleached kraft pulp
F	Never-dried CNC preserved in the freezer
F-FR	Frozen CNC suspensions defrost in the fridge
F-VA	Frozen CNC suspensions defrost in a vacuum furnace at 20ºC
F-40	Frozen CNC suspensions defrost in a bath at 40ºC
FBRM	Focused beam reflectance measurement

FWHM	Full width at half maximum of the diffraction peak
GT	Girard Reagent T
HNC	Hairy nanocrystalline cellulose
IEP	Isoelectric point
LCNC	Ligno-cellulose nanocrystals
LCNF	Ligno-cellulose nanofibers
LIQ	Never-dried CNC preserved in the fridge
LODP	Level-off polymerization degree
M10	Cell Growth medium: 20 g/L fructose, 5 g/L yeast extract, 3 g/L peptone
MAA	Mean aggregation area
MCC	Microcrystalline cellulose
MCL	Mean chord length
MFC	Microfibrillated cellulose
MFD	Maximum Feret Diameter
MG	Non-printed magazine
NC	Nanocellulose
NNLS	Non-negative least squares
NP	Non-printed newsprint
NP-B	Bleached non-printed newsprint
ONP	Old newsprint
OTR	Oxygen transmission rate
PAM	Polyacrylamide
PD	Polymerization degree
PDA	Photometric dispersion analysis
RP	Recycled paper
RS	Retention system
SD	Standard deviation
SEM	Scanning electron microscopy
SNCC	Sterically stabilized nanocrystalline cellulose
TEM	Transmission Electron Microscopy
TEMPO	(2,2,6,6-Tetramethylpiperidin-1-yl)oxyl
TI	Tensile Index
XRD	X-ray diffraction
η	Intrinsic viscosity
τ_D	Light intensity autocorrelation function decay


SUMMARY

SUMMARY

Papermaking is one of the oldest industries and the leading one in the application of recycling approaches. The increase in paper recyclability has been driven by economic and environmental factors, turning the paper sector into a reference of sustainable industry. Thus, recycling rate has increased year after year, reaching a record value of 72.3%, in Europe, in 2017. However, the recycled paper (RP) industry is continuously challenged by: (i) the growing quality requirements in terms of mechanical, physical and printing properties of paper products, (ii) the deterioration of recycled fibers as a consequence of the increasing number of recycling cycles, and (iii) the restrictions in the production costs. As a result of the above, this sector is looking for alternatives to further upgrade the quality of the paper products and to decouple it from the negative effects entailed by processing the fibers and adding paper and process aditives.

Nanocelluloses (NC) possess the inherent properties of cellulose, such as biodegradability, renewability and sustainability, and, additionally, they present several advantages, which include a high surface area, unique optical properties, lightweight, stiffness, high strength, etc. All these aspects have attracted the interest of both researchers and industries, shown by the exponential increase in the number of nanocellulose-related publications and patents

since 2010, especially in the last two years. According to the Journal Citation Reports, the number of articles published in 2018 amounted to 860.

The exceptional NC properties together with the fact that they present the same composition as paper, have driven these industries to regard NC as a possible solution for a number of the challenges described above. So far, the potential use of NC in papermaking has focused on improving paper quality in different aspects, such as strength, barrier properties or some special properties (flame retardant behavior or linting mitigation). Most of these studies have been focused on the use of cellulose nanofibers (CNF), while the potential of bacterial cellulose (BC) and cellulose nanocrystals (CNC) has been much less explored.

Thus, the main objective of this PhD thesis is to assess the potential of three types of nanocellulosic products to enhance the production of recycled paper. The NC considered in this work are: bacterial cellulose, cellulose nanocrystals and cationic hairy cellulose nanocrystals (CNCC). To attain the mentioned objective, the research has been divided into three lines:

1. The improvement of the mechanical properties of RP with BC.
2. The assessment of the dispersion degree of the CNC and its effect on RP.
3. The use of CNCC as a retention aid in paper production.

The aim of the first line of this PhD thesis is, therefore, the improvement of the mechanical properties of RP with the use of BC.

Despite the intensive research on the synthesis, characterization and application of BC, its industrial production is still limited due to its low productivity and the high cost of raw materials. The state of the art, reviewed in Publication I, summarizes the studies on BC production, considering the use of by-products as nutrients, the optimization of the culture method and the genetic modification of the strains to achieve a higher productivity. In addition, the possibilities of enhancing a desired property of BC for a specific use, either by varying the culture conditions or by using additives, are considered. Based on the state of the art, a genetic modification of the bacteria was proposed, with the objective of improving the BC production. In addition, these knowledge have been used to produce BC in static and agitated conditions and evaluate their application to improve the mechanical and physical properties of RP. On the other hand, a new BC production method was studied involving the in-situ culture of bacteria within the pulp so that the BC, produced at short culture times, produces an increase in paper strength. This approach could be used on-line to upgrade secondary fibers without fibrillation and dispersion steps.

Bacterial productivity has been proved to increase by some orders of magnitude through the rise of the intracellular levels of cyclic diguanylate (c-di-GMP, in charge of the exopolysaccharides synthesis) by the overexpression of DGC. This concept was applied in

this PhD thesis for *K. sucrofermentans* through the action of the gene pleD*. Three different methodologies were attempted for the cited purpose, using *E. coli β2163* donor strain: electroporation, and biparental and triparental conjugacion. It was proved that the gene pleD* was effectively introduced into the bacteria. However, neither the BC production nor the pellicle morphology were altered by this fact. Thus, it was concluded that the c-di-GMP levels of *K. sucrofermentans* were already at the maximum, failing the overexpression of the DGC by the gene pleD*. Consequently, the unmodified bacteria was used for the next studies.

Up to now, the improvement of virgin pulps with BC has been carried out by adding a BC membrane disintegrated at high speed. The approach followed in Publication II was different since BC nanofibers (BCNF) were produced by soft homogenization of disintegrated BC membranes and then added to RP pulp. When highly fibrillated NC is used as dry strengthening agent of paper, it usually induces an opposite trend on tensile and tear strengths: when one is increased, the other is reduced. Nevertheless, with the addition of low fibrillated BCNF, where some clusters of nanofibers coexist with individual nanofibers, this effect can be avoided. The best result was achieved with the addition of 3% BCNF, reaching increments in both tensile and tear indexes, as well as in strain at break (11.1; 7.6; and 66.8%, respectively). This synergistic improvement was related to a better paper flexibility. Due to size issues, the clusters were retained in the fiber network not only by hydrogen bonding, but also by physical retention within the gaps. In spite of this study pointing at the high potential of BC as strengthening agent, the approach described involves a high cost of BC production, resulting from the long culture time needed (around 7 days) and the high energy required to both, disintegrate and fibrillate the membranes, as well as disperse the nanofibers within the pulp.

In view of the above conclusions, a novel approach was proposed based on the in situ culture of bacteria with secondary fibers (Publication III). This could be an attractive alternative to reduce the associated costs while reaching similar benefits. Both agitated and static cultures were studied and compared in terms of their strengthening effect on the upgraded papers at different culture times. Results show that again, both tensile and tear indexes were improved when pulps cultivated in agitation were used (12.2% and 14.2%, respectively). In this study, bacteria coated the secondary fibers creating the BC on their surface and improving the quality of each individual fiber. In this way, the culture time needed to upgrade papers with the use of BC was reduced from 7 days to 12 h. Moreover, the energy costs associated to homogenization and dispersion were avoided. However, pulps cultured in static mode failed to improve RP properties, due to the fact that the BC was produced in a heterogeneous manner: while bacteria moved to the surface of the culture broth in search for oxygen, the added fibers tended to sediment.

The second line of this PhD thesis aims to characterize the aggregation state of CNC and to assess its effect on paper properties when they are used as dry-strengthening agents.

CNC have been traditionally produced from virgin fibers, namely wood, plants or by-products, and it was not until 2015 that the use of recycled fibers was considered for their production. Moreover, these few studies involved the application of intensive alkali and bleaching treatments to remove components other than cellulose, prior to a hydrolysis step. The hypothesis in this case is that, if a direct hydrolysis of secondary fibers could be conducted without a deterioration of the CNC effects on paper properties, CNC could be produced on-site at a much lower cost. In addition, the production of CNC from recycled fibers could take advantage of the availability of old newspapers, as consequence of the 28.3% decrease in the production of newsprint in the last five years in Europe.

In the Publication IV, CNC were directly produced from 100% RP. CNC yield and quality were assessed through lignin and ash determination, X-ray diffraction analysis, atomic force microscopy (AFM) and thermogravimetric analysis. The different composition of these papers, mainly containing cellulose, hemicelluloses, lignin, inks and mineral fillers, made CNC purity vary in the range of 77-93%. However, similar crystallinities (92-95%), polymerization degree (180) and aspect ratios (in the range of 50-120) were observed. This study proved, for the first time, the effective production of CNC from RP, without using a strong pretreatment to remove impurities. The results also showed that the hydrolysis yield and the CNC purity would not significantly affect the quality of the RP when these products were used as dry strengthening additives.

Achieving a high quality of CNC, however, is worth nothing if nanocrystals are not homogeneously distributed throughout the fiber network. Thus, the CNC dispersion degree and the way they are mixed within the furnish before paper formation is of utmost importance to attain positive effects in the final product. Taking this into consideration, operations typically used in RP mills, such as pulp disintegration or the use of dispersing agents, were applied to CNC and CNF to improve the homogeneity of their mixture within the fibers (Publication V). Pulping time, temperature and need for soaking were considered variables of study. Two dispersing agents were used directly to disperse the CNC and CNF suspensions prior to their application. In addition, two different retention systems were used: a three-component system (based on a coagulant, polyacrylamide and bentonite typically used in newsprint mills) and chitosan (as bioflocculant). Pulp soaking and long pulping times (60 min) favored the homogeneous mixture of both NC with the fibers, achieving increments in tensile index up to 30%. However, with the use of a low dose of a dispersing agent (0.003%), tensile index could still be increased up to 20.6%, avoiding the referred long pulping times. Hence, it was concluded that NC dispersion plays an important role on the enhancement of paper properties and is, therefore, a key parameter to study.

Nevertheless, the NC dispersion degree alone may not be the only important parameter in the improvement of paper properties with these nanoparticles. The nature of aggregates constituting the suspension may also play a relevant role. With this in view, the description of the aggregation state of CNC becomes necessary to understand how the type of aggregates, according to their morphology, cause distinctive effects. The hypothesis in this case is that CNC aggregation could be indirectly measured through the use of scattering techniques, such as dynamic light scattering (DLS), acquiring the data at different temperatures. This was indeed the focus of the article in preparation VIII, where the geometrical features of the particles present in CNC suspensions, extracted from AFM images, were correlated with DLS data. The light intensity autocorrelation function decay (τ_D) at different temperatures was considered for this purpose. The particles/aggregates observed in the AFM micrographs were classified into five groups attending to geometrical features, using unsupervised machine learning k-means clustering algorithm. Most of the particles were included in the group of smallest size, being presumably individual CNC. The relevance that each group had in the variability of the τ_D at different temperatures was determined through a variable importance analysis. The presence of a higher amount of particles in the groups of smaller size showed a higher impact on the τ_D at 50 ºC, where τ_D at the minimum temperature tested (10 ºC) was largely related to the quantity of medium aggregates. This first approach to describe the aggregation state of CNC suspensions could be further extended to extract the information of the aggregates directly from DLS data, without the need to resort to microscopy techniques. This new methodology paves the way to the development of a variety of possibilities for the CNC production and application at industrial scale.

Finally, the third line of this PhD thesis was conducted with the objective of using CNCC as retention additive to get a synergic effect and, thus, simplify the wet-end system of the paper production process at the time that paper quality increases.

Hairy nanocrystalline cellulose, a new family of NC having a crystalline shaft with amorphous regions at both ends, was recently discovered at the University of McGill. These particles combine the strength, lightness and cellulose-based composition of CNC, with the additional properties of the amorphous hair-like structures, which confer flocculant-like properties and electro-steric stability to the nanoparticles. Based on this knowledge, the possibility of using CNCC, produced through the cationization of the hairs, as retention aid in the production of paper was considered. With this hypothesis, NC could be used with a double objective as process and product additive, so that they could optimize retention and drainage, at the same time that paper properties could be improved.

First, the flocculation mechanism of these newly produced CNCC was assessed in a kaolinite suspension (Publication VI). Photometric dispersion analysis and focus beam reflectance measurements were used to monitor flocculation. Additionally, the average fractal

dimension (D_f) of the flocs formed was determined with a novel machine learning random forest regression model trained to interpret chord length distribution data. The maximum floc size and faster flocculation took place at the dosage corresponding to the isoelectric point (IEP), 25 - 30 mg/g, and reflocculation efficiency was around 50%. Hence, the flocculation mechanism of the CNCC/kaolinite system was identified as charge neutralization with reconformation of the flocs after breakage. The different D_f values measured on kaolinite/CNCC flocs suggested a relationship between particle conformation and CNCC dosage, presenting an opener structure when the CNCC dosage was between 10 and 20 mg/g.

Second, a filler suspension containing kaolinite and $CaCO_3$, the most common fillers used in papermaking, has been flocculated with CNCC with the aim of establishing differences or similarities with the previous study. CNCC were found to heteroflocculate fillers at a wide range of dosages, being the maximum floc size obtained with a CNCC dosage of 30 mg/g, which corresponded to that of the IEP, as in the previous study.

Finally, in the Publication VII, the CNCC were also used to flocculate a RP pulp containing the same proportion of fillers, in order to assess the flocculation of the full furnish. Additionally, pulp drainage, filler retention and mechanical properties of the produced papers were evaluated and compared with other RS. The optimum dosage in terms of flocculation efficiency and floc size was 20 mg/g. which corresponds to the IEP. At this dosage, pulp drainage was reduced by 78% and total retention was enhanced by 77%. The flocculation mechanism previously proposed was validated. An additional advantage of using CNCC is the fact that the mechanical properties of the final papers were not so noticeably reduced as with other RS typically used in RP mills.


RESUMEN EXTENDIDO

RESUMEN EXTENDIDO

La industria del papel es una de las más antiguas y la líder en el uso de productos reciclados. El motor del aumento en la reciclabilidad del papel ha sido principalmente impulsado por factores económicos y medioambientales. Por ello, el sector papelero es actualmente una referencia en sostenibilidad. Esto ha hecho que la tasa de reciclaje haya aumentado año tras año, alcanzando un valor record, en Europa, en 2017, del 72.3%. Sin embargo, la industria del papel reciclado (PR) está sometida a numerosos retos: (i) los altos requerimientos en la calidad del papel, especialmente en las propiedades mecánicas, físicas y de impresión, (ii) el deterioro de las fibras recicladas como consecuencia del alto número de ciclos de reciclado y (iii) las restricciones en los costes de producción. Como consecuencia, este sector está buscando alternativas que mejoren la calidad de los productos papeleros y que individualicen los efectos negativos que surgen del procesamiento de las fibras y del uso de aditivos de proceso.

Las nanocelulosas (NC) poseen las propiedades propias de la celulosa, como su biodegradabilidad, renovabilidad y sostenibilidad, y, además, presentan ventajas adicionales, donde se incluyen el alto área superficial, propiedades ópticas únicas, alta ligereza y resistencia, etc. Todo esto ha despertado el interés de un gran número de

investigadores e industrias, mostrado por un aumento exponencial del número de publicaciones y de patentes relacionadas con las NC desde el año 2010 y, especialmente, en los últimos dos años. De acuerdo con el *Journal Citation Reports*, el número de artículos publicados en 2018 fue de 860.

Estas propiedades excepcionales, junto con el hecho de que las NC están compuestas de los mismos componentes que el papel, hace que las industrias papeleras hayan pensado en estos materiales como una posible solución para muchos de los retos descritos anteriormente. Hasta ahora, el uso potencial de las NC en la industria papelera se ha centrado en la mejora de la calidad del papel en diferentes aspectos, que incluyen las propiedades mecánicas, barrera y algunas propiedades especiales (la mejora de la estabilidad térmica o la disminución del *linting*). La mayoría de estos estudios han sido llevados a cabo mediante el uso de nanofibras de celulosa (CNF), mientras que el potencial de la celulosa bacteriana (BC) y de los nanocristales de celulosa (CNC) ha sido mucho menos explorado.

Así, el principal objetivo de esta tesis doctoral es evaluar el potencial de tres tipos de productos nanocelulósicos para la mejora de la producción de papel reciclado. Las NC consideradas en este trabajo son: celulosa bacteriana, nanocristales de celulosa y nanocristales de celulosa *hairy* catiónicos (CNCC). Para desarrollar este objetivo, la investigación se ha dividido en tres bloques:

1. La mejora de las propiedades mecánicas del PR mediante el uso de BC.
2. El estudio del grado de dispersión de los CNC y su efecto en el PR.
3. El uso de los CNCC como agente de retención en la producción de PR.

El objetivo de la primera etapa de investigación es, por tanto, la mejora de las propiedades mecánicas del PR con el uso de BC.

A pesar de la intensiva investigación llevada a cabo sobre la síntesis, caracterización y aplicación de la BC, su producción industrial se encuentra aún limitada por su baja productividad y el alto coste de los nutrientes. El estado del arte, revisado en la Publicación I, recoge los estudios sobre la producción de la BC, considerando el uso de subproductos como nutrientes, la optimización del método de cultivo y la modificación genética de las cepas bacterianas con el objetivo de aumentar su productividad. Además, se han considerado las posibilidades de mejorar una propiedad determinada de la BC para un uso específico, mediante la variación de las condiciones de cultivo o el uso de aditivos. Basado en esta revisión, se ha realizado la modificación genética de las bacterias con el objetivo de aumentar la producción de BC. Además, se ha usado el conocimiento adquirido para producir BC en condiciones estáticas y agitadas, y se ha aplicado para la mejora de las propiedades mecánicas y físicas del PR. Por otro lado, se ha propuesto un nuevo método de producción de BC en el que las bacterias son cultivadas in situ con la pasta, de modo que la

BC pudiera mejorar las propiedades del PR a cortos tiempos de cultivo. Este nuevo enfoque podría ser usado para mejorar las fibras secundarias individualmente, evitando las etapas de dispersión y fibrilación.

Anteriormente, se había demostrado que la productividad bacteriana puede ser mejorada en varios órdenes de magnitud mediante el aumento de los niveles intracelulares de diguanilato cíclico (c-di-GMP, encargado de la síntesis de exopolisacáridos) por la sobreexpresión de DGC. Este concepto ha sido aplicado en esta tesis doctoral, donde el gen pleD* se introdujo en la cepa *K. sucrofermentans*. Se aplicaron tres metodologías diferentes, usando la cepa dadora *E. coli β2163*: electroporación, y conjugación biparental y triparental. Se probó que el gen fue introducido efectivamente en la cepa bacteriana. Sin embargo, no se observaron diferencias en la producción de BC ni en la morfología de las membranas producidas. Por ello, se concluyó que los niveles de c-di-GMP de la cepa *K. sucrofermentans* se encontraban en el máximo nivel, fallando la sobreexpresión del DGC por el gen pleD*. Consecuentemente, para los estudios posteriores se utilizó la cepa sin modificar.

Hasta ahora, la mejora de pastas vírgenes mediante el uso de BC ha sido llevada a cabo mediante la adición de membranas desintegradas a alta velocidad. Sin embargo, el enfoque de la Publicación II es diferente, ya que se produjeron nanofibras de BC (BCNF) mediante una homogeneización suave de las membranas de BC previamente desintegradas, y se añadieron a una pasta de PR. El uso de NC para mejorar la resistencia del papel se encuentra normalmente limitado por la disminución del índice de desgarro. La novedad de este trabajo es que la relación entre estos dos efectos ha sido eliminada debido a que algunos aglomerados de BCNF sin fibrilar están presentes junto con un bajo porcentaje de nanofibras individuales. Los mejores resultados se obtuvieron mediante la adición de un 3% de BCNF, consiguiendo mejoras en el índice de carga de rotura, de desgarro y en la elongación a rotura (11.1; 7.6; y 66.8%, respectivamente). Esta mejora sinérgica está relacionada con un aumento en la flexibilidad del papel. Debido a su tamaño, los aglomerados de BCNF fueron retenidos en la red fibrosa no solo por enlaces de puentes de hidrógeno, sino también por retención física en los huecos. A pesar de que este estudio demuestra el alto potencial de la BC como agente de resistencia, esta metodología conlleva altos costes asociados a la producción de BC, resultantes del largo tiempo de cultivo necesario (unos 7 días) y los altos requerimientos energéticos de desintegración y fibrilación de las membranas, además de la dispersión de las nanofibras con la pasta.

En este contexto, se ha planteado, como alternativa, el cultivo in situ de las bacterias con la suspensión de fibras (Publicación III). Esta opción podría reducir los costes descritos anteriormente mientras que se alcanzan beneficios similares. Se han estudiado cultivos en modo estático y agitado, comparando los beneficios que aportan al PR. Los resultados muestran que, de nuevo, ambos índices fueron mejorados cuando la pasta se cultivó con agitación (12.2% y 14.2%, en los índices de carga de rotura y tracción, respectivamente). Se

observó que las bacterias se situaron en la superficie de las fibras, donde produjeron la BC de tal forma que cubría las mismas. Se este modo se mejoró la calidad del papel mediante la mejora de la calidad de las fibras individuales. Debido a la mayor eficiencia del proceso, el tiempo de cultivo se consiguió reducir de 7 días (obtenido mediante homogeneización de membranas de BC) a 12 h, ahorrando al mismo tiempo muchos de los costes asociados a la dispersión de la BC. Estas mejoras únicamente se consiguieron con cultivos agitados, ya que se formaron sistemas heterogéneos en cultivos estáticos: las bacterias se movieron hacia la superficie en busca de oxígeno, mientras que las fibras originales sedimentaron.

El objetivo de la segunda etapa de la presente tesis doctoral fue la caracterización del estado de agregación de los CNC, y la evaluación del efecto que los agregados de CNC con diferente forma tienen en las propiedades mecánicas del PR.

Los CNC han sido tradicionalmente producidos a partir de fibra virgen, como madera, plantas o sub-productos, y no fue hasta 2015 cuando se consideró el uso de fibras recicladas como materia prima nanocelulósica. Estos estudios incluyen tratamientos alcalinos y de blanqueo para eliminar impurezas y aislar, de este modo, la celulosa para su posterior hidrólisis. La hipótesis en este caso es que, si se pudiera aplicar una hidrólisis directa a las fibras recicladas, sin que conlleve una disminución en los efectos que los CNC tienen en el PR, se podría producir y aplicar los CNC en la propia fábrica de papel a un coste mucho menor. Además, se podría aprovechar la cantidad de periódico ya usado y disponible, como consecuencia de la disminución de la producción de este producto en Europa (28.3%).

En la Publicación IV, se produjeron CNC directamente a partir de 100% PR. Se determinó el rendimiento y la calidad de los CNC mediante el análisis composicional, difracción de rayos X, microscopía de fuerzas atómicas (AFM) y análisis termogravimétrico. Los CNC obtenidos tuvieron unas propiedades similares en términos de cristalinidad (92-95%), grado de polimerización (180) y relación de aspecto (todos en el intervalo 50-120). Únicamente se encontraron diferencias en la pureza (77-93%) y en los rendimientos de hidrólisis (58-64%). Este estudio demostró, por primera vez, la producción efectiva de CNC a partir de PR, sin el uso de pretratamientos agresivos para eliminar impurezas. También se observó que la disminución en el rendimiento de hidrólisis y en la pureza de los CNC no afectaba significativamente a las propiedades del PR cuando estos fueron utilizados como agentes de resistencia en seco.

Por otra parte, tener unos CNC de alta calidad no es suficiente para la mejora del papel, si estos no están distribuidos homogéneamente en la red fibrosa. De este modo, se ha demostrado que una mayor dispersión de los CNC y de estos entre las fibras, es de gran importancia para conseguir unos efectos positivos en el producto final. Teniendo en cuenta estas consideraciones, se han utilizado algunas de las operaciones usadas comúnmente en las fábricas de PR, como son la desintegración o el uso de dispersantes, para conseguir suspensiones homogéneas tanto de CNC como de CNF (Publicación V). Se han variado el

tiempo y la temperatura de desintegración y se ha evaluado el uso de remojo en las propiedades finales del papel. Además, se han aplicado dos agentes de dispersión directamente en las suspensiones de CNC y CNF previo a su aplicación. Por último, se han estudiado dos agentes de retención: un sistema tricomponente (formado por un coagulante, una poliacrilamida y bentonita) y quitosano (como biofloculante). El remojo de las fibras con las NC y el empleo de largos tiempos de desintegración (60 min) favorecieron la mezcla de las NC con las fibras, consiguiendo incrementos en el índice de carga de rotura de hasta un 30%. Sin embargo, con el empleo de una cantidad mínima de dispersante (0.003%), se consiguió reducir el tiempo de desintegración de 60 a 10 min, a la vez que el índice de carga de rotura aumenta hasta un 20.6%. Así, se concluye que la dispersión de las NC juega un papel relevante en la mejora de los productos papeleros y es, por lo tanto, una variable clave a estudiar.

Sin embargo, conocer el grado de dispersión global de los CNC puede que no sea suficiente para describir los efectos que estos producen sobre los productos papeleros. De hecho, la naturaleza de los agregados podría tener también una gran influencia, ya que agregados de distinta morfología podrían causar diferentes problemas/beneficios. La hipótesis en este caso es que la agregación de los CNC podría ser indirectamente descrita a través del uso de técnicas de *scattering*, como por ejemplo difracción dinámica de la luz (DLS), recogiendo los datos a distintas temperaturas. Este fue, de hecho, el objetivo de la Publicación VI, donde los parámetros geométricos de las partículas/agregados presentes en las suspensiones de CNC, medidos mediante análisis de imágenes tomadas por microscopía de fuerzas atómicas (AFM), fueron correlacionados con datos extraídos mediante DLS. Para este propósito, se utilizó el tiempo al cual la función de autocorrelación empieza a caer (τ_D). Las partículas identificadas en las imágenes se clasificaron en cinco grupos mediante un modelo de aprendizaje automático sin supervisión, denominado *k-means clustering*. La mayoría de las partículas identificadas fueron clasificadas en el grupo de menor tamaño, siendo probablemente partículas individuales. Además, se hizo un análisis de importancia de variables donde se identificó la relevancia que cada grupo tiene en el resultado observado en las gráficas τ_D vs temperatura. La presencia de una mayor cantidad de partículas en los grupos de menor tamaño, mostró un mayor impacto en el valor del τ_D a 50 ºC, mientras el τ_D a la menor temperatura ensayada (10 ºC), fue fruto de una diferente cantidad de partículas pertenecientes al grupo de agregados de tamaño intermedio. Este estudio constituye un primer paso en la descripción del estado de agregación de CNC en suspensión, ya que se podría obtener esta información directamente de los datos extraídos mediante DLS, sin la necesidad de utilizar técnicas microscópicas. Esta nueva tecnología abriría el camino hacia el desarrollo de una gran variedad de posibilidades para la producción y aplicación de CNC a escala industrial.

Por último, el tercer bloque de esta tesis doctoral se centra en el uso de CNCC como agente de retención, para, así, simplificar el sistema de aditivos utilizado en el proceso de producción de papel, al mismo tiempo que mejorar la calidad del papel.

Los nanocristales de celulosa tipo *hairy*, una nueva familia de NC con un cuerpo cristalino y regiones amorfas a ambos extremos, fueron recientemente sintetizados en la Universidad de McGill. Estas partículas combinan la resistencia, ligereza y composición celulósica de los CNC, con las propiedades adicionales que les confieren los extremos amorfos: propiedades de floculante y estabilidad electro-estérica. Basado en este conocimiento, se planteó el uso de CNCC, como agente de retención en la producción de papel. Con esta hipótesis, los CNCC se podrían utilizar con un doble objetivo: como aditivos de proceso y de producto; de forma que mejoren la retención y el drenaje, al mismo tiempo que aumenten la calidad del papel.

En primer lugar, se evaluó el mecanismo de floculación de los CNCC en una suspensión de kaolin (Publicación VII). El proceso de floculación se monitorizó mediante análisis de dispersión fotométrica y medida por reflexión de haz enfocado. Se determinó la dimensión fractal de los flóculos formados, con el uso de un nuevo modelo de regresión de bosques aleatorios de aprendizaje automático. Con la dosis de 20-30 mg/g de CNCC se obtuvo el máximo tamaño de flóculo y la floculación más rápida, con una eficacia de refloculación del 50%, coincidiendo con el punto isoeléctrico. Por ello, se dedujo que el mecanismo de floculación de este sistema era neutralización de cargas con reconformación de los flóculos. Además, los diferentes valores de dimensión fractal sugieren una relación entre la conformación de las partículas y la dosis de CNCC, presentando una estructura más abierta cuando la dosis estaba entre 10 y 20 mg/g.

A continuación, se floculó una suspensión que contenía las cargas que son utilizadas mayoritariamente en estas industrias: kaolin y carbonato cálcico, con el objetivo de describir diferencias o similitudes con el estudio previo. Se encontró que los CNCC heteroflocularon los minerales en un amplio intervalo de dosis, encontrando el mayor tamaño de flóculo con una dosis de CNCC de 30 mg/g, correspondiendo, al igual que en el estudio anterior, al punto isoeléctrico.

Por último, en la Publicación VIII, se evaluó la floculación de la pasta completa (fibras y minerales), con los CNCC. Se determinó el efecto de la dosis de CNCC aplicada en el drenaje de la pasta, la retención de las cargas y las propiedades mecánicas de los papeles producidos, y se comparó con otros agentes de retención. La dosis óptima en términos de eficiencia de floculación y tamaño de flóculo fue 20 mg/g, que, de nuevo, correspondió al punto isoeléctrico. A esta dosis, se consiguió una reducción en el tiempo de drenaje del 78% y una mejora de la retención del 77%. Se validó, además, el mecanismo de floculación propuesto anteriormente. Una ventaja adicional de los CNCC comparados con otros sistemas de retención es que las propiedades mecánicas de los papeles finales no eran reducidas en gran medida, como por ejemplo ocurre con la poliacrilamida.

1. INTRODUCTION

1. INTRODUCTION

1.1. RECYCLED PAPER

Paper is one of the oldest and leading recycling material, mainly due to economic and environmental issues. Europe is the global leader in paper recycling, which achievements are based on voluntary agreements of the sector [1]. The recycling rate (utilization of paper for recycling plus the net trade of paper for recycling, compared to paper & board consumption) was 72.3% in 2017, with an increase of 20.5% since the year 2000 and close to the 74% goal for 2020 (CEPI 2017). A total of around 48.3 million tons of paper for recycling were used in this year for papermaking, which means a utilization rate of 52.4%. Among the different paper products, 55.7% was used for case materials, including paper and boards mainly used in the manufacture of corrugated board, and 18.9% was destined to produce newsprint and other graphic papers.

According to the European Declarations on Paper Recycling 2016-2020, although the industry has reached high levels in the recycling rate, different patterns in consumption, new technologies and diversifying application of paper-based solutions make it challenging to maintain these high recycling rates, which are now starting to reach the theoretical

maximum. For example, the demand for complex packaging solutions is heightening, thus finding more multi-material products on the market, which supposes an important challenge for recycling industries.

Due to the loss of fibers in the recycling paper chain, the use of virgin fibers is always required, which are often used in paper grades with strict quality requirements. On the other hand, the increase of recycling produces a decrease of the recycled paper (RP) quality due to the "hornification" process, which deteriorates the fibers each time they are recycled, reducing the inter-fiber bonding and the swelling ability of the fibers [1, 2].

Some paper mills use refining to enhance paper strength, but as recycled fibers are in a high degradation state, this technology is not usually applied to minimize their shortening [2]. Others use strengthening agents to reinforce recycled fibers when a moderate increment is needed. Some of these products are starch, acrylamide-based polymers, chitosan, gums, wood hemicelluloses or latex additives [3]. Recently, natural aids and nanomaterials are gaining prominence in this field due to environmental concerns and to the low dosages needed to reach high benefits [4]. Among them, the application of polyelectrolyte multilayer or the use of polyamines have been proved to work successfully at low dosages [3, 5]. In this context, the use of cellulose-based materials is receiving the interest of many researchers and papermaking industries. The use of NC as dry strengthening agent is much advantageous against, for example that of carboxymethyl cellulose (CMC), an amorphous water soluble polysaccharide mainly used for surface sizing or to improve wet strength of paper [3]. Advantages are due to the facts that crystallinity is maintained during the production process and that their chemical composition is the same than that of cellulose but in the nano-scale [6]. Additionally, NC have other particular properties, like a high surface area, unique optical properties, lightweight, stiffness and high strength, etc, that could induce additional benefits to paper quality [7].

The increasing interest in replacing plastics for the production of packages, bags and other products justifies the expansion of the paper recycling sector in the last years all around the world. On the contrary, the production of newspapers and magazines, has been highly affected by the increasing use of electronic media, due to their easy accessibility and to the fact that, in most cases, they are free of charge for the user. Thus, in the last five years, while the production of packaging papers in Europe has increased by 7.2%, the newsprint production has decreased by 28.3% (CEPI 2017). This is translated in a decrease in the utilization of paper for recycling for newspapers and magazines, as shown in Figure 1, reaching a value of 19.1% in 2017, while that for corrugated and kraft papers increased till 51.3%. This fact shows that newsprint mills are facing huge challenges in order to maintain their competitiveness [8]. As a consequence, some companies have shut down some production lines and other are looking for alternative market niches by developing improved and new products. In this context, the doctoral thesis presents alternatives to

improve the quality of the RP at the same time that a high added value sub-product could be produced.

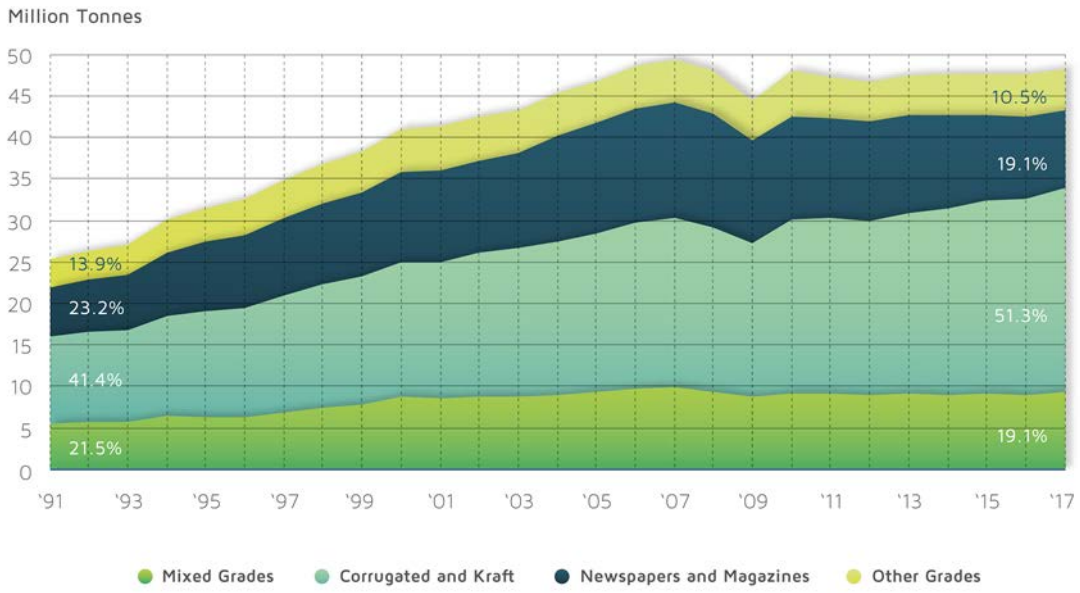

Figure 1. Utilization of paper for recycling by grade (CEPI 2017).

1.2. FROM CELLULOSE TO NANOCELLULOSE

Cellulose is the most available biopolymer on earth and the primary reinforcement component in the cell wall of plants [9]. It is produced not only by plants but also by fungus, bacteria and in less degree by tunicates (small and sessile marine animals). It is chemically defined as a linear homopolysaccharide composed of β-D-glucopyranose units linked together by β-1-4-glycosidic bonds. A chain can be formed by hundreds to thousands of glucose units.

Each cellulose fiber is formed by the union of fibrils, which are long thread-like bundle of molecules laterally stabilized by intermolecular hydrogen bonds [10]. Each elementary fibril can be considered as a string of cellulose crystals linked along the fibril axis by amorphous domains. The main portion of cellulose is of this type, which is called native cellulose or cellulose I, whereas cellulose II, III and IV are amorphous (being cellulose II the most stable). The proportion of the different cellulose types is related to its origin. Hence, cellulose from bacteria or tunicate is rich in Cellulose I whereas Cellulose II is mainly found in the cell wall of superior plants [10].

With the use of appropriate chemical, mechanical and/or enzymatic treatments, it is possible to reduce the size of cellulose in diameter or both diameter and length, up to the nano-scale following a top-down approach [11]. The term 'nanocellulose' generally refers

to cellulose materials having at least one dimension in the nanometer scale. Nanocellulose is also produced following a bottom-up approach in which bacteria produce glucose units that extruded out of their membrane and self-assembly forming the nanocellulose fibers.

NC have been classified into three main groups attending to their dimensions, functions, and preparation methods: cellulose nanofibers (CNF), cellulose nanocrystals (CNC), and bacterial cellulose (BC) (Figure 2). Recently, an ISO standard (ISO/TS 20477:2017: Nanotechnologies -- Standard terms and their definition for cellulose nanomaterial) has reviewed all nomenclature used for these NC and has standardized their use as the one of this thesis. These nanomaterials have grown in popularity owing to their exceptional properties for diverse applications. Some of the imperative properties of cellulose-based materials such as functionality, uniformity and durability can be improved with the use of NC. They present enhanced mechanical properties due to their high surface area, large water holding capacity and a reactive surface of –OH side groups, where almost any desired functional group can be provided [7].

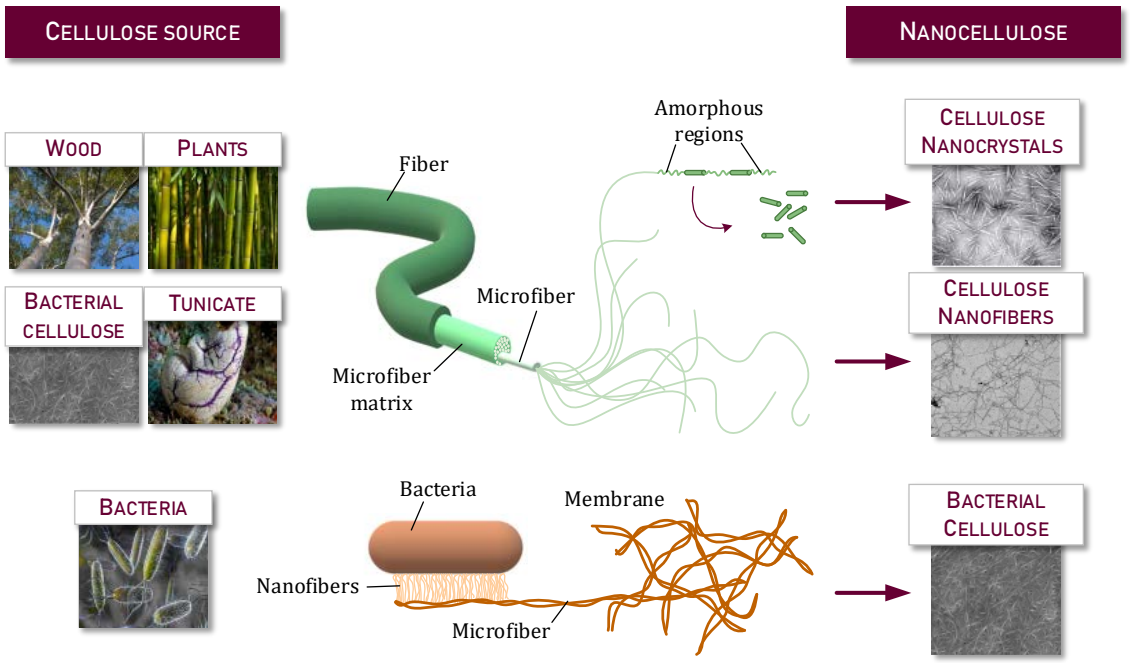

Figure 2. Schematic diagram of the origin and possible cellulose sources to produce the three main types of nanocellulose: cellulose nanocrystals, cellulose nanofibers and bacterial cellulose.

1.2.1 Cellulose nanofibers

The first isolation of microfibrillated cellulose (MFC) was published and patented in 1983 by Turbak, Snyder and Sandberg at the ITT Rayonier labs in Whippany, New Jersey, USA [12, 13]. They passed a wood pulp through a Manton-Gaulin homogenizer at high pressure followed by a high velocity decelerating impact. They described the product as a “gel type

material having properties distinguishable from all previously known celluloses". Since then, thousands of works have been published regarding new CNF isolation and characterization methods, and many application approaches [14-16].

CNF are, thus, the product of the destruction of the multi-level organization of natural fibers when they are submitter to high shearing forces. Currently, this involves two main steps: a pretreatment, where the cellulose fibers are frayed; and a mechanical treatment, where individual nanofibers are finally isolated in a gel-like macrostructure [17]. The properties of CNF depend not only on the production process but also on the raw material source and quality [18]. However, it has been recently demonstrated that the quality of the CNF is not always directly related to its effects [19].

1.2.1.1 Pretreatment

The main purpose of including a pretreatment within the process is to reduce mechanical disintegration costs [20]. Either enzymatic or chemical pretreatments have been proved to contribute positively to reduce the energy consumption in the mechanical treatment. However, they have a strong impact on CNF properties.

The use of enzymes to hydrolyze cellulose fibers has been conducted mainly with *cellulase*. However, they could be trapped by lignin, so high purity raw material is strictly necessary for a high hydrolysis yield [21]. With this pretreatment type, the strength of the gel network can be improved, inducing a high aspect ratio on the CNF and avoiding, at the same time, jams in the homogenizer [22].

Chemical pretreatments are, on the other hand, the most used in the CNF production, due to their higher reproducibility and to the fact that these modifications can confer to CNF special properties [17]. With the TEMPO-mediated oxidation ((2,2,6,6-Tetramethylpiperidin-1-yl)oxyl), the hydroxyl groups of the C6 of cellulose fibers are converted to carboxyl groups. With the use of this method, an almost transparent and highly viscous suspension is produced, with crystallinities of 65-95% [23]. In the case of the carboxymethylation, these hydroxyl groups are substituted by carboxymethyl groups (CH_2COOH) through the reaction of the cellulose fibers with monochloroacetic acid [7]. With this pretreatment, the fiber's charge is highly increased, making the fibrils easier to liberate. The cellulose surface charge could also be changed to positive, having the same effect on the subsequent treatments, but conferring a positive background, advantageous for some applications. This could be achieved through the introduction of quaternary ammonium groups to the hydroxyl groups of the cellulose [24].

1.2.1.2 Mechanical treatment

The most efficient techniques to isolate CNF are high-pressure homogenization, microfluidization and grinding, and, consequently, they are the most suitable for up-scaling

the CNF production. In a high-pressure homogenizer, the fibers suspension is pumped at high pressure through a spring-loaded valve assembly (Figure 3a). This valve makes rapid cycles of open-close, which makes the fibers be subjected to a large pressure drop with shearing and impact forces. These forces promote a high fibrillation of the fibers, which increase with the number of passes [17].

In the microfluidizer, the diluted pulp is pumped through z-shaped chambers (Figure 3b) where high shear forces convert the fibers into nanofibers. An advantageous issue against homogenization is the fact that plugging can be solved by using reverse flow through the chamber [25].

CNF produced through a friction grinding process is conducted by passing the cellulose fibers suspension through two nonporous ceramic grinding discs (Figure 3c). Only one grinding disc is rotating at high speed (rotor) while the other is kept fixed (stator), which causes high shear forces [17]. The principle for refining is similar, except that the gap clearance is larger than that of grinders, and the material is steel instead of ceramic. As this technology is simple and robust, it is easily scalable to industrial level.

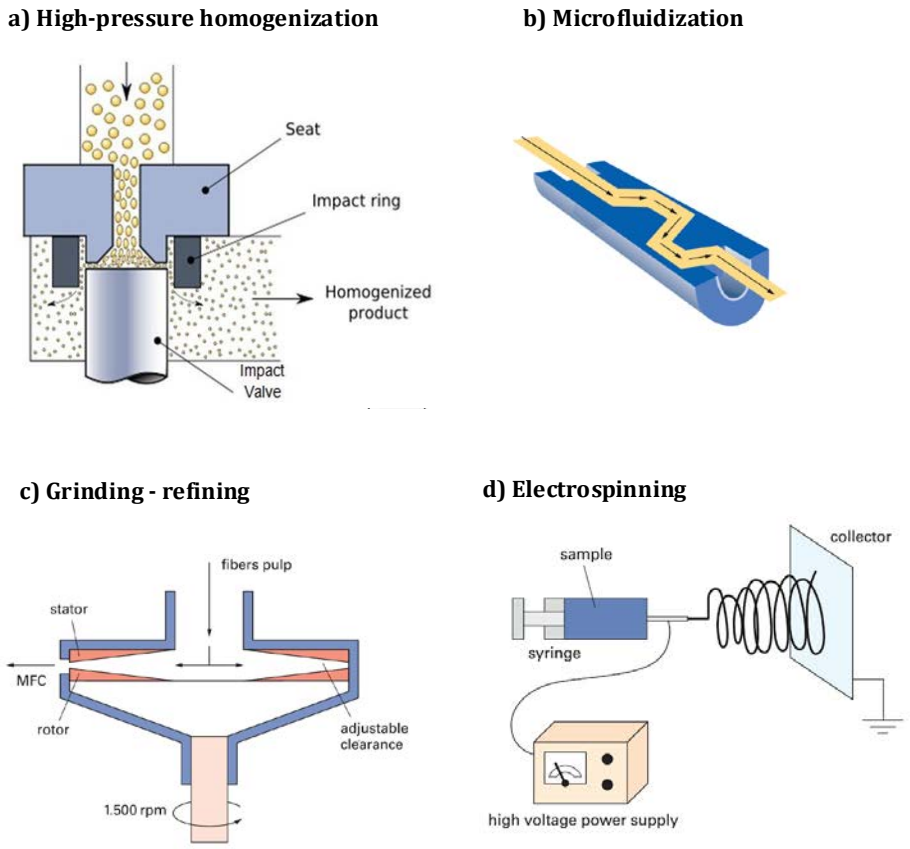

Figure 3. Mechanical treatments used for CNF production: a) Scheme of a high-pressure homogenizer; b) Details of the z-shaped interaction chamber of a microfluidizer (Microfluidics Inc. USA); c) Scheme of the friction grinding-refining process by grinding discs; d) electrospinning setup.

CNF can also be obtained by electrospinning, where only the diameter can be maintained constant from 100 nm to several microns. The principle of this technology differs from others since cellulose fibers have to be dissolved, instead of being directly deconstructed. The prepared solution is positively charged to high voltage, and passed from the orifice of the syringe to the collector (Figure 3d), what produces fibers in the submicron scale [26]. The main drawback of this technique is, indeed, the difficulty to find a suitable solvent to dissolve cellulose [17].

Additionally, other technologies have been proved to produce CNF of high quality, but their use is not as extended. Some of them are ultrasonication [27], cryocrushing [28], aqueous counter collision [29], ball milling [30] and twin-screw extrusion [31].

1.2.2 Bacterial cellulose

Despite BC has been observed for centuries in the production of vinegar, Kombucha tea and *nata de coco*, BC was firstly described by Brown [32], who found a jelly-like strong membrane on the surface of a vinegar fermentation broth. That strain was called *Acetobacter xylinus* and the extracellular polymer was identified as cellulose chemically pure and with identical molecular structure to that of the cellulose present in plants [33]. Since then, different bacterial strains have been identified to produce cellulose from different sugars and/or carbohydrates, such as those from the genus *Agrobacterium* [34, 35], *Pseudomonas* [36], *Rhizobium* [37, 38] and *Sarcina* [39]. However, only those of the *Komagataeibacter* (K) genus have been considered for industrial interests.

The strain *K. xylinus* is strictly aerobic, non-photosynthetic and able to transform glucose and other organic substrates into cellulose in a few days [40]. It is unique in its family for being able to convert carbohydrates into acetic acid during bacterial growth and cellulose production. Because of the respiratory metabolism of *K. xylinus*, it oxidizes ethanol to acetic acid and converts glucose into gluconic acid. All of these acid formations produce a decrease in the pH of the culture medium, especially under batch static culture [41, 42]. Most of the cellulose producing bacteria are gram-negative, rod-shaped and non-motile. In addition, a high proportion oxidizes ethanol and produces acid from glucose and other sugars.

It is believed that these types of bacteria produce cellulose because they try to protect themselves from ultraviolet radiation and harsh chemical environments [43]. The production mechanism starts by the extrusion of a cellulose chain by each pore of the cell wall, where 10-15 of them join together to create a nanofiber with a diameter of around 1.5 nm [44] (Figure 2). They self-assembly to form microfibers and then fibrillar ribbons are produced with an approximate width of 50-80 nm [45]. An overview of the network produced by bacteria is shown in Figures 2 and 4.

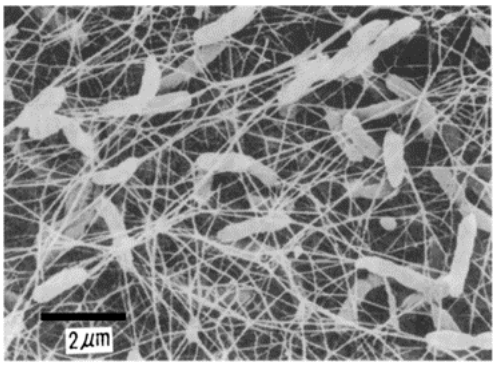

Figure 4. Scanning electron microscopy image of bacteria producing a BC pellicle.

According to the state of the art, the high shear stress suffered by bacterial cells with high agitation and aeration usually triggers a spontaneous mutation of bacteria of the genus *Komagataeibacter*, that deactivates the essential enzymes involved in the cellulose production, i.e. *phosphoglucomutase* and *uridine diphosphoglucose pyrophosphorylase* [46]. Because the modified cells (Cel-) grow faster than the cellulose producing cells (Cel+), the BC productivity resulted strongly reduced. However, there is some controversy in the literature, since Aydin et al. [47] analyzed the mutant ratio (number of Cel-/number of total cells) in these systems, which increased with the shaking rate and the number of batch, obtaining a maximum of 0.64 in the fifth batch at 200 rpm. On the other hand, Jung et al. [48] observed that with an impeller speed over 500 rpm, the Cel- in *K. hansenii PJK* disappeared. Due to the increasing interest of the scientific community in BC, many attempts have been conducted to isolate new strains that could have a higher productivity, but those of the genus *Komagataeibacter* are still considered as the most productive ones.

Several authors have also tried to modify genetically the BC producing bacteria, with the purpose of increasing the productivity or achieving the culture of bacteria in aerated and agitated systems without the production of the Cel-. A variety of methods have attempted to tune some strains, such as ultraviolet (UV) radiation [49], ethyl methanesulfonate [49], a high hydrostatic pressure treatment [50] and a disruption of the cellulase [51]. Results showed that the production of by-products obtained usually in these systems can be effectively reduced, but the BC macroscopic morphology could be affected.

In bacteria, the second messenger cyclic diguanylate (c-di-GMP) regulates the transition from a motile to a sedentary lifestyle. In this context, a higher concentrations of c-di-GMP improves the production of extracellular matrix components, such as exopolysaccharides, proteins, and, in our case, cellulose [52]. The c-di-GMP is synthesized from two molecules of GTP by the action of diguanylate cyclases (DGCs). It has been proved that artificial increments of the intracellular levels of c-di-GMP by the overexpression of DGCs often trigger phenotypes related to the synthesis of exopolysaccharides and biofilm formation [53]. Although this concept has been proved for some bacterial strains, such as

Sinorhizobium meliloti or *Pectobacterium atrosepticum*, their use in cellulose producing bacteria has not been explored yet.

Two major components have to be present in the culture media to allow bacteria to grow: carbon and nitrogen sources [54]. Typically, glucose has been the most used carbon source since it is not only presented as an energy source but also a cellulose precursor [55]. On the other hand, yeast extract and peptone are commonly used as nitrogen sources due to growth factors. Typically, to produce an appreciable amount of BC, a high amount of nutrients is required. Moreover, the use of these pure components suppose the production costs increase making thus the BC production almost inviable at industrial scale.

In this context, some researchers have proved the use of cost-effective media to feed bacteria and produce BC in the same proportion as using pure nutrients [56]. This is an interesting approach that contributes to the goals of circular economy. Some of them are glycerol from biodiesel or grape bagasse [57], konjac powder hydrolyzate [56], cotton cloth hydrolysate [58], orange juice [59], waste from beer fermentation broth [60] and pineapple or watermelon peels [61]. With the use of these media not only this purpose was achieved but it also induced an increment in the BC productivity. However, despite the promising results obtained with all these media, no comparison expressing culture conditions, nutrients, strain and productivity has been made, which difficult the applicability of these results due to the fragmentation of knowledge.

1.2.2.1 Culture method

There are many publications on the production of NC with different methods, showing that the properties of the produced BC are highly influenced by the culture conditions [62]. Thus, it is possible to reach a fit-for-use BC depending on its destiny [54]. Publication I reviews these papers as an attempt to identify the optimal production conditions and their relationship with the quality of the final product. The summary of the results of this study is shown in Table 1, where the different production methods are displayed and their main advantages and disadvantages have been identified.

The most used fermentation method to produce BC has been the static culture, since high yields have been reached. In this configuration, BC is created on the surface of the culture broth in the shape of a pellicle, which is denser on the side exposed to air. There are different hypothesis regarding this fact, like the creation of a support for living in different environments being prevented from drying, contamination and the lack of oxygen and food [63]. In addition, these pellicles hold bacteria to be in contact with the oxygen-rich air-media interface apart from protect themselves from ultraviolet light, retention of moisture and colonization of substrates [33, 64].

Table 1. Bacterial cellulose production configurations

Method/Equipment	Description	Advantages	Disadvantages	Ref.
a) Static culture 	BC produced in the shape of a pellicle or membrane at the surface of the culture broth.	• Compact and homogeneous pellicle • Low energy and investment expenses • BC with extremely high WHC[1] • Easy implementation for in-situ production of nanocomposites	• Long culture times: 5-20 days • Large space required	[60, 65]
b) Agitated culture: Shaken/impeller 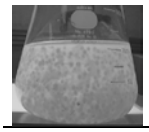	Culture media inoculated with bacteria and shaked 180-200 rpm or agitated with an impeller at 300-500 rpm	• Cost-effective • Suitable for economical scale production	• Shear stress converts microbial strains into Cel- mutants • BC is attached to the impeller, being difficult its recovery	[65]
c) Airlift bioreactors 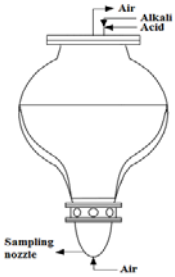	Culture media agitated through the air bubbling from the bottom	• Higher oxygen availability • Decreased power supply	• Aeration also causes the conversion of bacteria into Cel-. • Adhesion of BC to the top of the reactor • BC with low mechanical strength	[42]
	Spherical type bubble column bioreactor	• Low shear stress • Low concentrated solution state culture • High productivity	• Lower crystallinity • Lower mechanical properties • Lower DP	[66, 67]
d) Rotating disk bioreactor 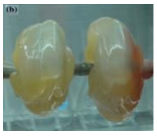	Disks rotating with their half area submerged in the inoculated medium. Low rotating speed in preferred (4 rpm)	• High contact with atmosphere: high oxygen availability • High productivity • Low production time: 3-4 days • Semi-continuous mode tried satisfactorily	• Lower mechanical properties of BC • Lower crystallinity	[68, 69]
e) Stirred tank reactor with a spin filter 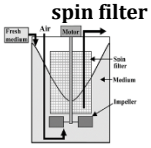	Agitated culture with the use of an impeller and a spin filter to collect all BC formed and the implementation of aeration (30 L/min)	• High cell density • High productivity	• Big amount of Cel+ cells converted in Cel-	[70]
f) Biofilm reactor 	PCS implemented in a biofilm reactor to increase the surface area of the impeller.	• High biomass density • Natural form of cell immobilization • Higher shear force than standard impellers at the same agitation speed • High productivity • High water retention on BC	• BC attached to the PCS: avoided with the addition of 2% CMC[2] to the culture media	[71-73]
g) Trickling bed reactor (TBR) 	Tank filled with corncobs where culture broth is pumped from bottom to the top at the same time than air	• High –OH associating degree • Increased oxygen supply • Decreased shear force • High biomass density • Higher DP • Higher WHC[1]	• More research needed	[74]

For industrial interests, batch or continuous mode would be more appropriate. One of the main drawbacks of this fermentation mode is the time needed by bacteria to get used to new fermentation conditions. Çakar et al. [75] optimized a static semicontinuous operation mode for *K. xylinus FC01*, finding the highest productivity by changing the culture volume with ½ ratio after 7 days. Fed-batch fermentation has been also tried by Bae et al. [76], who cultured *K. xylinus BPR2001* keeping the levels of sugar in 20 g/L by the addition of small amounts of molasses (6.3 g/h). An increment in the BC yield was also achieved.

1.2.2.2 Additives for increasing productivity and BC modifications

Different additives have been introduced in the culture medium to enhance BC productivity. For instance, alcohols [77], organic acids [78], agar [79, 80], thin stillage from rice wine distillery [81], CMC [82], 1-methylcyclopropene [83] and industrial-grade glucose [60].The highest increments in the BC productivity were achieved by the addition of 0.5% (w/v) n-butanol (increment of 56%) [84], 0.35% (w/v) succinic acid (increment of 80%) [78], 1.0% of CMC (increment of 530%) [82], 0.4% agar (increment of 71%) [80], 100 mg dextrose containing 0.14 mg 1-MCP in assigned days (day 1, day 2, day 4, day 6 and day 9) (increment of 25.4%) [83] and 1% industrial-grade glucose (increment of 65%) [60].

Sometimes, BC properties need to be enhanced for some applications with specific requirements. Thus, there are many research articles regarding BC modification for a specific application, either during bacteria culture or after BC isolation. A deep review of these papers was also included in the Publication I, and some of the possibilities are summarized below.

- Porosity: the BC membrane needs certain porosity to be used as wound dressing material to make sure that air and substrate penetrate into the skin [85]. It can be achieved by restricting the movement of bacteria during BC production through the application of oxygen in microgrooves or through the addition of potato starch or gelatin during culture [85-87]. In this way, the porous size was controlled for the future application.
- Adsorption capacity: it can be achieved by the modification of the membrane after culture with the use of amines [88], diethylenetriamine [89], phosphoric acid [90] and CMC [91], which introduce hydrophilic groups to the surface of the fibers.
- Electrically conducting material: a conductive nanomaterial can be added to the culture media. Among them, the most prominent are multiwalled carbon nanotubes [92], pyrrole [93] or polyaniline [94].
- Magnetic materials: The previous procedure was also used to develop magnetic materials for biomedical, magnetographic printing, data storage, anti-counterfeit and electronic applications [45].
- Thermal stability: it is a key property to enable the use of BC hydrogels as a drug-delivery system. Amin et al. [95] combined BC with acrylic acid to produce a hydrogel

by exposure to accelerated electron-beam irradiation, and they reached an accurate temperature control.

- Moisture: with the aim of delivering active substances into a wound, specific moisture is required to facilitate its penetration and an easy and painless dressing change [96]. An increase of 390% in water retention was obtained by Spaic et al. [97], through TEMPO-catalyzed oxidation of BC. In another study, swelling ability of a BC membrane modified with diclofenac was 6 times more than that of pure BC [98].
- Antimicrobial activity: It has to be improved for their application in biomedicine or food fields. The introduction of hyaluronic acid [99], poly(3-hidroxybutyrate) [100], silver particles [101] or titanium dioxide [102] into the culture media was found to effectively improve the antimicrobial activity of the scaffolds.
- Photochromic behavior: It is needed when they are desired to be applied as UV sensors. For this purpose, Hu et al. [103] modified the surface of the BC nanofibrils with spiropyran photochromes, and they observed that the color of the membrane was changed from colorless to pink, and was reversible.

1.2.3 Cellulose nanocrystals

CNC are the product of the extraction of crystalline domains from a cellulose material. This method focuses on dissolution of amorphous cellulose, typically in acid media. In 1951, Ranby, at the University of Uppsala, published the controlled sulfuric acid-catalyzed degradation of cellulose fibers to obtain a suspension of rod-like crystallites [104]. These studies woke up the interest of Derek Gray, who started to work on the CNC procedure method development in 1970s at the University of McGill. But it was not until 1992 when he and his colleague Jean-Francois Revol published their first work on extracting CNC from wood [105]. Since then, hundreds of works regarding the production, characterization, modification and application of CNC have been published around the world. Indeed, this product was considered of industrial use and there are already some companies that are producing and applying this material at industrial scale [106].

CNC have been traditionally produced by acid hydrolysis [107]. Some decades ago, Nickerson et al. [108] suggested that amorphous sections which join the crystallites in the longitudinal direction were attacked first, thus reducing its length. The proportion of these amorphous or disordered regions compared to crystallites is relatively small, so further hydrolysis will allow crystallites to remain as the only cellulose material. However, after several hours of further hydrolysis, it is assumed crystallites to hydrolyze into glucose. Despite both sulfuric and hydrochloric acids have been the most used for this purpose, other acids, like phosphoric or hydrobromic can be also used. However, the dispersibility of CNC produced from these acids is different. CNC obtained from sulfuric or phosphoric acid hydrolysis dispersed readily in water, due to the presence of sulfate or phosphate groups

on its surface. Nevertheless, those produced from hydrochloric or hydrobromic acid hydrolysis are not easily dispersible and they tend to flocculate [7].

The acid hydrolysis conditions were varied depending on the source of cellulose and purity of the sample [33]. Typically, when the purpose is to optimize reaction conditions, a pure cellulose material is used [109]. However, new tendencies are focused on using cellulose wastes or residues to obtain a high added value product at lower cost [110]. However, a high heterogeneity in the sample composition makes the conditions optimization a key process to obtain CNC with the maximum yield and appropriate properties. Table 2 presents some of the sources that have been used for CNC production.

Table 2. Cellulose sources for cellulose nanocrystals production

Cellulose source		Ref.	Cellulose source		Ref.
Wood	Softwood: pine, Douglas-fir	[111]	Agroforestry residues	Apple tree pruning	[112]
	Hardwood: eucalyptus, birch, poplar	[113]		Bioethanol residue	[114]
Non-woody plants and crops	Agave	[115]		Brewer's spent grains	[116]
	Bamboo	[117]		Cigarette filters	[118]
	Cotton	[119]		Coconut husk fibers	[120]
	Corncob	[121]		Cotton cloth waste	[122]
	Flax	[123, 124]		Garlic straw	[110]
	Hemp	[125]		Grape skins	[126]
	Humulus japonicus stem	[127]		Mango seed	[128]
	Kenaf bast fibers	[129]		Mengkuang leaves	[130]
	Mulberry	[131]		Oil palm biomass	[132]
	Okra fibers	[133]		Olive pomace	[116]
	Phormium tenax (harakeke)	[123]		Pea stalk	[112]
	Posidonia oceanica	[134]		Pineapple leaf	[135]
	Sisal	[136]		Plum seed shells	[137]
	Syngonanthus nitens (Capim dourado)	[138]		Potato peel	[139]
Animals/ bacteria	Bacteria	[140]		Rice (straw, husk…)	[141]
	Tunicates	[142]		Soy hulls	[143]
Others	Old corrugated containers (OCC)	[144]		Sugarcane bagasse	[145]
	Old newspapers (ONP)	[8]		Tomato peel	[146]
	Recycled pulp	[147]		Wheat straw	[116]
	Wastepaper	[148]			

In the case of cotton, BC and microcrystalline cellulose (MCC), as only cellulose is present, it can be directly hydrolyzed. However, when CNC are obtained from wood, agricultural residues or other types of biomass, not only cellulose is present but also extractives, hemicelluloses, lignin or inorganic particles. In these cases, to isolate the cellulose material, extractives (dewaxing) have to be removed with dichloromethane, acetone or ethanol/benzene, depending on the raw material [149]. Then, pectines and hemicelluloses are solubilized through an alkaline process, typically with NaOH or KOH [141]. Finally, several bleaching cycles are performed to remove the remaining amount of lignin [33].

These pretreatments facilitate the acid accessibility, but they increase considerably the yield loss. Moreover, the use of mineral acids as cellulose hydrolyzing agents usually triggers several disadvantages, such as high-energy consumption, toxicity and corrosion risk. New tendencies for CNC production are, therefore, focused on the isolation of CNC without a previous cellulose purification as well as the replacement of those acids by organic acids, ionic liquids or enzymes.

Due to the low water solubility of solid organic acids, they can be easily recovered after the reaction through crystallization at room temperature [196]. Chen, Zhu [197] proved the viability of producing carboxylated CNC and CNF from a bleached eucalyptus kraft pulp using oxalic acid. They increased the onset thermal degradation temperature and the produced CNC and CNF were longer due to the lower strength of these acids. As an attempt to avoid the typical pretreatments, Bian et al. [150] used maleic acid to produce ligno-CNC and ligno-CNF from two unbleached hardwood chemical pulps with different lignin contents. The yield of the CNC production was lower than 6%, but they fibrillated the non-hydrolyzed material to CNF. The ligno-CNC and ligno-CNF were more hydrophobic and thermally stable compared to lignin-free products, which opens new possibilities in other fields of applications.

Phosphotungstic acid, a heteropolyacid, was alternatively used to produce CNC, due to its relatively simple regeneration and notably less corrosive action than mineral acids [151]. The produced CNC formed stable hydrosols that after freeze-drying tend to agglomerate into different structures depending on the concentration.

Ionic liquids have been used as green solvents to dissolve cellulose, with an easy recovery after hydrolysis [152]. Recently, Iskak et al. [153] have produced CNC with a high yield, crystallinity and particle size under catalytic hydrolysis using ionic liquid. They found that the reaction temperature and time were the key variables affecting the yield and thermal properties of CNC.

On the other hand, the enzymatic hydrolysis has been also proposed to produce CNC due to its great potential for high saccharification efficiency and high penetration. With the use of

enzymatic hydrolysis, the environmental impact is reduced and the final products can be used in biomedical applications [154].

Despite all these attempts to improve CNC production, the most promising option is still sulfuric acid hydrolysis, but CNC are still expensive products and their industrial use has been focused of high value applications.

1.2.4 Hairy cellulose nanocrystalloids

As discussed, conventional CNC are produced by complete acid hydrolysis of the amorphous regions in cellulose fibers. The preferential reaction of chemicals with the disordered parts is not restricted to acid, but applies to almost all chemical reactions with cellulose fibers. As they are more kinetically accessible, most chemical modifications of cellulose fibers result in this preferential modification. This suggested a novel method to prepare NC: the amorphous regions could be solubilized, while, at the same time, leaving a sufficient number of cellulose chains attached to the ends of the crystalline domains. van de Ven et al. [155] shown that this is indeed possible. They converted cellulose to a water-soluble cellulose derivative by means of the reaction with periodate. The C2-C3 hydroxyl groups of the glucose units were converted into aldehydes, while simultaneously the C2-C3 bond was broken [156]. When periodate-oxidized fibers are heated to 80ºC, they fall apart in nanocrystalline cellulose with the amorphous regions still attached to both ends (Figure 5). They refer to the NC produced by this methodology as sterically stabilized nanocrystalline cellulose (SNCC) [157], since the dialdehyde modified cellulose chains (DAMC) protruding from both ends, provide steric stability.

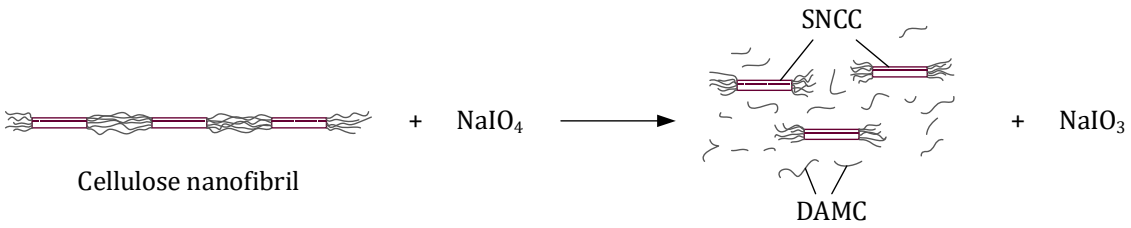

Figure 5. Periodate-oxidation reaction: from cellulose nanofibrils to sterically stabilized nanocrystalline cellulose (SNCC) and dissolved chemically modified cellulose chains (DAMC). Note that the modified cellulose only fall apart in SNCC and DAMC when the sample is heated to 80ºC.

The kinetic of the periodate reaction with fibers can be accelerated by adding an inert salt. For the reaction to occur, the negatively charged periodate ions have to penetrate the negatively charged pores of the fiber wall. Because of a Donnan equilibrium [158], the concentration of periodate in the pores is much lower than in the bulk. By adding salt, the

Donnan equilibrium is shifted, increasing the concentration of periodate in the pores, thus increasing the reaction rate.

Since the modified cellulose fibers remain intact prior heating, it is possible to separate chemicals by filtrating the sample. Thus, this NC production method is advantageous compared to the others. The produced iodate can be converted back to periodate by a simple reaction with hypochlorite under alkaline conditions, as previously reported [159]. Thus, although periodate is quite expensive, the high efficiency of the recovery cycle, near to 100%, reduces the cost of this reaction, which is mainly associated to the inexpensive cost of the hypochlorite.

Owing to the high reactivity of aldehyde groups, SNCC or DAMC may act as precious intermediates, which can be functionalized with other chemical groups. For instance, a chlorite oxidation of periodate-oxidized fibers results in carboxyl groups protruding from both ends. These charged chains provide electrostatic and steric (electrosteric) stability, thus they call these nanoparticles as electrosterically stabilized nanocrystalline cellulose (ENCC) [160].

On the other hand, a Schiff base reaction with a molecule bearing a primary amine ($R\text{-}NH_2$) results in the attachment of a group R of one's choice. In this way, Yang et al. [161] produced cationic hairy cellulose nanocrystalloids (CNCC) in which R carries a quaternary ammonium group. These CNCC are also electrosterically stabilized.

In the review article published in 2016 by van de Ven et al. [155], the synthesis of SNCC, ENCC, and CNCC was described in detail, as well as their characteristics, properties and their potential applications. Among them, their use as flocculant is of particular industrial interest. When CNC are used to bind to colloids and flocculate them, they are previously modified. However, as these hairy nanocrystals of cellulose (HNC) are easily functionalized on their edges after periodate oxidation, their bridging action could be conducted easily at low chemicals' consumption [155]. However, this concept, has not been studied deeply yet.

1.3. NANOCELLULOSE PROPERTIES

As it has been already mentioned, the NC properties are directly related to both the cellulose source and the production process. Since specific properties of CNF are detailed in previous publications [17, 19], we focused, in this case, on BC and CNC.

1.3.1 Morphology

The macroscopic morphology of BC mainly depends on the cultivation method, being in a form of pellicle when it is produced in static conditions, or in the form of irregular granules,

stellate and fibrous strands when the culture is agitated in either shake cultures or rotating disk systems. In addition, microscopic images also revealed morphological differences between both culture systems. The nanofibrils produced under static conditions are more extended and piled one above another in a crossing manner, and have a larger cross-sectional width. The cellulose pellicle obtained in agitated culture consists of entangled and curved nanofibrils. These morphological differences contribute to obtain different values of crystallinity and other important properties [162].

In the case of CNC and HNC, different microscopic analysis suggest that they are rod-shape with remarkable uniform width but with a wide distribution of lengths. Although the HNC have some amorphous chains on the edges of the crystalline shaft, they are not long enough to affect the total particle length.

BC nanofibrils have an average width of 1.5-4 nm while their length is extended to 1-9 μm [43]. However, although the width of an individual CNC or HNC is on the same magnitude order, their length is reduced up to that of the crystallites present in the cellulose origin. Thus, it can vary from 100 nm for CNC from cotton [122] to 1 μm for CNC from BC or tunicate [142].

1.3.2 Crystallinity

The crystallinity index (CrI) of a cellulose material and the dimensions of the crystallites have been the subject of extensive investigations for many years [163]. The CrI is the ratio of the diffraction portion from the crystalline part of the sample to the total diffraction of the same sample. The high crystallinity of BC synthesized under static culture is one of its most promising properties. Due to this fact, BC has exceptional mechanical and interfacial properties [71] compared to other cellulose materials. The average CrI value for BC varies between 84 and 89%, while that of cellulose with vegetal origin is in the range of 40 and 80% [65].

The value of CrI is of high relevance for CNC since it can be related to the degree of hydrolysis and then to the yield of reaction. Depending on the purity of the sample before hydrolysis, it can reach values up to 100% [164]. On average, values of 85-95% have been found in the literature [132].

1.3.3 Polymerization degree

The polymerization degree (PD) of NC varies depending on the source and treatment of the original cellulose fibre. It has been widely determined by diluting the cellulose sample in cupri-ethyene-diamine solution and measuring the intrinsic viscosity of the solution [8]. The Mark–Houwink–Sakurada equation is used to correlate values of intrinsic viscosity

with those for PD [165]. While the PD of wood cellulose are reported to be between 10000-15000, that of BC is quite lower, ranging from 2000 and 6000 [166].

Acid hydrolysis induces a rapid decrease in the cellulose PD, reaching the so-called level-off PD (LOPD) when hydrolysis yield is maximum. This LOPD has been found to correlate with the periodic crystal size along the longitudinal direction of cellulose chains of cellulose sources before hydrolysis [107]. In addition, LOPD strongly depends on cellulose origin, having the typical values of 160 for CNC from cotton [167], 300 from ramie fibers [168], 100-200 from bleached wood pulp [169], 180 from bamboo fibers [170] and much higher like 2000-6000 from BC [171].

1.3.4 Surface charge

Surface charge is a key parameter affecting the performance of the NC particles in several applications, such as imaging and drug delivery. A controlled surface charge not only improve the speed that NC are cleared out by the host system, but also they can increase colloidal stability in different fluids and avoid their aggregation in the presence of ionic agents [172].

Zeta potential has been used to evaluate the surface charge of nanoparticles and, then, to assess the degree of agglomeration of NC. A value of zeta potential smaller than -15 mV means the nanoparticles start to agglomerate, while higher than -30 mV shows enough bilateral repulsion and colloidal stability [173]. According to the literature, zeta potential values are around -46 mV for BCNF produced by TEMPO-mediated oxidation due to the carboxyl groups, -35 mV for CNC because of the sulfonate groups and -23 mV for ultrasonicated produced NC owing to its natural hydroxyl groups [173].

1.3.5 Mechanical properties

According to several studies, tensile strength of BC membranes is in the range of 200-2000 MPa, while Young's modulus is usually in the range of 15-140 GPa [166]. These excellent mechanical properties are directly due to their high DP and CrI, apart from nanofibril structure with high aspect ratio. Indeed, BC produced under static conditions shows the highest values of the cited interval, while that obtained under agitated culture presented the lowest values of the ranges for Young's modulus and tensile strength.

CNC have promising mechanical properties because of the removal of the amorphous parts of the nanofibers that increase the inter-chain hydrogen bonds in the crystalline regions, providing a strengthening effect. Its values for tensile strength (7500-7700 MPa) together with Young's modulus (130-250 GPa) [10, 164] are comparable with carbon fiber of TORAYCA® T1000G, one of the world's best mechanical properties material, with values of 6370 MPa for tensile strength and 294 GPa for Young's modulus [55].

1.3.6 Thermal properties

Research on the thermal stability of the cellulosic fibers is essential to stablish their applicability for composite technology, in which the processing temperature for thermoplastic polymers rises above 200ºC. In addition, both CNF and CNC have potential as rheology modifiers of some fluids like drilling fluids for use in oil wells or as additives in injection water for enhanced oil recovery. These NC will have, therefore, to support temperatures over 100ºC for days or even months [174].

In the case of BC, the combination of a high crystallinity and water content provide a good thermal stability, being able to be sterilized by an easy heating process like autoclaving [175]. This fact can suppose a great advantage in the biomedical field.

Crystalline structure of CNC is a key factor to describe their thermal stability since the cellulose chains are packed in a highly ordered manner through the strong hydrogen bonds preventing cellulose from melting and thus increasing the thermal stability [176]. However, CNC produced by sulfuric acid showed a two-stage degradation with an initial onset degradation around 120ºC and a second degradation around 225ºC, which induce the degradation of cellulose at lower temperature and lead to lower thermal stability [177].

1.3.7 Rheology

CNC display a wide set of phase behaviors with salt and pH, since they have an anisotropic shape and an electrical double layer that result in liquid crystallinity and self-assembly [178]. Thus, it would be possible to provide CNC with tunable rheological properties for a wide variety of applications. Some studied regions turned the suspension in a viscous fluid and viscoelastic soft solid, while others provoked regions of instability.

1.4. NANOCELLULOSE APPLICATIONS: RECYCLED PAPER

The applications of NC are linked to their properties, which include: light weight, nontoxicity, high strength and modulus, dimensional stability, thermal stability, high thermal conductivity, high optical transparency, low oxygen permeability, modest abrasively, and the fact that it is re-usable, recyclable, environmentally friendly, and biodegradable.

The potential markets for NC found in the literature have been classified into three different categories: high and low volume manufacturing processes and novel and emerging possibilities. The criteria to order the applications has been the volume of NC that would be required for the destined purpose. Thus, in the high volume manufacturing processes, the following industries are considered: nanocomposites [140, 179], paper and cartonboard

[180-182], cement [183, 184], textiles [185], food packaging [186, 187], food [188, 189] and water treatment [190, 191]. Low volume manufacturing processes include their use in medicine for tissue engineering, wound dressing, drug delivery or other minoritary purposes [192, 193], and cosmetics [194]. New potential uses of NC are being developed day after day, taking advantage of their capabilities, such as the modification of components rheolgy [195], their use as biosensors [196], in printed electronics [197] or in 3D printing [198].

The exceptional properties of the NC together with the fact that they are composed of the same components than paper, have awaked the interest of papermakers for NC as a possible solution for many of the paper recycling industry challenges [7]. The use of NC in this industrial sector has contributed significantly to improve paper quality in different aspects [187], such as mechanical properties [199], barrier properties [200] or some special properties, such as flame retardant behavior [201] or antimicrobial activity [202]. Moreover, there are several review articles which discuss and compare the different publications regarding the effect of NC on the paper production process [4, 10, 203, 204]. In most references, NC have been produced from virgin fibers.

Among the different applications of NC in papermaking, their use as dry strength [182] and coating [4] additives are the most predominant. Nevertheless, other options have been considered, such as their use as retention additive [205], for book restauration [206], for linting control [207] or as a vehicle to confer special characteristics, such as antimicrobial [202], electric [208] and fireproof [201] properties. However, all these studies have been carried out at lab-scale, and their up-scaling is still limited by several challenges regarding both NC themselves and some secondary effects on the production process. However, the forecasts predict that by 2020, the global use of NC in the paper and packaging sector could overcome 5 million tons per year, distributed in different uses as shown in Figure 6 [209].

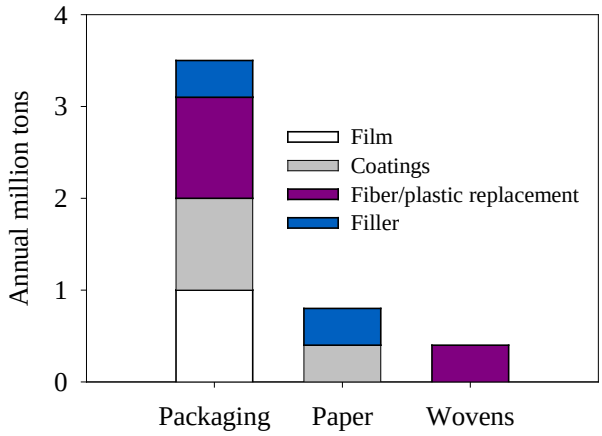

Figure 6. Annual tonnage estimates of nanocellulose material utilization by forest products subsector.

In 2014, Brodin et al. [4] identified the main drawbacks for the implementation of NC within the papermaking process. Since then, thousands of research studies have been published regarding new strategies to overcome these and other drawbacks. The challenges presented when NC is used in papermaking as strength or coating additive, to achieve upgraded barrier properties, both at lab-scale and to be scaled up to industrial level have been deeply analyzed and presented below. Moreover, the emerging strategies to solve these issues have been reviewed.

1.4.1 Challenges

One of the main challenges of the NC for this application is their high swelling ability. This would affect mainly to the barrier properties of the improved paper, as well as to the required energy for paper drying. In addition, there are other issues regarding the application of NC in the papermaking process, such as their dispersion within the pulp furnish, their retention within the fiber network and the consequent effect on drainage.

1.4.1.1 Nanocellulose production cost

Among the three main types of NC, the main interest of the researchers in this field has been focused on CNF [210]. The production of CNF requires breaking strong hydrogen bonds, made mainly by mechanical treatments of the pulp, with a chemical or enzymatic pretreatment that improve the fibrillation efficiency [211]. However, since the used chemicals are also of high cost and difficult to recover, the CNF production cost is still a limiting factor for their application [212].

In the case of CNC, as it was described previously, when the raw material presents other components than solely cellulose, they have to be removed prior acid hydrolysis in order to obtain a high reaction yield [213]. All these treatments not only decrease considerably the process yield, but also increase the production costs and the environmental impact.

On the other hand, to reach a high BC productivity, a high amount of nutrients and long culture times are required, facts that trigger a big increment in costs [214]. Furthermore, when bacteria are cultured in static mode, the BC is produced in the form of highly and strongly entangled nanofibrils [63]. These BC pellicles present a high difficulty to be separated into individual nanofibers, requiring high energy costs [199, 215].

Finally, HNC are produced through the oxidation of fibers with periodate and a posterior modification, depending on the final use. Although the cost of periodate is quite high, it has been demonstrated that an almost complete recovery and regeneration is possible. However, the reaction is conducted for a long time and the chemicals used to modify the oxidized fibers are also quite expensive. In addition, its first synthesis was carried out

recently, so deeper research is still needed to determine if they are able to improve paper properties.

1.4.1.2 High swelling behavior of nanocelluloses

Although the hydrogen-bonded structure of the NC films avoids a strong interaction with oils and greases, it affects negatively the gas and vapor permeability of the improved papers. According to the literature, the coating of paper with CNC can reduce the oxygen transmission rate (OTR) even below 1 mL/m^2·day·atm, mainly due to the decrement of the paper porosity [216]. However, the OTR will further increase with the presence of water or water vapor in the atmosphere, since oxygen can diffuse through adsorbed water. This increases the air and thus the oxygen permeability [217].

Despite the beneficial decrement of paper OTR, the water vapor permeability of papers made with a proportion of NC is high [218]. The temperature and relative humidity of the air were found the most influencing variables in this property: it rapidly increases when the relative humidity is higher than 25% and following Arrhenius law for temperature [219].

The OTR, water vapor permeability and oil-permeability of the papers upgraded by NC and its dependence with the relative humidity are strongly influenced by the impurities present in the NC and their functionalization. Theoretically, the presence of lignin should increase the hydrophobic character of paper, keeping good barrier properties even in presence of humidity. However, Spence et al. [18] proved that water vapor permeability increased with the lignin presence because of the weaker interactions among fibrils, which reduces the compactness of the network.

1.4.1.3 Nanocellulose dispersion in the pulp

When the aim of the NC application is to increase the mechanical properties of paper products, they are usually mixed with the pulp prior to paper formation. A rapid and high dispersion of the NC within the fibers would reduce the energy consumption for mixing, keeping optical properties and paper homogeneity, as well as improving the reinforcing efficiency.

CNF tend to form a network of nanofibers joint by hydrogen bonding, quite stable and strong enough to hinder their homogeneous dispersion. In this way, some clusters are present in the suspension even despite the fact that it appears to be homogeneous, so their reinforcing efficacy is less than the one expected [220, 221] and different conclusions can be extracted from different researchers. Moreover, these clusters could decrease the light scattering coefficient and thus the opacity of the sheet, as observed by Petroudy et al. [222].

Although CNC have not gel properties, they have a strong tendency to form aggregates in the longitudinally direction of the crystals by hydrogen bonding [107]. Nevertheless, when

sulfuric acid is used to hydrolyze cellulose, the surface hydroxyl groups of cellulose react to yield charged sulfate esters. They usually promote dispersion of the CNC in water. However, the substitution degree is not high enough to keep stable suspensions for a long time. Thus, they tend to flocculate and then sediment. This effect is even more pronounced when either hydrochloric or hydrobromic acid are used for CNC production [7]. These CNC aggregates could reduce the strengthening effect, and worsen the paper homogeneity and brightness.

Even though this fact, at present there is no consensual method to describe the aggregation state of these suspensions. Only Cherhal et al. [223] and Phan-Xuan et al. [224] studied the effect of charge density and ionic strength on the aggregation of the CNC particles through scattering techniques, but they did not focus on the characterization of their aggregates. Therefore, there is a first need to develop a method that quantifies and describes the dispersion of CNC products and, a second one, which optimizes the dispersion according to the final effect on the target application.

In the case of BC, as the most productive method is the static culture, entangled nanofibers in the shape of a membrane are obtained. However, for paper strengthen, nanofibers from the membrane must be separated into individuals [225, 226] i.e. by mechanical disintegration or acid hydrolysis [227]. This fact has been proved by Xiang et al. [228], who recently stated that a proper dispersion of BC within the paper matrix is of relevant importance to get reinforced paper sheets. It is possible that a homogeneous but not highly dispersed suspension of BC fibers, could suppose great benefits on paper properties without a high impact on NC production cost. However, no intense efforts have been made so far to study the effect of the fibrillation degree of BC membranes on papermaking properties.

1.4.1.4 Effect of nanocellulose on retention and drainage

The nano-size of the NC and their inherent anionic charge make them difficult to retain within the paper matrix without the use of a cationic aids [229, 230]. On the other hand, the NC retention into the fiber network usually causes a detrimental effect on the drainage rate, since the wet-web porosity is strongly reduced and the water binding is much greater [6, 229]. This fact decreases the productivity of the papermaking process and increases the energy consumption for pressing and drying. Overall, this is likely the most critical drawback for the implementation of NC at industrial scale and needs an individual study for each particular pulp [203].

Some authors support the idea that the addition of a suitable cationic agent can minimize the dependence of the NC retention and the pulp drainage [4]. Nevertheless, only a few works are focused on the study of the interactions of the NC with these systems and other components of the pulp [231, 232]. These authors proved that the appropriate retention system (RS) depends mainly on the NC surface charge. In addition, Lenze et al. [233] observed that the effect of the NC on drainage also depends on their length. Some of the

operation conditions of the papermaking industry could also affect in a big extent the NC retention and drainage time, such as pH and salt concentration, thus needing a further optimization [6]. Thus, the decoupling of retention and drainage effects when using NC is key for the implementation of these products at industrial scale.

1.4.2 Emerging possibilities

As described previously, there are many fields of application where either CNF or CNC could show their potential. Thus, new methodologies have been investigated in the last decades to reduce their production cost. In the case of CNF, mechanical, enzymatic and chemical treatments, as well as some of their combinations, have been studied. Most of the work on the enhancement of paper properties with NC has been carried out by application of these CNF on virgin pulps [234, 235]. However, the studies for recycled paper strengthening are more recent and, so far, most of them have been conducted with CNF, while the use of other NC, such as CNC, BC or CNCC, has not been explored deeply. Furthermore, these products could offer additional advantages on paper properties compared to CNF, since synergic effects could be obtained to decouple, for example, the effects on tensile index and tear index.

The procedure used to produce CNC has been extensively studied for decades, and even some companies are producing 300 ton/year of this product. However, the benefits observed from the application in mass of CNC in paper are quite lower than those observed typically with CNF. Thus, there may be other factors affecting this enhancement, possibly the dispersion of the particles. Although there is a clear acknowledgement about the CNC dispersion problems, there is a lack of information regarding how it affects to the paper strengthen ability. This fact is of utmost importance to optimize operational costs and maximize the effect of using NC.

In the case of BC; long and crystalline fibers are produced under static cultivation, which could potentially improve the paper strength. However, typically, long culture times with a high proportion of nutrients are needed to produce a worthwhile amount of BC. The in-situ culture of bacteria with other components triggers a reduction in the time required to produce a composite material, at the same time than a better conformability and homogeneity is obtained [236]. In this context, the in-situ culture of bacteria with cellulose fibers could improve their quality at short culture times and avoid BC dispersion problems. This approach has been seldom published for virgin pulps and deeper studies are needed [237, 238]. Furthermore, it has never been studied for recycled pulps. In addition, if low-cost nutrient sources, such as residues or sub-products, are used during the culture, the production costs could be reduced substantially.

CNCC could very likely flocculate most or all negatively stabilized colloids, like those present in the wet-end stage of the papermaking process. Such flocculant may, therefore, be used as

retention agent in papermaking by increasing the dewatering efficiency and lowering the cost of this rather expensive step, at the same time that mechanical properties of the final paper could be enhanced. However, this fact has not been proven yet. This new family of NC has been synthesized for the first time recently, so the production costs are still far from applicable. However, in view of the promising applications, it is possible that they can be reduced shortly.

The use of a multilayer coating in a determined order is presented as a potential alternative to improve barrier properties of paper. In this way, each of the applied layer will protect paper from the environment [239, 240].

- Clay or calcium carbonate, have been added between the paper and the NC layer, easing their retention and printing properties [241, 242].
- The use of hydrophobic coatings, such as shellac, over the NC layer, can protect the paper from the water and water vapor, keeping a low water permeability even at high humidity [243].
- The NC can also be combined with active functional aids to give special properties to the paper or board surface, for example antimicrobial, antioxidant, aromatic, flame retardant, electric and catalytic properties [197, 217, 244, 245].

An alternative option to the multilayer coating by the combination of NC and other components, is the own modification of the NC. In this way, the required amount of both components could be reduced without increasing in a big magnitude the thickness of the paper. However, the modification of the NC would provide likely only one additional characteristic to the NC, but when more than one property needs to be enhanced, different layers will be probably needed. Some of the methods to improve the hydrophobic behavior of the NC are the controlled hornification [246] or the addition of an alkyl ketene dimer sizing agent to the NC [247]. Also, oleophobization of the coated papers can be improved by the modification of NC with low surface energy substances, such as fluorocarbons [200] or O-acetyl-galactoglucomannan [248].

Recently, different studies support the idea that the alignment of CNC can improve both the stiffness and the strength of NC upgraded papers [249, 250]. Moreover, in the papermaking industry, cellulose fibers are mostly lengthwise orientated, to get a dimensional stability in this direction, even when they are subjected to big changes in moisture content [2]. Wet stretching [251], the use of fluid dynamics [252] and external magnetic [253] or electric fields [254] have proved to successfully improve the alignment of NC in the paper matrix.

In order to avoid the use of several compounds in the wet-end of the paper machine that could interact among them worsening the properties of the final paper, the modification of NC has been proposed. Since both fibers and fillers have negative charge at the working pH, the approach of cationizing NC could make them feasible to be used as a retentive agent at

the same time than increasing the mechanical performance, making the process more cost-efficient [255].

Another authors focused their research in the increment of the negative surface charge to increase the hydrogen bonding of the NC with the fibers. This contributes to enhance the performance of NC and reduces the required dose, limiting their effect on drainage. The increase of the anionicity of NC is carried out by means of introducing carboxymethyl, carboxylic or aldehyde groups in the NC structure.

A different methodology was proposed to apply NC to the pulp. This is done by adding the NC to the filler suspension for its pre-flocculation before mixing with the pulp. The NC interacts with the fillers producing a filler-NC complex, usually by means of adsorbing NC on the mineral particles. In this way, the retention of both NC and fillers is ensured, at the same time that drainage is not affected due to the addition of small particles that could block the dewatering.

Finally, a few studies focused on the reduction of the costs for each particular case, i.e. NC fits for use. In this context, the production of the required NC in the own paper mill would save transportation, drying and dispersion costs. Moreover, the on-site production of NC could be a promising alternative to help newsprint companies to maintain their competitiveness, not only to improve their own paper, but also to be sold to other companies.

On the other hand, the reduction in the cost of the raw material used for NC production, as well as the optimization of the NC production process would make the process more economic by the reduction of the NC associated costs.

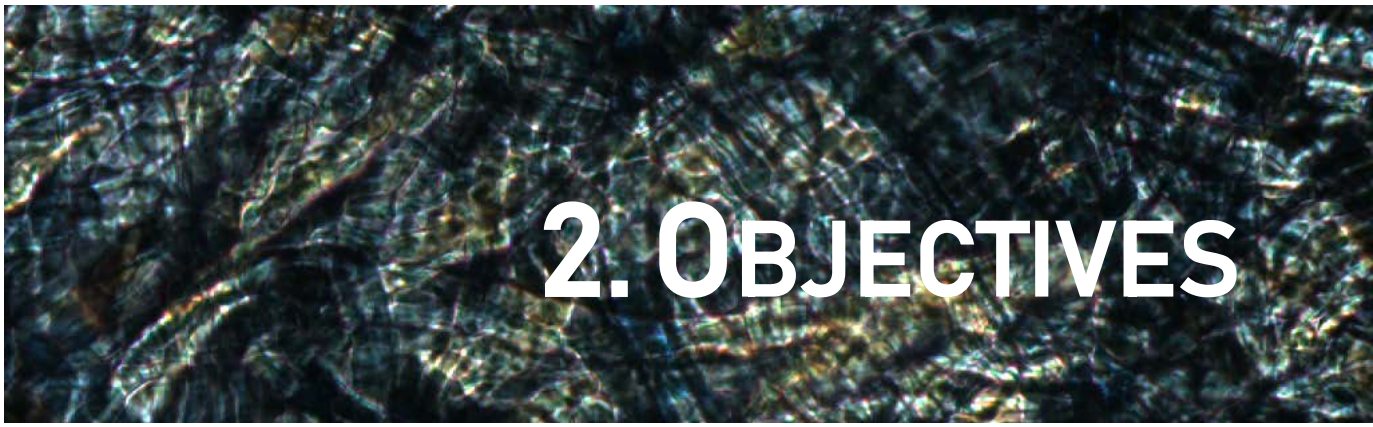
2. OBJECTIVES

2. OBJECTIVES

Paper recycling industry is facing severe challenges nowadays to maintain their competitiveness: (i) the deterioration of the recycled fibers as a consequence of the increasing recycling rate, (ii) the increasing requirements for mechanical, physical and printing properties and (iii) the restrictions in the production costs. The use of NC products in this sector could solve many of these challenges.

The most used NC in the papermaking sector is the CNF. However, even despite the high efforts of researchers and industries to reduce the costs associated to their production process, such as the high energy requirements, the high costs associated to chemicals as well as the difficulties found in their recovery and consequent reuse, their up-scaling is still far [212].

In this context, CNC are presented as great candidates to replace the CNF in the enhancement of the paper properties, since they are synthesized through a simple and much cheaper process, which consists of a hydrolysis reaction. Moreover, the chemicals used for their isolation are not expensive and they are easy to recover [256].

On the other hand, in view of the superior properties of the BC compared to those of vegetal origin cellulose, its use at low dosages could involve high benefits. Moreover, with the consequent nanofibrillation, nanocrystallization or even the in-situ culture of bacteria with the fibers, this impact could be further enhanced.

Finally, since the aldehyde groups present in HNC are highly reactive, it is easy to tune the particles to achieve fit-for-use nanoparticles. This fact together with the almost complete recovery of sodium periodate after the reaction, makes their production process be highly cost-effective. In papermaking, as most of colloids and fibers are negatively charged, the CNCC could be presented as an effective retention agent, facilitating the subsequent dewatering operations.

Thus, the global objective of this PhD is to assess the potential of three types of nanocellulosic products on the enhancement of the recycled paper production, focusing on BC, CNC and CNCC. For this purpose, the research has been divided into three specific objectives:

1. To improve the mechanical properties of RP by using BC.
2. To assess the dispersion degree of CNC suspensions and its effect on the RP quality.
3. To improve retention and paper drainage with the use of CNCC as a retention aid.

This research activity has resulted in 7 publications: 6 research publications and one review article; and the publication of several cross-sectional articles. In addition, there is one article in process of publication. Figure 7 shows a schematic diagram about the integration of the published studies in the present PhD thesis.

The main goal of the first line is the improvement of the RP quality, especially the mechanical properties, in terms of tensile (TI) and tear indexes, involving the use of BC.

First, a review article was published (Publication I), which focused on how to obtain and enhance a desired characteristic of the BC for a specific use. New isolated bacterial strains, some of them genetically modified to increase the productivity are reviewed. Improvements of the process, including new nutrient media, novel reactors and additives to increase the productivity, are compared with the use of standard media. Finally, a study of the BC properties produced by different methods and the potential enhancement of specific characteristics for different applications is included. Based on this study, the conditions to produce the BC at lab scale were defined as well as a new way to increase the bacteria productivity.

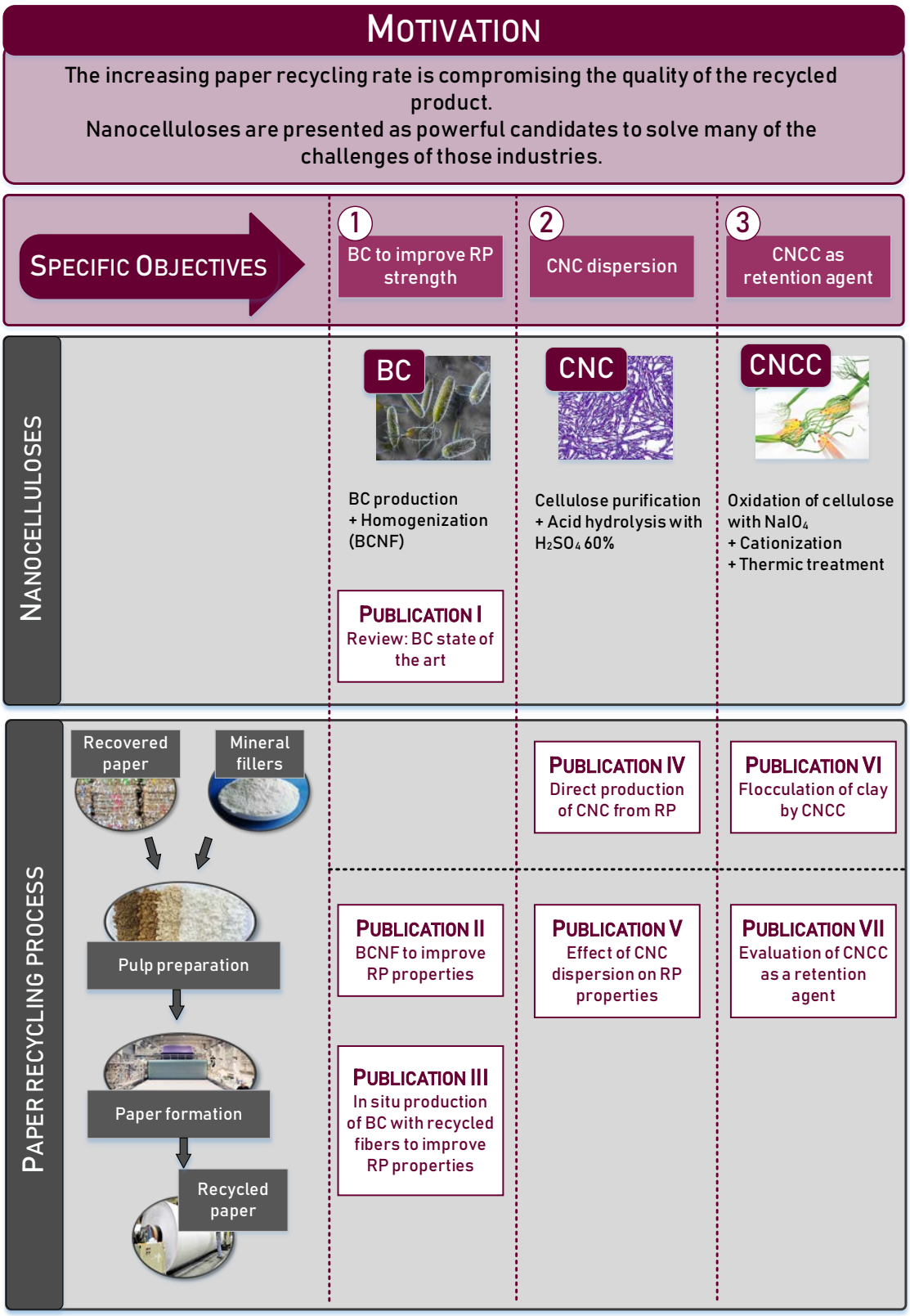

Figure 7. Schematic summary of the performed research to achieve the global objective of this thesis

- **Raising c-di-GMP intracellular levels of *K. sucrofermentans* to increase the BC production.** The overexpression of the DGC through the action of the gen PleD* could increase the c-di-GMP intracellular levels of this bacterial strain, increasing its productivity. The plasmid pJBpleD* is introduced in *Komagataeibacter* by three different methodologies, using the *E. coli* β2163 donor strain: electroporation, biparental conjugation and triparental conjugation. The presence of the mutant is corroborated by polymerase chain reaction (PCR). Both the modified and the wild-type bacteria are cultured under agitation and pH was determined each 24 h. The productivity is assessed through the final dry mass of BC ad the BC membranes are characterized by scanning electronic microscopy (SEM).

- **Addition of discrete amounts of nanofibrillated BC to the RP pulp.** With this method, the BC production line could be developed separately from the RP production process, and the BCNF could be added as a product additive. The objective of this study is, therefore, to improve RP properties by the addition of concrete proportions of BC nanofibers (BCNF). BCNF are obtained by a soft homogenization of the BC membranes produced under static culture of bacteria. Benefits in mechanical, physical and optical properties of the RP are assessed. Moreover, SEM, X-Ray diffraction (XRD) and ash measurements, are used to elucidate the mechanism of BCNF retention within the fiber network (Publication II).

- **In-situ production of BC with RP fibers.** Many operational costs, such as nanofibrillation or mixing with the pulp, could be avoided if the bacteria is let to grow and produce cellulose in a medium containing already the fibers. This second study aims to improve RP properties with the in-situ production of BC with the recycled fibers. This improved pulp is then mixed with the main pulp flow. The effect of the culture mode, in terms of static or agitated, on the RP properties is assessed. The mechanism that bacteria follow during culture in both methodologies is proposed. Finally, the effect of the culture volume and time on the improvement of these properties is evaluated (Publication III).

The second line of this PhD thesis aims to characterize the dispersion degree of CNC and assess its effect on RP properties when they are used as dry-strengthening agents.

The purpose of the Publication IV, is to determine the technical feasibility of producing CNC from recycled newsprint pulps (old newspapers (ONP) and the final product of the paper mill, NP). The direct production of the CNC without fillers removal and cellulose isolation is studied. Finally, the effect of the presence of impurities in the sample before hydrolysis on the quality of CNC is assessed.

Once they are produced, the CNC are added in mass to a RP furnish to study the effect of their dispersion on the mechanical properties of the RP. Thus, the focus of the Publication V is on the assessment of the effect that the aggregation state of the CNC has on the mechanical performance of the RP. Different mechanical and chemical methods are used for the CNC dispersion. Typical operations used in paper mills are also considered in order to evaluate if they are able to disperse effectively the NC in the pulp. Mechanical, physical and morphological properties of handsheets are determined to assess the effectivity of all these treatments.

There is a clear acknowledgement of the need of a method to determine the aggregation state of the CNC. The focus of the article in preparation VIII is indeed on the development of an easy method to describe the aggregation state of the CNC in water suspensions. The light intensity autocorrelation function decay (τ_D) at different temperatures determined through dynamic light scattering (DLS) is correlated with aggregation parameters detected by AFM image analysis. CNC individuals and their aggregates are grouped according to common geometrical features using unsupervised machine learning clustering. The contribution of each group on the variability of the DLS results is determined through variable importance analysis in randomized trees.

The third and last line of this PhD thesis was conducted with the objective of using CNCC as retention agent and thus simply the wet-end system of the RP production process.

The application of NC to improve RP properties in most cases causes a detrimental effect on the drainage [257]. Different retention and drainage additives are usually added to the wet-end to facilitate this operation. However, all these additives increase the complexity of the wet-end, and usually interact among them, thus needing a further study to optimize their implementation. The hypothesis in this case is that the use of a cationic NC could favor retention without affecting drainage. During the stay at the University of McGill in Canada, CNCC are produced and used as retention additive for the first time.

The objective of the Publication VI is to prove the effective flocculation of clay particles with CNCC and to assess the mechanism of action of these CNCC in flocculation operations. Flocculation monitoring is conducted by photometric dispersion analysis (PDA) at the University of McGill and laser reflectance (FBRM) at UCM. Zeta potential and supernatant turbidity removal, among others, are used to determine flocculation mechanism. Finally, the conformation of the clay/CNCC flocs is established through the measurement of their average fractal dimension in 2 and 3 dimensions (D_2 and D_f respectively). D_2 is obtained by processing optical microscopy images and a D_f is estimated through a novel machine learning random forest regression model that relates chord length distribution with D_f.

Once the flocculation mechanism of the CNCC is determined, their applicability as retention agent of a RP pulp is studied. The aim of the Publication VII, is, therefore, to study the effectivity of the CNCC to induce aggregation of a filler suspension (kaolinite/$CaCO_3$), a RP pulp and to assess their effect on drainage, solid retention and mechanical strength of the upgraded RP. Again, the conformation of the different fillers and fibers during flocculation is determined. An optimum dosage taking into account all these compromising issues is proposed. .

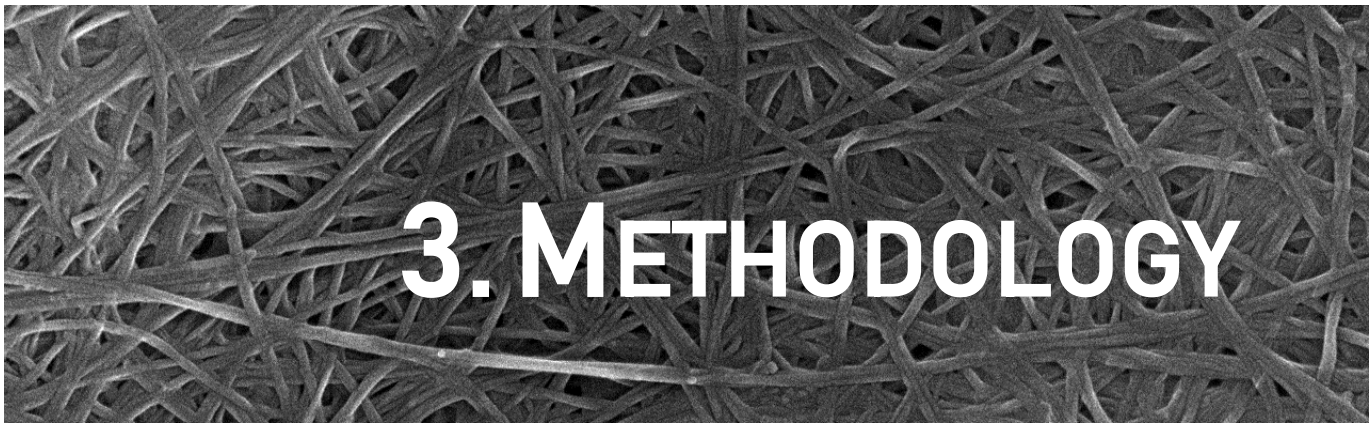

3. METHODOLOGY

3. METHODOLOGY

3.1 NANOCELLULOSE PRODUCTION

Three different types of NC have been mainly used for the studies carried out in the present thesis: BC, CNC and CNCC. A summary of the production and purification methods used are described below. CNF have been also used in the Publication V for comparison, so their production is also described briefly in this section.

3.1.1 Bacterial cellulose

The bacterial strain used for the production of BC was *Komagataeibacter sucrofermentans* CECT 7291, supplied by the Spanish Type Culture Collection (CECT). This bacteria has been selected because of its high productivity according to the literature [55].

Cell growth was carried out following the conditions recommended by the CECT, namely a medium composed of 20 g/L fructose, 5 g/L yeast extract and 3 g/L peptone (M10) in static mode at 30 °C for 4 days. Then, the produced pellicles of cellulose were cut in small pieces and shaken in a Multi Reax supplied by Heidolph (Schwabach, Germany) at 2000 rpm for 30

min. Cellulose pieces were removed from the bacterial suspension by gauze filtration. Then, it was centrifuged at 2900 *x g* for 10 min to separate bacteria from the nutrient medium. After removing the supernatant, bacteria were re-suspended in a saline solution: Ringer's solution (2.5 g/L NaCl, 0.105 g/L KCl, 0.12 g/L $CaCl_2 \cdot 2H_2O$, and 0.05g/L $NaHCO_3$) and centrifuged again in the same conditions. Bacteria were re-suspended in a small volume of Ringer´s solution and optical density was adjusted to 0.59-0.64 at the wavelength of 600 nm in a Cary 50 Conc UV-Visible spectrophotometer supplied by Varian Australia PTI LTD (Victoria, Australia).

For consequent cultures, 250 µL of the inoculum were added to each 100 mL of media. Two types of culture modes were used: static and agitated. In static culture, 100 mL of the inoculated medium were added to 140 x 20 mm Petri dishes and placed in an incubator. On the other hand, for agitated culture, 100 mL of the inoculated medium were placed in 250 mL Erlenmeyer beakers and placed in a Certomat IS orbital incubator manufactured by Sartorius Stedim Biotech GmbH (Goettingen, Germany) at 180 rpm. In all cases, culture was carried out at 30 °C for 7 days. Culture time was selected according to preliminary studies of productivity versus time. Finally, cellulose was purified by immersion in 1% NaOH at 90°C for 30 min and posterior washing with distilled water.

For the production of BCNF, the isolated BC was re-suspended in water at the final concentration of 1% (w/w), pulped for 60 min at 3000 rpm in a Messmer pulp disintegrator manufactured by Mavis Engineering Ltd. (London, UK), and homogenized through three batches at 600 bar in a laboratory homogenizer PANDA PLUS 2000, supplied by GEA Niro Soavi (Parma, Italy).

3.1.2 Cellulose Nanocrystals

The raw materials used for CNC production were:

- ONP, with an ISO Brightness of 45% and 14.5% (w/w) ash content, was prepared through the mixture of several commercial Spanish newsprints.
- NP, with an ISO Brightness of 56% and 14% (w/w) ash content, was kindly supplied by Holmen Paper (Madrid, Spain).
- *Eucalyptus globulus* ECF bleached kraft pulp (EUC), was kindly supplied by Torraspapel S.A. (Zaragoza, Spain).
- Microcrystalline cellulose (MCC), Avicel, was supplied by Sigma-Aldrich.

Recycled fibers present other components apart from cellulose, so a pretreatment was applied to purify the pulp. First, the pulp was disintegrated for 30 min at 3000 rpm at 1% (w/w) consistency in a Messmer pulp disintegrator manufactured by Mavis Engineering Ltd. (London, UK). Then, an alkali treatment was applied, consisting of suspending the pulp in 5% (w/w) NaOH and leaving it to react for 2 h at 125 °C. After that, several cycles of

washing with distilled water were developed by filtration till neutral pH was achieved. In a second step, 2% (w/v) NaClO was added to the pulp and the mixture was left to interact for 2 h at 125 °C. Again, the bleached pulp was washed with distilled water to reach neutral pH.

All pulps were dried overnight at 105 °C and then milled with a CT 293 Cyclotec supplied by FOSS A/S (Hillerød, Denmark), where milled particles have to pass through a sieve of 1 mm. Then, acid hydrolysis was conducted with 60% (w/w) H_2SO_4 at 45 °C. Acid concentration was selected according to preliminary tests, where a high hydrolysis yield was achieved avoiding, at the same time, the deterioration of the fibers and the conversion of cellulose into sugars. The ratio acid/pulp was set to 13.5 mL/g and the reaction was carried out for 90 min. After this time, the reaction was stopped by 10 times dilution of the mixture, and it was left to settle overnight. The sediment was washed by centrifugation with distilled water with a 3-16L centrifuge supplied by JP Selecta S.A. (Barcelona, Spain) at 4500 *x g* for 15 min until supernatant became turbid. Finally, to remove the excess of acid, the suspension was dialyzed against distilled water using tubing membranes made of regenerated cellulose with a molecular weight cut-off of 12000-14000 Da, supplied by Medicell International Ltd. (London, UK), until neutral pH was reached.

3.1.3 Hairy cellulose nanocrystals

A softwood kraft pulp, supplied by Domtar (Montreal, Canada), was used as raw material for HNC production. Two different types of HNC were produced: CNCC and ENCC (Figure 8).

In both cases, the procedure starts with the oxidation of the cellulose fibers with $NaIO_4$ to produce DAMC. First, the pulp was soaked in water and disintegrated at 3000 rpm for 10 min. Then, it was added to a solution of 0.98 g $NaIO_4$ and 0.78 g NaCl per gram of dry pulp and left to react for 24 h, stirring at 100 rpm at room temperature and with protection from light. After that time, 1 mL of ethylene glycol was added to quench the residual periodate [161]. Finally, the produced DAMC fibers were washed with distilled water by filtration.

To cationize the DAMC fibers and, therefore, produce the CNCC, the washed fibers were added to a solution containing 1 g of Girard reagent T (GT) and 2.4 g NaCl per gram of dry DAMC, and pH was adjusted to 4.5 with HCl [161]. After 24 h of stirring the mixture at room temperature, the cationic DAMC (CDAMC) were washed with abundant distilled water by filtration. The CDAMC at 1% of consistency were heated to 60 °C for 2 h. Finally, high intensity sonication was applied to the sample for 10 min, with an Ultrasonic Processor UP200H, supplied by Hielscher Ultrasonic GmbH (Teltow, Germany). To remove the non-fibrillated fraction and, therefore, isolate CNCC, the sample was centrifuged at 4500 *x g* for 10 min.

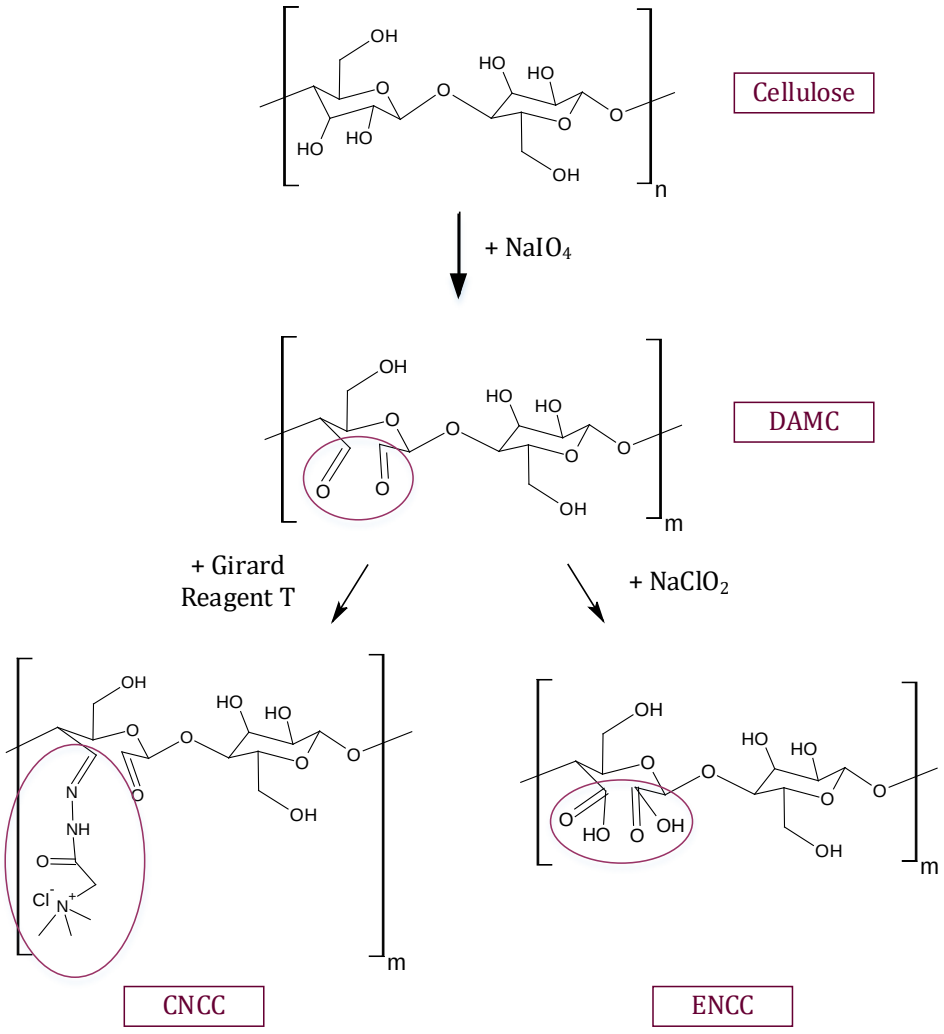

Figure 8. Chemical reactions carried out to produce two different types of hairy nanocrystalline cellulose (HNC): cationic HNC (CNCC) and electrosterically stabilized HNC (ENCC).

3.1.4 Cellulose Nanofibers

The CNF were produced from EUC pulp. First, pulp was oxidized by TEMPO-mediated oxidation using 5 mmol NaClO, 0.016 g 2,2,6,6-tetramethylpiperidine-1-oxyl radical (TEMPO) and 0.1 g NaBr per gram of dry pulp, using the procedure described by Saito et al. [23]. Briefly, the cellulose fibers were suspended at the concentration of 1% (w/w) in water containing TEMPO and NaBr, and the pH was adjusted to 10 with 0.5 M NaOH. Then, the required amount of NaClO was added to the suspension, keeping the reaction at room temperature while stirring at 500 rpm and maintaining the pH at 10. The reaction was conducted until no consume of NaOH was observed. Then, the oxidized pulp was washed with distilled water by filtration till neutral pH was achieved. After that, pulp consistency was adjusted to 1% (w/w) and it was homogenized through six passes at 600 bar with a PANDA PLUS 2000 laboratory homogenizer supplied by GEA Niro Soavi (Parma, Italy).

3.2. NANOCELLULOSE CHARACTERIZATION

3.2.1 Nanofibrillation degree

Nanofibrillation degree of BCNF and CNF was determined through the centrifugation of a 0.1% (w/w) sample at 4500 *x g* for 30 min. The ratio between the dry mass present in the supernatant respect to the initial sample was defined as the nanofibrillation degree.

3.2.2 Cationic demand

Cationic demand (CD) of CNC, BCNF and CNF samples was measured by colloidal titration with 0.00025 N poly-diallyl-dimethyl-ammonium chloride (PDADMAC), using a Charge Analysing System supplied by AFG Analytic GmbH (Leipzig, Germany). Then, CD was determined through Eq. (1).

$$CD = \frac{V_{PDADMAC} \cdot C_{PDADMAC}}{V_{sample} \cdot C_{sample}} \quad (1)$$

where $V_{PDADMAC}$ is the total volume of PDADMAC spent to reach zero charge, $C_{PDADMAC}$ is 0.00025 N, V_{sample} represents the volume of the sample suspension used in the test and C_{sample} means the concentration of the sample suspension.

3.2.3 Polymerization degree

PD of all NC was determined from the intrinsic viscosity (η) measurement, by the equation: $\eta = 0.42 \cdot PD$ valid for PD < 950 [165]. η was determined according to ISO 5351, with the method of dissolving cellulose in cupri-ethylene-diamine solution.

3.2.4 Crystallinity index and average crystalline dimension

Both Cr.I and average crystalline dimension (ACD) where calculated from data obtained by XRD spectra. A Philips X´Pert MPD X-Ray diffractometer with an autodivergent slit fitted with a graphite monocromator using Cu-Kα radiation, operated at 45 kV and 40 mA, was used for this purpose. XRD patterns were recorded in the range of 3-80° at the scanning speed of 1.5 °/min. The Cr.I was calculated through the Segal's method [258] by the Eq. (2).

$$Cr.I\ (\%) = \frac{I_{002} - I_{am}}{I_{002}} \cdot 100 \quad (2)$$

where I_{002}represents the intensity of the 002 plane at 2θ = 22.5° and I_{am} is the intensity of the amorphous scatter at 2θ = 18°.

ACD was defined as the perpendicular size to the diffracting plane represented by the maximum peak and determined through the Scherrer equation (Eq. (3)).

$$ACD = \frac{K \cdot \lambda}{\beta \cdot cos\theta} \quad (3)$$

where K is a dimensionless shape factor (normally 0.9), λ is the wavelength of the radiation in the diffraction experiment (λ = 0.15406 nm), β is the full width at half maximum of the diffraction peak (FWHM) in radians, and θ is its diffraction angle in radians.

3.2.5 Purity

Purity of CNC was determined as the remaining amount up to 100%, taking into account ash and lignin percentages, the main impurities still present after acid hydrolysis. Ash content was determined as the mass percentage of the sample after being submitted to 525 °C for 4 h, respect to the initial mass, following the ISO 1762. On the other hand, lignin content was measured indirectly through the Kappa number, according to Tappi 236 om-99, using the following equation: $Lignin\ (\%) = 0.13 \cdot Kappa\ number$ [259].

3.2.6 Morphology

CNC and HNC morphology and size was assessed through Atomic Force Microscopy (AFM) and Transmission Electron Microscopy (TEM). AFM was developed through two different equipments: i) an AFM MultiMode Nanoscope III A, from Bruker (Billerica, Massachusetts, USA) in tapping mode, belonging to the National Center of Electronic Microscopy of Spain in Madrid; ii) an AFM MultiMode 8, supplied by Bruker (Billerica, Massachusetts, USA) in PeakForce mode, belonging to the University of McGill (Montreal, Canada). For a better image resolution and particle fixing of the anionic NC, CNC, a drop of 20 µL of Poly-L-Lysine, a cationic agent, was deposited on a clean mica surface and left to dry at 60 °C. Then, a drop of 25 µL of CNC was deposited onto the cationic layer, left to dry at room temperature and then deposited in an oven at 60 °C overnight before analysis. In this way, aggregation of the CNC particles during drying in minimized. In the case of CNCC, as it is cationic itself, the procedure was developed without the application of Poly-L-Lysine. Both length and diameter distribution was determined using the NanoScope Analysis software.

NC morphology was also observed by TEM with a JEOL JEM 2100 at an accelerating voltage of 200 kV. A drop of sample was deposited on a copper grid and then stained with 2% (w/w) phosphotungstic acid for 2 min. It was left to dry at 60 °C overnight before imaging.

SEM was used to determine the morphology of BC pellicles, with a JEOL JSM 6335F at an accelerating voltage of 15 kV. Samples were previously dried overnight at 60 °C, placed onto a graphite slide and covered by a gold layer.

3.2.7 Thermogravimetric analysis

Thermal stability of CNC samples was assessed with an Exstar 6000 TG/DTA 6300 thermobalance, from Seiko Instruments Inc. (Chiba, Japan). The sample weight was recorded from 30 to 1000 °C at a heating rate of 10 °C/min with an air flow of 30 mL/min.

3.2.8 Hydrolysis yield

Hydrolysis yield of the CNC production was calculated as the proportion between the dry mass of the produced CNC and the dry mass of the sample before hydrolysis.

3.2.9 Dissolved amorphous cellulose

The amorphous cellulose proportion that is converted to sugars during acid hydrolysis was considered as dissolved amorphous cellulose (DAC), and determined through the chemical oxygen demand (COD) of the filtrated supernatant after hydrolysis. 2 mL of sample were added to Nanocolor COD 1500 tests, manufactured by Macherey-Nagel GmbH (Düren, Germany), and COD was obtained through the colorimetric method at 600 nm using an Aquamate-Spectrophotometer from Thermo-Scientific (Waltham, US). Assuming that all organic matter present in the suspension correspond to cellulose fractions, DAC can be calculated through the Equation (4) and (5).

$$DAC\ (mg/L) = \frac{COD}{1.185} = 2877.6 \cdot I^{600} \tag{4}$$

$$DAC\ (\%) = \frac{DAC\ (mg/L) \cdot V_{total}}{m_{b\ pret}} \cdot 100 \tag{5}$$

where V_{total} is the total volume after acid hydrolysis dilution and $m_{b\ pret}$ is the initial dry mass before pretreatment.

3.2.10 Aldehyde content

Oxidation degree of pulp achieved with $NaIO_4$ for HNC production was determined through the quantification of aldehyde groups [160]. The dialdehyde groups of DAMC were converted to oximes, employing a Schiff base reaction with hydroxylamine hydrochloride. Two suspensions were prepared: one with a known amount of DAMC in water and another with hydroxylamine hydrochloride at 5% (w/w). The pH of both suspensions was adjusted to 3.5. Then, the suspensions were mixed and the pH was controlled to 3.5 by the addition of 0.1 M NaOH. The reaction was finished when no change in pH was observed and aldehyde groups were determined by the consumption of the NaOH solution.

3.2.11 Cationic groups

The degree of cationization was determined through conductometric titration of the trimethylazanium chloride groups present in CDAMC with $AgNO_3$ 10 mM. The dossing and measurement were carried out automatically on a Metrohm 836 Titrando Instrument (Herisau, Switzerland). Around 0.05 g of CDAM (dry basis) were added to the titration beaker, and conductivity was recorded after the addition of 0.1 mL of $AgNO_3$ in 50 s intervals. It has been assumed the presence of one chloride counterion per trimethylammonium group. Initially, the conductivity starts decreasing while AgCl precipitates are forming, till all Cl^- are consumed. Afterwards, an increase in conductivity is observed. The amount of cationic groups present in the sample was determined through the amount spent of $AgNO_3$ before conductivity started to increase [161].

3.2.12 Zeta Potential

Zeta potential was measured with a ZetaPlus analyzer supplied by Brookhaven Instruments Corporation (New York, USA). 3 mL of sample at the concentration of 0.1% were placed into the cuvette. The cell was then immersed into the sample cuvette and it was placed inside the chamber. The result provided was the average value of at least 5 measurements.

3.2.13 Dynamic Light Scattering

The hydrodynamic diameter of the nanoparticles was assessed by a Brookhaven light scattering instrument BI9000 AT digital correlator (New York, USA). Scattered light intensity was recorded at 90ºC and 25ºC, of suspensions at 0.005%.

3.2.14 Carboxyl groups' determination

Carboxyl groups of ENCC were determined through conductometric titration on a Metrohm 836 Titrando instrument (Herisau, Switzerland). 0.05 g of ENCC in dry mass were added to 120 mL of deionized water and the pH was adjusted to 3.5 by adding 0.1 M HCl. Then, 0.1 mL of 10 mM NaOH were added per min, up to a pH of around 11 was achieved. The volume of NaOH spent in the part of the curve that represents weak acid on the titration graph was used to calculate carboxyl content through Equation (6).

$$Carboxyl\ content(mmol/g) = \frac{V_{NaOH} * C_{NaOH}}{m_{ENCC}} \quad (6)$$

where V_{NaOH} represents the NaOH volume spent in the second part of the titration graph, C_{NaOH} is the NaOH concentration used for titration and m_{ENCC} is the dry mass of ENCC used for this test.

3.2.15 Transmittance

Optical transmittance of CNF samples at the concentration of 0.1% (w/w) was determined from 400 to 800 nm using a Cary 50 Conc UV-Visible spectrophotometer supplied by Varian Australia PTI LTD (Victoria, Australia) [242].

3.3 GENETIC MODIFICATION OF BACTERIA

3.3.1 Bacterial mating

Bacterial growth was performed according to the procedure explained in the section 3.1.1. Once bacteria were suspended in water, they were submitted to a transformation with the objective of introducing the gen pleD*. This transformation was carried out by the *Plant-bacteria interactions* research group, at the *Estación experimental del Zaidín* belonging to the *Consejo Superior de Investigaciones Científicas* (EEZ-CSIC). Three different methodologies were used to transfer this gen from *E. coli β2163* holding pJB3pleD* to *K. sucrofermentans CECT 7291*: electroporation, biparental conjugation and triparental conjugation, following the protocols already published [52, 260]. The presence of the mutant was corroborated by polymerase chain reaction (PCR). Both the wild-type bacteria and the mutants were preserved at -80ºC.

3.3.2 Bacterial culture

To assess the productivity of all bacterial strains, including the wild-type and the mutants, they were grown in M10 for 4 days at 180 rpm of orbital agitation. To avoid the rejection of the gen by the mutants, the media was supplemented with tetracycline at the final concentration of 10 mg/L. Only the strains possessing the gen are able to survive and, therefore, produce BC in the presence of the antibiotic, so the effectivity of the modification was evaluated in this way.

After this period, bacteria were separated from the created BC and re-suspended in Ringer's solution following the procedure described in the section 3.1.1. Then, mutants were used to inoculate a medium composed M10 and tetracycline, while the wild-type was cultured with and without the supplementation of the antibiotic. After 7 days of cultivation at 30ºC in static mode, BC pellicles were extracted from the medium and sterilized following the methodology previously described.

pH was determined each 24 h of culture. Productivity was assessed through the determination of the dry mass of BC after their isolation per volume of culture. In addition, it was also determined each 24 h of culture. SEM micrographs of the dry BC pellicles after the 7 days of culture were obtained following the procedure described in the section 3.2.6.

3.4. PAPER STRENGTHENING

3.4.1 Handsheet formation

A mixture of 60% NP and 40% non-printed magazine (MG) was used to prepare the RP pulp to be improved [182]. Different procedures were used depending on the aim of the study and the type of NC.

In Publication II [215], different proportions of BCNF, namely 0.5, 1.5, 3 and 6% relative to the total dry weight, were added to the RP and diluted with hot water till a concentration of 1% (w/w). The mixture was pulped at 3000 rpm for 10 min in the standard disintegrator described previously. To retain the BCNF and improve handsheet formation, a three-component RS (CPAMB), typically used in newsprint mills, was used. The CPAMB was supplied by BASF (Ludwigshafen, Germany) and it is composed of a polyamine with a high molecular weight and a cationic charge density of 0.035 meq/g as coagulant; a PAM with a high molecular weight and a cationic charge density of 3.66 meq/g as flocculant, and a hydrated bentonite clay. After pulp disintegration, the polyamine was added at a concentration of 1.25 mg/g and stirred at 300 rpm for 15 min. Then, PAM and bentonite were added separated 30 s one after the other with continuous stirring at the dosage of 0.5 mg/g and 1.7 mg/g, respectively. Dosages were selected based on preliminary tests [261]. Handsheets were prepared at the basis weight of 60 g/m^2 in a normalized Rapid-Köthen handsheet former supplied by PTI (Vorchdorf, Austria) according to ISO 5269/2 (2004).

In Publication V [262], pulping conditions were varied to study the effect of the pulp and NC dispersion on the mechanical, physical and optical properties of the handsheets. Paper soaking before disintegration, pulping time (10 to 60 min) and water temperature (20 to 50 °C) were varied. For this study, a CNC and CNF dosage of 3 and 1.5%, respectively, were used. In addition, two dispersing agents were used for NC dispersion: (i) a synergistic mixture of a moisturizing and a detergent surfactant (D1), which is typically used during alkaline bleaching processes to facilitate the uniform impregnation of the fibers with the bleaching agent; and (ii) a moisturizing agent (D2), which facilitates the intimate contact between coatings and paper. Both dispersing agents were kindly supplied by NALCO (Naperville, USA). The dose interval for the dispersing additives (0.003-0.1 wt.%) was selected based on the supplier recommendation. Either D1 or D2 were added to the CNC or CNF suspensions and mixed for 2 min at high stirring speed. Then, the sample was disintegrated together with the pulp at a final consistency of 1% as previously described, for 10 min using hot water. The procedure developed for handsheet formation was the one already described, applying as RS not only CPAMB, but also chitosan (CH) of medium molecular weight dissolved at 1% (w/w), supplied by Sigma Aldrich. For CH application, 1 mg/g [261] were added to the pulp and stirred at 300 rpm for 30 min.

3.4.2 Handsheet characterization

Handsheets were always conditioned at 23 °C and 50% humidity for 24 h. Grammage was determined following the ISO 536. Mechanical (tensile and tear strength), physical (porosity and thickness) and optical (ISO Brightness and CIELAB colorimetric constants) properties were determined using an AUTOLINE 300 from Lorentzen & Wettre (Stockholm, Sweden). TI and tear index were calculated by dividing the tensile and tear strengths of the paper by its grammage. The bulk was calculated based on the ratio between the thickness and the grammage (ISO 534).

Homogeneity of the formed handsheets was determined through the standard deviation (SD) of 400 microgrammage measurements using a Beta formation tester manufactured by Ambertec (Espoo, Finland).

The morphology of the handsheets was analyzed by SEM with a JEOL JSM 6335F at an accelerating voltage of 15 kV. These analyses were carried out in the National Center of Electronic Microscopy of Spain.

In addition, XRD analysis of handsheets was carried out to evaluate the presence of the different mineral fillers in the paper matrix. Again, a Philips X'Pert MPD X-ray diffractometer with an autodivergent slit fitted with a graphite monochromator using Cu-Kα radiation operated at 45 kV and 40 mA was used.

Finally, the amount of the main fillers used in the paper industry, $CaCO_3$ and kaolinite, were determined through ash measurements at 525 °C and 900 °C, according to the ISO 1762 and the ISO 2144. As stated in the ISO 2144, both fillers does not decompose at 525 °C, but when they are submitted to 900 °C, only 56% of $CaCO_3$ and 86-89% of kaolinite are retained. Therefore, with these data the different filler contents have been calculated.

3.5. IN SITU PRODUCTION OF BACTERIAL CELLULOSE WITH RECYCLED FIBERS

A pulp suspension of 0.5% consistency was prepared by pulping RP (60% NP and 40% MG) at 3000 rpm for 10 min in the standard disintegrator. Then, 20 g/L fructose, 5 g/L yeast extract and 3 g/L peptone were added to the pulp suspension as nutrients and pH was adjusted to 6 by the addition of diluted HCl. The prepared suspension was autoclaved at 121 °C. Once it reached room temperature, 2.5 mL of the bacterial suspension, prepared as described previously, were added to inoculate each liter of pulp.

Both static and agitated culture were studied in order to assess which method is more favorable for the enhancement of RP mechanical properties. For static culture, 100 mL of the inoculated suspension were poured into 100 mL Petri dishes. For agitated culture, either 100 mL of the culture suspension were added to 250 mL Erlenmeyer flasks or 300 mL to

500 mL Erlenmeyer flasks, being placed into an orbital incubator at 180 rpm. Cultures were carried out at 30 °C for 6, 12, 24, 36 and 48h.

Different culture flasks at each time were autoclaved to remove bacteria and mixed with the corresponding amount of pulp to reach a total of 1 L at 1% of consistency. Then, the mixture was pulped at 3000 rpm for 10 min in a standard disintegrator described previously. The RS, CPAMB was added previously to handsheet formation. After that, handsheets were prepared as described in Section 3.3.1. Figure 9 shows a simplified scheme for an easier understanding of the process.

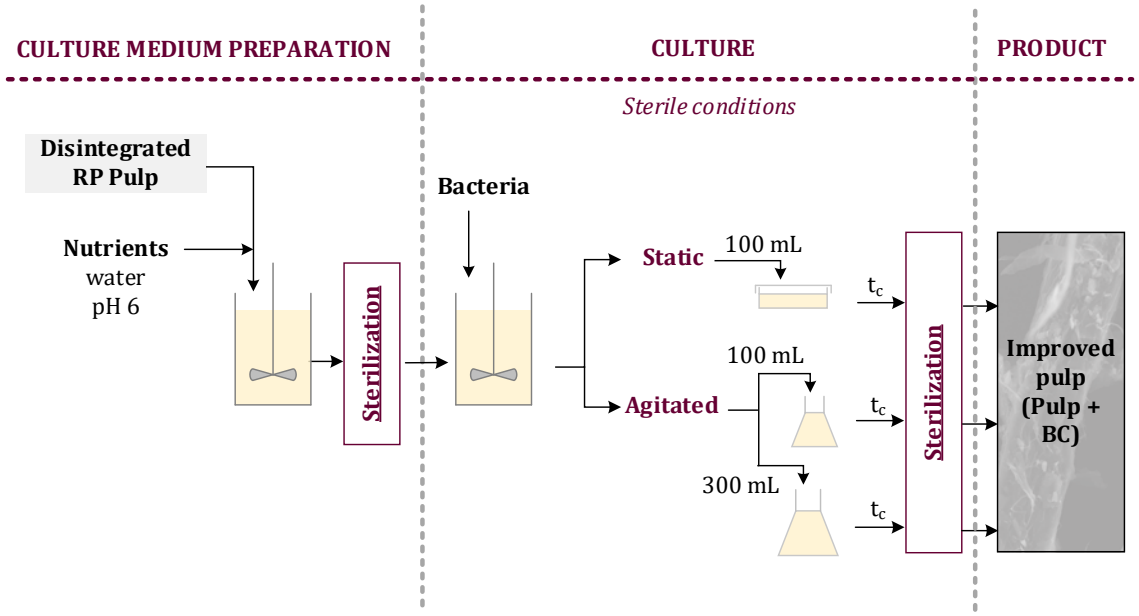

Figure 9. Procedure developed to culture bacteria in presence of fibers.

3.6. AGGLOMERATION STATE OF CELLULOSE NANOCRYSTALS

3.6.1 CNC conservation method

Recently produced CNC-EUC at 0.2% of concentration were conserved by 2 different methods: keeping the never-dried CNC in the fridge (LIQ) and freezing the sample with liquid nitrogen and keeping it in the freezer (F). The LIQ sample was used without further modification. However, the sample F was defrost by three different ways: the sample was placed in the fridge at 4ºC overnight (F-FR), in a vacuum furnace at 20ºC for 2 h (F-VA) and in a bath at 40ºC for 1 h (F-40).

3.6.2 Dynamic light scattering

Agglomeration state of CNC was monitored with DLS technique using a NanoBrook 90Plus supplied by Brookhaven Instruments Corporation (NY, USA). The equipment provides the hydrodynamic radius of spherical particles by the measurement of their Brownian motion at a determined temperature. The velocity of the Brownian motion is determined through the translational diffusion coefficient (D), which is also considered to determine the hydrodynamic diameter (d(H)) by the Stokes-Einstein equation (Eq (7)):

$$d(H) = \frac{kT}{3\pi\eta D} \tag{7}$$

Where k is the Boltzmann's constant, T is the absolute temperature and η is the viscosity.

The principle of this technique is shown in Figure 10. DLS technique measures the speed at which the particles are diffusing due to Brownian motion, by the measurement of the rate at which the intensity of the scattered light fluctuates when detected using a suitable optical arrangement. With a correlator, the signal is compared with itself at a particular point in time and a time much later, and thus the correlation function is constructed (Figure 11). The time at which the correlation starts to significantly decay is an indication of the mean size of the sample. Thus, the shorter τ_D and the steeper decay, the smaller and more monodisperse the sample is. From this point, different algorithms are used to transform the information from the correlation function into dimensional terms. The most used approach for this purpose is to fit a multiple exponential to the correlation function to obtain the distribution of particle sizes, such as the non-negative least squares (NNLS) or CONTIN [263].

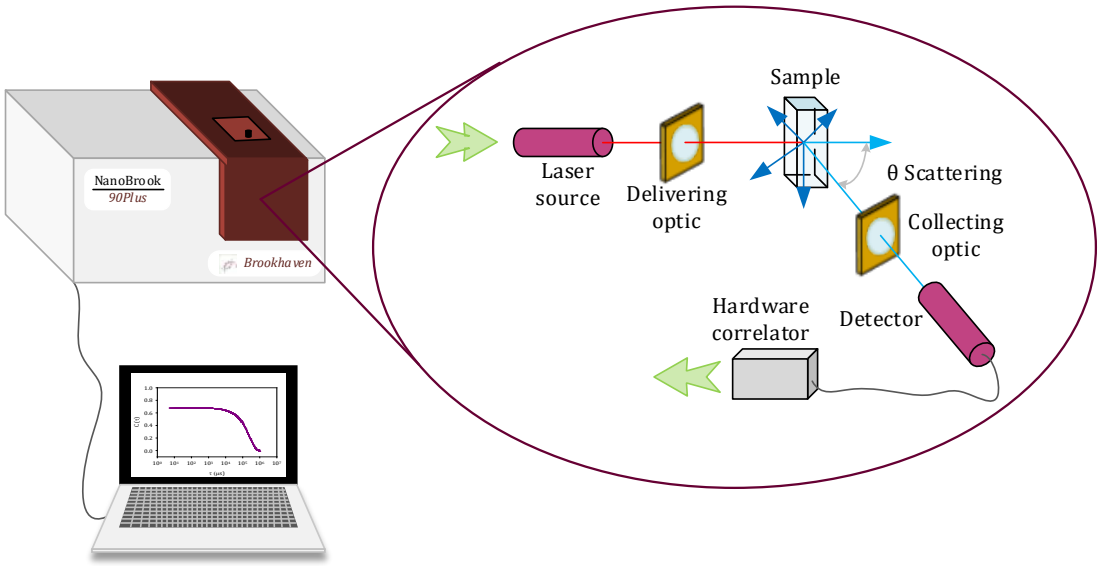

Figure 10. Principle of the DLS technique.

For this study, the mode forward scattering, detecting the scattering light at 15º and 640 nm, was chosen due to the presence of large particles, such as aggregates in solution. A set duration of 30 s with an equilibration time of 0 s were chosen for all experiments. No dust filter was applied due to the wide variety of sizes present in the sample.

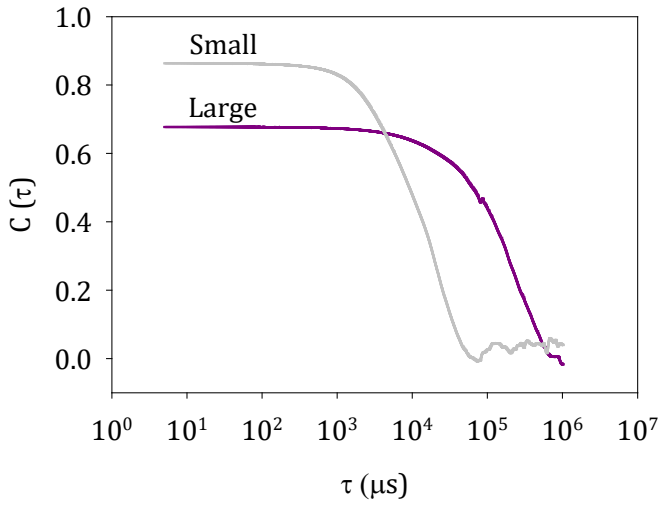

Figure 11. Typical correlogram from a sample containing large and small particles.

Three different concentrations of the CNC suspensions were used: 0.2%, 0.1% and 0.05%. Samples were sonicated for 30 min in an ultrasonic bath before analysis. Thereafter, 4 mL of the suspension were deposited on a glass cuvette and placed inside the chamber. Temperature was varied from 10 to 80ºC in intervals of 10ºC. 10 total measurements were made at each point with 50 s between them.

In this study, τ_D was defined as the time point at which the autocorrelation function has changed by 2% with respect to the mean of all previous values recorded.

3.6.3 AFM image analysis

Images taken by AFM were binarized and only the particles that were not intersecting with the border of the image were analyzed. The area, perimeter and maximum Feret diameter (MFD) in pixels were measured for each particle. Some additional parameters have been formed by the composition of these three, and are defined below.

Mean aggregation area (MAA). The compactness of a generic 2D object can be determined by the dimensionless ratio of the area vs perimeter^2. However, in the digital domain, where objects are represented as clusters of pixels, the latter relation becomes maximal for square shaped objects, thus defining a modified expression (Equation (8)) [264, 265].

$$MAA = \frac{1}{A_{total}} \sum \left(4 \cdot \frac{(Area)^{3/2}}{Perimeter} \right) \quad (8)$$

In the cited equation, the dimensionless ratio of each particle/cluster was multiplied by its area and the sum of all contributions was divided by the total area. In this way, the aggregated mass of nanocrystals can be estimated. On the other hand, the value of MAA could be an indicative of the spikiness of the particles in the suspension [266].

Two-dimensional fractal dimension (D_2). It was indirectly determined following the general expression : $A \propto r^{D_2}$, where A represents the total area of all primary particles present inside a circle of radius r [267]. Since the CNC individuals and aggregates are not spherical, the longest ferret of the clusters was used in place of r [268, 269]. Thus, the slope of the graph log (a) vs log (MFD) delivers the value of the average D_2.

Skewness. It was assigned to the symmetry or preferential spread of a size distribution to one side of the average value, being positive when it is on the left and negative in the opposite case [270]. The distribution is considered fine skewed when it is below -0.43, symmetrical when it is between -0.43 and +0.43 and coarsely skewed when it is over +0.43.

Kurtosis. It determines if the data of a normal distribution are heavy-tailed or light-tailed. When kurtosis is <1.70, the distribution is considered to be very platykurtic, platykurtic when it is between 1.70 and 2.55, mesokurtic between 2.55 and 3.70, leptokurtic between 3.70 and 7.40 and very leptokurtic when kurtosis was >7.40.

3.6.4 Unsupervised machine learning clustering

k-Means clustering was used to automatically classify the image elements according to their MFD, perimeter and surface area. First, the number of clusters (k) to consider in the sample was determined through the elbow method [271]. This method's output is the evolution of the sum of squared distances (inertia) of samples to their closest cluster as a function of the number of clusters. The number k is the one from which the addition of another cluster does not significantly improve the inertia value. Once this number k is chosen, the k-Means clustering algorithm is conducted, where the optimum centres that minimize the overall distance from points to their nearest centroids are found [272]. This analysis was carried out using the Scikit-learn Python module [273]. This classification was applied to all image elements taken as a whole considering their MFD, perimeter and area.

3.6.5 Variable importance analysis

Due to the challenging task to interpret the DLS graph, where the τ_D was plotted against the temperature, a variable importance analysis was carried out using extremely randomized trees (Extra-Trees) models. The Extra-Trees method is based on an ensemble of regression

trees whose main features are generated randomly [274]. Regression trees are machine-learning algorithmic models that predict the values of a response variable when presented with a set of data. With the application of the Extra-Trees models, irrelevant variables will have null importance, where a value of importance is delivered for those variables that have relevance on the results [275]. Extra-Trees analysis was carried out employing the Scikit-learn Python module [273].

Importance of both τ_D and their SD, at temperatures ranging from 10 to 50ºC, on the geometrical features of the k groups as well as on the aggregation parameters described from the AFM images was determined through the described method.

3.7 FILLERS FLOCCULATION BY HAIRY CELLULOSE NANOCRYSTALS

Firstly, a suspension of clay at 1 g/L in distilled water was prepared for flocculation tests by CNCC, adjusting the pH to 8.5 (Publication VI). Secondly, a combined suspension of 70% clay and 30% $CaCO_3$, simulating the proportion of these fillers in newsprint mills, was prepared, also at 1 g/L (Publication VII). The flocculation kinetic of clay and the system clay/$CaCO_3$ by CNCC was monitored by both PDA and FBRM.

3.7.1 Photometric dispersion analysis

PDA tests were carried out in a PDA 2000 manufactured by Rank Brothers (Cambridge, UK) in the University of McGill (Montreal, Canada). The output of the PDA is the ratio RMS to DC readings, where RMS is the root mean square of the fluctuations in transmitted light and DC makes reference to the average transmittance. When flocculation takes place, the value of RMS increase and DC slightly increase, increasing then the ratio RMS/DC. This value can be an indirect measurement of the size and number of flocs, and the initial slope can be considered as a measurement of the initial flocculation rate. The principle and operation of the PDA is shown in the Figure 12.

The experimental procedure starts with 200 mL of the flocculation suspension in a 600 mL beaker with magnetic stirring at 100 rpm. Using a standard 3 mm internal diameter tube, the suspension was pumped at 150 mL/min through the photocell of the PDA, flowing back to the test beaker. The concentration of either clay or clay/$CaCO_3$ was kept constant in all experiments, varying the CNCC dosage. After monitoring the initial suspension for 120 s, the required dosage of CNCC was added and the ratio RMS/DC was recorded for 10 min.

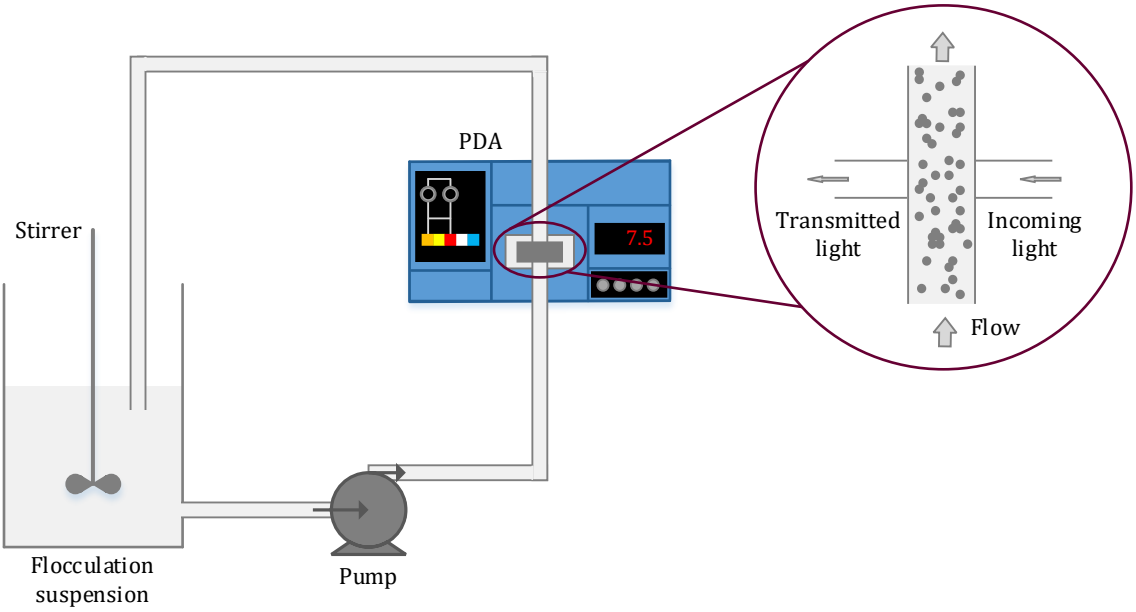

Figure 12. Schematic of the PDA set-up and the principle of the PDA measuring technique.

3.7.2 Focus beam reflectance measurement

The flocculation process was also assessed in real time observing the evolution of the corresponding suspension chord length distribution data. These data were gathered through a Focused beam reflectance measurement (FBRM) probe G400, supplied by Mettler Toledo (Columbus, USA). The FBRM can build a distribution of chord lengths that resembles the actual size distribution of particles in the corresponding suspension. The probe projects a rotating laser beam of known speed into the suspension and records the time during which the beam is intersecting a particle, which is then translated into a chord length, which is defined as the distance between the two edges of a particle [276]. In the present studies, the chord lengths detected were classified through the probe software in 200 size intervals organized logarithmically, ranging from 1 to 4000 μm, which could be grouped in different ways [277]. Figure 13 shows the experimental set-up for FBRM flocculation monitoring.

In order to compare the FBRM and PDA results, the FBRM probe was placed in a 600 mL beaker with 200 mL of the initial suspension under magnetic stirring at 100 rpm. After 120 s, the required CNCC dosage was added to the sample, recording the mean chord length (MCL) and the particle number every 5 s for 10 min. After the 10 min, the stirring speed was increased up to 350 rpm for 2 min in order to break the formed flocs. Then, the stirring speed was reduced to the initial speed, 100 rpm, for 4 min more to assess the reflocculation rate.

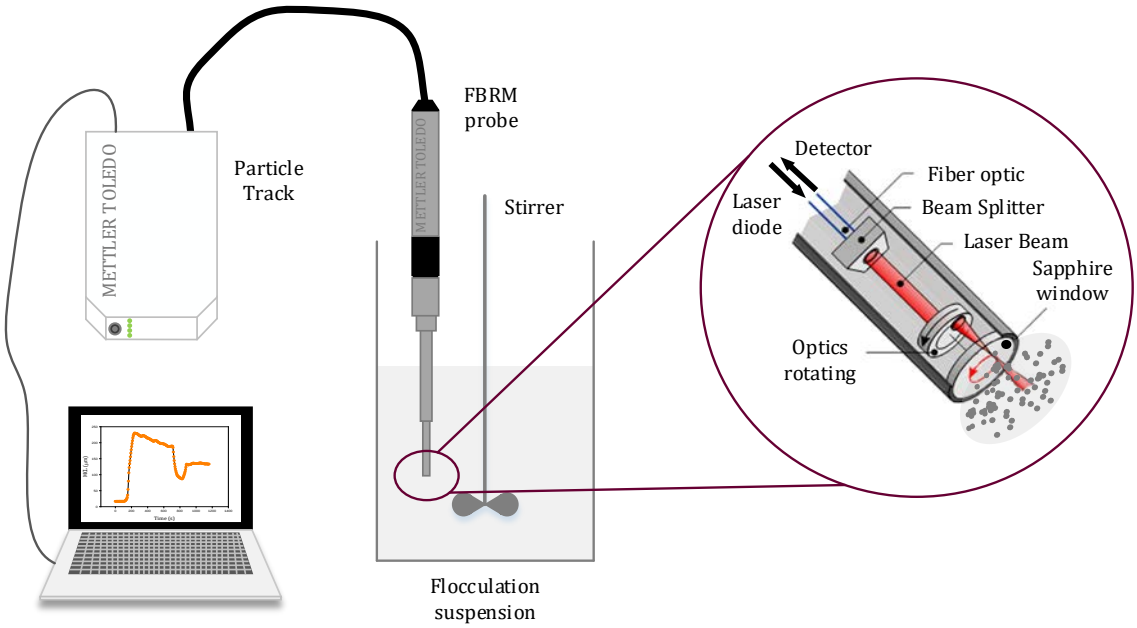

Figure 13. Schematic of the FBRM set-up and the principle of this measuring technique.

In the case of the Publication VII, a pulp made of disintegrated non-printed RP at the consistency of 0.5% was flocculated by CNCC and monitored by FBRM. The same experimental set-up as previously explained was used. However, in this case, stirring speed was adjusted to 200 rpm to ensure a complete homogenization of the suspension during CNCC dosage. To assess the reflocculation efficiency, shear rate was increased to 500 rpm and, then, decreased back to 200 rpm.

The flocculation stability has been calculated by Equation (9).

$$Flocculation\ stability\ (\%) = \frac{MCL_e - MCL_0}{MCL_m - MCL_0} \cdot 100 \quad (9)$$

where MCL_e is defined as the MCL after 10 min, MCL_0 is the MCL before CNCC addition and MCL_m the maximum MCL.

The refflocculation efficiency has been calculated by the Equation (10) [278].

$$Reflocculation\ efficiency\ (\%) = \frac{MCL_F - MCL_B}{MCL_e - MCL_B} \cdot 100 \quad (10)$$

where MCL_F is defined as the maximum MCL after the decrease of the stirring speed back to 100 rpm, and MCL_B is the MCL after breaking the flocs at high stirring speed (350 rpm).

3.7.3 Suspensions and flocs characterization

Zeta potential. To evaluate the isoelectric point (IEP) of the flocculated system, a fresh stock of the initial suspension was prepared and mixed with different amounts of CNCC. Then, zeta potential of these mixtures was determined after 5 min of agitation at the working pH (8.5), with a NanoBrook 90Plus supplied by Brookhaven Instruments Corporation (NY, USA).

Turbidity removal. Turbidity of the supernatant phase obtained after the flocculation trials was measured with a LP 2000-11 nephelometer supplied by Hanna Instruments (Rhode Island, USA), according to ISO 7027:2001. The turbidity of the initial suspension was also measured to calculate turbidity removal.

Optical microscopy. Optical microscopy was used to assess the flocs morphology using a Nikon ECLIPSE TE2000U (Tokio, Japan) and a Zeiss Axio Lab 10 microscope (Oberkochen, Germany). An aliquot of the sample was extracted directly from the flocculation beaker (at max MCL and reflocculated plateau) and a drop was placed onto cavity slides for analysis.

2D fractal dimension (D_2). D_2 was measured on microscopic images of the flocs. The images were processed and analyzed through the Fiji distribution of ImageJ 1.151h. Each microscopic photograph was converted into an 8-bit image and its contrast was adjusted to achieve a good definition of the flocs borders. Flocs were selected individually and copied into a separate image file. An automatic thresholding followed by a binarization was applied to each floc image. The fractal analysis was performed with the FracLac plugin of ImageJ using the default sampling sizes and 12 different grid positions. The D_2 output for each aggregate was the result of averaging the D_2 obtained in all grid positions.

3D fractal dimension (D_f). D_f was estimated by applying a machine learning random forest regression model [279] to the corresponding suspension chord length distribution data. Details on the methodology followed to implement the regression system can be found in the cited paper.

3.8. Retention and drainage

The effect of the CNCC on the drainage efficiency (Publication VII) was determined using a MütekTM DFR-05 supplied by Säffle (Sweden). 500 mL of a suspension of RP pulp at 0.5% consistency were added to the device and stirred for 90 s at 300 rpm. Then, the required CNCC dosage was added and left to flocculate for other 60 s. Immediately after, the stirring chamber was risen up and the suspension was filtrated by gravity through a 150 mesh. The drained weight was measured each 0.2 s for 240 s, and the drainage curve was plotted. The time spent in filtrating 300 g of sample was determined (W300) to compare the drainage efficiency of all experiments.

Retention was calculated indirectly based on the fibers, fines and filler losses present in the drained water. It was collected after finishing the drainage experiment, after 240 s. A known amount of the described sample was left to dry at 105ºC till constant weight, where the total solid content was determined. To get the amount of fibers or fines lost during draining, the dry sample was placed in a muffle furnace at 525ºC for 4 h, according to the ISO 1762. The total solid content minus that of ashes at 525ºC was considered as the percentage of drained fibers/fines. Finally, to differentiate between the retained kaolinite and $CaCO_3$, the sample was submitted to 900ºC in a muffle furnace according to the ISO 2144. It is considered that both fillers do not decompose at 525ºC, and 56% of $CaCO_3$ and 86-89% kaolinite remained in the sample at 900ºC. The calculation of the proportion of each mineral was developed according to these data.

4. Results and Discussion

4. RESULTS AND DISCUSSION

4.1. NANOCELLULOSE PRODUCTION AND CHARACTERIZATION

In view of the variety of NC types produced during this PhD thesis, a brief summary of their characterization is presented in Table 3.

A similar rod-like morphology was observed for all CNC and CNCC products, while BC presented a network structure, with much larger PD. Purity of the nanocellulosic material depended on that of the material used for their production, i.e. CNC from bleached pulps was 100% cellulose, while it was only 76% for CNC from ONP.

Hydrolysis yield varied in function of the ratio crystalline-amorphous cellulose of the raw material source. Thus, as eucalyptus, a hardwood, is more amorphous than, for example, softwoods, the hydrolysis yield of the CNC produced from this wood is only 8.5% compared to 64% for newsprint (typically composed of a mixture of both). This fact was also corroborated through the values determined of DAC, where it amounted to 58% for EUC pulps.

Table 3. Characterization data of all NC products used in this thesis. *Article in preparation

Property	BCNF	CNC				CNCC	CNF
		ONP	NP	NP-B	EUC		
Publication	II	IV	IV, V	IV	VIII*	VI, VII	V
Morphology	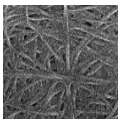	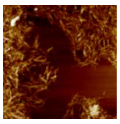	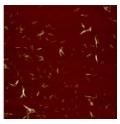	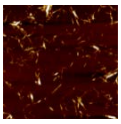	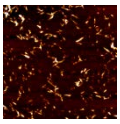	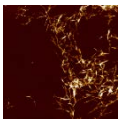	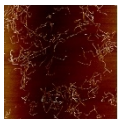
Nanofrillation Degree (%)	35.2	-	-	-	-	-	>95
CD (meq/g)	0.174	0.040	0.026	0.044	-	-	1.139
PD	1932	182	181	194	475	-	440
Cr.I (%)	98.4	92.6	93.4	94.8	93.3	-	-
ACD (nm)	-	32.5	41.2	45	-	-	-
Purity (%)	100	76	77.8	93.3	100	100	100
Diameter (nm)	2-30	2.9± 0.9	3.3± 2.9	4.4± 3.9	7.7± 2.1	4.7± 1.6	5-10
Length (nm)	-	371± 74	218± 48.6	356± 137	370± 170	380± 121	100-500
Hydrolysis Yield (%)	-	58.4	60.8	64.3	8.5	-	-
Full process yield (%)	-	58.4	60.8	34.6	8.5	35.3	-
DAC (%)	-	26.7	26.8	8.2	57.9	-	-
Aldehyde groups (mmol/g)	-	-	-	-	-	7.65	-
DLS size (nm)	-	-	-	-	-	326	-
Cationic groups (mmol/g)	-	-	-	-	-	1.31	-

4.2. BACTERIAL CELLULOSE TO IMPROVE RECYCLED PAPER STRENGTH

First, the bacteria was genetically modified with the objective of increasing the BC productivity. Second, the benefits that could be achieved through the addition of a mild-fibrillated BC to the RP pulp on the mechanical, physical and optical properties of the upgraded RP have been assessed. And third, in an attempt to reduce the costs associated to

the culture and homogenization, the in situ culture of bacteria with the RP fibers was studied and the benefits in the paper properties were quantified.

4.2.1 Genetic modification of bacteria

The BC production of the wild-type bacterial strain, *K. sucrofermentans*, in the medium containing tetracycline was negligible. In addition, there was a lack of BC in the cultures performed with the mutants created through electroporation and triparental configuration in the medium containing the antibiotic. Thus, from the three methodologies tried to modify the bacterial genetic, only the one carried out through the biparental conjugation was effective. Thus, the results presented in this section are those corresponding to the cited method.

Figure 14a shows the evolution of the BC production with the different strains: the wild-type in medium without antibiotic, and the modified with the vector (pJB3) and with both the vector and the gene (pJB3 pleD*) in medium with antibiotic. The produced BC started to be visible at shorter times for the wild-type bacteria, reaching the maximum of 3.6 g/L after 5 days of culture. However, the production of BC for the modified bacterial strain was not as high as expected previously, being even lower than the original one. After 5 days of culture, the production of all strains was kept almost invariable.

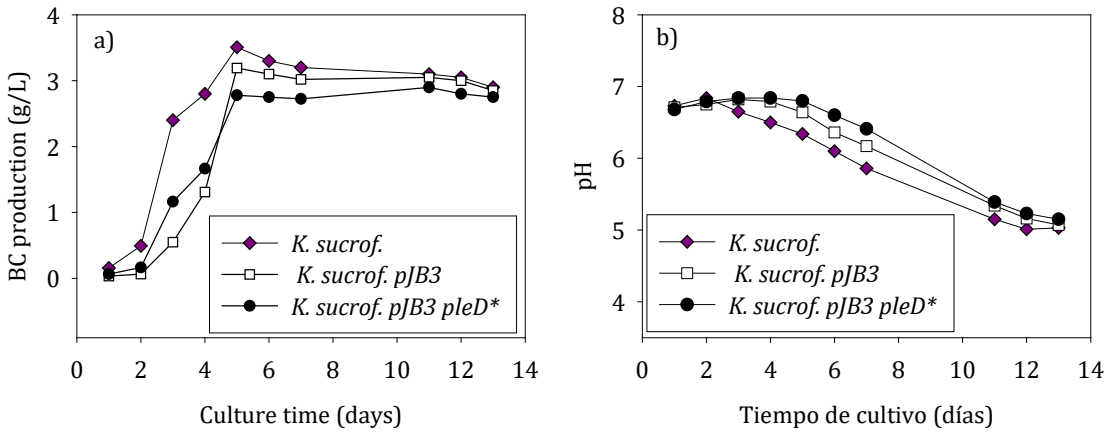

Figure 14. Evolution of a) BC production and b) pH, with the different strains, namely the wild-type, the one with the vector and the one with the gen pleD*.

This bacterial class converts carbohydrates into acetic acid during both bacterial growth and culture [40]. In addition, as a part of its respiratory metabolism, it oxidizes ethanol to acetic acid and converts glucose into gluconic acid [41]. All these acid formations produce a decrease in the pH of the culture broth, and it is even more pronounced in static cultivation [42]. Thus, the larger the BC production, the higher the decrement in the pH. This is indeed which is observed in Figure 14b: the pH of the culture broth from the wild-type bacterial

started to decrease at shorter times (after 3 days of cultivation). However, the bacteria modified with the gene pleD* was able to keep the neutral pH for around 7 days. It is possible that the presence of the antibiotic with the cited mutant decelerate its metabolism, reducing not only the production of BC, but also that of acid.

Presumably, both the BC production and the pH reduction with the inclusion of the gene pleD*, would be very similar to that of the wild-type if the antibiotic would not be present. However, it has been proved that the gene pleD* has been effectively introduced into the bacteria. Thus, it is possible that the c-di-GMP levels of K. sucrofermentans were already at the maximum, failing the overexpression of the DGC by the gene pleD*.

Despite this conclusion, SEM micrographs were obtained to assess if the morphological features of the produced BC pellicles presented any difference (Figure 15). A network structure of similar fiber diameter was observed for all samples.

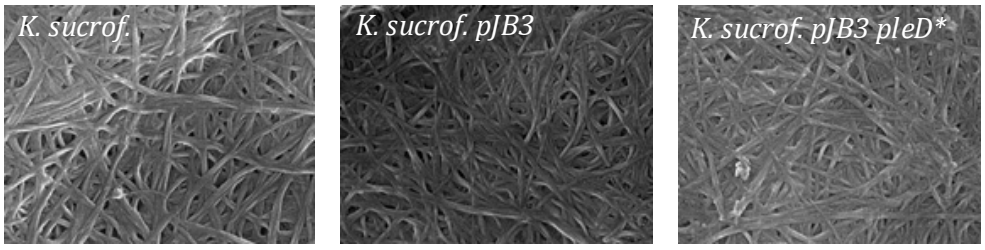

Figure 15. SEM micrographs of the BC pellicles produced through the wild-type strain (left), the one modified with the vector (middle) and the one modified with the gene (right).

Hence, it can be concluded that the presence of the gene pleD* in the *K. sucrofermentans* bacterial strain not only failed to improve the BC production levels, but also induced no difference in the morphological structure of the produced BC membranes. Therefore, the wild-type bacterial strain was used for the further studies carried out in this PhD thesis.

4.2.2 Mass application of low-fibrillated bacterial cellulose nanofibers

When BC is produced under static conditions, a pellicle on the surface is formed by the entanglement of bacteria during culture. These membranes are hard to disperse into individual nanofibers, what makes their application as reinforcement of materials a challenge.

In Publication II, BC membranes were synthesized in static culture and then fibrillated through homogenization, the typical procedure carried out to obtain vegetal CNF. Despite the application of these treatments, a low nanofibrillation degree was observed, being 35.2%. This fact means that some clusters of BC remain in the suspension, as well as some individual BCNF. This low nanofibrillation degree explains the value of CD shown in Table

3, with a value of 0.17 meq/g, compared to vegetal CNF, where CD values are around 0.46 meq/g [182]. However, both PD and Cr.I are much higher than either cellulose fibers or CNF, being 1932 and 98.4%, respectively. As the bacteria are free to move in the culture, they tend to move in a slow and direct way, forming therefore very long and crystalline nanofibers.

The presence of some clusters of BCNF as well as individual nanofibers can be observed in the SEM images of RP handsheets upgraded with different BCNF dosages (Figure 16). The BCNF clusters were identified by their homogeneous fibrils width and their entanglement described previously. However, the thin fibrils observed in the images may not only be due to the presence of some individual BCNF but also to some fines produced by the fibers deterioration during the recycling process.

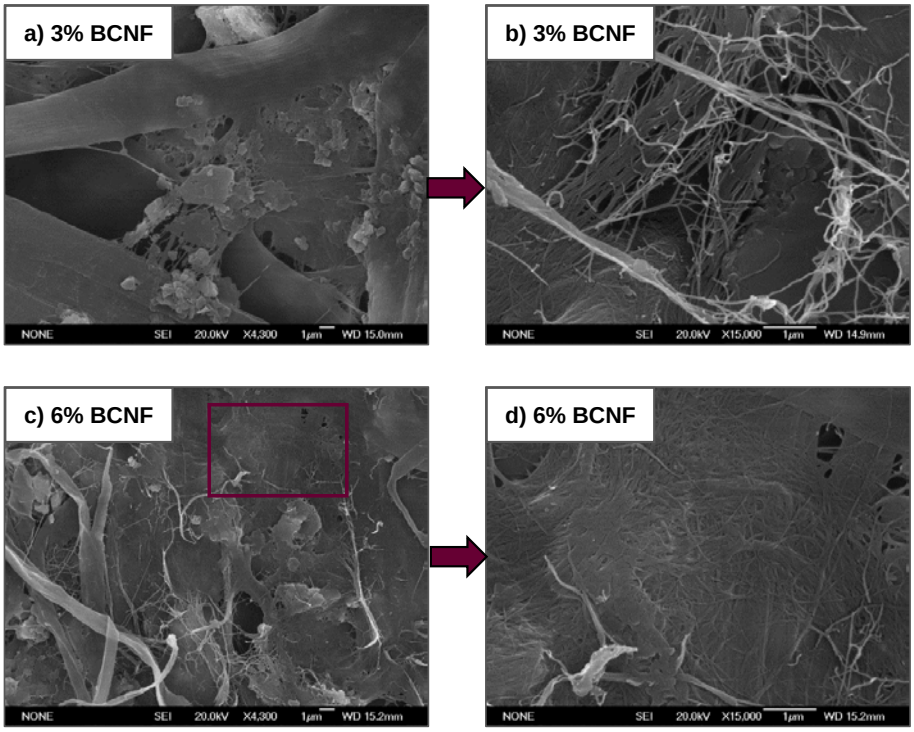

Figure 16. SEM images of RP handsheets improved with different BCNF dosages: a) and b) with 3% BCNF and c) and d) with 6% BCNF.

To assess the effect of the BCNF on the RP handsheets, TI and tear index were studied as mechanical properties, as well as porosity, beta formation and bulk as physical properties and ISO Brigthness and CIELAB color space as optical properties.

Figure 17 shows that the increase of the BCNF content in the RP induces an increment in both TI and tear index. With a BCNF concentration of more than 3%, the TI increases by more than 10%. However, the induced enhancement is quite lower than the one produced by vegetal CNF. For example, with the addition of 0.5% and 1.5% CNF of corn stalk and eucalyptus to the same RP, improvements of approximately 20% were obtained [182].

Nevertheless, the relevance of this study is that not only TI was enhanced, but also tear index (Figure 17). With 3% and 6% BCNF, tear index was improved by 7.6% and 10.1%, respectively. According to Hassan et al. [280], tear strength of paper is limited by the total numbers of fibers involved in the breaking of the handsheet, the fiber length and the number and strength of the interfiber bonds. Moreover, the number of fibers involved in the breaking process is related to the grammage and flexibility of the sheet. In rigid sheets, therefore, stress is concentrated in small areas, meaning only a few fibers are involved, while in flexible sheets, the force is transmitted from one fiber to another over a much larger area.

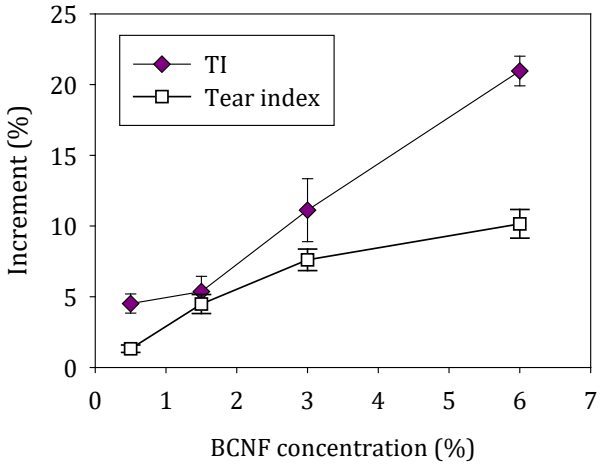

Figure 17. TI and tear index increments respect to the pulp without BCNF at different BCNF dosages.

Based on the described explanation, the more flexible the handsheets, the higher the tear index, which agrees with the results of this study. The reasons may be likely due to the lower number of hydrogen bonds formed between RP fibers and BCNF, compared to high fibrillated CNF, caused by the presence of some clusters. Thus, not only were formed stronger paper sheets, but also more flexible, favoring the transmission of the breaking force throughout the paper.

This is not the case for high fibrillated CNF, where typically an increase in TI triggers a decrement in tear strength [281]. Thus, Publication II shows a very important finding since this effect has been decoupled, allowing that both TI and tear index improve at the same time, with increasing BCNF concentrations. However, increasing concentrations of BCNF involve a concomitant increase in costs, mainly owing to chemical and energy expenses. In view of this explanation, with 3% BCNF, 10%, 7.6% and 66.8% of improvement in TI, tear index and strain at break can be obtained, at a minimum ratio improvement/BCNF dosage. This increment in strain at break also shows an upgraded elasticity of paper, mainly provided by the BCNF clusters.

Physical properties of upgraded handsheets, in terms of porosity, beta formation and bulk were also determined due to their importance in the runnability and printing quality of the paper. As shown in Figure 18, all these properties decrease their value with increasing concentration of BCNF. Since BCNF are retained at the gaps between fibers, porosity resulted decreased from 8.0 μm/Pa·s to 0.7 μm/Pa·s with a BCNF dosage of 6%. This is also a very interesting effect since a low porosity improves printing and barrier properties, factors very important for advanced paper applications.

The beta formation parameter is the SD of 400 microgrammage measurements, so a high value typically indicates a poor handsheet formation. Thus, beta formation indicates the homogeneity of the handsheets, and therefore the fibers and BCNF dispersion. In this study, beta formation decreased from 8.1 to 6.7 when 1.5% BCNF was added, keeping this value constant at higher dosages.

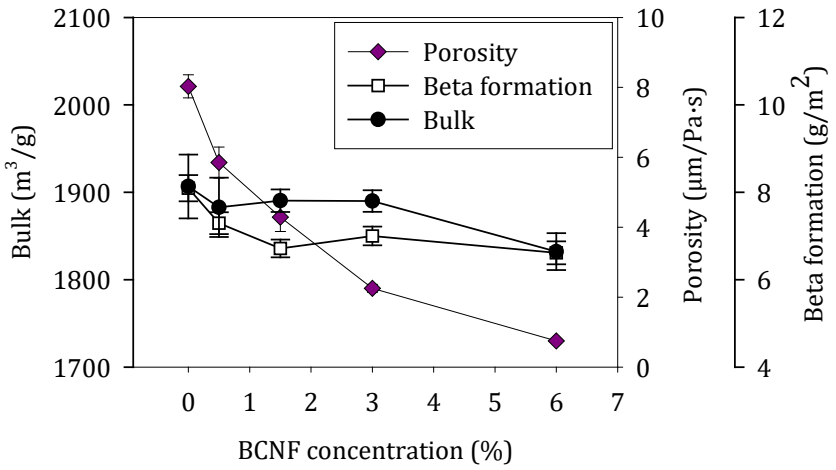

Figure 18. Evolution of physical properties of RP handsheets upgraded with different BCNF dosages: porosity, beta formation and bulk.

Bulk was also reduced with the addition of BCNF to the pulp, likely due to the replacement of the original fibers with the same weight of high quality nanofibers, which are situated at the gaps between macroscopic fibers, thus decreasing the thickness of handsheets with the same grammage. Nevertheless, a high concentration of BCNF (6%) was needed to affect the handsheet bulk, decreasing from 1890 to 1830. Finally, optical properties were found to vary in a higher extent when the BCNF dosage was below 1.5%, causing a detrimental effect in most of them. However, when the BCNF dosage was further increased, all of them kept constant.

Based on the images shown in Figure 16, it can be confirmed that the BCNF are retained in the gaps between fibers, linking the fibers of the pup and partially covering them. In addition, mineral fillers are retained in the handsheets in the proximity of the BCNF clusters.

Thus, the fillers were not only retained through chemical aids, but they were also hunted by a mesh formed by the BCNF clusters. To inquire if the mineral filler retention is favored by the presence of BCNF, the filler content in terms of both $CaCO_3$ and kaolinite (clay), was determined and showed in Figure 19.

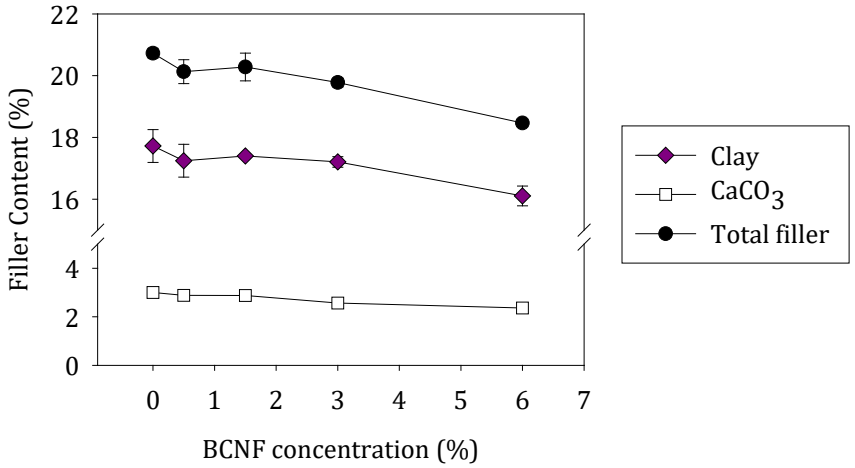

Figure 19. Mineral filler content in handsheets improved with different BCNF dosages.

For BCNF concentrations below 3%, the total filler content as well as the individual amount was kept almost constant compared to the initial value in the reference pulp without BCNF. However, they slightly decreased when the BCNF concentration is 6%, from 20.2 to 18.5%. To retain the mineral fillers within the fiber matrix, a RS was added at an optimized dosage. However, the BCNF interact likely with the RS, making this dose inadequate to retain both fillers and BCNF when the last is high. Moreover, as the specific surface area of BCNF is much higher compared to that of cellulose fibers, retention aids interact more favorably with the BCNF prior to recycled fibers. Then, the mineral fillers were situated more likely in the proximities of the BCNF clusters. When the BCNF dosage is 6% or higher, the dosage of the retention aids may not be high enough to retain both BCNF and mineral fillers. However, the reduction in the filler content in the final paper is not as high as expected due to the physical retention in the BCNF clusters. Therefore, an optimization of the wet-end aid, taking into account not only filler retention but also BCNF retention would be necessary to improve their efficiency.

4.2.3 In situ production of bacterial cellulose with recycled fibers

Despite the high enhancement of RP strength and flexibility, due to the increment in both TI and tear index, reached by the addition of low proportions of BCNF, the high culture time needed for the BC pellicle formation as well as the high energy demand for nanofibrillation, make this process still be a challenge with low applicability at industrial level. As alternative, the in-situ production of BC with the RP pulp has been studied, as summarized in

Publication III. This alternative could increase the mechanical performance of RP and reduce BC production time and cost.

Evolution of the handsheets TI and tear index with the culture time in both static and agitated modes is shown in Figure 20. The control experiments, referred to handsheets with the same amount of the cultured suspension but without being inoculated, were expressed in Figure 20 at zero time. Results show that both mechanical properties presented no variation when culture time was below 24 h for agitated cultures. It was stablished that cell growth gets a maximum after 24 h of culture, starting to increase the BC productivity in that moment [48]. However, when culture time was higher than 24 h, an increase in both indexes was observed. At 48 h of culture, the maximum increase was reached at the selected upgraded pulp/raw pulp (10%) ratio, meaning increments of 12.2% in TI and 14.2% in tear index. Therefore, the increase in both indexes with the addition of BCNF obtained in the Publication II was also observed in the present study. This behavior was assigned to the lower nanofibrillation degree of the BCNF, which was low compared to that of CNF. In this case, agitation caused the movement of the bacteria to the proximities of the fibers, producing the BC as small clusters of entangled individual nanofibers instead of a pellicle.

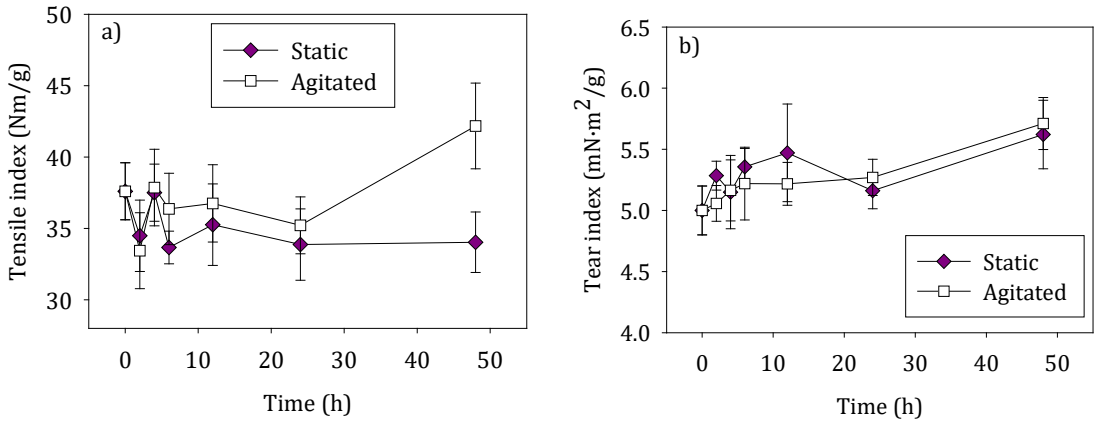

Figure 20. Effect of the culture time on the mechanical properties of paper in both static and agitated mode: a) tensile index and b) tear index.

This was not as positive for static cultures, where TI remained below the control value and with an irregular behavior for tear index. The lower movement of bacteria in static cultures limit the nutrients availability, thus decreasing the cell growth rate and, therefore, the BC productivity. In addition, while bacteria moved to the surface in search of oxygen, initial fibers tended to sediment. Thus, bonding between both types of fibers would probably happen during the mixing step, but seldom during culture. This fact makes difficult the improvement of the mechanical properties. A similar behavior was observed for strain at break results, where an irregular behavior characterizes the results for static cultures, while a final increment of 17.8% was obtained after 48 h of agitated culture.

Physical and optical properties of the handsheets were also evaluated. In both culture modes, porosity showed a decrement with the culture time, typical behavior of the NC fitting in the gaps between the fibers. The homogeneity of the handsheets in terms of beta formation, was more favorable for pulps upgraded by agitated culture. In this case, beta formation decreased with time, meaning that a more homogeneous paper is being produced with the increasing amount of BC. In the case of static culture, the formation of a pellicle of BCNF during culture at high culture time (48 h), triggered more irregular papers, thus keeping the initial value of beta formation or even increasing it at high culture time.

Optical properties were also affected by the addition of improved fibers to the pulp, reducing the ISO Brightness even at short times. This effect was assigned to the presence of residual nutrients in the hansheets, some of them of brown color, like yeast extract and peptone. Nutrients are supposed to pass through the filter while handsheets are being formed, but as the gaps between fibers are reduced by BC, some of them can remain in the papers, causing a detrimental effect in the optical properties.

With these results, a mechanism for the in-situ culture of bacteria with cellulosic fibers in both modes was proposed as shown in Figure 21. Before inoculation, RP fibers were distributed homogeneously in the culture broth for both culture methods. After that, a different mechanism between static and agitated culture is observed.

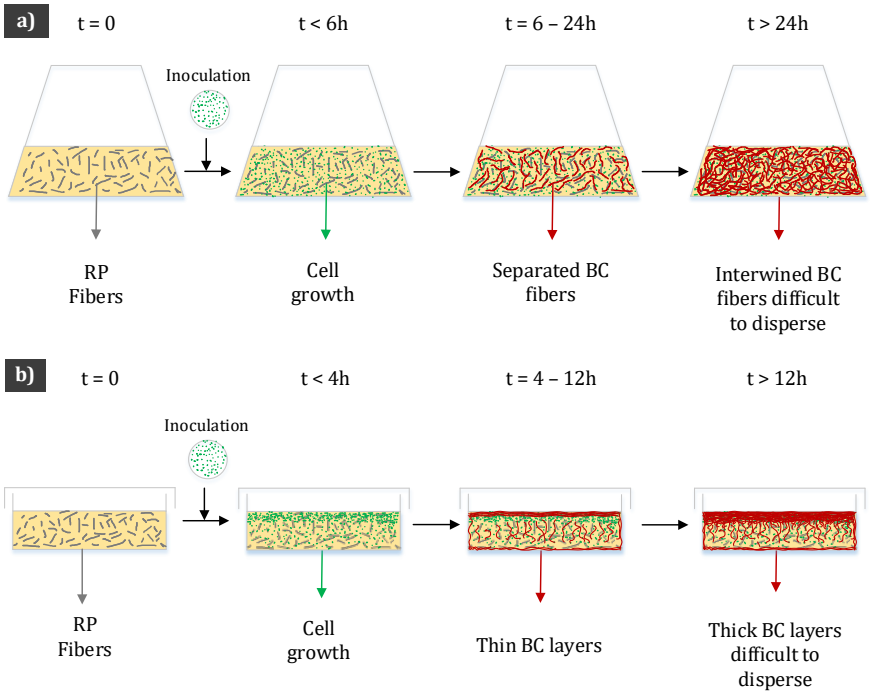

Figure 21. Proposed mechanism for in-situ culture of bacteria with cellulosic fibers in a) agitated mode and b) static mode.

In the case of agitated cultures, after 6 h the BC fibers started to make appearance. Considering the fact that aerobic bacteria move to places with high oxygen availability, it is highly probable that they tend to grow on the fibers surface. Thus, BC would coat the RP fibers, having preference for the damaged areas of the fibers, where they can serve as a support for bacteria. This fact can be observed in Figure 22, where a SEM micrograph of a handsheet produced with 10% of pulp upgraded by agitated culture is displayed. It is clearly observed how BC has coated the initial fibers, showing a smooth and homogeneous surface. At higher culture times, bacteria keep moving through the culture broth, joining the improved fibers among them. At a determined time between 6 and 24 h, this joints can be broken in the disintegrator, remaining separated fibers upgraded by BC. However, when the culture time was over 24 h, those networks are formed with a more compact and strong structure, being usually difficult to disperse (Figure 23c). Thus, big clusters of BC and recycled fibers remain after disintegration, forming heterogeneous handsheets with areas of a high amount of BC and others with lack of fibers or even holes.

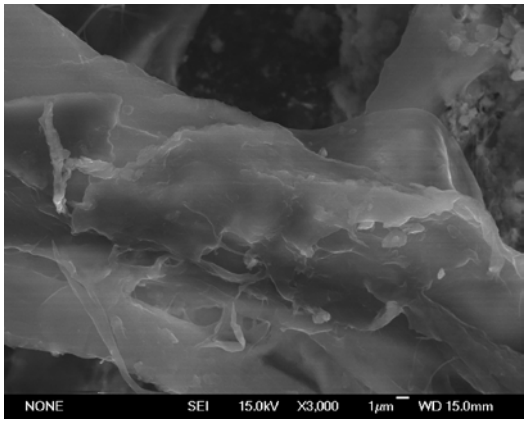

Figure 22. SEM micrograph of BC/recycled fibers handsheet produced by in-situ culture of bacteria in agitated mode after 48 h of culture.

On the other hand, static cultures always trigger irregular systems. In this case, bacteria tend to move to the surface of the culture broth in search of oxygen, while RP fibers tend to sediment by density difference (Figure 21b). As stated previously [43], cell growth is slower in static cultures, but as most of the bacteria are present in the surface of the culture broth, BC can be detected even before 4 h. When the culture time increased up to 12 h, a thicker BC pellicle with a denser surface in the side exposed to the air is formed (Figure 23e). After 48 h of culture, a thick and gelatinous membrane was produced at the top of the culture media, and a thinner but resistant membrane was also observed around the culture broth, wrapping all the fibers and medium inside (Figure 23f).

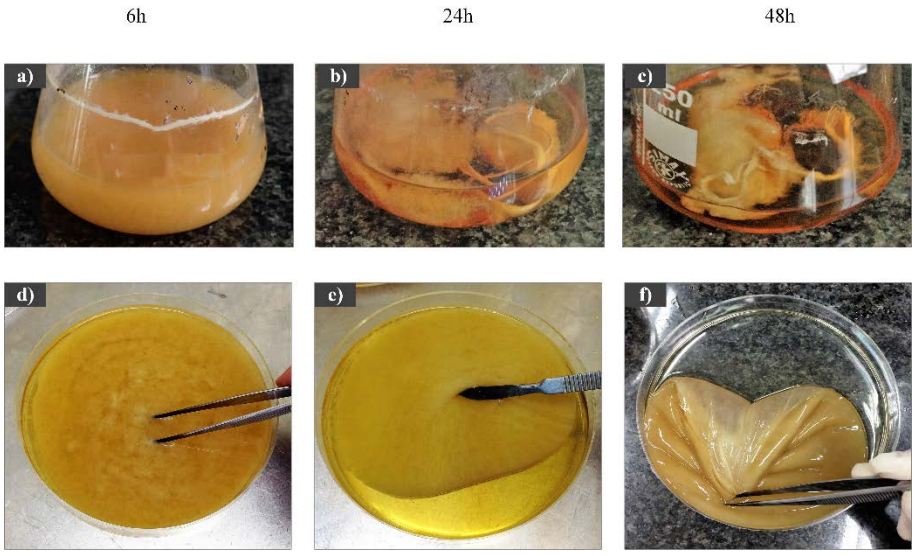

Figure 23. Images of agitated (a, b and c) and static (d, e and f) in-situ cultures after 6 h (a and d), 24 h (b and e) and 48 h (c and f) of culture time.

Taking all these aspects into account, it can be concluded that the in situ static culture of bacteria with fibers was faster than the agitated culture, but heterogeneous systems were produced. Thus, a deeper study about the effect of the culture volume on the mechanical, physical and optical properties of the handsheets was carried out in agitated mode.

As explained before, the residual amount of nutrients present in the handsheets were found to affect paper properties, so they were considered in all explanations. Nomenclature used for the study of the effect of the culture volume on the paper properties is showed in Table 4.

Table 4. Used nomenclature for each experiment, corresponding to different amounts of upgraded pulp, in a defined number of parallel culture flasks at different volumes.

Nomenclature	Upgraded pulp	Number of parallel culture flasks	Culture volume of each flask (mL)
5% (1)	5%	1	100
15% (3)	15%	3	100
15% (1)	15%	1	300
45% (3)	45%	3	300

TI results showed the tendency to improve when the amount of the upgraded pulp was further increased (Figure 24a). Fructose, the carbon source used in this study, is surrounded by hydroxyl groups, which makes possible the bond between them and the cellulose chains

by hydrogen bonding [282]. In this way, the porosity of the handsheets is reduced, increasing the TI of the material.

The same behavior for all developed experiments at different culture times was observed: first, TI was increased till a determined time (6 or 12 h) and then it was decreased due to the irregular formation of the handsheets, as explained previously. At the dosage of 5% (1), the maximum improvement was found at 12 h of culture, reaching an increment of 10.8% respect to the TI obtained with the addition of the same dosage at zero time. With the addition of the triple amount of the cultured pulp, 15% (3), TI reached the same value as the maximum TI for 5% (1) but 6 h before. However, the increment respect to the value at zero time was only 3.4%, meaning that the main factor affecting this property is the presence of nutrients.

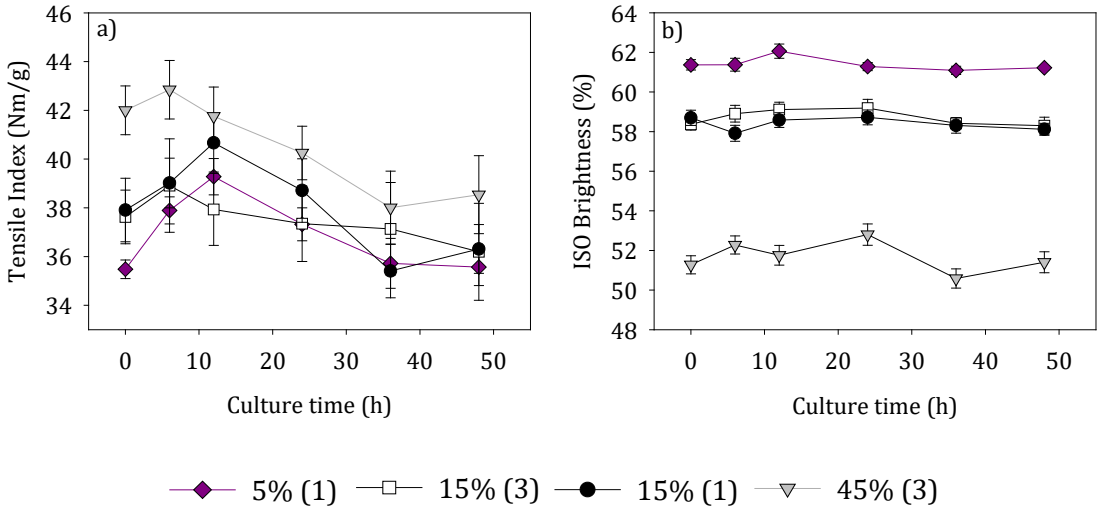

Figure 24. a) Tensile index and b) ISO Brightness of handsheets prepared with 5% (1), 15% (3), 15% (1) and 45% (3) of in-situ cultured bacteria.

Nevertheless, when the same volume was cultured in one single flask (15% (1)), the results were more satisfactory, reaching an increment of 7.4%. Although the enhanced oxygen availability should theoretically trigger an increasing BC production rate, reduced yields were obtained. According to Aydin et al. [47], the high shear stress suffered by bacterial cells with high agitation and aireation triggers a spontaneous mutation of bacteria of the genus *Komagataeibacter* which deactivates the essential enzymes involved in the cellulose production, i.e. *phosphoglucomutase* and *uridine diphosphoglucose pyrophosphorylase* [46]. As there is a wide oxygen availability in the smaller flasks, the probability of bacterial cells to mutate is higher, thus meaning a lower BC productivity and thus mechanical properties enhancement. This behavior described previously in the literature matches the results obtained for TI values at 15% (1), better than those at 15% (3), so it has been accepted.

Finally, at the dosage of 45% (3), only a slight improvement in TI was found after 6 h of culture. In this case, the high amount of residual nutrients present in the handsheets, induces a high increment in the TI. Moreover, the amount of BC produced may not be high enough to achieve deserving increments.

Regarding optical properties, ISO Brigthness showed a strong dependence with the dosage instead of the culture time (Figure 24b), which is again related closely to the amount of nutrients in the handsheets.

In view of the possibility that some BCNF can be loss during the removal of the medium components, the washing of the upgraded pulp before handsheet formation has been avoided. However, this issue would become a drawback for large scale fabrication, not only affecting paper properties, but also incrementing the microbiological population in the wastewater as well as easing the presence of deposits in some papermaking equipment. Hence, further studies would, therefore, be necessary to overcome this challenge before scaling-up this method.

4.3. CELLULOSE NANOCRYSTALS DISPERSION

First, CNC were produced from different RP and the effect that the different composition of the raw materials had on the properties and yields of CNC has been assessed.

As explained in the introduction, when sulfuric acid is used to hydrolyze cellulose, sulfate groups remain at the CNC surface, improving their stability in water suspensions [283]. However, this stability commonly declines over time, forming aggregates by hydrogen bonding that sediment at a determined aggregation degree and are difficult to re-disperse. This justifies that different effects can be observed with the same CNC product. Furthermore, CNC dispersion is an important bottleneck for their industrial application, since final results are not easily predictable. The effect of this aggregation state on the improvement of the mechanical properties of paper, as well as some efforts made to re-disperse them in the paper matrix are studied in detail in the Publication V.

In addition, some efforts have been made in order to assess the aggregation state of CNC through a DLS approach combined with image analysis made by AFM. This novel approach represents a new methodology of high interest for the industrial control of CNC quality and for its implementation in different applications.

4.3.1 Effect of raw material impurities on cellulose nanocrystals properties

The composition of the NP pulp depends on the needs of the printing companies, the availability of recycled fibers as well as the GDP of the country. In Europe, for example,

~98% newsprint presents a filler loading of 15-20% of the total dry mass. ONP is composed mainly of cellulose and hemicellulose, combined with a percentage of ash, lignin and inks that sums up to 25%.

In the Publication IV, recovered ONP composition was analyzed (Table 5). Results show the presence of 14.5% of ash, mainly composed of china clay and calcium carbonate, 9.1% of lignin and 76.4% of cellulose and hemicellulose. This raw material, when is recycled for the production of newsprint, is deinked and bleached, and, therefore, its composition varies slightly. In this study, NP presents 14% of ash and 6.5% of lignin. In our studies, in order to further purify the pulp before acid hydrolysis, two pretreatments based on alkali and bleaching steps, were applied, following the procedure described in 3.1.2 (NP-B). In this case, the ash and lignin contents were reduced up to 11.9% and 2%, respectively. Although the treatments are aggressive, and it is very likely that most of these components are removed, as the procedure includes several washing steps, some of the fibers are also lost, reducing the total mass of the pulp. In this way, the percentage of contaminants in the final pulp is not as low as expected.

Table 5. Composition of papers used as raw material for CNC production and that for produced CNC.

Type of paper	**Cellulose + Hemicellulose (%)**		**Ash (%)**		**Lignin (%)**	
	Raw material	CNC	Raw material	CNC	Raw material	CNC
ONP	76.4	76.0	14.5	11.5	9.1	12.5
NP	79.5	77.8	13.9	11.9	6.5	10.2
NP-B	86.0	93.3	11.9	5.7	2.0	0.93

When the cellulose pulps are submitted to acid hydrolysis, the amorphous cellulose is hydrolyzed to glucose. However, this is not the only component that is removed during this reaction, but also $CaCO_3$ is dissolved in acid pH, as well as a portion of lignin. This is the reason why the ash content is reduced in all produced CNC from RP (Table 5). This fact is more pronounced in CNC-NP-B, where this percentage decreases from 11.9% to 5.7%. This induced one to think that the main filler present in the NP-B pulp was $CaCO_3$, which was then dissolved during acid hydrolysis. This fact was also noted by XRD analysis, where an intense peak at 29.2° indicates the presence of $CaCO_3$ in a high proportion, compared to kaolinite, whose peaks, at 12.5° and 25°, denote its presence in a lower extent (Figure 25). As shown in Figure 25b, the peak showed for calcium carbonate in the NP-B pattern, disappear when CNC are isolated.

During acid hydrolysis, lignin fractionates into acid insoluble and acid soluble fractions. Due to the dissolution of amorphous cellulose and $CaCO_3$, the percentage of lignin in CNC-ONP

and CNC-NP increases respect to the initial pulps. However, in the case of CNC-NP-B, only a residual amount of lignin is present (0.9%), representing the acid insoluble fraction.

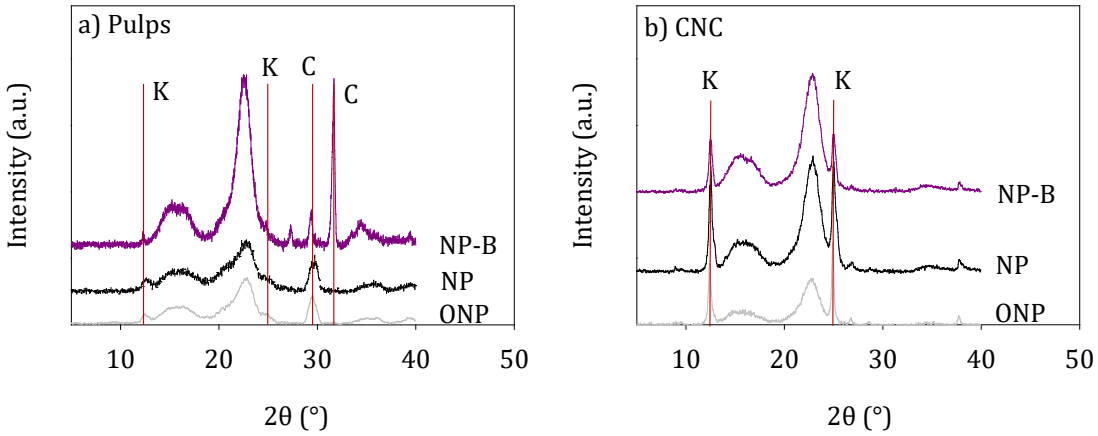

Figure 25. XRD patterns of a) NP-B, NP and ONP pulps and b) CNC-NP-B, CNC-NP and CNC-ONP. K and C represent the associated peaks to kaolinite and $CaCO_3$, respectively.

Depending on the final application of the CNC, the presence of the different impurities has to be taken into account. For example, the presence of lignin and inks has a direct impact on color, which could be a great inconvenient when special optical properties are required, like in graphic papers. On the other hand, in biomedical or electronic applications, the presence of determined fillers could suppose a deterioration of the quality of the device, and, furthermore, it could increase the toxicity of the final products.

Other important factors that would limit the application of the directly produced CNC, are the hydrolysis and the process yields. As shown in Table 3, the hydrolysis yield is higher for purer pulps before the acid hydrolysis treatment, finding the maximum for the pretreated sample (NP-B). However, with the application of both alkali and bleached treatments, a percentage of the cellulose fibers is lost, decreasing therefore the process yield. Compared to CNC-NP, the process yield of the CNC-NP-B decreases from 60.8% to 34.6%. This would mean a great increase not only in operational costs, but also in chemical expenses. As explained before, in most cases, depending on the final application of the CNC, this extra cost could not be afforded.

Other properties such as Cr.I, ACD, PD, morphology, size distribution and thermogravimetric analysis were also evaluated. In the case of Cr.I and PD, light variations were found. This fact would explain that the maximum hydrolysis yield was reached in all cases, removing almost completely the amorphous regions of the cellulose. Cr.I vary from 92.6 to 94.8%. Although PD of cellulose rapidly decreases when it is submitted to acid hydrolysis, the LOPD can be reached [107], which means only crystalline portions are present. This value was in this case 180.

According to the literature, higher ACD of cellulose particles means a higher purity and crystallinity in the CNC due to the narrowing of the crystallite size distribution [284]. This is exactly what occurs in the present study, where ACD of CNC-NP-B resulted in 45 nm compared to 32.5 nm for CNC-ONP. In addition, this parameter was also found to increase respect to the initial pulps.

Regarding size distribution, diameters of all produced CNC were found to be very close among them, while lengths vary in a higher extent. More specifically, CNC-NP-B were longer than CNC-NP mainly due to the higher aggregation of the first since their purity is much higher and, therefore, they are more likely to join by hydrogen bonding.

Thermogravimetric studies showed a difference behavior between samples before and after hydrolysis. While the first ones presented an endothermic peak at around 350 °C, where most of sample weight is loss, acid hydrolysis triggers a separation of the CNC decomposition in two steps: a first one at 200 °C and a second one at 370 °C. When temperature further increases, a lower but continuous mass loss occurred in TG curves of CNC, remaining a significant residue still after 1000 °C. The earlier degradation of CNC compared to pulp samples, has been assigned to the deposition of sulfate groups during H_2SO_4 hydrolysis, thus triggering a dehydration reaction [285].

4.3.2 Effect of CNC dispersion on the recycled paper mechanical properties improvement

The used method for preparing the NC and pulp furnish has a critical influence on the final paper properties, so it has to be considered to optimize paper quality. Different pulping conditions were used to assess the effect of this industrial operation on the improvement of the mechanical properties of paper by CNC. Furthermore, results were compared with those obtained by using CNF. Table 6 shows the identification of the tests carried out. Briefly, the use of overnight pulp soaking, and the variation of the pulping revolutions and temperature were studied to assess their effect on the mechanical, physical and optical properties. At industrial level, in a paper mill, 10 min of pulping at 50ºC are commonly used to disintegrate the recovered paper. As this step is required in the recycling process, taking advantage of it to efficiently disperse NC with the pulp would be a promising option.

Table 6. Pulping conditions used for each test.

Sample ID	Overnight soaking	Disintegration revolutions	Time (min)	Temperature (ºC)
A	No	30.000	10	50ºC
B	No	180.000	60	50ºC
C	Yes	180.000	60	20ºC

Two different RS have been used in this case: CPAMB and CH. The tendencies of the results with both RS were similar, but bigger differences between experiments were found for CPAMB, so graphs of the properties with this system are presented in Figure 26, as an example of the full study developed in the Publication V. CNF and CNC dosages were chosen based on preliminary tests in which a required increment of around 20% in mechanical properties was achieved, namely 1.5% CNF and 3% CNC [242].

No big differences were found among the TI results for all pulping conditions when no NC is used (Figure 26a). Regarding porosity, it underwent a high decrease when pulping time was increased from 10 to 60 min, no matter which retention additive was used (Figure 26b). This fact may be due to the reduction of the fibers size with the increasing pulping time, thus producing more fines that collaborate to form more compact handsheets. As a consequence, beta formation of handsheets was reduced with the increasing pulping time and the use of soaking, due to the reduction of porosity although TI remained constant.

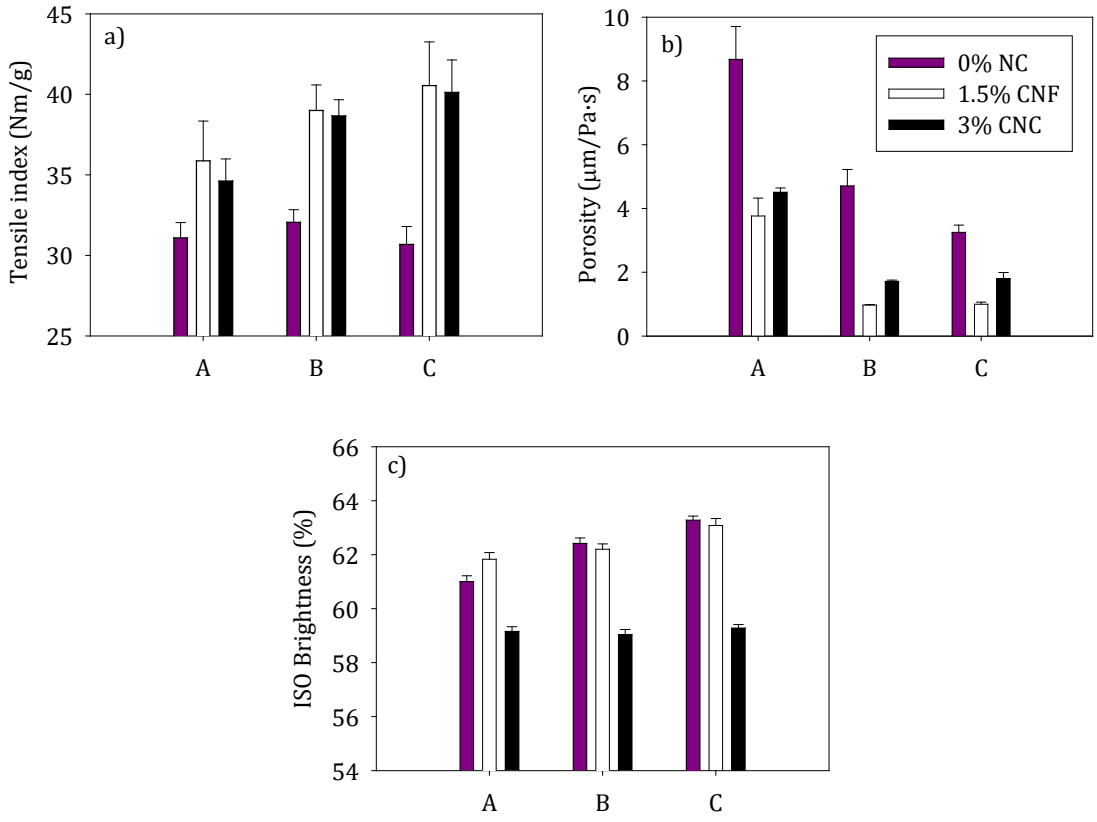

Figure 26. Effect of different pulping conditions on a) tensile index (TI), b) porosity and c) ISO brightness of handsheets without nanocellulose, 1.5% (w/w) CNF and 3% (w/w) CNC, using CPAMB as a retention system.

As expected, TI increased in a high extent when either CNF or CNC are added to the pulp matrix. Increments of 10, 20 and 30%, approximately, for A, B and C conditions were

obtained. This increment was higher when pulping time was increased from 10 to 60 min. This increment corresponded to a decrease in porosity, which was larger when pulping time increased, from -56 to -79 and -69%, for A, B and C conditions, respectively. A higher reduction in porosity when either CNF or CNC are added to the pulp is one of the signs of a good NC retention and a better NC dispersion.

Soaking hardly varied TI and porosity increments for the same pulping time (conditions B and C). Temperature during pulping was not therefore a key parameter to consider regarding the effective mixture and retention of NC in the fiber suspension, but pulping time was. Respect to beta formation measurements, it was observed that differences between all experiments were due to the used RS, instead of to the pulping conditions.

Generally, ISO brightness increases when more severe conditions were applied, namely B and C (Figure 26c). This was assigned to the higher swelling ability of the fibers, which was favored by the higher water temperature and the higher water-fiber contact time. This allows the fillers to penetrate into less accessible regions of the fibers, being easily retained in the wet-web and improving consequently the paper brightness. With the addition of CNF, brightness was kept almost invariable. Since CNF were produced from a bleached pulp, no effect on optical properties of handsheets was observed. However, in view of the direct hydrolysis carried out to produce CNC from a RP pulp, a brown color was observed, as shown in the Publication IV. This fact triggered a negative effect on the ISO Brightness of the handsheets, reducing this value by more than 2 points. Colorimetric constants induced that handsheets had a yellowness tendency, which is typically related to the presence of lignin in the sample.

With the aim of increasing the dispersion of the NC, two different dispersing agents were added to CNC prior to their addition to the pulp. CH was used as RS in view of their higher increments reached in the results showed previously. To assure an easy availability and reasonable costs for industrial implementation, commercial dispersing agents already used in paper mills were selected. Moisturizing and surfactants agents are typically used in this industry to control the deposit of slimes, to make ink particles hydrophobic during pulping, to clean felts, wires and machinery, to disperse some contaminants and to facilitate the impregnation of different components on the fibers [286]. Figure 27a shows an increasing increment in TI with the D1 dosage when no NC was used. However, this tendency is not as positive when CNC were included in the system, reaching values of TI lower than those of handsheets without CNC. A possible interaction between D1, CNC and the RS could have triggered a worsening in the TI of handsheets, so this dispersing agent was discarded for future assays.

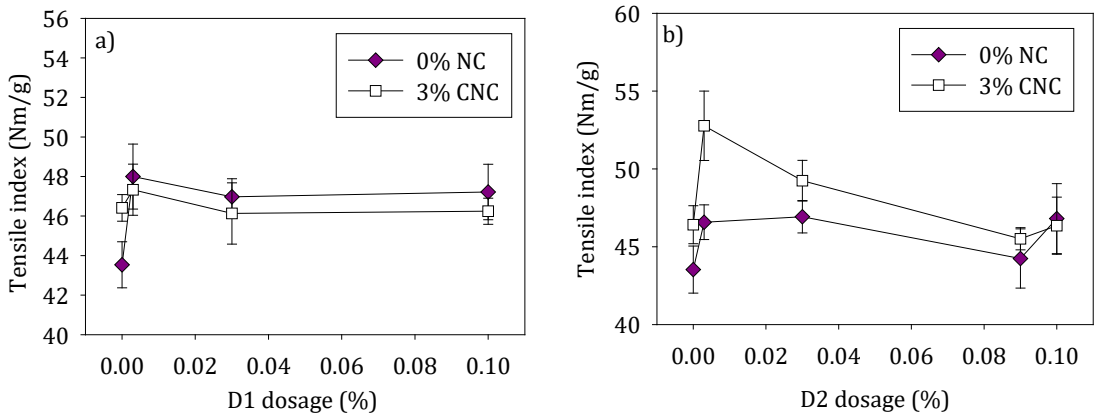

Figure 27. Effect of type and dosage of the dispersing agents: a) D1 and b) D2 on tensile index of the handsheets with 0% NC or 3% CNC using chitosan (CH) as a retention agent.

On the other hand, with the addition of D2 to the pulp, TI increased mainly due to the better dispersion of the fibers (Figure 27b). Moreover, when both CNC and D2 were combined and applied to the system, TI was further enhanced, reaching an increment of 21.8%, much higher than that obtained without the application of D2 (6.6%). D2 has been used in some paper mills to facilitate the intimate contact between the coating products and the paper. A coating is typically composed of a mixture of a binder, white pigments (mainly calcium carbonate, fine clay or talc) and water [286]. Although carboxylated styrene-butadiene, styrene-acrylonitrile or acrylic latexes have been used traditionally as binders, the use of NC is becoming more relevant as substitute of the cited components [4]. Thus, it could be expected that D2 could work effectively in the dispersion of NC.

Finally, as the maximum TI increment was obtained with D2, at the dosage of 0.003% (w/w) when using CNC and CH, this product was also tested with CNF and CPAMB. The effect of D2 on paper properties without NC for both RS was slightly different, mainly owing to the corresponding flocculation mechanism. With CPAMB, the presence of CNF increased the TI by 20.6% with the addition of D2, instead of 14.3% without dispersing agent. The same behavior was observed for CNC, were TI increased by 11.1% with D2 and 7.2% without it. With the use of CH, higher increments in TI were obtained for CNC previously dispersed by D2, 15.2% instead of 7.3%. However, CNF obtained similar results no matter if D2 is added or not (around 5% of increment in TI). Thus, it can be concluded that long pulping times could be avoided by the correct addition of a dispersant, as D2, and the adequate selection of the retention aid.

To sum up, when CPAMB is used as RS, both CNF and CNC provided a higher strength when D2 was added to the furnish for the same pulping conditions (A). However, the best TI values were obtained for long pulping time (conditions B and C). In the case of CH, similar results were obtained for CNF, although in the presence of CNC, the best results in TI were

those where D2 was added as dispersing agent at the conditions of the experiment A, at low pulping time.

4.3.3 Description of the CNC aggregation state

As shown previously, dispersion of CNC is of utmost importance to reduce operational costs and optimize the needed CNC dosage to get successful results. However, there is not an easy method to quantify the CNC dispersion. The focus of the article in preparation VIII is the development of an easy method to determine the aggregation state of the CNC in a water suspension. First, different aggregation parameters were defined through AFM image analysis, which is a useful technique but very time consuming. Figure 28 shows an example of the images for each of the conservation method used to preserve the CNC (nomenclature in Table 7). The heterogeneity of the images makes their qualitative analysis a challenging task. This is indeed why the elements present in the images have been analyzed individually in terms of area, perimeter and MFD. Some additional parameters derived from those described have been also considered, such as MAA, SD area, SD perimeter, SD MFD, as well as the distribution skewness and kurtosis.

Table 7. Nomenclature used for each experiment.

Nomenclature	Conservation method	Preparation method
LIQ	Never-dried at 4ºC	20ºC
F-FR	Frozen with liquid N_2	Defrost at 4ºC
F-VA	Frozen with liquid N_2	Defrost under vacuum at 20ºC
F-40	Frozen with liquid N_2	Defrost at 40ºC

The highest heterogeneity was found in F-40 and LIQ samples (Table 7), while the F-FR sample was more homogeneous according to SD area and SD MFD results. Skewness and kurtosis results revealed that all samples analyzed where coarse skewed, but with different grades. In the LIQ samples, the size distribution was lightly coarse skewed and very platykurtic, maybe due to the presence of more than one population. The opposite case was found for F-40 0.05%, where the size distribution was highly coarse skewed and very leptokurtic, showing the predominance of small particles in front of others.

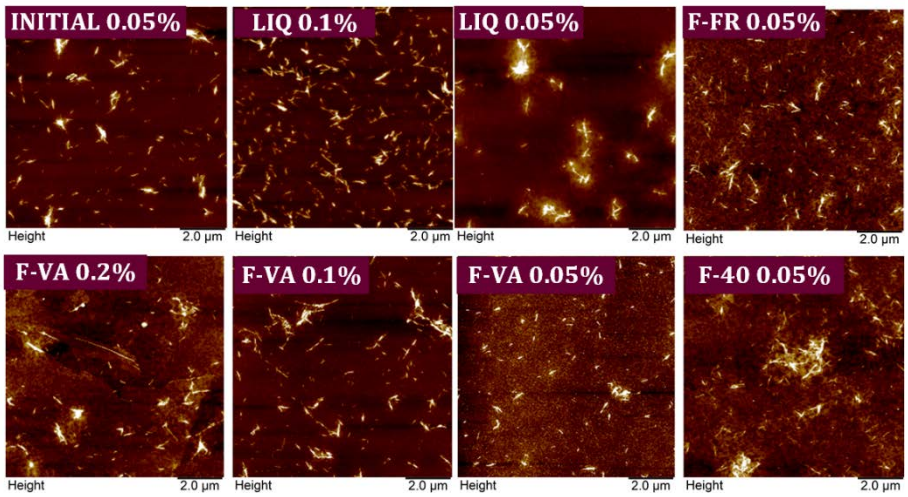

Figure 28.AFM images of examined samples.

D_2 was estimated from the representation of each element area and MFD. The slope of the cited graph can be interpreted as the average projected fractal dimension. The obtained values hardly varied from 1.6, except for the one corresponding to the sample F-FR 0.005% with a value of 1.44. Images in Figure 28 confirm this value, where individual nanocrystals and elongated aggregates are present.

4.3.3.1 Image elements clustering

The elbow method was used to classify the CNC individual particles and their aggregates into groups with similar geometrical features [271]. All elements were analyzed as a whole. Figure 29a depicts the evolution of the inertia as a function of the number of clusters considered. The optimum number of clusters was found to be five (Figure 29b). The groups were numbered according to the total number of elements belonging to them in decreasing order.

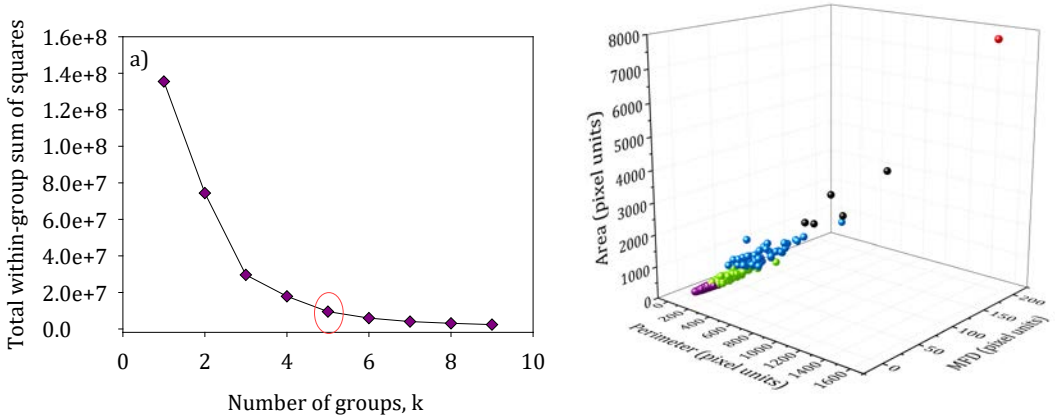

Figure 29. a) Evolution of the inertia with the number of groups considered. b) Groups of particles present in the study. Group 1 is presented in purple, Group 2 in green, Group 3 in blue, Group 4 in black and Group 5 in red.

Most of the elements (over 70%) were classified in the Group 1 (G1, in purple color), corresponding to particles with small area, perimeter and MFD. Given the position in the graph of this group, intuitively, this cluster would be associated to the CNC individuals. Then, four additional groups regarding different aggregation levels were identified. An increase in the percentage of particles corresponding to the G1 was observed when concentration was reduced, indicating a low aggregation extent. At any rate, the sum of the contributors to G1 and G2 was over 92%, indicating that most of the sample can be found as individual particles or small aggregates of few particles. From the results obtained for the particles clustering, it could be first stated that LIQ 0.1% sample was the most aggregated one, followed by LIQ 0.05% and F-VA 0.2%. On the other hand, F-VA 0.05% and F-FR 0.05% were the most homogeneous and less aggregated. Figure 30 shows the morphology of particles identified in each group.

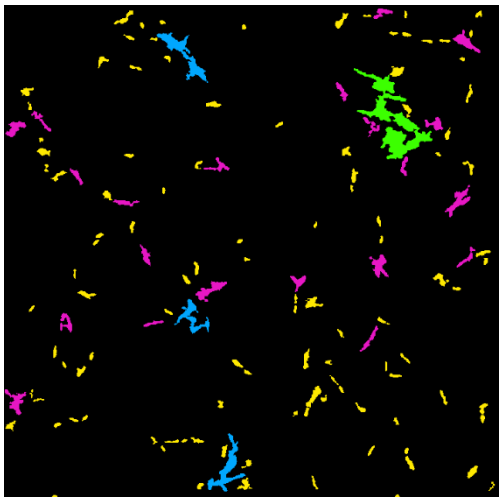

Figure 30. AFM image of F-40 0.05% with the groups identified by colors. Particles of G1 are shown in yellow, G2 in pink, G3 in blue and G4 in green.

4.3.3.2 Dynamic light scattering

Figure 31 shows the evolution of the τ_D with the temperature. At low temperatures, the thermal energy in the medium was likely insufficient to induce DLS-detectable motion in large or very spiky particles. The increase in the temperature would result in those particles are set in motion. Large particles in the distribution and those having a shape that limits their movement will remain virtually static. Temperature can, therefore, be seen as a size and shape filter acting on DLS measurements.

With an increase in the temperature, while the proportion of particles contributing to detectable motion will increase, aggregation will gain importance and some settling-prone aggregates will form, due to the higher collision probability that makes particles aggregate through hydrogen bonding. At large measuring times, the latter will likely sediment,

disappearing from the measurement field. The three simultaneous contributions of the aforementioned phenomena make the interpretation of DLS measurements a challenging task. In addition, at temperatures over 60 ºC, convection currents start to be significant in the cuvette [287]. This fact could induce non-random movement of particles, which would very likely compromise the correct interpretation of the Brownian motion.

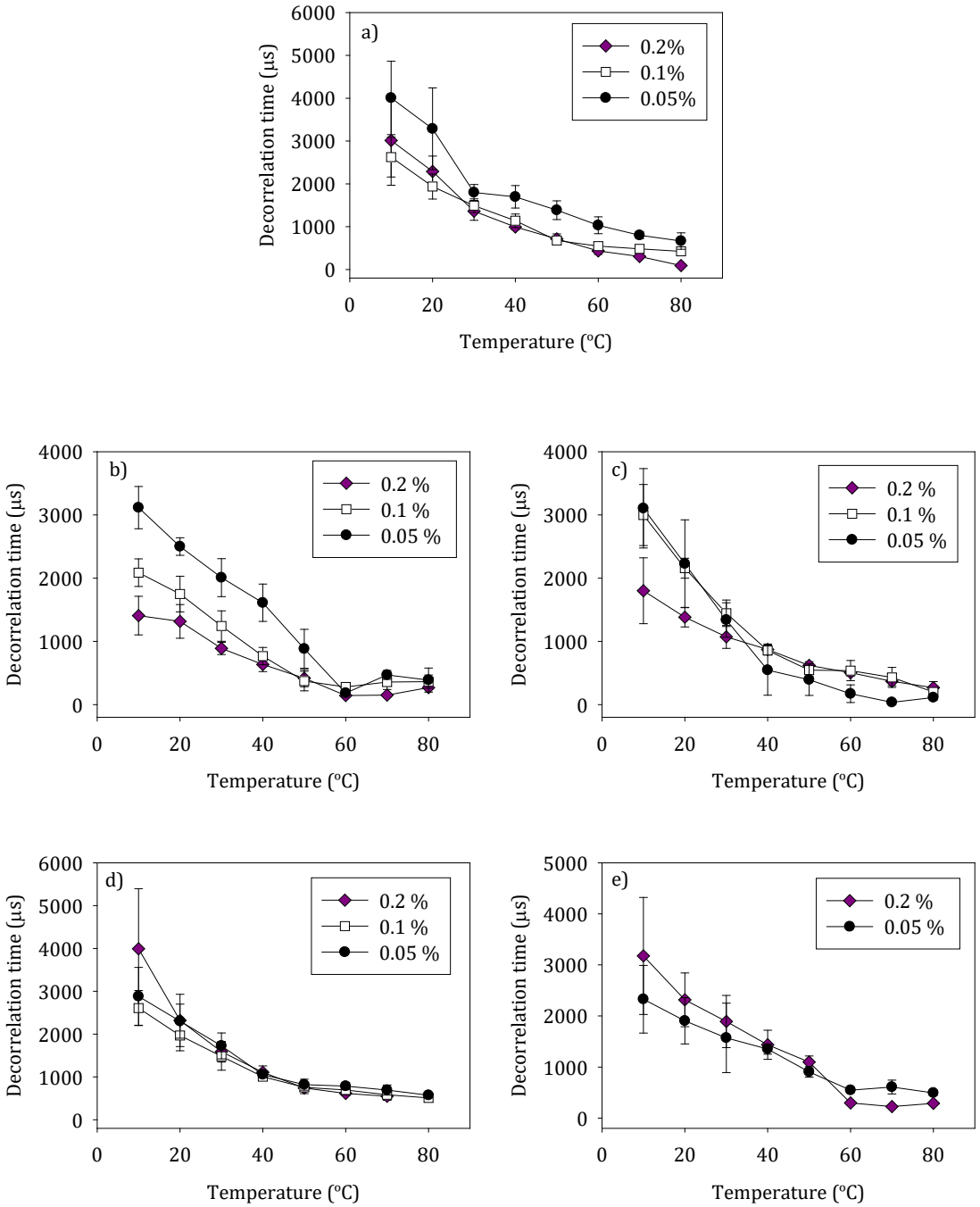

Figure 31. Evolution of the decorrelation time with the temperature for a) initial sample b) LIQ, c) F-FR, d) F-VA and e) F-40. Three CNC concentrations were tried: 0.2, 0.1 and 0.05%.

The SD of τ_D observed in the samples at 10 ºC could be attributable to the heterogeneity of particles present in the suspension, greater SDs indicating the presence of both aggregates and individual nanocrystals in the sample.

When the temperature was increased up to 30 ºC, τ_D dropped down to the half of the initial value, while SD was strongly reduced. It is probable that, at this temperature, the thermal energy available in the medium is sufficient to set most particles in random motion. Additionally, the rate of collisions between particles at this temperature will promote aggregation.

Finally, it can be firstly hypothesized that the value of the τ_D at 50ºC would be probably the value for the small aggregates present in the suspension.

4.3.3.3 Variable importance for DLS data interpretation

The aggregation parameters determined from AFM images as well as the group classification would correspond to the sample before the DLS experiment. Thus, it can be considered that samples with the same aggregation state would present a similar behavior during the analysis. Due to the high difficulties found to explain the DLS results, variable importance in extremely randomized trees was determined through the correlation of the data extracted from the formed groups and the AFM images with the DLS parameters. Figure 32 shows the contributions of each group in the τ_D and their SD at the temperatures considered.

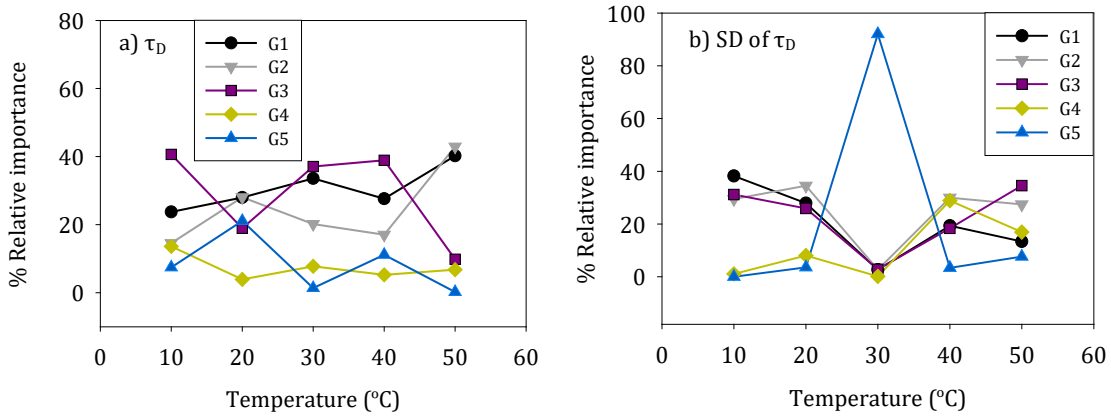

Figure 32. Group importance on the values of a) τ_D and b) SD of the τ_D at the different temperatures.

In general, the contributions of G4 and G5 are low, being predominant only the contribution of the G5 in a 92% to the SD τ_D at 30ºC. It is true that only one aggregate has been detected in AFM images corresponding to this group (G5), but there is a high probability that many others aggregates of similar geometry would be also present but not detected due to AFM equipment limitations. Then, this group has been considered for further explanations. As

particles contributing to G5 had a high volume, they probably sediment and thus will not appear in the following temperatures. Hence, this is likely the moment where the particles belonging to G4 showed their presence, in the SD 40ºC, with a percentage of 29%.

Contribution of G3 to τ_D at 10ºC stands out against the others with a percentage of 41%. One possible reasoning is the fact that, at this low temperature, only the movement of the small particles can be detected. Thus, particles of intermediate size, i.e. G3, could be the biggest ones that are detected at this temperature.

Finally, G1 and G2 showed a high impact on all variables studied. They were indeed the only contributors to τ_D at 50ºC at the same percentage. With the course of the experiment, many collisions would have likely provoked to form aggregates of higher size. Thus, it is highly possible that particles present at 50ºC were mostly those composed by the aggregation of particles from G1 and/or G2.

Variable importance was also determined taking into account the parameters obtained from AFM images. SD of τ_D at 30ºC showed the highest relevance when talking about spikiness (MAA), heterogeneity (SD area) and skewness. As G5 was considered the main responsible for these variations, it can be, therefore, stated that the high SD of the area, low spikiness and high skewness found in the samples was directly related with the presence of particles in the cited group.

Finally, D_2 of the particles/aggregates had more influence on the SD of the τ_D at low temperatures (10-20ºC). G1-G3 contributed by almost 100% to these values, due to the fact that small particles are the only ones that their movement can be detected at low temperature. As explained before, differences in the shape of the particles forming these groups, i.e. bonded parallel or as clusters, can be described directly by D_2.

This study shows that there is a direct relationship among the τ_D at different temperatures and the presence of CNC aggregates of different morphologies classified into groups. This first approach on the description of the aggregation state of the CNC could facilitate their characterization with an important reduction of the analysis time.

4.4. Hairy cellulose nanocrystals as retention additive

During the stay at the University of McGill, a new family of NC having a crystalline body and functionalized edges was developed, called HNC. In the case of CNCC, the edges present cationic charge. Thus, CNCC have been produced focusing on their application as a retention agent for fillers in the RP matrix. First, the flocculation of clay alone by CNCC has been studied, identifying the flocculation mechanism and evaluating the most effective dosage (Publication VI). After that, in a second study, the implementation of this product in the wet-end of the paper machine has been studied deeply. The hypothesis was that CNCC may have

a synergic effect on strength and retention. Thus, the study focused on the flocculation of both fillers ($CaCO_3$ and clay) as well as the retention and drainage effectivity and the determination of the mechanical properties (Publication VII).

4.4.1 Flocculation of kaolinite by cationic nanocrystalline cellulose

The first study was conducted through the flocculation of a kaolinite suspension with CNCC. Figure 33 shows the evolution of the ratio RMS/DC of the clay/CNCC system with time. The RMS/DC ratio provides the root mean square of the fluctuations in transmitted light and the average transmittance, indicating the relative floc size in arbitrary units [288]. After CNCC was added to the clay suspension, an extensive flocculation occurred. A high increment in the ratio was observed for dosages between 5 and 150 mg/g CNCC, increasing both the maximum value and the initial slope. More specifically, when dosage was between 10 and 100 mg/g, the RMS/DC ratio reached instantaneously the maximum measurement limit of the equipment (12.5), making a challenge the adequate monitoring of the clay flocculation at these dosages. This is indeed why these data are not shown in the cited figure.

During the first instants of the flocculation process, some of the primary particles start to agglomerate creating flocs of different size and shape, depending on the CNCC dosage. Thus, the average transmittance should increase slightly (Figure 33a). At low dosages, a coexistence of some clay particles with some small flocs may induce some fluctuations in transmitted light. Therefore, a very sensitive change in floc size is detected by PDA with a big change in the output ratio. In this way, when the change in size is much higher, the ratio would increase overpassing the maximum limit of the equipment, what makes difficult the flocculation monitoring by this method. Because of that, further experiments were carried out with the FBRM probe.

Regarding FBRM assays, Figure 33b shows that dosages below 5 mg/g does not induce a fast flocculation kinetic. However, when the CNCC dosage was higher than 5 mg/g, both maximum MCL and initial slope increase up to the maximum value, 240 μm and 3.1 μm/s, respectively, at the CNCC dosage interval of 10-25 mg/g. This fact was also observed by Chen et al. [289]. Finally, dosages higher than 30 mg/g induced smaller flocs with slower kinetics.

To understand the flocculation mechanism of the system clay/CNCC, zeta potential of fresh flocs as well as the turbidity of the supernatant has been determined and plotted in Figure 34. The adsorption of CNCC resulted in a decrease of the net negative charge of the clay suspension, reaching IEP at the CNCC dosage of 25-30 mg/g. Nevertheless, as observed in the turbidity reduction results (Figure 34), flocculation occurs in a much wider interval, showing more than 80% when the CNCC dosage was 7.5-75 mg/g. This observation suggests that differences in flocs MCL showed in Figure 33 are due to different flocs conformation rather than low flocculation efficiencies.

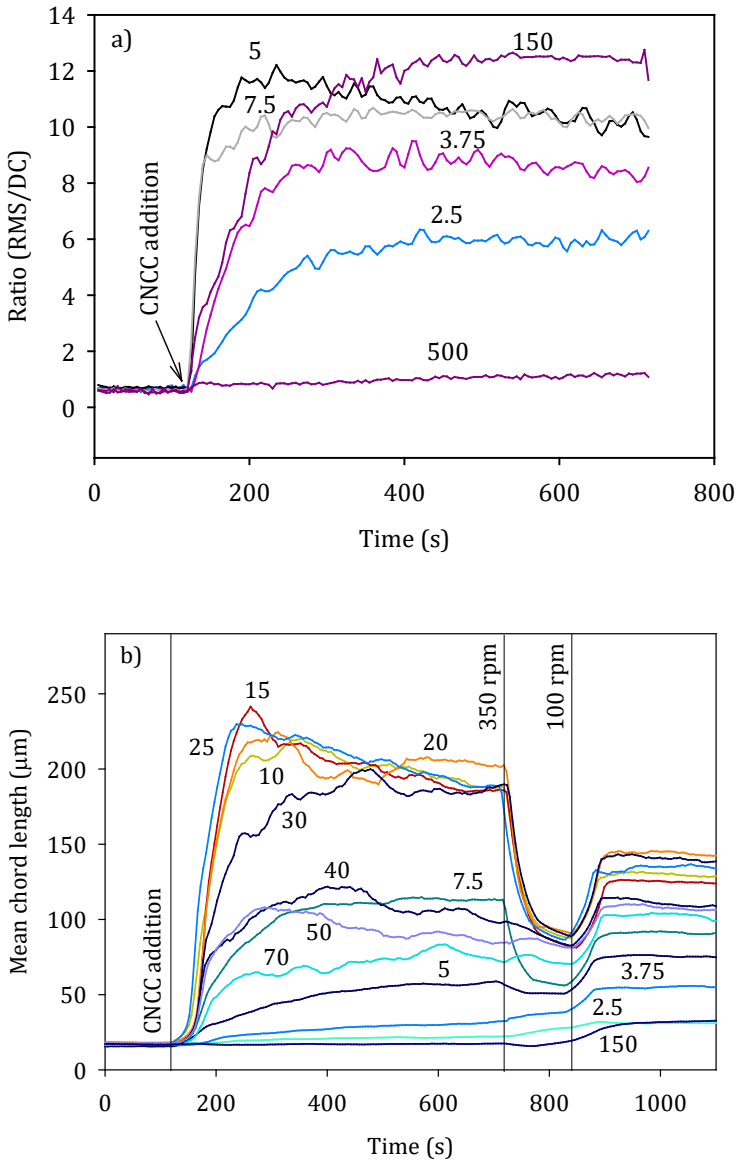

Figure 33. a) Clay flocculation with different CNCC dosages, monitored by PDA. b) MCL profiles of clay/CNCC experiments carried out by FBRM. Vertical lines in FBRM represent an external action on the experiment. Numbers indicated in the graph shows the CNCC dosage in mg/g.

Differences in the reflocculation efficiency could provide important information regarding the flocculation mechanism of the system. According to Yoon et al. [278], when clay/PDADMAC aggregates were exposed to high shear conditions, they were completely broken, but they were reflocculated immediately (over 70% of reflocculation efficiency) when shear conditions were decrerased again, which evidences a charge neutralization mechanism. In the case of clay/CPAM flocs, when they were exposed to high hydrodynamic shear, the bridging polymer (flocculation mechanism of CPAM) may undergo scission or

reconformation (patches formation) on the clay surface resulting in smaller and more compact flocs (with a reflocculation efficiency below 30%).

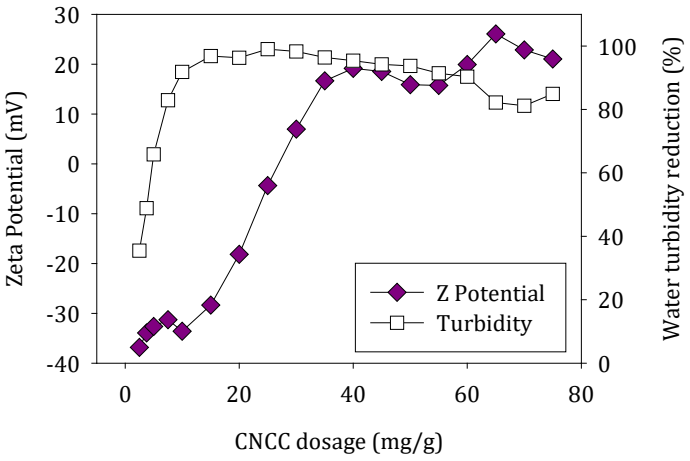

Figure 34. Zeta potential of recent flocs of clay at different CNCC dosages at the pH 8.5.

In this study, the values calculated for reflocculation efficiency, varying in the range of 40-62%, suggest that the flocculation mechanism of clay by CNCC is not purely charge neutralization nor bridge or patch formation. The present mechanism and its variations are likely due to the different patterns of attachment that CNCC and clay may undergo as a result of both species having different charge distribution in the same particle. Clay particles at pH 8.5 present a negative charge on the plane face of the particles, while it possess a slight positive charge on the borders. On the other hand, CNCC present a neutral crystalline body with positive charge at the edges.

To provide more details on the conformation of the particles during the flocculation process, the D_2 and D_f of the flocs at the maximum MCL and at the reflocculation step, at the different dosages, were determined and plotted in Figure 35. At the dosage of 10 mg/g, both D_2 and D_f reached the minimum value. As it can observed in Figure 35, a similar tendency between D_2 and D_f values was obtained, but higher differences were found using the three dimensional D_f, what makes easier to understand the 3D conformation of the particles. Taking into account the combination of the results observed for zeta potential, FBRM and D_f, three groups have been created to explain this behavior: dosages < 10 mg/g, dosages near the IEP (10-25 mg/g) and dosages >25 mg/g.

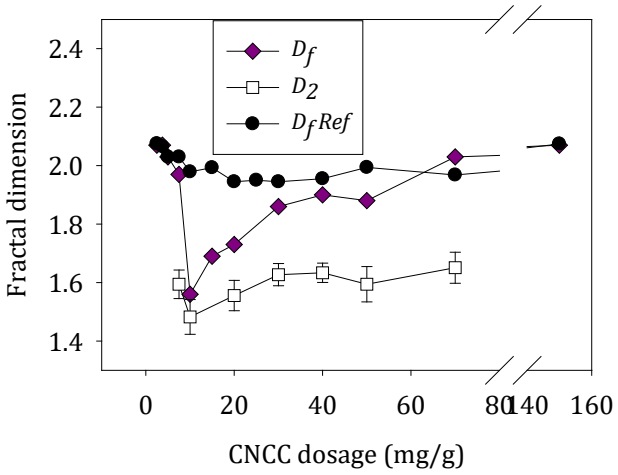

Figure 35. Variation of flocs D_2 and D_f calculated at maximum MCL and 2 minutes after reflocculation (D_f ref), with the CNCC dosage.

The proposed conformation has been represented in Figure 36. When the applied CNCC dosage is lower than 10 mg/g, the D_f has a value near 2, which means that compact flocs are being formed of small size (Figure 33b). This is probably due to the presence of two size populations: the initial clay agglomerates and the small flocs formed by clay/CNCC. It was also observed in Figure 33b, that the initial slope for this group is low, which is a typical behavior of high D_f flocs due to the higher amount of particles required to increase the characteristic length of the flocs. The spatial arrangement proposed for these aggregates would tend to the CNCC particles lying between both clay surfaces, forming a compact structure like the one showed at the left of Figure 36. The zeta potential in this case is apparently far from the IEP (-35 mV), but in view of the explained conformation, it is probable that the measured zeta potential corresponds to the one of the clay particles alone.

Generally, when flocs are more compact, they offer a higher resistance to be broken under high shear conditions, keeping the D_f almost invariable. In this experiment, it was observed that D_f calculated at the end of the flocculation experiment almost matches with the D_f obtained at the maximum MCL, so the structure of the flocs would be likely the same. Moreover, flocs are slightly broken when shear rate is increased, and bigger flocs are formed after reflocculation. It means that some free end of the CNCC is able to reach a free clay particle after decreasing the stirring rate, thus keeping compact structures but slightly bigger.

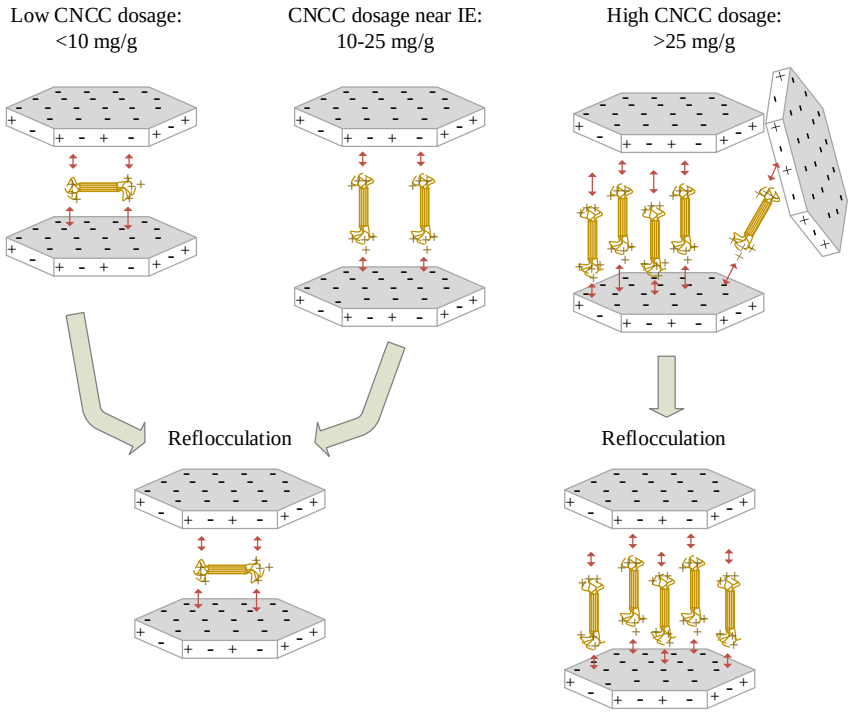

Figure 36. Proposed conformation of clay/CNCC flocs depending on the CNCC dosage.

According to the theory of flocculation mechanisms [290], flocs formed by polymer bridges are hard to break when stirring speed is increased, and when they are broken, polymer tends to reconformate as patches when the stirring speed is reduced. On the other side, patch mechanism creates softer flocs, which recover their size after being broken through shear stress. In this case, none of these mechanisms fully describe the behavior of flocculation for dosages below 10 mg/g. The main reason could be the fact that clay particles have flat shape instead of spherical as most of colloids, and CNCC are straight instead of flexible as traditional flocculants.

Results show that the D_f dropped to values around 1.6 when the zeta potential of the system was near the IEP, which means that a much opener structure with bigger gaps among the clay particles were being formed. Now, the possibility of a clay primary particle to locate a CNCC particle is higher, so the most probable conformation is the perpendicular position of both components, as shown in the middle scheme of Figure 36. Thus, longer structures are formed, which corresponds to faster flocculation kinetics. However, this low D_f triggers soft flocs, which break-up or re-configure relatively easy. When the shear rate is increased and afterwards decreased, the maximum size is not recovered and the D_f increases up to almost 2. Although these flocs are found to be near the IEP, a reflocculation efficiency of around 50% together with the soft flocs formed, suggests that neither polymer bridging nor charge neutralization fully explain the flocculation behavior.

Finally, when the CNCC dosage was over 25 mg/g, D_f values were over 1.9, meaning compact structures were being formed again. The flocculation process would probably start in the

same way as in the previous case, but as some CNCC can remain without joining to any clay particle, they might be attached to others forming compact flocs. This is shown in the right part of the Figure 36. Since the positive charges of clay particles on the borders are not very frequent at neutral pH, and the positive ends of the CNCC are much more active than their neutral body, this attachment by van der Waals forces would not happen until most of the negative areas of clay particles are fully covered. This point is found at the IEP.

This higher D_f triggers slower flocculation, which again matches FBRM results. As these aggregates are more compact, their structure does not extensively change when they are reflocculated at high shear stress. Therefore, D_f increases only slightly, from 1.9 to 2.0. When the CNCC dosage is increased over 25 mg/g, the IEP is overpassed, converting the total zeta potential of the system into positive. However, the efficiency of the flocculation, measured by the turbidity removal from the initial point, is still over 90% at the CNCC dosage of 25-60 mg/g, which means that almost all clay particles are being flocculated, despite the charge reversibility of the system.

Thus, new knowledge has been generated and the complex mechanism for the flocculation of kaolinite with CNCC has been elucidated. It is based on charge neutralization, where the maximum floc size and kinetic is found at the IEP, although it is highly efficient in a wide interval of dosages, from 7.5 to 75 mg/g. The size decrease after reflocculation can be explained by the different conformation that the CNCC and clay particles take after increasing the shear stress, but keeping the total charge of the system. However, the measurement of the flocs zeta potential is limited by the different configuration of the particles, obtaining values similar to the clay particles alone for low CNCC dosages, where CNCC are lying flat between clay particles.

4.4.2 Evaluation of cationic nanocrystalline cellulose as a retention additive

Considering the good results obtained for CNCC as flocculant, it was considered the possibility of using it as retention agent for RP pulp. In this way, a double benefit could be obtained, since both drainage and retention operations could be effectively improved at the same time that the wet-end system would remain much simplified. Furthermore, paper properties could be also improved.

For this study, a RP pulp was considered, containing 13.9% of fillers, being 30.4% $CaCO_3$ and 69.6% kaolin respect to the total filler content. First, the CNCC flocculation efficiency on a suspension of only fillers was assessed and compared to that obtained in the previous study, where only kaolinite was flocculated. Then, a complex pulp, containing fibers and fillers, was studied in terms of flocculation kinetic and efficacy on the subsequent operations, such as dewatering, fillers retention and handsheets mechanical properties.

4.4.2.1 Fillers flocculation

To assess the effectivity of the CNCC in promoting aggregation of fillers, a suspension made of $CaCO_3$ and kaolin at the described percentages was prepared. Flocculation was monitored by both PDA and FBRM instruments. Figure 37a shows the evolution of the ratio RMS/DC with the time at different CNCC dosages monitored by PDA. As shown in previous results with only kaolin (Figure 33), CNCC induced aggregation of the system kaolin/$CaCO_3$ in a very wide interval of dosages (5-220 mg/g). In this case, the maximum initial slope detected by PDA was found at the CNCC dosage of 20 mg/g, while experiments with only kaolin did not allow to determine this parameter due to instrument limitations (Figure 33a). Flocculation became slower when increasing the used CNCC dosage.

Although both kaolin and $CaCO_3$ had similar hydrodynamic diameters, 400 nm and 550 nm, respectively, they differ in shape and surface charge, what makes them move with a different trajectory during flocculation. Nevertheless, as both types of fillers are negatively charged (-32 mV for kaolin and -10.4 mV for $CaCO_3$), there is no energy barrier between them and CNCC. Thus, the rate of deposition of CNCC on filler particles is simply mass transport limited.

Maximum flocculation rates determined by FBRM were found from 20 to 80 mg/g (Figure 37b). Considering the FBRM graphs as well as zeta potential data (Figure 38), results have been classified into three groups and discussed separately: i) CNCC dosage <30 mg/g, ii) around 55 mg/g and iii) >80 mg/g.

In the first group, flocculation started immediately after the CNCC addition, but the flocs kept changing their conformation, reducing their MCL by around 75%. In the first instance, the CNCC would be probably standing up, bridging the different particles heterogeneously to end up lying down between them. Due to the small diameter of the nanoparticles, the gap between flocculated filler particles would be practically negligible, thus keeping the zeta potential of the system similar as the initial one.

Reflocculation efficiency for this group was lower than 40%. Bergaya et al. [291] determined that kaolinite particles at the working pH, 8.5, have a purely negative flat area with the borders presenting a mixed charge with positive and negative areas. This fact makes an initial agglomeration between kaolinite and $CaCO_3$ could be present before CNCC addition. With increasing shear, not only the flocs induced by CNCC could have been broken, but also those initially present. Then, newly formed negative surfaces will be now available, thus decreasing the bulk zeta potential (Figure 38) as well as the bulk floc size.

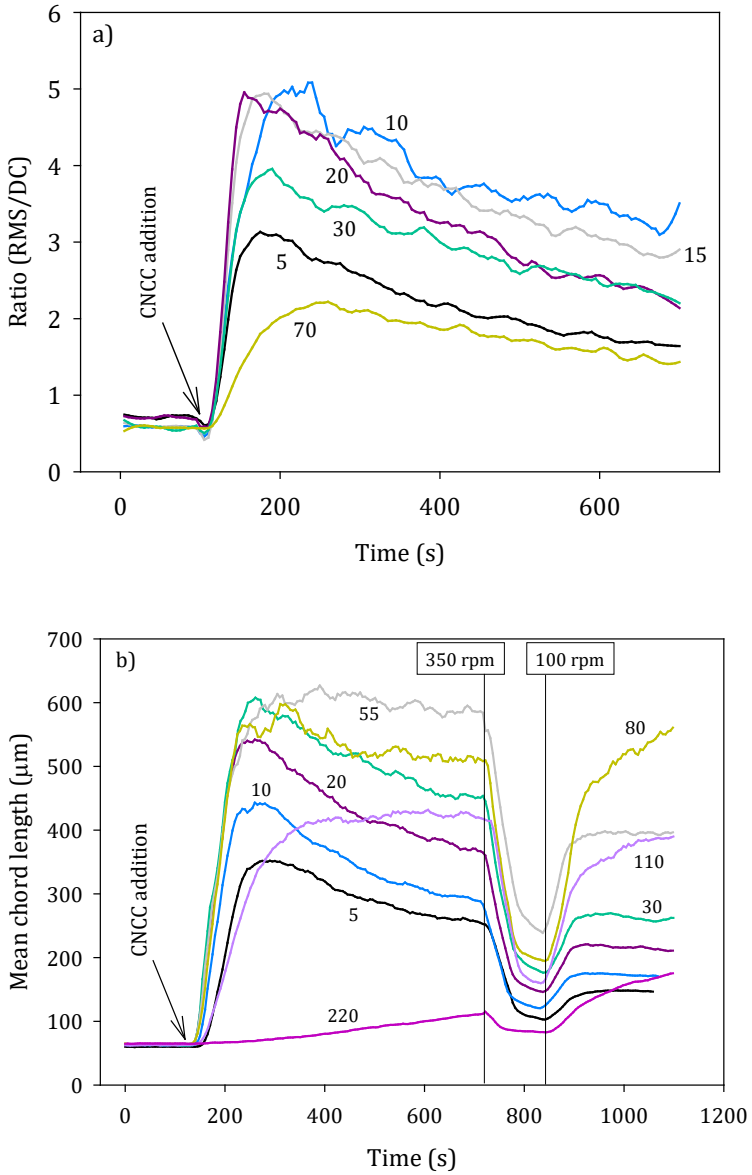

Figure 37. a) Evolution of the ratio (RMS/DC) of the flocculation of fillers with CNCC, monitored by PDA. b) MCL profiles of the experiments carried out by the flocculation of fillers using CNCC. Numbers indicated in the graph represent the CNCC dosage in mg/g. Vertical lines represent an external action on the experiment.

The IEP at both maximum MCL and reflocculation stages, was found to be at the CNCC dosage of 55 mg/g (second group). In this group, flocculation was again instantaneous but unlike the first group, flocs remained stable during the whole flocculation stage. Stable structures had been formed in two possible scenarios: fewer CNCC particles might have fallen down, thus preventing reconformation of flocs, and/or multiple CNCC could have bridged the filler particles, immobilizing them. Here, an equilibrium between floc formation and break-up was reached, indicated by a plateau in the MCL profile.

Initially, flocculation rates were determined by the adsorption of CNCC on fillers. However, after reflocculation, where aggregates size was recovered by 50%, one could be dealing mainly with collisions between "sticky" flocs, with different formation and break-up kinetics.

A quite different behavior was found in the third group (CNCC dosage > 80 mg/g). Here, the flocculation was retarded with the increasing CNCC dosage, probably caused by particle repulsion due to charge reversal. First, as said before, CNCC would attach orthogonally to the particles, creating flocs with an open structure. With the movement of the system, it is probable that some of them collided with the already formed flocs, forming a kind of structure that had a porous interior and an external surface with a highly positive charge density. After increasing the shear, the interior charge of the flocs would be accessible after floc breakage. Then, when the surface of a floc collides with the interior area of another, electrostatic attraction occurs forming new bonds and bigger flocs (Figure 37b). This was indeed the reason why positive charge observed at the maximum MCL was neutralized after reflocculation (Figure 38).

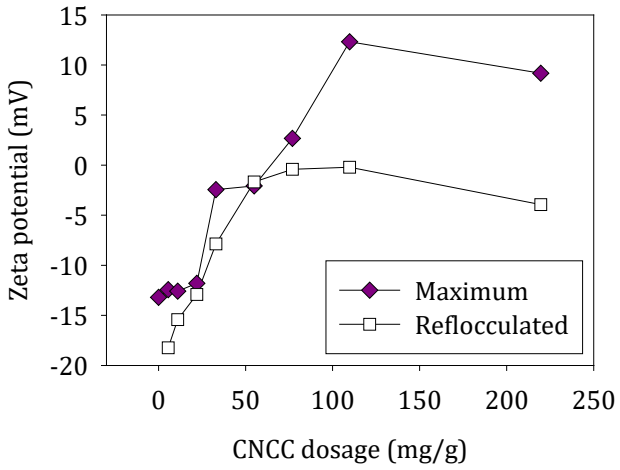

Figure 38. Zeta potential of flocs extracted from the FBRM experiments at the maximum MCL and at the reflocculation stage for different dosages of CNCC respect to the amount of fillers.

Optical microscopy images (Figure 39) show an increase in the floc size and compactness with the CNCC dosage till a maximum, observed at the IEP (55 mg/g). The opposite tendency was observed when the CNCC was further increased. Here, flocs became smaller and more spherical instead of composing elongated structures. A decrement in the floc size was observed in reflocculated flocs for the first and second groups. The opposite case was found for dosages over 110 mg/g, where the floc reconformation by the bonding between the exterior areas of the flocs and the released interior ones caused an increase in the floc size.

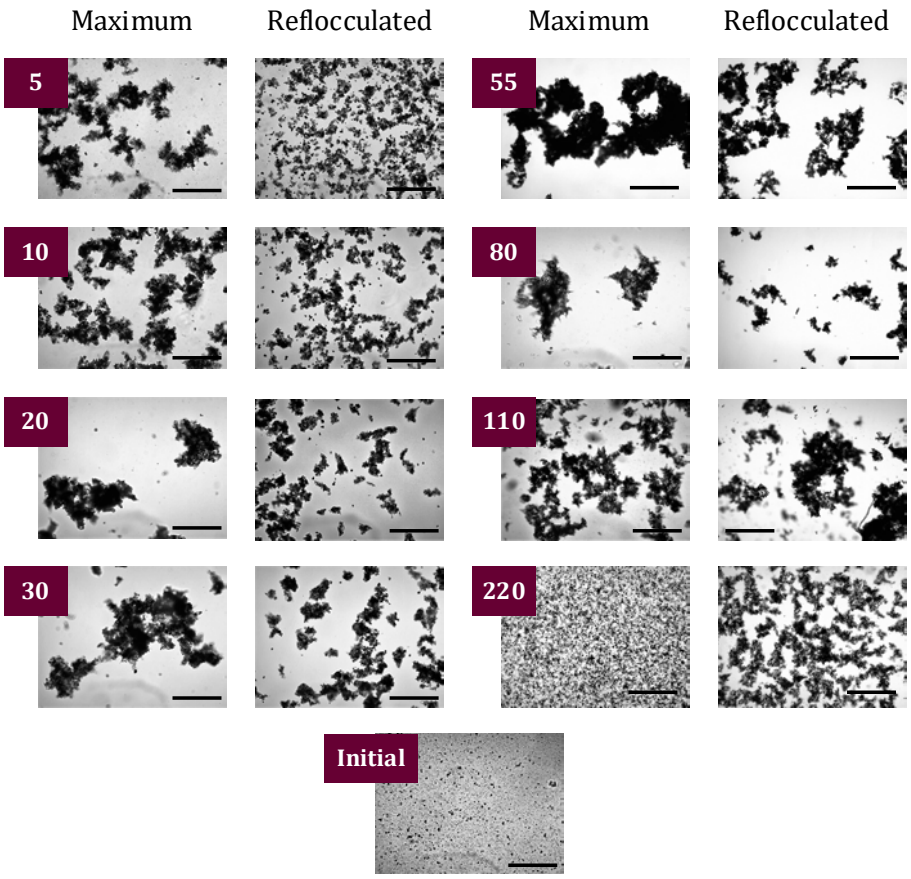

Figure 39. Optical microscope images of $CaCO_3$-clay flocs formed at different CNCC dosages at the maximum MCL point and at the reflocculation stage. Numbers indicated in the pictures represent the CNCC dosage corresponding to each experiment. Scale bar of the images for the initial sample and the CNCC dosages between 5.5 and 33 represent 500 µm, and those for CNCC dosages between 55 and 220 depict 1 mm.

As it was concluded in the previous study, where the CNCC were used to flocculate a kaolinite suspension, the main mechanism of action of the CNCC is charge neutralization. This is indeed the conclusion of this second study, where not only kaolinite but also $CaCO_3$ have been flocculated. However, when flocs were broken up and reflocculated, the positive charge changed to neutral and the floc size was increased. This is likely due to negative patches within the flocs, which became exposed upon floc break-up and which collided with positive (CNCC-covered) patches upon reflocculation, forming new CNCC bridges between the fillers.

4.4.2.2 Flocculation of recycled paper pulp

When CNCC is dosified to the full pulp containing fibers and fillers (13.9%), an increase in the CNCC dosage was translated into a consequent increase in the MCL, till a maximum of 76 µm at the CNCC dose of 20 mg/g (Figure 40). In this case, the CNCC dosage required to get the maximum MCL was hardly different to that used for kaolinite (15 mg/g) but quite

lower to that needed for kaolinite/$CaCO_3$ (30 mg/g). The maximum MCL was strongly reduced due to the presence of fibers with a diameter of around 30 μm. Since it is improbable that the fast rotating focused beam travels along the full length of a fiber, the MCL provided by the FBRM instrument is likely that of the diameter of the fibers [277, 292]. Hence, the MCL data displayed in the Figure 40 reflects an increase in the fiber width due to the attachment of filler particles together with the fines/fillers agglomerates size. Presumably there is a competition between filler flocculation and the deposition of filler aggregates on fibers. Fillers cannot grow till the same size, because they deposit on fibers before they can grow bigger.

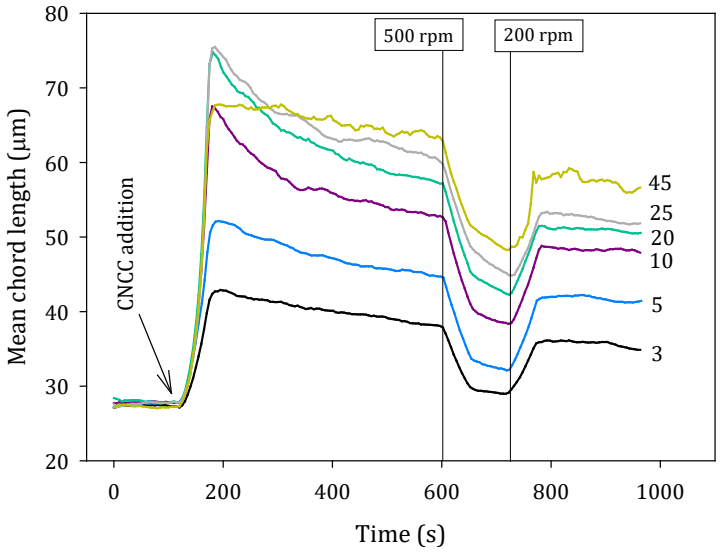

Figure 40. MCL profiles of the experiments carried out by the flocculation of RP pulp using CNCC. Numbers indicated in the graph represent the CNCC dosage in mg/g. Vertical lines represent an external action on the experiment.

Again, like in filler flocculation, the IEP was found at the CNCC dosage which induced the maximum MCL (20 mg/g). Pulp reflocculation efficiencies were around 80% for dosages below 10 mg/g, and decreased till 50% for dosages over 25 mg/g. When flocs were submitted to a high shear rate, fillers and fines situated among fibers were displaced and bonded to free areas of the fibers, thus increasing the width of the fibers but decreasing the filler floc size.

This fact was observed in images of the flocs in the suspension, as shown in Figure 41. While in the initial sample, the RP fibers, the fines and the fillers kept dispersed within the suspension, after the CNCC addition at the dosage which induced the maximum MCL, all fillers seemed to be coating the fibers, and, at the same time, serving as bridges that join some of the other fibers.

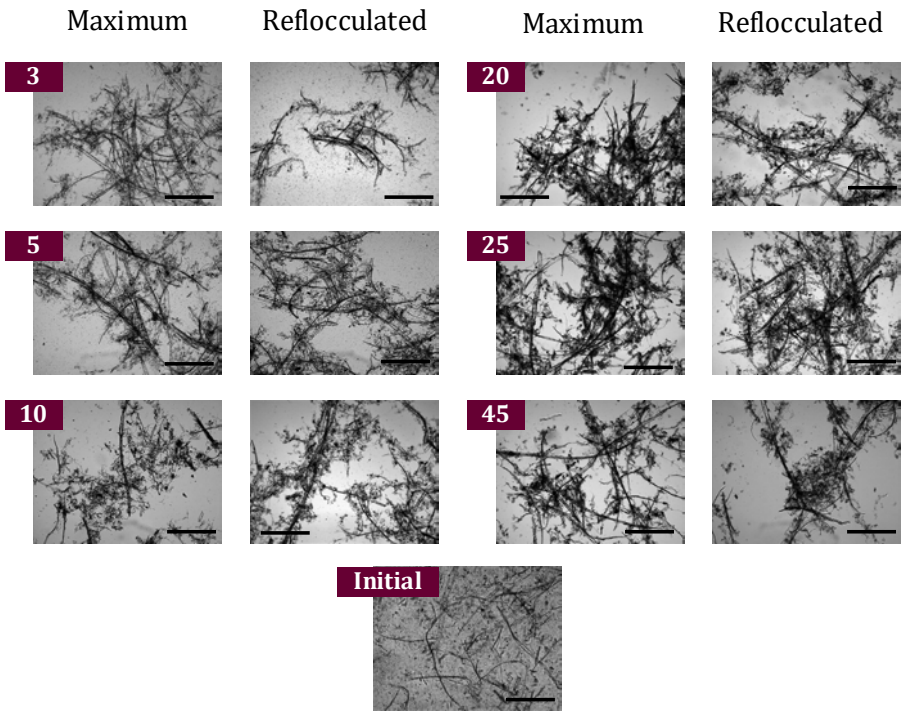

Figure 41. Optical microscope images of RP flocs at 5x magnification formed at different CNCC dosages at the maximum MCL point and at the reflocculation stage. Numbers indicated in the pictures represent the CNCC dosage corresponding to each experiment.

The results obtained in this study about the use of CNCC as flocculant of recycled pulp have been compared to the obtained previously, using other wet-end systems, and displayed in Table 8 [231]. For CNCC, the increase in MCL was maximum compared to these types of RS. The flocculation stability was similar to that of PVA (62%), but the reflocculation efficiency (60%) was intermediate between the low values of the dual RS (with a coagulant and CPAM) and cationic starch (25%), and the high value of PVA (78%). In addition, the maximum MCL was achieved at the IEP. However, in view of the rod-shape of the CNCC and their heterogeneous charge distribution, the conformation of the flocs could be constantly changing but without causing any effect to the bulk charge. Thus, it was deduced that CNCC in the presence of RP fibers acted through a charge neutralization mechanism in both flocculation and reflocculation stages, similar as the flocculation of only fillers. However, the floc stability is higher compared to traditional products used for this purpose and acting through charge neutralization mechanism, which may be an industrial advantage. Moreover, the dosage could be easily controlled by the on-line measurement of zeta potential.

Table 8. Comparison of results obtained with CNCC to those obtained with RS in the literature [231].

	CNCC	Dual RS	PVA	Cationic starch
Optimum Dose (mg/g)	20	3.5	30	20
Max. MCL (μm)	76	72	50	62
Floc stability (%)	62	72	60	50
Ref. efficiency (%)	60	25	78	28
Max MCL at the IEP?	YES	NO	-	-
	Charge neutralization	Bridging	Patch formation	Bridging

4.4.2.3 Retention, drainage and mechanical properties of RP

Traditionally, when NC have been used in mass, as dry strengthening agents of paper, drainage has usually slowed down [6]. This has been an important limitation since it affects the productivity of the machine if the speed has to be reduced. Many studies have been conducted in this line to solve these problems when CNF are included within the process [261].However, this drawback is not observed for CNCC, as shown in Figure 42a, where the W300 (time consumed for the filtration of 300 g of sample) was reduced by 78% at the CNCC dosage of 20 mg/g. In addition, the total drained water after 240 s was increased from 360 to 430 g. To assess which of the components present initially have been drained and not retained in the wet-web, the filtrated water has been analyzed (Figure 42b).

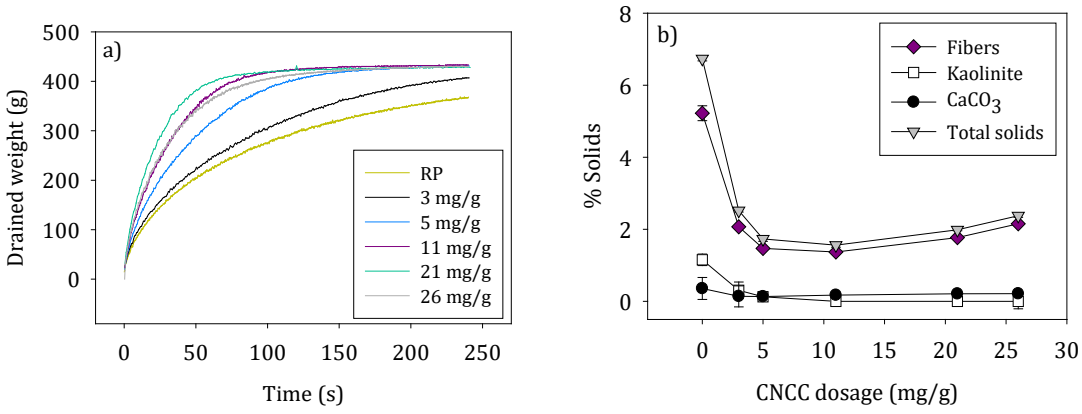

Figure 42. a) Evolution of the drained weight with time at different CNCC dosages, b) solids that passed through the mesh during the drainage experiments.

From the total solid content present during drainage experiments, 6.7% passed through the mesh when no CNCC was added to the suspension. After CNCC addition, these percentages were strongly reduced, reaching a minimum at the CNCC dosage of 10 mg/g, where the solid

retention reached 98.4%. As shown in the composition of the drained water, most of the drained solids was organic matter, i.e. fines.

When paper handsheets were prepared ad analyzed, it was observed that TI did not present much change when a low percentage of CNCC (5 mg/g) was added before handsheet formation (Figure 43). However, it was reduced for increasing dosages. Compared to other RS typically used in the papermaking industries, this worsening in the mechanical properties of the upgraded paper was not as worrying [261]. For example, TI was reduced by 31% with the dual RS composed of a coagulant and CPAM, or 17% with a CPAMB typically used in newsprint mills [261]. On the other hand, an additional advantage is that tear index remained almost invariable with the CNCC dosage, since in most cases, when TI increased, the tear index decreased consequently.

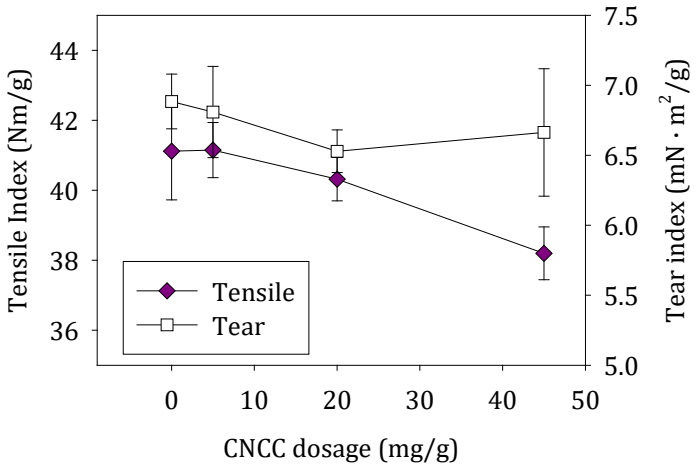

Figure 43. Effect of the CNCC dosage on the tensile and tear indexes of the produced handsheets.

To sum up, CNCC was found a useful retention agent that flocculate fillers and pulp suspensions effectively through a charge neutralization mechanism. With the implementation of CNCC to the wet-end, many of the usually present components can be substituted by just this one, which favors fillers and fibers retention at the same time that drainage is improved without a detrimental effect on paper mechanical properties. This represents a decoupling of the effects retention-drainage and a partial decoupling of the effects retention-paper properties, which prove the initial hypothesis.

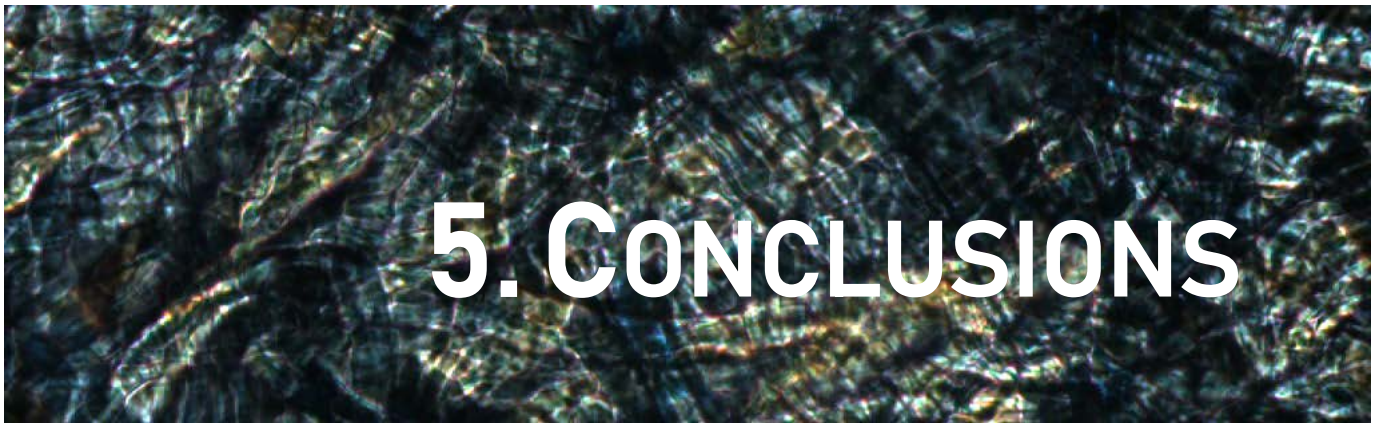

5. Conclusions

5. CONCLUSIONS

In this PhD thesis, the potential of three types of nanocellulosic products to improve the production of recycled paper has been established. BC was proved to be a great candidate to improve the mechanical properties of the RP. On the other hand, the high aggregation propensity of the CNC was found to be a key parameter to optimize and a new methodology has been developed for its quantification. Finally, the potential of using CNCC as process and product additive has been demonstrated, which opens new possibilities to simplify the wet-end of the paper machines.

In the first line of this PhD thesis, the improvement of the mechanical properties of RP with the use of BC was successfully demonstrated. The most productive bacterial strain and its most appropriate culture conditions were selected from a literature review. BC was produced in a nutrient-rich medium, in static mode, and mild-fibrillated, to be used in mass as dry strengthening additive. Finally, the novel in-situ culture of bacteria with the RP pulp approach was proposed and studied deeply. This last concept was proved for the first time, through the study of the main variables that could affect to their application.

- Genetic modification of *K. sucrofermentans* failed to induce an increase in its BC productivity. This was probably due to the fact that the c-di-GMP intracellular levels of this bacterial strain were already at the maximum level.
- BC has been proved to decouple the effect that CNF have on the tensile and tear indexes of the upgraded paper through the combined action of both individual BCNF together with some small clusters of BC. Thus, paper became more flexible through the improvement of both indexes and the strain at break.
- The BCNF retention mechanism was not only due to the hydrogen bonding of BCNF with the fibers, like in the case of high fibrillated CNF, but also to the physical retention of these clusters within the gaps. This fact, together with the high affinity between BCNF and fillers, due to the high specific surface area of BCNF, confirmed a higher filler retention in their proximities.
- The in situ production of BC has been successful in the case of agitated culture when the culture time was below 24 h: BC was found to cover the secondary fibers, compensating, thus, for the fiber damage suffered during the recycling process. At longer time, these coated fibers were interwoven forming tight clusters difficult to disperse that induced the production of heterogeneous papers.
    - Culture time was, therefore, a key parameter to optimize in view of the high dependence of the paper properties with the shape that BC acquires at different times.
    - Cultures in high volumes were more favorable to improve the mechanical properties: the dissolved oxygen concentration in the cultures with higher volume was suitable to avoid the shear stress and the diversion metabolic pathways towards the deactivation of the essential enzymes involved in the cellulose production.
- Although the presence of BC was detectable earlier in static than in agitated cultures (4 h compared to 12 h), heterogeneous systems were observed, thus failing to improve the properties of paper: BC was produced as a membrane floating on top of the culture, while all initial fibers sedimented.
- With the addition of 3% BCNF in mass to the RP pulp, TI, tear index and strain at break achieved increments of: 11.1%, 7.6% and 66.8%, respectively. On the other hand, papers upgraded with the BC produced in situ with the pulp for 12 h, reached increments of 24.3% in TI and 19.4% in strain at break with the addition of 15% of the cultured pulp. With this new approach, the culture time needed to reach the required improvements is much reduced (from 7 days to 12 h), while those costs associated with the BC dispersion are saved.

The second line of this PhD thesis allowed us to characterize the aggregation state of CNC and to assess its effect on paper properties when they are used as dry-strengthening additives. CNC were produced directly from RP, without a previous isolation of cellulose. These CNC were applied to RP, and the effect of their dispersion on

the mechanical properties of the final paper was assessed. Finally, a novel approach to characterize the aggregation state of CNC was established. This is important since there is not any methodology yet.

- The production of CNC from newspapers was proven to be a high value approach to maintain the competitiveness of newsprint mills.
    - CNC were produced through a direct acid hydrolysis to RP, without the use of the pretreatments typically applied to the pulp to isolate cellulose.
    - Despite the presence of some impurities in the CNC, neither the hydrolysis yield nor most of the properties resulted affected.
- The dispersion of CNC or CNF within the fibers had a high impact on RP mechanical properties.
    - A long pulping time (60 min) favored the homogeneous mixture of the NC with the fibers suspension, as well as their retention, reaching a maximum increment in TI of 30%.
    - However, an increase of up to 20.6% was achieved at much lower pulping times (10 min), with the use of dispersing agents.
- The aggregation state of CNC in water suspension has been characterized for the first time.
    - The behavior of the CNC during the determination of τ_D at different temperatures was proved to be related with the geometry of the particles and aggregates, as well as with the heterogeneity of the sample. This was attained through a variable importance analysis, correlating CNC geometrical parameters with the DLS data.
    - Particles/aggregates present in AFM images were automatically classified into five groups attending to morphological features. All samples studied had more than 70% of the particles in the group of smaller size, corresponding to CNC individuals.
    - Results revealed the two groups of smallest size had more relevance on the value of τ_D at 50 °C, while medium aggregates described variations of τ_D at 10 ºC.

Finally, in the third line of this PhD thesis, CNCC were proved as retention additive in recycled paper production, thus simplifying the wet-end system of the paper machine at the time that paper quality increases. First, the flocculation mechanism of the CNCC was studied in a kaolinite suspension. Then, the CNCC flocculation efficiency was additionally evaluated through the flocculation of the main fillers of RP mills: kaolinite and $CaCO_3$. Finally, a RP pulp was flocculated and drainage, retention and mechanical properties of the final RP were determined.

- CNCC was proved to achieve the aggregation of kaolinite particles, inducing faster flocculation with dosages close to the IEP, within the interval 10-30 mg/g, yielding flocs of a maximum MCL of 250 μm and turbidity removal values of over 80%.

    - Different types of aggregation were observed through the analysis of size and D_f, that depended on the CNCC dosage:
        - When it was <7.5 mg/g, compact (D_f = 2) and small flocs were formed, apparently away from the IEP.
        - At CNCC dosages between 10 and 25 mg/g, D_f dropped to 1.6, implying flocs of an opener structure and faster flocculation kinetics.
        - When dosage was over 25 mg/g, more complex and compact structures were found, with D_f over 1.9 and slow flocculation kinetics, with positive zeta potential values.
    - In the reflocculation stage, D_f reached an almost constant value around 2, meaning that the most stable conformation, being compact, was obtained.
    - Thus, it was concluded that the flocculation mechanism of the CNCC/kaolinite system was charge neutralization with reconformation of the flocs.
- CNCC were also found to flocculate successfully a suspension of fillers in a wide range of dosages.
    - The maximum MCL was found at the CNCC dosage of 30 mg/g, with a fast initial flocculation rate and being quite below the IEP (55 mg/g).
    - The process was found an example of heteroflocculation, since the rate of deposition on either kaolinite or $CaCO_3$ was simply mass transport limited.
    - At CNCC dosages well over the IEP, a different structure was observed, with an excess of positive charges on the outside surface of the flocs and some interior areas were charge was still negative. After their breakage, these interior areas interacted with the positive surface, forming bigger and more compact flocs.
- Finally, as it could be expected from these preliminary tests, CNCC also induced flocculation of RP components in a wide range of dosages.
    - Again, the maximum MCL was found at the IEP with a CNCC dosage of 20 mg/g.
    - Pulp drainage time was reduced by 78% and retention was improved by 77% with the addition of the cited CNCC dosage (20 mg/g).
    - Mechanical properties of the prepared handsheets were slightly reduced with the addition of the CNCC, but this worsening was not as relevant as with other RS (2.5% compared to 30%).
    - It can be finally concluded that CNCC could be effectively used as retention agent, increasing with the use of only one component the simplicity of the wet-end system.

FUTURE PERSPECTIVE

- The in-situ BC production with recycled fibers constitutes, therefore, a promising alternative to replace conventional paper strengthening agents. These results have the potential to be applied in industrial paper mills, employing pulp streams with the

application of low cost, non-exhaustive sterilization operations, such as ozone or ultraviolet radiation. In addition, with the use of fed-batch operation mode is possible to keep bacterial growth in stand-by while a portion is derived to be cultured with the pulp. Taking into account all these considerations as well as the use of low-cost nutrient medium, the process may be suitable for large scale production. However, more intensive research is needed to turn this hypothesis into reality.

- The use of dispersing agents could be a solution to one of the main challenges that are actually impeding the implementation of NC within the process: NC dispersion. On the other hand, although the study regarding the description of the aggregation state of CNC is merely descriptive, it constitutes a first attempt with the purpose to monitor on line the description of the aggregation state of CNC suspensions before their application. This could be attained through the development of a model that correlates the DLS data with the geometrical features of the particles, including samples of a wider variability. In this way, researchers and industries would not have the need to attend to microscopy techniques. Moreover, as the use of τ_D assumes no preferential particle shape, this approach could be extended to other nanoparticles that tend to bond and agglomerate with different morphologies.

- With the use of CNCC as a process and product additive, most of these agents typically used in the wet-end could be replaced by only this one component. This approach could be of utmost interest for those small recycled paper mills that are looking for simplicity. Nevertheless, deeper research is still needed to decouple completely the retention-paper properties effects.

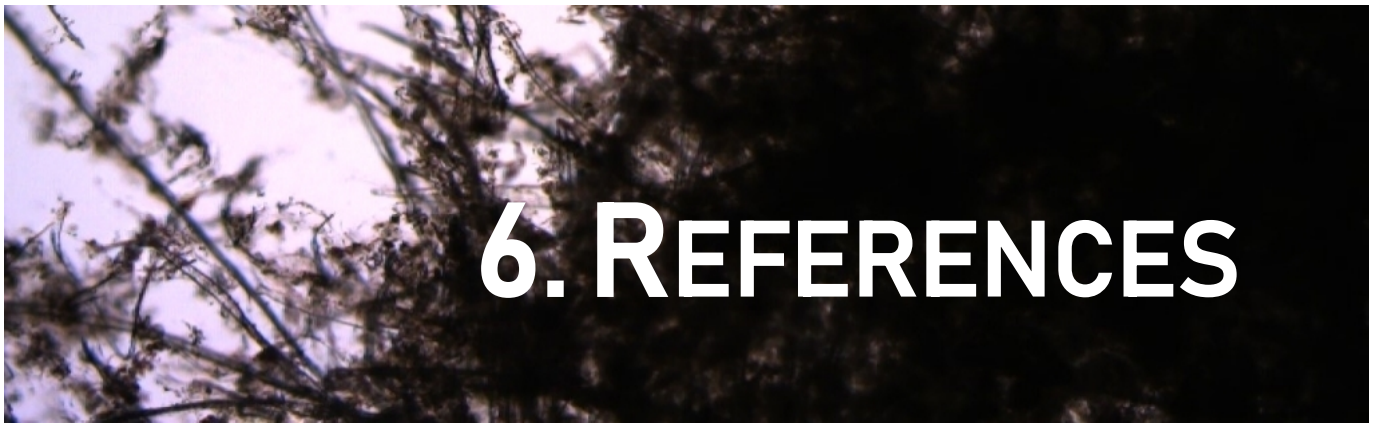

6. REFERENCES

6. REFERENCES

1. Blanco, A., R. Miranda, and M.C. Monte, *Extending the limits of paper recycling: improvements along the paper value chain.* Forest Systems, 2013. 22(3): p. 471-483.
2. Hubbe, M.A., R.A. Venditti, and O.J. Rojas, *What happens to cellulosic fibers during papermaking and recycling? A review.* BioResources, 2007. 2(4): p. 739-788.
3. Lindström, T., L. Wågberg, and T. Larsson. *On the nature of joint strength in paper-A review of dry and wet strength resins used in paper manufacturing*. in *13th fundamental research symposium*. 2005. The Pulp and Paper Fundamental Research Society Cambridge, UK.
4. Brodin, F.W., O.W. Gregersen, and K. Syverud, *Cellulose nanofibrils: Challenges and possibilities as a paper additive or coating material - A review.* Nordic Pulp & Paper Research Journal, 2014. 29(1): p. 156-166.
5. Hubbe, M.A., *Bonding between cellulosic fibers in the absence and presence of dry-strength agents–A review.* BioResources, 2007. 1(2): p. 281-318.
6. Taipale, T., et al., *Effect of microfibrillated cellulose and fines on the drainage of kraft pulp suspension and paper strength.* Cellulose, 2010. 17(5): p. 1005-1020.
7. Habibi, Y., *Key advances in the chemical modification of nanocelluloses.* Chemical Society Reviews, 2014. 43(5): p. 1519-1542.
8. Campano, C., et al., *Direct production of cellulose nanocrystals from old newspapers and recycled newsprint.* Carbohyd. Polym., 2017. 173: p. 489-496.
9. Klemm, D., et al., *Cellulose: Fascinating biopolymer and sustainable raw material.* Angewandte Chemie-International Edition, 2005. 44(22): p. 3358-3393.

10. Siqueira, G., J. Bras, and A. Dufresne, *Cellulosic Bionanocomposites: A Review of Preparation, Properties and Applications.* Polymers, 2010. 2(4): p. 728-765.
11. Mondal, S., *Preparation, properties and applications of nanocellulosic materials.* Carbohydrate Polymers, 2017. 163: p. 301-316.
12. Turbak, A.F., F.W. Snyder, and K.R. Sandberg, *Microfibrillated cellulose, a new cellulose product: properties, uses, and commercial potential*. Journal Name: J. Appl. Polym. Sci.: Appl. Polym. Symp.; (United States); Journal Volume: 37; Conference: 9. cellulose conference, Syracuse, NY, USA, 24 May 1982. 1983: ; ITT Rayonier Inc., Shelton, WA. Medium: X; Size: Pages: 815-827.
13. Turbak, A.F., F.W. Snyder, and K.R. Sandberg, *Microfibrillated cellulose*. 1983, Google Patents.
14. Dinand, E., et al., *Microfibrillated cellulose and method for preparing a microfibrillated cellulose*. 1999, Google Patents.
15. Makoui, K.B. and P.K. Chatterjee, *Cross-linked pore containing microfibrillated cellulose prepared by freezing and solvent exchange*. 1987, Google Patents.
16. Cavaille, J.-Y., et al., *Cellulose microfibril-reinforced polymers and their applications*. 2000, Google Patents.
17. Dufresne, A., *Nanocellulose: from nature to high performance tailored materials*. 2017: Walter de Gruyter GmbH & Co KG.
18. Spence, K.L., et al., *The effect of chemical composition on microfibrillar cellulose films from wood pulps: water interactions and physical properties for packaging applications.* Cellulose, 2010. 17(4): p. 835-848.
19. Balea, A., *Celulosa nanofibrilada y su aplicación en la industria papelera para la mejora de productos reciclados*, in *Chemical Engineering and materials department*. 2017, Complutense University of Madrid.
20. Tejado, A., et al., *Energy requirements for the disintegration of cellulose fibers into cellulose nanofibers.* Cellulose, 2012. 19(3): p. 831-842.
21. Berlin, A., et al., *Inhibition of cellulase, xylanase and β-glucosidase activities by softwood lignin preparations.* Journal of biotechnology, 2006. 125(2): p. 198-209.
22. Paakko, M., et al., *Enzymatic hydrolysis combined with mechanical shearing and high-pressure homogenization for nanoscale cellulose fibrils and strong gels.* Biomacromolecules, 2007. 8(6): p. 1934-1941.
23. Saito, T., et al., *Cellulose nanofibers prepared by TEMPO-mediated oxidation of native cellulose.* Biomacromolecules, 2007. 8(8): p. 2485-2491.
24. Zimmermann, T., N. Bordeanu, and E. Strub, *Properties of nanofibrillated cellulose from different raw materials and its reinforcement potential.* Carbohydrate Polymers, 2010. 79(4): p. 1086-1093.
25. Abdul Khalil, H.P.S., et al., *Production and modification of nanofibrillated cellulose using various mechanical processes: A review.* Carbohydrate Polymers, 2014. 99: p. 649-665.
26. Kim, C.-W., et al., *Structural studies of electrospun cellulose nanofibers.* Polymer, 2006. 47(14): p. 5097-5107.
27. Chen, W., et al., *Individualization of cellulose nanofibers from wood using high-intensity ultrasonication combined with chemical pretreatments.* Carbohydrate Polymers, 2011. 83(4): p. 1804-1811.
28. Chakraborty, A., M. Sain, and M. Kortschot, *Cellulose microfibrils: a novel method of preparation using high shear refining and cryocrushing.* Holzforschung, 2005. 59(1): p. 102-107.
29. Kose, R., et al., *"Nanocellulose" as a single nanofiber prepared from pellicle secreted by Gluconacetobacter xylinus using aqueous counter collision.* Biomacromolecules, 2011. 12(3): p. 716-720.
30. Baheti, V., R. Abbasi, and J. Militky, *Ball milling of jute fibre wastes to prepare nanocellulose.* World Journal of Engineering, 2012. 9(1): p. 45-50.

31. Ho, T.T.T., et al., *Nanofibrillation of pulp fibers by twin-screw extrusion.* Cellulose, 2015. 22(1): p. 421-433.
32. Brown, A.J., *XLIII.-On an acetic ferment which forms cellulose.* Journal of the Chemical Society, Transactions, 1886. 49(0): p. 432-439.
33. Dufresne, A., *Nanocellulose: from nature to high performance tailored materials*. 2012: Walter de Gruyter.
34. Barnhart, D.M., et al., *CelR, an ortholog of the diguanylate cyclase PleD of caulobacter, regulates Cellulose synthesis in Agrobacterium tumefaciens.* Applied and Environmental Microbiology, 2013. 79(23): p. 7188-7202.
35. Matthysse, A.G., et al., *The effect of cellulose overproduction on binding and biofilm formation on roots by Agrobacterium tumefaciens.* Molecular Plant-Microbe Interactions, 2005. 18(9): p. 1002-1010.
36. Ude, S., et al., *Biofilm formation and cellulose expression among diverse environmental Pseudomonas isolates.* Environmental Microbiology, 2006. 8(11): p. 1997-2011.
37. Ausmees, N., et al., *Structural and putative regulatory genes involved in cellulose synthesis in Rhizobium leguminosarum bv. trifolii.* Microbiology-Uk, 1999. 145: p. 1253-1262.
38. Robledo, M., et al., *Role of Rhizobium endoglucanase CelC2 in cellulose biosynthesis and biofilm formation on plant roots and abiotic surfaces.* Microbial Cell Factories, 2012. 11.
39. Yang, Y., et al., *Isolation and characteristics analysis of a novel high bacterial cellulose producing strain Gluconacetobacter intermedius CIs26.* Carbohydrate Polymers, 2013. 92(2): p. 2012-2017.
40. Kongruang, S., *Bacterial cellulose production by Acetobacter xylinum strains from agricultural waste products.* Applied Biochemistry and Biotechnology, 2008. 148(1-3): p. 245-256.
41. Ha, J.H., et al., *Bacterial cellulose production from a single sugar alpha-linked glucuronic acid-based oligosaccharide.* Process Biochemistry, 2011. 46(9): p. 1717-1723.
42. Lin, S.P., et al., *Biosynthesis, production and applications of bacterial cellulose.* Cellulose, 2013. 20(5): p. 2191-2219.
43. Huang, Y., et al., *Recent advances in bacterial cellulose.* Cellulose, 2014. 21(1): p. 1-30.
44. Ross, P., R. Mayer, and M. Benziman, *Cellulose biosynthesis and function in bacteria.* Microbiological Reviews, 1991. 55(1): p. 35-58.
45. Vitta, S. and V. Thiruvengadam, *Multifunctional bacterial cellulose and nanoparticle-embedded composites.* Current Science, 2012. 102(10): p. 1398-1405.
46. Nguyen, V.T., et al., *Spontaneous mutation results in lower cellulose production by a Gluconacetobacter xylinus strain from Kombucha.* Carbohydrate Polymers, 2010. 80(2): p. 337-343.
47. Aydin, Y.A. and N.D. Aksoy, *Isolation and characterization of an efficient bacterial cellulose producer strain in agitated culture: Gluconacetobacter hansenii P2A.* Applied Microbiology and Biotechnology, 2014. 98(3): p. 1065-1075.
48. Jung, J.Y., J.K. Park, and H.N. Chang, *Bacterial cellulose production by Gluconacetobacter hansenii in an agitated culture without living non-cellulose producing cells.* Enzyme and Microbial Technology, 2005. 37(3): p. 347-354.
49. Hungund, B.S. and S. Gupta, *Strain improvement of Gluconacetobacter xylinus NCIM 2526 for bacterial cellulose production.* African Journal of Biotechnology, 2013. 9(32): p. 5170-5172.
50. Wu, R.-Q., et al., *Mutagenesis induced by high hydrostatic pressure treatment: a useful method to improve the bacterial cellulose yield of a Gluconoacetobacter xylinus strain.* Cellulose, 2010. 17(2): p. 399-405.

51. Nakai, T., et al., *Formation of highly twisted ribbons in a carboxymethylcellulase gene-disrupted strain of a cellulose-producing bacterium.* Journal of bacteriology, 2013. 195(5): p. 958-964.
52. Perez-Mendoza, D., et al., *Novel mixed-linkage beta-glucan activated by c-di-GMP in Sinorhizobium meliloti (vol 112, pg E757, 2015).* Proceedings of the National Academy of Sciences of the United States of America, 2015. 112(27): p. E3632-E3632.
53. Pérez-Mendoza, D., et al., *N-Acetylglucosamine-dependent biofilm formation in Pectobacterium atrosepticum is cryptic and activated by elevated c-di-GMP levels.* Microbiology, 2011. 157(12): p. 3340-3348.
54. Santos, S.M., J.M. Carbajo, and J.C. Villar, *The effect of carbon and nitrogen sources on bacterial cellulose production and properties from Gluconacetobacter sucrofermentans CECT 7291 focused on its use in degraded paper restoration.* BioResources, 2013. 8(3): p. 3630-3645.
55. Campano, C., et al., *Enhancement of the fermentation process and properties of bacterial cellulose: a review.* Cellulose, 2016. 23(1): p. 57-91.
56. Hong, F. and K.Y. Qiu, *An alternative carbon source from konjac powder for enhancing production of bacterial cellulose in static cultures by a model strain Acetobacter aceti subsp xylinus ATCC 23770.* Carbohydrate Polymers, 2008. 72(3): p. 545-549.
57. Vazquez, A., et al., *Bacterial cellulose from simple and low cost production media by gluconacetobacter xylinus.* Journal of Polymers and the Environment, 2013. 21(2): p. 545-554.
58. Hong, F., et al., *Bacterial cellulose production from cotton-based waste textiles: enzymatic saccharification enhanced by ionic liquid pretreatment.* Bioresource Technology, 2012. 104: p. 503-508.
59. Kurosumi, A., et al., *Utilization of various fruit juices as carbon source for production of bacterial cellulose by Acetobacter xylinum NBRC 13693.* Carbohydrate Polymers, 2009. 76(2): p. 333-335.
60. Ha, J.H., et al., *Production of bacterial cellulose by a static cultivation using the waste from beer culture broth.* Korean Journal of Chemical Engineering, 2008. 25(4): p. 812-815.
61. Kumbhar, J., J. Rajwade, and K. Paknikar, *Fruit peels support higher yield and superior quality bacterial cellulose production.* Applied Microbiology and Biotechnology, 2015. 99(16): p. 6677-6691.
62. Hu, W.L., et al., *Functionalized bacterial cellulose derivatives and nanocomposites.* Carbohydrate Polymers, 2014. 101: p. 1043-1060.
63. Klemm, D., et al., *Nanocelluloses: A new family of nature-based materials.* Angewandte Chemie International Edition, 2011. 50(24): p. 5438-5466.
64. Williams, W.S. and R.E. Cannon, *Alternative environmental roles for cellulose produced by Acetobacter xylinum.* Applied and environmental microbiology, 1989. 55(10): p. 2448-2452.
65. Czaja, W., D. Romanovicz, and R.M. Brown, *Structural investigations of microbial cellulose produced in stationary and agitated culture.* Cellulose, 2004. 11(3-4): p. 403-411.
66. Song, H.J., et al., *Pilot-scale production of bacterial cellulose by a spherical type bubble column bioreactor using saccharified food wastes.* Korean Journal of Chemical Engineering, 2009. 26(1): p. 141-146.
67. Moon, S.-H., et al., *Comparisons of physical properties of bacterial celluloses produced in different culture conditions using saccharified food wastes.* Biotechnology and Bioprocess Engineering, 2006. 11(1): p. 26-31.
68. Kim, Y.J., et al., *Bacterial cellulose production by Gluconacetobacter sp RKY5 in a rotary biofilm contactor.* Applied Biochemistry and Biotechnology, 2007. 137: p. 529-537.

69. Lin, S.P., et al., *Semi-continuous bacterial cellulose production in a rotating disk bioreactor and its materials properties analysis.* Cellulose, 2014. 21(1): p. 835-844.
70. Jung, J.Y., et al., *Production of bacterial cellulose by Gluconacetobacter hansenii using a novel bioreactor equipped with a spin filter.* Korean Journal of Chemical Engineering, 2007. 24(2): p. 265-271.
71. Cheng, K.-C., J.M. Catchmark, and A. Demirci, *Enhanced production of bacterial cellulose by using a biofilm reactor and its material property analysis.* Journal of biological engineering, 2009. 3: p. 12.
72. Cheng, K.C., A. Demirci, and J.M. Catchmark, *Advances in biofilm reactors for production of value-added products.* Applied Microbiology and Biotechnology, 2010. 87(2): p. 445-456.
73. Cheng, K.C., J.M. Catchmark, and A. Demirci, *Effects of CMC Addition on Bacterial Cellulose Production in a Biofilm Reactor and Its Paper Sheets Analysis.* Biomacromolecules, 2011. 12(3): p. 730-736.
74. Lu, H.M. and X.L. Jiang, *Structure and Properties of Bacterial Cellulose Produced Using a Trickling Bed Reactor.* Applied Biochemistry and Biotechnology, 2014. 172(8): p. 3844-3861.
75. Çakar, F., et al., *Improvement production of bacterial cellulose by semi-continuous process in molasses medium.* Carbohydrate Polymers, 2014. 106: p. 7-13.
76. Bae, S. and M. Shoda, *Bacterial Cellulose Production by Fed-Batch Fermentation in Molasses Medium.* Biotechnology progress, 2004. 20(5): p. 1366-1371.
77. Mikkelsen, D., et al., *Influence of different carbon sources on bacterial cellulose production by Gluconacetobacter xylinus strain ATCC 53524.* Journal of applied microbiology, 2009. 107(2): p. 576-583.
78. Jung, H.I., et al., *Influence of glycerol on production and structural-physical properties of cellulose from Acetobacter sp V6 cultured in shake flasks.* Bioresource Technology, 2010. 101(10): p. 3602-3608.
79. Kim, S., et al., *Effect of viscosity-inducing factors on oxygen transfer in production culture of bacterial cellulose.* Korean Journal of Chemical Engineering, 2012. 29(6): p. 792-797.
80. Shah, N., J.H. Ha, and J.K. Park, *Effect of Reactor Surface on Production of Bacterial Cellulose and Water Soluble Oligosaccharides by Gluconacetobacter hansenii PJK.* Biotechnology and Bioprocess Engineering, 2010. 15(1): p. 110-118.
81. Wu, J.M. and R.H. Liu, *Thin stillage supplementation greatly enhances bacterial cellulose production by Gluconacetobacter xylinus.* Carbohydrate Polymers, 2012. 90(1): p. 116-121.
82. Cheng, K.C., J.M. Catchmark, and A. Demirci, *Effect of different additives on bacterial cellulose production by Acetobacter xylinum and analysis of material property.* Cellulose, 2009. 16(6): p. 1033-1045.
83. Hu, Y. and J.M. Catchmark, *Influence of 1-methylcyclopropene (1-MCP) on the production of bacterial cellulose biosynthesized by Acetobacter xylinum under the agitated culture.* Letters in Applied Microbiology, 2010. 51(1): p. 109-113.
84. Lu, Z.G., et al., *Effects of alcohols on bacterial cellulose production by Acetobacter xylinum 186.* World Journal of Microbiology & Biotechnology, 2011. 27(10): p. 2281-2285.
85. Yang, J.X., et al., *In situ fabrication of a microporous bacterial cellulose/potato starch composite scaffold with enhanced cell compatibility.* Cellulose, 2014. 21(3): p. 1823-1835.
86. Zang, S.S., et al., *Ordered manufactured bacterial cellulose as biomaterial of tissue engineering.* Materials Letters, 2014. 128: p. 314-318.
87. Chen, Y., et al., *Bacterial cellulose/gelatin composites: in situ preparation and glutaraldehyde treatment.* Cellulose, 2014. 21(4): p. 2679-2693.

88. Lu, M., et al., *Thermodynamics and kinetics of adsorption for heavy metal ions from aqueous solutions onto surface amino-bacterial cellulose.* Transactions of Nonferrous Metals Society of China, 2014. 24(6): p. 1912-1917.
89. Shen, W., et al., *Adsorption of Cu(II) and Pb(II) onto diethylenetriamine-bacterial cellulose.* Carbohydrate Polymers, 2009. 75(1): p. 110-114.
90. Oshima, T., et al., *Phosphorylated bacterial cellulose for adsorption of proteins.* Carbohydrate Polymers, 2011. 83(2): p. 953-958.
91. Chen, S.Y., et al., *Kinetic and thermodynamic studies of adsorption of Cu2+ and Pb2+ onto amidoximated bacterial cellulose.* Polymer Bulletin, 2009. 63(2): p. 283-297.
92. Yoon, S.H., et al., *Electrically conductive bacterial cellulose by incorporation of carbon nanotubes.* Biomacromolecules, 2006. 7(4): p. 1280-1284.
93. Muller, D., et al., *Chemical in situ polymerization of polypyrrole on bacterial cellulose nanofibers.* Synthetic Metals, 2011. 161(1-2): p. 106-111.
94. Muller, D., et al., *Electrically conducting nanocomposites: preparation and properties of polyaniline (PAni)-coated bacterial cellulose nanofibers (BC).* Cellulose, 2012. 19(5): p. 1645-1654.
95. Amin, M., et al., *Synthesis and characterization of thermo- and pH-responsive bacterial cellulose/acrylic acid hydrogels for drug delivery.* Carbohydrate Polymers, 2012. 88(2): p. 465-473.
96. Shezad, O., et al., *Physicochemical and mechanical characterization of bacterial cellulose produced with an excellent productivity in static conditions using a simple fed-batch cultivation strategy.* Carbohydrate Polymers, 2010. 82(1): p. 173-180.
97. Spaic, M., et al., *Characterization of anionic and cationic functionalized bacterial cellulose nanofibres for controlled release applications.* Cellulose, 2014. 21(3): p. 1529-1540.
98. Silva, N., et al., *Bacterial cellulose membranes as transdermal delivery systems for diclofenac: In vitro dissolution and permeation studies.* Carbohydrate Polymers, 2014. 106: p. 264-269.
99. Lopes, T.D., et al., *Bacterial cellulose and hyaluronic acid hybrid membranes: Production and characterization.* International Journal of Biological Macromolecules, 2014. 67: p. 401-408.
100. Cai, Z.J. and G. Yang, *Optical nanocomposites prepared by incorporating bacterial cellulose nanofibrils into poly(3-hydroxybutyrate).* Materials Letters, 2011. 65(2): p. 182-184.
101. Berndt, S., et al., *Antimicrobial porous hybrids consisting of bacterial nanocellulose and silver nanoparticles.* Cellulose, 2013. 20(2): p. 771-783.
102. Khan, S., et al., *Bacterial cellulose-titanium dioxide nanocomposites: nanostructural characteristics, antibacterial mechanism, and biocompatibility.* Cellulose, 2015. 22(1): p. 565-579.
103. Hu, W.L., et al., *Preparation and properties of photochromic bacterial cellulose nanofibrous membranes.* Cellulose, 2011. 18(3): p. 655-661.
104. Ranby, B.G., *Cellulose and muscle- The colloidal properties of cellulose micelles.* Discussions of the Faraday Society, 1951(11): p. 158-&.
105. Revol, J.F., et al., *Helicoidal self-ordering of cellulose microfibrils in aqueous suspension.* International Journal of Biological Macromolecules, 1992. 14(3): p. 170-172.
106. Celluforce. *Celluforce*. 2016; Available from: http://www.celluforce.com/.
107. Habibi, Y., L.A. Lucia, and O.J. Rojas, *Cellulose nanocrystals: chemistry, self-assembly, and applications.* Chemical reviews, 2010. 110(6): p. 3479-3500.
108. Nickerson, R.F. and J.A. Habrle, *CELLULOSE INTERCRYSTALLINE STRUCTURE - STUDY BY HYDROLYTIC METHODS.* Industrial and Engineering Chemistry, 1947. 39(11): p. 1507-1512.

109. Bondeson, D., A. Mathew, and K. Oksman, *Optimization of the isolation of nanocrystals from microcrystalline cellulose by acid hydrolysis.* Cellulose, 2006. 13(2): p. 171-180.
110. Kallel, F., et al., *Isolation and structural characterization of cellulose nanocrystals extracted from garlic straw residues.* Industrial Crops and Products, 2016. 87: p. 287-296.
111. Beck-Candanedo, S., M. Roman, and D.G. Gray, *Effect of reaction conditions on the properties and behavior of wood cellulose nanocrystal suspensions.* Biomacromolecules, 2005. 6(2): p. 1048-1054.
112. Garcia, A., et al., *The nanocellulose biorefinery: woody versus herbaceous agricultural wastes for NCC production.* Cellulose, 2017. 24(2): p. 693-704.
113. Liu, Y., et al., *A novel approach for the preparation of nanocrystalline cellulose by using phosphotungstic acid.* Carbohydrate polymers, 2014. 110: p. 415-422.
114. Oksman, K., et al., *Cellulose nanowhiskers separated from a bio-residue from wood bioethanol production.* Biomass & Bioenergy, 2011. 35(1): p. 146-152.
115. Rosli, N.A., I. Ahmad, and I. Abdullah, *Isolation and characterization of cellulose nanocrystals from Agave angustifolia fibre.* BioResources, 2013. 8(2): p. 1893-1908.
116. Martínez-Sanz, M., et al., *On the extraction of cellulose nanowhiskers from food by-products and their comparative reinforcing effect on a polyhydroxybutyrate-co-valerate polymer.* Cellulose, 2015. 22(1): p. 535-551.
117. Hu, Y., et al., *Preparation of cellulose nanocrystals and carboxylated cellulose nanocrystals from borer powder of bamboo.* Cellulose, 2014. 21(3): p. 1611-1618.
118. Ogundare, S.A., V. Moodley, and W.E. van Zyl, *Nanocrystalline cellulose isolated from discarded cigarette filters.* Carbohydrate Polymers, 2017. 175: p. 273-281.
119. Abu-Danso, E., et al., *Pretreatment assisted synthesis and characterization of cellulose nanocrystals and cellulose nanofibers from absorbent cotton.* International Journal of Biological Macromolecules, 2017. 102: p. 248-257.
120. Rosa, M.F., et al., *Cellulose nanowhiskers from coconut husk fibers: Effect of preparation conditions on their thermal and morphological behavior.* Carbohydrate Polymers, 2010. 81(1): p. 83-92.
121. Silvério, H.A., et al., *Extraction and characterization of cellulose nanocrystals from corncob for application as reinforcing agent in nanocomposites.* Industrial Crops and Products, 2013. 44: p. 427-436.
122. Wang, Z.H., et al., *Reuse of waste cotton cloth for the extraction of cellulose nanocrystals.* Carbohydrate Polymers, 2017. 157: p. 945-952.
123. Fortunati, E., et al., *Binary PVA bio-nanocomposites containing cellulose nanocrystals extracted from different natural sources: Part I.* Carbohydrate polymers, 2013. 97(2): p. 825-836.
124. Mujtaba, M., et al., *Utilization of flax (Linum usitatissimum) cellulose nanocrystals as reinforcing material for chitosan films.* International Journal of Biological Macromolecules, 2017. 104: p. 944-952.
125. Luzi, F., et al., *Production and characterization of PLA_PBS biodegradable blends reinforced with cellulose nanocrystals extracted from hemp fibres.* Industrial Crops and Products, 2016. 93: p. 276-289.
126. Lu, P. and Y.-L. Hsieh, *Cellulose isolation and core–shell nanostructures of cellulose nanocrystals from chardonnay grape skins.* Carbohydrate Polymers, 2012. 87(4): p. 2546-2553.
127. Jiang, Y.N., et al., *Preparation of cellulose nanocrystals from Humulus japonicus stem and the influence of high temperature pretreatment.* Carbohydrate Polymers, 2017. 164: p. 284-293.
128. Henrique, M.A., et al., *Valorization of an agro-industrial waste, mango seed, by the extraction and characterization of its cellulose nanocrystals.* Journal of environmental management, 2013. 121: p. 202-209.

129. Kargarzadeh, H., et al., *Effects of hydrolysis conditions on the morphology, crystallinity, and thermal stability of cellulose nanocrystals extracted from kenaf bast fibers.* Cellulose, 2012. 19(3): p. 855-866.
130. Sheltami, R.M., et al., *Extraction of cellulose nanocrystals from mengkuang leaves (Pandanus tectorius).* Carbohydrate Polymers, 2012. 88(2): p. 772-779.
131. Li, R., et al., *Cellulose whiskers extracted from mulberry: A novel biomass production.* Carbohydrate Polymers, 2009. 76(1): p. 94-99.
132. Haafiz, M.K.M., et al., *Isolation and characterization of cellulose nanowhiskers from oil palm biomass microcrystalline cellulose.* Carbohydrate Polymers, 2014. 103: p. 119-125.
133. Fortunati, E., et al., *Cellulose nanocrystals extracted from okra fibers in PVA nanocomposites.* Journal of Applied Polymer Science, 2013. 128(5): p. 3220-3230.
134. Fortunati, E., et al., *Processing of PLA nanocomposites with cellulose nanocrystals extracted from Posidonia oceanica waste: innovative reuse of coastal plant.* Industrial Crops and Products, 2015. 67: p. 439-447.
135. dos Santos, R.M., et al., *Cellulose nanocrystals from pineapple leaf, a new approach for the reuse of this agro-waste.* Industrial Crops and Products, 2013. 50: p. 707-714.
136. Trifol, J., et al., *Chemically extracted nanocellulose from sisal fibres by a simple and industrially relevant process.* Cellulose, 2017. 24(1): p. 107-118.
137. Frone, A.N., et al., *Isolation of cellulose nanocrystals from plum seed shells, structural and morphological characterization.* Materials Letters, 2017. 194: p. 160-163.
138. Siqueira, G., et al., *High reinforcing capability cellulose nanocrystals extracted from Syngonanthus nitens (Capim Dourado).* Cellulose, 2010. 17(2): p. 289-298.
139. Chen, D., et al., *Biocomposites reinforced with cellulose nanocrystals derived from potato peel waste.* Carbohydrate polymers, 2012. 90(1): p. 709-716.
140. Abu Ghalia, M. and Y. Dahman, *Fabrication and enhanced mechanical properties of porous PLA/PEG copolymer reinforced with bacterial cellulose nanofibers for soft tissue engineering applications.* Polymer Testing, 2017. 61: p. 114-131.
141. Johar, N., I. Ahmad, and A. Dufresne, *Extraction, preparation and characterization of cellulose fibres and nanocrystals from rice husk.* Industrial Crops and Products, 2012. 37(1): p. 93-99.
142. Zhang, T., et al., *Tunicate cellulose nanocrystals reinforced nanocomposite hydrogels comprised by hybrid cross-linked networks.* Carbohydrate polymers, 2017. 169: p. 139-148.
143. Neto, W.P.F., et al., *Extraction and characterization of cellulose nanocrystals from agro-industrial residue - Soy hulls.* Industrial Crops and Products, 2013. 42: p. 480-488.
144. Tang, Y.J., et al., *Extraction of cellulose nano-crystals from old corrugated container fiber using phosphoric acid and enzymatic hydrolysis followed by sonication.* Carbohydrate Polymers, 2015. 125: p. 360-366.
145. Teixeira, E.d.M., et al., *Sugarcane bagasse whiskers: Extraction and characterizations.* Industrial Crops and Products, 2011. 33(1): p. 63-66.
146. Jiang, F. and Y.L. Hsieh, *Cellulose nanocrystal isolation from tomato peels and assembled nanofibers.* Carbohydrate Polymers, 2015. 122: p. 60-68.
147. Filson, P.B. and B.E. Dawson-Andoh, *Sono-chemical preparation of cellulose nanocrystals from lignocellulose derived materials.* Bioresource Technology, 2009. 100(7): p. 2259-2264.
148. Danial, W.H., et al., *The reuse of wastepaper for the extraction of cellulose nanocrystals.* Carbohydrate Polymers, 2015. 118: p. 165-169.
149. Tappi, *Solvent extractives of wood and pulp; T 204 cm-97*. 2006, Tappi.
150. Bian, H.Y., et al., *Integrated production of lignin containing cellulose nanocrystals (LCNC) and nanofibrils (LCNF) using an easily recyclable di-carboxylic acid.* Carbohydrate Polymers, 2017. 167: p. 167-176.

151. Torlopov, M.A., et al., *Cellulose nanocrystals prepared in H3PW12O40-acetic acid system.* Cellulose, 2017. 24(5): p. 2153-2162.
152. Cheng, J.-Y. and Y.-H. Chu, *1-Butyl-2,3-trimethyleneimidazolium bis(trifluoromethylsulfonyl)imide ([b-3C-im][NTf2]): a new, stable ionic liquid.* Tetrahedron Letters, 2006. 47(10): p. 1575-1579.
153. Iskak, N.A.M., N.M. Julkapli, and S.B.A. Hamid, *Understanding the effect of synthesis parameters on the catalytic ionic liquid hydrolysis process of cellulose nanocrystals.* Cellulose, 2017. 24(6): p. 2469-2481.
154. Karim, Z., et al., *Necessity of enzymatic hydrolysis for production and functionalization of nanocelluloses.* Critical Reviews in Biotechnology, 2017. 37(3): p. 355-370.
155. van de Ven, T.G.M. and A. Sheikhi, *Hairy cellulose nanocrystalloids: a novel class of nanocellulose.* Nanoscale, 2016. 8(33): p. 15101-15114.
156. Guthrie, R., *The "dialdehydes" from the periodate oxidation of carbohydrates*, in *Advances in carbohydrate chemistry*. 1962, Elsevier. p. 105-158.
157. Yang, H., D.Z. Chen, and T.G.M. van de Yen, *Preparation and characterization of sterically stabilized nanocrystalline cellulose obtained by periodate oxidation of cellulose fibers.* Cellulose, 2015. 22(3): p. 1743-1752.
158. Overbeek, J.T., *The donnan equilibrium.* Prog. Biophys. Biophys. Chem, 1956. 6(1): p. 57-84.
159. Liimatainen, H., et al., *Regeneration and Recycling of Aqueous Periodate Solution in Dialdehyde Cellulose Production.* Journal of Wood Chemistry and Technology, 2013. 33(4): p. 258-266.
160. Yang , H., M.N. Alam, and T.G.M. van de Ven, *Highly charged nanocrystalline cellulose and dicarboxylated cellulose from periodate and chlorite oxidized cellulose fibers.* Cellulose, 2013. 20(4): p. 1865-1875.
161. Yang, H. and T.G.M. van de Ven, *Preparation of hairy cationic nanocrystalline cellulose.* Cellulose, 2016. 23(3): p. 1791-1801.
162. Dufresne, A., *Bacterial Cellulose*, in *Nanocellulose: From Nature to High Performance Tailored Materials*. 2012, Walter de Gruyter.
163. Park, S., et al., *Cellulose crystallinity index: measurement techniques and their impact on interpreting cellulase performance.* Biotechnology for Biofuels, 2010. 3: p. 10.
164. Moon, R.J., et al., *Cellulose nanomaterials review: structure, properties and nanocomposites.* Chemical Society Reviews, 2011. 40(7): p. 3941-3994.
165. Henriksson, M., et al., *Cellulose nanopaper structures of high toughness.* Biomacromolecules, 2008. 9(6): p. 1579-1585.
166. Iguchi, M., S. Yamanaka, and A. Budhiono, *Bacterial cellulose - a masterpiece of nature's arts.* Journal of Materials Science, 2000. 35(2): p. 261-270.
167. Leppanen, K., et al., *Structure of cellulose and microcrystalline cellulose from various wood species, cotton and flax studied by X-ray scattering.* Cellulose, 2009. 16(6): p. 999-1015.
168. Nishiyama, Y., et al., *Periodic disorder along ramie cellulose microfibrils.* Biomacromolecules, 2003. 4(4): p. 1013-1017.
169. Hamad, W.Y. and T.Q. Hu, *Structure-process-yield interrelations in nanocrystalline cellulose extraction.* Canadian Journal of Chemical Engineering, 2010. 88(3): p. 392-402.
170. Zhang, Y., et al., *Preparation and characterization of nanocrystalline cellulose from bamboo fibers by controlled cellulase hydrolysis*. Proceeding of the 4th International Conference on Pulping, Papermaking and Biotechnology, ed. Y. Jin, Z. Wang, and W. Wu. 2012, Nanjing: Nanjing Forestry Univ. 207-211.
171. Gardner, D.J., et al., *Adhesion and surface issues in cellulose and nanocellulose.* Journal of Adhesion Science and Technology, 2008. 22(5-6): p. 545-567.
172. Hosseinidoust, Z., et al., *Cellulose nanocrystals with tunable surface charge for nanomedicine.* Nanoscale, 2015. 7(40): p. 16647-16657.

173. Thakur, V.K., *Nanocellulose polymer nanocomposites: fundamentals and applications*. 2014: John Wiley & Sons.
174. Heggset, E.B., G. Chinga-Carrasco, and K. Syverud, *Temperature stability of nanocellulose dispersions.* Carbohydrate Polymers, 2017. 157: p. 114-121.
175. Qiu, K.Y. and A.N. Netravali, *A Review of Fabrication and Applications of Bacterial Cellulose Based Nanocomposites.* Polymer Reviews, 2014. 54(4): p. 598-626.
176. Tonoli, G., et al., *Cellulose micro/nanofibres from Eucalyptus kraft pulp: preparation and properties.* Carbohydrate polymers, 2012. 89(1): p. 80-88.
177. Jonoobi, M., et al., *Different preparation methods and properties of nanostructured cellulose from various natural resources and residues: a review.* Cellulose, 2015: p. 1-35.
178. Xu, Y., A.D. Atrens, and J.R. Stokes, *Rheology and microstructure of aqueous suspensions of nanocrystalline cellulose rods.* Journal of Colloid and Interface Science, 2017. 496: p. 130-140.
179. Dufresne, A., *Processing of Polymer Nanocomposites Reinforced with Polysaccharide Nanocrystals.* Molecules, 2010. 15(6): p. 4111-4128.
180. Brockman, A.C. and M.A. Hubbe, *Charge reversal system with cationized cellulose nanocrystals to promote dewatering of a cellulosic fiber suspension.* Cellulose, 2017. 24(11): p. 4821-4830.
181. Hioki, N., et al., *Bacterial Cellulose ; as a New Material for Papermaking.* JAPAN TAPPI JOURNAL, 1995. 49(4): p. 718-723.
182. Balea, A., et al., *Valorization of Corn Stalk by the Production of Cellulose Nanofibers to Improve Recycled Paper Properties.* BioResources, 2016. 11(2): p. 3416-3431.
183. Cao, Y., et al., *The influence of cellulose nanocrystal additions on the performance of cement paste.* Cement and Concrete Composites, 2015. 56: p. 73-83.
184. Mohammadkazemi, F., R. Aguiar, and N. Cordeiro, *Improvement of bagasse fiber-cement composites by addition of bacterial nanocellulose: an inverse gas chromatography study.* Cellulose, 2017. 24(4): p. 1803-1814.
185. Hu, L. and Y. Cui, *Energy and environmental nanotechnology in conductive paper and textiles.* Energy & Environmental Science, 2012. 5(4): p. 6423-6435.
186. He, X.J. and H.M. Hwang, *Nanotechnology in food science: Functionality, applicability, and safety assessment.* Journal of Food and Drug Analysis, 2016. 24(4): p. 671-681.
187. Azeredo, H.M.C., M.F. Rosa, and L.H.C. Mattoso, *Nanocellulose in bio-based food packaging applications.* Industrial Crops and Products, 2017. 97: p. 664-671.
188. Corral, M.L., et al., *Bacterial nanocellulose as a potential additive for wheat bread.* Food Hydrocolloids, 2017. 67: p. 189-196.
189. Yu, S.Y. and K.W. Lin, *Influence of Bacterial Cellulose (nata) on the Physicochemical and Sensory Properties of Frankfurter.* Journal of Food Science, 2014. 79(6): p. C1117-C1122.
190. Carpenter, A.W., C.F. de Lannoy, and M.R. Wiesner, *Cellulose Nanomaterials in Water Treatment Technologies.* Environmental Science & Technology, 2015. 49(9): p. 5277-5287.
191. Ge, S.J., et al., *Microalgae Recovery from Water for Biofuel Production Using CO2-Switchable Crystalline Nanocellulose.* Environmental Science & Technology, 2016. 50(14): p. 7896-7903.
192. Baah-Dwomoh, A., et al., *The feasibility of using irreversible electroporation to introduce pores in bacterial cellulose scaffolds for tissue engineering.* Applied Microbiology and Biotechnology, 2015. 99(11): p. 4785-4794.
193. Alkhatib, Y., et al., *Controlled extended octenidine release from a bacterial nanocellulose/Poloxamer hybrid system.* European Journal of Pharmaceutics and Biopharmaceutics, 2017. 112: p. 164-176.
194. Kawaguchi, I. and K. Nakamura, *Make-up tissue paper for removing cosmetics, comprises glycerin impregnated into a tissue paper which consists of pulp fiber, and*

bacterial cellulose entangled in the pulp interfiber forming a network structure. 2007, NAKAMURA K (NAKA-Individual) KAWAGUCHI I (KAWA-Individual). p. 10.
195. Sun, X.X., et al., *Cellulose Nanofibers as a Modifier for Rheology, Curing and Mechanical Performance of Oil Well Cement.* Scientific Reports, 2016. 6: p. 9.
196. Pirich, C.L., et al., *Piezoelectric immunochip coated with thin films of bacterial cellulose nanocrystals for dengue detection.* Biosensors & Bioelectronics, 2017. 92: p. 47-53.
197. Hoeng, F., A. Denneulin, and J. Bras, *Use of nanocellulose in printed electronics: a review.* Nanoscale, 2016. 8(27): p. 13131-13154.
198. Dutta, S., et al., *3D network of cellulose-based energy storage devices and related emerging applications.* Materials Horizons, 2017. 4(4): p. 522-545.
199. Chen, G.Q., et al., *Bioconversion of Waste Fiber Sludge to Bacterial Nanocellulose and Use for Reinforcement of CTMP Paper Sheets.* Polymers, 2017. 9(9): p. 14.
200. Aulin, C., M. Gallstedt, and T. Lindstrom, *Oxygen and oil barrier properties of microfibrillated cellulose films and coatings.* Cellulose, 2010. 17(3): p. 559-574.
201. Basta, A.H. and H. El-Saied, *Performance of improved bacterial cellulose application in the production of functional paper.* Journal of Applied Microbiology, 2009. 107(6): p. 2098-2107.
202. Wei, B., G.A. Yang, and F. Hong, *Preparation and evaluation of a kind of bacterial cellulose dry films with antibacterial properties.* Carbohydrate Polymers, 2011. 84(1): p. 533-538.
203. Osong, S.H., S. Norgren, and P. Engstrand, *Processing of wood-based microfibrillated cellulose and nanofibrillated cellulose, and applications relating to papermaking: a review.* Cellulose, 2016. 23(1): p. 93-123.
204. Boufi, S., et al., *Nanofibrillated cellulose as an additive in papermaking process: A review.* Carbohydrate Polymers, 2016. 154: p. 151-166.
205. Diab, M., et al., *Biobased polymers and cationic micro-fibrillated cellulose as retention and drainage aids in papermaking: Comparison between softwood and bagasse pulps.* Ind. Crops. Prod., 2015. 72: p. 34-45.
206. Santos, S.M., et al., *Paper reinforcing by in situ growth of bacterial cellulose.* Journal of Materials Science, 2017. 52(10): p. 5882-5893.
207. Balea, A., et al., *Effect of nanofibrillated cellulose to reduce linting on high filler-loaded recycled papers.* Appita J, 2016. 69(2): p. 148-156.
208. Du, X., et al., *Nanocellulose-based conductive materials and their emerging applications in energy devices - A review.* Nano Energy, 2017. 35: p. 299-320.
209. Cowie, J., et al., *Market projections of cellulose nanomaterial-enabled products--Part 2: Volume estimates.* TAPPI JOURNAL, Volume 13 Number 6, 2014; pp. 57-69., 2014. 13(6): p. 57-69.
210. Richmond, F., *Cellulose nanofibers use in coated paper*. 2014: The University of Maine.
211. Peng, B.L., et al., *Chemistry and applications of nanocrystalline cellulose and its derivatives: a nanotechnology perspective.* Canadian Journal of Chemical Engineering, 2011. 89(5): p. 1191-1206.
212. Delgado-Aguilar, M., et al., *Approaching a Low-Cost Production of Cellulose Nanofibers for Papermaking Applications.* Bioresources, 2015. 10(3): p. 5345-5355.
213. Dufresne, A., *Preparation of cellulose nanocrystals*, in *Nanocellulose: From Nature to High Performance Tailored Materials*. 2012, Walter de Gruyter.
214. Cacicedo, M.L., et al., *Progress in bacterial cellulose matrices for biotechnological applications.* Bioresource Technology, 2016. 213: p. 172-180.
215. Campano, C., et al., *Low-fibrillated Bacterial Cellulose Nanofibers as a sustainable additive to enhance recycled paper quality.* International Journal of Biological Macromolecules, 2018.

216. Rampazzo, R., et al., *Cellulose Nanocrystals from Lignocellulosic Raw Materials, for Oxygen Barrier Coatings on Food Packaging Films.* Packaging Technology and Science, 2017. 38(10): p. 645-661.
217. Lavoine, N., J. Bras, and I. Desloges, *Mechanical and Barrier Properties of Cardboard and 3D Packaging Coated with Microfibrillated Cellulose.* Journal of Applied Polymer Science, 2014. 131(8): p. 11.
218. Ferrer, A., L. Pal, and M. Hubbe, *Nanocellulose in packaging: Advances in barrier layer technologies.* Industrial Crops and Products, 2017. 95: p. 574-582.
219. Bedane, A.H., et al., *Water vapor transport properties of regenerated cellulose and nanofibrillated cellulose films.* Journal of Membrane Science, 2015. 493: p. 46-57.
220. Raj, P., et al., *Effect of polyelectrolyte morphology and adsorption on the mechanism of nanocellulose flocculation.* Journal of Colloid and Interface Science, 2016. 481: p. 158-167.
221. Raj, P., et al., *Effect of cationic polyacrylamide on the processing and properties of nanocellulose films.* Journal of Colloid and Interface Science, 2015. 447: p. 113-119.
222. Petroudy, S.R.D., et al., *Effects of bagasse microfibrillated cellulose and cationic polyacrylamide on key properties of bagasse paper.* Carbohydrate Polymers, 2014. 99: p. 311-318.
223. Cherhal, F., F. Cousin, and I. Capron, *Influence of charge density and ionic strength on the aggregation process of cellulose nanocrystals in aqueous suspension, as revealed by small-angle neutron scattering.* Langmuir, 2015. 31(20): p. 5596-5602.
224. Phan-Xuan, T., et al., *Aggregation behavior of aqueous cellulose nanocrystals: the effect of inorganic salts.* Cellulose, 2016. 23(6): p. 3653-3663.
225. Gao, W.-H., et al., *Properties of bacterial cellulose and its influence on the physical properties of paper.* BioResources, 2010. 6(1): p. 144-153.
226. Martinez-Sanz, M., A. Lopez-Rubio, and J.M. Lagaron, *Optimization of the Dispersion of Unmodified Bacterial Cellulose Nanowhiskers into Polylactide via Melt Compounding to Significantly Enhance Barrier and Mechanical Properties.* Biomacromolecules, 2012. 13(11): p. 3887-3899.
227. Fabra, M.J., et al., *Improving the barrier properties of thermoplastic corn starch-based films containing bacterial cellulose nanowhiskers by means of PHA electrospun coatings of interest in food packaging.* Food Hydrocolloids, 2016. 61: p. 261-268.
228. Xiang, Z., et al., *The reinforcement mechanism of bacterial cellulose on paper made from woody and non-woody fiber sources.* Cellulose, 2017. 24(11): p. 5147-5156.
229. Ahola, S., et al., *Effect of polymer adsorption on cellulose nanofibril water binding capacity and aggregation.* Bioresources, 2008. 3(4): p. 1315-1328.
230. Manninen, M., et al., *The effect of microfibrillated cellulose addition on drying shrinkage and dimensional stability of wood-free paper.* Nordic Pulp & Paper Research Journal, 2011. 26(3): p. 297-305.
231. Merayo, N., et al., *Interactions between cellulose nanofibers and retention systems in flocculation of recycled fibers.* Cellulose, 2017. 24(2): p. 677-692.
232. Ankerfors, M., T. Lindstrom, and G.G. Nordmark, *The effects of different types of wet-end added microfibrillated celluloses on the properties of paper made from bleached kraft pulp.* Nordic Pulp & Paper Research Journal, 2017. 32(3): p. 336-345.
233. Lenze, C.J., et al., *Intact and broken cellulose nanocrystals as model nanoparticles to promote dewatering and fine-particle retention during papermaking.* Cellulose, 2016. 23(6): p. 3951-3962.
234. Kumar, A., S. Singh, and A. Singh, *Comparative study of cellulose nanofiber blending effect on properties of paper made from bleached bagasse, hardwood and softwood pulps.* Cellulose, 2016. 23(4): p. 2663-2675.
235. Bharimalla, A.K., et al., *Micro/nano-fibrillated cellulose from cotton linters as strength additive in unbleached kraft paper: Experimental, semi-empirical, and mechanistic studies.* BioResources, 2017. 12(3): p. 5682-5696.

236. Yingkamhaeng, N., I. Intapan, and P. Sukyai, *Fabrication and Characterisation of Functionalised Superparamagnetic Bacterial Nanocellulose Using Ultrasonic-Assisted In Situ Synthesis.* Fibers and Polymers, 2018. 19(3): p. 489-497.
237. Surma-Slusarska, B., D. Danielewicz, and S. Presler, *Properties of Composites of Unbeaten Birch and Pine Sulphate Pulps with Bacterial Cellulose.* Fibres & Textiles in Eastern Europe, 2008. 16(6): p. 127-129.
238. Surma-Slusarska, B., S. Presler, and D. Danielewicz, *Characteristics of Bacterial Cellulose Obtained from Acetobacter Xylinum Culture for Application in Papermaking.* Fibres & Textiles in Eastern Europe, 2008. 16(4): p. 108-111.
239. Morseburg, K. and G. Chinga-Carrasco, *Assessing the combined benefits of clay and nanofibrillated cellulose in layered TMP-based sheets.* Cellulose, 2009. 16(5): p. 795-806.
240. Aulin, C., G. Salazar-Alvarez, and T. Lindstrom, *High strength, flexible and transparent nanofibrillated cellulose-nanoclay biohybrid films with tunable oxygen and water vapor permeability.* Nanoscale, 2012. 4(20): p. 6622-6628.
241. Pajari, H., et al. *Replacement of synthetic binders with nanofibrillated cellulose in board coating: pilot scale studies*. in *TAPPI international conference on nanotechnology for revenwable materials*. 2012.
242. Balea, A., et al., *Effect of Bleached Eucalyptus and Pine Cellulose Nanofibers on the Physico-Mechanical Properties of Cartonboard.* BioResources, 2016. 11(4): p. 8123-8138.
243. Hult, E.-L., M. Iotti, and M. Lenes, *Efficient approach to high barrier packaging using microfibrillar cellulose and shellac.* Cellulose, 2010. 17(3): p. 575-586.
244. Lin, N. and A. Dufresne, *Nanocellulose in biomedicine: Current status and future prospect.* European Polymer Journal, 2014. 59: p. 302-325.
245. Dumanli, A.G., *Nanocellulose and its Composites for Biomedical Applications.* Current Medicinal Chemistry, 2017. 24(5): p. 512-528.
246. Sharma, S., et al., *Thermally enhanced high performance cellulose nano fibril barrier membranes.* Rsc Advances, 2014. 4(85): p. 45136-45142.
247. Yuan, J.X., et al., *Effect of Wet-End Additives on the Results of Alkyl Ketene Dimer Sizing after Adding Bacterial Cellulose.* Bioresources, 2016. 11(4): p. 9280-9289.
248. Kisonen, V., et al., *Composite films of nanofibrillated cellulose and O-acetyl galactoglucomannan (GGM) coated with succinic esters of GGM showing potential as barrier material in food packaging.* Journal of Materials Science, 2015. 50(8): p. 3189-3199.
249. Sehaqui, H., et al., *Cellulose Nanofiber Orientation in Nanopaper and Nanocomposites by Cold Drawing.* Acs Applied Materials & Interfaces, 2012. 4(2): p. 1043-1049.
250. Reising, A.B., R.J. Moon, and J.P. Youngblood, *Effect of particle alignment on mechanical properties of neat cellulose nanocrystal films.* J-for-Journal of Science & Technology for Forest Products and Processes, 2012. 2(6): p. 32-41.
251. Torres-Rendon, J.G., et al., *Mechanical Performance of Macrofibers of Cellulose and Chitin Nanofibrils Aligned by Wet-Stretching: A Critical Comparison.* Biomacromolecules, 2014. 15(7): p. 2709-2717.
252. Hakansson, K.M.O., et al., *Hydrodynamic alignment and assembly of nanofibrils resulting in strong cellulose filaments.* Nature Communications, 2014. 5: p. 10.
253. Cranston, E.D. and D.G. Gray, *Formation of cellulose-based electrostatic layer-by-layer films in a magnetic field.* Science and Technology of Advanced Materials, 2006. 7(4): p. 319-321.
254. Gindl, W., et al., *Cellulose in Never-Dried Gel Oriented by an AC Electric Field.* Biomacromolecules, 2009. 10(5): p. 1315-1318.
255. Aguado, R., et al., *Cationic cellulosic derivatives as flocculants in papermaking.* Cellulose, 2017. 24(7): p. 3015-3027.

256. Gaddy, J.L. and E.C. Clausen, *Method of separation of sugars and concentrated sulfuric acid*. 1986, Google Patents.
257. Ottesen, V., K. Syverud, and O.W. Gregersen, *Mixing of cellulose nanofibrils and individual furnish components: Effects on paper properties and structure.* Nordic Pulp & Paper Research Journal, 2016. 31(3): p. 441-447.
258. Segal, L., et al., *An Empirical Method for Estimating the Degree of Crystallinity of Native Cellulose Using the X-Ray Diffractometer.* Textile Research Journal, 1959. 29(10): p. 786-794.
259. Tasman, J.E. and V. Berzins, *The Permanganate Consumption of Pulp Materials.* Tappi, 1957. 40(9): p. 691-704.
260. Pérez-Mendoza, D., et al., *Identification of functional mob regions in Rhizobium etli: evidence for self-transmissibility of the symbiotic plasmid pRetCFN42d.* Journal of bacteriology, 2004. 186(17): p. 5753-5761.
261. Merayo, N., et al., *Synergies between cellulose nanofibers and retention additives to improve recycled paper properties and the drainage process.* Cellulose, 2017. 24(7): p. 2987-3000.
262. Campano, C., et al., *Mechanical and chemical dispersion of nanocelluloses to improve their reinforcing effect on recycled paper.* Cellulose, 2018. 25(1): p. 269-280.
263. Sartor, M., *Dynamic light scattering.* University of California, San Diego, 2003: p. 2-21.
264. Farina, A., *Principles and methods in landscape ecology: towards a science of the landscape*. Vol. 3. 2008: Springer Science & Business Media.
265. Frohn, R.C. and R.D. Lopez, *Remote Sensing for Landscape Ecology: New Metric Indicators: Monitoring, Modeling, and Assessment of Ecosystems*. 2017: CRC Press.
266. Bogaert, J., et al., *Alternative area-perimeter ratios for measurement of 2D shape compactness of habitats.* Applied Mathematics and Computation, 2000. 111(1): p. 71-85.
267. Chakraborti, R.K., et al., *Changes in fractal dimension during aggregation.* Water Research, 2003. 37(4): p. 873-883.
268. Logan, B.E. and J.R. Kilps, *Fractal dimensions of aggregates formed in different fluid mechanical environments.* Water Research, 1995. 29(2): p. 443-453.
269. Gorczyca, B. and J. Ganczarczyk, *Image analysis of alum coagulated mineral suspensions.* Environmental Technology, 1996. 17(12): p. 1361-1369.
270. Blott, S.J. and K. Pye, *GRADISTAT: a grain size distribution and statistics package for the analysis of unconsolidated sediments.* Earth surface processes and Landforms, 2001. 26(11): p. 1237-1248.
271. Kodinariya, T.M. and P.R. Makwana, *Review on determining number of Cluster in K-Means Clustering.* International Journal of Computer Applications, 2013. 1(6): p. 90-95.
272. Kanungo, T., et al., *An efficient k-means clustering algorithm: Analysis and implementation.* IEEE Transactions on Pattern Analysis & Machine Intelligence, 2002(7): p. 881-892.
273. Pedregosa, F., et al., *Scikit-learn: Machine learning in Python.* Journal of machine learning research, 2011. 12(Oct): p. 2825-2830.
274. Geurts, P., D. Ernst, and L. Wehenkel, *Extremely randomized trees.* Machine learning, 2006. 63(1): p. 3-42.
275. Louppe, G., et al. *Understanding variable importances in forests of randomized trees*. in *Advances in neural information processing systems*. 2013.
276. Kumar, V., et al., *Real-Time Particle Size Analysis Using Focused Beam Reflectance Measurement as a Process Analytical Technology Tool for a Continuous Granulation-Drying-Milling Process.* Aaps Pharmscitech, 2013. 14(2): p. 523-530.
277. Blanco, A., et al., *Focused beam reflectant measurement as a tool to measure flocculation.* Tappi Journal, 2002. 1(10): p. 14-20.

278. Yoon, S.Y. and Y.L. Deng, *Flocculation and reflocculation of clay suspension by different polymer systems under turbulent conditions.* Journal of Colloid and Interface Science, 2004. 278(1): p. 139-145.
279. Lopez-Exposito, P., C. Negro, and A. Blanco, *Direct estimation of microalgal flocs fractal dimension through laser reflectance and machine learning.* Algal Res, 2019. 37: p. 240-247.
280. Hassan, E.A., M.L. Hassan, and K. Oksman, *Improving bagasse pulp paper sheet properties with microfibrillated cellulose isolated from xylanase-treated bagasse.* Wood and Fiber Science, 2011. 43(1): p. 76-82.
281. Jonoobi, M., A.P. Mathew, and K. Oksman, *Producing low-cost cellulose nanofiber from sludge as new source of raw materials.* Industrial Crops and Products, 2012. 40: p. 232-238.
282. Okar, D.A. and K. Zangger, *Hydrogen bonding in the fructose-2,6-bisphosphatase reaction correlates with activity.* Faseb Journal, 2007. 21(6): p. A1014-A1014.
283. Roman, M. and W.T. Winter, *Effect of sulfate groups from sulfuric acid hydrolysis on the thermal degradation behavior of bacterial cellulose.* Biomacromolecules, 2004. 5(5): p. 1671-1677.
284. Lu, P. and Y.-L. Hsieh, *Preparation and characterization of cellulose nanocrystals from rice straw.* Carbohydrate Polymers, 2012. 87(1): p. 564-573.
285. Wang, N., E. Ding, and R. Cheng, *Thermal degradation behaviors of spherical cellulose nanocrystals with sulfate groups.* Polymer, 2007. 48(12): p. 3486-3493.
286. Suhr, M., et al., *Best Available Techniques (BAT) Reference Document for the Production of Pulp, Paper and Board*, in *JRC Science and policy reports*, E. Commission, Editor. 2015, Institute for Prospective Technological Studies: Seville, Spain. p. 906.
287. HadjSadok, A., et al., *Characterisation of sodium caseinate as a function of ionic strength, pH and temperature using static and dynamic light scattering.* Food Hydrocolloids, 2008. 22(8): p. 1460-1466.
288. Gaudreault, R., et al., *Flocculation kinetics of precipitated calcium carbonate.* Colloids and Surfaces a-Physicochemical and Engineering Aspects, 2009. 340(1-3): p. 56-65.
289. Chen, D.Z. and T.G.M. van de Ven, *Flocculation kinetics of precipitated calcium carbonate induced by electrosterically stabilized nanocrystalline cellulose.* Colloids and Surfaces a-Physicochemical and Engineering Aspects, 2016. 504: p. 11-17.
290. Blanco, A., C. Negro, and J. Tijero, *Developments of flocculation in papermaking*. 2001: PIRA International.
291. Bergaya, F. and G. Lagaly, *General introduction: clays, clay minerals, and clay science.* Developments in clay science, 2006. 1: p. 1-18.
292. Wu, M.R. and T.G.M. van de Ven, *Flocculation and reflocculation: Interplay between the adsorption behavior of the components of a dual flocculant.* Colloids and Surfaces A: Physicochemical and Engineering Aspects, 2009. 341(1): p. 40-45.

7. Annex: Original publications

PUBLICATION I

Enhancement of the fermentation process and properties of bacterial cellulose: a review

Cristina Campano, Ana Balea, Angeles Blanco, Carlos Negro

Cellulose (2016) 23:57–91

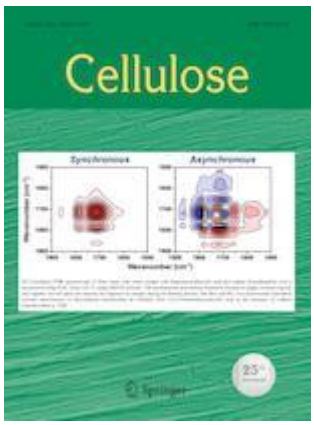

Impact factor 2016: ***3.417***

JCR, Materials Science, paper & wood, 1 out of 21, ***Q1***

Cellulose (2016) 23:57–91
DOI 10.1007/s10570-015-0802-0

REVIEW PAPER

Enhancement of the fermentation process and properties of bacterial cellulose: a review

Cristina Campano · Ana Balea · Angeles Blanco · Carlos Negro

Received: 1 August 2015 / Accepted: 26 October 2015 / Published online: 18 November 2015

Abstract Cellulose produced by bacteria (BC) has attracted increasing interest in view of its superior properties with respect to nanofibrillar structure, high purity and biocompatibility. Despite the intensive research, industrial production of BC has been limited, due to the low productivity, and the high cost of raw materials. This paper reviews the new approaches tried recently to get BC production feasible at large scale as the reduction in the quality of raw materials, the use of by-products and the optimization of the culture method. In addition, the new trends of enhancing specific properties of BC by varying culture conditions or by using additives have been reviewed. Thus, the paper presents how to obtain and enhance a desired property of BC for a specific use. This new approach will help researchers to develop new ideas in this field which will favour the commercialization of products made with BC and their industrial application.

Keywords Bacterial cellulose · *Gluconacetobacter xylinus* · Nanocellulose · *Gluconacetobacter hansenii* · *Komagataeibacter*

C. Campano · A. Balea · A. Blanco (✉) · C. Negro
Department of Chemical Engineering, Complutense University of Madrid, Avda. Complutense s/n, 28040 Madrid, Spain
e-mail: ablanco@ucm.es

Introduction

Cellulose produced by bacteria, has grown in popularity since its discovery in 1886 due to its special properties, such as high purity, an ultrafine and highly crystalline network structure, a superior mechanical strength, biodegradability, biocompatibility, large water-holding capacity (WHC) and good chemical stability (Santos et al. 2015; Shah et al. 2013). Because of these properties, BC is a promising material for many applications (Iguchi et al. 2000). These include strength reinforcement of polymeric materials or paper (Miao and Hamad 2013; Zimmermann et al. 2010), a thickening agent and food stabilizer (Shi et al. 2014), food packaging (Spence et al. 2010); biomaterial for manufacturing cosmetics (Kawaguchi and Nakamura 2007), artificial skin (Fu et al. 2013; Kingkaew et al. 2014), artificial blood vessels or tissue engineering (Gao et al. 2012; Klemm et al. 2001; Ramani and Sastry 2014; Scherner et al. 2014); diaphragms for loudspeakers (Ciechanska et al. 2002; Nishi et al. 1990) and for the preparation of optically transparent films (Palaninathan et al. 2014), electric conductors (Muller et al. 2012; Yoon et al. 2006) or magnetic materials (Charreau et al. 2013; Santos et al. 2015; Zhang et al. 2011).

BC was firstly described by Brown (1886), when he found a jelly-like strong membrane on the surface of a vinegar fermentation broth. That strain was called *Acetobacter xylinus*, but there are other bacteria able to produce cellulose, such as *Agrobacterium* (Barnhart

et al. 2013; Matthysse et al. 2005), *Pseudomonas* (Ude et al. 2006), *Rhizobium* (Ausmees et al. 1999; Robledo et al. 2012) and *Sarcina* (Yang et al. 2013).

Several studies have been developed to produce BC on an industrial scale, with a continuous or semicontinuous process, low-cost raw materials and small production of by-products. It is also necessary to have a high conversion of the carbon source into cellulose and a high BC productivity (Çakar et al. 2014). In order to know how to improve the fermentation process, some explanations about the mechanism of BC production have been made (Chawla et al. 2009; Huang et al. 2014b; Jonas and Farah 1998; Klemm et al. 2001; Pecoraro et al. 2007; Ross et al. 1991; Vandamme et al. 1998). The general idea is that for each pore in the cell walls of bacteria, a cellulose chain is produced where 10–15 of them join together to create a nanofibre with a diameter of approximately 1.5 nm (Ross et al. 1991). They self-assembly to form microfibres and then fibrillar ribbons are produced with an approximate width of 50–80 nm (Vitta and Thiruvengadam 2012). In Fig. 1, a strand (24 nm wide) is represented between the arrowheads, and a ribbon formed by some of them is being assembled. An overview of the network produced by bacteria is shown in Fig. 2.

Generally, the main factors affecting the composition, morphology and properties of BC are culture medium (nutrients and others), reactor design, temperature, oxygen availability, pH, final state and additives (Hu et al. 2014; Lee and Bismarck 2012; Ul-Islam et al. 2013b). The optimal design of the medium is not only important for the cell growth of microorganisms, but also for the stimulation of the cellulose formation (Chawla et al. 2009). Another key factor to improve is the reduction of the raw material costs. Some researchers are trying to increase or at least keep the productivity and yield with less expensive nutrients, e.g. by-products of other production processes. Static culture (SC) reactors have been largely used because of their high productivity, but some associated problems, like the large time of culture and the space required (Chawla et al. 2009; Song et al. 2009), support the use of other types of reactors: a rotating disk bioreactor (RDB) (Kim et al. 2007; Krystynowicz et al. 2002; Lin et al. 2014); a stirred tank reactor with a spin filter (Jung et al. 2007); a biofilm reactor (Cheng et al. 2009a, 2010, 2011); a spherical type bubble column bioreactor (Choi et al. 2009; Moon et al. 2006; Song et al. 2009); and a trickling bed reactor (TBR) (Lu and Jiang 2014).

There are many research articles and reviews about the characterization and properties of BC and its possible applications (Huang et al. 2014b; Lin et al. 2013a). However, the focus of this review is different since we consider how to obtain and enhance a desired characteristic for a specific use. New isolated bacterial strains, some of them genetically modified, to increase the productivity, have been reviewed. Improvements of the process, including new nutrient media, novel reactors and additives to increase the productivity, have also been compared with the use of standard media. Finally, a study of the properties of BC produced by different methods and the enhancement of specific characteristics and applications has been made. It is believed that this new approach about

Fig. 1 Scanning electron microscopy (SEM) of a *Komagataeibacter xylinus* bacteria producing a cellulose fibre (Reprinted from Hirai et al. 2002 with permission from Springer)

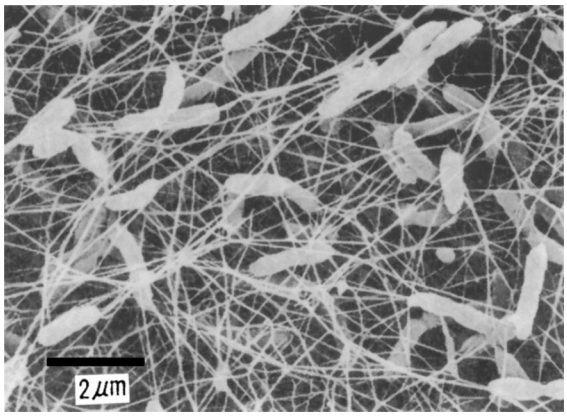

Fig. 2 SEM of bacteria producing a bacterial cellulose pellicle (Reprinted from Iguchi et al. 2000 with permission from Springer)

processing and applying BC will be a great advantage for those doing research in this field.

Bacterial strains characteristics, new trends in cellulose-negative mutants and genetic modification

Characteristics and behavior of bacterial strains

The main factor related to the productivity of BC is the type of bacteria (Zeng et al. 2014). Therefore, a review of the different characteristics and behavior of the BC producer strains isolated so far has been undertaken.

The bacterium *Acetobacter xylinum* (also known as *Gluconacetobacter xylinus*) (Oikawa et al. 1995a; Pecoraro et al. 2007) is currently called *Komagataeibacter (K). xylinus* (Kumbhar et al. 2015; Tsouko et al. 2015). Several attempts have been made to isolate this bacteria and other strains from fruits (Aydin and Aksoy 2014; Dellaglio et al. 2005; Kadere et al. 2008; Kojima et al. 1998; Lisdiyanti et al. 2001; Suwanposri et al. 2013), flowers (Lisdiyanti et al. 2001), fermented foods (Al-Gelawi et al. 2012; Aydin and Aksoy 2014; Hungund and Gupta 2010b; Lisdiyanti et al. 2001; Park et al. 2003), beverages (Jia et al. 2004), temple wash waters (Raghunathan 2013) and vinegar (Al-Gelawi et al. 2012; Aydin and Aksoy 2009, 2014; Castro et al. 2012; Kim et al. 2006; Sokollek et al. 1998; Son et al. 2002). The main characteristics of these isolates are showed in Table 1. The purpose of these investigations was to find a new type of bacteria with a higher yield of cellulose.

K. xylinus continues being the highest producer of BC so far. It is strictly aerobic, non-photosynthetic and able to transform glucose and other organic substrates into cellulose in a few days (Kongruang 2008). It is unique in its family for being able to convert carbohydrates into acetic acid during bacterial growth and cellulose production (Kongruang 2008). Because of the respiratory metabolism of *K. xylinus*, it oxidizes ethanol to acetic acid and converts glucose into gluconic acid. All of these acid formations produce a decrease in the pH of the culture medium, especially under batch SC (Ha et al. 2011; Kongruang 2008; Lin et al. 2013a). Moreover, the pH hardly varies when we talk about fed-batch cultivation. The reason could be the constant addition of fresh medium (Lin et al. 2013a; Shezad et al. 2010).

As it is shown in Table 1, all cellulose producing bacteria are gram-negative, rod-shaped and non-motile, except *K. persimmonis*, which presents motility (Hungund and Gupta 2010a). Almost all of them oxidize ethanol and produce acid from glucose and other sugars. Most of these bacteria need to be studied in more depth to evaluate the entire metabolic processes, both when they are growing or producing cellulose.

It is believed that the reason why these types of bacteria produce cellulose is because they try to protect themselves from ultraviolet (UV) radiation and harsh chemical environments (Huang et al. 2014b). When a new production method is developed, optimization of the oxygen demand is required, because of their aerobic mechanism.

Management of the cellulose-negative mutant

It is a general belief that agitated (AC) and aerated systems produce a decrease in the BC production because of the action of cellulose-negative mutants (Cel−), which become more enriched than the cellulose producing cells (Cel+) because they grow faster (Ha et al. 2008; Moon et al. 2006). Cel− are produced due to the shear stress generated either in these cultures or under these conditions and favour the production of by-products, which are different depending on the bacterial strain (Ha et al. 2008; Krystynowicz et al. 2002). However there is some controversy since Aydin and Aksoy (2014) analyzed the mutant ratio (number of Cel−/number of total cells) in these systems, increasing with the shaking rate and the number of batch, obtaining a maximum of 0.64 in the fifth batch with a speed of 200 rpm. However, Jung et al. (2005), using *K. hansenii PJK*, observed that with an impeller speed over 500 rpm, the population of Cel− disappeared.

In the case of *K. xylinus*, the by-product is a water-soluble polysaccharide (WSPS), usually called acetan, whose structure is similar to that of xanthan. It consists of glucose, mannose, glucuronic acid and rhamnose in a ratio of 4:1:1:1 (Ishida et al. 2002). However, when we talk about *K. hansenii*, a water-soluble oligosaccharide (WSOS) is the by-product (Jung et al. 2007; Lee et al. 2014; Park et al. 2003). Their colonies are distinguished by being bigger, round and mucous on Hestrin and Schramm medium (HS) in agar plates (Aydin and Aksoy 2014).

Table 1 Characteristics of bacterial cellulose producer strains isolated from different sources

Genus	Specie	Strain	Strain origin	Characteristics	Morphology	Colonies	Oxidation	Source of acid formation	Productivity (g/L)	References
Komagataeibacter	Xylinus	BPR 2002	Grape	Gram-negative, non-motile, aerobic, in pairs and in chain	Ellipsoidal to rod shapes, 0.6–0.8 × 1.0–3.0 μm	Cream to beige color and 2.5 to 3 mm in diameter	Ethanol, acetate	D-Glucose	–	Kojima et al. (1998)
		BPR 2003	Melon					–	–	Kojima et al. (1998)
		AS6	Wastes of vinegar fermentation					D-Glucose, sucrose, galactose, mannose and xylose	0.251	Aydin and Aksoy (2009)
		KJ-1	Rotten grape					–	7.2	Son et al. (2002)
		–	Vinegar and rotting fruits					D-Glucose, fructose, mannose and maltose.	5.1	Al-Gelawi et al. (2012)
	Hansenii	P2A	Vinegar fermentation waste, vinegar samples, and fresh and rotten fruits	Gram-negative, straight or slightly curved, singly or in pairs, non-motile	Rod shaped, 0.83–0.94 × 2.08–4.16 μm	Smooth, circular, convex, mucous, and cream- to beige-colored	Ethanol, acetate, lactate	D-Glucose, sucrose, galactose, mannose, sorbitol, rhamnose and xylose.	3.25	Aydin and Aksoy (2014), Park et al. (2003)
		AS7, AS14	Wastes of vinegar fermentation						0.187; 0.263	Aydin and Aksoy (2009)
		CGMCC 3917	Homemade vinegar/mutagenesis						–	Ge et al. (2011)
		–	Beleric myrobalan, fetid passionflower, lady's finger banana, star fruit, wild lemon and lychee						0.8	Suwanposri et al. (2013)
	Swingsii	DST GL01T	Apple fruit juice	Gram-negative, non-motile, occurring singly or in pairs	0.9 × 1.5–2.5 μm, coccoid rods	Pale yellow, smooth, viscous, convex, dense, with circular or irregular shape	–	D-Glucose, D-sorbitol, L-rhamnose	–	Dellaglio et al. (2005)
		–	Sapodilla and water melon						0.6	Suwanposri et al. (2013)
	Rhaeticus	DST GL02T	Apple fruit juice	Gram-negative, non-motile, occurring singly, in pairs or in short chains	0.9 × 1.5–2.5 μm, coccoid rods	Pale yellow, smooth, viscous, convex, dense, with circular or irregular shape	–	D-glucose, D-sorbitol, D-Arabinose	–	Dellaglio et al. (2005)
		–	Rambutan						0.5	Suwanposri et al. (2013)

Table 1 continued

Genus	Specie	Strain	Strain origin	Characteristics	Morphology	Colonies	Oxidation	Source of acid formation	Productivity (g/L)	References
	Oxydans	TQ-B2	Malt extract	Gram-negative	0.5–0.8 × 0.9–4.2 μm, ellipsoids or rods	–	Ethanol	D-Glucose	2.41	Jia et al. (2004)
	Oboediens	–	Governor's plum, mamao and water melon	Gram-negative and occurred singly or in pairs	–	Pale yellow, smooth, viscous, convex, dense, with circular or irregular shape	–	D-Glucose, D-sorbitol	0.7	Suwanposri et al. (2013)
	Persimmonis	GH-2	*Nata* (a desert)	Round, gram-negative, positive motility.	Thin long rod, 0.5 × 1.6 μm	Smooth to rough surface, pale white, translucent	–	–	6.71	Hungund and Gupta (2010a)
	–	DR-1	Temple wash waters	Gram-negative, individuals, pairs, chains or small clusters, motile, obligate aerobe	Short rods/cocco-bacilli in shape and mono and diplo-bacilli in arrangement under microscope	Circular, convex, regular shape, 3 mm diameter	–	D-Glucose, D-xylose, D-galactose, glycerol, lactose, maltose and sucrose	2.93	Raghunathan (2013)
	–	–	Coconut wine (mnazi)	Gram variable, strictly aerobic, motile on molten agar	Ellipsoidal to rod-shaped, straight or slightly curved	–	Ethanol, acetate, lactate	D-glucose, xylose, ribose, trehalose, melibiose, mannose and galactose.	–	Kadere et al. (2008)
	–	–	Grape, java plum, mangosteen, mamao, papaya, rambutan, sugar apple and wild lemon.	Gram-negative and occurred singly or in pairs	–	Pale yellow, smooth, viscous, convex, dense, with circular or irregular shape, rod-shaped	–	D-glucose, D-sorbitol	1	Suwanposri et al. (2013)
	–	–	Lychee and fetid passion flower	Gram-negative and occurred singly or in pairs	–	Pale yellow, smooth, viscous, convex, dense, with circular or irregular shape, rod-shaped	–	D-glucose, D-sorbitol	1	Suwanposri et al. (2013)
Enterobacter	Amnigenus	GH-1	Rotten apple	Gram-negative, ocurred singly, positive motility	Rod shaped, 0.5 × 1.5 μm	Round, raised elevation, smooth, cream color, translucent	–	–	4.1	Hungund and Gupta (2010b)

– means that these data are not mentioned in the selected article

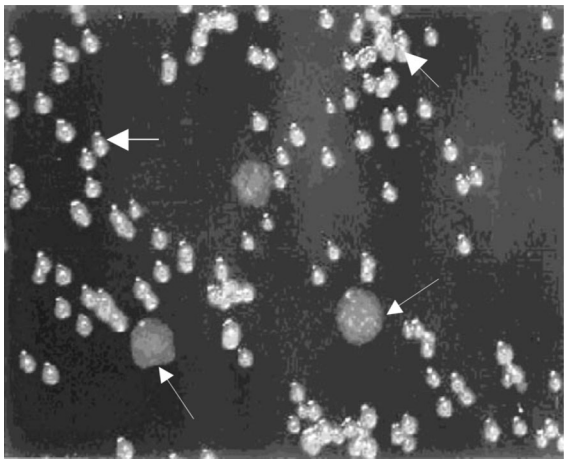

Fig. 3 Morphology of *Komagataeibacter xylinus E25* colonies grown on HS agar. *Thick arrows* indicate colonies of cellulose producing cells and thin arrows indicate colonies of cellulose negative mutants (Reprinted from Krystynowicz et al. 2002 with permission from Springer)

Because of the different morphology between Cel+ and Cel− colonies, as shown in Fig. 3, some authors have determined the amount of acetan in the produced pellicle to determine the purity of BC (Nguyen et al. 2008). In the experiment of Nguyen et al. (2008), solution-state proton nuclear magnetic resonance (H-NMR) spectroscopy was used for this purpose.

With the purpose of increasing the yield of the process, two lines of investigation have been reported: the first one consists of the exploitation of the by-product obtained by using it to produce more BC (Ha et al. 2011; Krystynowicz et al. 2002); and secondly, some authors have genetically modified the bacteria to avoid the production of this compound to produce BC (Kouda et al. 1997b; Naritomi et al. 2002).

Exploitation of the cellulose-negative mutant

In order not to waste the by-products, new trends are emerging to revert its production (Krystynowicz et al. 2002) by using it as an additive to avoid the production of higher amounts of WSPS in a new culture (Ha et al. 2011).

Krystynowicz et al. (2002) examined the capability of *K.* Cel− for spontaneous reversion into Cel+ forms. They isolated single characteristic Cel− colonies and allowed them to grow in fresh HS medium. They found when the number of transferred colonies to liquid medium increases, the number of Cel− reverting back to Cel+ is reduced. However, if a single Cel− colony was transferred, about 20 % of cells revert back to Cel+. Figure 3 shows both Cel+ producers and Cel− mutant morphologies, where the latter was found to be much bigger than Cel+ colonies. They also concluded that when the culture medium contained fructose rather than glucose enriched with ethanol as a carbon source, a decreased number of Cel− appeared.

Ha et al. (2011) evaluated the possibility of adding this WSOS into the culture medium in order to block its synthesis and increase BC production (from 7.4 to 10.5 g/L). Another advantage of this method is the enhancement of the mechanical and water release properties.

Since the production patterns of BC and acetan during the culture are similar, Ishida et al. (2002) investigated the relationship between their productivities. They generated a cell line that did not produce acetan (EP1) from wild-type *K. xylinus BPR2001*. This was then cultured in a medium containing acetan. Ishida et al. (2002) concluded that there is no relationship on the genetic level between acetan and BC syntheses.

More recently, Fang and Catchmark (2014) also studied the effect of hard to extract exopolysaccharides (HE-EPS) on BC synthesis by adding purified exopolysaccharides (EPS) to the medium. They observed that the only difference was in the crystal orientation, but not in crystallinity.

Genetic modification

Cel− have been proven to thrive in aerated and AC systems. However, it has also proven that BC can be produced in these conditions through genetic modification (Lin et al. 2013a). Taking advantage of this fact, an effective method to increase the BC productivity was found (up to 100 %) (Huang et al. 2014b). A variety of methods have attempted to genetically modify some strains, such as UV radiation (Hungund and Gupta 2010c), ethyl methanesulfonate (EMS) (Hungund and Gupta 2010c), a high hydrostatic pressure treatment (Wu et al. 2010) and a disruption of the cellulase (Nakai et al. 2013).

Some authors have experimented with a mutant strain of *K. xylinus BPR2001* called *K. xylinus* subsp. *Sucrofermentans BPR3001A*, which produces less WSPS (Kouda et al. 1997b; Naritomi et al. 2002).

Kouda et al. (1997b) studied the configuration of the agitator for maximum BC production, obtaining a value approximately 20 g/L after 48 h of culture at 1200 rpm with two impellers. This data is approximately 50 % higher than a culture of a bacterial strain without genetic modification under the same conditions. They also concluded in another study (Kouda et al. 1997a) that an enhanced BC production rate is achieved when the air flow rate is high and the partial pressure of carbon dioxide is low. Some years later, Naritomi et al. (2002) used this strain to develop a repeated-batch system, obtaining a BC productivity of 0.42 g/L h during at least 4 cycles of 48 h with a broth exchange ratio of 0.9.

A less effective attempt of increasing the productivity of BC was made by Hungund and Gupta (2010c), who demonstrated the viability of using UV radiation and EMS to modify *K. xylinus NCIM 2526* strain. They obtained an increase in the BC production of 30 % (3.92 g/L) using UV and 50 % (5.96 g/L) with the EMS method.

Wu et al. (2010) induced mutagenesis of *K. xylinus* strain with a high hydrostatic pressure treatment. An enhancement of BC production in the wet state was almost 100 % and a productivity of 158.56 g/L (wet weight). Some months later, they characterized it as *K. hansenii* subsp. nov.

More recently, Nakai et al. (2013) inhibited the cellulase (essential enzyme to produce cellulose) forming a carboxymethylcellulase to be experimented in BC production with *K. xylinus*. Not only was the production not enhanced but it decreased. However, highly twisted ribbons were obtained that could be used as a novel type of cellulose. With the objective of studying the cellulose–cellulase interactions, Moran-Mirabal (2013) utilized the application of fluorescent microscopy. Nevertheless, more intensive research is needed in order to use this method for this purpose (Suzuki et al. 2012a, b).

Another study about the function of the *acsD* gene, which is involved in BC biosynthesis through *K.* bacteria, was carried out by Mehta et al. (2015). They created an *acsD* disruption mutant in the *acsABCD* cellulose synthase operon of *K. xylinus* and observed that this protein is involved in the hierarchical orientation of cellulose fibres. This mutation resulted in highly efficient cellulose synthesis. Differences between the external morphology of BC films are shown in Fig. 4.

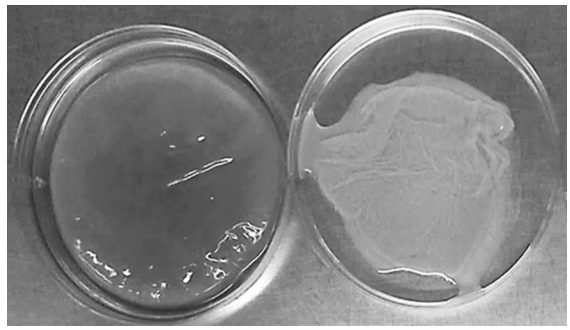

Fig. 4 Photographic comparisons of bacterial cellulose pellicles of wild type and the *acsDdm* mutant (Reprinted from Mehta et al. 2015 with permission from Springer)

Recent developments in fermentation methods

Generally, BC production process includes two steps: cell growth and culture. In the first case, the increase of bacterial cells is the main objective. However, when authors name culture as the process, they aim to the amount and quality of BC produced. Media can be optimized to improve either the cell number or the BC amount, depending on desired outcome.

K. xylinus has shown to have the ability to grow and produce cellulose on a variety of substrates. There have been many studies to investigate the optimal composition of the culture medium for each strain (Lin et al. 2013a).

Cell growth

A specific medium is necessary for the maximum cell growth of each strain. Table 2 displays typical optimal media required for different bacterial strains. Most of the bacterial strains are incubated for 24–72 h in HS medium (Hestrin and Schramm 1954) or corn steep liquor and fructose medium (CSL-Fru) (Bae et al. 2004) at 28–30 °C (Matsuoka et al. 1996) in SC (Hungund and Gupta 2010a) or shaking culture (Ha et al. 2008). The chosen nutrient medium is essential for maximum yield of biosynthesized cellulose with the increase of cell density (Jung et al. 2007; Krystynowicz et al. 2002).

As shown in Table 2, most of the researchers actually use the standard media (HS), which consists of: 20 g/L glucose, 5 g/L peptone, 5 g/L yeast extract, 2.7 g/L disodium phosphate (anhydrous) and 1.15 g/L citric acid (monohydrate) (Hestrin and Schramm

Table 2 Optimal growth medium of some bacterial strains

Genus and specie	Strain	Optimal medium	Time (h)	pH	Temp. (°C)	Type of culture	References
K. xylinus	K3	HS	48	5	30	Static	Nguyen et al. (2008)
	BPR 2001	CSL-Fru varied: 1.5 mL/L CSL	72	5	28	Static	Matsuoka et al. (1996)
	BPR 2001	CSL-Fru varied: 1.5 mL/L CSL	24	5	30	Shaking at 180 rpm	Bae and Shoda (2004)
	KU1	15 g/L D-mannitol, 5 g/L Polypeptone, 20 g/L yeast extract	48	5	30	Static	Oikawa et al. (1995b)
	FC01	HS	–	5	30	Static	Çakar et al. (2014)
	ATCC 53524	HS	48	5	30	Static	Mikkelsen et al. (2009)
	MTCC 2623	25 g/L mannitol, 5.0 g/L yeast extract and 3.0 g/L peptone	48	–	30	Shaking at 140 rpm	Dayal et al. (2013)
K. hansenii	PJK	HS varied: Glucose 10 g/L, yeast extract 10 g/L, peptone 7 g/L, acetic acid 1.5 mL/L, succinate 0.2 g/L and agar 15 g/L	24	5	30	Shaking at 200 rpm	Ha et al. (2008), Jung et al. (2005)
	NCIM 2529	HS	48	6	30	Shaking at 120 rpm	Mohite and Patil (2014)
K. sacchari	–	HS with agar 15 g/L	48	5	30	Static	Gomes et al. (2013)
K. persimmonis	GH-2	HS with 2 mL/L acetic acid, 5 mL/L ethanol and 0.2 g/L cycloheximide	24	6	30	Static	Hungund and Gupta (2010a)

1954). However, other authors vary concentration or add other compounds (Gomes et al. 2013; Hungund and Gupta 2010a). In the case of CSL-Fru, the composition is: 20 mL/L corn steep liquor (CSL), 40 g/L fructose, 1 g/L KH_2PO_4, 0.25 g/L $MgSO_4{\cdot}7H_2O$, 3.3 g/L $(NH_4)_2SO_4$, 3.6 mg/L $FeSO_4{\cdot}7H_2O$, 14.7 mg/L $CaCl_2{\cdot}2H_2O$, 2.42 mg/L $NaMoO_4{\cdot}2H_2O$, 1.73 mg/L $ZnSO_4{\cdot}7H_2O$, 1.39 mg/L $MnSO_4{\cdot}5H_2O$, 0.05 mg/L $CuSO_4{\cdot}5H_2O$, and 10 mL/L vitamin solution (Bae et al. 2004).

Novel nutrient sources

To stimulate the formation of cellulose, optimization of the media is important. It depends on the nutrients required for the microorganisms, the temperature, pH, type of culture and additives (Chawla et al. 2009; Shoda and Sugano 2005). Varying these parameters, a different composition, morphology and properties of the BC can be obtained (Hu et al. 2014; Krystynowicz et al. 2002).

Once the strains characteristics are known, new nutrient media are tried (Kurosumi et al. 2009; Zeng et al. 2011). To find the optimal nutrients for each strain, variations of the classical HS-medium are tested by varying the carbon or nitrogen sources. Generally, BC production has been made from glucose (Dayal et al. 2013; Hestrin and Schramm 1954), sucrose (Jaramillo et al. 2012), fructose (Jaramillo et al. 2013; Naritomi et al. 1998a, b; Yang et al. 1998), glycerol (Jung et al. 2010; Mikkelsen et al. 2009), mannitol (Dayal et al. 2013; Suwanposri et al. 2013) and arabitol (Mikkelsen et al. 2009; Oikawa et al. 1995a).

Glucose as a sole carbon source acts not only as an energy source but also as a cellulose precursor. It is converted into (keto) gluconic acids, what makes the glucose is of limited benefit for BC production, as there is a consequent decrease in the pH (Keshk and Sameshima 2006). It has a high cost for a relative low-yield and thus, limits its usefulness in industrial production. Thus, finding new cost-effective carbon and nitrogen sources from industrial wastes or byproducts of other processes for high-yield BC production has become a key issue (Hong and Qiu 2008).

Yeast extract and peptone are the most commonly used nitrogen sources in BC production because of

their nitrogen content and growth factors. New attempts to find an economic nitrogen source have been made (Lin et al. 2013a). The best candidate so far is CSL, not as it is the most effective (Matsuoka et al. 1996) but also because it has a buffering capacity (Noro et al. 2004) that helps to maintain the pH of the culture medium within the desired range (Lin et al. 2013a).

The most productive economic carbon sources are summarized in Table 3. They are compared to standard media under the same operation conditions. It is worth to mention that in order to make the process economically viable, not only the increase in the productivity is important but also the reduction in the price of the raw materials.

Generally, the best enhancements in productivity have been achieved by using konjac powder hydrolyzate (Hong and Qiu 2008) and waste from beer fermentation broth (WBFB) (Ha et al. 2008). In the first case, 35.3 g/L were achieved by using *K. xylinus ATCC 23770* in 8 days, getting a productivity of 4.42 g/L/day (an improvement of 207 % in comparison with the standard medium of glucose) (Hong and Qiu 2008). And secondly, when WBFB is used as substrate and *K. hansenii PJK* is used as a strain, an increase of 3000 % in the production of BC is produced (from 0.45 g/L in HS medium to 13.95 g/L) (Ha et al. 2008).

Another new idea was developed by Guo et al. (2013), who evaluated the possibility of using an enzymatic hydrolysate of SO_2-pretreated spruce wood to produce BC, but this requires a process of detoxification to eliminate inhibitors. Among all the experiments that they carried out, the best effects were achieved with activated charcoal, where the BC yield was 8.2 instead of 7.5 g/L obtained in a reference medium without inhibitors.

With the aim of converting cellulosic wastes into a richer carbon source, some pretreatments with dissolution agents such as NaOH/urea solution (Kuo and Lee 2009), *N*-methylmorpholine-*N*-oxide (NMMO) (Kuo and Lee 2009), ionic liquids 1-butyl-3-methylimidazolium chloride ([BMIM]Cl) (Kuo and Lee 2009), 1-allyl-3-methylimidazolium chloride ([AMIM]Cl) (Hong et al. 2012) and 85 % phosphoric acid (Kuo and Lee 2009) have been studied. These pretreatments resulted in 5–7-fold higher enzymatic hydrolysis rate and 7 times higher yield of fermentable sugars than untreated wastes. They are potential candidates to be employed in BC production process, as their use produces an increase of around 80 % compared with glucose. However, the cost of these dissolution agents has to reduce in order for it to be commercially viable (Hong et al. 2012).

Process improvement

In order to produce to an industrial level and have commercial application, large scale semicontinuous and continuous fermentation is needed. Depending on the final application, an optimal shape and composition with suitable BC properties at a maximum production is desirable. In this section, recent attempts to create a high BC production reactor are reviewed and compared to classical production methods.

Reactor

Currently, the fermentation methods that are proved to produce high yields are SC, AC and airlift reactors. However, some authors are trying to increase the amount of BC produced by developing new reactors (Krystynowicz et al. 2002; Moon et al. 2006).

In SC (Fig. 5), which is the most used method, BC is formed on the surface of shallow trays as a gelatinous pellicle, which has a denser surface on the side exposed to air (Chawla et al. 2009; Lin et al. 2013a; Song et al. 2009). BC produced in this culture presents some advantages, for instance, a more extensive interior surface area causes extremely high WHC (Huang et al. 2014b) or high speed of pellicle production (Chawla et al. 2009). On the opposite side, it usually takes 5–20 days (depending on the bacteria), which is not effective for industrial production, apart from the large space required (Chawla et al. 2009; Song et al. 2009).

AC (Fig. 6) seems an easy option to increase the mass transfer rate in terms of having low shear stress and a high oxygen transfer rate. However, as already mentioned, a non-cellulose mutant usually appears, thus lowering the BC productivity (Chawla et al. 2009; Huang et al. 2014b; Song et al. 2009).

In order to achieve the required oxygen demand, yet decreasing the power supply, airlift bioreactors have been tried (Kouda et al. 1997a). However, the adhesion of BC to the upper part of the reactor triggers homogeneity problems that reduce BC production (Krystynowicz et al. 2002). Furthermore, BC

Table 3 Comparison of productivity obtained with waste carbon source and standard media

Genus and specie	Strain	Time (days)	pH	Temp. (°C)	Type of reactor	Carbon source	Yield (g/L)	Productivity (g/L day)	Increm (%)	References
K. xylinus	NRRL B-42	14	5	28	Static	Glycerol from biodiesel	10	0.714	400	Vazquez et al. (2013)
						Grape bagasse	8	0.571	300	
						SM1	2	0.143		
	ATCC 23770	8	5	30	Static	Konjac powder hydrolyzate	35.3	4.41	207.0	Hong and Qiu (2008)
						SM2	11.5	1.44		
	BCRC 12334	7	6	30	Static	Thin stillage	3.05	0.436	−27.6	Wu and Liu (2013), Wu and Liu (2012)
						Thin stillage-HS	10.38	1.48	146.6	
						SM1	4.21	0.601		
	ATCC 23770	14	5	30	Static	Cotton cloth hydrolysate	10.8	0.771	83.1	Hong et al. (2012)
						SM2	5.9	0.421		
	NBRC 13693	14	6	30	Static	Orange juice	5.9	0.421	37.9	Kurosumi et al. (2009)
						SM3	4.28	0.306		
	ATCC 23770	7	5	30	Static	Fiber sludges from sulphate	6.23	0.890	27.1	Cavka et al. (2013)
						Fiber sludges from sulphite	4.65	0.664	−5.10	
						SM1	4.9	0.700		
	ATCC 23770	14	5	30	Static	Low-solids potato effluents	5.81	0.415	17.1	Thompson and Hamilton (2001)
						SM1	4.96	0.354		
	ATCC 10245	3	5	30	Static	H_2SO_4 heat treated sugar cane molasses	4.695	1.57	5.10	El-Saied et al. (2008)
						SM2	4.467	1.49		
	BPR 2001	3	5.09	25	Rotary shaker incubator	Maple syrup	1.51	0.503	−5.63	Zeng et al. (2011)
						SM4	1.6	0.533		
	BPR 2001	3	5	30	Jar fermentor	Molasses subjected to sulfuric acid	5.3	1.77	−29.3	Bae and Shoda (2004), Bae and Shoda (2005)
						SM5	7.5	2.50		
K. hansenii	PJK (KCTC 10505 BP)	14	5	30	Static	WBFB	13.95	0.996	3000	Ha et al. (2008)
						SM1	0.45	0.0321		
	MCM B-967	7	5	RT	Static	Pineapple peles	125[a]	17.8[a]	316	Kumbhar et al. (2015)
						Watermelon peles	100[a]	14.3[a]	233	
						SM1	30[a]	4.28[a]		

Table 3 continued

Genus and specie	Strain	Time (days)	pH	Temp. (°C)	Type of reactor	Carbon source	Yield (g/L)	Productivity (g/L day)	Increm (%)	References
K. pasteuria-nus	HBB6	7	6.5	30	Static	Beet molasses	0.03	0.00429	−30.2	Çoban and Biyik (2011)
						SM1	0.043	0.00614		
K. lovaniensis	HBB5					Beet molasses	0.023	0.00329	−39.5	
						SM1	0.038	0.00543		
K. sacchari	–	4	4.5	28	Static	Dry olive mill residue	0.85	0.213	−66	Gomes et al. (2013)
						SM1	2.5	0.625		

RT, room temperature; SM1, HS medium; SM2, glucose medium; SM3, synthetic media; SM4, fructose medium; SM5, CSL-Fru medium

[a] Wet weight

Fig. 5 Bacterial cellulose produced in static culture (Reprinted from Huang et al. 2014b with permission from Springer)

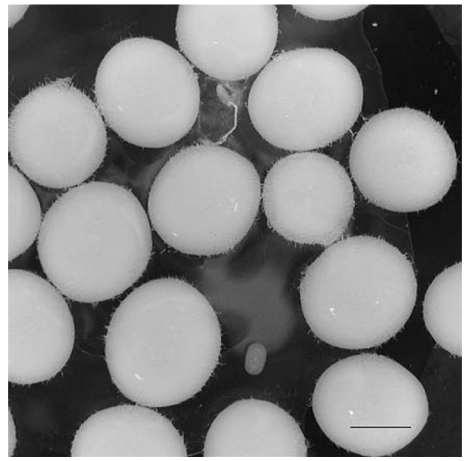

Fig. 6 Bacterial cellulose produced in agitated culture. *Scale bar* is 5 mm (Reprinted from Czaja et al. 2004 with permission from Springer)

pellets, which are produced not only in this type of reactor but also in AC, exhibit low mechanical strength in comparison with a BC pellicle (Lin et al. 2013a).

Aiming to achieve a better yield and to avoid all of these problems, new reactors are being investigated as summarized in Table 4.

In the last decade, a new fermentation reactor called RDB or rotating biological fermenter (RBF) (Fig. 7) has been increasingly used (Kim et al. 2007; Krystynowicz et al. 2002). As shown in Table 4, this enhances the productivity at the cost of reducing the

Table 4 Comparison of different reactors for bacterial cellulose production with static culture (classical method)

Reactor	Description	Preferred conditions	Characteristics	Compared with static culture	References
RDB or RBF (Fig. 7a, b)	Disks rotating with their half area submerged in the medium	High number of disks Low rotating speed (4 rpm) Surface/medium ratio of 0.71 cm^{-1}	Contact with atmosphere BC attached on the disks	Higher productivity: 0.47 g/L/day Less production time: from 12–20 to 3.5 days Lower Young's modulus: from 2.7 to 0.3 GPa Lower tensile strength: from 92 to 22.9 MPa Higher WHC at low centrifugation: from 60 to 400 g water/g BC	Kim et al. (2007), Krystynowicz et al. (2002), Serafica et al. (2002)
	Plastic composite disks (PCS) rotating	Maximum of five consecutive runs 5 days of a run	Semicontinuous operation mode	Higher productivity: 0.24 g/L/day Lower crystallinity: from 88.7 to 66.9 % Lower Young's modulus: from 3955.6 to 372.5 MPa Similar water content: 99.04 versus 98.66 %	Lin et al. (2014)
Stirred-tank reactor with a spin filter (Fig. 8)	Fermentor equipped with an impeller and a spin filter of stainless steel	pH 5 (controlled) 6 flat-blade turbine impeller at 500 rpm Periodical perfusion culture Aeration rate: 30 l/min	High cell density Big amount of Cel+ cells converted into Cel− mutants	Higher BC productivity: from 0.55 to 1.61 glL/day	Jung et al. (2007)
Biofilm reactor (Fig. 9a, b)	PCS implemented in a biofilm reactor	PCS blended with dried soybean hulls, defatted soybean flour, yeast extract, dried bovine red blood cells, and mineral salts 2.0 % of CMC	High biomass density Natural form of cell immobilization BC is attached on the PCS shaft and formed large chunks More shear force than standard impellers at the same agitation speed	Higher productivity: from 0.564 to 1.41 g/L/day Higher water retention: from 73 to 95 % Higher Young's modulus: from 286 to 2401 MPa Higher strain at break: from 0.8 to 1.4 % Higher crystallinity: from 85 to 93 %	Cheng et al. (2009a, 2010, 2011)
Spherical type bubble column bioreactor (Fig. 10)	Spherical reactor as airlift type	Aeration rate: 30 l/min	Low shear stress High oxygen transfer rate Low concentrated solution state culture	Higher productivity: from 1.9 to 2.27 g/L/day Lower crystallinity: from 86 to 79.6 % Lower tensile strength: from 17.15 to 11.66 MPa Lower degree of polymerization: from 20,150 to 16,800	Choi et al. (2009), Moon et al. (2006), Song et al. (2009)
TBR (Fig. 11)	Tank with a pump being in charge of moving the culture broth from the bottom to the top. Air is circulating at the same time. BC is periodically replaced by fresh feed		High –OH associating degree Increased oxygen supply Decreased shear force Greater ratio of surface to volume High biomass density	Higher polymerization degree: from 5590 to 6093 Higher purity: from 96.1 to 97.8 % Higher WHC: from 260 to 517 % Similar porosity: from 85.5 to 85.9 %	Lu and Jiang (2014)

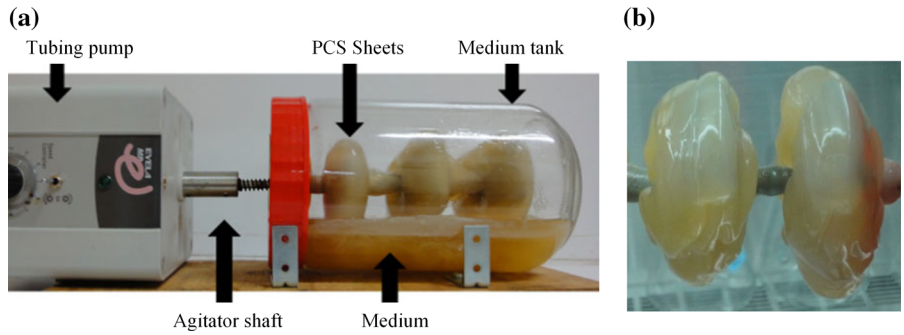

Fig. 7 **a** PCS-RDB reactor and **b** bacterial cellulose attached to the rotating disks (Reprinted from Lin et al. 2014 with permission from Springer)

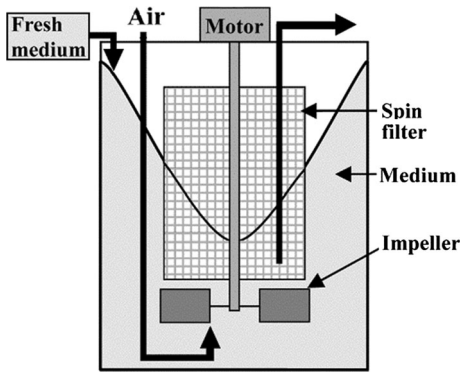

Fig. 8 Jar fermenter equipped with a spin filter (Reprinted from Jung et al. 2007 with permission from Springer)

BC mechanical properties. Owing to the low production time required, semi-continuous operation mode has been tried satisfactorily (Lin et al. 2014). In future, it may be possible to produce BC in a RDB through a continuous system. Dissanayake and Ismail (2013) have successfully developed a mathematical model to describe this reactor.

A higher productivity was achieved by Jung et al. (2007), who introduced a spin filter in a stirred tank reactor (Fig. 8) and raised this value to 1.61 g/L/day. However, more investigation is needed to avoid the conversion of Cel+ cells into Cel−.

After the addition of plastic composite supports (PCS) in a biofilm reactor (Fig. 9), Cheng et al. (2010) enhanced the productivity without any significant negative effect on the properties of BC. Besides, with the addition of 2.0 % carboxymethyl cellulose (CMC), the attachment of BC into the shaft is avoided (Cheng et al. 2011).

Within this list, the reactor which has reached the highest productivity (2.27 g/L/day) was a modified airlift-type bubble column bioreactor (Fig. 10) developed by Song et al. (Choi et al. 2009; Moon et al. 2006; Song et al. 2009). A low shear stress and high oxygen

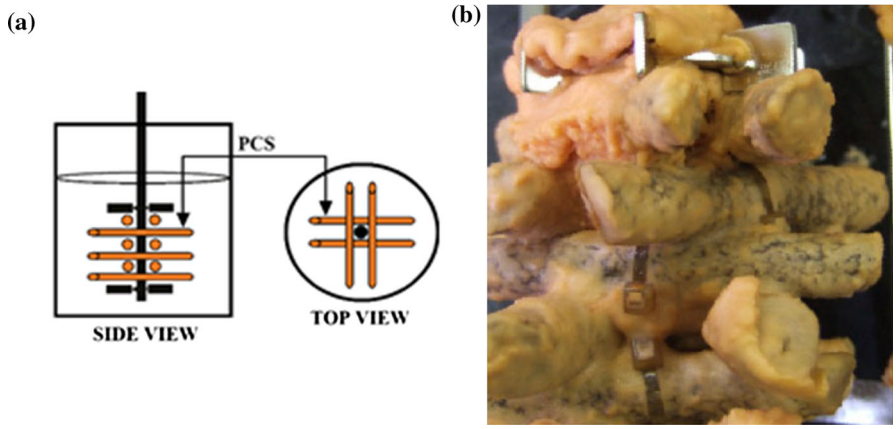

Fig. 9 **a** Plastic composite support implemented in a biofilm reactor and **b** bacterial cellulose attached to these supports (Reprinted from Cheng et al. 2010 with permission from Springer)

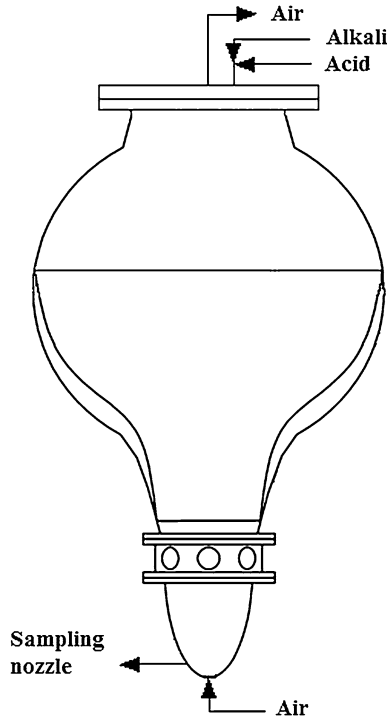

Fig. 10 Schematic diagram of a spherical type bubble column bioreactor (Inspired by Song et al. 2009)

rate were achieved. However, although mechanical properties, crystallinity and the degree of polymerization (DP) also decrease, the reduction is so insignificant that can be considered acceptable.

A novel cultivation method, trickling fermentation in a TBR (Fig. 11), has reached better results due to the characterization of BC as it is shown in Table 4. Nevertheless, more investigation about the optimal culture conditions is required, since properties and structure of BC are strictly connected with them and this system has not been studied in depth yet (Lu and Jiang 2014).

An additional inconvenience for the batch fermentation process is the long time required to restart a new culture, as bacteria take time to get used to new fermentation conditions. Therefore, a continuous fermentation process is needed, which has been intensively researched (Lin et al. 2013a). Naritomi et al. (Kouda et al. 2000; Naritomi et al. 1998a, 2002) designed a process to produce BC in a repeated-batch culture at a broth exchange ratio of 0.9 obtaining a BC production rate over 0.4 g/L/h. Figure 12 shows the high BC production in each batch, decreasing from the sixth cycle in advance.

Another attempt to enhance BC productivity was made by Çakar et al. (2014), who optimized a semi-continuous operation mode in SC by *K. xylinus FC01*. The highest productivity (1.637 g/L) was found from a ½ volume changing ratio in 7 days. This method is proving itself to be a better choice than continuous or batch processes.

Fed-batch fermentation has found to be another of the best solutions to the low productivity problem. Bae and Shoda (2004) performed intermittent and

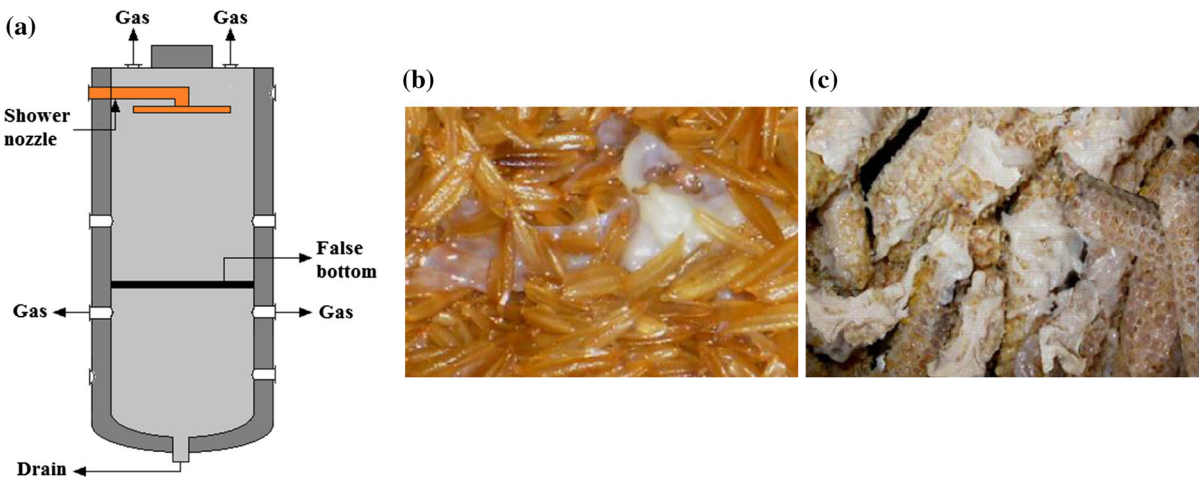

Fig. 11 **a** Schematic diagram of a trickling bed reactor. **b**, **c** Bacterial cellulose in trickling cultivation (Inspired and reprinted from Lu and Jiang 2014 with permission from Springer)

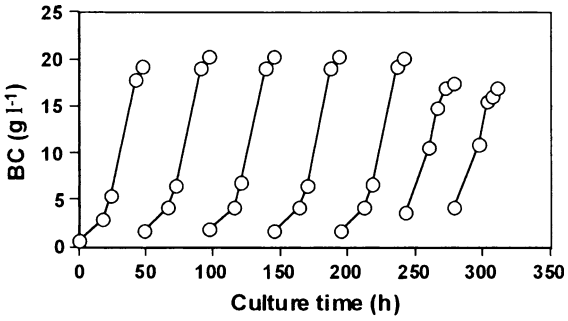

Fig. 12 Bacterial cellulose production by repeated-batch culture at a broth exchange ratio of 0.9 (Reprinted from Naritomi et al. 2002 with permission from Elsevier)

continuous fed-batch fermentations of *K. xylinus BPR2001* with a fresh molasses medium in order to maintain the levels of sugar concentration at around 20 g/L. Adding small amounts of molasses frequently, they obtained the best result of BC concentration (7.82 g/L in comparison with 5.3 g/L in batch fermentation) and cell growth. With these results they designed a continuous system adding a substrate rate of 6.3 g-sugar/h (7.16 g/L of BC).

Shezad et al. (2009) also investigated fed-batch cultivation by using WBFB and *K. hansenii PJK*. They obtained enhanced results after 30 days of cultivation: 350 g/L (wet weight) with a chemically defined medium, in comparison with around 125 g/L (wet weight) in batch cultivation in the same medium. After having found this method to increase productivity, they proceeded to characterize the BC sheets (Shezad et al. 2010). The crystallinity index was slightly reduced from 78 to 75.5 %; the DP was also decreased from 8011 to 7940; tensile strength was highly reduced from 76.7 to 19.8 MPa. Water was completely released after 64 h (batch) and 75 h (fed-batch); and WHC was found to be 273 (fed-batch) and 296 (batch) times its dry weight.

Additives for increasing productivity

Different additives have been introduced in the culture medium to enhance productivity. For instance, alcohols (Hestrin and Schramm 1954; Lu et al. 2011; Mikkelsen et al. 2009), organic acids (Jung et al. 2010; Lee et al. 2011), agar (Bae et al. 2004; Kim et al. 2012; Shah et al. 2010), thin stillage from rice wine distillery (Wu and Liu 2012), CMC (Cheng et al. 2009b), 1-methylcyclopropene (1-MCP) (Hu and Catchmark 2010) and industrial-grade glucose (Ha et al. 2008).

Lu et al. (2011) evaluated the effect of six different alcohols on the BC production rate by *K. xylinus 186*. The best result was obtained with 0.5 % (w/v) *n*-butanol added to the HS culture medium producing an increase of 56 % (1.326 g/L). Jung et al. (2010) added eight organic acids as co-substrate when *K.* sp. *V6* was used as a bacterial strain and glucose or glycerol was used as a substrate. The best effect was found by using 0.35 % (w/v) succinic acid (80 %, from 2.51 to 4.52 g/L). Around 1.0 % of CMC was found to be the optimal concentration of this additive to increase the productivity of BC by *K. xylinus*, with an increment of 530 %, from 1.3 to 8.2 g/L (Cheng et al. 2009b).

Agar has also been often used as an additive. Bae et al. (2004) concluded that an increase in the viscosity of the medium, dispersion of BC pellets and number of free cells produced by the addition of agar (0.4 % in *K. xylinus BPR2001*) enhance productivity. Shah et al. (2010) also evaluated the effect of this compound in the process and obtained an increase of the production of 71 % (from 3.194 to 5.472 g/L). Kim et al. (2012) finished their study stating that the increase in the viscosity produced by agar influenced the BC production more than the reduction of the oxygen transfer rate triggered.

A wastewater obtained from a rice wine distillery, called thin stillage, was used instead of distilled water in HS-medium by Wu and Liu (2012). They obtained a double profit: the productivity was enhanced 2.5-fold up to 10.38 g/L and the effluent was re-used rather than treated and discharged.

An improvement of 25.4 % of BC production by *K. xylinus JCM 9730* was achieved by adding 100 mg dextrose containing 0.14 mg 1-MCP in assigned days (day 1, day 2, day 4, day 6 and day 9) (Hu and Catchmark 2010).

Finally, in order to reduce the costs of production, Ha et al. (2008) produced BC using WBFB as substrate and *K. hansenii PJK* as bacterial strain. They added 1 % industrial-grade glucose to the culture broth, getting an increase of 65 %, from 8.46 to 13.95 g/L.

Table 5 Morphology and properties of bacterial cellulose compared with nanofibrillated cellulose and nanocrystalline cellulose

Properties	Parameters	BC			NFC		NCC		References (BC)	References (MFC)	References (NCC)
Morphology	Width (nm)	Nanofibril: 1.5–4 Fibril: 40			Nanofibril: 2–10 Fibril: 20–60		3–50		Gardner et al. (2008), Ross et al. (1991), Ruka et al. (2013)	Lavoine et al. (2012)	Peng et al. (2011)
	Length (μm)	1–9			>2		0.1–1		Huang et al. (2014b)	Lavoine et al. (2012)	Moon et al. (2011), Peng et al. (2011), Siqueira et al. (2010)
	Aspect ratio (L/w)	667–6000			>200		2–167				
Physical properties	Crystallinity	84–89 %			40–78 %		85–100 %		Czaja et al. (2004), Huang et al. (2014b)	Czaja et al. (2004), Huang et al. (2014b), Lavoine et al. (2012)	Moon et al. (2011)
	Polymerization degree (DP)	300–10,000			200–10,000		140–6000		Gardner et al. (2008), Surma-Slusarska et al. (2008b), Vitta and Thiruvengadam (2012)	Lavoine et al. (2012), Siro and Plackett (2010), Zimmermann et al. (2010)	Habibi et al. (2006)
	Structure	SC: 3D interwoven mesh			Web-like		Suspension of whiskers		Huang et al. (2014b), Ruka et al. (2013)	Lavoine et al. (2012)	Habibi et al. (2006)
		AC: amorphous agglomeration							Klemm et al.(2001), Pecoraro et al. (2007)		
	Porosity	Micro/nanopores			Micro/nanopores ~20 %		–		Vitta and Thiruvengadam (2012)	Lavoine et al. (2012), Vilaseca et al. (2014)	–
Thermal properties	Degradation stages	1st	2nd	3rd	1st	2nd	1st	2nd	El-Saied et al. (2008), Mohite and Patil (2014)	El-Saied et al. (2008), Mohite and Patil (2014)	El-Saied et al. (2008), Mohite and Patil (2014)
	Decomposition temperature range (°C)	250–399	399–500	500–561	272–366	372–510	274–354	448–522			
	Maximum weight loss temperature (°C)	350	496	525	333	499	333	521			
	Activation energy (kJ/mol)	96	167	794	238	95	246	364			
	Total activation energy (kJ/mol)	1058			334		609				
Mechanical properties	Tensile strength (MPa)	200–2000			2–2000		7500–7700		Gardner et al. (2008), Iguchi et al. (2000), Pecoraro et al. (2007), Vitta and Thiruvengadam (2012)	Lavoine et al. (2012), Siro and Plackett (2010), Vitta and Thiruvengadam (2012)	Moon et al. (2011)

Table 5 contiuned

Properties	Parameters	BC	NFC	NCC	References (BC)	References (MFC)	References (NCC)
		Young's modulus (GPa) 15–138	13–180	130–250		Eichhorn et al. (2010), Lavoine et al. (2012), Vitta and Thiruvengadam (2012)	Moon et al. (2011), Siqueira et al. (2010)
Water absorption properties	WHC	100–400	2–30	0.4–0.9	Mohite and Patil (2014), Shezad et al. (2010), Vitta and Thiruvengadam (2012)	Spence et al. (2010)	Tomer et al. (2001)
	Rehydration ability	Low	Low	–		Spence et al. (2010)	–
Optical properties	Light transmittance	>95 %	46–90 %	>90 %	(Huang et al. 2014b)	Siro and Plackett (2010), Spence et al. (2010)	Ma et al. (2011), Wang et al. (2013)
Acoustic properties	Sonic velocity	High (~ aluminum)	–	–	Iguchi et al. (2000)	–	–
	Dynamic loss	Low	–	–			
Other properties	Biocompatibility	Not enough antimicrobial activity	Not enough antimicrobial activity	–	George et al. (2014), Wu et al. (2014)	George et al. (2014), Wu et al. (2014)	–
	Biodegradability	High	High	–		George et al. (2014), Wu et al. (2014)	–
	Solubility[a]	NMMO Lithium chloride (LiCl)/*N*,*N*-dimethyl acetamide (DMAc) Ionic liquids N,Ndimethyl acetamide (DMAc)	$ZnCl_2(3H_2O)$ LiOH/urea/thiourea Hydrophobic organic solvents: hexane, toluene Dichloromethane *N*,*N*-dimethylformamide (DMF)		Chen et al. (2011b), Gao et al. (2011b), Lu and Shen (2011), Tome et al. (2011)	Gardner et al. (2008, George et al. (2014), Wu et al. (2014)	

[a] All cellulosic materials without modification present solubility in the same materials

Enhancement of morphology and properties of bacterial cellulose

Description and comparison of morphology and properties of bacterial cellulose with nanofibrillated cellulose and nanocrystalline cellulose

To get a better understanding about the specific properties of BC, they have been compared to those of nanofibrillated cellulose (NFC) and nanocrystalline cellulose (NCC). On one side, NFC is composed of nanofibrils with crystalline and amorphous parts and a high aspect ratio (L/w), obtained by a homogenization process (Jonoobi et al. 2015; Lavoine et al. 2012). Their properties depend on the cellulose origin, as eucalyptus (Negro et al. 2015), birch (Liu et al. 2014), cotton (Chen et al. 2014a; Li et al. 2014), corn (Merayo et al. 2014), agriculture residues (Chaker et al. 2014; Pelissari et al. 2014; Sehaqui et al. 2014; …) and the pretreatments of the raw material, which could be chemical [(2,2,6,6-tetramethylpiperidin-1-yl)oxyl (TEMPO) oxidation (Besbes et al. 2011), sulfonation (Liimatainen et al. 2013) and cationization (Pei et al. 2013)] or enzymatic (Hettrich et al. 2014; Paakko et al. 2007; Qing et al. 2013). On the other side, NCC is composed entirely of a crystalline structure and it is obtained by a chemical process of hydrolysis, typically with sulphuric acid. In that process, nanofibres are broken through the amorphous parts, remaining only whiskers of nano-size (Reiner 2008). Table 5 shows general characteristics of these three types of nanocelluloses.

Morphology

Generally, BC nanofibrils are extruded from the cytoplasmic membrane of the cells and aggregated into a ribbon-like fibril (Huang et al. 2014b; Ross et al. 1991; Ruka et al. 2013). This high aspect ratio (L/w) increases the surface area of the BC, which is a key factor to be used as a reinforcing material for an easy stress transfer (Huang et al. 2014b). Table 5 shows that typical sizes of BC nanofibrils are in the range of NFC, being longer than both vegetal NFC and NCC, whose length depends on the cellulose source (Jonoobi et al. 2015; Lavoine et al. 2012; Peng et al. 2011). The reason for the last comparison is the breaking mechanism of the nanofibers through acid hydrolysis in the amorphous regions, thus causing a reduction in the length but keeping a similar width (Moon et al. 2011) (Fig. 13).

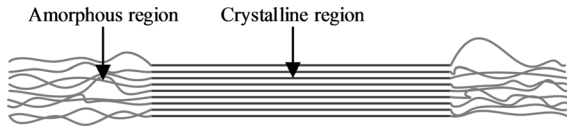

Fig. 13 Schematic cellulose nanofibril showing one of the suggested configurations of the crystalline and amorphous regions

Crystallinity

The crystal structure is one of the most promising properties of BC, inducing better mechanical and interfacial properties than that in plant cellulose (Huang et al. 2014b). It is composed of cellulose type I_α and I_β, that correspond respectively to triclinic and monoclinic unit cells (Huang et al. 2014b). The proportion of each one varies due to different culture conditions, so it can be modified if one changes the nutrient medium, type of reactor, pH or bacterial strain (Huang et al. 2014b). BC has found to be I_α-rich in a proportion of around 70–80 % (Huang et al. 2014b; Mohite and Patil 2014; Park et al. 2014; Sun et al. 2007). Nevertheless, higher plant cell wall cellulose and tunicates are composed mainly of cellulose type I_β with a similar percentage (Moon et al. 2011). The crystallinity index is observable in Table 5 and shows that NCC presents the highest value because of the removal of the amorphous parts (Moon et al. 2011). However, BC holds a superior value because of the nature of the cellulose produced from bacteria (Czaja et al. 2004).

Degree of polymerization

A factor related to the length and crystallinity of the nanocellulose is the DP, which is the number of the glucose units in a chain (Gardner et al. 2008). As it is understandable, the DP of BC is the highest, because of their long and crystalline nanofibrils, being followed by plant origin NFC and NCC (Habibi et al. 2006; Siro and Plackett 2010). Typical ranges are shown in Table 5.

Structure

BC produced in SC is usually presented as a three-dimensional interwoven mesh when it is viewed by SEM (Huang et al. 2014b; Ruka et al. 2013). However, an amorphous agglomeration is observed when AC is used (Klemm et al. 2001; Pecoraro et al. 2007). Its structure consists of micro/nanopores able to hold a variety of nanoparticles to form interesting nanocomposites for a wide range of applications (Vitta and Thiruvengadam 2012). A similar structure is obtained in vegetal NFC, where a web-like structure with micro/nanopores is also observed (Lavoine et al. 2012). However, NCC is presented as a suspension of whiskers in a chiral nematic ordered phase (Peng et al. 2011).

Thermal properties

The thermal properties of BC produced in a standard medium or low-cost medium (sugar cane molasses + CSL) have been compared to some plant cellulose, such as cotton linters, viscose wood pulp (VWP) and microcrystalline cellulose (MCC) (El-Saied et al. 2008). Their thermograms showed two degradation stages: the decomposition of cellulose caused the first stage (volatilization stage), while the second stage was due to the rapid volatilization and oxidation of char and the formation of a carbonaceous residue (carbonaceous stage). As it is shown in Table 5, BC starts the degradation process 22 and 24 °C before than VWP and MCC, but it finishes 33 and 45 °C respectively after them. However, maximum weight loss comes 17 °C before in the last two than in BC. Finally, the activation energy which is required to start the first degradation stage is much higher in case of VWP and MCC than of BC, being 142 and 150 °C higher than BC.

Mechanical properties

Krystynowicz et al. (2002) evaluated the mechanical properties of two forms of BC, obtaining a much higher Young's modulus and tensile strength for BC obtained in SC (SC–BC) than for BC produced in AC (AC–BC) (range in Table 5, where the maximum value corresponds to SC–BC and the minimum is similar to AC–BC). The differences between both structures together with the slightly smaller size of AC–BC nanofibrils, explain this behavior.

In both cases, these mechanical properties have been found to be superior to those of plant origin cellulose. According to several sources, a typical tensile strength of BC is in the range 200–2000 MPa (Gardner et al. 2008; Iguchi et al. 2000; Vitta and Thiruvengadam 2012), while Young's modulus is usually in the range 15–138 GPa (Gardner et al. 2008; Iguchi et al. 2000; Pecoraro et al. 2007; Vitta and Thiruvengadam 2012). The main reasons for the strength of BC include the high DP and crystallinity index of BC. Due to these mechanical properties, BC is used to reinforce other materials.

Plant origin NFC have resulted in having inferior mechanical properties to BC, mainly due to the lower length of their nanofibres, which decreases the surface area, and also because of the lower crystallinity (Lavoine et al. 2012).

However, NCC presents exceptional mechanical properties because of the removal of the amorphous parts of the nanofibres, which provides a strengthening effect. Its values for tensile strength (7500–7700 MPa) together with Young's modulus (130–250 GPa) (Moon et al. 2011; Siqueira et al. 2010) are comparable with carbon fiber of TORAYCA® T1000G, one of the world's best mechanical properties material, with values of 6370 MPa for tensile strength and 294 GPa for Young's modulus (TORAYCA® T1000G DATA SHEET). Nevertheless, because of their limited compatibility with typical matrixes and the difficulty in the dispersion step, the properties of the composites reinforced with NCC are far below what could be expected (Li et al. 2010).

Water absorption properties

BC is characterized by having a high WHC because of its very porous network that retains the water through hydrogen bonding. After Gelin et al. (2007) studied the water interaction properties in a BC gel, only 10 % of the 99 % (w/w) water contained in these hydrogels resulted in behaving like free bulk water, while the remaining 89 % was bounded to the nanofibril network. It has been proved that WHC varies depending on the cultivation method. For instance, BC produced in a RDB is able to hold almost five times

more water than that produced in SC (Krystynowicz et al. 2002).

WHC of vegetal NFC is low because of the lower surface area of the nanofibres to hold water. This argument is also valid in case of NCC, whose surface area is even less (Mohite and Patil 2014).

Optical properties

Light transmittance is another interesting property of BC to be used in optically transparent composites. High transference occurs because the wavelength of visible rays is higher than the nano-size of the fibres. BC composites can be applied in many applications such as display devices, coatings and lenses (Huang et al. 2014b).

In the case of vegetal NFC, it is possible to form large fiber fragments and aggregates that reduce the film transparency (Siro and Plackett 2010). NFC with low yields of homogenization process can also have low light transmittance values due to the possibility of that some fines or other compounds cause a high absorbance, thus reducing the value of the transmittance. This is why transmittance is usually related to the value of the yield of the process (Spence et al. 2010).

On the other hand, because of their high crystallinity and short length, NCC has proved to have a high light transmittance, usually higher than all types of NFC (Luna-Martinez et al. 2011; Yang et al. 2012).

Biocompatibility and biodegradability

As BC is biocompatible and biodegradable, it has been used in a wide range of applications in the biomedical field (George et al. 2014). However, one of the most important properties of a wound dressing, the antimicrobial activity, is not high enough in case of BC, NFC nor NCC (Wu et al. 2014). As it will be explained in the next section, several studies have been made in order to enhance this property by introducing some components with exceptional antimicrobial activities.

Enhancement of BC properties

For some applications, BC properties need to be enhanced. An example may be the high mechanical strength which is required to be used as a paper or plastic reinforcing additive, or the high WHC needed to keep the moisture content as a wound dressing material. Therefore, different additives or medium components have been added to the fermentative media to modify BC structural and physical properties in a specific way.

Morphology

Luo et al. (2014) have recently investigated the evolution of the structural properties when a BC scaffold is being processed. Although porosity, fiber diameter, fiber network structure, light transmittance and thickness of BC pellicles varied with the culture time until the 5th day, surface and crystal structure remain unchanged during the whole time of the culture. They also investigated the deposition of hydroxyapatite (HAp). Most of the results showed the same behavior as BC, except for the distribution of the HAp particles on the surface of BC nanofibres, where difference in the compactness of BC network provoked irregularities until 7th day of culture. They summarized their work with a controllable morphology of BC and BC/HAp by optimizing the culture time.

With the objective of investigating the effect of different polysaccharides on BC crystallinity, Park et al. (2014) used vibrational sum frequency generation (SFG) spectroscopy in BC/polysaccharide composites. Only with xylan, a reduction of crystallinity, by $\sim$55 % compared to the control sample, was obtained, while xyloglucan did it by $\sim$35 %. In the case of I_α, I_β allomorph amount, it was decreased with xyloglucan in the culture medium, from $\sim$60 to $\sim$20 %.

Biomedicine To be used as a wound dressing material, BC composite needs certain porosity to make sure that air and substrate penetrate into the skin (Yang et al. 2014).

Zang et al. (2014) prepared an ordered BC by restricting the movement of the bacteria through microgrooves and oxygen (Fig. 14). In this way, a structure of grid and strip was obtained, but a precise control is necessary. This could have potential interest in the biomedical field for tissue engineering as a scaffold in repair of nerve, skeleton and hamstring.

Yang et al. (2014) proposed to increase the porosity of the fibrous network of BC by using the gelatinization properties of potato starch (PS). When the

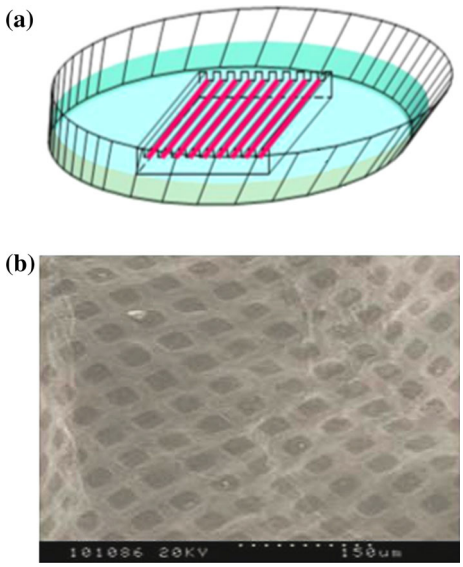

Fig. 14 Diagram for microgroove culture equipment and SEM of grid shaped bacterial cellulose (Reprinted from Zang et al. 2014 with permission from Elsevier)

composite was prepared with more than 1 % of PS, a double-stage structure with locally oriented nanofibres was presented, composed of a compact upper surface and transparent lower surface, thus improving the mechanical properties and pore size (until 40 μm).

With the aim of decreasing the porosity of a BC film, Chen et al. (2014b) added gelatin to the culture medium and treated the BC/gelatin composites with glutaraldehyde (GA) to crosslink BC fibrils and gelatin. They optimized the amounts of these two compounds to obtain good mechanical properties without decreasing the crystallinity index and swelling behavior, getting a value of 0.5 wt/v% gelatin, 1.0 wt/v% GA and 24 h of crosslinking time.

Explosives In view of BC's typical structure, which results in enhanced properties in comparison with plant cellulose, such as ultrafine and highly pure fiber network structure, it has been modified to be applied as an explosive. Sun et al. (2010) prepared BC nitrate (BCN) by introducing BC powder in nitrating solutions obtaining exceptionally promising results.

Membranes An ultrafine nanofiber network and a high specific surface area are pertaining to adsorption efficiency, high mechanical strength and good chemical stability. These properties are required when we talk about an adsorbing material (Huang et al. 2014b). Sun et al. (2007) concluded that BC obtained in SC has higher adsorption ability than that from shake culture. However, BC is characterized by having a low adsorption capacity and poor selectivity (Lu et al. 2014). To enhance this property, chemical modification has been investigated with amines (Lu et al. 2014), diethylenetriamine (Shen et al. 2009), phosphoric acid (Oshima et al. 2008, 2011) and CMC (Chen et al. 2009).

Lu et al. (2014) studied the metal ions-adsorption process by using amino-BC being BC chemically modified to be used in the water treatment field. They analyzed the thermodynamic, kinetic and mechanism of the adsorption, stating that both film and particle diffusion control the process of adsorption. As the reaction resulted in being endothermic, a higher adsorption rate was obtained with an increase in the temperature.

Sponges Generally, a relatively large pore size of a tissue engineering scaffold is necessary for cell ingrowth. In the case of BC, which its small pore size is characteristic, a treatment is needed to be used in this practical application.

Gao et al. (2011a) used the technique of emulsion freeze-drying (FD) to make a novel BC sponge. Large pores (from 20 to 1000 μm in diameter) and nano pores (down to 4 nm in diameter) were obtained with this method.

Conducting materials Because of its structural features, BC nanofibers have been evaluated for its use as support materials for lots of additives. When a conductive nanomaterial is added to the BC network, this non-conductive nanocellulose turns into a conductive material (Iguchi et al. 2000). This is why modified BC is an outstanding material to be used as a conductive material. Several studies have been carried out in order to prepare electrically conducting materials with multiwalled carbon nanotubes (MWCN) (Yoon et al. 2006), polydimethylsiloxane (PDMS) (Liang et al. 2012), pyrrole (PY) (Muller et al. 2011), aniline (Ani) or polyaniline (PAni) (Hu et al. 2011a; Lee et al. 2012; Marins et al. 2014; Muller et al. 2012; Wang et al. 2012), titanium oxide (Gutierrez et al. 2012, 2013), vanadium dioxide (Gutierrez et al. 2013), triethanolamine (TEA) (De Salvi et al. 2014) and grapheme (Feng et al. 2012).

Muller et al. (2011) developed a conducting BC material through in situ oxidative chemical polymerization of PY on the surface of BC nanofibres (with $FeCl_3$ as oxidant agent). They decreased the electrical resistivity from 9.1×10^{12} (BC) to 0.33 (composite) Ω cm due to the external coating of the nanofibres. Thermal stability was also enhanced for the same reason. This research group applied the same technique to prepare electrically conducting composites, but using Ani (Muller et al. 2012). The resultant material (BC/PAni) showed high electrical conductivity values (0.9 S/cm) and good mechanical properties (40 MPa). In both cases, nanoparticles coated the surface of BC nanofibers encapsulating them. In a later study (Marins et al. 2014), the effects of two oxidant agents, ammonium persulfate (APS) and $FeCl_3$ on the properties of the final BC/PAni membranes was investigated. Higher conductivity, improved absorption properties and a uniform, smooth coating is obtained in membranes prepared with $FeCl_3$ (Fig. 15).

Outstanding properties were achieved by Wang et al. (2012) because of the manipulation of the ordered flake-type nanostructure of composites consisting of BC and Pani. They used the technique of in situ polymerization of self-assembled Ani onto BC nanofibers and optimized the process. The obtained results were those of a supercapacitor: a high electrical conductivity of 5.1 S/cm and a mass-specific capacitance of 273 F/g at 0.2 A/g current density.

Due to the electrochemical properties of the carbonized BC (CBC), Huang et al. (2014a) decided to prepare a nanocomposite by immobilizing ultrafine-sized platinum nanoparticles on CBC to serve as an anode catalytic substrate for direct methanol fuel cells (DMFC). They showed better tolerance to poisonous species, higher methanol oxidation activity and stability than Pt/Vulcan (used to compare).

De Salvi et al. (2014) studied the influence of temperature on the ionic conductivity of membranes prepared by soaking BC membranes in TEA aqueous solutions and drying. An Arrhenius relation defined its behavior, showing an increment in the conductivity from 1.8×10^{-5} to 7.0×10^{-4} S/cm by increasing the temperature from 25 to 80 °C.

Magnetic materials Another approach of the micro/nanoporous spaces of the BC is to precipitate magnetic nanoparticles in order to form magnetic nanocomposites to be used for biomedical, magnetographic printing, data storage, anti-counterfeit and electronic applications (Vitta and Thiruvengadam 2012; Zhang et al. 2011).

To get flexible magnetic membranes of BC, Zhang et al. (2011) synthesized Fe_3O_4 nanoparticles in situ on the nanofibres and it was modified with fluoroalkyl silane (FAS). Amphiphobicity on the surface and superparamagnetic behavior with the saturation magnetization of 8.03 emu/g were demonstrated.

Ren et al. (2014) modified the conductive CBC with magnetic $CoFe_2O_4$ nanocrystals to create an electromagnetic nanocomposite by a solvothermal method. The best microwave absorption capacity was observed with a CBC/$CoFe_2O_4$ ratio of 10 wt%, where optimal reflection loss (RL) was −45 dB.

Nanocrystals of cellulose Because of the high aspect ratio and crystallinity, BC has been also used to produce nanocrystals or nanowhiskers through acid

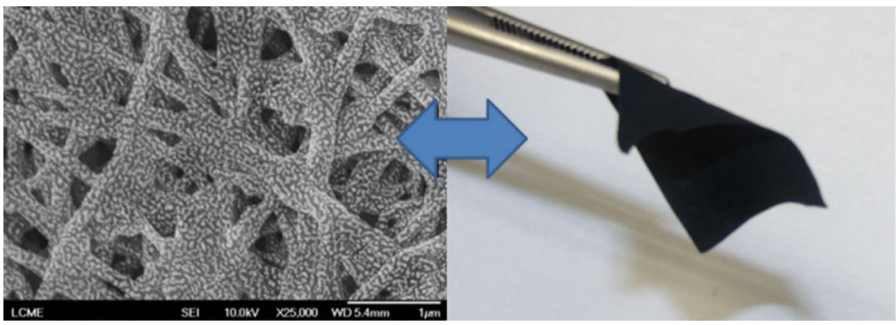

Fig. 15 Field-emission gun scanning electron microscope (FEG-SEM) of a bacterial cellulose membrane containing around 95 % Pani at the bacterial cellulose surface and macroscopic view of the BC/PAni(FeCl3) membrane (Reprinted from Marins et al. 2014 with permission from Springer)

hydrolysis (removing the amorphous parts of the nanofibrils) (Ambrosio-Martín et al. 2015; George and Siddaramaiah 2012; Huang et al. 2014b). They could be used in the nanocomposite field as a reinforcing element because of their stiffness and their comparatively lower density (Huang et al. 2014b).

BC nanocrystals (BCNC) has been modified and optimized in different ways for different purposes. For example, George and Siddaramaiah (2012) added BCNC to a gelatin matrix to form edible, biodegradable and high-performance nanocomposite films for food packaging applications.

Thermal properties

Biomedicine Thermal stability is a key property enabling the use of BC hydrogels as a drug-delivery system. Amin et al. (2012) combined BC with acrylic acid to produce a hydrogel by exposure to accelerated electron-beam irradiation at different doses. This material reduced the swelling in a human body at body temperature, so they concluded with a positive evaluation to be used for temperature-controlled delivery.

Papermaking As it has been already studied by Shafizadeh et al. (1978), flame-retardant compounds, such as those containing phosphorous, reduce the cellulose decomposition temperature and enhance char formation. Thus minimizes the formation of levoglucosan. In this way, Basta and El-Saied (2009) substituted glucose in the culture medium with glucose phosphate to enhance the flame resistance of BC, creating phosphate containing BC (PCBC). Both BC and PCBC were added into wood pulps making paper sheets and thermal degradation was investigated. With the presence of phosphate groups, they succeeded in increasing the resistivity to thermal decomposition and minimizing the formation of levoglucosan, controlling smoke generation and toxicity when burning. In addition, with the small amount of 5 % of these BC compounds added into wood pulp, strength and kaolin retention were significantly enhanced in the case of PCBC-pulp in comparison with BC-pulp sheets.

Mechanical properties

Despite the properties of dried BC, BC aerogels and their hydrated precursors have not provided sufficient compressive resistance for most commercial applications (Pircher et al. 2014). To reinforce BC aerogels, Pircher et al. (2014) incorporated four secondary polymers into the BC matrix. Composites of poly (methyl methacrylate) and BC (PMMA-BC) showed the best results: a Young's modulus of 3.28 MPa instead of 0.006 MPa of the BC aerogel and a tensile strength of 1513.1 kPa rather than 13 kPa of the BC aerogel.

Nanocomposites The nanofibrillar structure of BC together with its mechanical properties makes this material ideal to be used as a reinforcing material in a nanocomposite (Rosa et al. 2014; Ruka et al. 2013; Tomé et al. 2013). It has been largely used in this field for specific purposes in different ways: in situ synthesis (Ruka et al. 2013), or through impregnation method (ex situ).

Soykeabkaew et al. (2012) reinforced a starch matrix with BC using a film casting technique. They obtained a nanocomposite with markedly superior mechanical properties: a Young's modulus of 2.6 GPa (106-fold more than original matrix) and a tensile strength of 58 MPa (20-fold more); a glass transition temperature of 84.9 °C (35 °C more) and a thermal degradation temperature of 348.46 °C (40 °C more).

In another study, Rosa et al. (2014) prepared a green nanocomposite by grafting propylene oxide in dried BC with potassium hydroxide as the catalyst. BC nanofibres had a strong interfacial adhesion with the matrix, through a covalent bond. This material can be used as reinforced rigid polyurethane foams.

Biomedicine BC has also been used in the biomedical field to give the required mechanical properties to typical materials used as scaffolds for wound caring, artificial blood vessels or tissue engineering.

In order to maintain optimum pH levels during degradation of scaffolds for wound care and tissue engineering, therefore mimicking the mechanical properties of the human skin, Hu and Catchmark (2011) made bioabsorbable BC materials and introduced buffer ingredients and cellulases into their porous network. When they were hydrated with saline water (0.9 % NaCl), their mechanical properties behaved in a suitable way for wound caring: tensile strength of 18.65 MPa, extensibility of 7.04 % and a Young's modulus of 0.381GPa.

Due to the low mechanical properties of collagen, their applications in the biomedical field are limited. To enhance these properties, Albu et al. (2014) prepared composites of BC and collagen through different ways: by immersing BC pellicles in collagen gel (CG), collagen solution (CS) and hydrolyzed collagen (HC), and by mixing BC powder with solutions of collagen. Elastic modulus was enhanced by 4 (BC/HC and BC/CG in comparison with BC) and 60-fold (BC/CS compared to BC). This impressive enhancement of mechanical properties may be because of the easy access of collagen particles in dissolution to BC network.

Papermaking BC's mechanical properties together with its compatibility with wood cellulose make BC a potential candidate for being used as a reinforcing material in papermaking. Surma-Slusarska et al. (2008b) evaluated the suitability of using BC in papermaking composites. After a positive evaluation, they examined the structural and strength properties of composites of unbeaten, bleached birch and pine sulphate pulps with BC (Surma-Slusarska et al. 2008a). Composites obtained by culturing the strain with these suspended fibres had the best results. They increased the breaking length by 80 % compared to pure birch and pine pulps and the tear index by 200 % (compared to pure birch pulp) and 76 % (compared to pine pulp).

Cheng et al. (2011) prepared paper sheets from BC obtained in culture with CMC and wood pulp. Tensile strength was enhanced from 13 (regular paper) to 30 MPa (50 %-BC paper sheet) and Young's modulus was also increased from 14.3 (regular paper) to 23.5 MPa (50 %-BC paper sheet).

Food Due to its unique suspending, thickening, WHC, stabilizing and bulking properties, BC has been also applied into food (Shi et al. 2014; Yu and Lin 2014). Yu and Lin (2014) evaluated the characteristics of adding BC into pork frankfurters. When BC concentration increased, low textural hardness and shear values were obtained. A regular-fat frankfurter with 10–20 % high-fiber BC with acceptable sensory and textural traits was the final product.

Water absorption behavior

Some attempts to improve the capability of BC to rehydrate have been made by modifying the structure of BC to reduce the crystallinity (Chen et al. 2013). Lin et al. (2009) tried to enhance this ability by immersing BC with 0.5 % (w/w) enzymatically modified gelatin solution (EMG). The rehydration ratio of the nanocomposite was 3 (immersed 10 min) to 4 (immersed 7 h) times that of dried BC (16.5 %). A similar study about in situ modification of BC with CMC in culture with different strains was undertaken by Ma et al. (2014) and Chen et al. (2011a). With a small amount of CMC (0.01 %, w/v), BC produced by *Enterobacter sp. FY-07* increased its rehydration ability and WHC by 43.3 and 31.0 %, respectively, causing a reduction in the crystallinity of more than 39.8 % (Fig. 16).

Biomedicine With the aim of delivering active substances into a wound, specific moisture is required to facilitate its penetration and an easy and painless dressing change (Shezad et al. 2010). Because of the high liquid absorbency and hygienic nature, BC has been widely used in this way. In the case of Meftahi et al. (2010), they immersed cotton gauze samples in the BC culture medium to coat them, producing an increase in the WHC of 33 %.

A 390 % increase in water retention was obtained by Spaic et al. (2014), by TEMPO-catalyzed oxidation of BC. They observed that this property was pH dependent and increased by fivefold when the pH changes from 1 to 7.

Several attempts have been made to explore the behavior of these systems in human or animal skins with different drugs. Recently, Silva et al. (2014) investigated the incorporation of diclofenac sodium salt in BC membranes as novel nanostructured transdermal delivery systems. Swelling capacity of BC/diclofenac was 6 times more than that of pure BC. The permeation rates were similar to that of commercial patches but significantly lower than that of a commercial gel.

Huang et al. (2010) modified in situ the structure of BC to enhance its ability to rehydrate. The best result was obtained with CMC, which reduced the crystallinity from 70.5 to 45.4 %, thus causing an increase in the rehydration ability from around 13.5 to 19 % (after 10 min) and from 16 to 23 % (after 7 h).

Tome et al. (2011) also chemically modified BC to make its surface hydrophobic. They used several anhydrides and hexanoyl chloride suspended in an ionic liquid. They obtained a hydrophobic surface without modification of the ultrastructure.

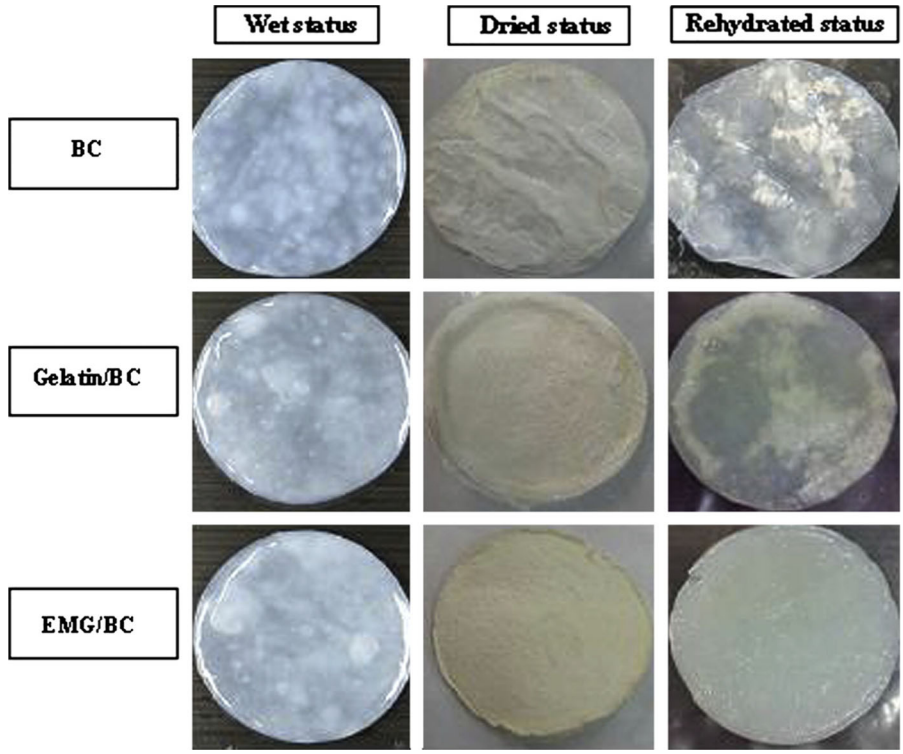

Fig. 16 Appearance of bacterial cellulose, gelatin/bacterial cellulose and enzymatically modified gelatin/bacterial cellulose before and after freeze-drying and rehydration (Reprinted from Lin et al. 2009 with permission from Elsevier)

Biocompatibility (antimicrobial activity)

As it is said in the previous section, some modifications have to be made to BC to enhance its antimicrobial activity. Some of them are with hyaluronic acid (HA) (Lopes et al. 2014), poly(3-hidroxybutyrate) (PHB) (Cai and Yang 2011; Cai et al. 2011; Martínez-Sanz et al. 2015; Ruka et al. 2014), silver (Ag) nanoparticles (Berndt et al. 2013; Feng et al. 2014; George et al. 2014; Li et al. 2015; Wu et al. 2014), chitosan (Kingkaew et al. 2014; Lai et al. 2014; Lin et al. 2013b), titanium dioxide (Khan et al. 2015), montmorillonite (MMT) (Ul-Islam et al. 2013a) and benzalkonium chloride (Wei et al. 2011).

Biomedicine With the purpose of preparing a scaffold for tissue regeneration, Lopes et al. (2014) introduced HA on BC production on different days of the fermentation (first, third or sixth day). When HA is added on the first day, more hydrophobic membranes were produced than that of native BC, but if it is added on the sixth day, the hydrophilic character increases. Crystallinity (60–68 % on the third day of addition) and thermal stability increased when the addition of HA was delayed.

Cai et al. (2011) prepared a biocompatible nanocomposite by impregnating BC into PHB so it can be applied in the tissue engineering field. They used BC due to its biocompatibility and nanofibrillar structure, which enhanced PHB crystallinity, tensile strength (130 %) and elongation (100 %). In another study (Cai and Yang 2011), they also improved the thermal stability of PHB from 195 to 250 °C, tensile strength by 150 %, elongation at break by 300 % and Young's modulus by 120 %.

Ruka et al. (2013) altered the morphology and properties of BC by adding PHB to the culture medium to make a fully degradable nanocomposite system. Tensile properties increased, but crystallinity (79–52 %) decreased.

Ag nanoparticles have been studied for their antimicrobial activity, apart from their extremely developed specific surface. In this case, BC network

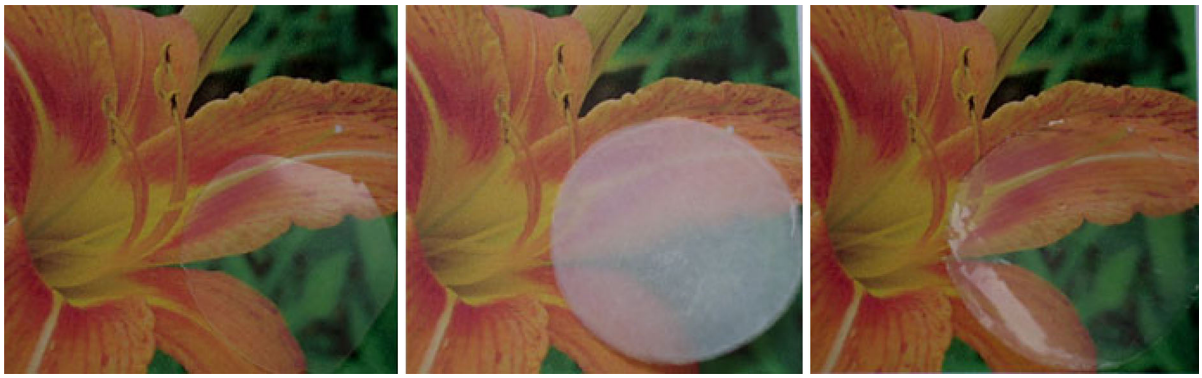

Fig. 17 Photographs of cured epoxidized soybean oil matrix, bacterial cellulose and cured ESO/BC composite films (Reprinted from Retegi et al. 2012 with permission from Springer)

serves as a template for the precipitation of Ag nanoparticles through different methods (Li et al. 2015). Wu et al. (2014) created Ag-BC material by soaking purified BC in a solution of silver ammonia. They demonstrated with two tests modelled on rat wounds of different degree that it may be possible to decrease inflammation and promote scald wound healing.

Another material that may potentially be used in the biomedical field is chitosan. Lin et al. (2013b) prepared BC-chitosan membranes and experimented its effects on rat models. Through histological examinations, they demonstrated that wounds treated with these membranes epithelialized and regenerated faster than those treated with BC. Kingkaew et al. (2014) evaluated the influence of the molecular weight (MW) of chitosan in all produced films showed antibacterial activities against *Staphylococcus aureus* and *Aspergillus niger* when MW was higher, but against *Escherichia coli* no inhibitory effect was shown. However, the growth of human skin cells was favored when MW of chitosan was low.

Wei et al. (2011) prepared an antibacterial dry film by immersing a FD-BC film in a benzalkonium chloride solution with another FD process. 24 h of a constant and prolonged antimicrobial activity especially against Staphylococcus aureus and Bacillus subtilis was achieved. This procedure could be carried out with other antimicrobial agents instead of benzalkonium chloride, such as antibiotics, Ag antibiotic agents and antimicrobial surfactants (Khan et al. 2015).

Food The main roles of active packaging is to protect food products from the environment, which extends their shelf life. By adding antibacterial agents, like enhanced BC, industry takes advantage of this antibacterial activity without variation of the packages that are normally used (Gao et al. 2014).

E-polylysine (EPL) was used to coat the surfaces of BC nanofibres through a crosslinking method to enhance the antibacterial activity of BC by Gao et al. (2014). There was effective antibacterial activity against *Escherichia coli* and *Staphylococcus aureus* when the EPL concentration was high.

Optical properties

With the aim of preparing photochromic BC nanofibrous membranes, Hu et al. (2011b) modified the surface of BC nanofibers with spiropyran photochromes. When they are subjected to UV irradiation, their color changed from colorless to pink, and returned again to colorless by visible light.

Composites with high stiffness and good ductility were obtained when the BC network structure was incorporated onto a matrix of epoxidized soybean oil (ESO) by Retegi et al. (2012). Resulting films presented high transparency, with an only loss of transmittance of 15 % in the nanocomposites. This can be observed in Fig. 17.

Gutierrez et al. (2013) developed a new method to produce conductive BC composites through a

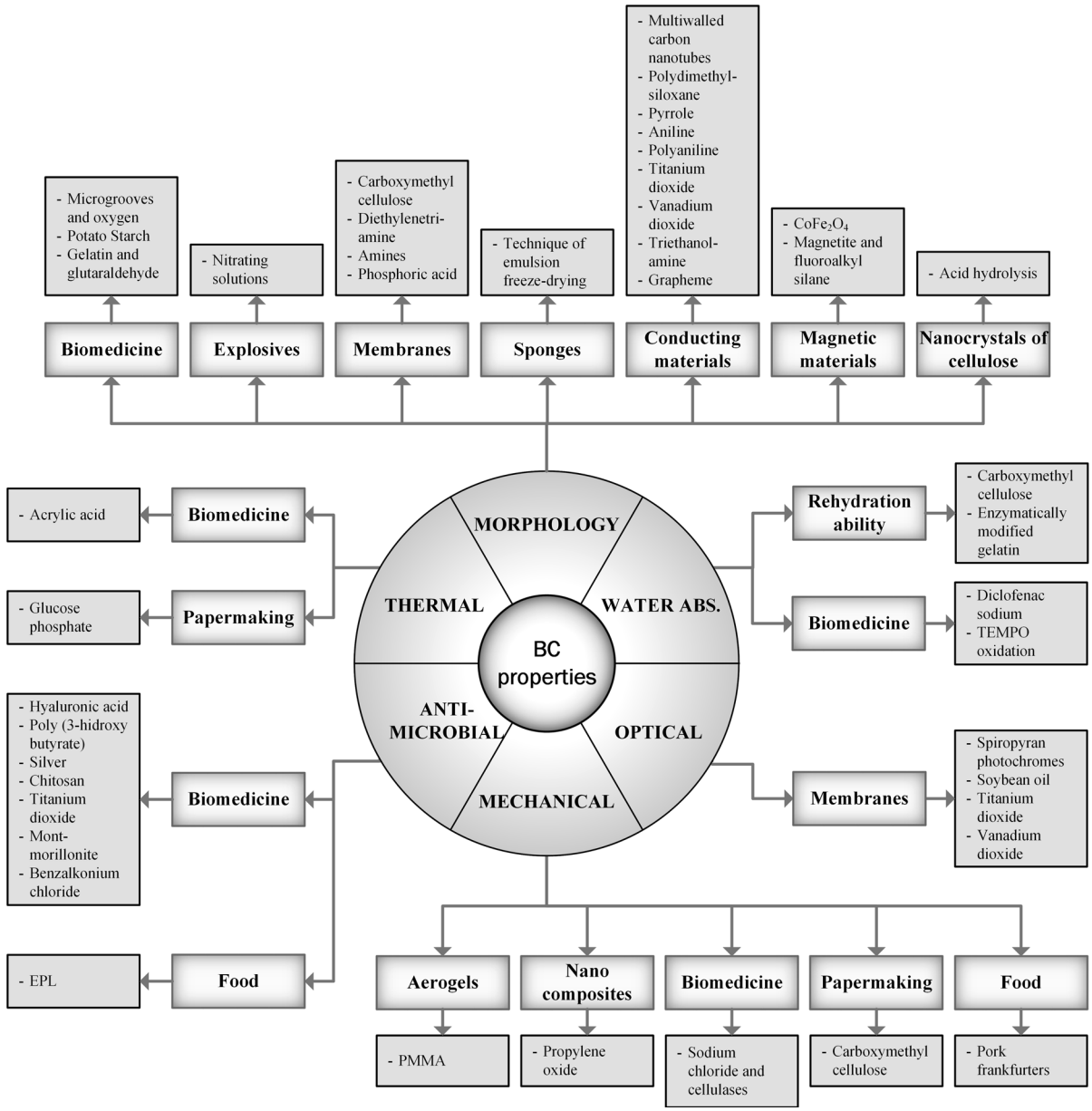

Fig. 18 Schematic diagram of main applications and modifications of bacterial cellulose depending on the property which is desired to be enhanced

diffusion step of sol–gel titanium or vanadium oxide nanoparticles via the orbital incubator. Nanopapers of a Young's modulus of 6 GPa were obtained when a mixture of vanadium and titanium oxide were applied. They possessed the reversible photochromic properties characteristic of vanadium oxide, so these nanopapers could be used for optical applications.

Conclusions

In view of its unique properties, such as nanofibril structure, high porosity, purity, crystallinity, mechanical properties, WHC and good antimicrobial activity, BC is presented as a promising candidate to substitute plant origin cellulose when specific applications are

required. However, BC has to deal with some technical issues before it can be scaled up to industrial level. These include its relative high cost, low solubility and hydrophobicity. Different studies are being carried out to overcome these problems. However, the expense of BC production due to the low productivity and the high-cost of raw materials limits its applications.

Fed-batch operation mode is a possible solution to these production process issues, since the constant addition of fresh medium to the culture broth makes bacteria continue producing cellulose. Another promising method is repeated-batch culture, where a ratio of culture broth is extracted to another medium in order to get a semi-continuous process. Both mechanisms have resulted higher yields. If genetic modification of the bacteria and a low-cost nutrient medium are added to these methods, the process may be suitable for a larger scale. However, more intensive research is needed to turn this hypothesis into reality.

To get an easier overview of the different modifications of BC to be used in a specific application, a complete diagram with most of substances considered in this review has been developed (Fig. 18).

Acknowledgments The authors wish to acknowledge the financial support of the SPANISH MINISTRY OF ECONOMY AND COMPETITIVENESS through the project "NANOSOL PAPELREC" (Ref. CTQ2013-48090-C2-1-R) and the Grant of C. Campano (BES-2014-068177).

References

Albu MG, Vuluga Z, Panaitescu DM, Vuluga DM, Casarica A, Ghiurea M (2014) Morphology and thermal stability of bacterial cellulose/collagen composites. Cent Eur J Chem 12:968–975

Al-Gelawi MH, Hameed ND, Jasim HM (2012) Isolation, identification and the role of plasmid of cellulose producing *Gluconacetobacter xylinus*. J Plant Mol Biol Biotechnol 3:16–20

Ambrosio-Martín J, Fabra MJ, Lopez-Rubio A, Lagaron JM (2015) Melt polycondensation to improve the dispersion of bacterial cellulose into polylactide via melt compounding: enhanced barrier and mechanical properties. Cellulose 22:1201–1226

Amin M, Ahmad N, Halib N, Ahmad I (2012) Synthesis and characterization of thermo- and pH-responsive bacterial cellulose/acrylic acid hydrogels for drug delivery. Carbohyd Polym 88:465–473

Ausmees N, Jonsson H, Hoglund S, Ljunggren H, Lindberg M (1999) Structural and putative regulatory genes involved in cellulose synthesis in *Rhizobium leguminosarum bv. trifolii*. Microbiology 145:1253–1262

Aydin YA, Aksoy ND (2009) Isolation of cellulose producing bacteria from wastes of vinegar fermentation. WCECS 2009: World congress on engineering and computer science, vols I and II. Int Assoc Engineers-Iaeng, Hong Kong

Aydin YA, Aksoy ND (2014) Isolation and characterization of an efficient bacterial cellulose producer strain in agitated culture: *Gluconacetobacter hansenii P2A*. Appl Microbiol Biotechnol 98:1065–1075

Bae S, Shoda M (2004) Bacterial cellulose production by fed-batch fermentation in molasses medium. Biotechnol Progr 20:1366–1371

Bae SO, Shoda M (2005) Production of bacterial cellulose by *Acetobacter xylinum BPR2001* using molasses medium in a jar fermentor. Appl Microbiol Biotechnol 67:45–51

Bae S, Sugano Y, Shoda M (2004) Improvement of bacterial cellulose production by addition of agar in a jar fermentor. J Biosci Bioeng 97:33–38

Barnhart DM, Su SC, Baccaro BE, Banta LM, Farrand SK (2013) CelR, an ortholog of the diguanylate cyclase PleD of *caulobacter*, regulates Cellulose synthesis in *Agrobacterium tumefaciens*. Appl Environ Microbiol 79: 7188–7202

Basta AH, El-Saied H (2009) Performance of improved bacterial cellulose application in the production of functional paper. J Appl Microbiol 107:2098–2107

Berndt S, Wesarg F, Wiegand C, Kralisch D, Müller F (2013) Antimicrobial porous hybrids consisting of bacterial nanocellulose and silver nanoparticles. Cellulose 20:771–783

Besbes I, Alila S, Boufi S (2011) Nanofibrillated cellulose from TEMPO-oxidized eucalyptus fibres: effect of the carboxyl content. Carbohyd Polym 84:975–983

Brown AJ (1886) XLIII.-On an acetic ferment which forms cellulose. J Chem Soc Trans 49:432–439

Cai ZJ, Yang G (2011) Optical nanocomposites prepared by incorporating bacterial cellulose nanofibrils into poly(3-hydroxybutyrate). Mater Lett 65:182–184

Cai ZJ, Yang GA, Kim J (2011) Biocompatible nanocomposites prepared by impregnating bacterial cellulose nanofibrils into poly(3-hydroxybutyrate). Curr Appl Phys 11:247–249

Çakar F, Özer I, Aytekin AO, Sahin F (2014) Improvement production of bacterial cellulose by semi-continuous process in molasses medium. Carbohyd Polym 106:7–13

Castro C, Zuluaga R, Alvarez C, Putaux JL, Caro G, Rojas OJ, Mondragon I, Ganan P (2012) Bacterial cellulose produced by a new acid-resistant strain of *Gluconacetobacter genus*. Carbohyd Polym 89:1033–1037

Cavka A, Guo X, Tang S-J, Winestrand S, Jönsson LJ, Hong F (2013) Production of bacterial cellulose and enzyme from waste fiber sludge. Biotechnol Biofuels 6:25

Chaker A, Mutje P, Vilar MR, Boufi S (2014) Agriculture crop residues as a source for the production of nanofibrillated cellulose with low energy demand. Cellulose 21: 4247–4259

Charreau H, Foresti ML, Vazquez A (2013) Nanocellulose patents trends: a comprehensive review on patents on cellulose nanocrystals, microfibrillated and bacterial cellulose. Recent Pat Nanotechnol 7:56–80

Chawla PR, Bajaj IB, Survase SA, Singhal RS (2009) Microbial cellulose: fermentative production and applications. Food Technol Biotechnol 47:107–124

Chen SY, Zou Y, Yan ZY, Shen W, Shi SK, Zhang X, Wang HP (2009) Carboxymethylated-bacterial cellulose for copper and lead ion removal. J Hazard Mater 161:1355–1359

Chen HH, Chen LC, Huang HC, Lin SB (2011a) In situ modification of bacterial cellulose nanostructure by adding CMC during the growth of *Gluconacetobacter xylinus*. Cellulose 18:1573–1583

Chen Y, Zhang YM, Ke FY, Zhou JH, Wang HP, Liang DH (2011b) Solubility of neutral and charged polymers in ionic liquids studied by laser light scattering. Polymer 52:481–488

Chen H-H, Lin S-B, Hsu C-P, Chen L-C (2013) Modifying bacterial cellulose with gelatin peptides for improved rehydration. Cellulose 20:1967–1977

Chen WS, Abe K, Uetani K, Yu HP, Liu YX, Yano H (2014a) Individual cotton cellulose nanofibers: pretreatment and fibrillation technique. Cellulose 21:1517–1528

Chen Y, Zhou X, Lin Q, Jiang D (2014b) Bacterial cellulose/gelatin composites: in situ preparation and glutaraldehyde treatment. Cellulose 21:2679–2693

Cheng K-C, Catchmark JM, Demirci A (2009a) Enhanced production of bacterial cellulose by using a biofilm reactor and its material property analysis. J Biol Eng 3:12

Cheng KC, Catchmark JM, Demirci A (2009b) Effect of different additives on bacterial cellulose production by *Acetobacter xylinum* and analysis of material property. Cellulose 16:1033–1045

Cheng KC, Demirci A, Catchmark JM (2010) Advances in biofilm reactors for production of value-added products. Appl Microbiol Biotechnol 87:445–456

Cheng KC, Catchmark JM, Demirci A (2011) Effects of CMC addition on bacterial cellulose production in a biofilm reactor and its paper sheets analysis. Biomacromolecules 12:730–736

Choi CN, Song HJ, Kim MJ, Chang MH, Kim SJ (2009) Properties of bacterial cellulose produced in a pilot-scale spherical type bubble column bioreactor. Korean J Chem Eng 26:136–140

Ciechanska D, Struszczyk H, Kazimierczak J, Guzinska K, Pawlak M, Kozlowska E, Matusiak G, Dutkiewicz M (2002) New electro-acoustic transducers based on modified bacterial cellulose. Fibres Text East Eur 10:27–30

Çoban EP, Biyik H (2011) Evaluation of different pH and temperatures for bacterial cellulose production in HS (Hestrin-Scharmm) medium and beet molasses medium. Afr J Microbiol Res 5:1037–1045

Czaja W, Romanovicz D, Brown RM (2004) Structural investigations of microbial cellulose produced in stationary and agitated culture. Cellulose 11:403–411

Dayal MS, Goswami N, Sahai A, Jain V, Mathur G, Mathur A (2013) Effect of media components on cell growth and bacterial cellulose production from *Acetobacter aceti MTCC 2623*. Carbohyd Polym 94:12–16

De Salvi DTB, Barud HS, Pawlicka A, Mattos RI, Raphael E, Messaddeq Y, Ribeiro SJL (2014) Bacterial cellulose/triethanolamine based ion-conducting membranes. Cellulose 21:1975–1985

Dellaglio F, Cleenwerck I, Felis GE, Engelbeen K, Janssens D, Marzotto M (2005) Description of *Gluconacetobacter swingsii sp nov* and *Gluconacetobacter rhaeticus sp nov*., isolated from Italian apple fruit. Int J Syst Evol Microbiol 55:2365–2370

Dissanayake D, Ismail FM (2013) Mathematical modeling of bacterial cellulose production by *Acetobacter xylinum* using rotating biological fermentor. In: Proceedings 27th European conference on modelling and simulation ECMS 2013. European Council Modelling and Simulation, Nottingham

Eichhorn SJ, Dufresne A, Aranguren M, Marcovich NE, Capadona JR, Rowan SJ, Weder C, Thielemans W, Roman M, Renneckar S, Gindl W, Veigel S, Keckes J, Yano H, Abe K, Nogi M, Nakagaito AN, Mangalam A, Simonsen J, Benight AS, Bismarck A, Berglund LA, Peijs T (2010) Review: current international research into cellulose nanofibres and nanocomposites. J Mater Sci 45:1–33

El-Saied H, El-Diwany AI, Basta AH, Atwa NA, El-Ghwas DE (2008) Production and characterization of economical bacterial cellulose. Bioresources 3:1196–1217

Fang L, Catchmark JM (2014) Characterization of water-soluble exopolysaccharides from *Gluconacetobacter xylinus* and their impacts on bacterial cellulose crystallization and ribbon assembly. Cellulose 21:3965–3978

Feng YY, Zhang XQ, Shen YT, Yoshino K, Feng W (2012) A mechanically strong, flexible and conductive film based on bacterial cellulose/graphene nanocomposite. Carbohyd Polym 87:644–649

Feng J, Shi Q, Li W, Shu X, Chen A, Xie X, Huang X (2014) Antimicrobial activity of silver nanoparticles in situ growth on TEMPO-mediated oxidized bacterial cellulose. Cellulose 21:4557–4567

Fu LN, Zhang J, Yang G (2013) Present status and applications of bacterial cellulose-based materials for skin tissue repair. Carbohyd Polym 92:1432–1442

Gao CA, Wan YZ, Yang CX, Dai KR, Tang TT, Luo HL, Wang JH (2011a) Preparation and characterization of bacterial cellulose sponge with hierarchical pore structure as tissue engineering scaffold. J Porous Mat 18:139–145

Gao QY, Shen XY, Lu XK (2011b) Regenerated bacterial cellulose fibers prepared by the NMMO center dot H_2O process. Carbohyd Polym 83:1253–1256

Gao C, Yan T, Dai K, Wan Y (2012) Immobilization of gelatin onto natural nanofibers for tissue engineering scaffold applications without utilization of any crosslinking agent. Cellulose 19:761–768

Gao C, Yan T, Du J, He F, Luo HL, Wan YZ (2014) Introduction of broad spectrum antibacterial properties to bacterial cellulose nanofibers via immobilising epsilon-polylysine nanocoatings. Food Hydrocoll 36:204–211

Gardner DJ, Oporto GS, Mills R, Samir M (2008) Adhesion and surface issues in cellulose and nanocellulose. J Adhes Sci Technol 22:545–567

Ge HJ, Du SK, Lin DH, Zhang JN, Xiang JL, Li ZX (2011) *Gluconacetobacter hansenii* subsp nov., a High-Yield Bacterial Cellulose Producing Strain Induced by High Hydrostatic Pressure. Appl Biochem Biotechnol 165:1519–1531

Gelin K, Bodin A, Gatenholm P, Mihranyan A, Edwards K, Stromme M (2007) Characterization of water in bacterial cellulose using dielectric spectroscopy and electron microscopy. Polymer 48:7623–7631

George J, Siddaramaiah (2012) High performance edible nanocomposite films containing bacterial cellulose nanocrystals. Carbohyd Polym 87:2031–2037

George J, Kumar R, Sajeevkumar VA, Ramana KV, Rajamanickam R, Abhishek V, Nadanasabapathy S, Siddaramaiah (2014) Hybrid HPMC nanocomposites containing bacterial cellulose nanocrystals and silver nanoparticles. Carbohyd Polym 105:285–292

Gomes FP, Silva N, Trovatti E, Serafim LS, Duarte MF, Silvestre AJD, Neto CP, Freire CSR (2013) Production of bacterial cellulose by *Gluconacetobacter sacchari* using dry olive mill residue. Biomass Bioenergy 55:205–211

Guo X, Cavka A, Jonsson LJ, Hong F (2013) Comparison of methods for detoxification of spruce hydrolysate for bacterial cellulose production. Microb Cell Fact 12:14

Gutierrez J, Tercjak A, Algar I, Retegi A, Mondragon I (2012) Conductive properties of TiO_2/bacterial cellulose hybrid fibres. J Colloid Interface Sci 377:88–93

Gutierrez J, Fernandes SCM, Mondragon I, Tercjak A (2013) Multifunctional hybrid nanopapers based on bacterial cellulose and sol-gel synthesized titanium/vanadium oxide nanoparticles. Cellulose 20:1301–1311

Ha JH, Shehzad O, Khan S, Lee SY, Park JW, Khan T, Park JK (2008) Production of bacterial cellulose by a static cultivation using the waste from beer culture broth. Korean J Chem Eng 25:812–815

Ha JH, Shah N, Ul-Islam M, Khan T, Park JK (2011) Bacterial cellulose production from a single sugar alpha-linked glucuronic acid-based oligosaccharide. Process Biochem 46:1717–1723

Habibi Y, Chanzy H, Vignon MR (2006) TEMPO-mediated surface oxidation of cellulose whiskers. Cellulose 13:679–687

Hestrin S, Schramm M (1954) Synthesis of cellulose by *Acetobacter xylinum*. 2. Preparation of freeze-dried cells capable of polymerizing glucose to cellulose. Biochem J 58:345

Hettrich K, Pinnow M, Volkert B, Passauer L, Fischer S (2014) Novel aspects of nanocellulose. Cellulose 21:2479–2488

Hirai A, Tsuji M, Horii F (2002) TEM study of band-like cellulose assemblies produced by *Acetobacter xylinum* at 4 degrees C. Cellulose 9:105–113

Hong F, Qiu KY (2008) An alternative carbon source from konjac powder for enhancing production of bacterial cellulose in static cultures by a model strain *Acetobacter aceti* subsp. *xylinus ATCC 23770*. Carbohyd Polym 72:545–549

Hong F, Guo X, Zhang S, S-f Han, Yang G, Jönsson LJ (2012) Bacterial cellulose production from cotton-based waste textiles: enzymatic saccharification enhanced by ionic liquid pretreatment. Bioresour Technol 104:503–508

Hu Y, Catchmark JM (2010) Influence of 1-methylcyclopropene (1-MCP) on the production of bacterial cellulose biosynthesized by *Acetobacter xylinum* under the agitated culture. Lett Appl Microbiol 51:109–113

Hu Y, Catchmark JM (2011) In vitro biodegradability and mechanical properties of bioabsorbable bacterial cellulose incorporating cellulases. Acta Biomater 7:2835–2845

Hu WL, Chen SY, Yang ZH, Liu LT, Wang HP (2011a) Flexible electrically conductive nanocomposite membrane based on bacterial cellulose and polyaniline. J Phys Chem B 115:8453–8457

Hu WL, Liu SP, Chen SY, Wang HP (2011b) Preparation and properties of photochromic bacterial cellulose nanofibrous membranes. Cellulose 18:655–661

Hu WL, Chen SY, Yang JX, Li Z, Wang HP (2014) Functionalized bacterial cellulose derivatives and nanocomposites. Carbohyd Polym 101:1043–1060

Huang HC, Chen LC, Lin SB, Hsu CP, Chen HH (2010) In situ modification of bacterial cellulose network structure by adding interfering substances during fermentation. Bioresour Technol 101:6084–6091

Huang Y, Wang TH, Ji MZ, Yang JZ, Zhu CL, Sun DP (2014a) Simple preparation of carbonized bacterial cellulose-Pt composite as a high performance electrocatalyst for direct methanol fuel cells (DMFC). Mater Lett 128:93–96

Huang Y, Zhu CL, Yang JZ, Nie Y, Chen CT, Sun DP (2014b) Recent advances in bacterial cellulose. Cellulose 21:1–30

Hungund BS, Gupta S (2010a) Improved production of bacterial cellulose from *Gluconacetobacter persimmonis GH-2*. J Microbial Biochem Technol 2:127–133

Hungund BS, Gupta SG (2010b) Production of bacterial cellulose from *Enterobacter amnigenus GH-1* isolated from rotten apple. World J Microbiol Biotechnol 26:1823–1828

Hungund BS, Gupta S (2010c) Strain improvement of *Gluconacetobacter xylinus NCIM 2526* for bacterial cellulose production. Afr J Biotechnol 9:5170–5172

Iguchi M, Yamanaka S, Budhiono A (2000) Bacterial cellulose—a masterpiece of nature's arts. J Mater Sci 35:261–270

Ishida T, Sugano Y, Nakai T, Shoda M (2002) Effects of acetan on production of bacterial cellulose by *Acetobacter xylinum*. Biosci Biotechnol Biochem 66:1677–1681

Jaramillo R, Tobio W, Escamilla J (2012) Effect of sucrose in the production of cellulose by *Gluconacetobacter xylinus* in static culture. Rev MVZ Córdoba 17:3004–3013

Jaramillo R, Perna O, Revollo AB, Arrieta C, Escamilla E (2013) Effect of different concentrations of fructose on bacterial cellulose production in static culture. Rev Colomb Cienc Anim 5:116–130

Jia SR, Ou HY, Chen GB, Choi DB, Cho KA, Okabe M, Cha WS (2004) Cellulose production from *Gluconobacter oxydans TQ-B2*. Biotechnol Bioprocess Eng 9:166–170

Jonas R, Farah LF (1998) Production and application of microbial cellulose. Polym Degrad Stabil 59:101–106

Jonoobi M, Oladi R, Davoudpour Y, Oksman K, Dufresne A, Hamzeh Y, Davoodi R (2015) Different preparation methods and properties of nanostructured cellulose from various natural resources and residues: a review. Cellulose 22:935–969

Jung JY, Park JK, Chang HN (2005) Bacterial cellulose production by *Gluconacetobacter hansenii* in an agitated culture without living non-cellulose producing cells. Enzyme Microb Technol 37:347–354

Jung JY, Khan T, Park JK, Chang HN (2007) Production of bacterial cellulose by *Gluconacetobacter hansenii* using a novel bioreactor equipped with a spin filter. Korean J Chem Eng 24:265–271

Jung HI, Jeong JH, Lee OM, Park GT, Kim KK, Park HC, Lee SM, Kim YG, Son HJ (2010) Influence of glycerol on production and structural-physical properties of cellulose from *Acetobacter sp V6* cultured in shake flasks. Bioresour Technol 101:3602–3608

Kadere TT, Miyamoto T, Oniang'o RK, Kutima PM, Njoroge SM (2008) Isolation and identification of the genera *Acetobacter* and *Gluconobacter* in coconut toddy (mnazi). Afr J Biotechnol 7:2963–2971

Kawaguchi I, Nakamura K (2007) Make-up tissue paper for removing cosmetics, comprises glycerin impregnated into a tissue paper which consists of pulp fiber, and bacterial cellulose entangled in the pulp interfiber forming a network structure. JP2009077752-A; JP4314292-B2

Keshk S, Sameshima K (2006) The utilization of sugar cane molasses with/without the presence of lignosulfonate for the production of bacterial cellulose. Appl Microbiol Biotechnol 72:291–296

Khan S, Ul-Islam M, Khattak W, Ullah M, Park J (2015) Bacterial cellulose-titanium dioxide nanocomposites: nanostructural characteristics, antibacterial mechanism, and biocompatibility. Cellulose 22:565–579

Kim SY, Kim JN, Wee YJ, Park DH, Ryu HW (2006) Production of bacterial cellulose by *Gluconacetobacter sp RKY5* isolated from persimmon vinegar. Appl Biochem Biotechnol 131:705–715

Kim YJ, Kim JN, Wee YJ, Park DH, Ryu HW (2007) Bacterial cellulose production by *Gluconacetobacter* sp. *RKY5* in a rotary biofilm contactor. Appl Biochem Biotechnol 137:529–537

Kim S, Li H, Oh I, Kee C, Kim M (2012) Effect of viscosity-inducing factors on oxygen transfer in production culture of bacterial cellulose. Korean J Chem Eng 29:792–797

Kingkaew J, Kirdponpattara S, Sanchavanakit N, Pavasant P, Phisalaphong M (2014) Effect of molecular weight of chitosan on antimicrobial properties and tissue compatibility of chitosan-impregnated bacterial cellulose films. Biotechnol Bioprocess Eng 19:534–544

Klemm D, Schumann D, Udhardt U, Marsch S (2001) Bacterial synthesized cellulose—artificial blood vessels for microsurgery. Prog Polym Sci 26:1561–1603

Kojima Y, Tonouchi N, Tsuchida T, Yoshinaga F, Yamada Y (1998) The characterization of acetic acid bacteria efficiently producing bacterial cellulose from sucrose: the proposal of *Acetobacter xylinum* subsp. *nonacetoxidans* subsp. nov. Biosci Biotechnol Biochem 62:185–187

Kongruang S (2008) Bacterial cellulose production by *Acetobacter xylinum* strains from agricultural waste products. Appl Biochem Biotechnol 148:245–256

Kouda T, Naritomi T, Yano H, Yoshinaga F (1997a) Effects of oxygen and carbon dioxide pressures on bacterial cellulose production by *Acetobacter* in aerated and agitated culture. J Ferment Bioeng 84:124–127

Kouda T, Yano H, Yoshinaga F (1997b) Effect of agitator configuration on bacterial cellulose productivity in aerated and agitated culture. J Ferment Bioeng 83:371–376

Kouda T, Naritomi M, Naritomi T, Yano H, Yoshinaga F (2000) Process for continuously preparing bacterial cellulose. Google Patents

Krystynowicz A, Czaja W, Wiktorowska-Jezierska A, Gonçalves-Miśkiewicz M, Turkiewicz M, Bielecki S (2002) Factors affecting the yield and properties of bacterial cellulose. J Ind Microbiol Biot 29:189–195

Kumbhar J, Rajwade J, Paknikar K (2015) Fruit peels support higher yield and superior quality bacterial cellulose production. Appl Microbiol Biotechnol 99:6677–6691

Kuo C-H, Lee C-K (2009) Enhancement of enzymatic saccharification of cellulose by cellulose dissolution pretreatments. Carbohyd Polym 77:41–46

Kurosumi A, Sasaki C, Yamashita Y, Nakamura Y (2009) Utilization of various fruit juices as carbon source for production of bacterial cellulose by *Acetobacter xylinum NBRC 13693*. Carbohyd Polym 76:333–335

Lai C, Zhang S, Chen X, Sheng L (2014) Nanocomposite films based on TEMPO-mediated oxidized bacterial cellulose and chitosan. Cellulose 21:2757–2772

Lavoine N, Desloges I, Dufresne A, Bras J (2012) Microfibrillated cellulose—its barrier properties and applications in cellulosic materials: a review. Carbohyd Polym 90:735–764

Lee K-Y, Bismarck A (2012) Susceptibility of never-dried and freeze-dried bacterial cellulose towards esterification with organic acid. Cellulose 19:891–900

Lee K-Y, Quero F, Blaker J, Hill CS, Eichhorn S, Bismarck A (2011) Surface only modification of bacterial cellulose nanofibres with organic acids. Cellulose 18:595–605

Lee H-J, Chung T-J, Kwon H-J, Kim H-J, Tze W (2012) Fabrication and evaluation of bacterial cellulose-polyaniline composites by interfacial polymerization. Cellulose 19:1251–1258

Lee KY, Buldum G, Mantalaris A, Bismarck A (2014) More than meets the eye in bacterial cellulose: biosynthesis, bioprocessing, and applications in advanced fiber composites. Macromol Biosci 14:10–32

Li DS, Liu ZY, Al-Haik M, Tehrani M, Murray F, Tannenbaum R, Garmestani H (2010) Magnetic alignment of cellulose nanowhiskers in an all-cellulose composite. Polym Bull 65:635–642

Li Y, Li GZ, Zou YL, Zhou QJ, Lian XX (2014) Preparation and characterization of cellulose nanofibers from partly mercerized cotton by mixed acid hydrolysis. Cellulose 21:301–309

Li Z, Wang L, Chen S, Feng C, Chen S, Yin N, Yang J, Wang H, Xu Y (2015) Facilely green synthesis of silver nanoparticles into bacterial cellulose. Cellulose 22:373–383

Liang HW, Guan QF, Zhu Z, Song LT, Yao HB, Lei X, Yu SH (2012) Highly conductive and stretchable conductors fabricated from bacterial cellulose. NPG Asia Mater 4:6

Liimatainen H, Visanko M, Sirvio J, Hormi O, Niinimaki J (2013) Sulfonated cellulose nanofibrils obtained from wood pulp through regioselective oxidative bisulfite pretreatment. Cellulose 20:741–749

Lin SB, Hsu CP, Chen LC, Chen HH (2009) Adding enzymatically modified gelatin to enhance the rehydration abilities and mechanical properties of bacterial cellulose. Food Hydrocolloid 23:2195–2203

Lin SP, Calvar IL, Catchmark JM, Liu JR, Demirci A, Cheng KC (2013a) Biosynthesis, production and applications of bacterial cellulose. Cellulose 20:2191–2219

Lin WC, Lien CC, Yeh HJ, Yu CM, Hsu SH (2013b) Bacterial cellulose and bacterial cellulose-chitosan membranes for wound dressing applications. Carbohyd Polym 94:603–611

Lin SP, Hsieh SC, Chen KI, Demirci A, Cheng KC (2014) Semi-continuous bacterial cellulose production in a rotating disk bioreactor and its materials properties analysis. Cellulose 21:835–844

Lisdiyanti P, Kawasaki H, Seki T, Yamada Y, Uchimura T, Komagata K (2001) Identification of *Acetobacter* strains isolated from Indonesian sources, and proposals of *Acetobacter syzygii* sp. nov., *Acetobacter cibinongensis* sp. nov., and *Acetobacter orientalis* sp nov. J Gen Appl Microbiol 47:119–131

Liu J, Korpinen R, Mikkonen KS, Willfor S, Xu CL (2014) Nanofibrillated cellulose originated from birch sawdust after sequential extractions: a promising polymeric material from waste to films. Cellulose 21:2587–2598

Lopes TD, Riegel-Vidotti IC, Grein A, Tischer CA, Faria-Tischer PCD (2014) Bacterial cellulose and hyaluronic acid hybrid membranes: production and characterization. Int J Biol Macromol 67:401–408

Lu HM, Jiang XL (2014) Structure and properties of bacterial cellulose produced using a trickling bed reactor. Appl Biochem Biotechnol 172:3844–3861

Lu XK, Shen XY (2011) Solubility of bacteria cellulose in zinc chloride aqueous solutions. Carbohyd Polym 86:239–244

Lu ZG, Zhang YY, Chi YJ, Xu N, Yao WY, Sun B (2011) Effects of alcohols on bacterial cellulose production by *Acetobacter xylinum 186*. World J Microbiol Biotechnol 27:2281–2285

Lu M, Zhang YM, Guan XH, Xu XH, Gao TT (2014) Thermodynamics and kinetics of adsorption for heavy metal ions from aqueous solutions onto surface amino-bacterial cellulose. Trans Nonferrous Met Soc China 24:1912–1917

Luna-Martinez JF, Hernandez-Uresti DB, Reyes-Melo ME, Guerrero-Salazar CA, Gonzalez-Gonzalez VA, Sepulveda-Guzman S (2011) Synthesis and optical characterization of ZnS-sodium carboxymethyl cellulose nanocomposite films. Carbohyd Polym 84:566–570

Luo HL, Zhang J, Xiong GY, Wan YZ (2014) Evolution of morphology of bacterial cellulose scaffolds during early culture. Carbohyd Polym 111:722–728

Ma H, Zhou B, Li HS, Li YQ, Ou SY (2011) Green composite films composed of nanocrystalline cellulose and a cellulose matrix regenerated from functionalized ionic liquid solution. Carbohyd Polym 84:383–389

Ma T, Zhao Q, Ji K, Zeng B, Li G (2014) Homogeneous and porous modified bacterial cellulose achieved by in situ modification with low amounts of carboxymethyl cellulose. Cellulose 21:2637–2646

Marins JA, Soares BG, Fraga M, Muller D, Barra GMO (2014) Self-supported bacterial cellulose polyaniline conducting membrane as electromagnetic interference shielding material: effect of the oxidizing agent. Cellulose 21:1409–1418

Martínez-Sanz M, Vicente A, Gontard N, Lopez-Rubio A, Lagaron J (2015) On the extraction of cellulose nanowhiskers from food by-products and their comparative reinforcing effect on a polyhydroxybutyrate-co-valerate polymer. Cellulose 22:535–551

Matsuoka M, Tsuchida T, Matsushita K, Adachi O, Yoshinaga F (1996) A synthetic medium for bacterial cellulose production by *Acetobacter xylinum* subsp. *sucrofermentans*. Biosci Biotech Biochem 60:575–579

Matthysse AG, Marry M, Krall L, Kaye M, Ramey BE, Fuqua C, White AR (2005) The effect of cellulose overproduction on binding and biofilm formation on roots by *Agrobacterium tumefaciens*. Mol Plant-Microbe Interact 18:1002–1010

Meftahi A, Khajavi R, Rashidi A, Sattari M, Yazdanshenas ME, Torabi M (2010) The effects of cotton gauze coating with microbial cellulose. Cellulose 17:199–204

Mehta K, Pfeffer S, Brown RM Jr (2015) Characterization of an *acsD* disruption mutant provides additional evidence for the hierarchical cell-directed self-assembly of cellulose in *Gluconacetobacter xylinus*. Cellulose 22:119–137

Merayo N, Fuente E, Mutjé P, Negro C (2014) Uso de NFC a partir de pasta de eucalipto y residuos de maíz para mejorar la resistencia del papel reciclado. Paper presented at the XXVII Congreso Interamericano y Colombiano de Ingeniería Química, Cartagena de Indias

Miao CW, Hamad WY (2013) Cellulose reinforced polymer composites and nanocomposites: a critical review. Cellulose 20:2221–2262

Mikkelsen D, Flanagan B, Dykes G, Gidley M (2009) Influence of different carbon sources on bacterial cellulose production by *Gluconacetobacter xylinus strain ATCC 53524*. J Appl Microbiol 107:576–583

Mohite BV, Patil SV (2014) Physical, structural, mechanical and thermal characterization of bacterial cellulose by *G-hansenii NCIM 2529*. Carbohyd Polym 106:132–141

Moon S-H, Park J-M, Chun H-Y, Kim S-J (2006) Comparisons of physical properties of bacterial celluloses produced in different culture conditions using saccharified food wastes. Biotechnol Bioprocess Eng 11:26–31

Moon RJ, Martini A, Nairn J, Simonsen J, Youngblood J (2011) Cellulose nanomaterials review: structure, properties and nanocomposites. Chem Soc Rev 40:3941–3994

Moran-Mirabal J (2013) The study of cell wall structure and cellulose–cellulase interactions through fluorescence microscopy. Cellulose 20:2291–2309

Muller D, Rambo CR, Recouvreux DOS, Porto LM, Barra GMO (2011) Chemical in situ polymerization of polypyrrole on bacterial cellulose nanofibers. Synth Met 161:106–111

Muller D, Mandelli JS, Marins JA, Soares BG, Porto LM, Rambo CR, Barra GMO (2012) Electrically conducting nanocomposites: preparation and properties of polyaniline (PAni)-coated bacterial cellulose nanofibers (BC). Cellulose 19:1645–1654

Nakai T, Sugano Y, Shoda M, Sakakibara H, Oiwa K, Tuzi S, Imai T, Sugiyama J, Takeuchi M, Yamauchi D (2013) Formation of highly twisted ribbons in a carboxymethylcellulase gene-disrupted strain of a cellulose-producing bacterium. J Bacteriol 195:958–964

Naritomi T, Kouda T, Yano H, Yoshinaga F (1998a) Effect of ethanol on bacterial cellulose production from fructose in continuous culture. J Ferment Bioeng 85:598–603

Naritomi T, Kouda T, Yano H, Yoshinaga F (1998b) Effect of lactate on bacterial cellulose production from fructose in continuous culture. J Ferment Bioeng 85:89–95

Naritomi T, Kouda T, Yano H, Yoshinaga F, Shigematsu T, Moriumura S, Kida K (2002) Influence of broth exchange ratio on bacterial cellulose production by repeated-batch culture. Process Biochem 38:41–47

Negro C, Merayo N, Seara M, Balea A, Fuente Edl, Blanco A (2015) Effect of NFC added in mass to a recycled pulp on the flocculation process. Paper presented at the 10th European Congress of Chemical Engineering, Nice, France

Nguyen VT, Flanagan B, Gidley MJ, Dykes GA (2008) Characterization of Cellulose Production by a

Gluconacetobacter xylinus Strain from Kombucha. Curr Microbiol 57:449–453

Nishi Y, Uryu M, Yamanaka S, Watanabe K, Kitamura N, Iguchi M, Mitsuhashi S (1990) The structure and mechanical properties of sheets prepared from bacterial cellulose. 2. Improvement of the mechanical properties of sheets and their applicability to diaphragms of electroacoustic transducers. J Mater Sci 25:2997–3001

Noro N, Sugano Y, Shoda M (2004) Utilization of the buffering capacity of corn steep liquor in bacterial cellulose production by *Acetobacter xylinum*. Appl Microbiol Biotechnol 64:199–205

Oikawa T, Morino T, Ameyama M (1995a) Production of cellulose from D-Arabitol by *Acetobacter xylinum KU-1*. Biosci Biotechnol Biochem 59:1564–1565

Oikawa T, Ohtori T, Ameyama M (1995b) Production of cellulose from D-mannitol by *Acetobacter xylinum KU-1*. Biosci Biotechnol Biochem 59:331–332

Oshima T, Kondo K, Ohto K, Inoue K, Baba Y (2008) Preparation of phosphorylated bacterial cellulose as an adsorbent for metal ions. React Funct Polym 68:376–383

Oshima T, Taguchi S, Ohe K, Baba Y (2011) Phosphorylated bacterial cellulose for adsorption of proteins. Carbohyd Polym 83:953–958

Paakko M, Ankerfors M, Kosonen H, Nykanen A, Ahola S, Osterberg M, Ruokolainen J, Laine J, Larsson PT, Ikkala O, Lindstrom T (2007) Enzymatic hydrolysis combined with mechanical shearing and high-pressure homogenization for nanoscale cellulose fibrils and strong gels. Biomacromolecules 8:1934–1941

Palaninathan V, Chauhan N, Poulose AC, Raveendran S, Mizuki T, Hasumura T, Fukuda T, Morimoto H, Yoshida Y, Maekawa T, Kumar DS (2014) Acetosulfation of bacterial cellulose: an unexplored promising incipient candidate for highly transparent thin film. Mater Express 4:415–421

Park JK, Park YH, Jung JY (2003) Production of bacterial cellulose by *Gluconacetobacter hansenii PJK* isolated from rotten apple. Biotechnol Bioprocess Eng 8:83–88

Park YB, Lee CM, Kafle K, Park S, Cosgrove DJ, Kim SH (2014) Effects of plant cell wall matrix polysaccharides on bacterial cellulose structure studied with vibrational sum frequency generation spectroscopy and X-ray diffraction. Biomacromolecules 15:2718–2724

Pecoraro É, Manzani D, Messaddeq Y, Ribeiro SJL (2007) Chapter 17—bacterial cellulose from *Gluconacetobacter xylinus:* preparation, properties and applications. In: Gandini MNBA (ed) Monomers, polymers and composites from renewable resources. Elsevier, Amsterdam, pp 369–383

Pei AH, Butchosa N, Berglund LA, Zhou Q (2013) Surface quaternized cellulose nanofibrils with high water absorbency and adsorption capacity for anionic dyes. Soft Matter 9:2047–2055

Pelissari FM, Sobral PJD, Menegalli FC (2014) Isolation and characterization of cellulose nanofibers from banana peels. Cellulose 21:417–432

Peng BL, Dhar N, Liu HL, Tam KC (2011) Chemistry and applications of nanocrystalline cellulose and its derivatives: a nanotechnology perspective. Can J Chem Eng 89:1191–1206

Pircher N, Veigel S, Aigner N, Nedelec JM, Rosenau T, Liebner F (2014) Reinforcement of bacterial cellulose aerogels with biocompatible polymers. Carbohyd Polym 111: 505–513

Qing Y, Sabo R, Zhu JY, Agarwal U, Cai ZY, Wu YQ (2013) A comparative study of cellulose nanofibrils disintegrated via multiple processing approaches. Carbohyd Polym 97: 226–234

Raghunathan D (2013) Production of microbial cellulose from the new bacterial strain isolated from temple wash waters. Int J Curr Microbiol App Sci 2:275–290

Ramani D, Sastry TP (2014) Bacterial cellulose-reinforced hydroxyapatite functionalized graphene oxide: a potential osteoinductive composite. Cellulose 21:3585–3595

Reiner RS (2008) Cellulose Nanocrystals: preparation and processing. Paper presented at the international conference on nanotechnology for the Forest Products Industry, St. Louis, Missouri, USA

Ren Y, Li SR, Dai B, Huang XH (2014) Microwave absorption properties of cobalt ferrite-modified carbonized bacterial cellulose. Appl Surf Sci 311:1–4

Retegi A, Algar I, Martin L, Altuna F, Stefani P, Zuluaga R, Gañán P, Mondragon I (2012) Sustainable optically transparent composites based on epoxidized soy-bean oil (ESO) matrix and high contents of bacterial cellulose (BC). Cellulose 19:103–109

Robledo M, Rivera L, Jimenez-Zurdo JI, Rivas R, Dazzo F, Velazquez E, Martinez-Molina E, Hirsch AM, Mateos PF (2012) Role of *Rhizobium endoglucanase CelC2* in cellulose biosynthesis and biofilm formation on plant roots and abiotic surfaces. Microb Cell Fact 11:125

Rosa JR, da Silva ISV, de Lima CSM, Neto WPF, Silverio HA, dos Santos DB, Barud HD, Ribeiro SJL, Pasquini D (2014) New biphasic mono-component composite material obtained by partial oxypropylation of bacterial cellulose. Cellulose 21:1361–1368

Ross P, Mayer R, Benziman M (1991) Cellulose biosynthesis and function in bacteria. Microbiol Rev 55:35–58

Ruka DR, Simon GP, Dean KM (2013) In situ modifications to bacterial cellulose with the water insoluble polymer poly-3-hydroxybutyrate. Carbohyd Polym 92:1717–1723

Ruka D, Simon G, Dean K (2014) Harvesting fibrils from bacterial cellulose pellicles and subsequent formation of biodegradable poly-3-hydroxybutyrate nanocomposites. Cellulose 21:4299–4308

Santos SM, Carbajo JM, Quintana E, Ibarra D, Gomez N, Ladero M, Eugenio ME, Villar JC (2015) Characterization of purified bacterial cellulose focused on its use on paper restoration. Carbohyd Polym 116:173–181

Scherner M, Reutter S, Klemm D, Sterner-Kock A, Guschlbauer M, Richter T, Langebartels G, Madershahian N, Wahlers T, Wippermann J (2014) In vivo application of tissue-engineered blood vessels of bacterial cellulose as small arterial substitutes: proof of concept? J Surg Res 189:340–347

Sehaqui H, de Larraya UP, Liu P, Pfenninger N, Mathew AP, Zimmermann T, Tingaut P (2014) Enhancing adsorption of heavy metal ions onto biobased nanofibers from waste pulp residues for application in wastewater treatment. Cellulose 21:2831–2844

Serafica G, Mormino R, Bungay H (2002) Inclusion of solid particles in bacterial cellulose. Appl Microbiol Biotechnol 58:756–760

Shafizadeh F, Lai YZ, McIntyre CR (1978) Thermal-degradation of 6-chlorocellulose and cellulose zinc chloride mixture. J Appl Polym Sci 22:1183–1193

Shah N, Ha JH, Park JK (2010) Effect of reactor surface on production of bacterial cellulose and water soluble oligosaccharides by *Gluconacetobacter hansenii PJK*. Biotechnol Bioprocess Eng 15:110–118

Shah N, Ul-Islam M, Khattak WA, Park JK (2013) Overview of bacterial cellulose composites: a multipurpose advanced material. Carbohyd Polym 98:1585–1598

Shen W, Chen SY, Shi SK, Li X, Zhang X, Hu WL, Wang HP (2009) Adsorption of Cu(II) and Pb(II) onto diethylenetriamine-bacterial cellulose. Carbohyd Polym 75:110–114

Shezad O, Khan S, Khan T, Park JK (2009) Production of bacterial cellulose in static conditions by a simple fed-batch cultivation strategy. Korean J Chem Eng 26:1689–1692

Shezad O, Khan S, Khan T, Park JK (2010) Physicochemical and mechanical characterization of bacterial cellulose produced with an excellent productivity in static conditions using a simple fed-batch cultivation strategy. Carbohyd Polym 82:173–180

Shi ZJ, Zhang Y, Phillips GO, Yang G (2014) Utilization of bacterial cellulose in food. Food Hydrocolloid 35:539–545

Shoda M, Sugano Y (2005) Recent advances in bacterial cellulose production. Biotechnol Bioprocess Eng 10:1–8

Silva N, Rodrigues AF, Almeida IF, Costa PC, Rosado C, Neto CP, Silvestre AJD, Freire CSR (2014) Bacterial cellulose membranes as transdermal delivery systems for diclofenac: in vitro dissolution and permeation studies. Carbohyd Polym 106:264–269

Siqueira G, Bras J, Dufresne A (2010) Cellulosic bionanocomposites: a review of preparation, properties and applications. Polymers 2:728–765

Siro I, Plackett D (2010) Microfibrillated cellulose and new nanocomposite materials: a review. Cellulose 17:459–494

Sokollek SJ, Hertel C, Hammes WP (1998) Cultivation and preservation of vinegar bacteria. J Biotechnol 60:195–206

Son C, Chung S, Lee J, Kim S (2002) Isolation and cultivation characteristics of *Acetobacter xylinum KJ-1* producing bacterial cellulose in shaking cultures. J Microbiol Biotechnol 12:722–728

Song HJ, Li HX, Seo JH, Kim MJ, Kim SJ (2009) Pilot-scale production of bacterial cellulose by a spherical type bubble column bioreactor using saccharified food wastes. Korean J Chem Eng 26:141–146

Soykeabkaew N, Laosat N, Ngaokla A, Yodsuwan N, Tunkasiri T (2012) Reinforcing potential of micro- and nano-sized fibers in the starch-based biocomposites. Compos Sci Technol 72:845–852

Spaic M, Small D, Cook J, Wan W (2014) Characterization of anionic and cationic functionalized bacterial cellulose nanofibres for controlled release applications. Cellulose 21:1529–1540

Spence KL, Venditti RA, Rojas OJ, Habibi Y, Pawlak JJ (2010) The effect of chemical composition on microfibrillar cellulose films from wood pulps: water interactions and physical properties for packaging applications. Cellulose 17:835–848

Sun DP, Zhou LL, Wu QH, Yang SL (2007) Preliminary research on structure and properties of nano-cellulose. J Wuhan Univ Technol Mat Sci Ed 22:677–680

Sun DP, Ma B, Zhu CL, Liu CS, Yang JZ (2010) Novel Nitrocellulose Made from Bacterial Cellulose. J Energ Mater 28:85–97

Surma-Slusarska B, Danielewicz D, Presler S (2008a) Properties of composites of unbeaten birch and pine sulphate pulps with bacterial cellulose. Fibres Text East Eur 16:127–129

Surma-Slusarska B, Presler S, Danielewicz D (2008b) Characteristics of Bacterial Cellulose Obtained from *Acetobacter Xylinum* Culture for Application in Papermaking. Fibres Text East Eur 16:108–111

Suwanposri A, Yukphan P, Yamada Y, Ochaikul D (2013) Identification and biocellulose production of *Gluconacetobacter* strains isolated from tropical fruits in Thailand. Maejo Int J Sci Technol 7:70–82

Suzuki S, Hirai A, Horii F (2012a) Formation and structure of the complexes of sub-elementary fibrils of bacterial cellulose with fluorescent brightener molecules. Cellulose 19:1607–1618

Suzuki S, Suzuki F, Kanie Y, Tsujitani K, Hirai A, Kaji H, Horii F (2012b) Structure and crystallization of sub-elementary fibrils of bacterial cellulose isolated by using a fluorescent brightening agent. Cellulose 19:713–727

Thompson DN, Hamilton MA (2001) Production of bacterial cellulose from alternate feedstocks. In: Twenty-second symposium on biotechnology for fuels and chemicals. Springer, Berlin, pp 503–513

Tome LC, Freire MG, Rebelo LPN, Silvestre AJD, Neto CP, Marrucho IM, Freire CSR (2011) Surface hydrophobization of bacterial and vegetable cellulose fibers using ionic liquids as solvent media and catalysts. Green Chem 13:2464–2470

Tomé L, Fernandes SM, Perez D, Sadocco P, Silvestre AD, Neto C, Marrucho I, Freire CR (2013) The role of nanocellulose fibers, starch and chitosan on multipolysaccharide based films. Cellulose 20:1807–1818

Tomer G, Patel H, Podczeck F, Newton JM (2001) Measuring the water retention capacities (MRC) of different microcrystalline cellulose grades. Eur J Pharm Sci 12:321–325

TORAYCA® T1000G DATA SHEET

Tsouko E, Kourmentza C, Ladakis D, Kopsahelis N, Mandala I, Papanikolaou S, Paloukis F, Alves V, Koutinas A (2015) Bacterial cellulose production from industrial waste and by-product streams. Int J Mol Sci 16:14832–14849

Ude S, Arnold DL, Moon CD, Timms-Wilson T, Spiers AJ (2006) Biofilm formation and cellulose expression among diverse environmental *Pseudomonas* isolates. Environ Microbiol 8:1997–2011

Ul-Islam M, Khan T, Khattak W, Park J (2013a) Bacterial cellulose-MMTs nanoreinforced composite films: novel wound dressing material with antibacterial properties. Cellulose 20:589–596

Ul-Islam M, Khattak W, Kang M, Kim S, Khan T, Park J (2013b) Effect of post-synthetic processing conditions on structural variations and applications of bacterial cellulose. Cellulose 20:253–263

Vandamme EJ, De Baets S, Vanbaelen A, Joris K, De Wulf P (1998) Improved production of bacterial cellulose and its application potential. Polym Degrad Stabil 59:93–99

Vazquez A, Foresti ML, Cerrutti P, Galvagno M (2013) Bacterial cellulose from simple and low cost production media by *gluconacetobacter xylinus*. J Polym Environ 21:545–554

Vilaseca F, Gonzalez I, Alcala M, Chinga-Carrasco G, Vilaseca F, Boufi S, Mutje P (2014) From paper to nanopaper: evolution of mechanical and physical properties. In: Ongoing modification of cellulose nanofibers and their potential appications, Madrid, Spain

Vitta S, Thiruvengadam V (2012) Multifunctional bacterial cellulose and nanoparticle-embedded composites. Curr Sci 102:1398–1405

Wang HH, Zhu EW, Yang JZ, Zhou PP, Sun DP, Tang WH (2012) Bacterial cellulose nanofiber-supported polyaniline nanocomposites with flake-shaped morphology as supercapacitor electrodes. J Phys Chem C 116:13013–13019

Wang QQ, Zhu JY, Considine JM (2013) Strong and optically transparent films prepared using cellulosic solid residue recovered from cellulose nanocrystals production waste stream. ACS Appl Mater Interfaces 5:2527–2534

Wei B, Yang GA, Hong F (2011) Preparation and evaluation of a kind of bacterial cellulose dry films with antibacterial properties. Carbohyd Polym 84:533–538

Wu JM, Liu RH (2012) Thin stillage supplementation greatly enhances bacterial cellulose production by *Gluconacetobacter xylinus*. Carbohyd Polym 90:116–121

Wu J-M, Liu R-H (2013) Cost-effective production of bacterial cellulose in static cultures using distillery wastewater. J Biosci Bioeng 115:284–290

Wu R-Q, Li Z-X, Yang J-P, Xing X-H, Shao D-Y, Xing K-L (2010) Mutagenesis induced by high hydrostatic pressure treatment: a useful method to improve the bacterial cellulose yield of a *Gluconoacetobacter xylinus strain*. Cellulose 17:399–405

Wu J, Zheng YD, Wen XX, Lin QH, Chen XH, Wu ZG (2014) Silver nanoparticle/bacterial cellulose gel membranes for antibacterial wound dressing: investigation in vitro and in vivo. Biomed Mater 9:12

Yang YK, Park SH, Hwang JW, Pyun YR, Kim YS (1998) Cellulose production by *Acetobacter xylinum BRC5* under agitated condition. J Ferment Bioeng 85:312–317

Yang H, Tejado A, Alam N, Antal M, van de Ven TGM (2012) Films Prepared from Electrosterically Stabilized Nanocrystalline Cellulose. Langmuir 28:7834–7842

Yang Y, Jia JJ, Xing JR, Chen JB, Lu SM (2013) Isolation and characteristics analysis of a novel high bacterial cellulose producing strain *Gluconacetobacter intermedius CIs26*. Carbohyd Polym 92:2012–2017

Yang JX, Lv XG, Chen SY, Li Z, Feng C, Wang HP, Xu YM (2014) In situ fabrication of a microporous bacterial cellulose/potato starch composite scaffold with enhanced cell compatibility. Cellulose 21:1823–1835

Yoon SH, Jin HJ, Kook MC, Pyun YR (2006) Electrically conductive bacterial cellulose by incorporation of carbon nanotubes. Biomacromolecules 7:1280–1284

Yu SY, Lin KW (2014) Influence of Bacterial Cellulose (nata) on the Physicochemical and Sensory Properties of Frankfurter. J Food Sci 79:C1117–C1122

Zang SS, Sun Z, Liu K, Wang G, Zhang R, Liu BF, Yang G (2014) Ordered manufactured bacterial cellulose as biomaterial of tissue engineering. Mater Lett 128:314–318

Zeng XB, Small DP, Wan WK (2011) Statistical optimization of culture conditions for bacterial cellulose production by *Acetobacter xylinum BPR 2001* from maple syrup. Carbohyd Polym 85:506–513

Zeng M, Laromaine A, Roig A (2014) Bacterial cellulose films: influence of bacterial strain and drying route on film properties. Cellulose 21:4455–4469

Zhang W, Chen SY, Hu WL, Zhou BH, Yang ZH, Yin N, Wang HP (2011) Facile fabrication of flexible magnetic nanohybrid membrane with amphiphobic surface based on bacterial cellulose. Carbohyd Polym 86:1760–1767

Zimmermann T, Bordeanu N, Strub E (2010) Properties of nanofibrillated cellulose from different raw materials and its reinforcement potential. Carbohyd Polym 79:1086–1093

PUBLICATION II

Low-fibrillated bacterial cellulose nanofibers as a sustainable additive to enhance recycled paper quality

Cristina Campano, Noemi Merayo, Carlos Negro, Angeles Blanco

International Journal of Biological Macromolecules (2018) 114: 1077–1083

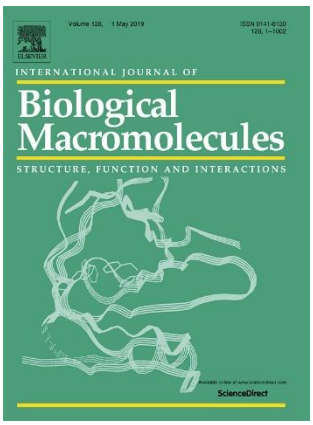

Impact factor 2017: ***3.909***

JCR, Polymer Science, 10 out of 87, ***Q1***

International Journal of Biological Macromolecules 114 (2018) 1077–1083

Contents lists available at ScienceDirect

International Journal of Biological Macromolecules

journal homepage: http://www.elsevier.com/locate/ijbiomac

Low-fibrillated bacterial cellulose nanofibers as a sustainable additive to enhance recycled paper quality

Cristina Campano, Noemi Merayo, Carlos Negro, Ángeles Blanco *

Department of Chemical Engineering, Complutense University of Madrid, Avda. Complutense s/n, 28040 Madrid, Spain

ARTICLE INFO

Article history:
Received 19 January 2018
Received in revised form 26 March 2018
Accepted 27 March 2018
Available online 29 March 2018

Keywords:
Bacterial cellulose nanofibers
Improved recycled paper properties
Retention mechanism

ABSTRACT

Bacterial cellulose is a biological macromolecule synthesized by bacteria of high purity and crystallinity. Bacterial cellulose nanofibers (BCNF) have been produced by soft homogenization and added to a recycled pulp to improve its quality. The benefits of BCNF on mechanical, physical and optical paper properties have been quantified and the retention mechanism of the BCNF in the paper network has been proposed. The use of BC to improve paper strength is usually limited by the decrease of tear index. The novelty of this work is that these two effects are decoupled by the addition of BCNF of low fibrillation (35.2%). In this way, some BCNF clusters are produced together with the individual nanofibers. Thus, with the addition of 3% BCNF, tensile and tear indexes as well as strain at break were improved by 11.1, 7.6, and 66.8%, respectively. Furthermore, the clusters were retained in the fiber network not only by hydrogen bonding, but also by physical retention within the gaps. Therefore, the addition of BCNF not only increases the mechanical properties of paper but also makes the handsheets more flexible and facilitates filler retention.

1. Introduction

Paper is the most recycled material in the world, and it is actually one of the best alternatives to replace plastics in the production of packages and bags. However, there are some challenges that recycled paper industry has to deal with. The most limiting is to keep the mechanical, physical and printing requirements of the product at the same time that the quality of the recycled paper is decreasing [1].

Nanocellulose is a biodegradable material that can contribute to an effective improvement of paper quality [2], and bacterial cellulose (BC), in particular, has superior properties than nanocelluloses of vegetal origin. Its high purity is one of the main distinctive of this biological macromolecule, since vegetal cellulose is always combined with hemicellulose and lignin, between other less abundant compounds [3]. In addition, its nanometric diameter but micrometric fiber length provide it a high surface area along with a high resistance, crystallinity and degree of polymerization and thus average molecular weight [4]. The BC is extruded by aerobic bacterial strains, especially of the genus *Komagataeibacter*, that are mainly isolated from rotten fruits and wastes of vinegar fermentation [5].

When these bacteria are cultured in static mode, they create a membrane on the surface of the culture broth due to their natural movement in search of oxygen. This membrane is a structurally stable hydrogel composed of a nanofiber network that contains fibers with diameters between 20 and 100 nm and up to 99% water in its structure [4]. Although these membranes have been widely used without further modification, e.g. for the fabrication of organic light emitting diodes or scaffolds for tissue engineering [6,7], the nanofibers must be separated to use them as strengthening agents of a matrix [8]. Between the used methods for BC application, high speed disintegration at 16,000 r/min [9,10] effectively improve the mechanical properties of different virgin pulps, such as unbleached softwood [9] and hardwood kraft pulp [10] unbeaten birch and pine sulfate pulps [11] between others [12]. High speed disintegrated BC has been also used to improve other properties of paper, such as the flame retardant behavior of a softwood pulp [13]. This treatment produces a microfibrillation of the cellulose, getting ribbons with diameters in the range of 40–60 nm. On the other hand, it is also possible to obtain a nanofibrillation of the BC by acid hydrolysis, typical procedure used to isolate vegetal-derived cellulose nanocrystals (CNC) [5]. However, to the best knowledge of the authors, BC has not been nanofibrillated by high-pressure homogenization for any application. In this paper the enhancement of paper properties and, thus, recycled paper is studied.

The use of BC to improve tensile strength of paper is limited by the consequent decrease of tear index. The novelty of this work is the use of low fibrillated BC nanofibers (BCNF) with the presence of individual nanofibers and small unfibrillated clusters that can decouple this two effects. In this way, new opportunities to improve paper properties are foreseen. These BCNF have been produced from a soft homogenization of BC membranes, obtained through the culture of *Komagataeibacter sucrofermentans* in static mode. The benefits of the addition of different

* Corresponding author.
E-mail address: ablanco@ucm.es (Á. Blanco).

https://doi.org/10.1016/j.ijbiomac.2018.03.170
0141-8130/

proportions of BCNF on the mechanical, physical and optical properties of a recycled paper have been assessed. Moreover, scanning electronic microscopy (SEM), X-Ray diffraction (XRD) and ash measurements, were used to elucidate the mechanism of BCNF retention within the fiber network.

2. Experimental section

2.1. Materials

Komagataeibacter sucrofermentans CECT 7291, obtained from the Spanish Type Culture Collection (CECT), was the cellulose-producing bacterial strain used in this study. A three-component retention system frequently used in newsprint mills was supplied by BASF (Ludwigshafen, Germany): polyamine with a high molecular weight and a cationic charge density of 0.035 meq/g as coagulant; polyacrylamide (PAM) with a high molecular weight and a cationic charge density of 3.66 meq/g as flocculant; and hydrated bentonite clay. All other reagents and nutrients were of analytical grade and were supplied by Sigma-Aldrich.

2.2. Preparation and characterization of BCNF

Cell growth was carried out in a medium composed of 20 g/L fructose, 5 g/L yeast extract and 3 g/L peptone (M10) in static mode at 30 °C for 4 days. Then, the produced cellulose was removed to isolate bacteria in a high population as described by Santos, et al. [14].

When BC pellicles were isolated, they were suspended in water at a concentration of 1%, pulped for 60 min at 3000 rpm and homogenized in three batches at 600 bar in a laboratory homogenizer (PANDA PLUS 2000, supplied by GEA Niro Soavi, Parma, Italy) to obtain the BCNF.

Nanofibrillation degree, cationic demand (CD) and polymerization degree (PD) were determined as described by Merayo, et al. [15]. Nanofibrillation degree was determined through centrifugation of a suspension of 0.1 wt% BCNF at 4500 ×*g* for 30 min. Nanofibrillation degree was calculated by the ratio between the remaining amount of BCNF in the supernatant and the total amount of BCNF [16]. CD was measured by colloidal titration using a Charge Analysing System (CAS) supplied by AFG Analytic GmbH (Leipzig, Germany). 0.00025 N poly-diallyl-dimethyl-ammonium chlorides (PDADMAC) was used as standard titration reagent. Then, CD was calculated through the Eq. (1).

$$CD = \frac{V_{PDADMAC} \cdot C_{PDADMAC}}{V_{sample} \cdot C_{sample}} \quad (1)$$

where $V_{PDADMAC}$ corresponds to the volume of PDADMAC spent in the titration, V_{Sample} means the volume of the suspension of BCNF used in the test, $C_{PDADMAC}$ is 0.00025 N and C_{sample} is the concentration of BCNF during the titration. PD of the BCNF was calculated through the determination of limiting viscosity number (η) according to ISO 5351/1, where the method in cupri-ethylene-diamine (CED) solution was used. Then, PD was related to η using $\eta = 0.42 \cdot PD$ when $PD < 950$ and $\eta = 2.28 \cdot PD^{0.76}$ when $PD > 950$ [17,18].

Crystallinity index (Cr·I) was examined through XRD using a Philips X'Pert MPD X-ray diffractometer with an autodivergent slit fitted with a graphite monochromator using Cu-Kα radiation operated at 45 kV and 40 mA. XRD patterns were recorded from 3 to 80° at a scanning speed of 0.64°/min. Segal's method was used to calculate Cr·I, according to Eq. (2) [19].

$$Cr.I\ (\%) = \frac{I_{002} - I_{am}}{I_{002}} \cdot 100 \quad (2)$$

I_{002} is the intensity of the 002 interference at $2\theta = 22.5°$ and I_{am} is the intensity of the amorphous scatter at $2\theta = 18°$.

2.3. Handsheet preparation and characterization

A mixture of 60% old newsprint and 40% old magazine was used to prepare the recycled paper to simulate a newsprint furnish. Different proportions of BCNF, 0.5, 1.5, 3 and 6% relative to the total dry weigh, were added to the paper and diluted with hot water to reach a final concentration of 1 wt%. The mixture was pulped using a Messmer pulp disintegrator (Mavis Engineering Ltd., London, UK) at 3000 rpm for 10 min. After disintegration, the polyamine was added to the pulp at a concentration of 1.25 mg/g and stirred at 300 rpm for 15 min. The PAM and the bentonite were added separated 30 s one after the other with continuous stirring. Handsheets were prepared with a basis weight of 60 g/m^2 in a normalized Rapid-Köthen handsheet former (PTI, Vorchdorf, Austria) according to ISO 5269/2 (2004).

Handsheets were conditioned at 23 °C and 50% humidity for 24 h. Grammage was determined following ISO 536. Mechanical, physical and optical characterizations were performed using an AUTOLINE 300 from Lorentzen & Wettre (Stockholm, Sweden). Tensile (TI) and tear indexes were calculated by dividing the tensile and tear strengths of the paper by its grammage. In addition, the physical properties of porosity, beta formation and thickness were measured. Homogeneity of the formed handsheets was determined through the standard deviation of 400 microgrammage measurements using a Beta formation tester (Ambertec, Espoo Finland). The bulk was calculated based on the ratio between the thickness and grammage.

The morphology of the handsheets was analyzed by SEM with a JEOL JSM 6335F at an accelerating voltage of 15 kV. These analyses were carried out in the National Center of Electronic Microscopy of Spain.

In addition, XRD analysis of handsheets was carried out to evaluate the presence of the different mineral fillers in the paper matrix. Again, a Philips X'Pert MPD X-ray diffractometer with an autodivergent slit fitted with a graphite monochromator using Cu-Kα radiation operated at 45 kV and 40 mA was used.

Finally, the main fillers used in the paper industry, $CaCO_3$ and kaolinite, were determined through ash measurements at 525 °C and 900 °C, according to ISO 1762 and ISO 2144. As stated in ISO 2144, both fillers does not decompose at 525 °C, but when they are submitted to 900 °C, only 56% of CaCO3 and 86–89% of kaolinite are retained. Therefore, the calculation of the filler contents has been made according to these proportions.

3. Results and discussion

3.1. BCNF characterization

The characterization results of the BCNF are shown in Table 1. The high entanglement of bacteria during culture, leads to the formation of membranes composed by a resistant network of nanofibers. The strength of the BC membranes causes a great difficulty in the production of highly fibrillated suspensions of BCNF. Thus, a low nanofibrillation degree has been observed, being 35.2%; as a result, some BCNF clusters were added to the handsheets as well as individual nanofibers.

This low nanofibrillation degree also explains the low value of cationic demand, being 0.174 meq/g, compared to typical values for high fibrillated CNF, which are in the order of 0.465 meq/g [16]. As expected, PD and Cr·I values were much higher than either any cellulose fibers or CNF obtained in the literature [20]. It is mainly due to the static culture

Table 1
Results of BCNF characterization.

Property	Units	Value
Nanofibrillation degree	%	35.2
Cationic demand	meq/g	0.174
PD	–	1932
Cr·I	%	98.4

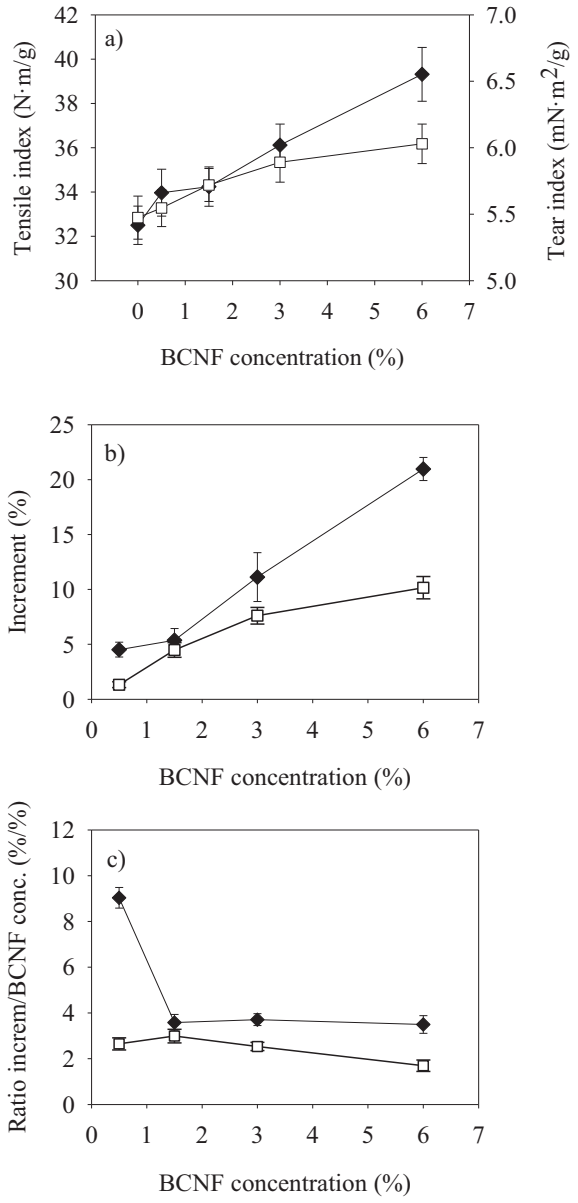

Fig. 1. Evolution of a) tensile and tear indexes, b) relative improvements in tensile and tear indexes and c) ratio between the improvements in the tensile and tear indexes to BCNF concentration versus BCNF concentration. Symbols on the graphs represent the following: ♦ tensile index and □ tear index.

of bacteria, which allows them to move in a slow and direct way, forming very long and crystalline nanofibers [5].

3.2. Effect of BCNF concentration on mechanical properties of recycled paper

Fig. 1a shows that increasing BCNF content tended to an increase in the TI of the recycled paper. The addition of low concentrations of BCNF (0.5–1.5%) caused the TI to increase by approximately 5% (Fig. 1b). Higher concentrations of BCNF further improved the TI (11 and 21% at concentrations of 3 and 6%, respectively). These improvements are slightly lower than those obtained with vegetable-derived CNF. For example, an improvement of approximately 20% in TI was obtained with the addition of 0.5% and 1.5% CNF from corn stalk and eucalyptus, respectively [16]. This may be due to the strong intermolecular attraction between BCNF due to hydrogen bonding and entanglement of bacteria during the culture process, which makes BC difficult to separate into individual nanofibers. Therefore, the low nanofibrillation degree, 35.2% (Table 1) compared to 86% for corn CNF and >95% for eucalyptus CNF [16], resulted in a smaller effect on paper strength. However, the effect might not only be due to the nanofibrillation degree but also to the different mechanisms of action of BCNF compared to CNF.

The tear index increased with increasing concentrations of BCNF from 5.5 without BCNF to 5.9 mN·m²/g with 3% BCNF and to 6.0 mN·m²/g with 6% BCNF (Fig. 1a). These data represent improvements of 7.6 and 10.1%, respectively (Fig. 1b). According to Hassan, et al. [21], tear strength of paper is determined by the total number of fibers involved in the breaking of the handsheet, the fiber length and the number and strength of the interfiber bonds. They also explained that the number of fibers involved in the breaking process is related to the grammage and flexibility of the sheet. Thus, in rigid sheets, stress

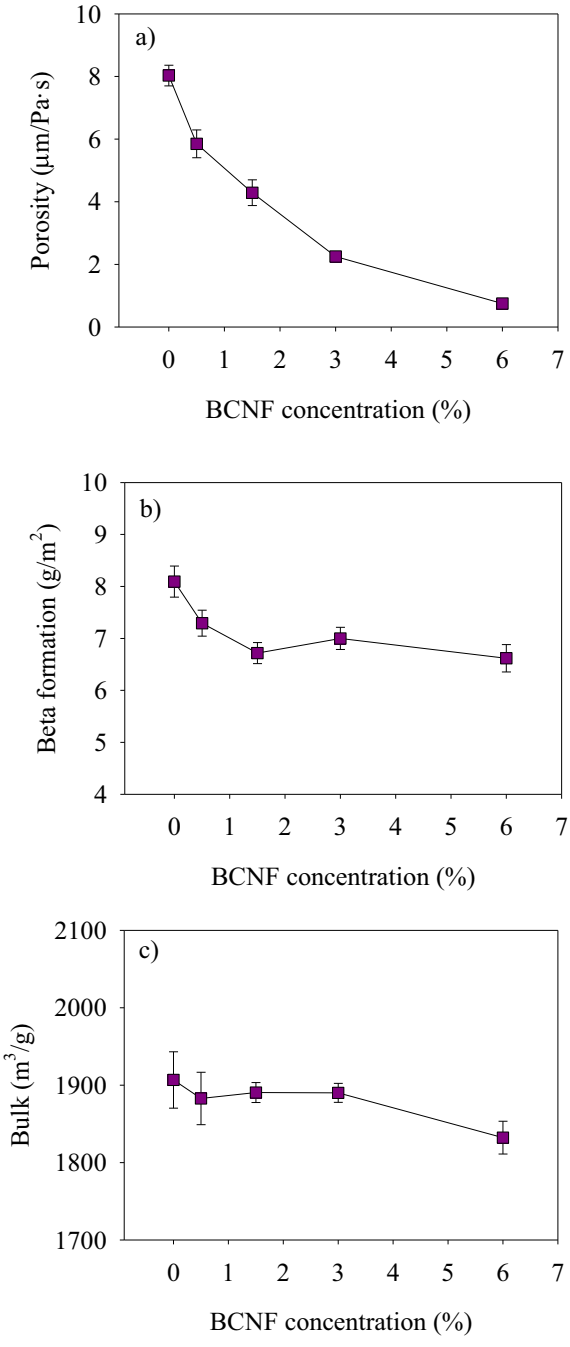

Fig. 2. Evolution of physical properties of handsheets with changes in BCNF concentration: a) porosity, b) grammage standard deviation and c) bulk.

is concentrated in small areas, meaning only a few fibers are involved, but when sheets are more flexible, the force is transmitted from one fiber to another over a much larger area. In their study, the tear index was not affected by microfibrillated cellulose (MFC) when MFC content was lower than 30%, but it was strongly decreased when the concentration was higher than 30%. They explained that the large number of hydrogen bonds could be the reason for this decrease.

Based on that explanation, the more flexible the handsheets, the higher the tear index, which agrees with the results in this study. Thus, because BCNF clusters are added to the pulp instead of individual nanofibers, the number of hydrogen bonds formed between fibers is not as high as it was with CNF. Therefore, BCNF interacted with fibers, not only making stronger composites but also making the paper more flexible and favoring the transmission of the breaking force throughout the paper. However, when the degree of nanofibrillation is higher, the TI increases at low concentrations, but the tear index is strongly affected [16,22]. These results are in accordance with different studies in which CNF were added to deinked pulps [23] or thermo-mechanical pulps [24].

In this study, this relationship has been decoupled, thus both TI and tear index were improved with increasing concentrations of BCNF. However, increasing concentrations of BCNF also involve a concomitant increase in costs. The cost mainly includes both chemical and energy expenses. Therefore, generally the maximum TI and tear index obtained with the minimum BCNF concentration is desired. This has to be optimized based on the needs of each industrial paper product. The ratios between the improvements in strength (TI or tear index) and the increases in the BCNF concentrations were calculated as shown in Fig. 1c. The maximum ratio of TI/BCNF concentration (9.0%/%) was obtained at the BCNF concentration of 0.5%, decreased until 3.6%/% at a concentration of 1.5%, and then remained constant thereafter (BCNF concentrations of 3 and 6%). Therefore, concentrations of 1.5% or higher have the same ability to improve TI. However, slight differences were found in the ratio of tear index/BCNF concentration. For the lower concentrations of BCNF evaluated, 0.5, 1.5 and 3%, the ratios varied in the range of 2.6–3.0%/% and then decreased down to 1.7%/% when the concentration of BCNF increased to 6%.

Although 0.5% of BCNF resulted in the highest ratio among the increases in TI and the concentration of BCNF used, this concentration only cause a 5% increase in TI, which may be not enough to justify the use of BCNF. When looking for improvements of 10–20%, the efficacy of using 1.5% BCNF is the same as using 6%. Therefore, if greater improvements in TI are desired, the BCNF concentration should be increased up to at least 3% to improve the TI by at least 10%.

Strain at break obtained from tensile strength measurements was improved with increasing concentrations of BCNF, and reached a value of 1.37% with 6% BCNF compared to 0.82% without them. Therefore, BCNF not only enhanced the strength of the paper but also provided the paper with some elasticity. This behavior is consistent with the results of Yousefi, et al. [25], who improved paper with BCNF and obtained a TI of 142.3 Nm/g instead of 11.2 Nm/g and a strain at break of 6.5% instead of 1.5% for nanopaper and regular paper, respectively.

3.3. Effect of BCNF concentration on physical and optical properties of paper

Physical and optical properties of the handsheets were also measured due to the importance of those properties for the machine runnability and printing quality of the paper. It has been previously reported that for CNF [20], porosity decreased with increasing concentrations of BCNF since they are retained at the gaps between fibers (Fig. 2a). With the addition of only 0.5% BCNF, the porosity decreased from 8.0 to 5.8 μm/(Pa·s), and it reached 0.7 μm/(Pa·s) at a BCNF concentration of 6%. This result also indicates that BCNF are being retained in the handsheets and are not lost during paper formation. The decrease

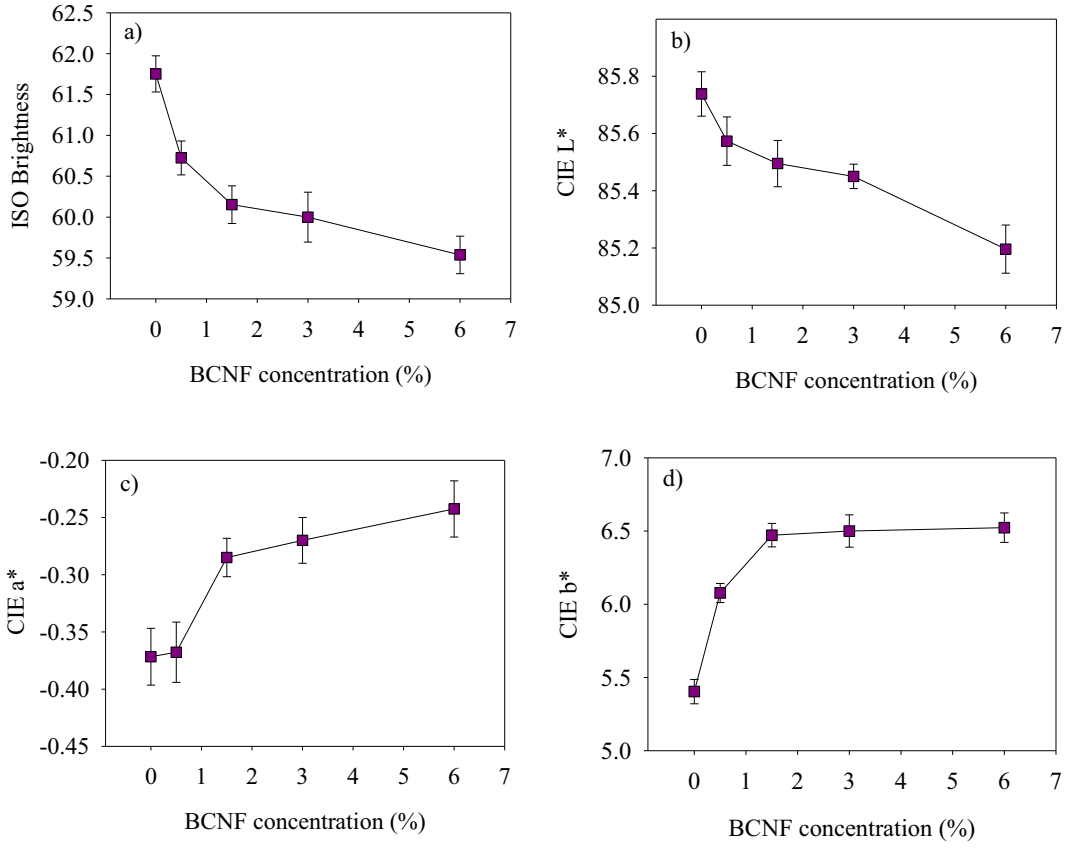

Fig. 3. Evolution of optical properties of handsheets with BCNF concentration: a) ISO Brightness, b) CIE L*, c) CIE a* and d) CIE b*.

in porosity improves printing properties and barrier paper properties which is very important for advanced paper applications.

Because beta formation is the standard deviation of 400 microgrammage measurements, higher values indicate poorer handsheet formation. In this study, beta formation decreased when the concentration of BCNF was low, from 8.1 to 7.3 and 6.7 g/m^2 at concentrations of 0, 0.5 and 1.5%, respectively (Fig. 2b). However, higher concentrations of BCNF did not further improve handsheet formation. Therefore, the reduction in porosity did not affect the homogeneity of the paper, since most of the pores were covered homogeneously by BCNF. Thus, the quality of handsheet formation was maintained at BCNF concentrations higher than 1.5%, although porosity was further reduced.

The bulk of the handsheets decreased when a concentration of 6% BCNF was used (Fig. 2c). This behavior is likely due to the replacement of the original fibers with the same amount of high-quality nanofibers, which are situated at the gaps between macroscopic fibers thus decreasing the thickness of handsheets with the same grammage. A concentration of 6% BCNF was needed to affect handsheet bulk and, at that concentration, the bulk decreased to 1830 compared to 1890 m^3/g when no BCNF were added. Up to a concentration of 3% BCNF, the bulk was constant. According to the results of beta formation, the high standard deviations for the measurements in which there was a low BCNF concentration (0 and 0.5%) indicate a high variation of thickness and therefore worse formation.

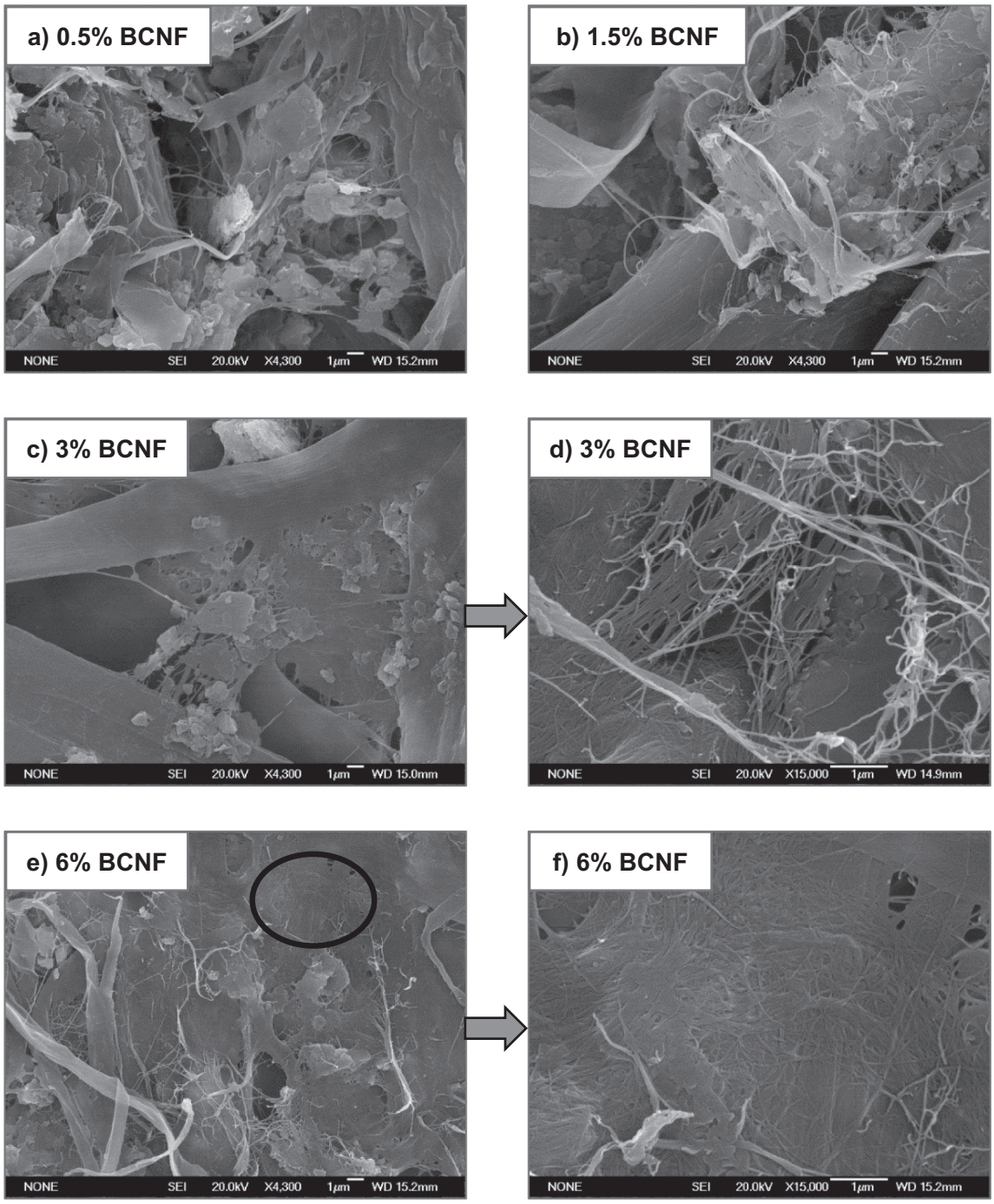

Fig. 4. SEM images of the handsheets with different concentrations of BCNF: a) 0.5% BCNF, b) 1.5% BCNF, c) and d) 3% BCNF, and e) and f) 6% BCNF.

Fig. 3 shows the evolution of optical properties with increasing concentrations of BCNF. ISO-brightness was affected by the presence of BCNF, and it was reduced from 61.7% to 60.7% with only 0.5% BCNF. However, with concentrations of 1.5% or greater, the reduction was less pronounced; however, it decreased to an ISO-brightness of 59.5% with 6% BCNF. Balea, et al. [16] suggested that this is because brightness is measured through the light reflectance produced by fibers, fines and fillers at the paper sheets, and the small size of the CNF and BCNF makes them disperse or reflect only a small amount of visible radiation. Therefore, brightness decreased with the addition of these nanocelluloses.

Colorimetric constants are also considered important properties for the quality of the final paper, and they usually need to be within a limited range that varies depending on the requirements of the company. In this case, CIE L* decreased and CIE a* and CIE b* increased with increasing concentrations of BCNF. Therefore, according to the CIELAB color space, increasing concentrations of BCNF made the handsheets appear more black, red and yellow. This color tendency was strongly affected by concentrations below 1.5% BCNF and remained more stable thereafter (Fig. 3).

Considering these data, low concentrations of BCNF did not strongly affect the physical and optical properties of paper, but deviations in thickness were still high and the increase in the TI was low. The optimum concentration in terms of efficacy in increasing mechanical properties proposed before (0.5% BCNF) is no longer viable since porosity, beta formation and deviation in thickness measurement are still high and can be improved. Therefore, considering the obtained improvements in the mechanical indexes and physical and optical properties, the recommended concentration is 3% BCNF. At this concentration, the TI increased by 11.1%, strain at break was enhanced in 66.8%, tear index increased 7.6%, porosity decreased from 8.0 to 2.2 μm/Pa·s, beta formation reached its minimum value of 7.0 g/m^2, bulk was kept almost constant at 1890 m^3/g and brightness and colorimetric constants remained almost constant at concentrations higher than 1.5% BCNF. The improvement in the formation, even at the highest studied concentration (6%) is due to the mechanism of retention of BCNF in the fiber network.

3.4. Hypothesis of the BCNF retention mechanism to enhance the paper strength

The mechanism traditionally proposed for the retention of vegetal CNF in the paper sheets is based on their interaction with the components of the pulp, mainly fibers and fines, through hydrogen bonding, in the presence of mineral fillers [26]. This was observed in the FESEM images of Hii, et al. [26], where highly fibrillated CNF are bonded with the fibers of the pulp.

BCNF are retained within the fiber network not only because of the hydrogen bonding between nanofibers and fibers but also because of their retention within the gaps between macroscopic fibers and on the fibers surface. This is due to their low degree of nanofibrillation, only 35.2%, which means that BCNF were added as clusters of nanofibers, more than individual nanofibers. Since these clusters are tightly bound by both hydrogen bonding and entanglement of BCNF during bacterial culture, they strengthen the handsheets and make them more flexible as shown in Fig. 1.

To confirm this hypothesis, the handsheets surfaces were analyzed by SEM (Fig. 4). At low concentration of BCNF (Fig. 4a and b), it is difficult to identify BCNF clusters in the micrographs of the handsheets among the mixture of fibers, fines and fillers. The thin fibrils observed in these images may not only be due to the presence of some individual BCNF but also to some deteriorated fibers because of the recycling process, which causes fibrillation of fibers. This is clearly shown in the study by Delgado-Aguilar, et al. [23] in which they observed the change in fiber size triggered by beating.

When the BCNF concentration was increased up to 3% (Fig. 4c and d), some BCNF clusters start to be visible. They were identified because of the homogeneous width of BCNF and their entanglement. These images confirm the initial hypothesis proposed that these BCNF are retained in the gaps between fibers, linking the fibers of the pulp and partially covering them. In addition, mineral fillers are retained in the handsheets in the proximity of the BCNF clusters. Thus, not only chemical retention through flocculants takes place, but also a physical retention because of the gap filling with the nanofibers net.

The covering effect of BCNF on recycled fibers is clearly observed when their concentration increased up to 6% BCNF (Fig. 4 e and f) and it can be considered an improvement of the recycled fibers. These BCNF clusters are linked together to form a microscopic web that acts like a membrane easing filler retention, in view of the very small pore size.

Results from XRD analysis are represented in Fig. 5, where typical cellulose I associated peaks, obtained at 2θ = 15–17°, 22.5° and 35° are shown [27]. The other peaks in the XRD pattern indicate the presence of other crystalline materials. They correspond to the two mineral fillers used in the recycled paper industry: kaolinite and calcium carbonate. The peak at around 29.5° is the most intense peak of the XRD pattern of $CaCO_3$. On the other side, the observed peaks at 12.5° and 25° in all samples are attributed to kaolinite [28]. However, this material has many other minority peaks associated to its pattern, which cannot be observed due to the presence of the other components. Therefore, the quantification of the filler contents in each sample made through *The International Centre for Diffraction Data database* (ICDD) is not reliable. Moreover, no big difference between samples can be extracted from Fig. 5.

Then, filler content has been determined through ISO standards and showed in Fig. 6. Both $CaCO_3$ and kaolinite contents are kept almost constant when concentration of BCNF is below 3%. However, they slightly decreased when the BCNF concentration is 6%, from 20.3 to 18.5%. The found reason is that the dose of the retention aids has been optimized to retain mineral fillers within the paper sheet. However, BCNF probably interact with the retention system, thus, this dose is adequate to retain both fillers and BCNF, when the last is not high.

However, as the specific surface area of BCNF is much higher than that of cellulose fibers, retention aids interact with these nanofibers as well as with the mineral fillers prior to recycled fibers. Thus, the retention of mineral fillers is favorable in the proximities of BCNF as showed in SEM images (Fig. 4). When the dose of BCNF is below 3%, both BCNF and mineral fillers are retained within the paper network. However, when BCNF concentration is increased to 6%, the amount of retention

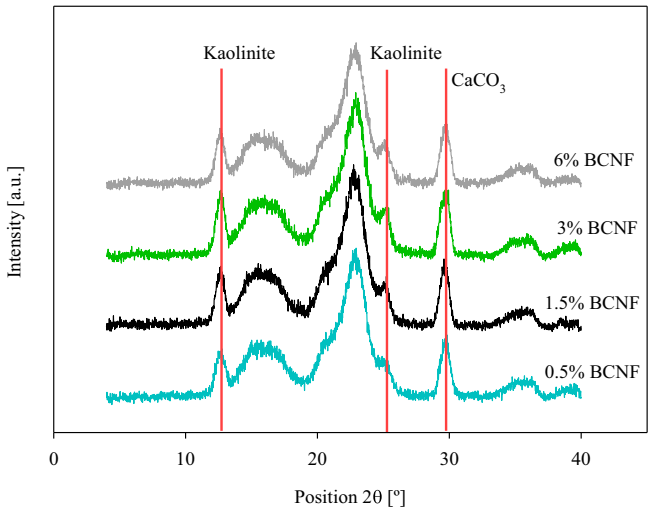

Fig. 5. XRD patterns of papers enhanced with different BCNF concentrations. Red vertical lines show the different positions for the mineral fillers of recycled paper: kaolinite and $CaCO_3$. (For interpretation of the references to color in this figure legend, the reader is referred to the web version of this article.)

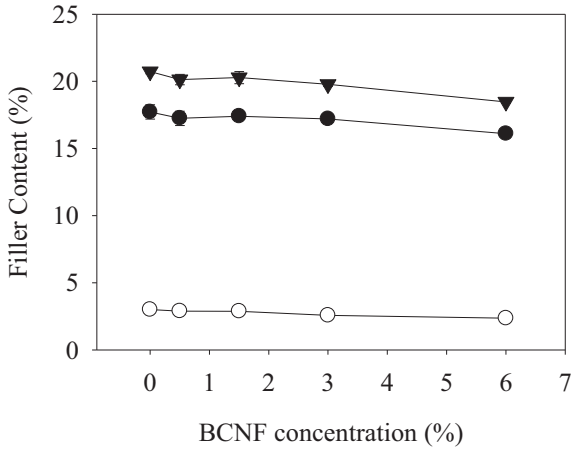

Fig. 6. Mineral filler contents in handsheets prepared at different BCNF concentrations. Symbols on the graphs represent the following: ○ $CaCO_3$ filler content (%), ● kaolinite filler content (%) and ▼ total mineral filler content (%).

aids is not high enough to allow the chemical retention of all mineral fillers. Despite this fact, the reduction in the mineral filler content is not as high since they are physically retained by the BCNF clusters. Therefore, an optimization of the wet-end aids, taking into account not only the filler retention but also the BCNF addition would be necessary to improve the drainage step and reduce costs [29]. Then, a deeper research on the synergy between the retention system and the strength additives is still needed.

4. Conclusions

BCNF have been produced by a soft homogenization treatment of BC pellicles and applied to a recycled pulp in order to enhance the properties of the produced paper. The improvement of tensile strength of paper by BC is limited by the decrease of tear index. The novelty of this work is the use of low fibrillated BCNF with the presence of individual nanofibers as well as small clusters that decouple these two effects. This makes paper sheets more flexible and facilitates the retention of mineral fillers in the proximities of the BCNF clusters. By the addition of 3% BCNF, all measured mechanical properties have been improved: TI by 11.1%, tear index by 7.6% and strain at break by 66.8%. In addition, the optical properties of the produced papers are kept as high as the unmodified paper when BCNF concentration was below 1.5%. Finally, a high homogeneity is observed in the produced handsheets according to the beta formation, the porosity and the bulk results.

The BCNF retention mechanism is not only due to the hydrogen bonding of BCNF with the fibers, like in the case of high fibrillated CNF, but also to the physical retention of these clusters within the gaps. This fact together with the high affinity between BCNF and fillers due to the high specific surface area of BCNF, confirm a higher filler retention in their proximities, as observed in SEM images.

Acknowledgements

Authors wish to acknowledge the Spanish Ministry of Economy and Competitiveness for the financial support of this study by the projects CTQ2013-48090-C2-1-R and CTQ2017-85654-C2-2-R, as well as the grant of C. Campano (BES-2014-068177).

References

[1] T. Lindström, L. Wågberg, T. Larsson, On the nature of joint strength in paper-A review of dry and wet strength resins used in paper manufacturing, 13th Fundamental Research Symposium, The Pulp and Paper Fundamental Research Society Cambridge, UK 2005, pp. 457–562.
[2] S.H. Osong, S. Norgren, P. Engstrand, Processing of wood-based microfibrillated cellulose and nanofibrillated cellulose, and applications relating to papermaking: a review, Cellulose 23 (1) (2016) 93–123.
[3] A. Dufresne, Bacterial Cellulose, Nanocellulose: From Nature to High Performance Tailored Materials, Walter de Gruyter, 2012.
[4] D. Klemm, F. Kramer, S. Moritz, T. Lindström, M. Ankerfors, D. Gray, A. Dorris, Nanocelluloses: a new family of nature-based materials, Angew. Chem. Int. Ed. 50 (24) (2011) 5438–5466.
[5] C. Campano, A. Balea, A. Blanco, C. Negro, Enhancement of the fermentation process and properties of bacterial cellulose: a review, Cellulose 23 (1) (2016) 57–91.
[6] C. Legnani, C. Vilani, V.L. Calil, H.S. Barud, W.G. Quirino, C.A. Achete, S.J.L. Ribeiro, M. Cremona, Bacterial cellulose membrane as flexible substrate for organic light emitting devices, Thin Solid Films 517 (3) (2008) 1016–1020.
[7] W.H. Tang, S.R. Jia, Y.Y. Jia, H.J. Yang, The influence of fermentation conditions and post-treatment methods on porosity of bacterial cellulose membrane, World J. Microbiol. Biotechnol. 26 (1) (2010) 125–131.
[8] M. Martinez-Sanz, A. Lopez-Rubio, J.M. Lagaron, Optimization of the dispersion of unmodified bacterial cellulose nanowhiskers into polylactide via melt compounding to significantly enhance barrier and mechanical properties, Biomacromolecules 13 (11) (2012) 3887–3899.
[9] T. Tabarsa, S. Sheykhnazari, A. Ashori, M. Mashkour, A. Khazaeian, Preparation and characterization of reinforced papers using nano bacterial cellulose, Int. J. Biol. Macromol. 101 (2017) 334–340.
[10] H. Shibazaki, S. Kuga, F. Onabe, Mechanical properties of papersheet containing bacterial cellulose, Jpn. TAPPI J. 48 (12) (1994) 1621–1630.
[11] B. Surma-Slusarska, D. Danielewicz, S. Presler, Properties of composites of unbeaten birch and pine sulphate pulps with bacterial cellulose, Fibres Text. East. Eur 16 (6) (2008) 127–129.
[12] K.C. Cheng, J.M. Catchmark, A. Demirci, Effects of CMC addition on bacterial cellulose production in a biofilm reactor and its paper sheets analysis, Biomacromolecules 12 (3) (2011) 730–736.
[13] A.H. Basta, H. El-Saied, Performance of improved bacterial cellulose application in the production of functional paper, J. Appl. Microbiol. 107 (6) (2009) 2098–2107.
[14] S.M. Santos, J.M. Carbajo, J.C. Villar, The effect of carbon and nitrogen sources on bacterial cellulose production and properties from Gluconacetobacter sucrofermentans CECT 7291 focused on its use in degraded paper restoration, Bioresources 8 (3) (2013) 3630–3645.
[15] N. Merayo, A. Balea, E. de la Fuente, Á. Blanco, C. Negro, Interactions between cellulose nanofibers and retention systems in flocculation of recycled fibers, Cellulose 24 (2) (2017) 677–692.
[16] A. Balea, N. Merayo, E. Fuente, M. Delgado-Aguilar, P. Mutje, A. Blanco, C. Negro, Valorization of corn stalk by the production of cellulose nanofibers to improve recycled paper properties, Bioresources 11 (2) (2016) 3416–3431.
[17] M. Marx-Figini, Significance of the Intrinsic Viscosity Ratio of Unsubstituted and Nitrated Cellulose in Different Solvents, 72(1), 1978 161–171.
[18] M. Henriksson, L.A. Berglund, P. Isaksson, T. Lindstrom, T. Nishino, Cellulose nanopaper structures of high toughness, Biomacromolecules 9 (6) (2008) 1579–1585.
[19] L. Segal, J.J. Creely, A.E. Martin, C.M. Conrad, An empirical method for estimating the degree of crystallinity of native cellulose using the x-ray diffractometer, Text. Res. J. 29 (10) (1959) 786–794.
[20] A. Balea, Á. Blanco, M.C. Monte, N. Merayo, C. Negro, Effect of bleached eucalyptus and pine cellulose nanofibers on the physico-mechanical properties of cartonboard, Bioresources 11 (4) (2016) 8123–8138.
[21] E.A. Hassan, M.L. Hassan, K. Oksman, Improving bagasse pulp paper sheet properties with microfibrillated cellulose isolated from xylanase-treated bagasse, Wood Fiber Sci. 43 (1) (2011) 76–82.
[22] M. Jonoobi, A.P. Mathew, K. Oksman, Producing low-cost cellulose nanofiber from sludge as new source of raw materials, Ind. Crop. Prod. 40 (2012) 232–238.
[23] M. Delgado-Aguilar, I. Gonzalez, M.A. Pelach, E. De La Fuente, C. Negro, P. Mutje, Improvement of deinked old newspaper/old magazine pulp suspensions by means of nanofibrillated cellulose addition, Cellulose 22 (1) (2015) 789–802.
[24] O. Eriksen, K. Syverud, O. Gregersen, The use of microfibrillated cellulose produced from kraft pulp as strength enhancer in TMP paper, Nord. Pulp Pap. Res. J. 23 (3) (2008) 299–304.
[25] H. Yousefi, M. Faezipour, S. Hedjazi, M.M. Mousavi, Y. Azusa, A.H. Heidari, Comparative study of paper and nanopaper properties prepared from bacterial cellulose nanofibers and fibers/ground cellulose nanofibers of canola straw, Ind. Crop. Prod. 43 (2013) 732–737.
[26] C. Hii, O.W. Gregersen, G. Chinga-Carrasco, O. Eriksen, The effect of MFC on the pressability and paper properties of TMP and GCC based sheets, Nord. Pulp Pap. Res. J. 27 (2) (2012) 388–396.
[27] Q.H. Xu, Y. Gao, M.H. Qin, K.L. Wu, Y.J. Fu, J. Zhao, Nanocrystalline Cellulose from Aspen Kraft Pulp and its Application in Deinked Pulp, 60, 2013 241–247.
[28] C. Campano, R. Miranda, N. Merayo, C. Negro, A. Blanco, Direct production of cellulose nanocrystals from old newspapers and recycled newsprint, Carbohydr. Polym. 173 (2017) 489–496.
[29] N. Merayo, A. Balea, E. de la Fuente, Á. Blanco, C. Negro, Synergies Between Cellulose Nanofibers and Retention Additives to Improve Recycled Paper Properties and the Drainage Process, 24(7), 2017 2987–3000.

PUBLICATION III

In situ production of bacterial cellulose to economically improve recycled paper properties

Cristina Campano, Noemi Merayo, Carlos Negro, Angeles Blanco

International Journal of Biological Macromolecules (2018) 118: 1532–1541

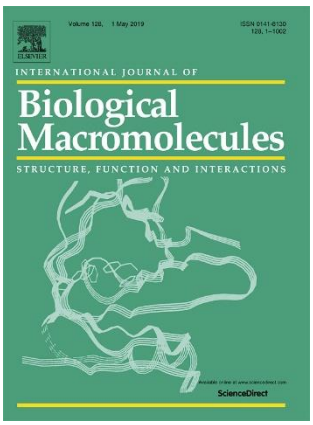

Impact factor 2017: ***3.909***

JCR, Polymer Science, 10 out of 87, ***Q1***

International Journal of Biological Macromolecules 118 (2018) 1532–1541

Contents lists available at ScienceDirect

International Journal of Biological Macromolecules

journal homepage: http://www.elsevier.com/locate/ijbiomac

In situ production of bacterial cellulose to economically improve recycled paper properties

Cristina Campano, Noemi Merayo, Carlos Negro, Angeles Blanco *

Department of Chemical Engineering, Complutense University of Madrid, Avda. Complutense s/n, 28040 Madrid, Spain

ARTICLE INFO

Article history:
Received 25 May 2018
Received in revised form 27 June 2018
Accepted 30 June 2018
Available online 5 July 2018

Keywords:
Bacterial cellulose
Recycled paper
Strength
In situ culture
Mechanical properties
Industrial application

ABSTRACT

This study focusses on the in-situ production of bacterial cellulose in recycled pulps to increase the quality of fibers in the suspension. The effect of different dosages of the upgraded pulp on the mechanical, physical and optical properties of handsheets was assessed. Papers produced with pulps cultivated in agitation exhibited increments in both tensile and tear indexes of 12.2% and 14.2%, respectively. Thus, flexibility of the paper was also improved. On the other hand, pulps enhanced with static culture fail to improve tensile index of paper, while tear index was increased by 12.4%. The production mechanism for both types of culture was proposed. In agitated culture, bacteria were found to coat the primary fibers, improving their quality. In the case of static culture, heterogeneous systems were observed since recycled fibers tended to sediment while bacteria moved to the surface of the culture broth in search of oxygen. Hence, the in situ production of BC with recycled fibers can, therefore, be an alternative to replace conventional paper strengthening agents. The results attained indicate that the in-situ production of upgraded pulps can be implemented in paper mills cultivating pulp streams sterilized through low cost, non-exhaustive operations, such as ozone or ultraviolet radiation.

1. Introduction

Recycled paper (RP) global demand has increased in recent years, worsening the quality of the recovered paper [1]. As consequence of the fiber hornification process in each recycling cycle, the paper mechanical properties are negatively affected [2,3]. A lower inter-fiber and filler-fiber bonding capacity, and a reduction in the ability to swell when fibers are re-suspended in water are produced, which reduce the paper strength [4]. Recently, paper strengthening agents based on nanocelluloses have been increasingly used, even though their production is still expensive and nanocellulose fiber dispersion is still an issue [3].

Bacterial cellulose (BC) presents several advantages compared to plant cellulose, such as high purity, high polymerization degree and high crystallinity [5,6]. These exceptional properties make BC a great candidate to be used as strengthening agent of several materials [7]. It can be obtained by aerobic bacteria of the genus *Komagataeibacter*, mainly isolated from rotten fruits and wastes of the vinegar fermentation [8]. Between all culture methods, static and agitated modes have been the most used due to their simplicity and high yield [9]. In static cultures, bacteria tend to move towards the surface of the culture broth. Thus, BC is synthesized on the surface of shallow trays as a pellicle with higher density on the side exposed to air [10]. In view of this behavior, a large space is required to reach a worthwhile amount, fact that usually makes this type of process difficult to scale-up [5]. With the implementation of agitation, the mass transfer rate is improved, increasing the oxygen availability within the whole culture broth [11]. However, some authors have published different studies about the appearance of a genetic mutation of bacteria of the described genus, due to the high shear stress provoked by high agitation and aeration [12,13]. According to these authors, this spontaneous mutation deactivates essential enzymes involved in the cellulose synthesis, reducing the cellulose production rate [14]. In this sense, bacteria synthesize other water-soluble polysaccharides with lower strength such as acetan, levan or xylan, which are composed of the same starter molecule than BC [15].

Between the different strategies used to obtain composites made of BC, the in-situ culture of bacteria with other components is found the most useful [16]. This fact could trigger a reduction in the required time to produce a nanocomposite, as well as a better and more compact conformability [17]. In this way, mechanical and barrier properties, as well as water holding capacity of the materials added to the culture broth have been improved. BC has been in-situ produced with potato starch [18], poly-3-hydroxybutyrate [16], bentonite [19], graphene oxide [20,21], glyoxal [22], carboxymethyl cellulose [23,24], gelatin [25] and carbon nanotubes [26].

Material strengthening by BC in-situ production presents several advantages compared to the addition of cellulose nanofibers (CNF) and cellulose nanocrystals (CNC) to the same materials, which can be

* Corresponding author.
E-mail address: ablanco@ucm.es (A. Blanco).

https://doi.org/10.1016/j.ijbiomac.2018.06.201
0141-8130/

grouped in the minimization of costs [10]. Nutrients cost can be reduced to almost zero by using industrial residues or wastes containing sugars, such as konjac powder hydrolyzate [27] or waste from beer fermentation broth [13], which also contributes to the circular economy aims.

However, this approach has been seldom published in the papermaking field, and deeper studies are necessary before considering its industrial implementation [28,29]. In this work, the in-situ production of BC with recycled fibers to improve the mechanical properties of RP has been studied. First, the effect of the culture mode, in terms of static or agitated methodologies, on the mechanical, physical and optical properties has been assessed. Moreover, a production mechanism for both methods has been proposed. Finally, different culture volumes and times have been studied to assess the influence of the oxygen availability. These results provide new insights for the papermaking application on the culture modes, as well as on the main variables affecting the BC productivity (culture and time volume).

2. Materials and methods

2.1. Materials

The bacterial strain *Komagataeibacter sucrofermentans* CECT 7291, used in this study, was obtained from the Spanish Type Culture Collection (CECT). To retain the fibers, a three-component retention system (C-F-B), commonly used in paper mills, was selected. Polyamine (C) with a high molecular weight and a cationic charge density of 0.035 meq/g was used as coagulant; polyacrylamide (F) with a high molecular weight and a cationic charge density of 3.66 meq/g was used as flocculant; and hydrated bentonite clay (B) was used as microparticle. These products were supplied by BASF (Ludwigshafen, Germany). Recycled newsprint (NP) and magazine papers (MG) were kindly supplied by Holmen Paper (Madrid, Spain). Nutrients, such as fructose, yeast extract and peptone, as well as other reactants like NaCl, KCl, $CaCl_2 \cdot 2H_2O$, $NaHCO_3$ and NaOH were of analytical grade and supplied by Sigma-Aldrich.

2.2. Bacterial growth and culture media preparation

Cell growth and bacteria isolation were developed according to the procedure previously described [30]. The bacterial suspension was prepared with Ringer's solution by adjusting optical density to 0.59–0.64 at the wavelength of 600 nm.

A pulp suspension of 0.5% consistency was prepared by pulping 60% NP and 40% MG papers using a Messmer pulp disintegrator (Mavis Engineering Ltd., London, UK) at 3000 rpm for 10 min [3]. Then, 20 g/L fructose, 5 g/L yeast extract and 3 g/L peptone were added to the pulp suspension and pH was adjusted to 6 by the addition of diluted HCl. The prepared suspension was autoclaved at 121 °C. Once it reached room temperature, 2.5 mL of the bacterial suspension were added to inoculate each liter of pulp.

2.3. In-situ culture

For static culture, 100 mL of the inoculated suspension were poured into 100 mL Petri dishes and let to culture at 30 °C. For agitated culture, either 100 mL of the culture suspension were added to 250 mL Erlenmeyer flasks or 300 mL to 500 mL Erlenmeyer flasks, being placed into a Certomat IS orbital incubator manufactured by Sartorius Stedim Biotech GmbH (Goettingen, Germany) at 180 rpm and 30 °C. Cultures were carried out for 6, 12, 24, 36 and 48 h, autoclaving the samples at each time before using it to prepare handsheets. Fig. 1a shows a simplified scheme for an easier understanding of the process.

2.4. Handsheets formation

To assess the effect of the culture mode on the mechanical, physical and optical properties of paper, different culture flasks at each time were autocleaved to remove bacteria and mixed with the corresponding amount of pulp to reach a total of 1 L at 1% of consistency. Developed experiments and nomenclature used for each case are shown in Table 1. Then, the mixture was pulped at 3000 rpm for 10 min. The retention system, (1.25 mg/g of C, 0.5 mg/g of F and 1.7 mg/g of B) was added previously to handsheet formation. Then, handsheets with a basis weight of 60 g/m^2 (ISO 5269/2 (2004)) were prepared with a normalized Rapid-Köthen handsheet former (PTI, Vorchdorf, Austria). A schematic view of the procedure is shown in Fig. 1b.

2.5. Handsheet characterization

Handsheet grammage was determined according to ISO 536. Formation homogeneity was evaluated by the standard deviation of 400 microgrammage measurements by using a Beta formation tester (Ambertec, Espoo Finland). Mechanical, physical and optical properties, such as tensile and tear strengths, strain at break, porosity, thickness, ISO Brightness, and CIE L*, a* and b* were measured with an AUTOLINE 300 from Lorentzen & Wettre (Stockholm, Sweden). Tensile (TI) and tear indexes were determined as the ratio between the corresponding strength and its grammage.

Morphology of the handsheets was analyzed by scanning electron microscopy (SEM), with a JEOL JSM 6335F at an accelerating voltage of 15 kV. These analyses were carried out at the *National Center of Electronic Microscopy of Spain*.

3. Results and discussion

3.1. Effect of culture mode on paper properties

3.1.1. Mechanical properties

Handsheets prepared at the dosage of 10% (2) by both static and agitated cultures were used in order to compare the effect of the culture mode on the paper properties. Evolution of the handsheets TI with the culture time is shown in Fig. 2a. Before 24 h of culture, handsheets prepared with improved fibers cultured in both static and agitated modes, presented a similar behavior. The control experiment (handsheets with the same amount of the cultured suspension but without being inoculated) was 37.6 Nm/g, represented in Fig. 2a as zero time. Results are in agreement with data from Jung et al. [31], who stablished that cell growth gets a maximum after 24 h of culture, starting to increase the BC productivity in that moment.

At 48 h of incubation, TI of handsheets increased up to 42.2 Nm/g for agitated culture, meaning an increase of 12.2%. At this time, the number of cell colonies keeps constant, thus increasing the BC productivity. However, this is not as positive for static cultures, where TI remained below the control value (34.1 Nm/g). The lower movement of bacteria in static cultures limits the nutrients availability, thus decreasing the cell growth rate and therefore the BC productivity. However, it is highly likely that increasing the culture time, handsheets TI will be enhanced since the BC produced by static cultures usually presents better properties in terms of crystallinity and fibers length.

It is well known that tensile and tear strengths are compromised when CNF are added as strengthening agents, since when one is improved the other is negatively affected [32]. This fact has been assigned to the high number of hydrogen bonds between CNF and paper fibers [33]. However, as it was observed in a previous study [30], when nanofibrillation was not so high, not only hydrogen bonding drives the retention of nanocellulose, but also physical retention in the fiber gaps. In this case, the BCNF clusters added to the pulp not only reinforced the paper, but also made the paper more flexible by favoring

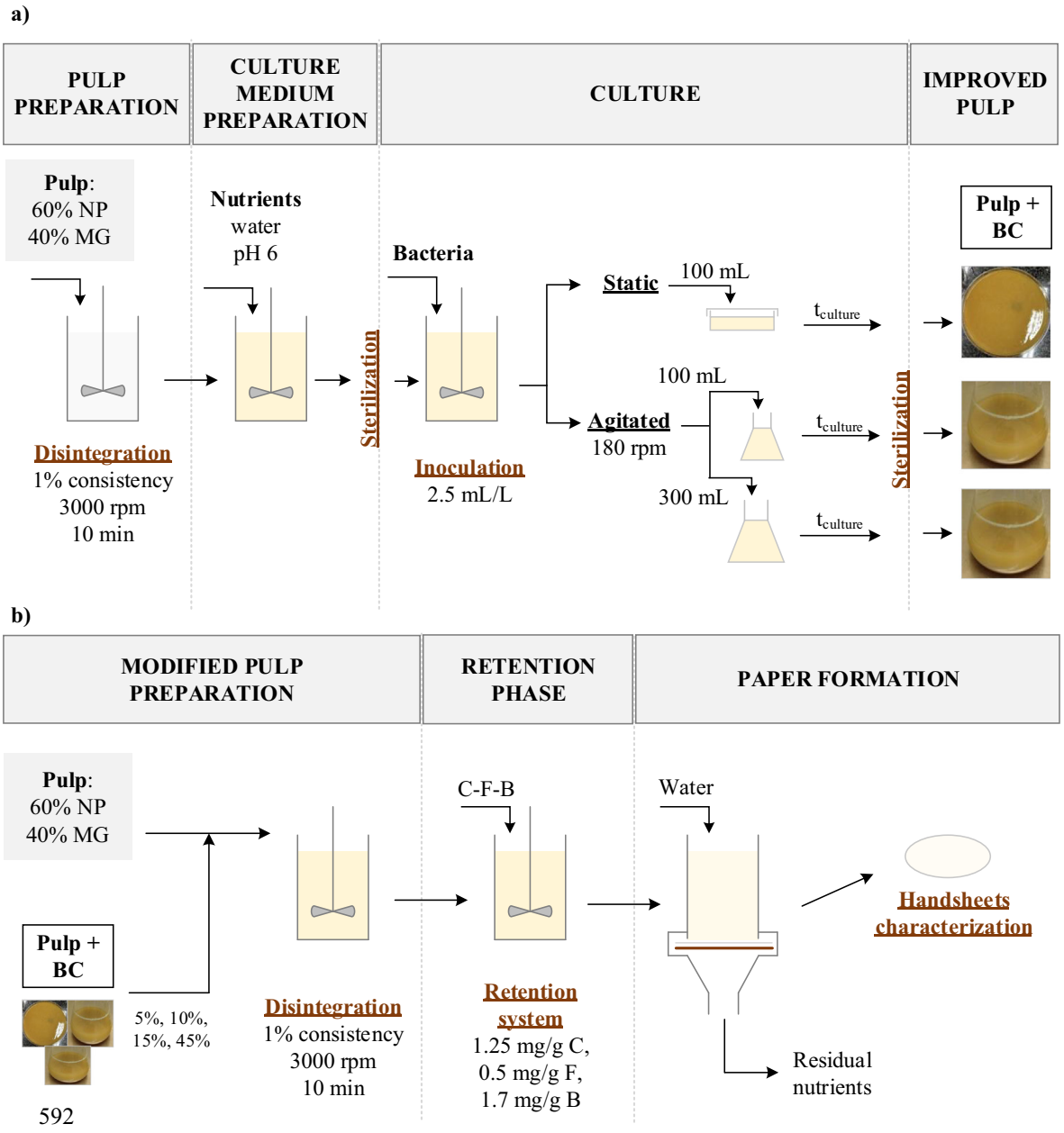

Fig. 1. a) Procedure developed to culture bacteria in presence of fibers, and b) procedure carried out to form handsheets at different proportions of the improved fibers composed of pulp and BC.

the transmission of the breaking force throughout the paper and, consequently, improving the tear index.

In this study, tear index of handsheets was improved with the culture time in both agitated and static systems (Fig. 2b). Comparing with Fig. 2a, tear index variation results inversely related to TI when culture is carried out in static mode. However, in the case of agitated culture, TI remained almost invariable when time was below 24 h, while tear index kept increasing until 48 h (reaching a maximum increment of 14.2% at 48 h).

As it was explained before, BC produced in static mode formed a web on the surface of the culture broth [8]. On the other side, primary cellulose fibers were likely to sediment. Then, the bonding between BC and primary fibers could have taken place during the pulping after mixing with the pulp, but seldom during the culture.

On the opposite side, it seems that in agitated culture, bacteria had preference to grow on the surface of the cellulose fibers, probably having a higher oxygen availability. In this way, BC could have been synthetized as coating of these fibers, not only by hydrogen bonding but also as a physical covering. This fact triggers a higher handsheets flexibility, since the inter-fiber force transmission is developed in a larger area [33].

Table 1
Used nomenclature for each experiment, corresponding to different amounts of improved pulp, in a defined number of parallel culture flasks at different volumes.

Nomenclature	Improved pulp	Number of parallel culture flasks	Culture volume of each flask
5% (1)	5%	1	100 mL
10% (2)	10%	2	100 mL
15% (3)	15%	3	100 mL
15% (1)	15%	1	300 mL
45% (3)	45%	3	300 mL

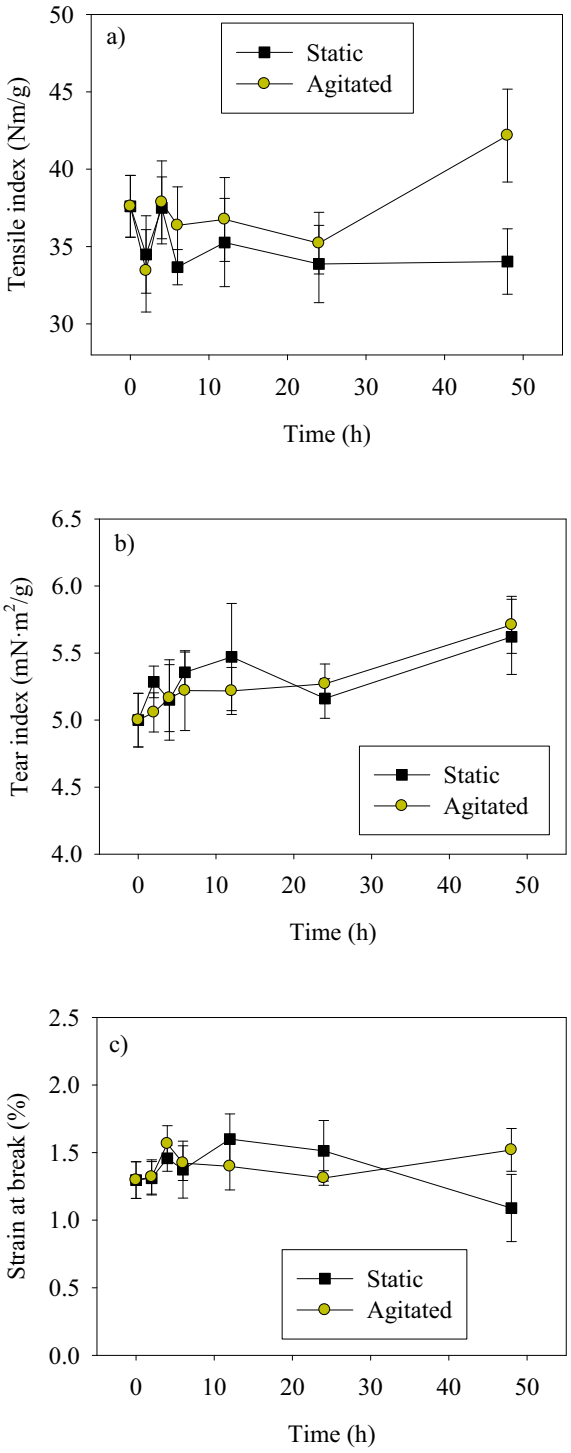

Fig. 2. Effect of culture time on the mechanical properties of paper in both static and agitated mode: a) tensile index, b) tear index and c) strain at break.

Strain at break results are represented in Fig. 2c. When BC was produced in static culture, strain at break increased by 24.1% the first 12 h, but it was reduced by 15.5% after 48 h of culture compared to the initial value. This fact could be related to the irregular formation of the handsheets, since the synthetized BC pellicles were difficult to disperse [30]. However, in agitated culture, strain at break increased by 8.5%, when time was below 24 h, and by 17.8% at 48 h, with also agrees with the higher flexibility found based on TI and tear index results.

Other important issue that can affect the mechanical performance of paper is the fact that the BC produced by the two cell culture methods is different [8]. Static cultures provide a higher BC crystallinity and length since bacteria are free to move through the surface of the culture broth. These two factors would induce a significant enhancement in paper strength if the BC nanofibers could be completely disperse. However, this is one of the main drawbacks of culturing bacteria in static mode, due to the high entanglement of nanofibers in the BC pellicle [30]. On the other hand, more amorphous and short chains of BC are produced in agitated systems, due to the shearing of the culture broth that can break BC nanofibers while they are being formed. In view of these properties, a worse improvement would be expected for agitated cultures compared to static. However, a higher nanofiber dispersion could be reached, thus allowing a greater effect of BC on the paper mechanical performance.

3.1.2. Physical properties

Nanocelluloses are known to decrease the porosity of handsheets since they are mainly fitted within the gaps between fibers, forming a more compact structure, thus improving barrier properties [34]. As shown in Fig. 3a, porosity of handsheets formed by culturing the pulp in static mode presented a decreasing tendency with culture time. However, porosity decreased in a smoother way in the case of agitated cultures, reaching a decrement of 44.6% when culture time was 48 h.

Beta formation measurement shows the homogeneity of the handsheets as the standard deviation of the microgrammage measured in different points of the sample. According to Fig. 3b, formation of handsheets prepared with the static cultured improved pulp was more homogeneous when time was below 24 h, since beta formation decreased by 15.7%. However, the formation of a pellicle of BCNF during culture at high culture time (48 h) triggered more irregular papers, increasing the beta formation index by 2% compared to the initial sample.

In the case of agitated cultures, beta formation presented a smoother decreasing tendency, meaning that the production of BC was carried out homogeneously within the pulp. Even at low culture times, below 6 h, this parameter was reduced by 12.2%, and by 20% at 48 h. These results for agitated cultures present a high advantage respect to those of static mode, since the control of the handsheet properties can be carried out in a more confidence way.

Fig. 3c shows the evolution of the handsheets bulk with the culture time. The bulk is defined as the ratio between the thickness and the grammage. In this case, a similar behavior was observed between both static and agitated cultures, decreasing the value of this parameter at short times followed by an increase after 12 h. The first reduction was assigned to the replacement of the original fibers by improved fibers of either BC alone (static mode) or fibers covered by BC (agitated mode). It resulted in a reduction of the handsheet thickness while keeping the grammage without variation [35]. Then, when culture time was 48 h, the bulk further increased by 6.2% and 2.8% for static and agitated cultures, respectively. Depending on the final use of the paper, a low bulk could be inconvenient, since it entails a low paper manageability [1]. Therefore, a further optimization should be carried out in the case of newsprint, magazine or office papers.

3.1.3. Optical properties

Optical properties were also affected by the addition of improved fibers to the pulp, reducing the ISO Brightness of handsheets when the pulp was cultured even for short times (Fig. 4a). This effect could be assigned to the presence of nutrients in the handsheets, some of them of brown color (yeast extract and peptone). Nutrients are supposed to pass through the filtering mesh when handsheets are being formed, due to the small particle size. However, as BC fibers diameter is in the nano-scale, some nutrient particles can remain as impurities within the paper, thus causing a detrimental effect on optical properties. This fact was much more intense at high culture time (48 h), since it was reduced by 3.5 and 4.7 points for static and agitated cultures, respectively. As the produced BC amount through static mode is lower than in

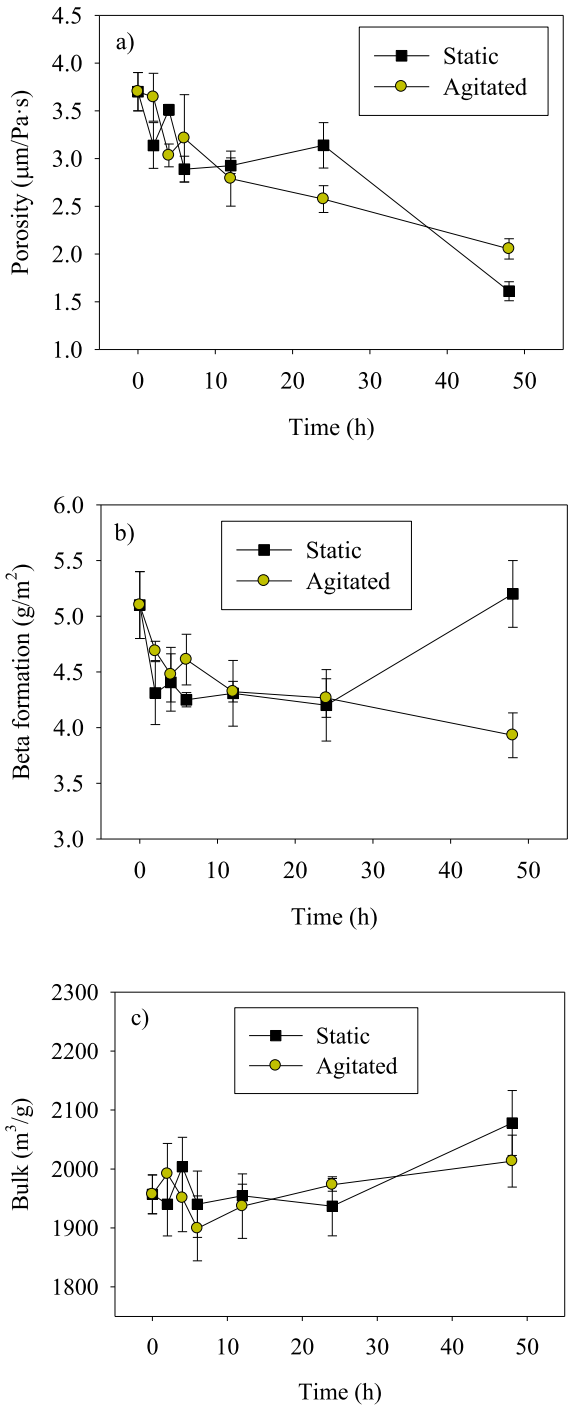

Fig. 3. Effect of culture time on the physical properties of paper in both static and agitated mode: a) porosity, b) beta formation and c) bulk.

agitated mode, the nutrients present in these handsheets are scarcer and thus ISO Brightness is not as affected.

The colorimetric constants showed a narrow trend between the values for static and agitated cultures. In this way, CIE L* and CIE b* decreased by 2.2 and 1.5 points, respectively, after 2 h of culture (Fig. 4b and d). It means that handsheets were tending to black and blue colors with the longer culture time. Respect to CIE a* (Fig. 4c), it was not very affected by the nutrients present within the paper, varying slightly in the range of −0.32 to −0.4. The reason for this decrement in CIE a*

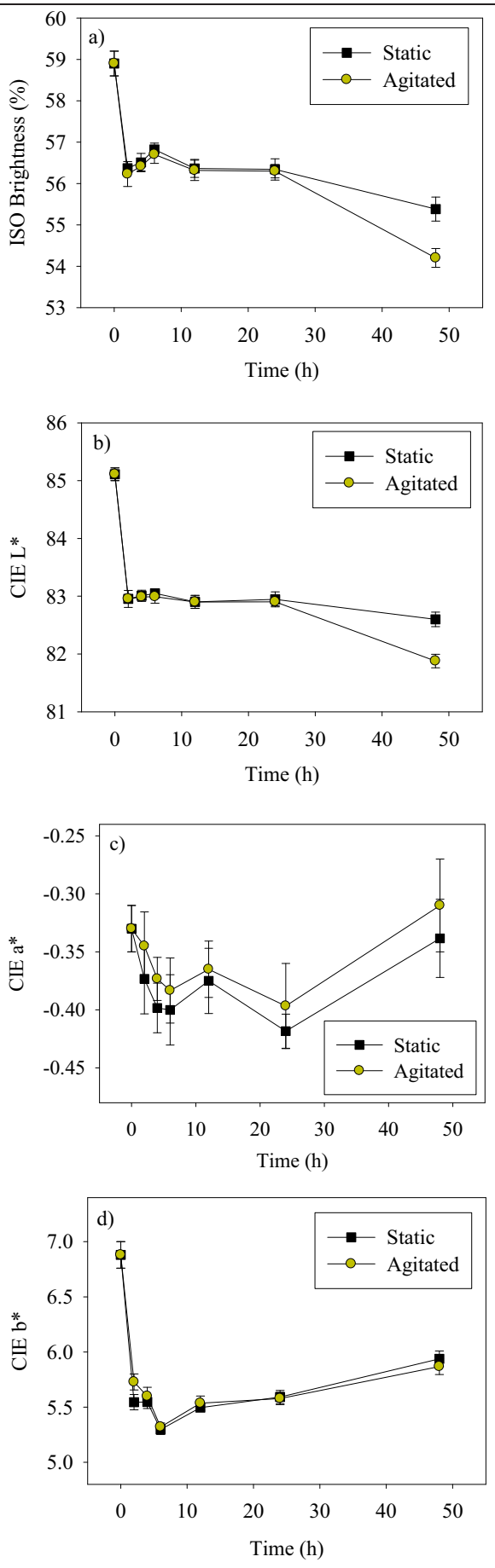

Fig. 4. Effect of culture time on the optical properties of paper in both static and agitated mode: a) ISO brightness, b) CIE L*, c) CIA a* and d) CIE b*.

could be mainly due to the darkness of the culture media. Nevertheless, as it can be observed, the darkness of the handsheets is not as important as the color change.

3.2. Static and agitated culture: production mechanism

A schematic illustration of BC synthesis in the presence of fibers for both agitated and static cultures is shown in Fig. 5.

In the case of agitated culture (Fig. 5a), RP fibers are distributed homogeneously through the culture broth at zero time, as observed in Fig. 6a, where a macroscopic view of the culture broth is displayed. After the pulp was inoculated, mainly cell growth took place for the first 6 h of culture. However, when the culture time was over 6 h, the BC fibers started to make appearance (Fig. 6b). Considering the fact that aerobic bacteria have the preference for zones with high oxygen availability, it is highly probable that they tend to grow on the fibers surface. Thus, BC would be likely synthesized as a coating of these fibers, fixing the flaws of the recycled fibers. With the orbital agitation of the culture, bacteria keep moving through the broth while they are producing BC, so finally a network composed of coated fibers was created. When this network was further disintegrated, the improved fibers could be separated. Then, mechanical properties of handsheets are highly probable to be improved.

Moreover, when culture time was over 24 h, those networks are formed with a more compact and strong structure, being usually difficult to separate (Fig. 6c). Therefore, big clusters are the result of the pulp disintegration, with heterogeneous shape and composition. Then, irregular handsheets with areas of a high amount of BC and others with lack of fibers or even holes are obtained. As a conclusion, it can be confirmed that culture time is a key parameter for the in-situ production of BC with recycled fibers by agitated culture, and has to be optimized to reach a worth improvement in paper mechanical properties.

In the case of static culture, while recycled fibers tended to sediment, bacteria moved to the surface of the culture broth in search of oxygen (Fig. 5b). In this case, as published previously [11], cell growth is slower, but as most of bacteria are concentrated on the surface of the liquid phase, BC production can be detected even before 4 h of culture. At this time, a BC thin gelatinous pellicle is observed, as shown in Fig. 6d. When the culture time increased to more than 12 h, a thicker BC pellicle with a denser surface on the side exposed to air is formed [10]. Fig. 6e showed as the BC pellicle adsorbed almost all the fibers added to the culture, deducing that not only BC was being produced on the surface of the culture broth, but also on the surface of the Petri dish (although in a lower extent). This fact was observed in Fig. 6f, when after 48 h of culture, a thick and gelatinous membrane was produced at the top of the culture and a thinner but resistant membrane was also formed around the culture broth, wrapping all the fibers and medium inside (Fig. 6f).

SEM images of the handsheets formed by the combination of agitated cultured pulp at the dosage of 10% (2) and recycled fibers are shown in Fig. 7. When handsheets were formed before the inoculation of the pulp (shown in graphs as 0 h), individual primary fibers were observed with some mineral fillers attached to their surface. Also, it is worth mentioning that these fibers show a rough surface, mainly due to the deterioration caused by the recycling cycles. As explained before, when bacteria were cultured with the pulp for 6 h, some BC fibers were produced as a coating of these fibers, easing the attachment of the mineral fillers within the paper sheet. At higher culture time, some bridges of BC were detected between recycled fibers. Finally, it is observed in

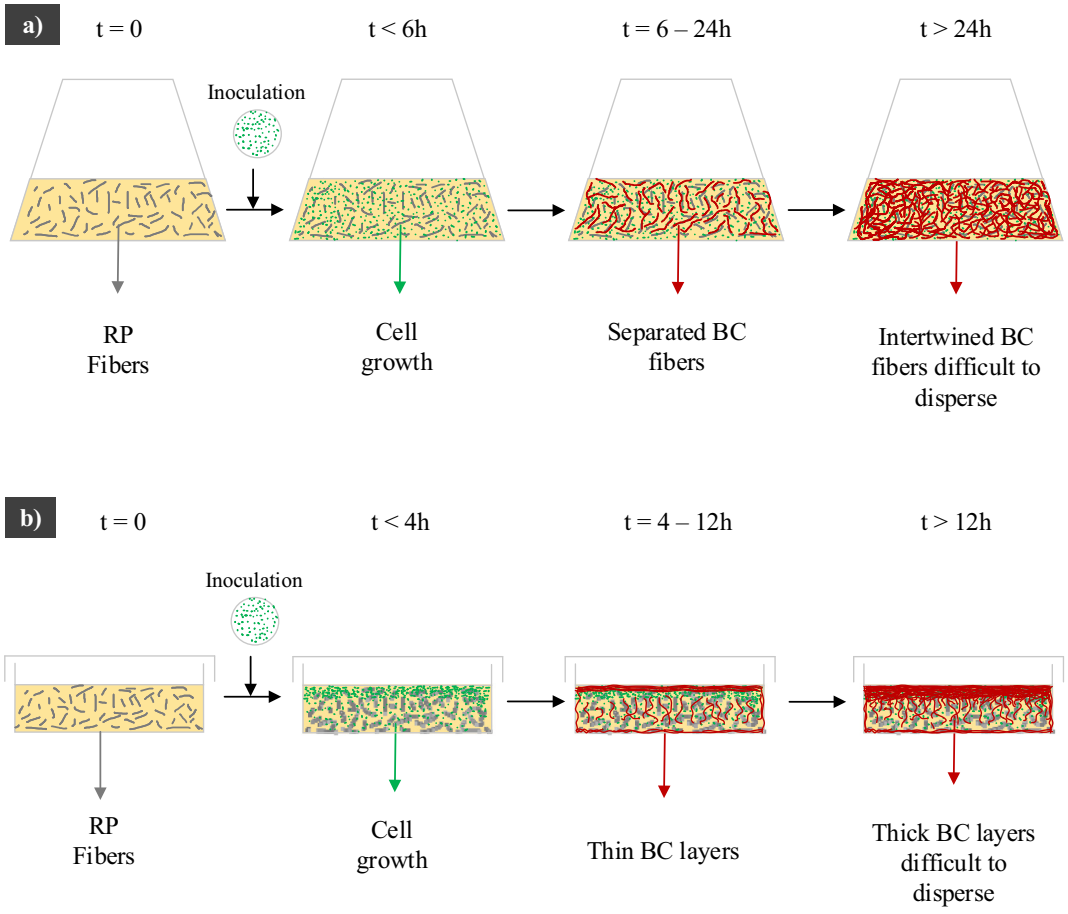

Fig. 5. Proposed mechanism for in-situ culture of bacteria with cellulosic fibers in a) agitated mode and b) static mode.

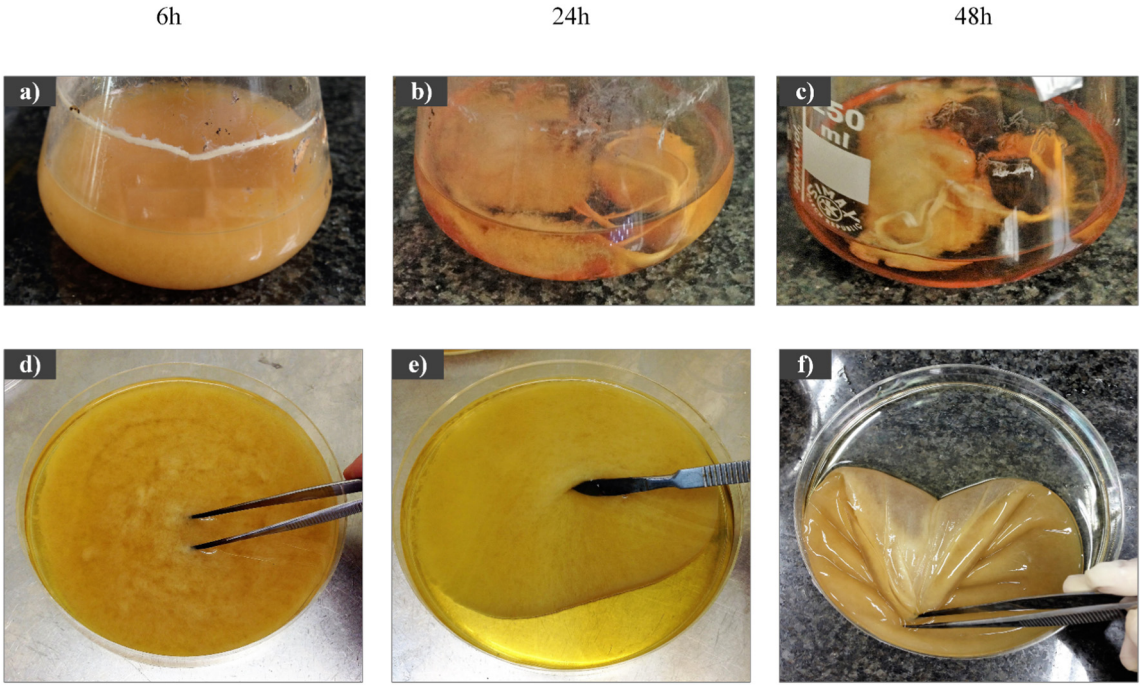

Fig. 6. Images of agitated (a, b and c) and static (d, e and f) in-situ cultures after 6 (a and d), 24 (b and e) and 48 h (c and f) of culture time.

Fig. 7 at 48 h that not only the fibers were covered, but also they were joint by BC, which is shown in the micrographs as a smooth and homogeneous surface.

Taking all these aspects into account, it can be concluded that static culture of bacteria in-situ with fibers was faster than agitated culture, but heterogeneous systems were produced. In addition, the formed BC pellicles were difficult to disintegrate, which caused a bad handsheet formation, as well as a mechanical properties worsening. On the other side, agitated cultures resulted in efficient systems, since BC was found to cover the primary recycled fibers, compensating for the fiber damage. Moreover, the enhanced paper flexibility observed previously when pure BC was added as a strength additive to the pulp [30] was also found in this culture mode. Therefore, a deeper study of the effect of the culture volume on mechanical, physical and optical properties of the RP was carried out in agitated mode.

3.3. Effect of the culture volume on paper properties

Nutrients were supposed to pass through the filter when handsheets were being formed, due to their small size, together with the fact that they were dissolved. However, the residual amount present in handsheets was observed to affect paper properties, so they were taken into account for all explanations.

Zero time values showed in Fig. 8 were those obtained with the addition of cultured pulp without inoculation at the different dosages. They show the tendency of TI to improve with a higher dosage of the cultured pulp. Thus, for the dosages of 5%, 15% and 45%, TI increased by 8.5%, 15.3% and 28.4% compared to handsheets made of pulp without nutrients. Fructose, the carbon source used in this study, is surrounded by hydroxyl groups, which makes possible the bond between them and the cellulose chains by hydrogen bonding [36]. In this way, the size of gaps among the cellulose fibers are reduced, thus increasing the tensile strength of the material.

When the cultured pulp dosage was 5% (1), the handsheets TI was found to increase with the culture time for the first hours, reaching improvements of 6.8% and 10.8% at 6 and 12 h. After that, TI decreased due to the heterogeneous formation of the handsheets, which concentrated the improved fibers with BC in a specific area of the handsheets. This behavior was related to the BC production mechanism in agitated culture previously explained, since the improvement in mechanical properties was deceased after 24 h.

With the addition of the triple amount of the cultured pulp, 15% (3), TI reached 39.0 Nm/g, which is the same value as the maximum TI for 5% (1), but 6 h before. However, the increment respect to the value at zero time was only 3.4%, meaning that the main parameter affecting the enhancement in the mechanical properties was the amount of nutrients present within the handsheets. Thus, although the dosage was triplicate, TI was not as improved as expected.

Nevertheless, when the same volume was cultured in one single flask (15% (1)), the results were more satisfactory. The highest TI value was obtained at 12 h (40.7 Nm/g), reaching an increment of 7.4% compared to the TI for zero time at this dosage. Then, after 24 h of culture, the TI increment was strongly reduced to 2.1% and even reaching a decrement after that. As mentioned before, the formation of a high amount of BC difficult to disperse together with a lower amount of nutrients could be the causes of this worsening.

Compared to 15% (3), a higher enhancement in the mechanical performance was achieved for culture times below 24 h. Although the enhanced oxygen availability should theoretically trigger an increasing BC production rate, reduced yields have been also previously reported [37]. According to Aydin and Aksoy [12], the high shear stress suffered by bacterial cells with high agitation and aeration triggers a spontaneous mutation of bacteria of the genus *Komagataeibacter* which deactivates the essential enzymes involved in the cellulose production, i.e. phosphoglucomutase and uridine diphosphoglucose pyrophosphorylase [14]. As there is a wide oxygen availability in the smaller flasks, the probability of bacterial cells to mutate is higher, thus meaning a lower BC productivity and thus mechanical properties enhancement. This behavior described previously in the literature matches the better results obtained for TI values at 15% (1) than those at 15% (3), so it has been accepted.

Finally, at the dosage of 45% (3), only a slight improvement in TI (1.9%) was found after 6 h of culture. In this case, the high amount of residual nutrients present in the handsheets induces a high increment in the TI. In addition, the BC amount produced during culture was not high enough to achieve deserving increments, probably also masked

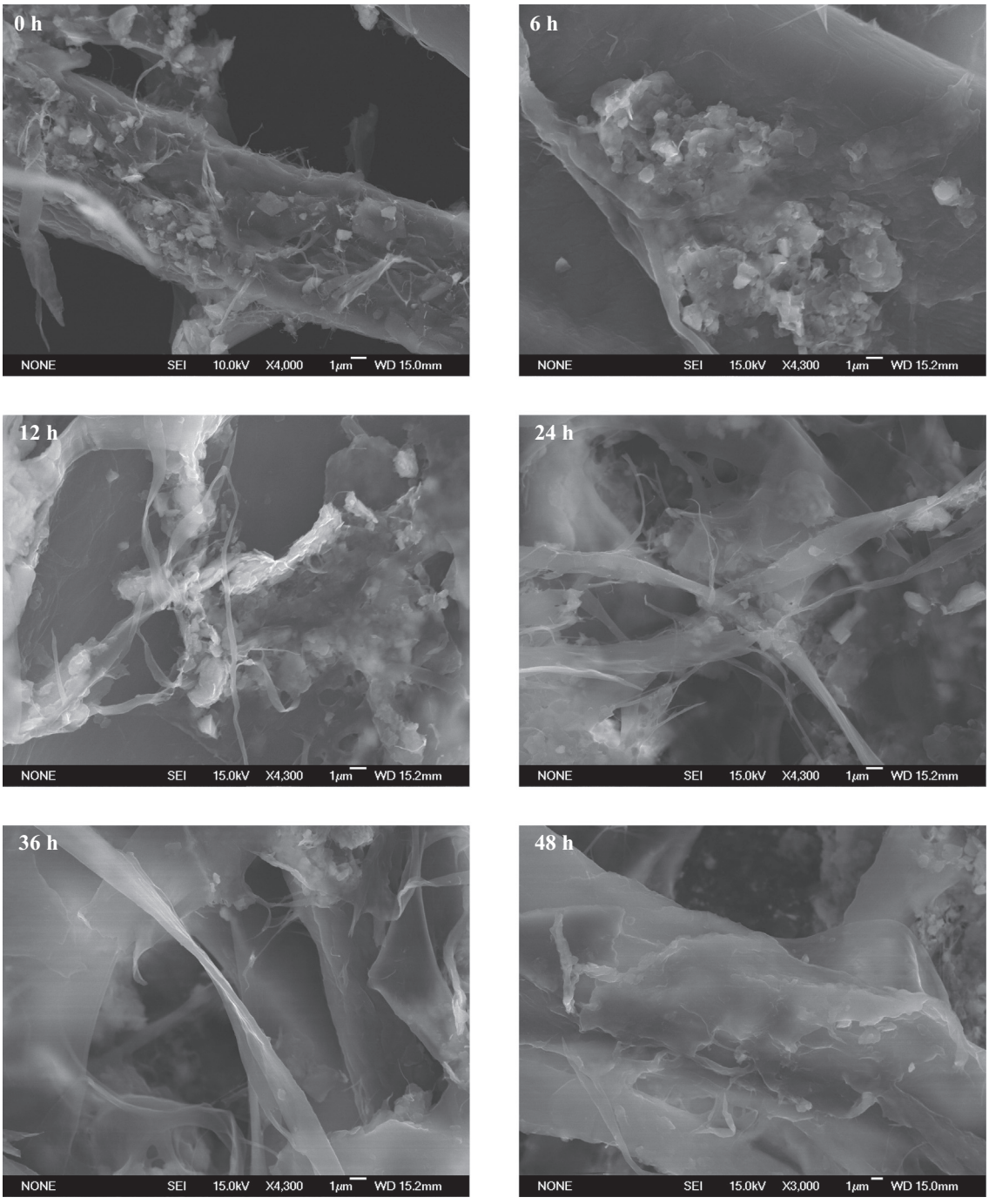

Fig. 7. SEM micrographs of BC/recycled fibers handsheets produced by in-situ culture of bacteria in agitated mode.

by the reinforcing effect of fructose in handsheets. Moreover, even a worsening in mechanical properties was observed for culture time longer than 12 h. The consumption of nutrients by bacteria together with the bad handsheets formation due to the numerous clusters of BC, was the responsible of this decrement.

This behavior agreed with the proposed mechanism of in situ culture for agitated systems, without observing any improvement in mechanical properties when culture time was higher than 24 h. Interestingly, when culture was carried out in just one flask, either 100 mL or 300 mL, TI results presented a similar behavior, increasing at the first stage, getting a maximum at 12 h of culture, and decreasing after that time. However, when both dosages were triplicated, TI values did not follow the same tendency at all, but increased at 6 h and decreased after that time.

Strain at break was also increased at high dosages of in-situ cultured pulp at zero time (Fig. 9). Thus, when the dosage was 5%, it was decreased by 9.3%, while it was increased by 4.6% and 28.7% at the dosages of 15% and 45%. As TI results, strain at break increased due to the higher number of hydrogen bonds between several units of fructose and cellulose. In this way, tensile strength was increased as well as the flexibility of the handsheets, as previously described [30].

The variation of the strain at break values with time at the dosage of 5% (1) matched with the TI behavior. At 6 h of culture, it increased by 11.1%, getting a maximum in 12 h with an improvement of 17.9%.

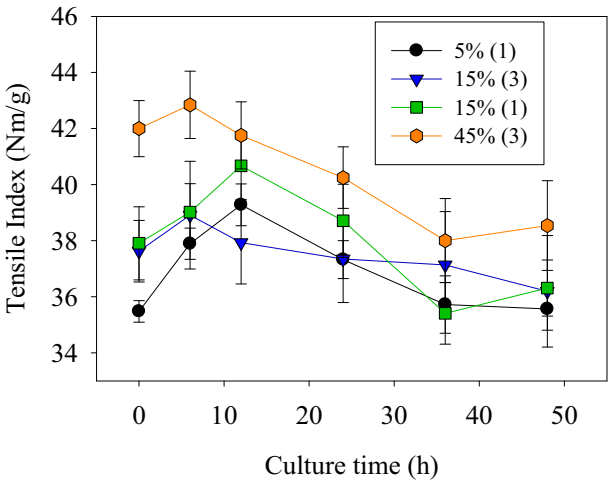

Fig. 8. Tensile index of handsheets prepared with 5% (1), 15% (3), 15% (1) and 45% (3) of in situ cultured bacteria.

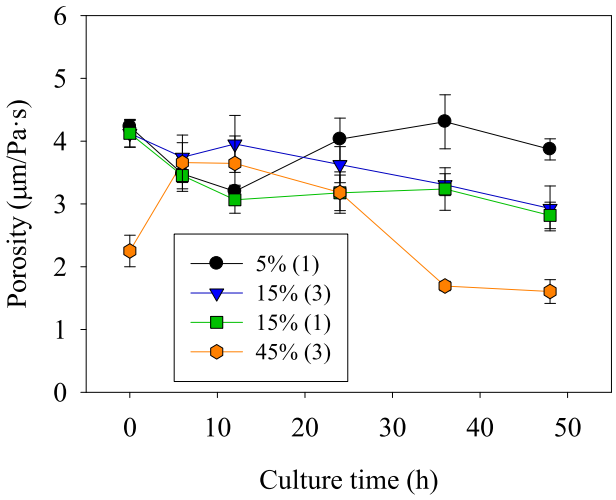

Fig. 10. Porosity of handsheets prepared with 5% (1), 15% (3), 15% (1) and 45% (3) of pulp in-situ cultured by bacteria.

However, when a 15% (3) of cultured pulp was added to the pulp, a maximum increment of 11.8% was found at 6 h of culture, decreasing after that time. Compared to 15% (1), while TI was highly improved, strain at break was almost similar. Then, the BC produced could be the driver for the enhancement in TI, but not for the strain at break improvement. In addition, the high error bars show low confidence data. Finally, at a high dosage of 45% (3), while strain at break at zero time was further improved, it was decreased with the culture time, what is explained by the higher amount of BC and the nutrients consumption. Then, while TI results were so dependent on the BC production, strain at break seems to be affected in a high extent by the amount of residual nutrients in the handsheets.

Porosity of handsheets was traditionally found to decrease by the addition of different nanocelluloses, since they fit the gaps between fibers [3]. Therefore, it was expected this parameter to be reduced with the culture time while the BC production is developed. In addition, as fructose is bonded to fibers by hydrogen bonds, and both TI and strain at break were increased by this residual component, porosity should be reduced. This is indeed what happened according to Fig. 10, where increments of −5.2% and −49.4% were found for dosages of 15% and 45% at zero time, respectively. This explanation also agrees with the results observed for 5% (1), 15% (3) and 15% (1) with time. However, results for 45% (3) differ from the previous results. While TI slightly increased during the first 6 h of culture, porosity also increased by 62.7%. Then, it strongly decreased after 24 h of culture, until values were below the one of zero time (decrement of 28.8%). The reason for that behavior could be the ease of the nutrients to be retained within the BC network, forming an impermeable area.

Finally, Fig. 11 showed a strongly dependence of the dosage with the optical properties and not with culture time (Fig. 11). Then, when the dosage was 5% (1), the ISO brightness was 61.4%, being reduced to 58.3% and 52.0% for the dosages of 15% and 45%.

Due to the possibility that some BC nanofibers can be loss during the removal of the medium components because of their small size, washing of the pulp has been avoided. However, this issue would become a drawback for large scale fabrication, not only affecting paper properties, but also incrementing the microbiological population in the wastewater as well as easing the presence of deposits in some papermaking equipment. Hence, further studies would, therefore, be necessary to overcome this challenge before scaling-up this method.

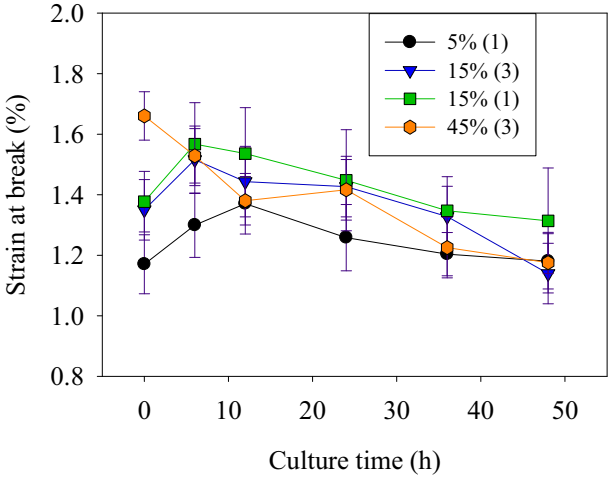

Fig. 9. Strain at break of handsheets prepared with 5% (1), 15% (3), 15% (1) and 45% (3) of pulp in-situ cultured by bacteria.

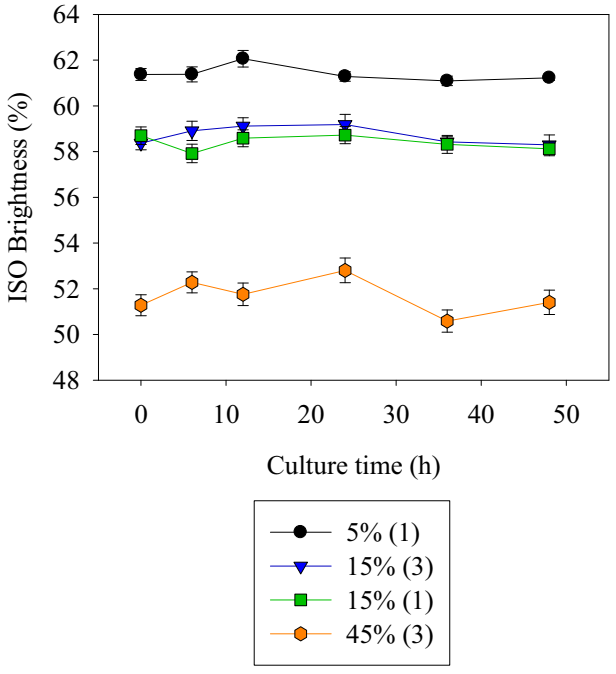

Fig. 11. ISO Brightness of handsheets prepared with 5% (1), 15% (3), 15% (1) and 45% (3) of pulp in-situ cultured by bacteria.

4. Conclusions

The viability of the in situ culture of bacteria of the genus *Komagataeibacter* with recycled fibers to reinforce paper has been demonstrated. The presence of BC was verified in all experiments, being observed earlier in static culture.

In this latter case, BC was produced as a thick membrane floating on top of the layer of sedimented primary fibers, thus failing to improve the properties of paper. In agitated cultures, the production of BC appeared to present two stages: first, BC was found to cover the primary fibers, compensating thus for the fiber damage suffered during the recycling process; at a later time, these coated fibers were interwoven forming tight clusters difficult to disperse and producing heterogeneous papers. Agitated cultures showed capacity to improve mechanical properties of paper, but only in the first stage.

The BC production in agitated media in the first stage enhanced paper flexibility, which is not obtained using the traditional CNF or CNC. A maximum improvement in the mechanical properties was obtained at 12 h for the addition of 15% (1), reaching increments of 24.3% in TI and 19.4% in strain at break. Owing to the different mechanisms and improvement percentages, culture time was found a key parameter to be optimized.

Probably due to the combination of the correct hydrodynamic environment and culture volume, the dissolved oxygen concentration in the cultures with higher volume was suitable to avoid the shear stress and the diversion metabolic pathways towards the deactivation of the essential enzymes involved in the cellulose production. This shear stress was suffered by bacteria in cultures with small volume, thus reducing the BC productivity.

In view of the results, the in-situ BC production with recycled fibers constitutes a promising alternative to replace conventional strengthening agents. These results have the potential to be applied in industrial paper mills, employing pulp streams with the application of low cost, non-exhaustive sterilization operations, such as ozone or ultraviolet radiation. Further studies must be carried out to substitute nutrients by waste streams and thus reduce the costs.

Acknowledgements

The authors wish to acknowledge the financial support of the Spanish Ministry of Economy and Competitiveness by the projects CTQ2013-48090-C2-1-R and CTQ2017-85654-C2-2-R, as well as the grant of C. Campano (BES-2014-068177). The authors wish also to acknowledge the Community of Madrid through the RETO-PROSOST-CM Programme (S2013/MAE-2907).

References

[1] A. Blanco, R. Miranda, M.C. Monte, Extending the limits of paper recycling: improvements along the paper value chain, For. Syst. 22 (3) (2013) 471–483.
[2] I. Čabalová, F. Kačík, A. Geffert, D. Kačíková, The effects of paper recycling and its environmental impact, Environ. Manag. (2011) 329–350.
[3] C. Campano, N. Merayo, A. Balea, Q. Tarrés, M. Delgado-Aguilar, P. Mutjé, C. Negro, A. Blanco, Mechanical and chemical dispersion of nanocelluloses to improve their reinforcing effect on recycled paper, Cellulose 25 (1) (2017) 269–280.
[4] M.A. Hubbe, Prospects for maintaining strength of paper and paperboard products while using less forest resources: a review, Bioresources 9 (1) (2013) 1634–1763.
[5] P.R. Chawla, I.B. Bajaj, S.A. Survase, R.S. Singhal, Microbial cellulose: fermentative production and applications, Food Technol. Biotechnol. 47 (2) (2009) 107–124.
[6] J.R. Rosa, I.S.V. da Silva, C.S.M. de Lima, W.P.F. Neto, H.A. Silverio, D.B. dos Santos, H.D. Barud, S.J.L. Ribeiro, D. Pasquini, New biphasic mono-component composite material obtained by partial oxypropylation of bacterial cellulose, Cellulose 21 (3) (2014) 1361–1368.
[7] S.H. Osong, S. Norgren, P. Engstrand, Processing of wood-based microfibrillated cellulose and nanofibrillated cellulose, and applications relating to papermaking: a review, Cellulose 23 (1) (2016) 93–123.
[8] C. Campano, A. Balea, A. Blanco, C. Negro, Enhancement of the fermentation process and properties of bacterial cellulose: a review, Cellulose 23 (1) (2016) 57–91.
[9] M. Rajinipriya, M. Nagalakshmaiah, M. Robert, S. Elkoun, Importance of agricultural and industrial waste in the field of nanocellulose and recent industrial developments of wood based nanocellulose: a review, ACS Sustain. Chem. Eng. 6 (3) (2018) 2807–2828.
[10] S.P. Lin, I.L. Calvar, J.M. Catchmark, J.R. Liu, A. Demirci, K.C. Cheng, Biosynthesis, production and applications of bacterial cellulose, Cellulose 20 (5) (2013) 2191–2219.
[11] Y. Huang, C.L. Zhu, J.Z. Yang, Y. Nie, C.T. Chen, D.P. Sun, Recent advances in bacterial cellulose, Cellulose 21 (1) (2014) 1–30.
[12] Y.A. Aydin, N.D. Aksoy, Isolation and characterization of an efficient bacterial cellulose producer strain in agitated culture: *Gluconacetobacter hansenii* P2A, Appl. Microbiol. Biotechnol. 98 (3) (2014) 1065–1075.
[13] J.H. Ha, O. Shehzad, S. Khan, S.Y. Lee, J.W. Park, T. Khan, J.K. Park, Production of bacterial cellulose by a static cultivation using the waste from beer culture broth, Korean J. Chem. Eng. 25 (4) (2008) 812–815.
[14] V.T. Nguyen, B. Flanagan, D. Mikkelsen, S. Ramirez, L. Rivas, M.J. Gidley, G.A. Dykes, Spontaneous mutation results in lower cellulose production by a *Gluconacetobacter xylinus* strain from Kombucha, 80 (2) (2010) 337–343.
[15] S.-H. Moon, J.-M. Park, H.-Y. Chun, S.-J. Kim, Comparisons of physical properties of bacterial celluloses produced in different culture conditions using saccharified food wastes, 11 (1) (2006) 26–31.
[16] D.R. Ruka, G.P. Simon, K.M. Dean, In situ modifications to bacterial cellulose with the water insoluble polymer poly-3-hydroxybutyrate, Carbohydr. Polym. 92 (2) (2013) 1717–1723.
[17] N. Yingkamhaeng, I. Intapan, P. Sukyai, Fabrication and characterisation of functionalised superparamagnetic bacterial nanocellulose using ultrasonic-assisted in situ synthesis, Fiber. Polym. 19 (3) (2018) 489–497.
[18] J.X. Yang, X.G. Lv, S.Y. Chen, Z. Li, C. Feng, H.P. Wang, Y.M. Xu, In situ fabrication of a microporous bacterial cellulose/potato starch composite scaffold with enhanced cell compatibility, Cellulose 21 (3) (2014) 1823–1835.
[19] B. Wang, G.X. Qi, C. Huang, X.Y. Yang, H.R. Zhang, J. Luo, X.F. Chen, L. Xiong, X.D. Chen, Preparation of bacterial cellulose/inorganic gel of bentonite composite by in situ modification, Indian J. Microbiol. 56 (1) (2016) 72–79.
[20] W.K. Zhu, W. Li, Y. He, T. Duan, In-situ biopreparation of biocompatible bacterial cellulose/graphene oxide composites pellets, Appl. Surf. Sci. 338 (2015) 22–26.
[21] Y.Y. Feng, X.Q. Zhang, Y.T. Shen, K. Yoshino, W. Feng, A mechanically strong, flexible and conductive film based on bacterial cellulose/graphene nanocomposite, Carbohydr. Polym. 87 (1) (2012) 644–649.
[22] C. Castro, N. Cordeiro, M. Faria, R. Zuluaga, J.L. Putaux, I. Filpponen, L. Velez, O.J. Rojas, P. Ganan, In-situ glyoxalization during biosynthesis of bacterial cellulose, Carbohydr. Polym. 126 (2015) 32–39.
[23] H.H. Chen, L.C. Chen, H.C. Huang, S.B. Lin, In situ modification of bacterial cellulose nanostructure by adding CMC during the growth of *Gluconacetobacter xylinus*, Cellulose 18 (6) (2011) 1573–1583.
[24] T. Ma, Q. Zhao, K. Ji, B. Zeng, G. Li, Homogeneous and porous modified bacterial cellulose achieved by in situ modification with low amounts of carboxymethyl cellulose, Cellulose 21 (4) (2014) 2637–2646.
[25] Y. Chen, X. Zhou, Q. Lin, D. Jiang, Bacterial cellulose/gelatin composites: in situ preparation and glutaraldehyde treatment, Cellulose 21 (4) (2014) 2679–2693.
[26] S. Park, J. Park, I. Jo, S.P. Cho, D. Sung, S. Ryu, M. Park, K.A. Min, J. Kim, S. Hong, B.H. Hong, B.S. Kim, In situ hybridization of carbon nanotubes with bacterial cellulose for three-dimensional hybrid bioscaffolds, Biomaterials 58 (2015) 93–102.
[27] F. Hong, K.Y. Qiu, An alternative carbon source from konjac powder for enhancing production of bacterial cellulose in static cultures by a model strain *Acetobacter aceti subsp xylinus* ATCC 23770, Carbohydr. Polym. 72 (3) (2008) 545–549.
[28] B. Surma-Slusarska, D. Danielewicz, S. Presler, Properties of composites of unbeaten birch and pine sulphate pulps with bacterial cellulose, Fibres Text. East. Eur. 16 (6) (2008) 127–129.
[29] B. Surma-Slusarska, S. Presler, D. Danielewicz, Characteristics of bacterial cellulose obtained from *Acetobacter xylinum* culture for application in papermaking, Fibres Text. East. Eur. 16 (4) (2008) 108–111.
[30] C. Campano, N. Merayo, C. Negro, A. Blanco, Low-fibrillated bacterial cellulose nanofibers as a sustainable additive to enhance recycled paper quality, Int. J. Biol. Macromol. 114 (2018) 1077–1083.
[31] J.Y. Jung, J.K. Park, H.N. Chang, Bacterial cellulose production by *Gluconacetobacter hansenii* in an agitated culture without living non-cellulose producing cells, Enzym. Microb. Technol. 37 (3) (2005) 347–354.
[32] M. Jonoobi, A.P. Mathew, K. Oksman, Producing low-cost cellulose nanofiber from sludge as new source of raw materials, Ind. Crop. Prod. 40 (2012) 232–238.
[33] E.A. Hassan, M.L. Hassan, K. Oksman, Improving bagasse pulp paper sheet properties with microfibrillated cellulose isolated from xylanase-treated bagasse, Wood Fiber Sci. 43 (1) (2011) 76–82.
[34] H.M.C. Azeredo, M.F. Rosa, L.H.C. Mattoso, Nanocellulose in bio-based food packaging applications, Ind. Crop. Prod. 97 (2017) 664–671.
[35] F.W. Brodin, O.W. Gregersen, K. Syverud, Cellulose nanofibrils: challenges and possibilities as a paper additive or coating material - a review, Nord. Pulp Pap. Res. J. 29 (1) (2014) 156–166.
[36] D.A. Okar, K. Zangger, Hydrogen bonding in the fructose-2,6-bisphosphatase reaction correlates with activity, FASEB J. 21 (6) (2007) A1014.
[37] M. Shoda, Y. Sugano, Recent advances in bacterial cellulose production, 10 (1) (2005) 1–8.

PUBLICATION IV

Direct production of cellulose nanocrystals from old newspapers and recycled newsprint

Cristina Campano, Ruben Miranda, Noemi Merayo, Carlos Negro, Angeles Blanco

Carbohydrate Polymers (2017) 173: 489–496

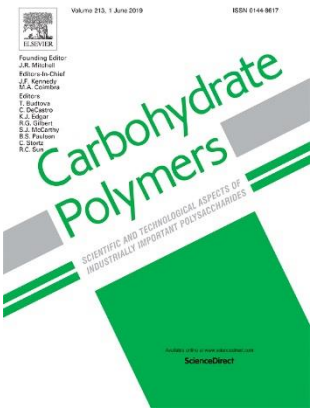

Impact factor 2017: ***5.158***

JCR, Polymer Science, 7 out of 87, ***Q1***

Carbohydrate Polymers 173 (2017) 489–496

Contents lists available at ScienceDirect

Carbohydrate Polymers

journal homepage: www.elsevier.com/locate/carbpol

Direct production of cellulose nanocrystals from old newspapers and recycled newsprint

Cristina Campano, Ruben Miranda, Noemi Merayo, Carlos Negro, Angeles Blanco*

Department of Chemical Engineering, Complutense University of Madrid, Avda. Complutense s/n, 28040 Madrid, Spain

ARTICLE INFO

Article history:
Received 28 March 2017
Received in revised form 11 May 2017
Accepted 24 May 2017
Available online 27 May 2017

Keywords:
Cellulose nanocrystals
Newsprint
Recycled paper
Process yield
Alkali and bleaching pretreatments
Old newspapers

ABSTRACT

Cellulose nanocrystals (CNC) are high added value products which can be used in many applications. In this research, CNC were directly produced from two recycled papers: old newspapers (ONP) and 100% recycled newsprint (NP). CNC were also obtained from NP by previously isolating the cellulose particles by alkali and bleaching treatments. CNC yield and quality was assessed through lignin and ash determination, X-ray diffraction analysis, atomic force microscopy and thermogravimetric analysis. Not only crystallinities resulted similar (92–95%), but also aspect ratios (L/d) (each in the range of 50–120). However, different CNC purities and hydrolysis and process yields were obtained. Thus, CNC purity decreased from 93 to 77%, hydrolysis yield was reduced from 64 to 58% but process yield strongly improved from 35 to 60% when no pretreatment was used. Therefore, this study proves the viability of the direct production of CNC from recycled papers.

1. Introduction

Cellulose, the most abundant renewable and naturally occurring polymer, has been used for nearly 150 years either as raw fibers or after some modifications. Cellulose consists of linear bonds of glucose as monosaccharide $(C_6H_{10}O_5)_n$, conforming both crystalline and amorphous regions (Mohamed, Salleh, Jaafar, Asri, & Ismail, 2015). Last can be removed by acid hydrolysis, remaining the crystalline part, which is known CNC, with a rod-like morphology (Habibi, Lucia, & Rojas, 2010).

In the last decades, the paper became one of the most recycled products with a recycling rate of 71.5% in Europe (CEPI 2015). However, paper industry is suffering an important crisis. In last years, while the demand of packaging papers is increasing continuously, the use of newsprint and some other graphic papers is decreasing. For example the production of packaging papers in Europe increased 7.2% in the last five years, while newsprint production decreased in 28.3% (CEPI 2015). This fact supposes huge challenges for the newsprint mills in order to maintain their competitiveness. As a consequence some companies have shut down production lines and others are looking for other market niches by developing new products and high added value products (Delgado-Aguilar, Tarres, Pelach, Mutje, & Fullana-i-Palmer, 2015). In this sense, the on-site production of nanocellulose can be a very promising alternative.

CNC are growing in popularity since their first isolation by Ranby in 1951, through a sulfuric acid hydrolysis of cellulose fibers (Ranby, 1951). These CNC exhibit many advantages compared to cellulose fibers, such as high strength, high surface area, unique optical properties, lightweight, stiffness, etc. Not only their properties and wide application prospects have attracted a high interest, but also their inherent renewability and sustainability (Habibi, 2014).

CNC can be prepared from any single source containing cellulose, such as wood pulps (Du et al., 2016; Hu et al., 2014), plant sources such as ramie or cotton (Csiszar, Kalic, Kobol, & Ferreira, 2016; Peresin, Habibi, Zoppe, Pawlak, & Rojas, 2010), food byproducts or wastes such as rice straw or rice husk (Lu & Hsieh, 2012; Mart&nez-Sanz, Vicente, Gontard, Lopez-Rubio, & Lagaron, 2015) or bacterial cellulose (Campano, Balea, Blanco, & Negro, 2016). To the best knowledge of the authors, only two recent references have studied the technical feasibility of using recycled paper as raw material to produce CNC (Danial et al., 2015; Mohamed et al., 2015). This cellulose source presents some advantages compared to wood pulps, such as the high availability and the low cost.

CNC production from recycled paper has been made after isolation of cellulose fibers by using intensive treatments. On the one side, Danial et al. (2015) boiled ONP for more than 12 h for two times, treating the resulting pulp with 5% (w/v) NaOH and followed by 2% (v/v) NaClO treatment. On the other side, Mohamed et al. (2015) used wastepaper, but they removed the printed areas of

* Corresponding author.
E-mail addresses: ccampano@ucm.es (C. Campano), rmiranda@ucm.es (R. Miranda), nmerayoc@ucm.es (N. Merayo), cnegro@ucm.es (C. Negro), ablanco@ucm.es (A. Blanco).

http://dx.doi.org/10.1016/j.carbpol.2017.05.073
0144-8617/

ONP, thus really using non-printed newsprint (NP). They applied an alkali treatment with 5 wt% NaOH at 125 °C for 2 h followed by a bleaching treatment with 2% (w/v) $NaClO_2$ at 125 °C for other 2 h, repeating this step until a white pulp was obtained. In addition, the used newsprint seems to be free of fillers, which is not the most typical case. In Europe, for example, ~98% of newsprint is produced from recovered paper and filler loadings are usually in the 15–20% range.

This work aims to determine the technical feasibility of producing CNC directly from recycled papers (ONP and NP) with fillers and without a previous isolation of cellulose fibers. To compare, a two-step pretreatment similar to the antecedents in the literature, based on an alkali treatment and a bleaching step has been applied to NP (NP-B). Thus, the effect of the presence of impurities in sample before hydrolysis on the quality of CNC has been assessed.

2. Experimental

2.1. Materials

ONP with an ISO brightness of 45% and 14.5 wt% ash content and NP with an ISO brightness of 56% and 14.0 wt% ash content were used as raw materials. Microcrystalline cellulose (MCC), Avicel, was used as reference of pure cellulosic material, supplied by Sigma-Aldrich. Chemicals used for acid hydrolysis and alkali treatment, H_2SO_4 and NaOH, were supplied by Sigma Aldrich (analytical reagent grade) and used without further modification. Furthermore, NaClO used for bleaching as a 10% w/v solution (technical grade), was supplied by Panreac.

2.2. Methods

Different CNC were prepared:

- ONP: direct acid hydrolysis.
- NP: direct acid hydrolysis.
- NP-B: Two-step pretreatment (alkali and bleaching treatments, similar to antecedents on literature) to NP, followed by acid hydrolysis. The purpose is to assess the effect of pretreatment on CNC properties and process yield.
- MCC: direct acid hydrolysis. These CNC were prepared to compare the effect of the raw material on CNC properties.

2.2.1. Two-step pretreatment

Alkali and bleaching treatments were applied to NP resulting in NP-B, adapting the procedure of Mohamed et al. (2015). Briefly, NP was disintegrated for 30 min at 3000 rpm, using a Messmer pulp disintegrator (Mavis Engineering Ltd, London, UK). Then, it was treated with 5 wt% NaOH for 2 h at 125 °C. After that, pulp was washed with distilled water. Then, 2% (w/v) NaClO was added and left to interact for 2 h at 125 °C. After, it was subsequently washed with distilled water to reach constant pH. NP-B pulp was dried overnight at 105 °C and then it was milled through an IKA analysis grinder A10 (IKA-Werke Gmbh, Staufen, Germany).

2.2.2. CNC production

After milling ONP, NP, NP-B and MCC, acid hydrolysis of dry milled samples was carried out with 60 wt% H_2SO_4 at 45 °C. This acid concentration was selected based on the study of Chen et al. (2015) in which the yield is maximized while minimizing conversion of CNC to sugars. The ratio between acid and extracted cellulose was set at 13.5 mL/g and the reaction time was 90 min, based on preliminary tests. First, 200 mL of prepared H_2SO_4 solution were slowly added during 2 min to avoid overheating of dry milled sample. Then, it was agitated in glass beaker on a thermostatic bath with an impeller covered by Teflon at 500 rpm. After the reaction time, mixture was diluted 10 times with distilled water to stop the reaction and left to settle overnight. The sediment was washed four times by centrifugation using a 3–16L centrifuge (JP Selecta S.A, Barcelona, Spain) at 4500*g* for 15 min to remove excess of acid. Finally, the suspension was dialyzed against distilled water using tubing membranes made of regenerated cellulose with a molecular weight cut-off of 12000–14000 Da (Medicell International Ltd, London, UK), until neutral pH was reached. All experiments were carried out by triplicate.

2.3. CNC characterization

2.3.1. CNC purity

After acid hydrolysis and dialysis, different proportion of ash and lignin can be present together with CNC. The amount of mineral fillers in the different CNC was measured through ash content at 525 °C following ISO 1762. Lignin content was measured indirectly by Kappa number according to Tappi 236 om-99 using the following equation: $Lignin\,(\%) = 0.13 \cdot Kappanumber$ (Tasman & Berzins, 1957). The remaining percentage up to 100% corresponds to the value of CNC purity.

2.3.2. Crystallinity index and average crystalline dimension

X-ray diffraction (XRD) spectra was obtained using a Philips X'Pert MPD X-Ray diffractometer with an autodivergent slit fitted with a graphite monocromator using Cu-Kα radiation operated at 45 kV and 40 mA. XRD patterns were recorded from 3 to 80° at a scanning speed of 1.5°/min. Crystallinity index (Cr.I) was determined using Segal's method (Segal, Creely, Martin, & Conrad, 1959) by the Eq. (1).

$$Cr.I\,(\%) = \frac{I_{002} - I_{am}}{I_{002}} \cdot 100 \quad (1)$$

Where I_{002} is the intensity of the 002 plane at $2\theta = 22.5°$ and I_{am} is the intensity of the amorphous scatter at $2\theta = 18°$.

ACD was determined by the widely-used Scherrer Eq. (2).

$$ACD = \frac{K \cdot \lambda}{\beta \cdot cos\theta} \quad (2)$$

Where ACD is the perpendicular size to the diffracting plane represented by the maximum peak, K is a dimensionless shape factor (normally 0.9), λ is the wavelength of the radiation in the diffraction experiment (λ = 0.15406 nm), β is the full width at half maximum (FWHM) of the diffraction peak in radians and θ is its diffraction angle also in radians (French & Cintron, 2013).

2.3.3. Polymerization degree

PD was determined from intrinsic viscosity (η), by the following equation: $\eta = 0.42 \cdot PD$ valid for $PD < 950$ (Henriksson, Berglund, Isaksson, Lindstrom, & Nishino, 2008). η was measured by the method of dissolving cellulose in cupri-ethyene-diamine (CED) solution, according to ISO 5351.

2.3.4. Morphology

Surface morphology and size distribution were determined using Atomic Force Microscopy (AFM) with an AFM multimode Nanoscope III A (Bruker), in tapping mode. A drop of a solution of 0.05% of consistency was deposited on a clean mica surface and left to dry overnight at room temperature before analysis.

2.3.5. Thermogravimetric analysis

Thermal stability was assessed using a Seiko Exstar 6000 TGA/DTA thermobalance, measuring the sample weight from 30 to 1000 °C at a heating rate of 10 °C/min with an air flow of 30 mL/min.

2.4. Yields

2.4.1. Hydrolysis yield

Hydrolysis yield was calculated by Eq. (3).

$$\text{Hydrolysis yield}\ (\%) = \frac{m_{CNC}}{m_{b\,hydr.}} \cdot 100 \quad (3)$$

Where m_{CNC} is the dry mass of the produced CNC (with the remaining impurities) and $m_{b\,hydr.}$ is the dry mass of sample before hydrolysis.

2.4.2. Process yield

CNC or process yield was determined by the ratio of m_{CNC} and the initial dry mass before pretreatment ($m_{b\,pret.}$) (Eq. (4)).

$$\text{Process yield}\ (\%) = \frac{m_{CNC}}{m_{b\,pret.}} \cdot 100 \quad (4)$$

2.4.3. Pretreatment losses

This percentage mainly includes the amount of lignin, hemicellulose and mineral fillers removed during the pretreatment, although the loss of some cellulose fibers is also possible. The mass loss during pretreatment was determined through the Eq. (5).

$$\text{Pretreatment losses}(\%) = \frac{m_{b\,pret.} - m_{b\,hydr.}}{m_{b\,pret.}} \cdot 100 \quad (5)$$

2.4.4. Hydrolysis mass loss

The mass loss during hydrolysis was determined by the sum of two values: dissolved amorphous cellulose and losses during hydrolysis. Dissolved amorphous cellulose (DAC) was determined through chemical oxygen demand (COD) of the filtrated supernatant after hydrolysis. Nanocolor® COD 1500 test method (Macherey-Nagel GmbH) and a Thermo Aquamate UV–vis spectrophotometer were used to obtain the COD value. Assuming that all present organic materials correspond to cellulose, DAC can be calculated from the following equation: $DAC\,(mg/L) = COD/1.185 = 2877.6 \cdot I^{600}$ obtained by Wang et al. (2012) through calibration with MCC. To be consistent with the rest of the calculations, a percentage value has been determined (Eq. (6)).

$$DAC = \frac{DAC \cdot V_{total}}{m_{b\,pret.}} \cdot 100 \quad (6)$$

Where V_{total} is the total volume when hydrolysis mixture is diluted 10 times.

Hydrolysis losses were determined through the remaining amount until 100%, mainly composed of dissolved $CaCO_3$ and cellulose losses. Eq. (7) shows the formula used to calculate this value.

$$\text{Hydrolysis losses}(\%) = 100 - \text{Process yield} - \text{Pretreatment losses} - DAC \quad (7)$$

3. Results and discussion

3.1. CNC purity

Since raw materials of this study are not pure cellulose, their main components, cellulose + hemicellulose, lignin and ash were determined, both before and after hydrolysis (Fig. 1).

The most used mineral fillers in papermaking are kaolin and calcium carbonate, while others such as talc or titanium dioxide are used in a lower extent (Lourenco, Gamelas, & Ferreira, 2014). As expected, the initial ash content of ONP and NP is almost the same, around 14%. However, after the two-step pretreatment, it is reduced to around 12%. The main cause is the loss of these mineral fillers in the filtration step after each treatment.

During acid hydrolysis, not only amorphous cellulose is dissolved but also $CaCO_3$ (soluble at acid pH). Therefore, ash contents in CNC samples are reduced to 11.5, 11.9 and 5.7%, for CNC-ONP, CNC-NP and CNC-NP-B, respectively. Presence of fillers was also verified through XRD analyses (showed in Section 3.2), where kaolinite and $CaCO_3$ were identified in the raw materials, while kaolinite was the only mineral filler present in CNC samples.

Lignin is present in most recycled papers, including ONP and NP. Lignin is removed from the pulp for producing papers with high optical properties, but only partially for newsprint, which must be produced as economically as possible. Results show that the amount of lignin in NP is lower than in ONP (6.5% vs. 9.1% Fig. 1a) because of its partial removal during recycling. However, differently to bleached chemical pulps, where lignin is virtually removed, mechanical or deinking pulps used for newsprint production can still present a high amount of lignin. Bleaching of NP (NP-B) reduced the lignin content to 2%.

During acid hydrolysis, lignin fractionates into an acid insoluble and acid soluble fractions. Due to dissolution of amorphous cellulose, percentage of lignin referred to the total amount of CNC in CNC-ONP and CNC-NP increased from 9.1 to 12.5% and from 6.5 to 10.2%, respectively. However, when CNC are produced from NP-B, lignin content is reduced due to the solubilization of acid soluble lignin is higher than dissolution of amorphous cellulose. In this case, only a residual amount of 0.9% is present. In case of repeating the bleaching process a second time, the percentage of lignin would be practically zero. It occurs with CNC-MCC, in which raw material is pure cellulose. However, the acid insoluble lignin remained after hydrolysis approximately in the same amount.

From Fig. 1b, it is clearly observed how a better quality in sample before hydrolysis produced a higher CNC purity. This value is similar in CNC-ONP, and CNC-NP (76.0% and 77.8%, respectively). However, this percentage not only includes cellulose but also hemicellulose since both ONP and NP have typically a cellulose/hemicellulose ratio between 1 and 2.2 (Sun & Cheng, 2002). Because of hemicellulose removal during alkali pretreatment, dissolution of lignin during bleaching and calcium carbonate during acid hydrolysis, CNC-NP-B purity increased up to 93.3%, considered as the percentage of cellulose. Depending on the final application of these CNC, CNC purity has to be taken into account.

The amount of lignin has a direct impact in color, which could limit their application when high optical properties are required. Fig. 2 shows physical appearance of dry sample before hydrolysis and the obtained CNC dispersions. The black color of CNC-ONP corresponds to remaining inks used in newspapers printing, mainly black, which masked color of other components. In the case of NP and CNC-NP, a brown color indicates the presence of lignin in the sample. As it has been previously explained, percentage of lignin in this sample (10.2%) is much higher than 0.9% corresponding to CNC-NP-B. However, a lighter color but still beige has been obtained instead of white obtained for CNC-MCC, probably due to the presence of a residual amount of lignin.

3.2. Crystallinity and average crystalline dimension

Typical crystalline cellulose associated peaks are obtained in MCC spectra $2\theta = 15–17^\circ$, 22.5° and 35° (Fig. 3a), confirming its high degree of crystallinity in a cellulose I structure (Xu et al., 2013). Peak at around 29.5° in raw materials is due to the presence of $CaCO_3$, which is the most intense peak other than cellulose of their XRD spectra. As it is soluble in acid media, it is not detected in CNC samples (Fig. 3b). There are also observed peaks at 12.5° and 25° in both raw materials and CNC, which are attributed to kaolinite. In CNC these peaks are more intense due to the increase of its relative amount in CNC samples by removal of amorphous parts of cellulose and $CaCO_3$.

Initial Cr.I value for ONP (85.9%) and NP (86.5%) are in accordance with Mohamed et al. (2015). They used non-printed areas of ONP, i.e. NP and obtained 82.0% of Cr.I. An increment in Cr.I is obtained

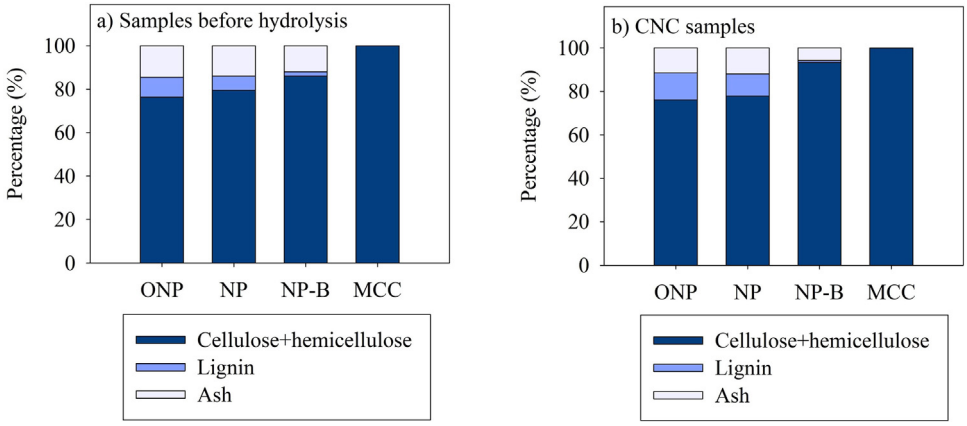

Fig. 1. Proportion of cellulose + hemicellulose, lignin and ash in a) samples before hydrolysis and b) obtained CNC.

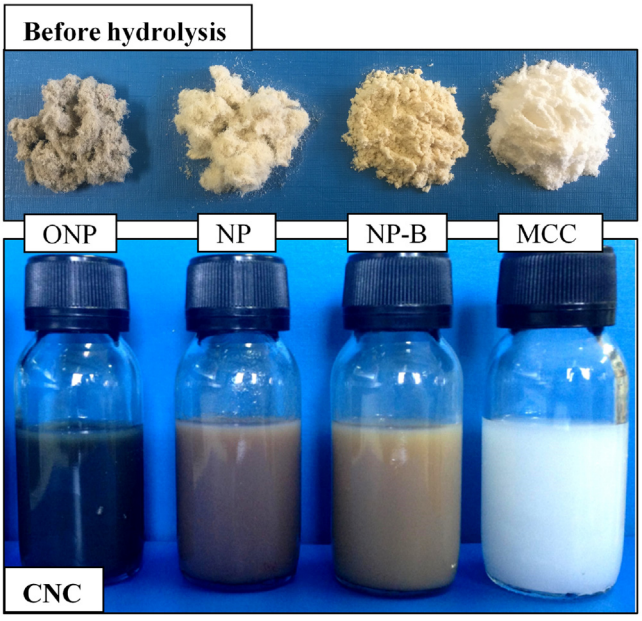

Fig. 2. Macroscopic images of sample before hydrolysis at the top and obtained CNC at the bottom for ONP, NP, NP-B and MCC.

when NP is bleached (NP-B), due to partial removal of hemicellulose and lignin (Sheltami, Abdullah, Ahmad, Dufresne, & Kargarzadeh, 2012), reaching 90.6% of Cr.I.

After hydrolysis, Cr.I increases in all cases as expected. CNC-ONP show lower value of Cr.I than CNC-NP (92.6% and 93.4%, respectively), mainly due to the slightly lower hydrolysis yield. In addition, according to Donnet (1993), typical used inks are oxidized in acid media, thus consuming some amount of H_2SO_4. Therefore, less amorphous cellulose is removed from raw materials, reaching a lower Cr.I. The subsequent acid hydrolysis of NP-B is favored by purity, reaching a value of Cr.I of 94.8%, very close to that of CNC-MCC (95.5%). However, the increase in Cr.I was not the same in all cases, those being 6.7, 7 and 4.2 percentage units for CNC-ONP, CNC-NP and CNC-NP-B, respectively. In case of CNC-MCC, the degree of Cr.I improvement is lower (3.9 percentage units) since the maximum value has been reached near that of raw material (91.6%) (Dufresne, 2012). These values are in accordance with Danial et al. (2015), whose CrI increased 10.1 percentage units after hydrolysis using ONP as raw material. However, as pretreatments of Mohamed et al. (2015) were much more aggressive, increment in CrI after acid hydrolysis is much lower, only 1.7 percentage units.

It is supposed that higher ACD of cellulose is observed when purity is higher due to the narrowing of the crystallite size distribution (Lu & Hsieh, 2012). Therefore, ACD values increase with purity, being 7.5, 10.3 and 12 nm for ONP, NP and NP-B and 32.5, 41.2 and 45 nm for their respective CNC. In all cases, ACD increases with acid hydrolysis treatment, due to that higher removal of amorphous cellulose favors aggregation of CNC. These values also checked the higher efficiency of the CNC production process when purer is the sample before hydrolysis.

3.3. Polymerization degree

It is well known PD of cellulose decreases rapidly when acid hydrolysis takes place, until the so-called level-off PD (LOPD) is reached, which depends on the cellulose origin. A higher LOPD con-

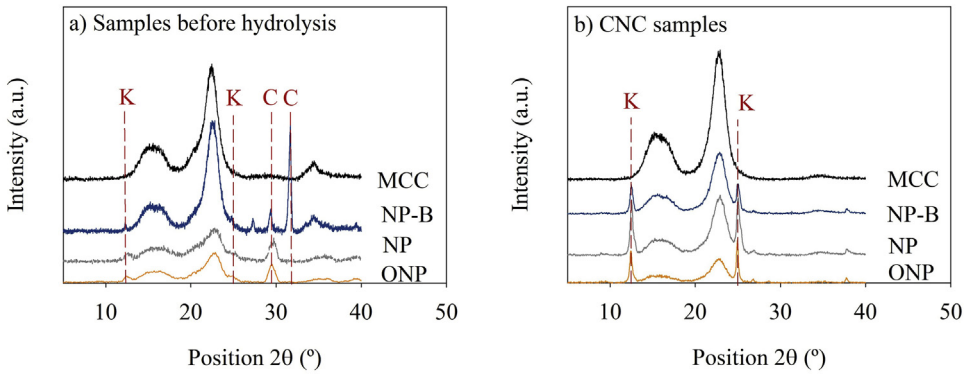

Fig. 3. XRD patterns of a) MCC, NP-B, NP and ONP and b) CNC-MCC, CNC-NP-B, CNC-NP and CNC-ONP. *K is representing kaolinite and C means $CaCO_3$.

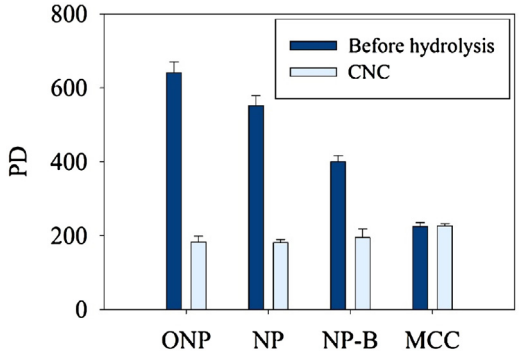

Fig. 4. PD of samples before hydrolysis and obtained CNC.

fers better strength properties when CNC are applied to different matrixes (Habibi et al., 2010).

ONP and NP had different PD, being 640 and 550, respectively (Fig. 4). The reason could be related with the number of recycling cycles and ageing as explained by Čabalová, Kač&k, Geffertand, and Kač&ková (2011). Including a pretreatment, polymer length and therefore PD is reduced from 551 to 400 (Fig. 4), mainly caused by the action of chemicals. However, CNC obtained from ONP, NP and NP-B present similar PD: 182, 181 and 194, respectively. The main reason for this behavior can be that LOPD might have been reached. On the other side, when MCC is used to prepare CNC, PD is not affected (225), thus acid hydrolysis only triggered a reduction in diameter, not in length.

These results are in accordance with Hamad and Hu (2010), who got a PD value of 100 for CNC produced from a commercial softwood kraft pulp, and with Zhang, Lu, Chenand, & Lv (2012) who obtained 174 from bamboo fibers.

3.4. Morphology and size distribution

CNC obtained from ONP present a high degree of aggregation as it is shown in Fig. 5. Presence of inks or lignin can be cause this behavior, being difficult to distinguish in AFM images if a single or CNC aggregates are observed. However, CNC obtained from NP and NP-B show better dispersion and thinner appearance due to removal of some impurities. On the contrary, due to the high purity of CNC-MCC, they also tend to aggregate, but in this case, hydrogen bonding seems to be the cause, what makes CNC size very difficult to determine.

As being composed of lower amount of lignin, production of CNC from NP-B is more effective than ONP and NP, thus more surface area in the CNC was obtained. In terms of size, CNC-ONP have 2.94 ± 0.99 nm wide and 371.18 ± 74.15 nm long (Aspect ratio (L/D) between 50 and 200), while CNC-NP are found to be 3.26 ± 2.90 nm wide and 218.22 ± 48.64 nm long (L/D ratio between 50 and 90). As it is deduced from a representative image of CNC-ONP (Fig. 5a), it is difficult to give a correct length due to the high agglomeration. CNC-NP-B dimensions were 4.40 ± 3.91 nm wide and 356.27 ± 137.28 nm long (L/D ratio between 50 and 120). The reason why length of CNC-NP-B is much higher than that of CNC-NP could be the aggregation between CNC individuals. These values are similar to those reported for CNC isolated from NP by Mohamed et al. (2015), where they had 5.78 ± 2.14 nm wide and 121.42 ± 32.51 nm long (aspect ratio of 5–40), and from ONP by Danial et al. (2015), who reached an average value of ~4 nm wide and ~170 nm long (average aspect ratio of 42). A higher aspect ratio is achieved in all CNC produced in this study compared to those in the literature. When these CNC are applied to reinforce different matrixes, a higher aspect ratio can suppose a higher increment in strength.

3.5. Thermogravimetric analysis

TG/DTG studies were carried out to compare thermal stability of the different samples. Samples before hydrolysis present an endothermic peak at around 350 °C where most of sample is loss (Fig. 6a and c). However, acid hydrolysis triggers a separation of this sample decomposition in two steps: the first at 200 °C and the second at 370 °C (Fig. 6b and d). After this temperature, a lower but continuous mass loss occurred in TG curves of CNC, remaining a significant residue still after 1000 °C.

The initial weight loss between 100 and 130 °C of all samples was assigned to evaporation of residual water and volatile matter in samples (Sheltami et al., 2012). Peak at around 750 °C of ONP and NP DTG curves (Fig. 6c) was identified as $CaCO_3$ (Sanders & Gallagher, 2002), confirming that it is only present in raw materials but not in CNC.

Lignin has shown to be difficult to decompose in nitrogen atmosphere. However, in air atmosphere it usually decompose between 430 and 540 °C (Canetti, Bertini, De Chirico, & Audisio, 2006). Therefore, when lignin is removed through pretreatments, maximum decomposition peak moved to lower temperatures, from 352 °C for ONP and NP to 316 °C for NP-B (Fig. 6c).

All CNC samples started an earlier degradation than raw materials mainly caused by deposition of sulfate groups during H_2SO_4 hydrolysis, thus triggering a dehydration reaction (Wang, Ding, & Cheng, 2007). However, despite ONP and NP TGs are quite similar, their behavior after acid hydrolysis is different. While first DTG peak of ONP is about 220 °C at a decomposition rate of around −12%/min, that of NP is almost 30 °C lower (around 190 °C) and mass loss rate is around third (−4%/min). Since the main difference between these two raw materials is ink content, it has been assumed that this impurity has caused this behavior. Typical used inks in newsprint industries are based on mineral oils (Biedermann & Grob, 2010), which can react with sulfuric acid changing the decomposition profile.

When lignin and hemicelluloses are removed from NP and CNC are produced, first maximum degradation temperature (T_{max1}) increases from 190 to 209 °C (due to hemicelluloses removal) and second peak temperature (T_{max2}) decreases almost 60 °C (from 367 to 307 °C) because of lignin removal. The results obtained for CNC-NP-B are in accordance with Mohamed et al. (2015), obtaining almost the same TG/DTG curves.

Residues at 600 °C were analyzed to compare with existing literature. These residues were different in ONP (30.0%) compared to NP (26.0%), because of their different inherent composition. As during two-step pretreatment hemicellulose and lignin are removed, but ash content is very similar, residue at 600 °C of NP-B increases up to 32.1%. It has been demonstrated that sulfate groups introduced at the surface of CNC act as flame retardant as well as reduce thermal stability (Roman & Winter, 2004). For that reason, residue at 600 °C increases after acid hydrolysis treatment. This value for CNC-NP-B is exactly the same as that obtained by Mohamed et al. (2015) (31.3%), who used a similar procedure and the same raw material (NP). It is quite similar to that of CNC-MCC (31.3 and 29.5%, respectively), what indicates their similar composition, only differing in ash content: 5.7% compared to 0.1%, respectively.

3.6. Yields

Since ONP and NP composition is similar, hydrolysis yields resulted in close values, 60.8 and 58.4%, respectively (Fig. 7a). However, with the inclusion of the two-step pretreatment, this yield increased up to 64.3%. The main reason is the removal of impurities during pretreatment, favoring the access of acid to cellulose. In addition, as MCC is purely a crystalline cellulose material, hydrolysis yield is considerably higher (75%). In comparison with

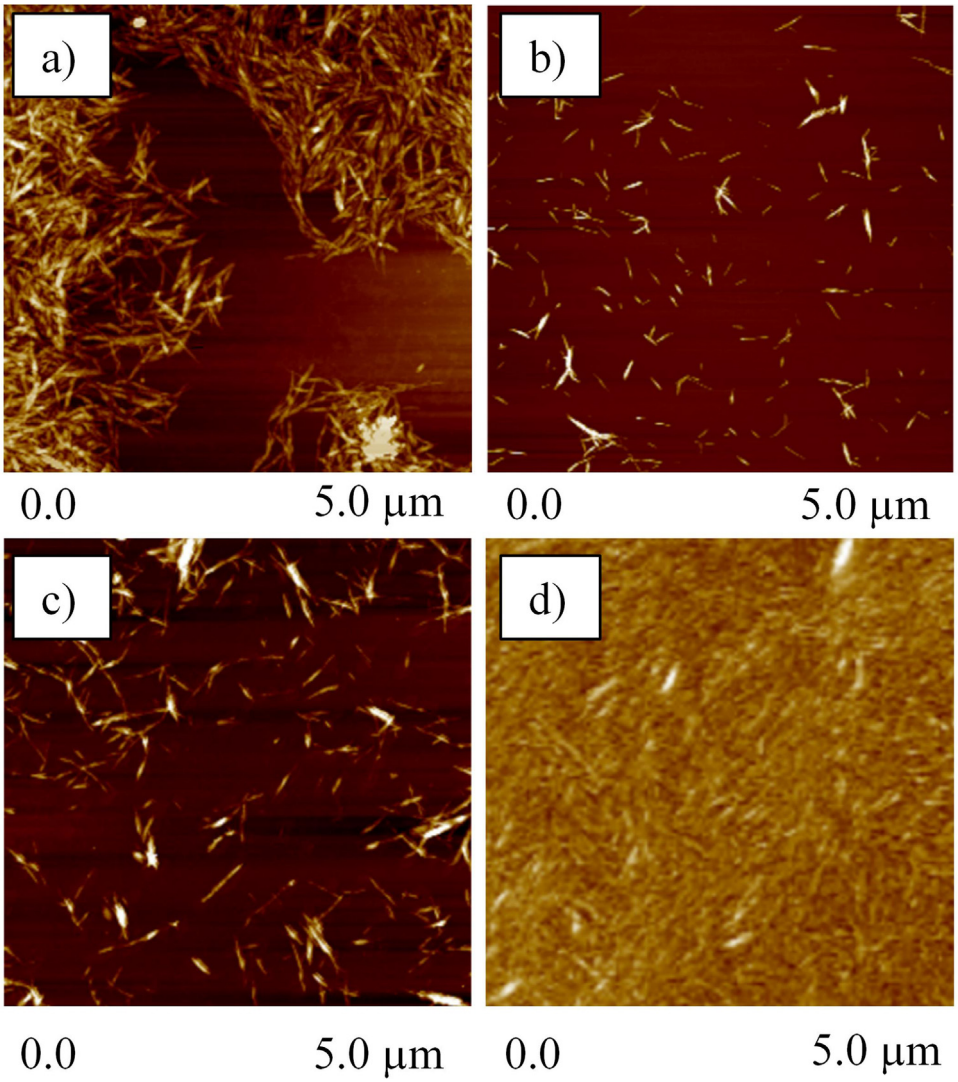

Fig. 5. AFM images of a) CNC-ONP, b) CNC-NP, c) CNC-NP-B and d) CNC-MCC.

bibliographic values, hydrolysis yield of 60.8% for CNC-NP is slightly higher than that obtained by Mohamed et al. (2015) (54.6%), who obtained CNC from NP. In addition, it has been demonstrated that lower quality materials can be used to prepare CNC with a hydrolysis yield comparable to that obtained by Wang et al. (2012), who used a bleached Kraft eucalyptus pulp and obtained a value of 58.7%.

As it has been observed in other CNC properties, slight differences have been found between ONP and NP process yields, varying between 58.4 and 60.8%, respectively (Fig. 7b). Nevertheless, a better quality raw material (MCC) improved the process yield from 60.8 to 75%. The main reason is the cellulose purity of different raw materials, so that when it is pure (MCC), process yield is considered the theoretical maximum according to Chen et al. (2015), who ensure that it is possible to reach a process yield of more than 70% from a bleached eucalyptus pulp. In CNC-NP-B, process yield decreased to 34.6% due to removal not only of impurities, but also the loss of cellulose and other compounds during pretreatments. Nevertheless, this yield is almost double to that obtained by Danial et al. (2015), who use ONP as raw material to produce CNC of similar quality to CNC-NP-B and obtained a process yield of ca. 19%. Mohamed et al. (2015) used NP, but pretreatment losses were not considered in the process yield (they only calculated hydrolysis yield), thus no comparisons can be done.

DAC values are higher when quality of raw material is lower, thus meaning that more amorphous cellulose is present in its structure. As shown in Fig. 7b, 26.8% of NP was amorphous cellulose, being almost the same amount to that of ONP (26.7%) but more than twice as MCC (11.7%). Pretreatment losses value includes removed lignin, hemicellulose, some mineral fillers and cellulose loss during two-step pretreatment. Mohamed et al. (2015) reduced hemicellulose content from 15.33% to 0.28% and lignin amount from 29.46 to 0.89% by using a similar pretreatment. The sum of these two percentages is 44.79%, which makes the 46.2% obtained in the present study, a reasonable percentage for pretreatment losses of NP-B.

3.7. Comparison of results

CNC produced directly from ONP and NP present similar properties (Table 1). The main differences are based on the presence of inks in ONP, which entails a residuary black color in CNC-ONP.

However, there is an increment in CNC quality when the two-step pretreatment is included in the process. Briefly, CNC-NP-B present higher purity (93.3% compared to 77.8%), Cr.I (94.8% compared to 93.4%), PD (194 and 181), aspect ratio (50–120 compared to 50–90, respectively) and hydrolysis yield (64.3 compared to 60.8%) than CNC-NP.

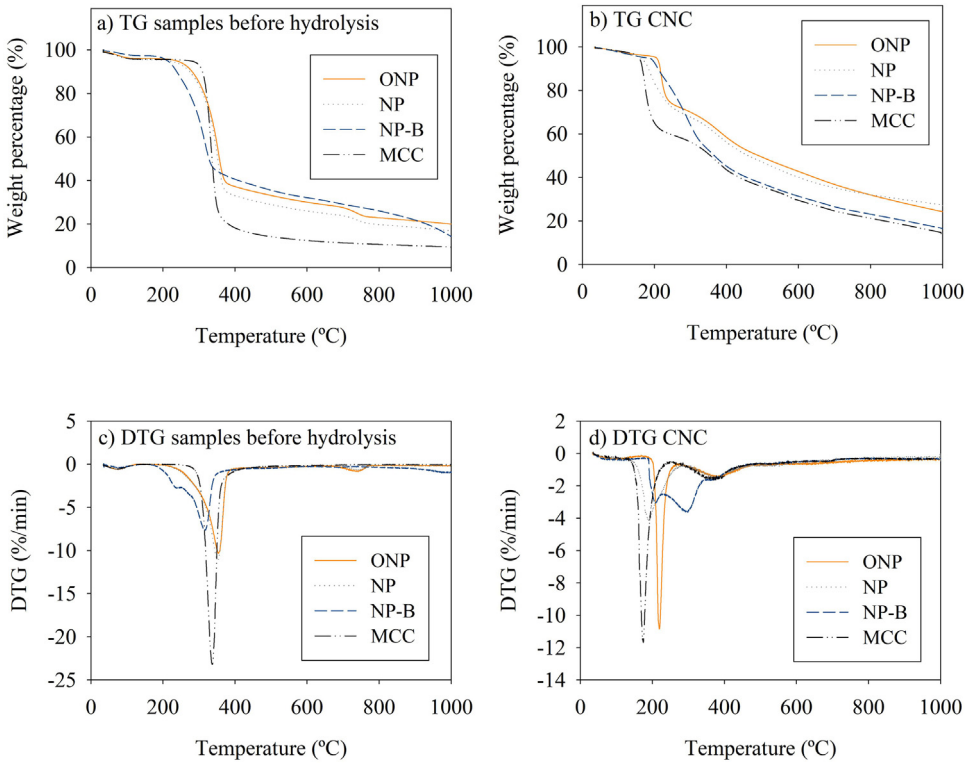

Fig. 6. TG curves of a) samples before hydrolysis and b) produced CNC and DTG curves of c) samples before hydrolysis and d) CNC.

Table 1
Comparison of CNC properties produced from ONP, NP, NP-B and MCC.

	CNC-ONP	CNC-NP	CNC-NP-B	CNC-MCC
CNC purity (%)	76.0	77.8	93.3	99.9
Ash 525 °C (%)	11.5	11.9	5.7	0.1
Lignin (%)	12.5	10.2	0.9	0.0
Color	Black	Brown	Beige	White
Cr.I (%)	92.6	93.4	94.8	95.5
ACD (nm)	32.5	41.2	45	54.9
PD	182	181	194	226
Aspect ratio	50-200	50-90	50-120	2-70*
Hydrolysis yield (%)	58.4	60.8	64.3	75.0
Process yield (%)	58.4	60.8	34.6	75

* Bibliographic data (Elazzouzi-Hafraoui et al., 2007).

Although CNC-ONP have lower quality than the other CNCs of this study due to the higher levels of inks and lignin, their production cost is much lower and the process yield higher than other approaches to produce CNCs. First, the raw material is cheaper (around 100 €/ton) and the cost of chemicals for alkaline and bleaching treatments are saved. Furthermore, as the removal of impurities is not carried out before hydrolysis, process yield is also higher. This is a very interesting approach to obtain "low-cost" CNCs which can be used in certain applications where the quality requirements are not so high, i.e. for paper and board production.

CNC-NP are produced from a better quality raw material, with no inks and a lower content on lignin, but its cost is also higher (around 500 €/ton). However, as direct production of CNC was used, costs related to pretreatments are still saved while higher process yields are obtained compared to other approaches followed in literature. Then, quality of CNC-NP is improved compared to CNC-ONP.

Finally, in the case of CNC-NP-B, cost increases not only by the use of NP but also due to the high chemical and energy consume during pretreatments. In addition, there is a significantly lower process yield compared to the other two previous approaches (35% vs. around 60%) due to the extensive removal of impurities before acid hydrolysis. The quality of CNC-NP-B is of course greater, however, the associated costs for its production are much higher than any of the other two direct approaches for obtaining CNC. Furthermore, it is questionable the sustainability of these production processes in which pretreatment losses are so high. It is probably a better option to use high quality raw materials such as virgin fibers to avoid all these losses and use recycled fibers in other less demanding uses such as newsprint production in which the yields are significantly higher.

4. Conclusions

To the best knowledge of the authors, CNC have been only produced with a previous isolation of cellulose particles. This purification treatments suppose an increment in costs due to chemical and energy consumption and the low process yield because of the high pretreatment losses. However, this study proves the viability of a direct production of CNC from recycled papers.

CNC produced from ONP and NP present similar properties. However, the cost of ONP is around five times lower than that of NP. Therefore, in applications where presence of inks is not a problem, i.e. for example high-strength papers, CNC produced from ONP would be an interesting option to improve their properties at low cost.

On the other side, CNC-NP-B present a higher purity and quality compared to CNC-ONP and CNC-NP. Despite the increment in costs because of the lower process yield, CNC-NP-B is still a more economic option than CNC-MCC, where the cost of raw material is strongly higher. In addition, their properties are quite similar, opening their range of applications.

Therefore, each produced CNC can be applied in different applications, depending on quality requirements. When high quality CNC are needed, CNC-NP-B will be the best candidate. However, applications where presence of impurities is not an inconvenience, like packaging paper and cardboard or fibercement, CNC-ONP and

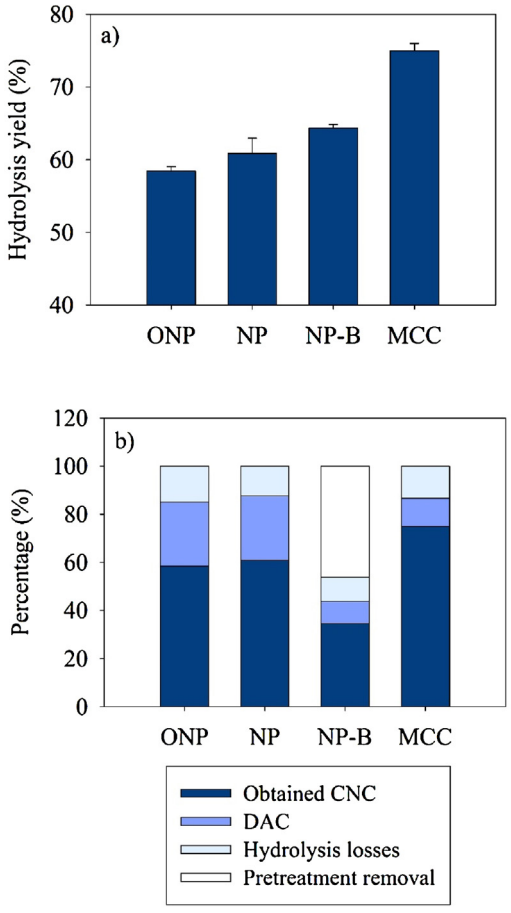

Fig. 7. a) Hydrolysis yield and b) Process yield, DAC, hydrolysis losses and pretreatment removal percentages referred to initial dry mass of papers of all obtained CNC.

CNC-NP can be used due to their lower cost, thus promoting an extended use of CNC and avoiding a large volume of ONP being used in less sustainable applications.

Acknowledgements

This study has been supported by the project "NANOSOLPAPEL-REC" (Ref. CTQ2013-48090-C2-1-R) and the grant of C. Campano (BES-2014-068177), from the Spanish Ministry of Economy and Competitiveness. Authors also wish to acknowledge Francisco Caballero and Cristina Villagrasa for their collaboration in the experimental work.

References

Biedermann, M., & Grob, K. (2010). Is recycled newspaper suitable for food contact materials? Technical grade mineral oils from printing inks. *European Food Research and Technology*, *230*(5), 785–796.

Čabalová, I., Kačík, F., Geffert, A., & Kačíková, D. (2011). The effects of paper recycling and its environmental impact. *Environmental Management in Practice*, 329–350.

Campano, C., Balea, A., Blanco, A., & Negro, C. (2016). Enhancement of the fermentation process and properties of bacterial cellulose: A review. *Cellulose*, *23*(1), 57–91.

Canetti, M., Bertini, F., De Chirico, A., & Audisio, G. (2006). Thermal degradation behaviour of isotactic polypropylene blended with lignin. *Polymer Degradation and Stability*, *91*(3), 494–498.

Chen, L. H., Wang, Q. Q., Hirth, K., Baez, C., Agarwal, U. P., & Zhu, J. Y. (2015). Tailoring the yield and characteristics of wood cellulose nanocrystals (CNC) using concentrated acid hydrolysis. *Cellulose*, *22*(3), 1753–1762.

Csiszar, E., Kalic, P., Kobol, A., & Ferreira, E. D. (2016). The effect of low frequency ultrasound on the production and properties of nanocrystalline cellulose suspensions and films. *Ultrasonics Sonochemistry*, *31*, 473–480.

Danial, W. H., Majid, Z. A., Muhid, M. N. M., Triwahyono, S., Bakar, M. B., & Ramli, Z. (2015). The reuse of wastepaper for the extraction of cellulose nanocrystals. *Carbohydrate Polymers*, *118*, 165–169.

Delgado-Aguilar, M., Tarres, Q., Pelach, M. A., Mutje, P., & Fullana-i-Palmer, P. (2015). Are cellulose nanofibers a solution for a more circular economy of paper products? *Environmental Science & Technology*, *49*(20), 12206–12213.

Donnet, J.-B. (1993). *Carbon black: Science and technology*. CRC Press.

Du, H. S., Liu, C., Mu, X. D., Gong, W. B., Lv, D., Hong, Y. M., et al. (2016). Preparation and characterization of thermally stable cellulose nanocrystals via a sustainable approach of FeCl3-catalyzed formic acid hydrolysis. *Cellulose*, *23*(4), 2389–2407.

Dufresne, A. (2012). *Nanocellulose: From nature to high performance tailored materials*. Walter de Gruyter.

Elazzouzi-Hafraoui, S., Nishiyama, Y., Putaux, J.-L., Heux, L., Dubreuil, F., & Rochas, C. (2007). The shape and size distribution of crystalline nanoparticles prepared by acid hydrolysis of native cellulose. *Biomacromolecules*, *9*(1), 57–65.

French, A. D., & Cintron, M. S. (2013). Cellulose polymorphy, crystallite size, and the Segal Crystallinity Index. *Cellulose*, *20*(1), 583–588.

Habibi, Y., Lucia, L. A., & Rojas, O. J. (2010). Cellulose nanocrystals: Chemistry, self-assembly, and applications. *Chemical Reviews*, *110*(6), 3479–3500.

Habibi, Y. (2014). Key advances in the chemical modification of nanocelluloses. *Chemical Society Reviews*, *43*(5), 1519–1542.

Hamad, W. Y., & Hu, T. Q. (2010). Structure-process-yield interrelations in nanocrystalline cellulose extraction. *Canadian Journal of Chemical Engineering*, *88*(3), 392–402.

Henriksson, M., Berglund, L. A., Isaksson, P., Lindstrom, T., & Nishino, T. (2008). Cellulose nanopaper structures of high toughness. *Biomacromolecules*, *9*(6), 1579–1585.

Hu, Y., Tang, L., Lu, Q., Wang, S., Chen, X., & Huang, B. (2014). Preparation of cellulose nanocrystals and carboxylated cellulose nanocrystals from borer powder of bamboo. *Cellulose*, *21*(3), 1611–1618.

Lourenco, A. F., Gamelas, J. A. F., & Ferreira, P. J. (2014). Increase of the filler content in papermaking by using a silica-coated PCC filler. *Nordic Pulp & Paper Research Journal*, *29*(2), 240–245.

Lu, P., & Hsieh, Y.-L. (2012). Preparation and characterization of cellulose nanocrystals from rice straw. *Carbohydrate Polymers*, *87*(1), 564–573.

Martínez-Sanz, M., Vicente, A., Gontard, N., Lopez-Rubio, A., & Lagaron, J. (2015). On the extraction of cellulose nanowhiskers from food by-products and their comparative reinforcing effect on a polyhydroxybutyrate-co-valerate polymer. *Cellulose*, *22*(1), 535–551.

Mohamed, M. A., Salleh, W. N. W., Jaafar, J., Asri, S., & Ismail, A. F. (2015). Physicochemical properties of green nanocrystalline cellulose isolated from recycled newspaper. *Rsc Advances*, *5*(38), 29842–29849.

Peresin, M. S., Habibi, Y., Zoppe, J. O., Pawlak, J. J., & Rojas, O. J. (2010). Nanofiber composites of polyvinyl alcohol and cellulose nanocrystals: Manufacture and characterization. *Biomacromolecules*, *11*(3), 674–681.

Ranby, B. G. (1951). Cellulose and muscle—The colloidal properties of cellulose micelles. *Discussions of the Faraday Society*, *11*, 158.

Roman, M., & Winter, W. T. (2004). Effect of sulfate groups from sulfuric acid hydrolysis on the thermal degradation behavior of bacterial cellulose. *Biomacromolecules*, *5*(5), 1671–1677.

Sanders, J. P., & Gallagher, P. K. (2002). Kinetic analyses using simultaneous TG/DSC measurements: Part I: Decomposition of calcium carbonate in argon. *Thermochimica Acta*, *388*(1–2), 115–128.

Segal, L., Creely, J. J., Martin, A. E., & Conrad, C. M. (1959). An empirical method for estimating the degree of crystallinity of native cellulose using the X-ray diffractometer. *Textile Research Journal*, *29*(10), 786–794.

Sheltami, R. M., Abdullah, I., Ahmad, I., Dufresne, A., & Kargarzadeh, H. (2012). Extraction of cellulose nanocrystals from mengkuang leaves (Pandanus tectorius). *Carbohydrate Polymers*, *88*(2), 772–779.

Sun, Y., & Cheng, J. (2002). Hydrolysis of lignocellulosic materials for ethanol production: A review. *Bioresource Technology*, *83*(1), 1–11.

Tasman, J. E., & Berzins, V. (1957). The permanganate consumption of pulp materials. *Tappi*, *40*(9), 691–704.

Wang, N., Ding, E., & Cheng, R. (2007). Thermal degradation behaviors of spherical cellulose nanocrystals with sulfate groups. *Polymer*, *48*(12), 3486–3493.

Wang, Q. Q., Zhu, J. Y., Reiner, R. S., Verrill, S. P., Baxa, U., & McNeil, S. E. (2012). Approaching zero cellulose loss in cellulose nanocrystal (CNC) production: Recovery and characterization of cellulosic solid residues (CSR) and CNC. *Cellulose*, *19*(6), 2033–2047.

Xu, Q. H., Gao, Y., Qin, M. H., Wu, K. L., Fu, Y. J., & Zhao, J. (2013). Nanocrystalline cellulose from aspen kraft pulp and its application in deinked pulp. *International Journal of Biological Macromolecules*, *60*, 241–247.

Zhang, Y., Lu, X. B., Chen, W., & Lv, W. J. (2012). *Preparation and characterization of nanocrystalline cellulose from bamboo fibers by controlled cellulase hydrolysis*. Nanjing: Nanjing Forestry Univ.

PUBLICATION V

Mechanical and chemical dispersion of nanocelluloses to improve their reinforcing effect on recycled paper

Cristina Campano, Noemi Merayo, Ana Balea, Quim Tarrés, Marc Delgado-Aguilar, Pere Mutjé, Carlos Negro, Angeles Blanco

Cellulose (2018) 25: 269–280

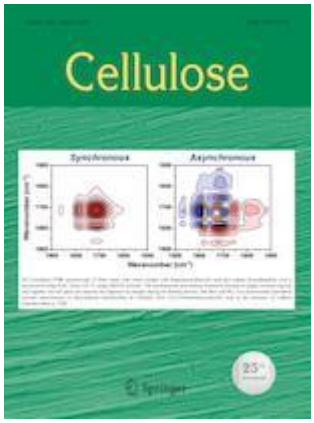

Impact factor 2017: ***3.809***

JCR, Materials Science, paper & wood, 1 out of 21, ***Q1***

Cellulose (2018) 25:269–280
https://doi.org/10.1007/s10570-017-1552-y

ORIGINAL PAPER

Mechanical and chemical dispersion of nanocelluloses to improve their reinforcing effect on recycled paper

Cristina Campano · Noemí Merayo · Ana Balea · Quim Tarrés · Marc Delgado-Aguilar · Pere Mutjé · Carlos Negro · Ángeles Blanco

Received: 19 September 2017 / Accepted: 30 October 2017 / Published online: 2 November 2017

Abstract The use of nanocelluloses as strength-enhancing additives in papermaking is widely known since both cellulose nanofibers (CNF) and nanocrystals (CNC) present similar composition than paper but their exceptional properties in the nanometer scale confers a paper quality enhancement. However, some agglomeration problems in CNF and CNC through hydrogen bonding cause a lower improvement of mechanical properties of paper. Therefore, a better dispersion of both nanocelluloses can maximize their effect on paper properties, thus reducing the needed dose to get the same increment in tensile strength and then reducing material costs. To ease the implementation of these nanocelluloses in the production process of recycled paper, typically used operations of these industries have been used. Among them, those devoted to improve the homogeneous mixture of nanocellulose in the pulp suspension have been assessed. Firstly, pulping conditions were studied, including pulping time, temperature and need for soaking as variables. Secondly, some dispersing agents used in papermaking were considered, studying the effect of different types and doses. The highest tensile strength of paper was achieved by applying long pulping times (60 min), getting increments up to 30% with the use of soaking and polyacrylamide as retention system. However, with the use of a low dose of a dispersing agent (0.003%), tensile index can be still increased up to 20.6% avoiding these long times. This study can be of great interest of those researchers trying to implement the use of nanocelluloses as strength additive in papermaking.

C. Campano · N. Merayo (✉) · A. Balea · C. Negro · Á. Blanco
Department of Chemical Engineering, Complutense University of Madrid, Avda Complutense s/n, 28040 Madrid, Spain
e-mail: nmerayoc@ucm.es

C. Campano
e-mail: ccampano@ucm.es

A. Balea
e-mail: anabalea@ucm.es

C. Negro
e-mail: cnegro@ucm.es

Á. Blanco
e-mail: ablanco@ucm.es

Q. Tarrés · M. Delgado-Aguilar · P. Mutjé
Group LEPAMAP, Department of Chemical Engineering, University of Girona, c/M. Aurèlia Campmany 61, 17071 Girona, Spain
e-mail: joaquimagusti.tarres@udg.edu

M. Delgado-Aguilar
e-mail: m.delgado@udg.edu

P. Mutjé
e-mail: pere.mutje@udg.edu

Keywords Reinforcement · Cellulose nanofibers · Cellulose nanocrystals · Dispersion · Strength · Recycled paper

Introduction

In 2015, the recycling rate in Europe reached the value of 71.5% with a total utilization of paper for recycling of 47.7 million tons (CEPI 2015). However, the increasing number of recycling cycles triggers different consequences: (1) the reduction in the inter-fiber bonding and filler retention capacity; (2) the reduction in the ability of the fibers to swell; and 3) the detriment of the mechanical properties (Delgado-Aguilar et al. 2015; Hubbe 2013). Since major constituents of nanocellulose are almost the same as those of pulps used in papermaking industries, their compatibility, as well as their characteristics, will increase the number of hydrogen bonds in the fiber network and, therefore, the strength of paper (Balea et al. 2016a).

The term "nanocellulose" includes different types of cellulose nanomaterials: cellulose nanocrystals (CNC), cellulose nanofibers (CNF) and bacterial cellulose. On the one side, when acid hydrolysis is applied to cellulose, amorphous regions are dissolved, remaining the crystalline domains of nano-size or CNC (Habibi et al. 2010). Some of the advantages of CNC, compared to cellulose fibers, are the self-assembly, the very high strength due to their high crystallinity, the high functionalization for their inherently high surface area, the unique optical properties and lightweight (Habibi 2014). Therefore, CNC have been used to reinforce pulp suspensions (Coccia et al. 2014; Salam et al. 2013; Sun et al. 2015). When sulfuric acid is used to hydrolyze the cellulose, sulfate groups remain at the CNC surface, improving their stability in water suspensions (Roman and Winter 2004). However, stability commonly declines over time, forming aggregates that sediment and are difficult to re-disperse. Consequently, not only is the effect of CNC on paper strength influenced by the cellulose source and the production process of CNC, but also by the effective mixture of CNC within the fiber suspension. This effect has not been studied yet.

On the other side, through a mechanical defibrillation, it is possible to reduce the diameter of cellulose, keeping long the nanofiber length. When this treatment is applied, CNF are obtained. CNF are distinguished from CNC by having higher aspect ratio (> 200 in CNF compared to 2–170 in CNC), lower crystallinity index (40–78% compared to 85–100%), higher water absorption capacity and lower light transmittance (Campano et al. 2016). To reach a high defibrillation yield, pulp has to be homogenized at consistencies between 1 and 3 wt%. This confers a stable gel structure, which is more difficult to mix homogeneously with the pulp suspension than in the case of having individual nanofibers (Osong et al. 2016). Although there are several studies supporting the ability of CNF to reinforce both virgin (Gonzalez et al. 2012; Petroudy et al. 2014; Taipale et al. 2010) and recycled pulps (Balea et al. 2016a, b; Delgado-Aguilar et al. 2015), no studies have been published on the effect of the mixture CNF-pulp suspension on the paper properties.

Therefore, the mixture of CNC or CNF with the pulp suspension during papermaking continues being a challenge. In this work, both mechanical and chemical methods have been applied in order to improve dispersion of CNC and CNF in a matrix of recycled paper. Then, pulping conditions and the addition of dispersing agents have been assessed, and mechanical, physical and morphology of handsheets have been measured.

Experimental

Production and characterization of CNC

CNC were produced from non-printed newsprint (NPN) made of 100% recycled paper with an ISO brightness of 56% and 14.0 wt% ash content. NPN was chosen as raw material for CNC production to ease the implementation of this process on-site the newsprint paper mill (Campano et al. 2017). NPN was milled with an IKA analysis grinder A10 (IKA-Werke Gmbh, Staufen, Germany), and passed through a 20-mesh sieve. Then, dry milled NPN was acid hydrolyzed following typical hydrolysis conditions (Chen et al. 2015). Briefly, 13.5 mL of 60 wt% H_2SO_4 were added per gram of dry milled NPN and the hydrolysis was carried out with mechanical stirring at 500 rpm, at 45 °C during 90 min. After that, the mixture was diluted 10 times and left to settle overnight. Then, supernatant was discarded and

sediment was washed using several centrifugation cycles at 4500×g for 10 min (JP Selecta S.A, Barcelona, Spain) until turbid supernatant was observed. Finally, the sample was dialyzed using membranes of regenerated cellulose with a molecular weight cut-off of 12,000–14,000 Da (Medicell International Ltd, London, UK) until neutral pH was achieved. A final CNC suspension of a concentration of around 1% was obtained.

Hydrolysis yield was determined as the proportion of produced dry CNC versus initial dry matter. CNC purity was considered as the 100% of sample minus ash and lignin percentages, being the main impurities of the CNC sample. Ash percentage was determined by subjecting the sample at 525 °C, according to ISO 1762 (2015). Lignin was measured through Kappa number according to Tappi 236 om-99. The relation between lignin and kappa number was described by Tasman and Berzins (1957) with Eq. (1).

$$Lignin\,(\%) = 0.13 \cdot Kappa\,number \quad (1)$$

Crystallinity index (Cr.I) was determined through X-ray diffraction (XRD) with a Philips X'Pert MPD X-ray diffractometer with an autodivergent slit fitted with a graphite monocromator using Cu-Kα radiation operated at 45 kV and 40 mA. XRD pattern was recorded from 4° to 40° at a scanning speed of 1.5° min^{-1}. Segal's method was used to determine Cr.I (Segal et al. 1959) (Eq. 2):

$$Cr.I\,(\%) = \frac{I_{200} - I_{am}}{I_{200}} \cdot 100 \quad (2)$$

where I_{002} is the intensity of the 200 plane at $2\theta = 22.5°$ and I_{am} is the intensity of the amorphous scatter at $2\theta = 18°$ (French 2014). Resulting XRD pattern has been previously published and discussed (Campano et al. 2017).

Degree of polymerization (DP) was calculated from the intrinsic viscosity (η) of the CNC suspensions, determined according to ISO 5351 standard (2010). η was obtained by measuring the elution time of the cellulose–copper ethylenediamine complex through a capillary viscometer, adapted according to Henriksson et al. (2008) and Marx-Figini (1978). The relation between η and DP can be described by one of the two distinct Mark–Houwink–Sakurada (MHS) equations (Eqs. 3, 4), depending on the magnitude of the DP value:

$$\eta = 0.42 \cdot DP\ (\text{when } DP < 950) \quad (3)$$

$$\eta = 2.28 \cdot DP^{0.76}\ (\text{when } DP > 950) \quad (4)$$

Morphology was observed through Atomic Force Microscopy (AFM) using an AFM multimode Nanoscope III A (Bruker) in tapping mode with a FESP probe oscillating at 86.5 kHz. A drop of never-dried CNC with a consistency of 0.05% was deposited on mica surface and left to dry before analysis. Microscopic analyses were carried out at the National Centre of Electronic Microscopy at the Complutense University of Madrid. Table 1 lists the properties of CNC produced in this study.

Cationic demand (CD) was measured through colloidal titration of the CNC suspension (0.05–0.1 wt%) with 0.001 N polyDADMAC on a Mütek PCD04 particle charge detector (BTG Instruments GmbH, Herrsching, Germany).

Production and characterization of CNF

A never-dried, refined *Eucalyptus globulus* ECF bleached kraft pulp, which is a common source used to produce CNF, with a Canadian Standard Freeness of 540.8 mL was used as raw material to produce CNF. This pulp was obtained from Torraspapel S.A. (Zaragoza, Spain). First, pulp was oxidized through TEMPO-mediated oxidation with 5 mmol of NaClO per gram of dry sample following the procedure of Saito et al. (2007). The oxidized pulp was washed with distilled water using dilution-filtration cycles until pH was around 7. After that, pulp consistency was adjusted to 1% and homogenized through six passes at 600 bar, using a PANDA PLUS 2000 laboratory homogenizer manufactured by GEA Niro Soavi

Table 1 Characterization of CNC

	Units	Value
Hydrolysis yield	wt%	60.8
Purity	wt%	77.8
Ash content	wt%	11.9
Lignin content	wt%	10.2
Cr.I	%	93.4
DP	Monomeric units	181
CD	meq g^{-1}	0.026

(Parma, Italy). The degree of oxidation of the pulp was determined by measuring the amount of carboxyl groups by conductimetric titration of pulp after TEMPO-mediated oxidation and cleaning, but before homogenization (Table 2). The amount of carboxyl groups was determined from the curve of conductivity versus amount (mL) of sodium hydroxide added following the method developed by Habibi et al. (2006).

CNF were also characterized by determining the CD, the yield of nanofibrillation, the transmittance and DP (Table 2). Yield of nanofibrillation was determined by centrifugation of a diluted CNF suspension (0.1 wt%) at 4500×*g* for 30 min in order to isolate the nanofibrillated fraction in the supernatant from the non-fibrillated one deposited in the sediment. Optical transmittance of the diluted CNF (0.1 wt%) was measured between 400 and 800 nm with a Cary 50 Conc UV–visible spectrophotometer (Varian Australia PTI LTD, Victoria, Australia). DP and morphology of CNF was determined following the same procedure previously described for CNC ("Production and characterization of CNC" section). In this case, CNF suspension was prepared by further dilution with distilled water (0.01 wt%) to allow measuring individual CNF from the AFM images. Figure 1 shows the AFM images of both CNC and CNF suspensions. AFM image of CNF suspension shows a high degree of fibrillation, showing diameters of a few nanometers with several micrometers of length. Moreover, CNF bundles are also present, forming and entangled network. On the other hand, CNC were cylindrical in shape with 5–10 nm in width and shorter than CNF in length (100–500 nm in length) because acid treatment of the cellulose fibers dissolve the amorphous regions releasing the individual crystallites. Consequently, the aspect ratio of the CNC was lower than CNF.

Table 2 Characterization of CNF

	Units	Value
Carboxyl Groups	mmol g^{-1}	0.59
Yield of nanofibrillation	%	> 95
Transmittance at 800 nm	%	83.5
DP	Monomeric units	440
CD	meq g^{-1}	1.139

Additives

Two commercial dispersing agents were selected in this study: (1) A synergistic mixture of a moisturizing and a detergent surfactant (D1), which is typically used during the alkaline bleaching process to facilitate the uniform impregnation of the fibers with the bleaching agent; and (2) A moisturizing agent (D2), which facilitates the intimate contact between coatings and paper. Both dispersing agents were kindly supplied by NALCO (Naperville, USA). The dose interval for the dispersing additives (0.003–0.1 wt%) was selected based on the supplier recommendation.

Two different retention additives were assessed in this study: (1) A three-component system (CPAM),

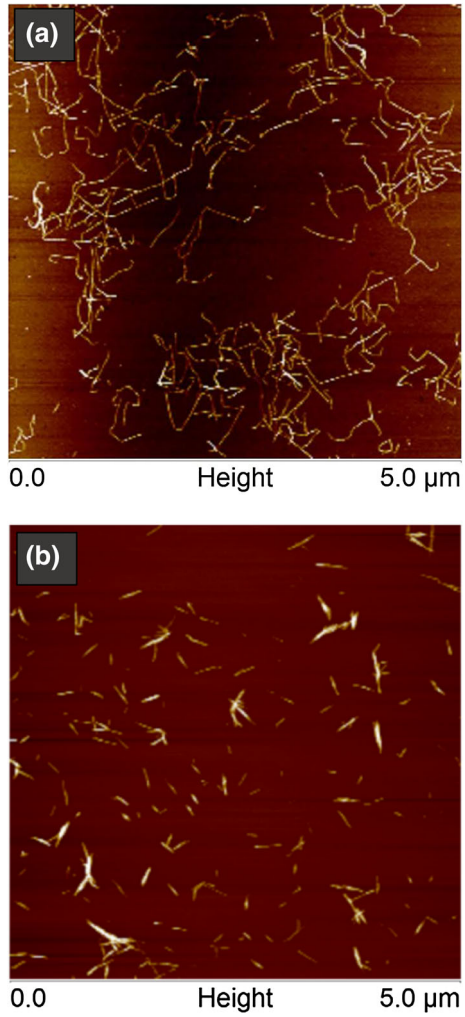

Fig. 1 AFM images of **a** CNF (5 × 5 µm) and **b** CNC (5 × 5 µm)

supplied by BASF (Ludwigshafen, Germany), and composed of a coagulant (a polyamine with cationic charge density of 0.035 meq g^{-1} and high molecular weight), a flocculant (a cationic polyacrylamide with high molecular weight and cationic charge density of 3.66 meq g^{-1}) and hydrated bentonite clay. Coagulant was added after dilution (1:100) of commercial solution. Cationic polyacrylamide and bentonite have concentrations of 3.5 and 34 g L^{-1}, respectively. (2) Chitosan from crab shells (CH) was supplied by Sigma-Aldrich (Steinheim, Germany) with a cationic charge density of 4.79 meq g^{-1} and low molecular weight, was also studied as an alternative biodegradable single retention additive (Fatehi et al. 2010). The chitosan solution was prepared at 1% by dissolving chitosan in a solution of glacial acetic acid in ultrapure water subject to mechanical stirring at 400 rpm for 1 h. The chitosan solution was left to settle for 24 h before use.

Doses of 1.25 mg coagulant g^{-1} of dried pulp, 0.5 mg flocculant g^{-1} of dried pulp, 1.7 mg bentonite g^{-1} of dried pulp and 1 mg CH g^{-1} of dried pulp were used for the laboratory experiments. The doses were selected based on industrial recommendations and previous studies (Merayo et al. 2017b).

Cellulose pulp

Pulp was prepared by disintegration of 20 g of dry 100% recovered paper (RP) with the corresponding amount of CNF or CNC in a total volume of 2 l, with tap water, using a Messmer pulp disintegrator (Mavis Engineering Ltd, London). RP was prepared with a mixture of 60 wt% old newspaper (ONP) and 40 wt% old magazine (OMG), both unprinted and kindly supplied by Holmen Paper Madrid (Madrid, Spain). Based on literature, a dose of 1.5 wt% CNF was selected as the optimum dose to improve the mechanical properties of the recycled paper (Balea et al. 2016b). In case of CNC suspensions, 3 wt% CNC was selected, since previous tests showed similar increments in tensile index (TI) than those using 1.5 wt% CNF. Pulping conditions selected to study the dispersion were varied as shown in Table 3.

When dispersing agents were studied, they were added to the CNC (or CNF) and mixed during 2 min. Then the sample was disintegrated together with the RP at a final consistency of 1% with a Messmer pulp disintegrator (Mavis Engineering Ltd., London, England) for 30,000 revolutions and hot water ($\sim$ 50 °C), based on the ISO 5263-1 standard (2013).

Sheet preparation and characterization

Firstly, either CNC or CNF are stirred with the selected dose of dispersing agents for 5 min at high shearing rate. After that, the prepared suspension is added to the pulp and disintegrated for the specific time of each test. Once the recycled pulp was disintegrated, it was mixed with the corresponding retention additive (CPAM or CH) and handsheets were prepared with a basis weight of 60 g m^{-2} in a normalized Rapid-Köthen sheet former from PTI (Vorchdorf, Austria), following the ISO standard 5269-2 (2004). The pulp was transferred to the stock chamber of the Rapid Köthen sheet former just after the 30 s of mixing with the retention additive. These handsheets were conditioned in a weather chamber at 23 °C and 50% humidity for 24 h before mechanical characterization.

Tear and tensile strengths were measured using an AUTOLINE 300 from Lorentzen and Wettre (Stockholm, Sweden), following the ISO standards 1974 (2012) and 1924-3 (2014), respectively. Tear index and TI were calculated using the average grammage of the handsheets. Optical properties were measured according to the ISO standards 2470-1 (2012) and ISO 11664-4 (2008). Formation was measured with a Beta Formation Tester (BFT) from Ambertec Oy (Espoo, Finland), which provides a standard deviation of the basis weight of the sheet.

Table 3 Pulping conditions used for each test

Sample ID	Overnight soaking	Speed (revolutions)	Pulping time (min)	Water temperature (°C)
A	No	30,000	10	$\sim$ 50
B	No	180,000	60	$\sim$ 50
C	Yes	180,000	60	$\sim$ 20

Results and discussion

Effect of pulping conditions on recycled paper properties adding nanocellulose

Not only did the mixture of nanocelluloses in the pulp affect the paper properties, but also the pulping conditions. Therefore, the reference with no nanocelluloses was needed to evaluate the effect of pulping conditions independently of the nanocelluloses addition. Different methods have been used to form a homogeneous mixture between the nanocelluloses and the original pulp. They vary from short stirring times with diluted CNF suspensions, 0.014–1% CNF (Ahola et al. 2008; Taipale et al. 2010), to long disintegration times, for 180,000 revolutions (Gonzalez et al. 2012). In the case of CNC, less literature is available about their application in paper, only one reference has been found (Sun et al. 2015), where CNC are stirred for 1 min at 800 rpm. The used method for nanocelluloses and pulp conjugation has a big influence on the final properties of paper, so it has to be considered to obtain a good quality paper.

10 min of pulping (30,000 rev) are commonly used at industrial conditions in the paper mill, which implies temperatures around 50 °C. Therefore, these conditions were selected as the basis (A). Since pulping step is unavoidable, taking advantage of it to efficiently conjugate nanocelluloses with the pulp is a promising option. Starting at lab scale, longer pulping times have been assessed, as well as swelling of fibers overnight before pulping.

Differences between paper properties prepared with the addition of CPAM or CH are related to the different flocculation mechanism of these additives. Whereas CPAM works through a bridging mechanism (Merayo et al. 2017a), in which flocs have an extended conformation, CH seems to form more compact flocs. Thus, CPAM is very effective to improve drainage process, but affects negatively TI regardless the pulping conditions. On the other hand, CH resulted in handsheets with higher TI, lower porosity and better formation. However, both of them were characterized by their cationic nature, facilitating the retention of fibers, fines and fillers, as well as anionic nanocelluloses. The presence of carboxyl groups in the CNF prepared by TEMPO-oxidation increased the anionicity of the CNF, measured as CD (Table 2), which is clearer if it is compared to CD of CNC (Table 1). Therefore, the presence of carboxyl groups in the CNF will facilitate the retention of CNF in the paper.

In the case of using CPAM, no differences were found in TI between the three methods when no nanocelluloses are used (Fig. 2a). Nevertheless, when CH is used as additive, the increase in the pulping time (B and C) favored the disintegration of the pulp increasing TI (Fig. 2b). Regarding porosity, it underwent a high decrease when pulping time was increased from 10 to 60 min, no matter which retention additive was used (Fig. 3). That is due to the reduction in the size of the fibers, probably increasing the amount of fines in the pulp suspension, which collaborate to form more compact handsheets. Consequently, beta formation results of handsheets prepared with CPAM (Fig. 4a) shows a better homogeneity, agreeing with

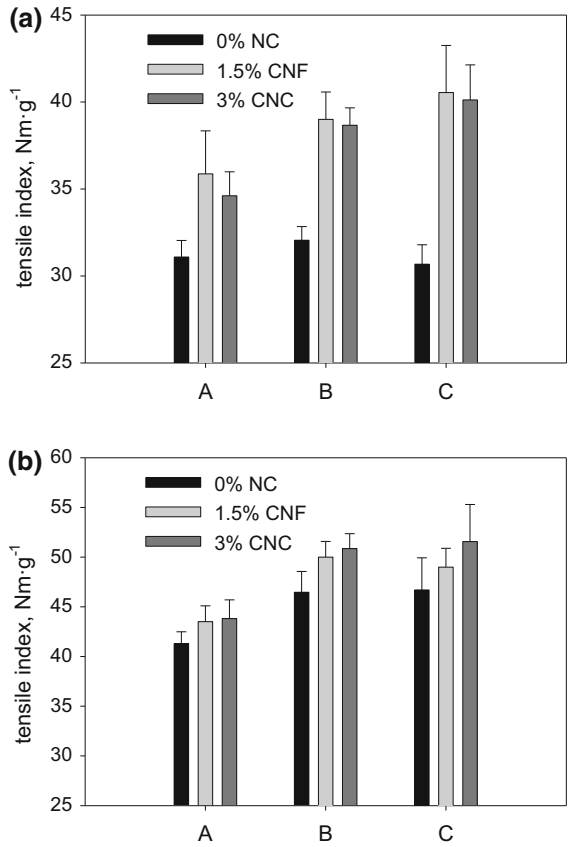

Fig. 2 Effect of different pulping conditions on tensile index (TI) of the handsheets with 1.5 wt% CNF or 3 wt% CNC, when **a** three-component retention system and **b** chitosan were added to the recycled pulp. (*A*) Not soaking, time = 10 min, T = 50 °C; (*B*): not soaking, time = 60 min, T = 50 °C; (*C*) soaking, time = 60 min, T = 20 °C

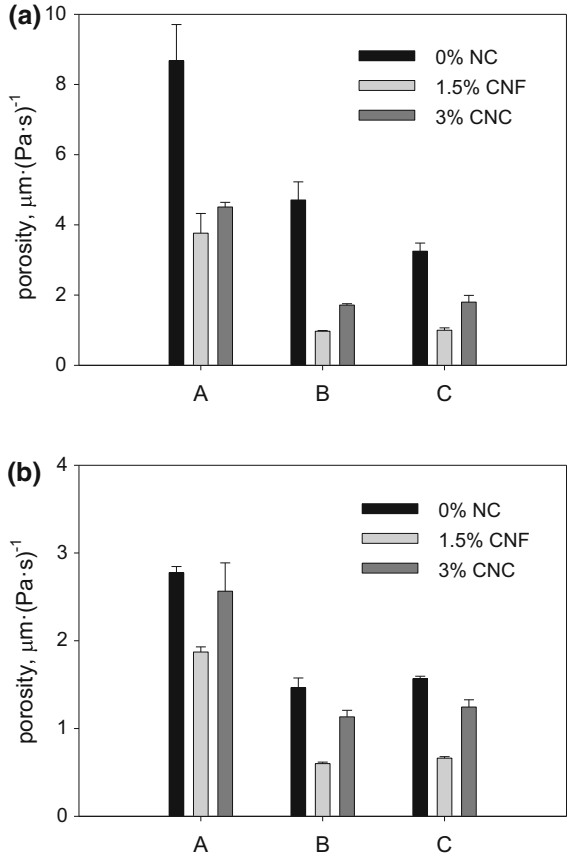

Fig. 3 Effect of different pulping conditions on porosity of the handsheets with 1.5 wt% CNF or 3 wt% CNC, when **a** three-component retention system and **b** chitosan were added to the recycled pulp. (*A*) Not soaking, time = 10 min, T = 50 °C; (*B*) not soaking, time = 60 min, T = 50 °C; (*C*) soaking, time = 60 min, T = 20 °C

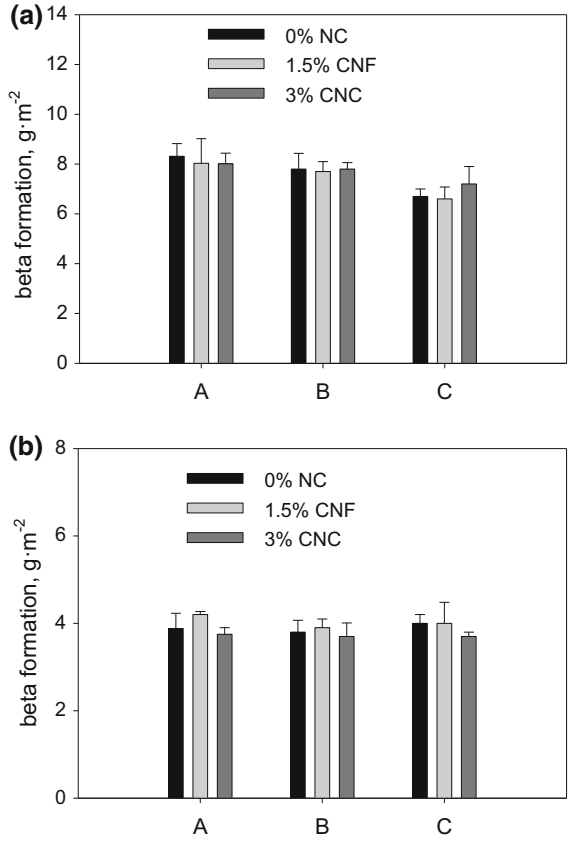

Fig. 4 Effect of different pulping conditions on beta formation of the handsheets with 1.5 wt% CNF or 3 wt% CNC, when **a** three-component retention system and **b** chitosan were added to the recycled pulp. (*A*) Not soaking, time = 10 min, T = 50 °C; (*B*) not soaking, time = 60 min, T = 50 °C; (*C*) soaking, time = 60 min, T = 20 °C

the increment in TI and decrement in porosity. However, pulping conditions did not vary handsheets formation when they are produced with CH (Fig. 4).

The effect of the addition of both CNC and CNF was directly dependent on the retention additive used. In both cases, TI increased with the addition of nanocelluloses, although improvement in the case of CPAM was higher, reaching increments in TI of 10, 20 and 30%, approximately, applying A, B and C pulping conditions for CPAM, respectively. In the case of using CH, 6, 8 and 10% increments were obtained (Fig. 2). The changes in the conditions applied during pulping were usually more evident when CPAM was used as retention additive because the scope for improvements was higher. TI of CH with no nanocellulose is already high, so not much relative improvement can be expected with the addition of either CNC or CNF. However, similar behaviors were observed varying pulping conditions with both retention additives.

Increments in TI with the addition of nanocelluloses were higher when pulping time increased from 10 to 60 min (Fig. 2), according with a higher decrease in porosity, from −56 to −79 and −69%, for A, B and C conditions with CPAM, respectively (Fig. 3a). A reduction in porosity when either CNC or CNF are added is one of the signs of better dispersion of these nanocelluloses. Porosity of handsheets prepared with conditions A were much higher in all cases. However, when pulping time was increased (B), porosity decreased to half without nanocellulose, only due to the effect of pulping time (Fig. 3). If CPAM is

used as retention additive, porosity was generally much higher since drainage was much favored. However, with the addition of CNF and CNC, porosity decreased drastically, reaching the highest reductions when conditions B were applied. In these cases, porosity was decreased from 4.7 to 1.7 and 0.9 μm $(Pa\ s)^{-1}$ for CNC and CNF, respectively. While CNF continued decreasing porosity in more than 30% using CH, no significant variation was found in porosity when CNC are added to the pulp (Fig. 3b). The lower retention of these CNC on the matrix can be the cause for the lower decrement in porosity, due to their lower size compared to CNF.

As the fiber network porosity decreases (longer pulping time), the effect of nanocelluloses on a further reduction of porosity is higher due to the lower size of the pores between fibers, blocked with nanocellulose. Higher porosity of the handsheets implies that nanocelluloses reduces the porosity but to a lesser extent. On the other hand, the retention of nanocelluloses can be affected not only by the size of the pores, but also by the mixture of nanocellulose within the pulp.

At the same pulping time (conditions B and C) similar results in TI were observed, around 40 and 50 N m g^{-1} for CPAM and CH, respectively. As a conclusion, temperature during pulping did not affect the mixture of nanocelluloses, whereas pulping time was an important parameter to consider regarding effective mixture and retention of nanocelluloses in the fiber suspension.

Measurements of beta formation indicate the standard deviation of grammage in a matrix of 400 micrograms measurements. Therefore, the higher values of beta formation indicate a worse sheet formation. As shown in Fig. 4, measurements of beta formation depend mainly on the retention additive used, instead of the addition of CNF or CNC, being better the formation with CH than CPAM. Porosity results were in accordance with these values since a higher porosity induced more deviation between next points of the handsheets.

Generally, brightness increased with pulping time and soaking (conditions C, Table 4). It is mainly due to swelling of the fibers that allowed these impurities to be more available to the water penetration, thus favoring their dissolution and subsequent removal in drained water during the handsheet formation. In addition, values obtained with CPAM were slightly higher than those of the handsheets prepared with CH, resulting in around 0.5 points more in cases A and B, and 1.5 points more in C. Although these differences

Table 4 Effect of different pulping conditions on optical properties of the handsheets with 1.5 wt% CNF or 3 wt% CNC, when (a) three-component retention system and (b) chitosan were added to the recycled pulp

		Three-component retention system			Chitosan		
		0%	1.5% CNF	3.0% CNC	0%	1.5% CNF	3.0% CNC
A: Not soaking, t = 10 min, T = 50 °C							
Brightness	(%)	61.00 ± 0.22	61.83 ± 0.25	59.16 ± 0.17	60.59 ± 0.65	61.54 ± 0.43	58.65 ± 0.64
CIE L	–	85.55 ± 0.10	85.59 ± 0.11	84.46 ± 0.09	85.51 ± 0.23	85.49 ± 0.17	84.30 ± 0.24
CIE a*	–	− 0.39 ± 0.02	− 0.36 ± 0.01	− 0.21 ± 0.02	− 0.45 ± 0.03	− 0.37 ± 0.02	− 0.22 ± 0.02
CIE b*	–	5.83 ± 0.09	5.07 ± 0.06	5.62 ± 0.03	6.12 ± 0.23	5.20 ± 0.13	5.85 ± 0.21
B: Not soaking, t = 60 min, T = 50 °C							
Brightness	(%)	62.42 ± 0.20	62.2 ± 0.20	59.04 ± 0.19	61.81 ± 0.63	61.90 ± 0.40	58.08 ± 0.46
CIE L	–	85.85 ± 0.09	85.87 ± 0.08	84.59 ± 0.07	85.78 ± 0.20	85.65 ± 0.09	84.23 ± 0.16
CIE a*	–	− 0.45 ± 0.02	− 0.43 ± 0.02	− 0.27 ± 0.03	− 0.54 ± 0.02	− 0.45 ± 0.02	− 0.28 ± 0.02
CIE b*	–	4.98 ± 0.07	4.60 ± 0.02	5.97 ± 0.08	5.44 ± 0.24	5.55 ± 0.20	6.28 ± 0.18
C: Soaking, time = 60 min, T = 20 °C							
Brightness	(%)	63.28 ± 0.15	63.08 ± 0.26	59.28 ± 0.13	62.04 ± 0.96	61.35 ± 0.35	58.40 ± 0.58
CIE L	–	85.94 ± 0.07	85.84 ± 0.13	84.54 ± 0.06	85.53 ± 0.33	85.26 ± 0.22	84.22 ± 0.22
CIE a*	–	− 1.02 ± 0.03	− 1.01 ± 0.02	− 0.18 ± 0.02	− 1.10 ± 0.07	− 1.14 ± 0.07	− 0.17 ± 0.03
CIE b*	–	4.30 ± 0.07	4.40 ± 0.10	5.65 ± 0.03	4.78 ± 0.33	4.95 ± 0.31	5.95 ± 0.19

are not significant, this tendency has already observed by other authors and could be due to the brownish color of the chitosan suspension (Fernandes et al. 2011). CNF kept almost constant brightness, comparing with initial paper, using either CPAM or CH. Since CNF were produced from a fully bleached pulp, no effect on optical properties of handsheets with CNF was observed. However, due to the direct hydrolysis without a previous isolation of cellulose of the recycled paper, a brown color was observed in CNC and therefore optical properties of those handsheets have been negatively affected. More specifically, brightness was reduced from 61 to 59.2% with CPAM (reduction of 1.8 points) and from 60.6 to 58.6% with CH (reduction of 2 points). It seems that brightness was more affected by the addition of a dark component than the pulping conditions.

Colorimetric constants changed when either CNF or CNC were applied. In the case of CNF with CPAM, the variation in these parameters is traduced in blueness tendency. However, when CH is used, CNF addition with A conditions tends to green and blue appearance, but increasing pulping time (B and C), CNF trigger greenness and yellowness tendency. On the other side, CNC caused an increment in CIE b*, which is typically related with the presence of lignin in paper, coming from the 10.2% of lignin present in CNC (Heitner 1993).

Effect of adding dispersing agents on recycled paper using nanocellulose

Addition of dispersing agents leads to different behaviors, depending on which of them was used. To assure easy availability and reasonable costs of dispersing agents for industrial implementation, commercial agents already used in papermaking industry were selected. Moisturizing and surfactant agents are typically used in this industry to control the deposit of slimes, to make ink particles hydrophobic during pulping, to clean felts, wires and machinery and to disperse some substances and to facilitate the impregnation of different components on the fibers (Suhr et al. 2015).

Different doses of the two dispersing agents were applied to assess the effect of nanocellulose on the paper properties. Figure 5a shows an increase in TI with the addition of different amounts of D1 to the pulp. However, this tendency was not observed when

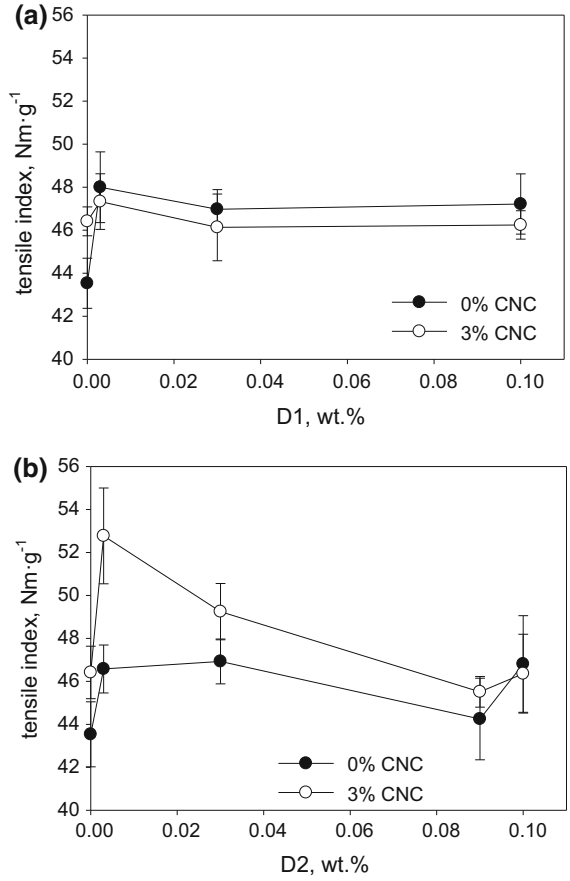

Fig. 5 Effect of type and dose of dispersing agent on tensile index (TI) of the handsheets with 3 wt% CNC when chitosan were added to the recycled pulp. **a** D1; **b** D2

D1 were added to the pulp with CNC, reaching values of TI lower than those of handsheets with only D1. The addition of D1 to the pulp with 0% CNC favored the efficient dispersion of the fibers throughout the network, thus improving mechanical properties. The effect of CNC and D1 by separate was not synergistic when they were used together. That could be explained by means of the mechanism of CNC to increase TI of the paper, which can act similarly to a dispersing agent, thus, there is not a combination of mechanisms that led to a further improvement in TI. On the other hand, since D1 is typically used in paper mills to facilitate the uniform impregnation of fibers with the bleaching agent, the interaction of fibers with CNC and the type of flocs formed can be affected, leading to worse effect of CNC on the handsheets. Therefore, it can be concluded that D1 does not get to

disperse CNC, so it has been discarded for future assays.

With the addition of only D2 to the pulp, TI was increased mainly due to the better dispersion of the fibers (Fig. 5b). Moreover, when both CNC and a low dose of D2 (0.003%) were combined and then applied, TI was further enhanced from 43.4 Nm g^{-1} (neither CNC nor D2) to 52.8 Nm g^{-1}, getting an increment of 21.8%. That increment was much higher than the obtained without the addition of D2 (from 43.4 to 46.4 Nm g^{-1}, increment of 6.6%). This dispersing agent has been typically used in some paper mills as moisturizing agent to facilitate the intimate contact between some coatings and paper. Most of the used coatings are composed of a mixture of a binder, white pigments (mainly calcium carbonate, fine clay or talc) and water (Suhr et al. 2015). Although traditionally carboxylated styrene-butadiene, styrene-acrylonitrile or acrylic latexes have been used as binders (Suhr et al. 2015), recently nanocelluloses are becoming more relevant (Brodin et al. 2014). Therefore, it was expected that D2 could effectively disperse CNC suspensions in the paper sheets.

Due to the promising results obtained with D2 at the dose of 0.003% respect to dry mass of paper, it has been chosen for further assays with both nanocelluloses in the presence of CPAM and CH using the pulping conditions A (Fig. 6). The effect of D2 on paper properties without nanocelluloses for both retention systems has found to be slightly different, mainly owing to the corresponding flocculation mechanism. With CPAM, CNF increased in 20.6% the TI with the addition of D2 (Fig. 6a), instead of 14.3% without dispersing agent (Fig. 2a). The same behavior was observed for CNC, were TI increased in 11.1% with D2 (Fig. 6a) and 7.2% without it (Fig. 2a). With the use of CH, higher increments in TI were obtained for CNC previously dispersed by D2 (15.2 (Fig. 6a) instead of 7.3% (Fig. 2b). However, CNF obtained similar results no matter if D2 is added or not (around 5% of increment in TI). It can be concluded that long pulping times could be avoided by adding the adequate dispersing and retention agent.

Comparing these results with those obtained at the best pulping conditions of each retention system, different conclusions can be proposed. In the case of using CPAM, both CNF and CNC provided higher increments in TI with D2 (Fig. 6a) compared to the same pulping conditions (A) without dispersant, but

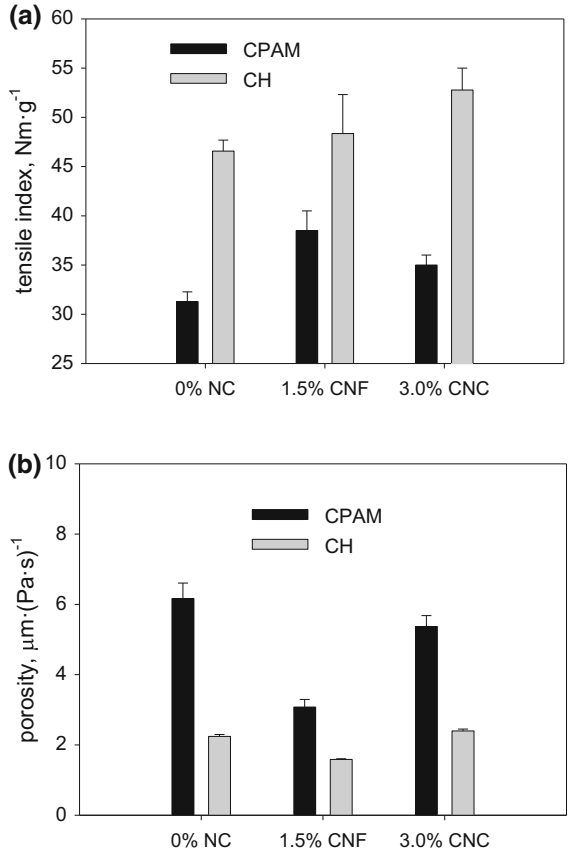

Fig. 6 Effect of 0.003 wt% D2 agent on **a** tensile index (TI), **b** porosity of the handsheets with 1.5 or 3 wt% CNC when a three-component retention additive or chitosan were added to the recycled pulp

the best TI values were obtained with the increment of the pulping time (conditions B and C, Fig. 2). This behavior was kept for CNF retained with CH (Figs. 2, 6). Nevertheless, when CH is used to retain CNC, the best results were obtained with the addition of D2 at pulping conditions A (Fig. 6a).

Porosity was reduced in 3 points with CNF using CPAM and 0.5 points using CH (Fig. 6b). With both CPAM and CH, CNF addition decreased porosity values to the half with pulping conditions B and C (Fig. 3) compared to conditions A and D2 (Fig. 6b), which agrees with higher retention of the CNF and thus TI value. However, in the case of CNC, porosity was not much affected by the addition of CNC with D2, keeping similar values to those of handsheets with no nanocellulose (Fig. 6b). Compared to data from Fig. 3, porosity of handsheets prepared with pulping

conditions A and D2 (Fig. 6b) was always higher than that of handsheets without the dispersant use.

Conclusions

Pulping conditions have an important impact on the homogeneous mixture of CNF and CNC in the fibers suspension, thus on their retention, although that also depends on the retention additive used. In the case of using CPAM, the highest TI was achieved by pulping during 60 min with both CNC and CNF, which could be attributed to the homogeneous mixture of the nanofibers in the fibers suspension because the large amount of pulping time did not increased the TI without the addition of nanocelluloses. Less differences were found when the retention system used was CH. In this case, the increase of pulping time led to an increase in TI without nenocellulose addition. Both CNC and CNF achieved slightly further increase in TI, obtaining the higher values when CNC were pulped during 60 min. The main advantages of using a dispersing agent is the reduction of pulping time (from 60 to 10 min), letting the papermaking mills work with similar conditions to those used without nanocellulose addition, and the easier industrial implementation of this option to achieve an homogeneous mixture of nanocellulose in the fiber suspension. However, due to the high influence of the type of nanocellulose, the retention additive and the dispersing agent, further studies must be performed to assess the viability of the different combinations.

Acknowledgments The authors wish to thank the Economy and Competitiveness Ministry of Spain for the support of the project with reference CTQ2013-48090-C2-1-R and the Grant of C. Campano (BES-2014-068177).

References

Ahola S, Myllytie P, Osterberg M, Teerinen T, Laine J (2008) Effect of polymer adsorption on cellulose nanofibril water binding capacity and aggregation. BioResources 3:1315–1328

Balea A, Blanco Á, Monte MC, Merayo N, Negro C (2016a) Effect of bleached eucalyptus and pine cellulose nanofibers on the physico-mechanical properties of cartonboard. BioResources 11:8123–8138

Balea A, Merayo N, Fuente E, Delgado-Aguilar M, Mutje P, Blanco A, Negro C (2016b) Valorization of corn stalk by the production of cellulose nanofibers to improve recycled paper properties. BioResources 11:3416–3431

Brodin FW, Gregersen OW, Syverud K (2014) Cellulose nanofibrils: challenges and possibilities as a paper additive or coating material—a review. Nord Pulp Pap Res J 29:156–166

Campano C, Balea A, Blanco A, Negro C (2016) Enhancement of the fermentation process and properties of bacterial cellulose: a review. Cellulose 23:57–91

Campano C, Miranda R, Merayo N, Negro C, Blanco A (2017) Direct production of cellulose nanocrystals from old newspapers and recycled newsprint. Carbohydr Polym 173:489–496

CEPI (2015). Key statistics. European Pulp and Paper Industry

Chen LH, Wang QQ, Hirth K, Baez C, Agarwal UP, Zhu JY (2015) Tailoring the yield and characteristics of wood cellulose nanocrystals (CNC) using concentrated acid hydrolysis. Cellulose 22:1753–1762

Coccia V, Cotana F, Cavalaglio G, Gelosia M, Petrozzi A (2014) Cellulose nanocrystals obtained from *Cynara cardunculus* and their application in the paper industry. Sustainability 6:5252–5264

Delgado-Aguilar M, Gonzalez I, Pelach MA, De La Fuente E, Negro C, Mutje P (2015) Improvement of deinked old newspaper/old magazine pulp suspensions by means of nanofibrillated cellulose addition. Cellulose 22:789–802

Fatehi P, Kititerakun R, Ni YH, Xiao HN (2010) Synergy of CMC and modified chitosan on strength properties of cellulosic fiber network. Carbohydr Polym 80:208–214

Fernandes SCM, Freire CSR, Silvestre AJD, Neto CP, Gandini A (2011) Novel materials based on chitosan and cellulose. Polym Int 60:875–882

French AD (2014) Idealized powder diffraction patterns for cellulose polymorphs. Cellulose 21:885–896

Gonzalez I, Boufi S, Pelach MA, Alcala M, Vilaseca F, Mutje P (2012) Nanofibrillated cellulose as paper additive in eucalyptus pulps. BioResources 7:5167–5180

Habibi Y (2014) Key advances in the chemical modification of nanocelluloses. Cellulose 43:1519–1542

Habibi Y, Chanzy H, Vignon MR (2006) TEMPO-mediated surface oxidation of cellulose whiskers. Cellulose 13:679–687

Habibi Y, Lucia LA, Rojas OJ (2010) Cellulose nanocrystals: chemistry, self-assembly, and applications. Chem Rev 110:3479–3500

Heitner C (1993) Light-induced yellowing of wood-containing papers—an evolution of the mechanism. In: Heitner C, Scaiano JC (eds) Photochemistry of lignocellulosic materials, vol 531. ACS symposium series. American Chemical Society, Washington, pp 2–25

Henriksson M, Berglund LA, Isaksson P, Lindstrom T, Nishino T (2008) Cellulose nanopaper structures of high toughness. Biomacromol 9:1579–1585

Hubbe MA (2013) Prospects for maintaining strength of paper and paperboard products while using less forest resources: a review. BioResources 9:1634–1763

Marx-Figini M (1978) Significance of the intrinsic viscosity ratio of unsubstituted and nitrated cellulose in different solvents. Die Angew Makromol Chem 72:161–171

Merayo N, Balea A, de la Fuente E, Blanco Á, Negro C (2017a) Interactions between cellulose nanofibers and retention

systems in flocculation of recycled fibers. Cellulose 24:677–692

Merayo N, Balea A, de la Fuente E, Blanco Á, Negro C (2017b) Synergies between cellulose nanofibers and retention additives to improve recycled paper properties and the drainage process. Cellulose 24:2987–3000

Osong SH, Norgren S, Engstrand P (2016) Processing of wood-based microfibrillated cellulose and nanofibrillated cellulose, and applications relating to papermaking: a review. Cellulose 23:93–123

Petroudy SRD, Syverud K, Chinga-Carrasco G, Ghasemain A, Resalati H (2014) Effects of bagasse microfibrillated cellulose and cationic polyacrylamide on key properties of bagasse paper. Carbohydr Polym 99:311–318

Roman M, Winter WT (2004) Effect of sulfate groups from sulfuric acid hydrolysis on the thermal degradation behavior of bacterial cellulose. Biomacromol 5:1671–1677

Saito T, Kimura S, Nishiyama Y, Isogai A (2007) Cellulose nanofibers prepared by TEMPO-mediated oxidation of native cellulose. Biomacromol 8:2485–2491

Salam A, Lucia LA, Jameel H (2013) A novel cellulose nanocrystals-based approach to improve the mechanical properties of recycled paper. ACS Sustain Chem Eng 1:1584–1592

Segal L, Creely JJ, Martin AE, Conrad CM (1959) An empirical method for estimating the degree of crystallinity of native cellulose using the X-ray diffractometer. Text Res J 29:786–794

Suhr M, Klein G, Kourti I, Rodrigo Gonzalo M, Giner Santonja G, Roudier S, Delgado Sancho L (2015) Best available techniques (BAT) reference document for the production of pulp, paper and board. Institute for Prospective Technological Studies, Seville. https://doi.org/10.2791/370629

Sun B, Hou Q, Liu Z, Ni Y (2015) Sodium periodate oxidation of cellulose nanocrystal and its application as a paper wet strength additive. Cellulose 22:1135–1146

Taipale T, Osterberg M, Nykanen A, Ruokolainen J, Laine J (2010) Effect of microfibrillated cellulose and fines on the drainage of kraft pulp suspension and paper strength. Cellulose 17:1005–1020

Tasman JE, Berzins V (1957) The permanganate consumption of pulp materials. Tappi 40:691–704

PUBLICATION VI

Hairy cationic nanocrystalline cellulose as a novel flocculant of clay

Cristina Campano, Patricio Lopez-Exposito, Angeles Blanco, Carlos Negro, Theo G.M. van de Ven

Journal of Colloid and Interface Science (2019) 545:153-161

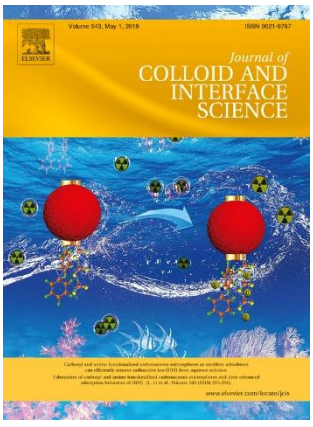

Impact factor 2017: ***5.091***

JCR, Chemistry, Physical, 33 out of 146, ***Q1***

Journal of Colloid and Interface Science 545 (2019) 153–161

Contents lists available at ScienceDirect

Journal of Colloid and Interface Science

journal homepage: www.elsevier.com/locate/jcis

Regular Article

Hairy cationic nanocrystalline cellulose as a novel flocculant of clay

Cristina Campano [a,1], Patricio Lopez-Exposito [b], Angeles Blanco [b], Carlos Negro [b], Theo G.M. van de Ven [a,*]

[a] Department of Chemistry, Pulp and Paper Research Centre, and Quebec Centre for Advances Materials, McGill University, 3420 University Street, Montreal, Quebec H3A 2A7, Canada
[b] Department of Chemical Engineering, Complutense University of Madrid, Avda. Complutense s/n, 28040 Madrid, Spain

GRAPHICAL ABSTRACT

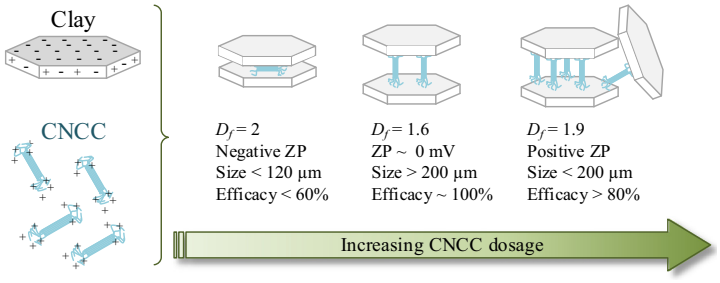

ARTICLE INFO

Article history:
Received 11 December 2018
Revised 27 February 2019
Accepted 28 February 2019
Available online 1 March 2019

Keywords:
Hairy nanocellulose
Cationic nanocrystals
Flocculation
Clay
Fractal dimension
Conformation

ABSTRACT

Hypothesis: The present paper investigates, for the first time, the potential of cationic hairy cellulose nanocrystals (CNCC) to induce the flocculation of a model suspension of kaolinite. CNCC belong to a brand new family of nanocelluloses characterized for presenting a crystalline rod-like body and functionalized amorphous chains at both ends. Given that these chains can be easily tuned, these nanocelluloses present a high potential as fit-to-purpose flocculants.
Experiments: CNCC were produced through periodate oxidation, cationization and thermal treatment of cellulose. Flocculation was monitored by both photometric dispersion analysis and laser reflectance. Flocs were characterized by the determination of zeta potential, supernatant turbidity removal and optical microscopy. A recently developed machine learning random forest regression model was used to estimate fractal dimension (D_f) from chord length distribution data.
Findings: Although a high efficiency was achieved for CNCC dosages between 7.5 and 75 mg/g, the maximum floc size and the fastest flocculation were found near the isoelectric point (10–30 mg/g). Thus, CNCC acted through charge neutralization mechanism. The model used to estimate flocs D_f was found very successful to describe the flocculation process. The clay/CNCC flocs D_f values suggest a relation between floc conformation and CNCC dosage, presenting an opener structure when closer to the isoelectric point.

1. Introduction

Cationic hairy cellulose nanocrystals (CNCC) have been recently developed by Yang and van de Ven [1]. These nanoparticles have the exceptional properties of other nanocelluloses while also presenting areas with a high density of positive charge that can potentially induce the aggregation of colloidal materials.

* Corresponding author.
E-mail addresses: ccampano@ucm.es (C. Campano), plopezex@ucm.es (P. Lopez-Exposito), ablanco@ucm.es (A. Blanco), cnegro@ucm.es (C. Negro), theo.vandeven@mcgill.ca (T.G.M. van de Ven).
[1] Permanent address: Department of Chemical Engineering, Complutense University of Madrid, Avda. Complutense s/n, 28040 Madrid, Spain.

https://doi.org/10.1016/j.jcis.2019.02.097
0021-9797/

CNCC are produced by making a cellulose pulp react with sodium periodate in controlled conditions, employing less than 6.17 mM $NaIO_4$/g cellulose for 42 h. Such conditions guarantee that the crystalline sections of cellulose remain unaltered while the amorphous parts are oxidized to a given extent according to the quantity of oxidant used [2]. This oxidation causes the C2-C3 bonds within glucose units to break, thus giving place to 2,3- dialdehyde groups [3]. The product of that reaction is then subject to a Schiff base reaction that binds a desired group (-R) to the aldehyde positions. The properties of the resulting nanoparticles can be tuned by choosing the nature of the -R group. Since cellulose dialdehyde is soluble in water, a thermal treatment after the Schiff base reaction induces the solubilization of the amorphous parts that join consecutive crystalline sections. This releases individual nanocrystals that still present some amorphous regions attached at both ends. The particular structure and chemical nature of hairy nanocellulose produced with the referred approach were confirmed by Chen and van de Ven [2].

The use of periodate as oxidizing agent has several advantages compared to mineral acids used to produce conventional cellulose nanocrystals (CNC). One of the most fascinating properties is that the fibers keep their initial size while heat is not applied, allowing an easy recovery of periodate as iodate when fibers are washed [4]. This increases the sustainability of this method thus reducing total production cost, compared to traditional nanocelluloses.

Kaolinite is used as a common thickening agent in a variety of industrial sectors [5], due, among other factors, to its low price, low abrasiveness and good availability [6,7]. This aluminum silicate is applied in paper, ceramic, paint, plastic, rubber, and cracking catalyst industries [8,9]. Kaolinite has been widely studied as a model species to assess the performance and aggregation mechanism of new flocculants [5]. Kaolinite particles are usually shaped as slim sheets of triclinic crystals with pseudo hexagonal morphology [8]. For example, the addition of fillers in papermaking industries is widely used in office graphic papers to reduce the materials cost and improve specific properties of paper [9].

Synthetic polyelectrolytes, such as cationic or anionic polyacrylamides, and polyethylene imines, are the most used flocculants [10]. They are usually adapted to the specific conditions of each particular industry by selecting their molecular weight, charge density and by optimizing their dosage [10].

In this work, CNCC were produced and used to flocculate kaolinite particles, with the aim of assessing the flocculation mechanism. Flocculation monitoring was performed by photometric dispersion analysis (PDA) and laser reflectance. Zeta potential and supernatant turbidity removal were determined. Furthermore, a brand new machine learning random forest regression model was used to estimate 3D fractal dimension (D_f) of flocs from chord length distribution data. To check the effectivity of the model, the 2D fractal dimension (D_2) was estimated through the acquisition and processing of optical images. The use of CNCC and the model employed to describe flocs D_f could be of high relevance not only for the papermaking industry, but also for many other processes involving flocculation.

2. Materials and methods

2.1. Materials

The raw material used for CNCC preparation was a softwood kraft pulp supplied by Domtar, Canada. Kaolinite (Sigma Aldrich) was used as a model for clay. Chemicals used for the different reactions, sodium (meta) periodate, GT [(2-hydrazinyl- 2-oxoethyl)-trimethylazanium chloride, GT], ethylene glycol, hydroxylamine hydrochloride, $AgNO_3$, hydrochloric acid (0.1 M) and sodium hydroxide (0.1 M) were supplied by Sigma Aldrich (analytical reagent grade) and used without further modification. Propanol and sodium chloride were purchased from ACP Chemicals Inc.

2.2. Preparation of cationic hairy nanocrystalline cellulose (CNCC)

CNCC were prepared through a three-step treatment based on the procedure proposed by Yang and van de Ven [1]: oxidation of the pulp with $NaIO_4$ to produce DAMC (Fig. S1a); cationization of the DAMC to produce cationic DAMC (CDAMC) (Fig. S1b) and finally a heat treatment to nanofibrillate the CDAMC and thus produce CNCC.

2.2.1. Dialdehyde modified cellulose (DAMC) production

Initially, 20 g of dried softwood kraft pulp were soaked and disintegrated at 3000 rpm for 10 min. Then, the disintegrated pulp was added to a solution of 19.6 g $NaIO_4$ and 15.6 g of NaCl was prepared. The reaction was conducted for 24 h while stirring at room temperature and protecting the reaction mixture from any light with some layers of aluminum foil. Upon reaching the end of the 24 h period, 20 mL ethylene glycol were added to quench the residual periodate [1]. The produced DAMC fibers were washed by filtration.

2.2.2. Cationization of dialdehyde modified cellulose (CDAMC)

Washed DAMC fibers were added to a solution containing 1 g GT and 2.4 g NaCl per gram of dry DAMC. pH was adjusted to 4.5 with HCl. After 24 h of stirring at room temperature, the CDAMC were washed by filtration.

2.2.3. Preparation of nanocellulose

Never-dried CDAMC were adjusted to a consistency of 1% with water and stirred at 60 °C for 2 h. After that, high intensity sonication was applied for 10 min with an Ultrasonic Processor UP200H, supplied by Hielscher, Germany. To remove the non-fibrillated fraction, the sample was centrifuged at 5000 rpm for 10 min.

2.3. CNCC characterization

2.3.1. Aldehyde content

Cellulose oxidation degree achieved with $NaIO_4$ was determined through the quantification of aldehyde groups. The dialdehyde groups of DAMC were converted to oximes employing a Schiff base reaction with hydroxylamine hydrochloride following the procedure described by Yang, Alam and van de Ven [11].

2.3.2. Yield

Process yield was calculated as the proportion between the final dry mass of CNCC and the initial amount of pulp before all reactions. The rest of the pulp was that of the dissolved cellulose plus that lost during the washing steps.

Nanocellulose yield was calculated as the ratio between the final dry mass of the supernatant after centrifugation and the initial dry mass before centrifugation.

2.3.3. Cationic groups

The degree of cationization was determined through conductometric titration of the trimethylazanium chloride groups present in CDAMC with $AgNO_3$ 10 mM. The dosing and measurement were carried out automatically on a Metrohm 836 Titrando Instrument (Herisau, Switzerland). Around 0.05 g of CDAMC (dry basis) were added to the titration beaker, and conductivity was recorded after the addition of 0.1 mL of $AgNO_3$ in 50 s intervals. It has been assumed the presence of one chloride counterion per trimethylammonium group. Initially, the conductivity starts decreasing while

AgCl precipitates are forming, till all Cl^- are consumed. Afterwards, an increase in conductivity is observed.

2.3.4. Zeta potential

Zeta potential was measured with a ZetaPlus analyzer supplied by Brookhaven Instruments Corporation (New York, USA). CNCC and clay samples were measured on solutions at 0.1%.

2.3.5. Atomic force microscopy (AFM)

Surface morphology and particle dimension of CNCC were determined by atomic force microscopy (AFM) with a MultiMode 8 from Bruker, in PeakForce mode. A drop of 20 μL of a CNCC suspension of 0.005% consistency was deposited on a clean mica surface and left to dry at room temperature and then deposited in an oven at 60 °C overnight before analysis. Both length and diameter distribution were determined using the NanoScope Analysis software. 20 individual particles were measured to determine the average size and standard deviation.

2.3.6. Dynamic light scattering (DLS)

The effective diameter of CNCC and clay particles was assessed by a Brookhaven light scattering instrument BI9000 AT digital correlator. Scattered light intensity was recorded at 90° and 25 °C, of suspensions at 0.005%.

2.4. Flocculation of clay by CNCC

2.4.1. Photometric dispersion analysis (PDA)

The flocculation kinetics of clay by CNCC was monitored by PDA (PDA 2000, Rank Brothers, Cambridge, UK). The output of this equipment is the ratio of RMS to DC readings, where RMS is the root mean square of the fluctuations in transmitted light and DC makes reference to the average transmittance. When flocculation takes place, the value of RMS increase and DC slightly increase, increasing then the ratio RMS/DC. This value can be an indirect measurement of the size and number of flocs, and the initial slope can be considered as a measurement of the initial flocculation rate. The principle and operation of the PDA is shown in a previously published paper [12].

The experimental procedure starts with 200 mL of a clay suspension at 1 g/L of concentration and pH 8.5, in a 600 mL beaker with magnetic stirring at 100 rpm. Using a standard 3 mm internal diameter tube, the suspension was pumped at 150 mL/min through the photocell of the PDA, flowing back to the test beaker. The concentration of clay was kept constant in all experiments, varying the CNCC dosage. After monitoring the clay suspension for 120 s, the required amount of CNCC was added and the ratio RMS/DC was recorded for 10 min more.

2.4.2. Focused beam reflectance measurement

The flocculation process was also assessed in real time observing the evolution of the corresponding suspension mean chord length (MCL) [13]. These data were gathered through a focused beam reflectance measurement probe (FBRM) M500L, supplied by Mettler Toledo (Columbus, USA). The FBRM can build a distribution of chord lengths that resembles the actual size distribution of particles in the corresponding suspension. The probe projects a rotating laser beam of known speed into the suspension and records the time during which the beam is intersecting a particle. This is then translated into a chord length, which is defined as the distance between the two edges of a particle [14]. In the present study, the chord lengths detected were classified through the probe software in 200 size intervals organized logarithmically, ranging from 1 to 4000 μm [15].

In order to compare FBRM and PDA results, the FBRM probe was placed in a 600 mL beaker with 200 mL of the clay suspension (1 g/L) under magnetic stirring at 100 rpm. After 120 s, the required CNCC dose was added to the sample, recording the MCL and the particle number every 5 s for 10 min. After the 10 min, stirring speed was increased up to 350 rpm for 2 min in order to break the formed flocs. Then, stirring speed was reduced to the initial speed, 100 rpm, for 4 min more to assess the reflocculation rate.

The flocculation stability was calculated by Eq. (1).

$$\textit{Flocculation stability}\ (\%) = \frac{MCL_e - MCL_0}{MCL_m - MCL_0} \cdot 100 \quad (1)$$

where MCL_e is defined as the MCL after 10 min, MCL_0 is the MCL before CNCC addition and MCL_m the maximum MCL [16].

The reflocculation efficiency was calculated by the following equation Eq. (2) [17]:

$$\textit{Reflocculation efficiency}\ (\%) = \frac{MCL_F - MCL_B}{MCL_e - MCL_B} \cdot 100 \quad (2)$$

where MCL_F is defined as the maximum MCL after the decrease of the stirring speed back to 100 rpm, and MCL_B is the MCL after breaking the flocs at high stirring speed (350 rpm).

2.5. Flocs characterization

2.5.1. Zeta potential

To evaluate the isoelectric point (IEP) of the system clay/CNCC, a fresh stock of clay suspension (1 g/L) was prepared and mixed with different amounts of CNCC. Then, zeta potential of these mixtures was determined after 5 min of agitation at the working pH (8.5).

2.5.2. Turbidity removal

Turbidity of the supernatant phase obtained after the flocculation trials was measured with a LP 2000-11 nephelometer supplied by Hanna Instruments, according to ISO 7027:2001. The turbidity of clay suspension was also measured to calculate the turbidity removal from the water suspension.

2.5.3. Scanning electron microscopy (SEM)

Scanning electron microscopy (SEM) images were obtained with a JEOL JSM 6335F at an accelerating voltage of 15 kV. These analyses were carried out at the National Center of Electronic Microscopy of Spain.

2.5.4. Optical microscopy

Optical microscopy was used to assess flocs morphology through a Nikon ECLIPSE TE2000U (Tokio, Japan).

2.5.5. Fractal dimension (D_f)

D_2 was measured on microscopic images taken with a Zeiss Axio Lab 10 microscope. The images were processed and analyzed through the Fiji distribution of ImageJ 1.151 h. Each microscopic photograph was converted into an 8-bit image and its contrast was adjusted to achieve a good definition of flocs' borders. Flocs were selected individually and copied into a separate image file. An automatic thresholding followed by a binarization was applied to each floc image. The fractal analysis was performed with the FracLac plugin of ImageJ using the default sampling sizes and 12 different grid positions. The D_2 output for each aggregate was the result of averaging the D_2 obtained in all grid positions.

D_f was estimated by applying a machine learning random forest regression model [18] to the corresponding suspension chord length distribution data. Details on the methodology followed to implement the regression system can be found in the cited paper.

3. Results and discussion

3.1. CNCC characterization

According to the reactions schemes in Fig. S1, 1 mol of $NaIO_4$ reacts with 1 mol of glucose monomer to produce 1 mol of DAMC with 2 aldehyde groups. Based on the amount of pulp used and assuming a 100% consumption of $NaIO_4$, the theoretical maximum degree of oxidation (DO) and thus aldehyde content is 1.48 and 9.24 mmol/g, respectively. However, the DO and the measured aldehyde content was 0.64 and 3.84 mmol/g, respectively. This translates into a reaction conversion of 41.5%. These results agree with the study of Chen and van de Ven [2] in which the variation of the efficiency of $NaIO_4$ oxidation of pulp with time is presented.

After cationization and heat treatment, the process yield was 54.9%. Hence, the remaining 45.1% corresponded to the mass lost during the washing steps performed after each reaction. After all treatments (periodate and Girard reactions and the thermal treatment), most of the sample still remained in the form of fibers (Fig. S2a), and only 2.1% was CNCC (nanocellulose yield of 3.8%). However, after application of high intensity sonication, these fibers were converted into smaller particles, presumably CNCC, that were not visible under optical microscopy (Fig. S2b). With this treatment, the nanocellulose yield was increased from 3.8% to 98.9%.

Charge content of CNCC calculations, made from Fig. S3, indicated a cationic group's amount of 1.31 mmol/g. The theoretical maximum, assuming 100% conversion with the used mass of GT, was calculated to be 3.92 mmol/g. The determined reaction conversion is 33.42%, which implies that a 66.68% DAMC monomers were not substituted. Since the aldehyde content of DAMC fibers was 3.84 mmol/g, on average, less than 1 cationic group was attached to each dialdehyde group.

The zeta potential of CNCC was +14.5 mV, which is consistent with Yang and van de Ven [1], who obtained +27 mV of zeta potential with 1.68 mmol/g of cationic groups. This cationic charge is high enough to use this product as cationic flocculant.

The morphology of the CNCC is shown in Fig. 1. A rod-like morphology is generally observed in the micrographs, similar to that of traditional sulfuric acid produced CNC [19]. Although the hairs are not detectable with this technology, their presence has been confirmed in a previous study through DLS and acoustic attenuation [2,20]. The fact that hairs are protruding from the ends is also proved in papers [21,22]. Since there are not steric impediments among the sulfuric acid produced CNC, they usually tend to agglomerate in the longitudinal direction through hydrogen bonding [23]. However, in the case of CNCC, they seem to aggregate by joining the end of the crystals, positively charged, with the body of other particles, which is lightly negative. This can be observed in the pictures, where even some of the particles are bonded forming a cross structure between them.

The nanocrystals size, estimated through the measurement of different CNCC individual elements on the AFM images, was, on average, 4.7 ± 1.6 nm wide and 380 ± 120 nm long. In addition, the effective particle diameter obtained by DLS on a diluted suspension of CNCC was 326 ± 8 nm. This size is estimated considering the particles as spheres, so compared to length and width measured from the micrographs, it should be between both values.

The straight morphology of the CNCC, resembling that of CNC, may indicate that most of amorphous regions have been dissolved. However, the average diameter obtained through DLS, 326 nm, is much larger than that obtained previously for periodate and chlorite oxidized cellulose fibers: 200 nm in salt free water and reduced to 100 nm with salt [11]. This allows for the possibility of finding some doublets in the sample, consisting of two crystalline parts with an amorphous region in between.

3.2. Clay flocculation by CNCC: PDA

Fig. 2a shows the flocculation kinetics of clay by different CNCC dosages, monitored by PDA. The RMS/DC ratio indicates the relative floc size in arbitrary units [24]. At zero time, only clay particles are present in the suspension, which are quite agglomerated as shown in Fig. S4a. These agglomerates, of 18 μm on average, are created due to the double charge distributed on the particle surface (Fig. S4b) [25]. In all cases, the initial value of the ratio was set to 0.7 so that this parameter has enough margin to increase before the equipment maximum limit is reached (12.5). After CNCC was added, an extensive flocculation of clay occurred. When CNCC dosage increased from 2.5 to 7.5 mg/g, both initial slope and maximum values (plateau) increased, as observed in Fig. 2b. However, when the CNCC dosage was over 10 mg/g, the RMS/DC ratio reached instantaneously the maximum measurement limit of the equipment, impeding the adequate monitoring of clay flocculation. Therefore, the plateau values observed in Fig. 2b are the same for these dosages, and are indicated with arrows pointing up meaning that the real plateau values are higher than 12.5. Although the plateau value is also 12.5 for the CNCC dosage of 150 mg/g clay, the initial slope decreases from 1.2 to 0.1 s^{-1}, which means that the

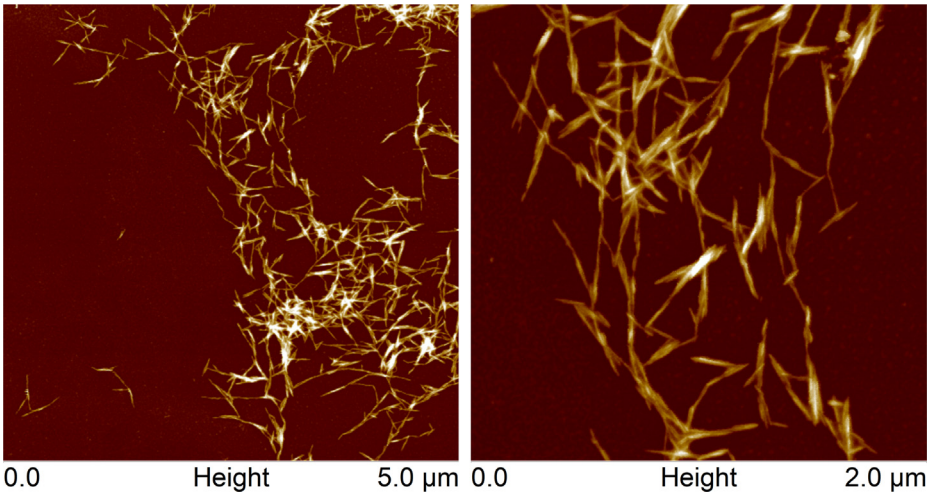

Fig. 1. AFM height images' of CNCC.

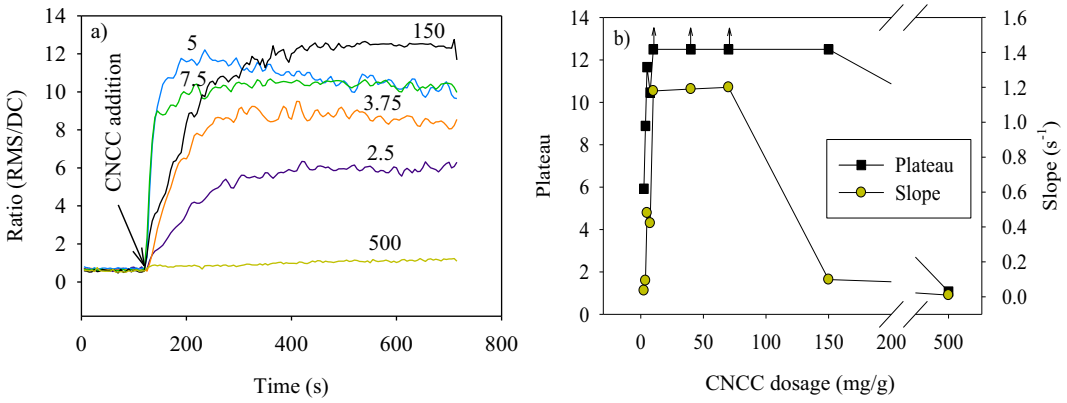

Fig. 2. (a) Clay flocculation with CNCC dosages between 2.5 and 500 mg/g-clay, monitored by PDA. The numbers on the graph lines correspond to the CNCC dosage related to the amount of clay present during the experiment in mg/g. The curves of the PDA monitoring for dosages between 10 and 100 have not been represented since an instantaneous step reaching the detection limit of the equipment (12.5) occurs. (b) Plateau and initial slope of clay flocculation experiments at different CNCC dosages, monitored by PDA. Arrows pointing up show that the real value is higher than the one represented, but it cannot be determined by this method.

flocculation efficiency is being reduced, probably due to an excess of positive charges in the system.

When flocculation occurs, some of the primary particles would agglomerate by the action of CNCC, thus the average transmittance should increase slightly. When the CNCC dosage is below 7.5 mg/g, a coexistence of some primary particles and some small flocs is observed. Then, many fluctuations in transmitted light are present, even despite there are some primary particles distributed through the sample. Therefore, a very sensitive change in floc size is detected by PDA with a large increase in the output ratio. This explanation justifies the impediment of measuring the ratio when floc size is very high.

3.3. Clay flocculation by CNCC: FBRM

In order to study the floc behavior and to assess the flocculation mechanism, FBRM experiments have been carried out (Fig. 3). When CNCC are added to the clay sample, flocculation starts to be perceivable through an increase in the MCL accompanied by a reduction in the number of particles. At low CNCC dosages (below 5 mg/g), the MCL varies but with very slow kinetics. When the

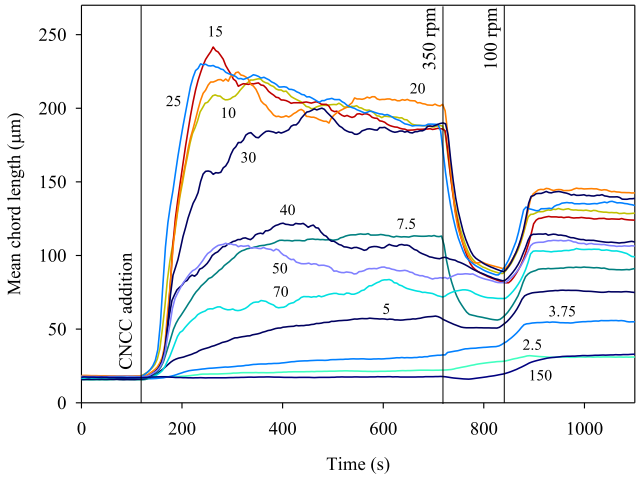

Fig. 3. Mean chord length (MCL) profiles of different CNCC dosages obtained with FBRM. The numbers in the figure indicate the CNCC dosage related to the amount of clay present during the experiment in mg/g. Vertical lines represent an external action on the experiment: first, CNCC addition, second, an increment in the stirring speed from 100 rpm to 350 rpm, and third, a reduction in the stirring speed from 350 rpm back to 100 rpm.

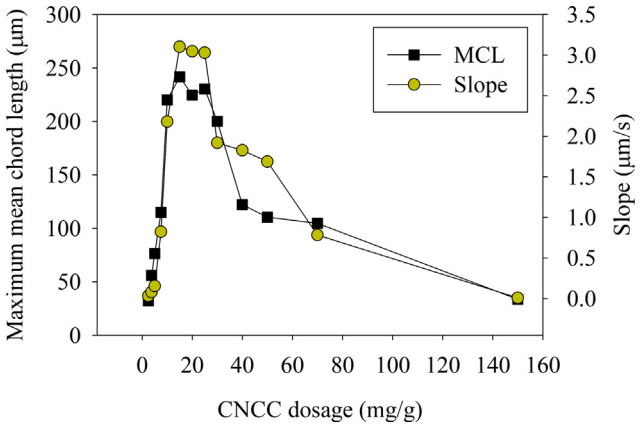

Fig. 4. Data extracted from FBRM experiments: Plateau and initial slope of clay flocculation experiments with CNCC, monitored by FBRM.

dosage of CNCC employed was greater than 5 mg/g, both maximum MCL and initial slope increased up to a maximum value at the CNCC dosage interval of 10–25 mg/g as displayed in Fig. 4. The maximum MCL and slope observed were 240 µm and 3.1 µm/s respectively, when applying a CNCC dosage of 15 mg/g. When the addition of CNCC surpassed 30 mg/g clay, the flocculation kinetics started to be slower, resulting in smaller flocs. The largest clay/CNCC aggregates obtained correspond to the fastest flocculation kinetics as shown in Fig. 4, which was also observed by Chen and van de Ven [26].

The zeta potential of clay/CNCC fresh flocs is shown in Fig. 5a. The adsorption of CNCC resulted in a decrease of the net negative charge of clay particles, reaching the IEP or zero point charge when the CNCC dosage was 25–30 mg/g. In spite of this later fact, flocculation occurred in a much wider interval of CNCC dosages as the assessment of the supernatant turbidity reduction points out. As observed in Fig. 5a, the reduction in turbidity was over 80% when the CNCC were added at a dosage within the interval 7.5–75 mg/g. This observation suggests that differences in floc sizes observed in Fig. 3 are due to different floc conformations rather than to low flocculation efficiencies.

Yoon and Deng [17] observed that when clay/PDADMAC aggregates were exposed to high shear conditions, they were completely broken, decreasing floc size almost down to the initial size. Yet, they were reflocculated immediately (over 70% of reflocculation

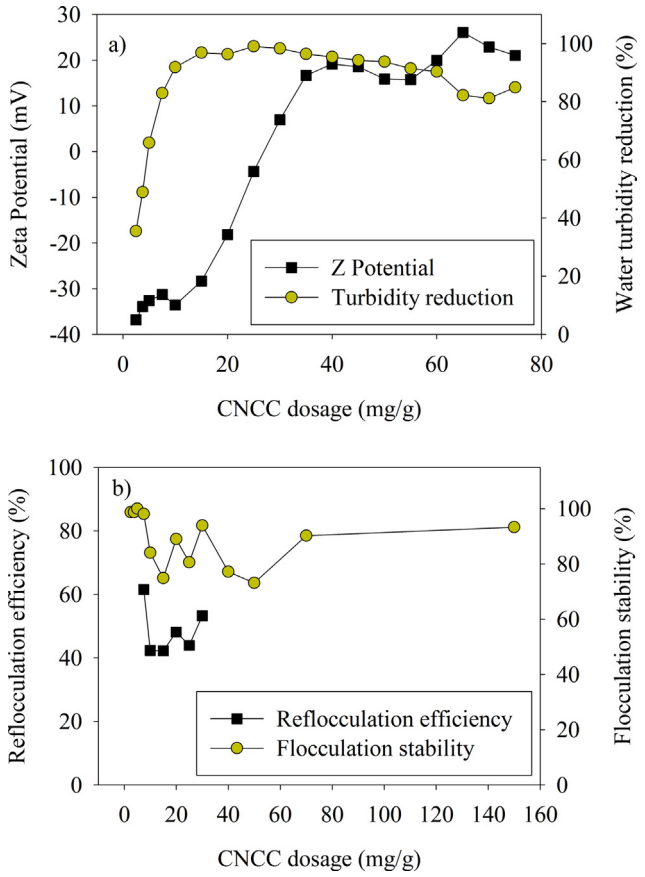

Fig. 5. (a) Zeta potential of recent flocs of clay at different CNCC dosages at pH 8.5 and (b) reflocculation efficiency and flocculation stability of flocs of clay with different CNCC dosages.

efficiency) when shear conditions were lowered again, which evidenced a charge neutralization mechanism. In the case of clay/CPAM flocs, when they were broken by exposure to high hydrodynamic shear, the bridging polymer (flocculation mechanism of CPAM) may undergo scission or reconformation (patches formation, with higher compactness) on the clay surface resulting in a loss of its initial flocculation ability (with a reflocculation efficiency below 30%) [17].

Both flocculation stability and reflocculation efficiency results are shown in Fig. 5b. Only when CNCC was added at dosages within the interval 7.5–30 mg/g, the flocs were broken with the high stirring speed and thus the reflocculation efficiency could be calculated. As displayed in Fig. 5b, the reflocculation ability of clay/CNCC flocs lies between 40 and 62% depending on the dosage, being 45% at the IEP (25 mg/g clay). These results suggest that the flocculation of clay by CNCC is not purely charge neutralization mechanism nor bridge or patch formation. The present mechanism and its variations were likely due to the different patterns of attachment that CNCC and clay may undergo as a result of both species having different charge distribution in the same particle (Fig. S4).

Regarding flocculation stability, the clay/CNCC flocs formed with all CNCC dosages presented stability values over 70% (Fig. 5b). This decrement in the MCL size with the time can be related to the reconformation of the polymer chains on the clay particles surface and/or to the break-up of the formed flocs [27]. To assess the validity of this argument, the evaluation of floc shape indicators, such as D_f is required.

3.4. Clay flocculation by CNCC: Flocs conformation

To assess the effect of the CNCC dosage on the conformation of the flocs, the flocs D_2 and D_f at the maximum MCL and at the reflocculation stage were estimated for each experiment (Fig. 6). D_2 reached a minimum value, 1.48, when CNCC was dosed at 10 mg/g. These variations agree with those of D_f obtained from a machine learning random forest regression model recently published, which correlates the average D_f of flocs with CLD at the steady state obtained by FBRM [18]. In the case of the D_f values, similar tendencies but higher differences between CNCC dosages were found, what made it easier to understand the 3D conformation of clay primary particles flocculated by CNCC.

As described above, the flocculation behavior was found to vary in three different ways depending on the CNCC dosage: <10 mg/g, 10–25 mg/g and >25 mg/g. Hence, the discussion of the floc conformation has been developed separately.

When the applied CNCC dosage is lower than 10 mg/g, the D_f was around 2, which means that compact flocs were being formed by a low number of primary particles. In this case, the size of flocs obtained by FBRM was low (Fig. 3), probably due to two size populations: the small clay agglomerates and the small flocs formed by clay and CNCC (Fig. 7a). In addition, flocculation kinetic seemed to be much slower for a higher D_f due to the larger quantity of particles required to distinctively increase the characteristic length of flocs (Fig. 3). The proposed spatial arrangement for these aggregates would start with both ends of a CNCC particle attaching to the flat area of two clay particles. However, as this structure is not inherently stable since it has a high number of degrees of freedom, the CNCC particle most likely would tend to lie between both clay surfaces, forming a compact floc like the one shown at the left of Fig. 8. The zeta potential of flocs in this dosage interval (below 10 mg/g) is apparently far from the IEP, but due to the explained conformation, it is likely that the measured zeta potential corresponds to the one of clay particles, since the CNCC would be inside a sandwich structure. Therefore, the real zeta potential would be higher than −35 mV, which is the average value for these measurements.

Generally, when flocs are more compact, they offer a higher resistance to be broken under high shear conditions, which increases their reflocculation efficiency, keeping the D_f almost invariable. Flocs were slightly broken when shear rate was increased, but bigger flocs were formed after reflocculation. It is possible that some free ends of the CNCC were able to reach a free clay particle after decreasing the stirring rate, thus keeping compact structures of similar D_f but slightly larger (Fig. 7e).

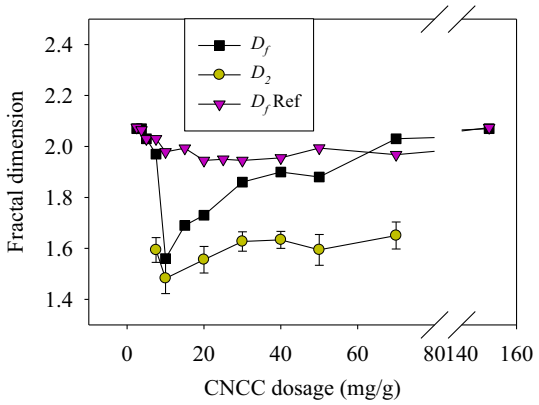

Fig. 6. Variation of flocs D_2 and D_f calculated at maximum MCL with the CNCC dosage, and 2 min after reflocculation (D_f Ref).

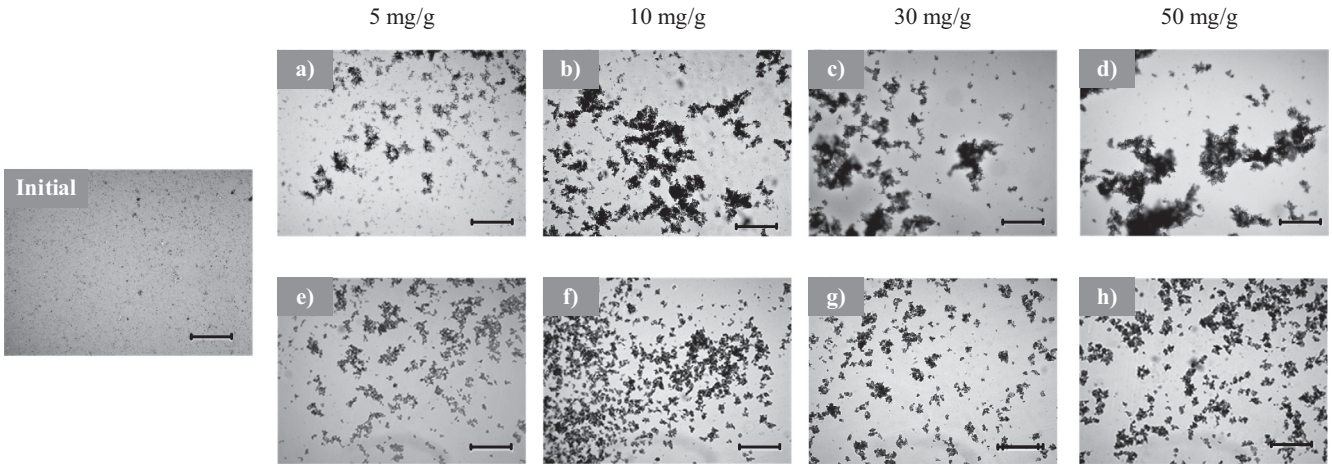

Fig. 7. Optical microscope images of clay/CNCC flocs at 5× magnification and different CNCC dosages: (a) and (d) 5 mg/g, (b) and (f) 10 mg/g, (c) and (g) 30 mg/g and (d) and (h) 50 mg/g. (a), (b), (c) and (d) pictures were taken at the MCL, while (e), (f), (g) and (h) images were taken after reflocculation. Scale bar on the images represent 100 μm.

When the CNCC dosage applied was between 10 and 25 mg/g, D_f dropped to values around 1.6, which means that a much opener structure with larger gaps among the clay particles were being formed. Now, the possibility of a clay primary particle to locate a CNCC particle is higher, so the most probable conformation is the perpendicular position of both components, as shown in the middle scheme of Fig. 8. Thus, longer structures are formed (Fig. 7b).

As explained by van de Ven [28], flocs with low D_f have faster flocculation kinetics than those with high D_f. However, the stability of these flocs is lower, thus they tend to re-conform into more compact and stable structures that correspond to higher D_f values. These flocs were, therefore, soft flocs, which break-up or re-configure with relative ease. If an elongated floc breaks up and attaches to another floc, the MCL would decrease and D_f would increase. This was the case of clay/CNCC aggregates at this CNCC dosage interval, where big flocs were formed almost instantaneously, but after reaching a maximum, the MCL slightly decreased until reaching a plateau (Fig. 3). When the shear rate was increased and afterwards decreased, the maximum size was not recovered and D_f increased up to almost 2. This means that a more compact

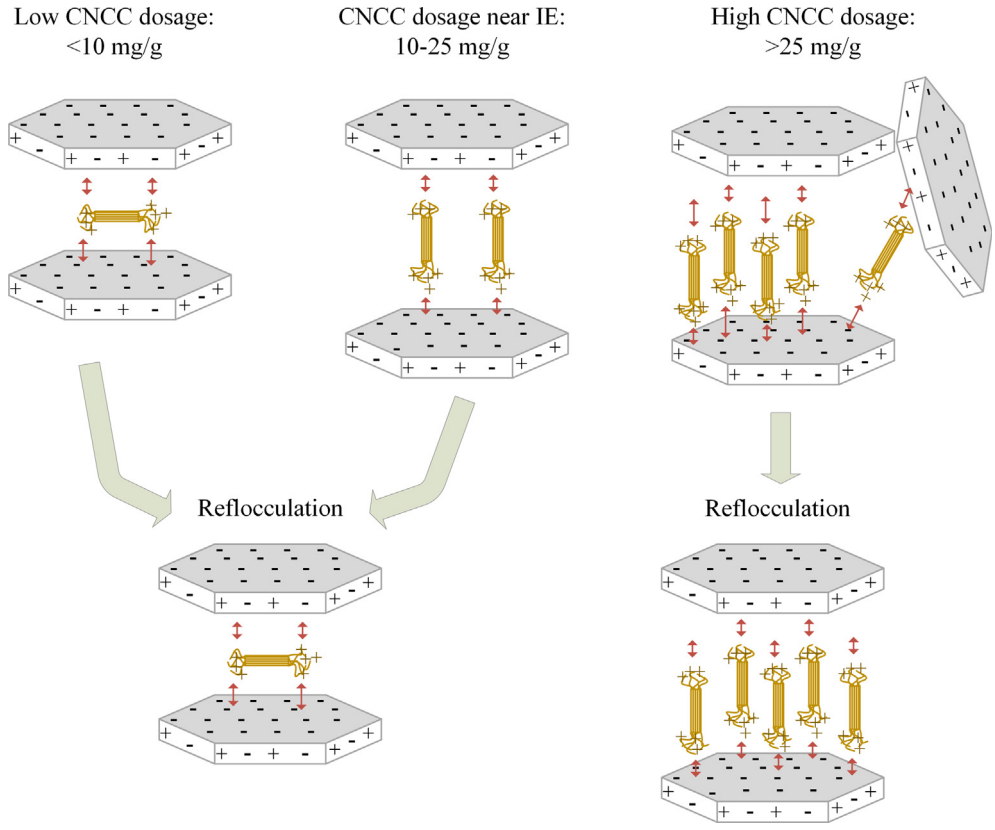

Fig. 8. Proposed conformation of clay/CNCC flocs depending on the CNCC dosage.

structure is being formed, which probably could match the final structure of flocs if the flocculation experiments were carried out for a longer time.

Finally, when the CNCC dosage was over 25 mg/g, D_f values were over 1.9, meaning compact structures were being formed again (Fig. 6). At this point, the number of CNCC particles may be higher than that of clay primary particles. The flocculation process would probably start in the same way as in the previous case, but as some CNCC could remain without joining to any clay particle, they might be attached to others forming compact flocs. This is shown in the right part of the Fig. 8. This conformation would have a large D_f since flocs were more compact, as well as larger (Fig. 7c and d). Since the positive charges of clay particles on the borders are not very frequent at neutral pH, and the positive ends of the CNCC are much more active than their neutral body, this attachment by van der Waals forces would not happen until most of the negative areas of clay particles were fully covered. It was observed that this would happen when CNCC dosage exceeds a value of 25 mg/g. At this point, it was found the IEP, which means most of the charges have been neutralized.

As these aggregates were more compact, their structure did not extensively change when they were reflocculated at high shear stress. Therefore, D_f increased only slightly, from 1.9 to 2.0. When the CNCC dosage was increased over 25 mg/g, the IEP was overpassed, reverting the bulk charge. However, the efficiency of the flocculation, measured by the turbidity removal from the initial point, was still over 90% at the CNCC dosage of 25–60 mg/g, which possibly means almost all clay particles were being flocculated, despite the charge reversibility of the system.

Finally, it is worth mentioning that for all CNCC dosages, when a high shear stress was applied and then reset to the initial one, D_f reached an almost constant value around 2 and a similar size, which indicates that the most stable conformation has been reached (Fig. 8).

Hence, the mechanism proposed in this study combines properties of both charge neutralization and bridges formation. This mechanism is different to that obtained previously, since the maximum floc size and kinetic are found at the IEP (typical of charge neutralization), but flocs were neither soft nor hard: the reflocculation efficiency was around 50%, what indicated that they rearranged their conformation after breakage (typical of bridging mechanism that turns into patches). In the case of chitosan and low charge density cationic polyacrylamide, they flocculate kaolinite mainly through a bridging mechanism, where large and hard flocs are created far from the IEP. These flocs are not much broken under shear and they recover their size by around 20% when it is released, due mainly to the reconformation of the particles [29]. However, in the case of Poly(diallyldimethylammonium chloride) (PDADMAC), a charge neutralization mechanism is observed, where smaller but softer flocs are formed at the IEP, that break almost completely under shear and recover over 90% of the initial size [17].

4. Conclusions

A novel CNCC cationic flocculant has been produced and evaluated in the flocculation of clay suspensions. The results prove that CNCC are highly effective in achieving the aggregation of clay particles, reaching high flocculation efficiencies over a wide interval of CNCC dosages (7.5–75 mg/g). The fastest flocculation processes were found when it was dosed within the interval 10–30 mg/g, corresponding to the IEP. However, the MCL before flocs breakup was not achieved after reflocculation, driving to reconformation of the CNCC/clay. Thus, a complex charge neutralization mechanism was proposed, different to that obtained previously [17,30–32].

The particular charge distribution nature of both CNCC and clay may lead to various types of aggregation, depending on the proportion between them. The D_f of the CNCC/clay flocs determined by a machine learning random forest regression model [18] was a very useful and easy tool to determine the spatial configuration patterns of the aggregates. They were classified in three main groups based on CNCC dosage. When it was 7.5 mg/g or lower, compact ($D_f = 2$) and small flocs were formed, apparently away from the IEP. Secondly, when CNCC dosage was 10–25 mg/g, D_f dropped to 1.6, implying flocs of an opener structure and faster flocculation kinetics. Finally, more complex and compact structures were found when CNCC dosage was over 25 mg/g, with D_f over 1.9 and slow flocculation kinetics, with zeta potential values over +10 mV.

It is worth mentioning that after reflocculating the clay/CNCC flocs, D_f reaches an almost constant value around 2, meaning that the most stable conformation has been reached. It is also confirmed in all cases, that flocs will tend to achieve a compact structure with time.

Finally, it can be concluded that, in the view of the results, CNCC constitutes a candidate to replace conventional wet-end retention aids, not only since it may avoid the detrimental effect of traditional polymers on paper mechanical strength [33], but also because it enables to tune the characteristics of the flocs formed to suit the industry requirements by adequately choosing the quantity of the CNCC added over a very ample interval of effective dosages.

Acknowledgements

Authors thank the Spanish Ministry of Economy and Competitiveness for the funding of the projects (Ref. CTQ2013-48090-C2-1-R and CTQ2017-85654-C2-2-R), the grant of C. Campano (BES-2014-068177) and the mobility funding (EEBB-I-17-12595); and the Community of Madrid for funding the RETO-PROSOST-CM (S2013/MAE-2907). Theo van de Ven acknowledges support of a NSERC Discovery grant (42686-13).

Appendix A. Supplementary material

Supplementary data to this article can be found online at https://doi.org/10.1016/j.jcis.2019.02.097.

References

[1] H. Yang, T.G.M. van de Ven, Cellulose 23 (3) (2016) 1791–1801.
[2] D.Z. Chen, T.G.M. van de Ven, Cellulose 23 (2) (2016) 1051–1059.
[3] Q.X. Hou, W. Liu, Z.H. Liu, L.L. Bai, Ind. Eng. Chem. Res. 46 (23) (2007) 7830–7837.
[4] H. Liimatainen, J. Sirvio, H. Pajari, O. Hormi, J. Niinimaki, J. Wood Chem. Technol. 33 (4) (2013) 258–266.
[5] B.R. Sharma, N.C. Dhuldhoya, U.C. Merchant, J. Polym. Environ. 14 (2) (2006) 195–202.
[6] W.M. Bundy, J.N. Ishley, Appl. Clay Sci. 5 (5) (1991) 397–420.
[7] B. Alince, T.G.M. van de Ven, J. Colloid Interface Sci. 155 (2) (1993) 465–470.
[8] M. Mihai, E.S. Dragan, Colloids Surf., A 346 (1) (2009) 39–46.
[9] A. Balea, A. Blanco, N. Merayo, C. Negro, Appita J. 69 (2) (2016) 148–156.
[10] M. Diab, D. Curtil, N. El-shinnawy, M.L. Hassan, I.F. Zeid, E. Mauret, Ind. Crops. Prod. 72 (2015) 34–45.
[11] H. Yang, M.N. Alam, T.G.M. van de Ven, Cellulose 20 (4) (2013) 1865–1875.
[12] D.Z. Chen, T.G.M. van de Ven, Colloid Surf. A-Physicochem. Eng. Asp. 506 (2016) 789–793.
[13] A. Blanco, C. Negro, A. Hooimeijer, J. Tijero, Appita J. 49 (2) (1996) 113–116.
[14] V. Kumar, M.K. Taylor, A. Mehrotra, W.C. Stagner, AAPS PharmSciTech. 14 (2) (2013) 523–530.
[15] A. Blanco, E. De la Fuente, C. Negro, M.C. Monte, J. Tijero, Tappi J. 1 (10) (2002) 14–20.
[16] N. Merayo, A. Balea, E. de la Fuente, Á. Blanco, C. Negro, Cellulose 24 (2) (2017) 677–692.
[17] S.Y. Yoon, Y.L. Deng, J. Colloid Interface Sci. 278 (1) (2004) 139–145.
[18] P. Lopez-Exposito, C. Negro, A. Blanco, Algal Res. 37 (2019) 240–247.

[19] C. Campano, R. Miranda, N. Merayo, C. Negro, A. Blanco, Carbohyd. Polym. 173 (2017) 489–496.
[20] S. Safari, A. Sheikhi, T.G.M. van de Ven, J. Colloid Interface Sci. 432 (2014) 151–157.
[21] H. Yang, T.G.M. van de Ven, Biomacromolecules 17 (6) (2016) 2240–2247.
[22] M. Tavakolian, J. Lerner, F. Medina, J. Frances, T.G. van de Ven, A. Kakkar, J. Colloid Interface Sci. (2019).
[23] F. Cherhal, F. Cousin, I. Capron, Langmuir 31 (20) (2015) 5596–5602.
[24] R. Gaudreault, N. Di Cesare, D. Weitz, T.G.M. van de Ven, Colloid Surf. A-Physicochem. Eng. Asp. 340 (1–3) (2009) 56–65.
[25] F. Bergaya, G. Lagaly, Developments Clay Sci. 1 (2006) 1–18.
[26] D.Z. Chen, T.G.M. van de Ven, Colloid Surf. A-Physicochem. Eng. Asp. 504 (2016) 11–17.
[27] M.G. Rasteiro, F.A.P. Garcia, P. Ferreira, A. Blanco, C. Negro, E. Antunes, Powder Technol. 183 (2) (2008) 231–238.
[28] T.G.M. van de Ven, Colloidal Hydrodynamics, Academic Press, 1989.
[29] J. Li, S. Jiao, L. Zhong, J. Pan, Q. Ma, Colloids Surf., A 428 (2013) 100–110.
[30] M.H. Gorakhki, C.A. Bareither, Appl. Clay Sci. 114 (2015) 593–602.
[31] M.S. Zbik, R.S.C. Smart, G.E. Morris, J. Colloid Interface Sci. 328 (1) (2008) 73–80.
[32] R. Divakaran, V.N. Sivasankara Pillai, Water Res. 35 (16) (2001) 3904–3908.
[33] N. Merayo, A. Balea, E. de la Fuente, Á. Blanco, C. Negro, Cellulose 24 (7) (2017) 2987–3000.

PUBLICATION VII

Hairy cationic nanocrystalline cellulose as retention additive in recycled paper

Cristina Campano, Patricio Lopez-Exposito, Angeles Blanco, Carlos Negro, Theo G.M. van de Ven

https://doi.org/10.1007/s10570-019-02494-x

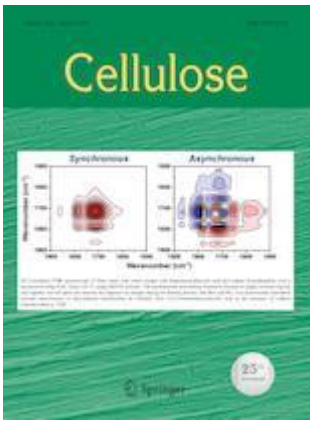

Impact factor 2017: ***3.809***

JCR, Materials Science, paper & wood, 1 out of 21, ***Q1***

Cellulose
https://doi.org/10.1007/s10570-019-02494-x

ORIGINAL RESEARCH

Hairy cationic nanocrystalline cellulose as retention additive in recycled paper

Cristina Campano · Patricio Lopez-Exposito · Angeles Blanco · Carlos Negro · Theo G. M. van de Ven

Received: 2 January 2019 / Accepted: 8 May 2019

Abstract Hairy cellulose nanocrystalloids (HNC) are a brand new family of nanocellulose characterized by having functionalized amorphous poles joined by a crystalline shaft. In this paper we hypothesize that cationic HNC (CNCC) could be used as an effective retention agent in papermaking. To investigate this, we first flocculated a suspension of only fillers, namely kaolinite and $CaCO_3$, and second, a suspension of recycled fibers, with CNCC. It was monitored by photometric dispersion analysis and laser focused beam reflectance. The flocculation mechanism was assessed by means of zeta potential, reflocculation efficiency, flocculation stability and optical microscopy. Finally, the effect of CNCC on drainage, retention and paper mechanical properties was studied. CNCC were found to heteroflocculate fillers at a wide range of dosages, finding a maximum floc size at a dosage of 30 mg/g. On the other hand, the maximum floc size when flocculating the pulp suspension, was found at a lower CNCC dosage (20 mg/g). In this case, fillers were being attached to the exterior surface of the fibers. In both systems, the maximum size increment was observed at the isoelectric point, so a charge neutralization mechanism was proposed. The addition of CNCC not only improved filler retention, but also pulp drainage by reducing these times. Moreover, although mechanical properties of the handsheets were affected by the presence of CNCC, this effect was much lighter than that caused by traditionally used retention systems. Hence, CNCC could replace many additives used in the wet-end of a paper machine, thus simplifying its operation.

C. Campano · P. Lopez-Exposito · A. Blanco (✉) · C. Negro
Department of Chemical Engineering, Complutense University of Madrid, Avda. Complutense s/n, 28040 Madrid, Spain
e-mail: ablanco@ucm.es

T. G. M. van de Ven
Department of Chemistry, Pulp and Paper Research Centre, and Quebec Centre for Advances Materials, McGill University, 3420 University Street, Montreal, QC H3A 2A7, Canada

Published online: 20 May 2019

Graphical abstract

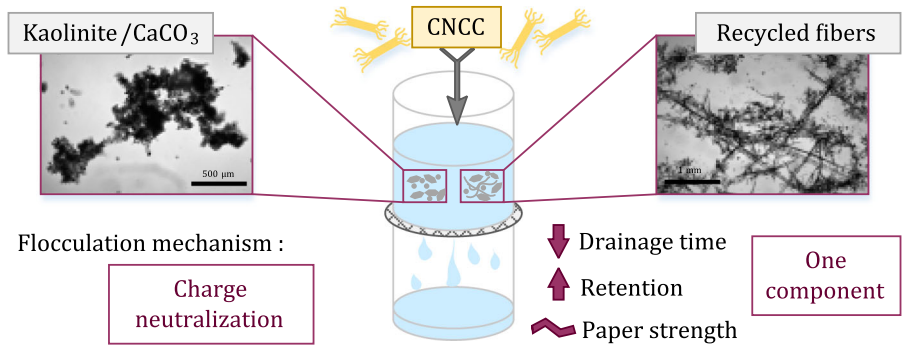

Keywords Hairy cationic nanocrystalline cellulose · Recycled paper · Retention system · Fillers flocculation · Drainage and retention · Fibers flocculation

Introduction

Paper is one of the oldest and leading recycling industries, mainly due to economic and environmental issues (Blanco et al. 2013). In Europe, the recycling rate achieved 72.3% in 2017, which represent an increase of 20.5% since the year 2000 (CEPI 2017). Typically, recycled newsprint paper presents a filler loading of 15–20% that reduces considerably the costs of the process (Raymond et al. 2004). Additionally, they also enhance the optical properties, as well as some physical properties such as bulk and smoothness. Nevertheless, their retention needs the addition of a retention system (RS) of cationic charge (Diab et al. 2015).

The mineral fillers used most frequently are kaolin and calcium carbonate, while others such as talc or titanium dioxide are also used but to a lower extent (Lourenco et al. 2014). Kaolin and talc are often used in view of their low price, but they might not fulfill the optical requirements. While $CaCO_3$, in the form of precipitated calcium carbonate, is increasingly used to increase paper brightness.

One of the main consequences of the increasing recycling rate is the deterioration of the fibers during the different chemical, mechanical and thermic treatments (Hubbe et al. 2007; Miranda and Blanco 2010). To increase the mechanical strength of the paper, different strengthening agents are being used. Among the emerging trends is the use of nanocellulose (Habibi 2014). Cellulose nanofibers (CNF), cellulose nanocrystals (CNC) and bacterial cellulose have a high potential to improve mechanical, barrier and some special properties (Balea et al. 2016a; Campano et al. 2018a, b; Yousefi et al. 2013). However, the application of nanocellulose in the papermaking process is associated with a detrimental effect on drainage (Merayo et al. 2017a; Taipale et al. 2010).

Hairy cellulose nanocrystalloids are a brand new family of nanocellulose obtained by a periodate oxidation of cellulose. They present amorphous edges joined by a crystalline shaft (van de Ven and Sheikhi 2016). These edges can be functionalized with different agents to confer special behavior. When those are modified through a Schiff base reaction with a cationic agent, these amorphous regions acquire a positive charge, while maintaining a neutral crystalline body (Yang and van de Ven 2016). They have been called previously cationic hairy cellulose nanocrystalloids (CNCC). Although other types of hairy cellulose nanocrystalloids, such as sterically and electrosterically stabilized nanocrystalline cellulose (SNCC and ENCC, respectively), have been proved to flocculate calcium carbonate particles (Chen and van de Ven 2016a, b), the use of CNCC as flocculant has not been reported yet. In view of their positive surface charge, located on the amorphous regions of the particles, they could potentially be used as a RS during papermaking at the time that the nanocellulose improves paper properties.

In this study, the applicability of the CNCC as a retention agent for recycling paper (RP) industries was assessed. We hypothesized that CNCC could replace

wet-end additives typically used in papermaking industries, such as coagulants, polyacrylamides, bentonites, starches, etc., improving the critical operations of drainage and filler retention, as well as the mechanical properties of the final paper. For this purpose, we first study the flocculation efficiency of the CNCC in a suspension containing both kaolinite and calcium carbonate. Photometric dispersion analysis and laser reflectance were used to monitor the flocculation process. Thereafter, CNCC were also assayed to flocculate a suspension made of RP containing these fillers. Finally, their effect on the pulp drainage, fillers retention and mechanical properties of the final paper was studied.

Materials and methods

Materials

The raw material used for CNCC preparation was a softwood kraft pulp supplied by Domtar, Canada. Deinked newspaper with an ISO brightness of 56% and 14.0 wt% ash content was used as model of RP, and it was kindly supplied by Holmen Paper Madrid. Chemicals used for the different reactions, sodium (meta) periodate, GT [(2-hydrazinyl-2-oxoethyl)-trimethylazanium chloride, GT], ethylene glycol, hydroxylamine hydrochloride, $AgNO_3$ and hydrochloric acid (0.1 M) and sodium hydroxide (0.1 M) were supplied by Sigma Aldrich (analytical reagent grade) and used without further modification. Propanol and sodium chloride were purchased from ACP Chemicals Inc. Kaolinite and precipitated calcium carbonate were supplied by Sigma Aldrich. Kaolinite has a zeta potential in suspension of − 32.1 mV and an average diameter of 460 nm. On the other hand, precipitated calcium carbonate presented a zeta potential of − 18.3 mV and an average diameter of 4.5 μm.

Production and characterization of CNCC

The procedure followed to produce CNCC has been adapted from Yang and van de Ven (2016). First, the pulp was soaked in water and disintegrated at 3000 rpm for 10 min. Then, it was added to a solution of 0.98 g $NaIO_4$ and 0.78 g NaCl per gram of dry pulp and left to react for 24 h, stirring at 100 rpm at room temperature and with protection from light. After that time, 1 mL of ethylene glycol was added to quench the residual periodate. Finally, the produced dialdehyde modified cellulose (DAMC) fibers were washed with distilled water by filtration.

Second, the DAMC fibers were cationized by means of reaction with 1 g GT and 2.4 g NaCl per gram of dry DAMC, and pH was adjusted to 4.5 with HCl. After 24 h of reaction under stirring conditions at room temperature, the cationic DAMC (CDAMC) were washed with abundant water by filtration and submitted to a thermic treatment at 60 °C for 2 h. Finally, high intensity sonication was applied to the sample for 10 min, with an Ultrasonic Processor UP200H, supplied by Hielscher Ultrasonic GmbH (Teltow, Alemania). To remove the non-fibrillated fraction and therefore isolate the CNCC, the sample was centrifuged at 5000 rpm for 10 min.

The aldehyde content of the DAMC fibers was determined according to Yang et al. (2013). The process yield was calculated as the ratio between the final dry mass of CNCC and the initial amount of pulp. To assess the nanofibrillation degree, the proportion between the dry mass of the supernatant after centrifugation and the initial dry mass before this step was determined.

The cationization degree of the CNCC was determined by means of conductometric titration of the trimethylazanium chloride groups with 10 mM $AgNO_3$. The analysis was conducted on a Metrohm 836 Titrando Instrument (Herisau, Switzerland). Zeta potential of the CNCC sample at 0.1% concentration was measured with a ZetaPlus analyzer supplied by Brookhaven Instruments Corporation (New York, USA).

Morphology and particle size was assessed by atomic force microscopy (AFM) with a MultiMode 8 from Bruker, in PeakForce mode. A drop of 20 μL of 0.005% CNCC was deposited on a clean mica surface and left to dry at room temperature. Then, it was placed in an oven at 60 °C overnight before analysis. Characterization results of the CNCC particles are shown in Table 1.

RP fillers determination and characterization

$CaCO_3$ and kaolinite percentages were determined through ash measurements of the RP at 525 °C and 900 °C, according to ISO 1762 and ISO 2144. As stated in ISO 2144, both fillers do not decompose at

Table 1 Results for CNCC characterization

Property	Value	Units
Aldehyde groups	3.84	mmol/g
$NaIO_4$ reaction conversion	41.5	%
Process yield	54.9	%
Nanofibrillated yield	54.3	%
Cationic groups	1.31	mmol/g
Cationization reaction conversion	33.4	%
Zeta Potential	+ 14.5	mV
Width	4.67 ± 1.56	nm
Length	379 ± 121	nm

525 °C, but after the treatment at 900 °C, only 56% of $CaCO_3$ and 86-89% of kaolinite are retained. Therefore, the calculation of the filler contents has been made according to these proportions. The amount of fillers present in the RP was 13.9%, of which 30.4% was $CaCO_3$ and 69.6% kaolin. The zeta potential of kaolinite was found to be − 32 mV and its equivalent spherical diameter, determined by dynamic light scattering (DLS), was 400 nm. $CaCO_3$ at the same conditions had a zeta potential of − 10.4 mV and an equivalent spherical diameter of 550 nm.

Flocculation of fillers induced by CNCC

The flocculation kinetics of fillers with CNCC was monitored by Photometric dispersion analysis (PDA) and laser reflectance. PDA experiments were performed with a PDA 2000, supplied by Rank Brothers (Cambridge, UK). This equipment provides the ratio of RMS to DC, where RMS is the root mean square of the fluctuations in transmitted light and DC refers to the average transmittance. With increasing floc size, the RMS/DC ratio (a measure of the fluctuations in light transmittance relative to the average transmittance) increases, indicating flocculation is taking place. More details can be found in a previously published study (Chen and van de Ven 2016b).

A suspension of 1 g/L containing 70% kaolinite and 30% $CaCO_3$ was prepared for the flocculation studies. These percentages were close to those obtained from the initial amount of mineral fillers and the amount obtained from ash measurements. 200 mL of the described suspension were placed in a 600 mL beaker stirred by magnetic agitation at 100 rpm. The suspension was pumped at 150 mL/min with a standard 3 mm internal diameter tube, through the photocell of the PDA, flowing back to the test beaker. After 120 s of measurement, a CNCC dose was added to the suspension, recording the RMS/DC ratio each 5 s for 10 min.

In addition, the flocculation efficiency was also assessed in real time by the evolution of the mean chord length (MCL) using a focused beam reflectance measurement (FBRM) M500L, manufactured by Mettler Toledo (Columbus, USA) (Blanco et al. 1996). The probe projects a rotating laser beam at a fixed speed into the sample suspension and records the time that the beam is intersecting with a particle, which is being translated into a chord length (Kumar et al. 2013). In the present study, the probe software classified the detected chord lengths in 200 size intervals organized logarithmically, ranging from 1 to 4000 μm (Blanco et al. 2002).

200 mL of the filler suspension were poured in a 600 mL beaker and stirred at 100 rpm. After 120 s of monitoring, the required CNCC dosage was added to the suspension and the MCL was recorded each 5 s for 10 min. After that, the stirring speed was increased to 350 rpm for 2 min and then decreased back to 100 rpm for 4 min more.

The flocculation stability was determined from Eq. (1)

$$Flocculation\ stability(\%) = \frac{MCL_e - MCL_0}{MCL_m - MCL_0} \cdot 100 \quad (1)$$

where MCL_e is defined as the MCL after 10 min, MCL_0 is the MCL before CNCC addition and MCL_m the maximum MCL.

The refflocculation efficiency was calculated by Eq. (2) (Yoon and Deng 2004).

$$Reflocculation\ efficiency(\%) = \frac{MCL_F - MCL_B}{MCL_e - MCL_B} \cdot 100 \quad (2)$$

where MCL_F is defined as the maximum MCL after the decrease of the stirring speed back to 100 rpm, and MCL_B is the MCL after breaking the flocs at high stirring speed (350 rpm).

Flocculation of RP with CNCC

Flocculation of RP pulps suspensions were only monitored by FBRM since the size of the fibers does not allow them to flow through the tube of the PDA. In this case, a suspension of disintegrated RP at a consistency of 0.5% was prepared. The initial stirring speed was set to 200 rpm to ensure a complete homogenization of the suspension, then increased to 500 rpm and decreased back to 200 rpm.

Floc characterization

Zeta potential

An aliquot of the formed flocs during the FBRM experiments was extracted from the beaker at the maximum flocculation point and at the reflocculation stage. The zeta potential of these samples was determined with a NanoBrook 90Plus supplied by Brookhaven Instruments Corporation (NY, USA).

Optical microscopy

An extra aliquot was extracted at the same points than the described above, for image analysis. Optical microscopy was used, through a Zeiss Axio Lab 10 microscope (Oberkochen, Germany).

Drainage and retention assessment

The efficiency of CNCC on pulp drainage was determined with a MütekTM DFR-05 supplied by (Säffle, Sweden). First, 500 mL of a RP suspension at 0.5% consistency was added to the agitation chamber and stirred at 300 rpm for 90 s. Then, the CNCC at the required dosage was added and after other 60 s, the suspension was filtrated by gravity through a 150 mesh. The drained weight was monitored each 0.2 s for 240 s. To compare the efficiency of the different experiments, the time spent in the filtration of 300 g of the sample was determined (W300).

Drained samples were collected to determine the retention of solids in the paper wet-web. A known amount of a collected sample was left to dry at 105 °C overnight and the total solid content was determined. Then, the dry sample was placed in a muffle furnace at 525 °C for 4 h, to determine the mineral filler content according to ISO 1762. Finally, to differentiate between kaolinite and $CaCO_3$ contents, ash at 900 °C was determined according to ISO 2144. Again, it was assumed that both fillers do not decompose at 525 °C, but 56% of $CaCO_3$ and 86–89% kaolinite remained in the sample at 900 °C.

Handsheet formation and characterization

RP was disintegrated at 1% of consistency for 1 h. Then, different proportions of CNCC were added to the pulp, [5, 20 and 45 mg/g (0.5, 2 and 4.5%, respectively)], and stirred for 60 s. Then, handsheets of a basis weight of 60 g/m^2 were formed in a normalized Rapid-Köthen handsheet former (PTI, Vorchdorf, Austria), according to ISO 5269/2 (2004).

The formed handsheets were conditioned at 23 °C and 50% humidity for 24 h before grammage determination, according to ISO 536. Tensile and tear strengths were determined according to ISO 1924-2 and ISO 1974, and their indexes were calculated dividing the strengths by their corresponding basis weight.

The proportion of solids that were retained during handsheet formation was determined through the relation between the dry weight after and before formation. Similarly, filler retention was calculated as the proportion between the amount of fillers present in the prepared handsheets and that contained in the pulp before paper formation.

Results and discussion

Fillers flocculation

Figure 1 shows the evolution of the ratio between RMS and DC with time at different CNCC dosages. As described previously, the RMS/DC ratio indicates the relative size in arbitrary units of the suspension. With PDA technology, a very sensitive change in the floc size is detected.

Results showed an almost instantaneous flocculation after the addition of CNCC for all dosages assayed (Fig. 1). The initial slope increased with the CNCC dosage until reaching a maximum with 20 mg/g after 35 s of measurement. Although the ratio caught up a similar value for the dosages of 10 and 15 mg/g, a higher slope, indicating a higher flocculation rate, is often desired. Higher CNCC dosages induced a slower

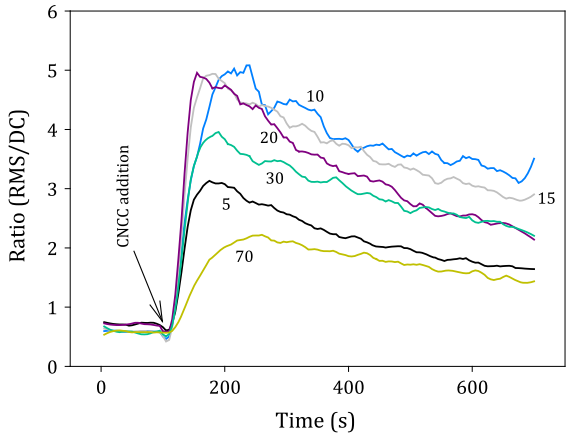

Fig. 1 Evolution of the ratio (RMS/DC) of the flocculation of clay and calcium carbonate with CNCC dosages between 5 and 70 mg/g monitored by PDA. Numbers presented in the graph show the CNCC dosage used for each experiment in mg/g

flocculation with smaller flocs. Although a higher process efficiency was accomplished for the described dosages, flocculation took place for a very wide range of dosages, namely 5–70 mg/g. Thus, a more in depth study of the floc size and flocculation trajectory was performed with FBRM.

The flocculation of kaolin and $CaCO_3$ induced by CNCC as measured by FBRM is shown in Fig. 2a, which shows MCLs for various CNCC dosages. It can be seen that maximum flocculation rates are observed for dosages between 20 and 80 mg CNCC/g fillers, as the initial slopes are identical within experimental error. This is different from the observations made with the PDA, where the fastest flocculation was found at 20 mg/g. This could be due to a bias in PDA measurements towards larger particles, which scatter more light.

Considering the FBRM graphs as well as the data extracted from these experiments, which were zeta potential at the maximum MCL and at the reflocculation stage and the reflocculation efficiency (Fig. 2), results have been classified into three different groups in terms of CNCC dosage: (a) < 30 mg/g, (b) around 55 mg/g and (c) > 80 mg/g. They have been discussed separately, considering the three different behaviors observed in Fig. 2.

In the first group flocculation started immediately after the CNCC addition, but the MCL decreased after reaching the maximum value, with floc stability of around 75%. The zeta potential measured at the maximum MCL resulted in a value very similar to that of the initial suspension, reaching a value near zero at a dosage of 30 mg/g. Two simultaneous steps contributed to the flocculation process: floc formation and break-up, usually resulting in a dynamic equilibrium associated with a plateau at long times (Chen and van de Ven 2016a). However, in this group, a plateau was not observed, instead a maximum was noted, indicating that the conformation (structure) of the flocs initially formed changed with time. A possible explanation for this behavior could be a change in the way that the CNCC were being deposited on the kaolin/$CaCO_3$ particle surfaces. The CNCC would be likely standing up in the first instance, with the positive hairs contacting the negative filler surfaces, bridging the different particles. Subsequently they would lie down between them, thus decreasing the gap between flocculated filler particles (provided there is enough spaced), since this is the most stable form. This is likely to occur since the CNCC amount was not high enough to cover completely all the particles. Thus, since most CNCC particles are bridging fillers, the outside of all particles is little affected, resulting in a zeta potential (Fig. 2b) similar as the initial one.

Both fillers had different hydrodynamic diameters, being 460 nm for kaolin and 4500 nm for $CaCO_3$. In addition, they differ in shape and surface charge, what makes them move with a different trajectory during flocculation. On the one hand, particles of kaolin have an active plane surface with thin borders ($\sim$ 100 nm) and a bulk zeta potential of $-$ 32 mV. On the other hand, $CaCO_3$ are porous and round with a bulk zeta potential of $-$ 18.3 mV. Since both types of particles are negatively charged, there is no energy barrier between (cationic) CNCC and filler. Thus, the rate of deposition of CNCC on filler particles is simply mass transport limited.

When shear rate is increased to 350 rpm and then ceased back to 100 rpm, flocs did not reach the initial size, decreasing their MCL with a reflocculation efficiency lower than 40%. As observed by Bergaya and Lagaly (2006), kaolinite particles present a charge distributed heterogeneously over the particles. At the working pH of this study, 8.5, the flat area of the particles is completely negative, while the borders present an almost neutral charge, with some negative and some positive spaces. Thus, an initial agglomeration between kaolinite and $CaCO_3$ could be present, showing a MCL bigger than the one that would

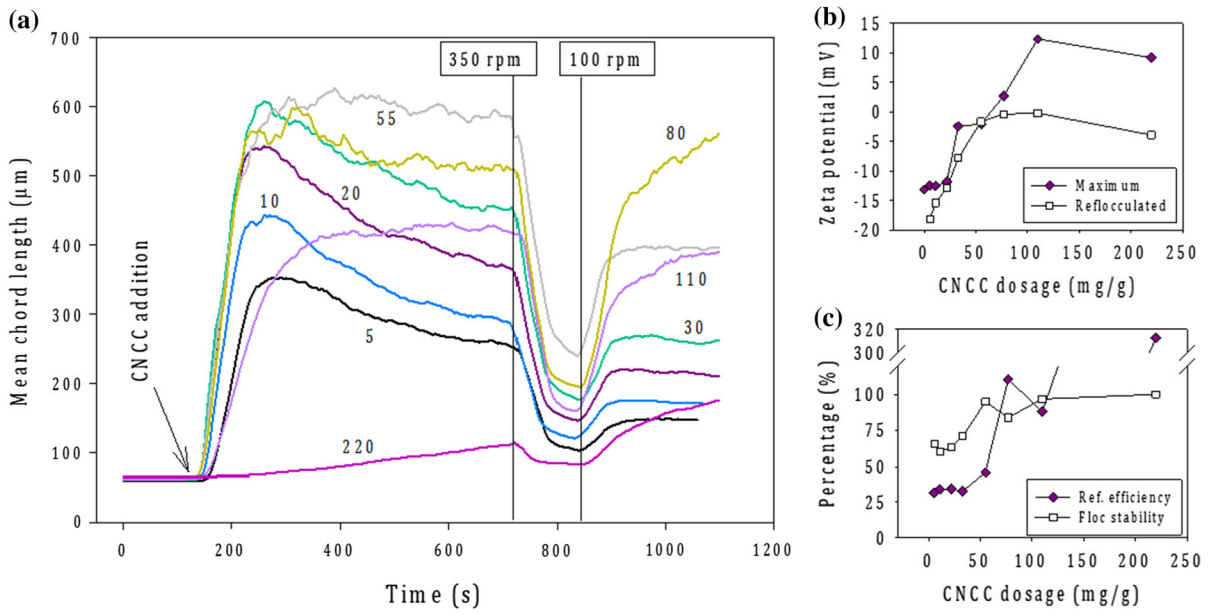

Fig. 2 **a** Mean chord length (MCL) profiles of flocs produced in the flocculation of clay and $CaCO_3$ using CNCC. Numbers indicated in the graph represent the CNCC dosage used for each experiment, expressed in mg/g. Vertical lines represent an external action on the experiment: first, CNCC addition after 100 s, increasing the shear rate to 350 rpm and third, the reduction in the stirring speed back to 100 rpm. **b** Zeta potential of flocs extracted from the FBRM experiments at the maximum MCL and at the reflocculation stage for different dosages of CNCC and **c** Reflocculation efficiency and flocculation stability of flocs at different CNCC dosages

correspond for completely dispersed suspensions. With increasing shear, not only the flocs induced by CNCC can be broken, but also those initially present. Then, newly formed negative surfaces are now available, thus decreasing the bulk zeta potential (Fig. 2b) as well as the bulk floc size.

At a CNCC dosage of 55 mg/g, a dosage corresponding to the second group alluded to above, the zeta potential was close to zero at both maximum MCL and reflocculation stages. In the second group flocculation started immediately after the CNCC addition as before, but in this case, flocs remained stable for about 10 min of observation. As in the previous group, flocculation started likely by the orthogonal deposition of the CNCC on the flat surfaces of the kaolin and $CaCO_3$. However, as the used dosage is higher, flocs could evolve in two ways: fewer CNCC particles may have fallen down, thus preventing reconformation of flocs or multiple CNCC particles could have bridged the fillers, forming stable structures. Here, an equilibrium between floc formation and break-up was reached, indicated by a plateau in the MCL profile.

As the stability of flocs was higher at this dosage, the flocs were also broken when shear rate was increased, but much less than in the previous scenario. After reducing the shear, flocs recovered their size by 50%. It is probable that when flocs were broken, the CNCC remained attached by one end to either a kaolin or a $CaCO_3$ particle, while the other edge was free. Since the released spots on the particle were quite small considering the diameter of the CNCC, there was a low probability that the free CNCC edges filled the gaps in the same way as before. Thus broken flocs would maintain a similar shape and size in the reflocculation stage, recovering only 50% of the size reached before the deflocculation stage. Also initially flocculation rates are determined by adsorption of CNCC on fillers. During reflocculation we deal mainly with collisions between "sticky" flocs, with different formation and break-up kinetics.

Finally, when the CNCC dosage was higher than 80 mg/g, namely the third group, the behavior was quite different to those described previously. Here, the flocculation was retarded with the increasing CNCC dosage. Charge reversal was probably the cause for this slowness. Hence, initial flocs of small size were

formed, where charge was not distributed homogenously in the structure. First, as said before, CNCC would attach orthogonally to the particles, creating open flocs. As the particles were moving continuously, it is probable that some of them collided with the already formed floc, forming a kind of structure that had a porous interior and an external surface with a highly positive charge density. As the zeta potential only measures the charge of the external surface, a positive zeta potential was measured (Fig. 2b). Nevertheless, these flocs were broken at a higher shear rate, making the interior charge accessible so that when the surface of one floc collides with another, they create bonding by electrostatic attraction resulting in bigger flocs. This fact was observed in the FBRM graphs (Fig. 2a), where MCL was increased to values even larger than before breaking the flocs, without reaching a plateau. Positive charges measured at the maximum MCL were neutralized in the reflocculating stage, obtaining zeta potentials near the IEP.

Optical microscopy was used to test these explanations. Figure 3 shows an increasing floc size at the maximum MCL when CNCC dosage was further increased, till a maximum was obtained at a dosage of 55 mg/g (IEP). An increasing compactness in the flocs was also observed by the darkness of the flocs (Rasteiro et al. 2008). However, when the CNCC dosage is further increased beyond the IEP, flocs were becoming smaller and more spherical instead of forming elongated structures such as at the IEP.

After the reflocculation stage, the floc size decreased for the first and second group of dosages, matching with the low reflocculation efficiency found before. The opposite case was found for dosages over 110 mg/g, where the floc reconformation by the bonding between the exterior areas of the flocs and the released interior ones caused an increase in the floc size.

As can be concluded from this study, the mechanism of action of these CNCC is likely charge neutralization. The fact that the maximum floc size was obtained at the IEP and that there was a charge reversal with higher CNCC dosages are characteristic points of the charge neutralization mechanism. Hence the initial flocculation appears to be due to charge neutralization. However, when samples were broken up and reflocculated, the positive charge changed to neutral and the floc size was increased. This is likely due to negative patches within the flocs, which became exposed upon floc break-up and which collided with positive (CNCC-covered) patches upon reflocculation, forming CNCC bridges between the fillers. The flocs formed in the initial stage seemed to be soft, in view of the pronounced decrease in the floc MCL when the shear rate was increased. They did not recover their final size after re-establishing the initial shear rate, which implies that the flocs changed their structure under high shear, presumably by reducing the floc size by forcing CNCC particles, which bridged fillers in a perpendicular orientation, to lay flat.

Flocculation of recycled paper

Figure 4a shows the evolution of the MCL with time when different CNCC dosages were added to the pulp. Again, an immediate increase in the floc size was observed even when a low amount of CNCC was added. An increase in the CNCC dosage was translated into a consequent increase in the MCL, till a maximum of 76 μm was reached at a CNCC dose of 20 mg/g. Compared to the maximum MCL observed in the flocculation experiments with only kaolinite and $CaCO_3$, 620 μm (Fig. 2a), this was much lower. However, in pulp fiber suspension MCL measures mainly the diameter of the fibers since it is unlikely that the fast rotating focused beam travels along the full length of a fiber (Blanco et al. 2002; Wu and van de Ven 2009) and hence the MCL of the pulp flocculation measured by FBRM probably reflects an increase in the fiber width together with the fines/fillers agglomerates size. Presumably the floc size is lower in the presence of RP, because there is a competition between filler flocculation and the deposition of filler aggregates on fibers. Fillers cannot grow till the same size, because they deposit on fibers before they can grow bigger.

This fact matches with the images taken by optical microscopy (Fig. 5). It was observed in the picture of the initial sample that the RP fibers, the fines and the fillers remained dispersed in the suspension. However, after CNCC addition, fillers and fines contained positive CNCC particles on their surface, allowing them to deposit on the fibers increasing the effective diameter of the fibers, and consequently the MCL. At the dosages that the maximum MCL was obtained, 20 and 25 mg/g, the fillers seem to be coating the fibers,

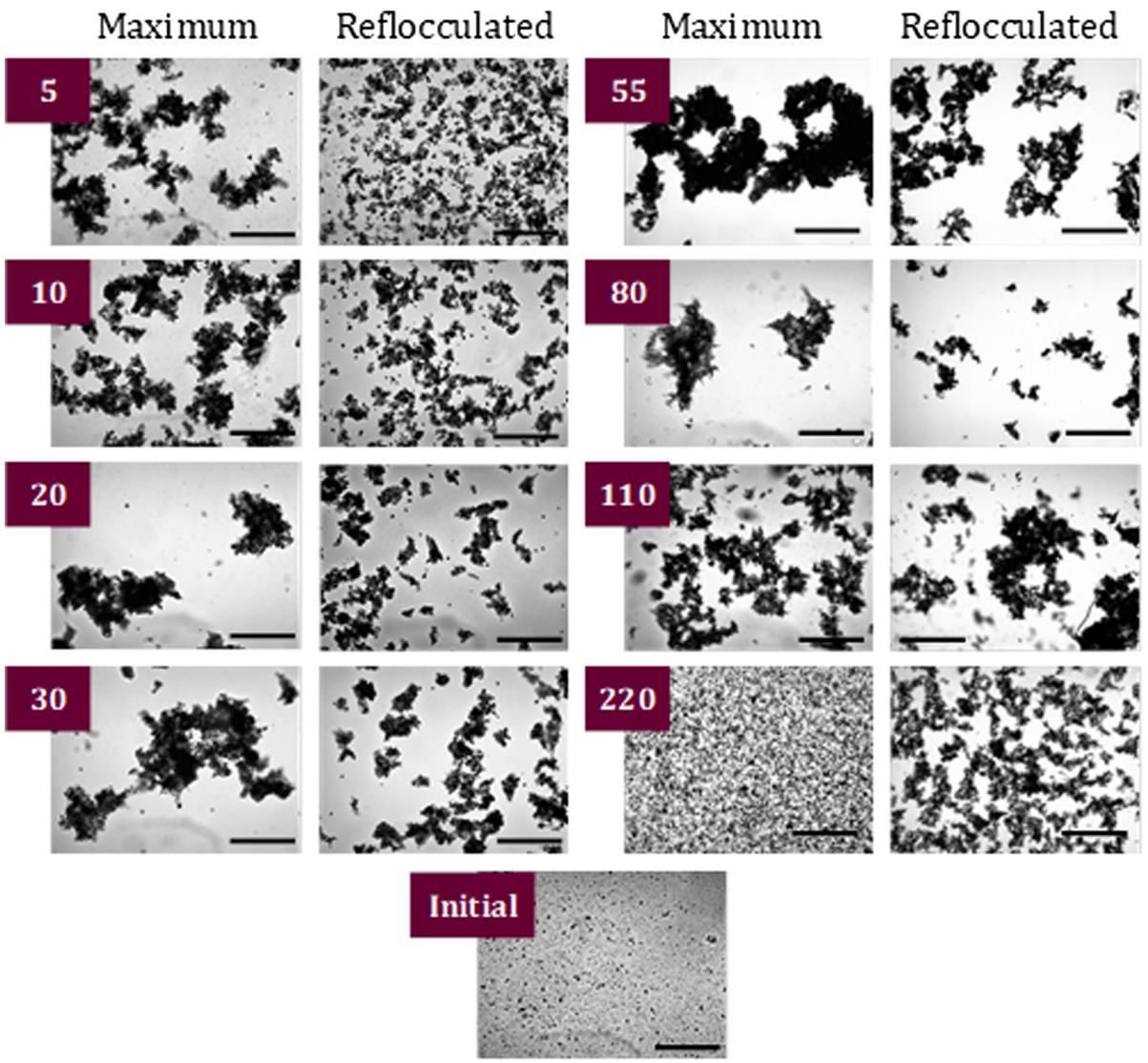

Fig. 3 Optical microscope images of $CaCO_3$–clay flocs formed at different CNCC dosages at the maximum MCL point and at the reflocculation stage. Numbers indicated in the pictures represent the CNCC dosage corresponding to each experiment. Scale bar of the images for the initial sample and the CNCC dosages between 5.5 and 33 represent 500 µm, and those for CNCC dosages between 55 and 220 depict 1 mm

and at the same time serving as bridges that join some of the fibers forming a kind of web as shown in Fig. 5.

The zeta potential was again determined at the flocculation and reflocculation stages (Fig. 4b). From a negative charge of -34 mV of the initial pulp, the zeta potential was increased with increasing CNCC dosage, till reaching the IEP at the CNCC dosage of 20 mg/g. However, in this case, the charge was not reversed when the dosage was further increased, but was maintained around the IEP. Looking at the zeta potential values for the reflocculated samples, a negative charge possibly hidden inside the flocs may have been released, thus provoking a decrease in the bulk charge.

The tests carried out with CNCC dosages lower than 25 mg/g induced floc stabilities of around 65%, and higher percentages for larger CNCC concentrations (Fig. 4c). Reflocculation efficiencies were found to vary with the CNCC dosage (Fig. 4c), being around 80% for dosages below 10 mg/g, and decreasing till

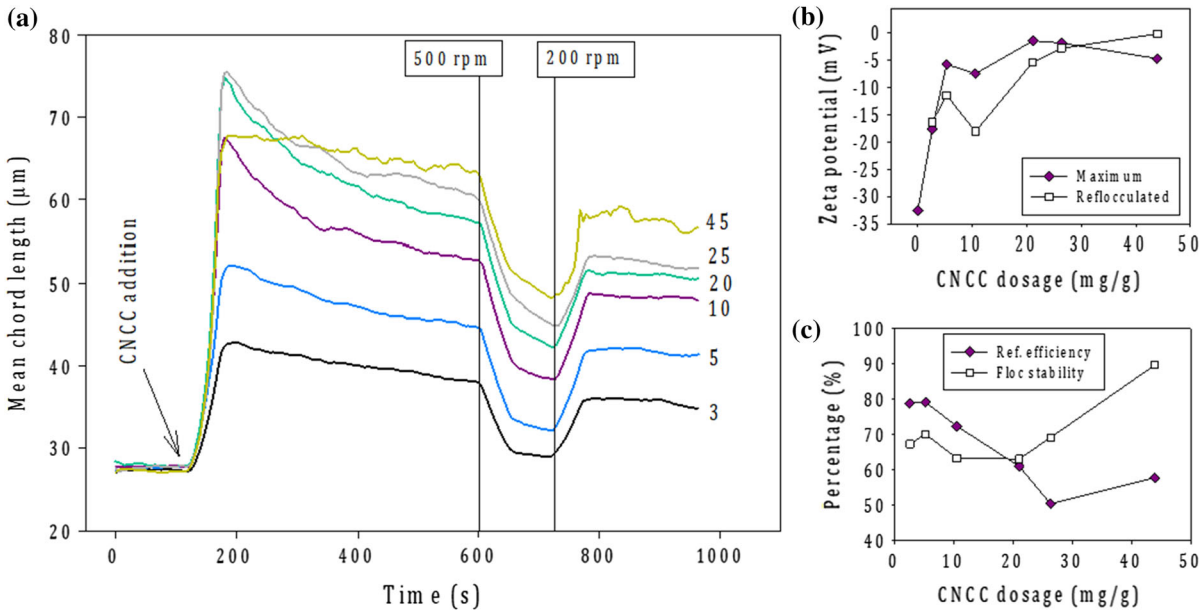

Fig. 4 **a** Mean chord length (MCL) profiles of flocs formed by the flocculation of RP using CNCC. Numbers indicated in the graph represent the CNCC dosage in mg/g. Vertical lines represent an external action on the experiment: first, CNCC addition at 200 rpm, second, increasing in the shear rate to 500 rpm and third, the reducing the stirring speed back to 200 rpm. **b** Zeta potential of flocs extracted from the FBRM experiments at the maximum MCL and at the reflocculation stage for different dosages of CNCC respect to the amount of RP, and **c** reflocculation efficiency and flocs stability of flocs at different CNCC dosages

50% for dosages over 25 mg/g. As observed in Fig. 5, when flocs are submitted to a high shear rate, fillers and fines situated among fibers are displaced and bonded to free areas of the fibers, thus increasing the width of the fibers but decreasing the floc size.

These results were compared to those obtained with some of the RS used traditionally in papermaking industries, such as a dual RS (DRS) composed of a coagulant and cationic polyacrylamide (PAM), polyvinylamine (PVA) or cationic starch (Merayo et al. 2017a). With the use of DRS, the maximum MCL was 72 µm, and it was achieved with 3.5 mg PAM/g. This increment was similar to that obtained with CNCC, but in this case with 20 mg/g. However, the floc stability achieved with CNCC was 62%, quite low compared to that of DRS, which was 72%. The proposed mechanism for DRS was bridging formation in view of the difference in dosage for optimum flocculation and for reaching the IEP, together with the low reflocculation efficiency, which was 25%. In contrast for CNCC, the maximum increment in the MCL was achieved at the IEP and the refflocculation efficiency was 60%.

For PVA, a lower flocculation efficiency was obtained, with a maximum MCL of 50 µm at the dosage of 30 mg/g. In this case, the floc stability was quite similar to that achieved by CNCC, but with a higher reflocculation efficiency, 78%. The proposed flocculation mechanism for this type of flocculant was patch formation (Merayo et al. 2017a).

Finally, for cationic starch 20 mg/g was needed to achieve the maximum MCL, with a value of 62 µm. Similar to DRS, a low reflocculation efficiency of 28% and a floc stability of 50% was obtained. The authors proposed that flocculation occurred due to bridging (Merayo et al. 2017a).

For CNCC, the increase in MCL was maximum compared to these types of RS. The flocculation stability was similar to that of PVA (62%), but the reflocculation efficiency (60%) was intermediate between the low values of DRS and cationic starch (25%), and the high value of PVA (78%). In addition, the maximum MCL was achieved at the IEP. The flocculation mechanism was, therefore, neither bridging nor patch formation. Similar to the flocculation in the absence of RP, the flocculation mechanism for the

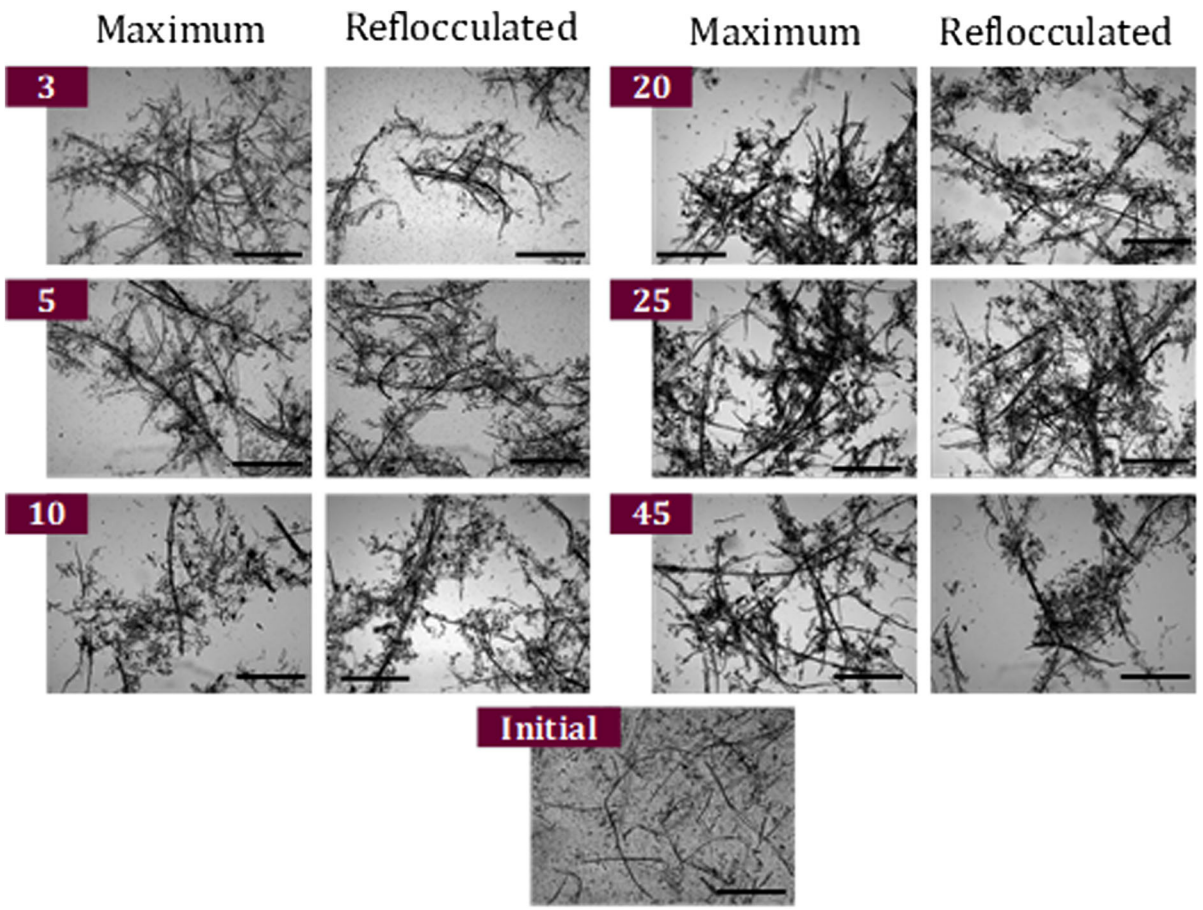

Fig. 5 Optical microscope images of RP flocs at 5 × magnification formed at different CNCC dosages at the maximum MCL point and at the reflocculation stage. Numbers indicated in the pictures represent the CNCC dosage corresponding to each experiment. Scale bar present in the images represent 1 mm

initial flocculation was charge neutralization. However, due to the rod-shape of the CNCC and their particular charge distribution having positive areas at the poles of the particles, it is probable that when the shear rate was increased, some of the particles that were standing up before, turned into particles lying flat, keeping the bulk charge unchanged but with smaller flocs. This could be the reason why reflocculation efficiency was 60%, implying that broken flocs did reform, but with an altered floc conformation, also shown in Fig. 5. Thus, it was deduced that the CNCC in the presence of RP acted through a charge neutralization mechanism in both flocculation and reflocculation stages, similar as the flocculation in the absence of RP.

Drainage and retention

The use of nanocellulose as a dry strengthening agent in paper has commonly resulted in a worsening of drainage (Taipale et al. 2010). However, with the use of the appropriate RS, this operation could be improved (Merayo et al. 2017b), but their implementation requires a previous optimization of the systems, which increases the complexity of the wet-end. We hypothesized that CNCC alone could partially fulfill all these requirements, and this is indeed what it is observed in Fig. 6.

As it could be expected from the flocculation tests, the pulp drainage time was reduced with the use of CNCC. The highest efficiency was found at the CNCC dosage of 20 mg/g, also the one with higher flocculation efficiency and that induced bigger flocs. At the

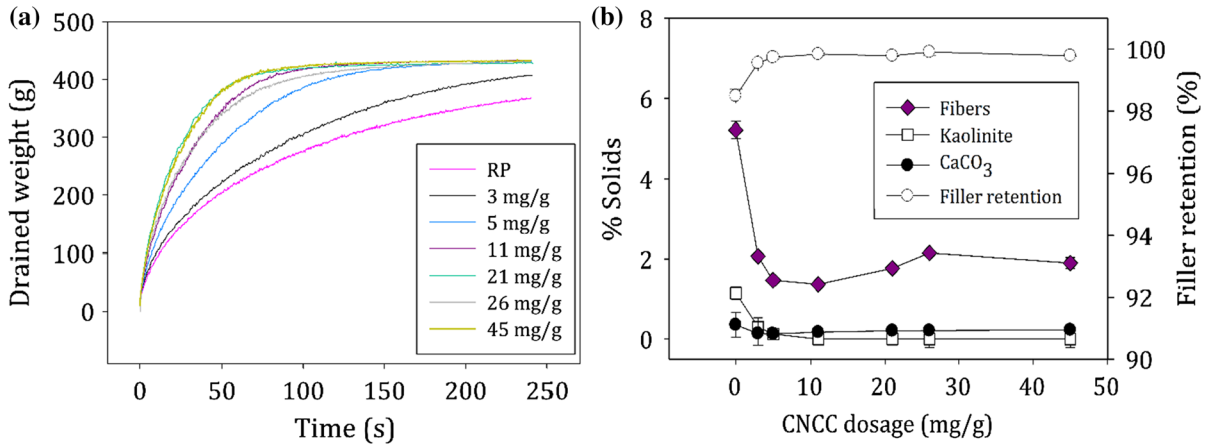

Fig. 6 **a** Evolution of the drained weight with time at different CNCC dosages, **b** solids that passed through the mesh during the drainage experiments and filler retention of the corresponding pad

cited dosage, the W300 (time consumed with the filtration of 300 g of the sample) was reduced from 122 to 26 s (78%), while the total drained weight increased by 15% (from 360 to 430 g). For all CNCC dosages tested, drainage time was reduced and the total drained water was increased, always reaching a constant value of 430 g. This improvement was reached even despite the high water retention capacity of the CNCC. The large floc size induced by CNCC together with the fact that CNCC are positioned inside the flocs, bridging the particles, and not on the surface, counteract the inherent high water retention capacity of the nanocelluloses.

Figure 6b shows the filler retention as well as the percentage of solids that passed through the mesh during the drainage experiments. From the total solid content present during drainage experiments, 6.7% passed through the mesh when no CNCC was added to the suspension. The non-retained solids consisted of 77% organics, likely fines, 17% kaolinite and 7% $CaCO_3$. When the CNCC dosage was increased, these percentages were strongly reduced, reaching a minimum at the CNCC dosage of 10 mg/g. At this dosage, the total drained solids was reduced to 1.6%, implying a solid retention of 98.4%. As shown in Fig. 6b, all kaolinite was retained inside the cake, while a low percentage of $CaCO_3$ passed through the mesh, but most of the drained sample was organic matter, i.e. fines. Results show that some fines flocculate with $CaCO_3$ without incorporation of kaolin. Perhaps this is due to the smaller size of kaolin. All fillers flocculate, but $CaCO_3$ is larger, thus being more easily removed from a fiber or an aggregate. When the CNCC dosage was higher than the IEP (20 mg/g), both drainage and solid retention efficiencies decreased. At these dosages, the charge of the system was reversed and some of the floc sizes were not large enough to be retained in the network.

These results were compared to those published previously by Merayo et al. (2017b), where the drainage and retention of the same RP was studied by the addition of different RS. Quite lower W300 values were obtained for CNCC compared to experiments carried out with either CPAM, CH or PVA. Although the CNCC reduced the drainage time by a large amount, it was smaller than results described previously (Merayo et al. 2017b). In these last assays, the W300 reached a value lower than 10 s with 1 mg/g CPAM, CH and 20 mg/g PVA. However, filler retention was much improved compared with that obtained with these RS: it was increased from 70% to 85% with CPAM, 82% with PVA and around 75% for CH and cationic starch (Merayo et al. 2017b), while it reached values near 98% with the use of CNCC.

The lower drainage efficiency of the CNCC could be ascribed to the location of the positive charges on the flocculant, which favors deposition of CNCC on fillers and fibers in a perpendicular orientation. Another relevant factor is the rigid rod-like shape of CNCC, instead of being flexible like CPAM or PVA. Chitosan, like cellulose is quite rigid, but when it is dissolved it has a persistence length of 22 nm (Terbojevich et al. 1991), compared to the CNCC characteristic length of 380 nm. Moreover, it was observed

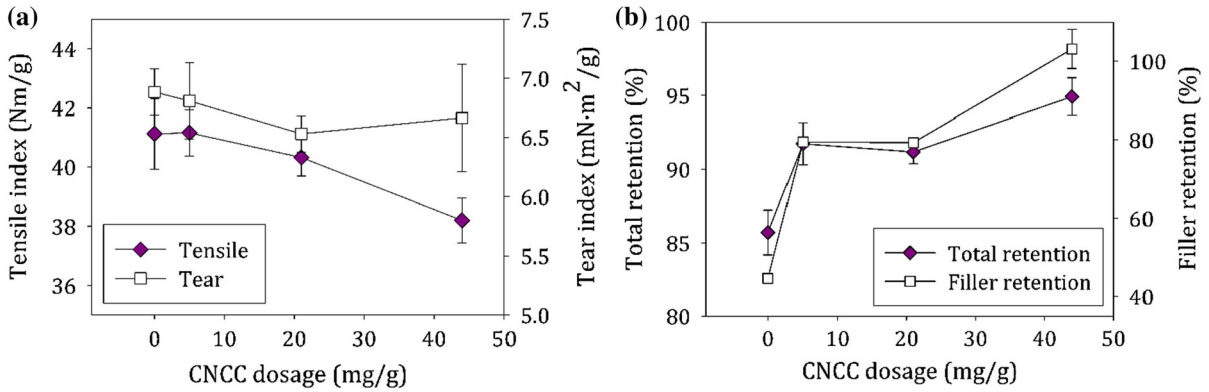

Fig. 7 **a** Effect of the CNCC dosage on the tensile and tear indexes of the produced handsheets and **b** total retention of solids and fillers in the prepared handsheets at different CNCC dosages

in optical images (Fig. 5) that all fillers were flocculated but some of them remained separated from the fibers. Hence it is likely that these non-attached flocs are trapped in the porous fiber web during papermaking, thus worsening the drainage time.

Mechanical properties

The effect on mechanical performance of RP upon CNCC addition was determined (Fig. 7). The tensile index did not present much change when the CNCC dosage was low (5 mg/g), while it further decreased with increasing dosage. This negative effect could have been caused by the increased presence of fillers in the paper (Fig. 7b), which avoids an effective and continuous bonding between fibers. However, most of the RS used typically in papermaking industries, such as CPAM or PVA, worsen paper strength to a much larger extent (Merayo et al. 2017b). The difference between CNCC and these other RS, could be ascribed to the fact that they are cellulosic and crystalline materials, and, therefore, have a high inherent strength (Habibi et al. 2010). In addition, the CNCC would most probably attach to the fillers and fibers in a perpendicular orientation, which may have induced a more open structure, harming paper formation. In this context, when a low CNCC dosage is used, a more homogenous and porous paper would be created, as shown in Fig. 5. In this case, the tensile index of the papers is not much affected. Nevertheless, the use of higher CNCC dosages induced a higher attraction of the CNCC-filler flocs to the fibers, with a filler retention of around 100%, covering them almost completely and reducing the possibilities of hydrogen bonding among them. This led to more open structures, similar as explained for lower dosages, but in this case, as the floc size observed is much higher, the sheet formation could have been harmed.

On the other hand, CNCC made no difference to the tear index (6.6 to 6.9 mN m^2/g). Usually, when highly fibrillated nanocellulose is added to a bleached pulp matrix, even at very low dosages, with or without fillers, the tensile index is enhanced, whereas the tear index is decreased (Balea et al. 2016b; Delgado-Aguilar et al. 2015), i.e. these indexes follow an opposite trend. It is believed that the reason why both indexes react oppositely with the use of nanocellulose is the larger number of hydrogen bonds among the different components induced by nanocellulose (Hassan et al. 2011). This effect is beneficious for tensile index but not for tear index, which is determined through the total number of fibers involved in the breaking of the paper, the fiber length and the number and strength of the interfiber bonds. In this case, both indexes follow the same trend with the increase in the CNCC dosage, decreasing slightly. Nevertheless, no clear conclusions could be drawn for the dosage of 45 mg/g in view of the large deviations.

Conclusions

The use of the CNCC as RS was studied through the addition of different percentages of this flocculant to a RP pulp. CNCC were found to flocculate successfully a suspension of only fillers in a wide range of dosages.

The maximum MCL was found at the CNCC dosage of 30 mg/g, increasing the floc size with a high slope and being quite below the IEP (55 mg/g). As both kaolin and $CaCO_3$ are negatively charged, there is no energy barrier between CNCC and filler. Thus, the rate of deposition was simply mass transport limited, and the process is an example of heteroflocculation.

When the applied CNCC dosage was larger than at the IEP, heterogeneous flocs were formed, having an excess of positive charges on the outside surface of the flocs and some interior spots were charge was not neutralized. When the shear rate was increased and reduced again, these negative areas interacted with the exterior part of other flocs, forming new flocs of larger size and compactness.

CNCC also induced flocculation of RP components in a wide range of dosages. The maximum MCL was found at a CNCC dosage lower than that obtained for fillers alone (20 mg/g), with a value of 75 µm. As the FBRM determines the width of the fibers, an increase in the MCL implies that fillers are being attached to the exterior surface of the fibers, as also shown in optical images. Due to the fact that the maximum MCL was found at the IEP, the flocculation mechanism before floc break-up was charge neutralization. A refloculation efficiency of 60% implied that broken flocs were anew formed but with an altered floc conformation. Again, the maximum MCL reached in this stage was at the IEP, which makes us come up with the same flocculation mechanism of charge neutralization.

Finally, the pulp drainage time was reduced by 78%, improving the retention by 77% with the addition of 20 mg/g CNCC. With the use of CNCC as a retention agent, not only flocculation of the RP components is much favored, but also the drainage and the retention can be improved without a detrimental effect on mechanical properties. Hence, their use stands out against other RS (Merayo et al. 2017a, b; Taipale et al. 2010), since only one agent could fulfill most of these requirements, increasing the simplicity of the wet-end system.

Acknowledgments Authors thank the Spanish Ministry of Economy and Competitiveness for the funding of the projects (Ref. CTQ2013-48090-C2-1-R and CTQ2017-85654-C2-2-R), the grant of C. Campano (BES-2014-068177) and the mobility funding (EEBB-I-17-12595); and the Community of Madrid for funding the RETO-PROSOST-CM (S2013/MAE-2907). Theo van de Ven acknowledges support of a NSERC Discovery grant (42686-13).

References

Balea A, Blanco A, Merayo N, Negro C (2016a) Effect of nanofibrillated cellulose to reduce linting on high filler-loaded recycled papers. Appita J 69:148–156

Balea A, Merayo N, Fuente E, Delgado-Aguilar M, Mutje P, Blanco A, Negro C (2016b) Valorization of corn stalk by the production of cellulose nanofibers to improve recycled paper properties. BioResources 11:3416–3431

Bergaya F, Lagaly G (2006) General introduction: clays, clay minerals, and clay science. Dev Clay Sci 1:1–18

Blanco A, Negro C, Hooimeijer A, Tijero J (1996) Polymer optimization in paper mills by means of a particle size analyser: an alternative to zeta potential measurements. Appita J 49:113–116

Blanco A, De la Fuente E, Negro C, Monte MC, Tijero J (2002) Focused beam reflectant measurement as a tool to measure flocculation. Tappi J 1:14–20

Blanco A, Miranda R, Monte MC (2013) Extending the limits of paper recycling: improvements along the paper value chain. For Syst 22:471–483. https://doi.org/10.5424/fs/2013223-03677

Campano C et al (2018a) Mechanical and chemical dispersion of nanocelluloses to improve their reinforcing effect on recycled paper. Cellulose 25:269–280. https://doi.org/10.1007/s10570-017-1552-y

Campano C, Merayo N, Negro C, Blanco A (2018b) In situ production of bacterial cellulose to economically improve recycled paper properties. Int J Biol Macromol 118:1532–1541. https://doi.org/10.1016/j.ijbiomac.2018.06.201

Chen DZ, van de Ven TGM (2016a) Flocculation kinetics of precipitated calcium carbonate (PCC) with sterically stabilized nanocrystalline cellulose (SNCC). Colloid Surf A-Physicochem Eng Asp 506:789–793. https://doi.org/10.1016/j.colsurfa.2016.07.058

Chen DZ, van de Ven TGM (2016b) Flocculation kinetics of precipitated calcium carbonate induced by electrosterically stabilized nanocrystalline cellulose. Colloid Surf A-Physicochem Eng Asp 504:11–17. https://doi.org/10.1016/j.colsurfa.2016.05.023

Delgado-Aguilar M, Gonzalez I, Pelach MA, De La Fuente E, Negro C, Mutje P (2015) Improvement of deinked old newspaper/old magazine pulp suspensions by means of nanofibrillated cellulose addition. Cellulose 22:789–802. https://doi.org/10.1007/s10570-014-0473-2

Diab M, Curtil D, El-shinnawy N, Hassan ML, Zeid IF, Mauret E (2015) Biobased polymers and cationic micro-fibrillated cellulose as retention and drainage aids in papermaking: comparison between softwood and bagasse pulps. Ind Crop Prod 72:34–45. https://doi.org/10.1016/j.indcrop.2015.01.072

Habibi Y (2014) Key advances in the chemical modification of nanocelluloses. Chem Soc Rev 43:1519–1542. https://doi.org/10.1039/c3cs60204d

Habibi Y, Lucia LA, Rojas OJ (2010) Cellulose nanocrystals: chemistry, self-assembly, and applications. Chem Rev 110:3479–3500. https://doi.org/10.1021/cr900339w

Hassan EA, Hassan ML, Oksman K (2011) Improving bagasse pulp paper sheet properties with microfibrillated cellulose

isolated from xylanase-treated bagasse. Wood Fiber Sci 43:76–82

Hubbe MA, Venditti RA, Rojas OJ (2007) What happens to cellulosic fibers during papermaking and recycling? A review. BioResources 2:739–788

Kumar V, Taylor MK, Mehrotra A, Stagner WC (2013) Real-time particle size analysis using focused beam reflectance measurement as a process analytical technology tool for a continuous granulation-drying-milling process. AAPS PharmSciTech 14:523–530. https://doi.org/10.1208/s12249-013-9934-4

Lourenco AF, Gamelas JAF, Ferreira PJ (2014) Increase of the filler content in papermaking by using a silica-coated PCC filler. Nord Pulp Paper Res J 29:240–245

Merayo N, Balea A, de la Fuente E, Blanco Á, Negro C (2017a) Interactions between cellulose nanofibers and retention systems in flocculation of recycled fibers. Cellulose 24:677–692. https://doi.org/10.1007/s10570-016-1138-0

Merayo N, Balea A, de la Fuente E, Blanco Á, Negro C (2017b) Synergies between cellulose nanofibers and retention additives to improve recycled paper properties and the drainage process. Cellulose 24:2987–3000

Miranda R, Blanco Á (2010) Environmental awareness and paper recycling. Cellul Chem Technol 44:431–449

Rasteiro M, Garcia F, Ferreira P, Blanco A, Negro C, Antunes E (2008) Evaluation of flocs resistance and reflocculation capacity using the LDS technique. Powder Tecnol 183:231–238

Raymond L, Turcotte R, Gratton R (2004) The challenges of increasing filler in fine paper. Pap Technol 45:34–40

Taipale T, Osterberg M, Nykanen A, Ruokolainen J, Laine J (2010) Effect of microfibrillated cellulose and fines on the drainage of kraft pulp suspension and paper strength. Cellulose 17:1005–1020. https://doi.org/10.1007/s10570-010-9431-9

Terbojevich M, Cosani A, Conio G, Marsano E, Bianchi E (1991) Chitosan: chain rigidity and mesophase formation. Carbohydr Res 209:251–260

van de Ven TGM, Sheikhi A (2016) Hairy cellulose nanocrystalloids: a novel class of nanocellulose. Nanoscale 8:15101–15114. https://doi.org/10.1039/c6nr01570k

Wu MR, van de Ven TGM (2009) Flocculation and reflocculation: interplay between the adsorption behavior of the components of a dual flocculant. Colloid Surf A-Physicochem Eng Asp 341:40–45. https://doi.org/10.1016/j.colsurfa.2009.03.034

Yang H, van de Ven TGM (2016) Preparation of hairy cationic nanocrystalline cellulose. Cellulose 23:1791–1801. https://doi.org/10.1007/s10570-016-0902-5

Yang H, Alam MN, van de Ven TGM (2013) Highly charged nanocrystalline cellulose and dicarboxylated cellulose from periodate and chlorite oxidized cellulose fibers. Cellulose 20:1865–1875. https://doi.org/10.1007/s10570-013-9966-7

Yoon SY, Deng YL (2004) Flocculation and reflocculation of clay suspension by different polymer systems under turbulent conditions. J Colloid Interface Sci 278:139–145. https://doi.org/10.1016/j.jcis.2004.05.011

Yousefi H, Faezipour M, Hedjazi S, Mousavi MM, Azusa Y, Heidari AH (2013) Comparative study of paper and nanopaper properties prepared from bacterial cellulose nanofibers and fibers/ground cellulose nanofibers of canola straw. Ind Crop Prod 43:732–737. https://doi.org/10.1016/j.indcrop.2012.08.030